$\Xi_c(3055)$ DECAY MODES

	Mode	Fraction (Γ_i/Γ)
Γ_1	$\Sigma^{++}K^-$	seen
Γ_2	ΛD^+	seen

$\Xi_c(3055)$ BRANCHING RATIOS

$\Gamma(\Lambda D^+)/\Gamma(\Sigma^{++}K^-)$ Γ_2/Γ_1

VALUE	DOCUMENT ID		TECN	COMMENT
5.09±1.01±0.76	KATO	16	BELL	721 and 103 evts

$\Xi_c(3055)$ REFERENCES

KATO	16	PR D94 032002	Y. Kato *et al.*	(BELLE Collab.)
KATO	14	PR D89 052003	Y. Kato *et al.*	(BELLE Collab.)
AUBERT	08J	PR D77 012002	B. Aubert *et al.*	(BABAR Collab.)

$\Xi_c(3080)$

$I(J^P) = \frac{1}{2}(?^?)$ Status: ***

$\Xi_c(3080)$ MASSES

$\Xi_c(3080)^+$ MASS

VALUE (MeV)	EVTS	DOCUMENT ID		TECN	COMMENT
3077.2±0.4 OUR AVERAGE					
3077.9±0.9	596	KATO	16	BELL	e^+e^- Υ region
3077.0±0.4±0.2	403 ± 60	AUBERT	08J	BABR	$e^+e^- \approx 10.58$ GeV
• • • We do not use the following data for averages, fits, limits, etc. • • •					
3076.9±0.3±0.2	210 ± 30	KATO	14	BELL	See KATO 16
3076.7±0.9±0.5	326 ± 40	CHISTOV	06	BELL	See KATO 14

$\Xi_c(3080)^0$ MASS

VALUE (MeV)	EVTS	DOCUMENT ID		TECN	COMMENT
3079.9±1.4 OUR AVERAGE Error includes scale factor of 1.3.					
3079.3±1.1±0.2	90 ± 27	AUBERT	08J	BABR	$e^+e^- \approx 10.58$ GeV
3082.8±1.8±1.5	67 ± 20	CHISTOV	06	BELL	$e^+e^- \approx \Upsilon(4S)$

$\Xi_c(3080)$ WIDTHS

$\Xi_c(3080)^+$ WIDTH

VALUE (MeV)	EVTS	DOCUMENT ID		TECN	COMMENT
3.6±1.1 OUR AVERAGE Error includes scale factor of 1.5.					
3.0±0.7±0.4	596	KATO	16	BELL	e^+e^- Υ region
5.5±1.3±0.6	403 ± 60	AUBERT	08J	BABR	$e^+e^- \approx 10.58$ GeV
• • • We do not use the following data for averages, fits, limits, etc. • • •					
2.4±0.9±1.6	210 ± 30	KATO	14	BELL	See KATO 16
6.2±1.2±0.8	326 ± 40	CHISTOV	06	BELL	See KATO 14

$\Xi_c(3080)^0$ WIDTH

VALUE (MeV)	EVTS	DOCUMENT ID		TECN	COMMENT
5.6±2.2 OUR AVERAGE					
5.9±2.3±1.5	90 ± 27	AUBERT	08J	BABR	$e^+e^- \approx 10.58$ GeV
5.2±3.1±1.8	67 ± 20	CHISTOV	06	BELL	$e^+e^- \approx \Upsilon(4S)$

$\Xi_c(3080)$ DECAY MODES

	Mode	Fraction (Γ_i/Γ)
Γ_1	$\Lambda_c^+ \overline{K}\pi$	seen
Γ_2	$\Sigma_c(2455)\overline{K}$	seen
Γ_3	$\Sigma_c(2455)^{++}K^-$	seen
Γ_4	$\Sigma_c(2520)^{++}K^-$	seen
Γ_5	$\Sigma_c(2455)\overline{K} + \Sigma_c(2520)\overline{K}$	seen
Γ_6	$\Lambda_c^+ \overline{K}$	not seen
Γ_7	$\Lambda_c^+ \overline{K}\pi^+\pi^-$	not seen
Γ_8	ΛD^+	seen

$\Xi_c(3080)$ BRANCHING RATIOS

$\Gamma(\Sigma_c(2455)\overline{K})/\Gamma(\Lambda_c^+\overline{K}\pi)$ Γ_2/Γ_1

VALUE	DOCUMENT ID		TECN	COMMENT
0.45±0.06 OUR AVERAGE				
0.45±0.05±0.05	AUBERT	08J	BABR	in $\Lambda_c^+ K^-\pi^+$
0.44±0.12±0.07	AUBERT	08J	BABR	in $\Lambda_c^+ K_S^0\pi^-$

$\Gamma(\Sigma_c(2520)^{++}K^-)/\Gamma(\Sigma_c(2455)^{++}K^-)$ Γ_4/Γ_3

VALUE	DOCUMENT ID		TECN	COMMENT
1.07±0.27±0.04	KATO	16	BELL	234 and 176 evts

$[\Gamma(\Sigma_c(2455)\overline{K}) + \Gamma(\Sigma_c(2520)\overline{K})]/\Gamma(\Lambda_c^+\overline{K}\pi)$ Γ_5/Γ_1

VALUE	DOCUMENT ID		TECN	COMMENT
0.89±0.12 OUR AVERAGE				
0.95±0.14±0.06	AUBERT	08J	BABR	in $\Lambda_c^+ K^-\pi^+$
0.78±0.21±0.05	AUBERT	08J	BABR	in $\Lambda_c^+ K_S^0\pi^-$

$\Gamma(\Lambda D^+)/\Gamma(\Sigma_c(2455)^{++}K^-)$ Γ_8/Γ_3

VALUE	DOCUMENT ID		TECN	COMMENT
1.29±0.30±0.15	KATO	16	BELL	186 and 176 evts

$\Xi_c(3080)$ REFERENCES

KATO	16	PR D94 032002	Y. Kato *et al.*	(BELLE Collab.)
KATO	14	PR D89 052003	Y. Kato *et al.*	(BELLE Collab.)
AUBERT	08J	PR D77 012002	B. Aubert *et al.*	(BABAR Collab.)
CHISTOV	06	PRL 97 162001	R. Chistov *et al.*	(BELLE Collab.)

$\Xi_c(3123)$

$I(J^P) = ?(?^?)$ Status: *

OMITTED FROM SUMMARY TABLE

A peak in the $\Sigma_c(2520)^{++}K^- \to \Lambda_c^+ K^-\pi^+$ mass spectrum with a significance of 3.6 standard deviations. KATO 14 finds no evidence for this state.

$\Xi_c(3123)$ MASSES

$\Xi_c(3123)^+$ MASS

VALUE (MeV)	EVTS	DOCUMENT ID		TECN	COMMENT
3122.9±1.3±0.3	101 ± 35	AUBERT	08J	BABR	$e^+e^- \approx 10.58$ GeV

$\Xi_c(3123)$ WIDTHS

$\Xi_c(3123)^+$ WIDTH

VALUE (MeV)	EVTS	DOCUMENT ID		TECN	COMMENT
4.4±3.4±1.7	101 ± 35	AUBERT	08J	BABR	$e^+e^- \approx 10.58$ GeV

$\Xi_c(3123)$ REFERENCES

KATO	14	PR D89 052003	Y. Kato *et al.*	(BELLE Collab.)
AUBERT	08J	PR D77 012002	B. Aubert *et al.*	(BABAR Collab.)

Ω_c^0

$I(J^P) = 0(\frac{1}{2}^+)$ Status: ***

The quantum numbers have not been measured, but are simply assigned in accord with the quark model, in which the Ω_c^0 is the *ssc* ground state.

Ω_c^0 MASS

VALUE (MeV)	EVTS	DOCUMENT ID		TECN	COMMENT
2695.2± 1.7 OUR FIT Error includes scale factor of 1.3.					
2695.2$^{+\ 1.8}_{-\ 1.6}$ OUR AVERAGE Error includes scale factor of 1.3. See the ideogram below.					
2693.6± 0.3$^{+1.8}_{-1.5}$	725	SOLOVIEVA	09	BELL	$\Omega^-\pi^+$ in $e^+e^- \to \Upsilon(4S)$
2694.6± 2.6±1.9	40	[1] CRONIN-HEN..01		CLE2	$e^+e^- \approx 10.6$ GeV
2699.9± 1.5±2.5	42	[2] FRABETTI	94H	E687	γBe, $\overline{E}_\gamma = 221$ GeV
• • • We do not use the following data for averages, fits, limits, etc. • • •					
2705.9± 3.3±2.0	10	[3] FRABETTI	93	E687	γBe, $\overline{E}_\gamma = 221$ GeV
2719.0± 7.0±2.5	11	[4] ALBRECHT	92H	ARG	$e^+e^- \approx 10.6$ GeV
2740 ±20	3	BIAGI	85B	SPEC	Σ^-Be 135 GeV/c

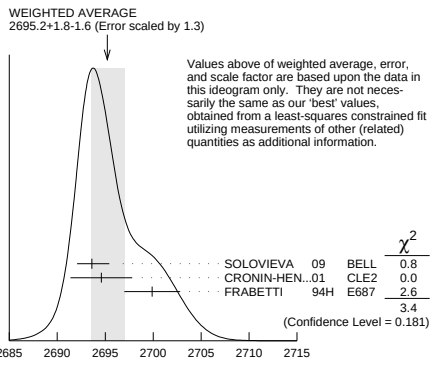

[1] CRONIN-HENNESSY 01 sees 40.4 ± 9.0 events in a sum over five channels.

[2] FRABETTI 94H claims a signal of 42.5 ± 8.8 $\Sigma^+ K^- K^- \pi^+$ events. The background is about 24 events.
[3] FRABETTI 93 claims a signal of 10.3 ± 3.9 $\Omega^- \pi^+$ events above a background of 5.8 events.
[4] ALBRECHT 92H claims a signal of 11.5 ± 4.3 $\Xi^- K^- \pi^+ \pi^+$ events. The background is about 5 events.

Ω_c^0 MEAN LIFE

VALUE (10^{-15} s)	EVTS	DOCUMENT ID		TECN	COMMENT
69±12 OUR AVERAGE					
72±11±11	64	LINK	03C	FOCS	$\Omega^- \pi^+$, $\Xi^- K^- \pi^+ \pi^+$
55^{+13+18}_{-11-23}	86	ADAMOVICH	95B	WA89	$\Omega^- \pi^- \pi^+ \pi^+$, $\Xi^- K^- \pi^+ \pi^+$
86^{+27}_{-20}±28	25	FRABETTI	95D	E687	$\Sigma^+ K^- K^- \pi^+$

Ω_c^0 DECAY MODES

Mode	Fraction (Γ_i/Γ)	Confidence level

No absolute branching fractions have been measured.
The following are branching *ratios* relative to $\Omega^- \pi^+$.

Cabibbo-favored ($S = -3$) decays — relative to $\Omega^- \pi^+$

Γ_1	$\Omega^- \pi^+$	**DEFINED AS 1**	
Γ_2	$\Omega^- \pi^+ \pi^0$	1.80±0.33	
Γ_3	$\Omega^- \rho^+$	>1.3	90%
Γ_4	$\Omega^- \pi^- 2\pi^+$	0.31±0.05	
Γ_5	$\Omega^- e^+ \nu_e$	2.4 ±1.2	
Γ_6	$\Xi^0 \overline{K}^0$	1.64±0.29	
Γ_7	$\Xi^0 K^- \pi^+$	1.20±0.18	
Γ_8	$\Xi^0 \overline{K}^{*0}$, $\overline{K}^{*0} \to K^- \pi^+$	0.68±0.16	
Γ_9	$\Xi^- \overline{K}^0 \pi^+$	2.12±0.28	
Γ_{10}	$\Xi^- K^- 2\pi^+$	0.63±0.09	
Γ_{11}	$\Xi(1530)^0 K^- \pi^+$, $\Xi^{*0} \to \Xi^- \pi^+$	0.21±0.06	
Γ_{12}	$\Xi^- \overline{K}^{*0} \pi^+$	0.34±0.11	
Γ_{13}	$\Sigma^+ K^- K^- \pi^+$	<0.32	90%
Γ_{14}	$\Lambda \overline{K}^0 K^0$	1.72±0.35	

Ω_c^0 BRANCHING RATIOS

A few early but now obsolete measurements have been omitted. See K.A. Olive, et al. (Particle Data Group), Chinese Physics **C38** 070001 (2014).

$\Gamma(\Omega^- \pi^+ \pi^0)/\Gamma(\Omega^- \pi^+)$ Γ_2/Γ_1

VALUE	EVTS	DOCUMENT ID		TECN	COMMENT
1.80±0.33 OUR AVERAGE		Error includes scale factor of 1.9.			
2.00±0.17±0.11	403	YELTON	18	BELL	$e^+ e^- \to \Upsilon(4S)$, +higher
1.27±0.31±0.11	64	AUBERT	07AH	BABR	$e^+ e^- \approx \Upsilon(4S)$

$\Gamma(\Omega^- \rho^+)/\Gamma(\Omega^- \pi^+ \pi^0)$ Γ_3/Γ_2

VALUE	CL%	DOCUMENT ID		TECN	COMMENT
>0.71	90	[1] YELTON	18	BELL	$e^+ e^- \to \Upsilon(4S)$, +higher

[1] This submode fraction is evaluated from a background-subtracted signal in a mass plot. Result ignores interference effects and systematic uncertainties, which YELTON 18 claim are both small.

$\Gamma(\Omega^- \pi^- 2\pi^+)/\Gamma(\Omega^- \pi^+)$ Γ_4/Γ_1

VALUE	EVTS	DOCUMENT ID		TECN	COMMENT
0.31±0.05 OUR AVERAGE					
0.32±0.05±0.02	108	YELTON	18	BELL	$e^+ e^- \to \Upsilon(4S)$, +higher
0.28±0.09±0.01	25	AUBERT	07AH	BABR	$e^+ e^- \approx \Upsilon(4S)$

$\Gamma(\Omega^- \pi^+)/\Gamma(\Omega^- e^+ \nu_e)$ Γ_1/Γ_5

VALUE	EVTS	DOCUMENT ID		TECN	COMMENT
0.41±0.19±0.04	11	AMMAR	02	CLE2	$e^+ e^- \approx \Upsilon(4S)$

$\Gamma(\Xi^0 \overline{K}^0)/\Gamma(\Omega^- \pi^+)$ Γ_6/Γ_1

VALUE	EVTS	DOCUMENT ID		TECN	COMMENT
1.64±0.26±0.12	98	YELTON	18	BELL	$e^+ e^- \to \Upsilon(4S)$, +higher

$\Gamma(\Xi^0 K^- \pi^+)/\Gamma(\Omega^- \pi^+)$ Γ_7/Γ_1

VALUE	EVTS	DOCUMENT ID		TECN	COMMENT
1.20±0.16±0.08	168	YELTON	18	BELL	$e^+ e^- \to \Upsilon(4S)$, +higher

$\Gamma(\Xi^0 \overline{K}^{*0}, \overline{K}^{*0} \to K^- \pi^+)/\Gamma(\Xi^0 K^- \pi^+)$ Γ_8/Γ_7

VALUE	EVTS	DOCUMENT ID		TECN	COMMENT
0.57±0.10	95	[1] YELTON	18	BELL	$e^+ e^- \to \Upsilon(4S)$, +higher

[1] This submode fraction is evaluated from a background-subtracted signal in a mass plot. Result ignores interference effects and systematic uncertainties, which YELTON 18 claim are both small.

$\Gamma(\Xi^- \overline{K}^0 \pi^+)/\Gamma(\Omega^- \pi^+)$ Γ_9/Γ_1

VALUE	EVTS	DOCUMENT ID		TECN	COMMENT
2.12±0.24±0.14	349	YELTON	18	BELL	$e^+ e^- \to \Upsilon(4S)$, +higher

$\Gamma(\Xi^- K^- 2\pi^+)/\Gamma(\Omega^- \pi^+)$ Γ_{10}/Γ_1

VALUE	EVTS	DOCUMENT ID		TECN	COMMENT
0.63±0.09 OUR AVERAGE		Error includes scale factor of 1.4.			
0.68±0.07±0.03	278	YELTON	18	BELL	$e^+ e^- \to \Upsilon(4S)$, +higher
0.46±0.13±0.03	45	AUBERT	07AH	BABR	$e^+ e^- \approx \Upsilon(4S)$

$\Gamma(\Xi(1530)^0 K^- \pi^+, \Xi^{*0} \to \Xi^- \pi^+)/\Gamma(\Xi^- K^- 2\pi^+)$ Γ_{11}/Γ_{10}

VALUE	EVTS	DOCUMENT ID		TECN	COMMENT
0.33±0.09	74	[1] YELTON	18	BELL	$e^+ e^- \to \Upsilon(4S)$, +higher

[1] This submode fraction is evaluated from a background-subtracted signal in a mass plot. Result ignores interference effects and systematic uncertainties, which YELTON 18 claim are both small.

$\Gamma(\Xi^- \overline{K}^{*0} \pi^+)/\Gamma(\Xi^- K^- 2\pi^+)$ Γ_{12}/Γ_{10}

VALUE	EVTS	DOCUMENT ID		TECN	COMMENT
0.55±0.16	136	[1] YELTON	18	BELL	$e^+ e^- \to \Upsilon(4S)$, +higher

[1] This submode fraction is evaluated from a background-subtracted signal in a mass plot. Result ignores interference effects and systematic uncertainties, which YELTON 18 claim are both small.

$\Gamma(\Sigma^+ K^- K^- \pi^+)/\Gamma(\Omega^- \pi^+)$ Γ_{13}/Γ_1

VALUE	CL%	EVTS	DOCUMENT ID		TECN	COMMENT
<0.32	90	17	YELTON	18	BELL	$e^+ e^- \to \Upsilon(4S)$, +higher

$\Gamma(\Lambda \overline{K}^0 \overline{K}^0)/\Gamma(\Omega^- \pi^+)$ Γ_{14}/Γ_1

VALUE	EVTS	DOCUMENT ID		TECN	COMMENT
1.72±0.32±0.14	95	YELTON	18	BELL	$e^+ e^- \to \Upsilon(4S)$, +higher

Ω_c^0 REFERENCES

YELTON	18	PR D97 032001	J. Yelton *et al.*	(BELLE Collab.)
PDG	14	CP C38 070001	K. Olive *et al.*	(PDG Collab.)
SOLOVIEVA	09	PL B672 1	E. Solovieva *et al.*	(BELLE Collab.)
AUBERT	07AH	PRL 99 062001	B. Aubert *et al.*	(BABAR Collab.)
LINK	03C	PL B561 41	J.M. Link *et al.*	(FNAL FOCUS Collab.)
AMMAR	02	PRL 89 171803	R. Ammar *et al.*	(CLEO Collab.)
CRONIN-HEN...	01	PRL 86 3730	D. Cronin-Hennessy *et al.*	(CLEO Collab.)
ADAMOVICH	95B	PL B358 151	M.I. Adamovich *et al.*	(CERN WA89 Collab.)
FRABETTI	95D	PL B357 678	P.L. Frabetti *et al.*	(FNAL E687 Collab.)
FRABETTI	94H	PL B338 106	P.L. Frabetti *et al.*	(FNAL E687 Collab.)
FRABETTI	93	PL B300 190	P.L. Frabetti *et al.*	(FNAL E687 Collab.)
ALBRECHT	92H	PL B288 367	H. Albrecht *et al.*	(ARGUS Collab.)
BIAGI	85B	ZPHY C28 175	S.F. Biagi *et al.*	(CERN WA62 Collab.)

$\Omega_c(2770)^0$

$I(J^P) = 0(\frac{3}{2}^+)$ Status: ***

The natural assignment is that this goes with the $\Sigma_c(2520)$ and $\Xi_c(2645)$ to complete the lowest mass $J^P = \frac{3}{2}^+$ SU(3) sextet, part of the SU(4) 20-plet that includes the $\Delta(1232)$. But J and P have not been measured.

$\Omega_c(2770)^0$ MASS

The mass is obtained from the mass-difference measurement that follows.

VALUE (MeV)	DOCUMENT ID
2765.9±2.0 OUR FIT	Error includes scale factor of 1.2.

$\Omega_c(2770)^0 - \Omega_c^0$ MASS DIFFERENCE

VALUE (MeV)	EVTS	DOCUMENT ID		TECN	COMMENT
$70.7^{+0.8}_{-0.9}$ OUR FIT					
$70.7^{+0.8}_{-1.0}$ OUR AVERAGE					
$70.7\pm0.9^{+0.1}_{-0.9}$	54 ± 9	SOLOVIEVA	09	BELL	$\Omega_c^0 \gamma$ in $e^+ e^- \to \Upsilon(4S)$
70.8±1.0±1.1	105 ± 22	AUBERT,BE	06I	BABR	$e^+ e^- \approx \Upsilon(4S)$

$\Omega_c(2770)^0$ DECAY MODES

The $\Omega_c(2770)^0 - \Omega_c^0$ mass difference is too small for any strong decay to occur.

	Mode	Fraction (Γ_i/Γ)
Γ_1	$\Omega_c^0 \gamma$	presumably 100%

$\Omega_c(2770)^0$ REFERENCES

SOLOVIEVA	09	PL B672 1	E. Solovieva *et al.*	(BELLE Collab.)
AUBERT,BE	06I	PRL 97 232001	B. Aubert *et al.*	(BABAR Collab.)

$\Omega_c(3000)^0$ $I(J^P) = ?(?^?)$ Status: ***

$\Omega_c(3000)^0$ MASS

VALUE (MeV)	EVTS	DOCUMENT ID		TECN	COMMENT
3000.4±0.2±0.1±0.3	1.3k	[1] AAIJ	17AH	LHCB	*pp* at 7, 8, 13 TeV

[1] The third error is the uncertainty on the Ξ_c^+ mass. (AAIJ 17AH gave $^{+0.3}_{-0.5}$ MeV here, but as of 2018 it is ±0.3.)

$\Omega_c(3000)^0$ WIDTH

VALUE (MeV)	EVTS	DOCUMENT ID		TECN	COMMENT
4.5±0.6±0.3	1.3k	AAIJ	17AH	LHCB	*pp* at 7, 8, 13 TeV

$\Omega_c(3000)^0$ DECAY MODES

	Mode	Fraction (Γ_i/Γ)
Γ_1	$\Xi_c^+ K^-$	seen

$\Omega_c(3000)^0$ BRANCHING RATIOS

$\Gamma(\Xi_c^+ K^-)/\Gamma_{total}$ Γ_1/Γ

VALUE	DOCUMENT ID		TECN	COMMENT
seen	AAIJ	17AH	LHCB	*pp* at 7, 8, 13 TeV

$\Omega_c(3000)^0$ REFERENCES

AAIJ	17AH	PRL 118 182001	R. Aaij *et al.*	(LHCb Collab.)

$\Omega_c(3050)^0$ $I(J^P) = ?(?^?)$ Status: ***

$\Omega_c(3050)^0$ MASS

VALUE (MeV)	EVTS	DOCUMENT ID		TECN	COMMENT
3050.2±0.1±0.1±0.3	970	[1] AAIJ	17AH	LHCB	*pp* at 7, 8, 13 TeV

[1] The third error is the uncertainty on the Ξ_c^+ mass. (AAIJ 17AH gave $^{+0.3}_{-0.5}$ MeV here, but as of 2018 it is ±0.3.)

$\Omega_c(3050)^0$ WIDTH

VALUE (MeV)	CL%	DOCUMENT ID		TECN	COMMENT
<1.2	95	AAIJ	17AH	LHCB	*pp* at 7, 8, 13 TeV

$\Omega_c(3050)^0$ DECAY MODES

	Mode	Fraction (Γ_i/Γ)
Γ_1	$\Xi_c^+ K^-$	seen

$\Omega_c(3050)^0$ BRANCHING RATIOS

$\Gamma(\Xi_c^+ K^-)/\Gamma_{total}$ Γ_1/Γ

VALUE	DOCUMENT ID		TECN	COMMENT
seen	AAIJ	17AH	LHCB	*pp* at 7, 8, 13 TeV

$\Omega_c(3050)^0$ REFERENCES

AAIJ	17AH	PRL 118 182001	R. Aaij *et al.*	(LHCb Collab.)

$\Omega_c(3065)^0$ $I(J^P) = ?(?^?)$ Status: ***

$\Omega_c(3065)^0$ MASS

VALUE (MeV)	EVTS	DOCUMENT ID		TECN	COMMENT
3065.6±0.1±0.3±0.3	1.74k	[1] AAIJ	17AH	LHCB	*pp* at 7, 8, 13 TeV

[1] The third error is the uncertainty on the Ξ_c^+ mass. (AAIJ 17AH gave $^{+0.3}_{-0.5}$ MeV here, but as of 2018 it is ±0.3.)

$\Omega_c(3065)^0$ WIDTH

VALUE (MeV)	EVTS	DOCUMENT ID		TECN	COMMENT
3.5±0.4±0.2	1.74k	AAIJ	17AH	LHCB	*pp* at 7, 8, 13 TeV

$\Omega_c(3065)^0$ DECAY MODES

	Mode	Fraction (Γ_i/Γ)
Γ_1	$\Xi_c^+ K^-$	seen

$\Omega_c(3065)^0$ BRANCHING RATIOS

$\Gamma(\Xi_c^+ K^-)/\Gamma_{total}$ Γ_1/Γ

VALUE	DOCUMENT ID		TECN	COMMENT
seen	AAIJ	17AH	LHCB	*pp* at 7, 8, 13 TeV

$\Omega_c(3065)^0$ REFERENCES

AAIJ	17AH	PRL 118 182001	R. Aaij *et al.*	(LHCb Collab.)

$\Omega_c(3090)^0$ $I(J^P) = ?(?^?)$ Status: ***

$\Omega_c(3090)^0$ MASS

VALUE (MeV)	EVTS	DOCUMENT ID		TECN	COMMENT
3090.2±0.3±0.5±0.3	2.0k	[1] AAIJ	17AH	LHCB	*pp* at 7, 8, 13 TeV

[1] The third error is the uncertainty on the Ξ_c^+ mass. (AAIJ 17AH gave $^{+0.3}_{-0.5}$ MeV here, but as of 2018 it is ±0.3.)

$\Omega_c(3090)^0$ WIDTH

VALUE (MeV)	EVTS	DOCUMENT ID		TECN	COMMENT
8.7±1.0±0.8	2.0k	AAIJ	17AH	LHCB	*pp* at 7, 8, 13 TeV

$\Omega_c(3090)^0$ DECAY MODES

	Mode	Fraction (Γ_i/Γ)
Γ_1	$\Xi_c^+ K^-$	seen

$\Omega_c(3090)^0$ BRANCHING RATIOS

$\Gamma(\Xi_c^+ K^-)/\Gamma_{total}$ Γ_1/Γ

VALUE	DOCUMENT ID		TECN	COMMENT
seen	AAIJ	17AH	LHCB	*pp* at 7, 8, 13 TeV

$\Omega_c(3090)^0$ REFERENCES

AAIJ	17AH	PRL 118 182001	R. Aaij *et al.*	(LHCb Collab.)

$\Omega_c(3120)^0$ $I(J^P) = ?(?^?)$ Status: ***

$\Omega_c(3120)^0$ MASS

VALUE (MeV)	EVTS	DOCUMENT ID		TECN	COMMENT
3119.1±0.3±0.9±0.3	480	[1] AAIJ	17AH	LHCB	*pp* at 7, 8, 13 TeV

[1] The third error is the uncertainty on the Ξ_c^+ mass. (AAIJ 17AH gave $^{+0.3}_{-0.5}$ MeV here, but as of 2018 it is ±0.3.)

$\Omega_c(3120)^0$ WIDTH

VALUE (MeV)	CL%	DOCUMENT ID		TECN	COMMENT
<2.6	95	AAIJ	17AH	LHCB	*pp* at 7, 8, 13 TeV

$\Omega_c(3120)^0$ DECAY MODES

	Mode	Fraction (Γ_i/Γ)
Γ_1	$\Xi_c^+ K^-$	seen

$\Omega_c(3120)^0$ BRANCHING RATIOS

$\Gamma(\Xi_c^+ K^-)/\Gamma_{\text{total}}$ Γ_1/Γ

VALUE	DOCUMENT ID		TECN	COMMENT
seen	AAIJ	17AH	LHCB	pp at 7, 8, 13 TeV

$\Omega_c(3120)^0$ REFERENCES

AAIJ 17AH PRL 118 182001 R. Aaij *et al.* (LHCb Collab.)

DOUBLY CHARMED BARYONS ($C = +2$)

$\Xi_{cc}^{++} = u\,c\,c$, $\Xi_{cc}^{+} = d\,c\,c$, $\Omega_{cc}^{+} = s\,c\,c$

Ξ_{cc}^{+}

$I(J^P) = ?(?^?)$ Status: *

OMITTED FROM SUMMARY TABLE

This would presumably be an isospin-1/2 particle, a ccu Ξ_{cc}^{++} and a ccd Ξ_{cc}^{+}. However, opposed to the evidence cited below, the BABAR experiment has found no evidence for a Ξ_{cc}^{+} in a search in $\Lambda_c^+ K^- \pi^+$ and $\Xi_c^0 \pi^+$ modes, and no evidence of a Ξ_{cc}^{++} in $\Lambda_c^+ K^- \pi^+ \pi^+$ and $\Xi_c^0 \pi^+ \pi^+$ modes (AUBERT,B 06D). Nor have the BELLE (CHISTOV 06, KATO 14) or LHCb (AAIJ 13CD) experiments found any evidence for this state.

Ξ_{cc}^{+} MASS

VALUE (MeV)	EVTS	DOCUMENT ID		TECN	COMMENT
3518.9±0.9 OUR AVERAGE					
3518 ±3	6	[1] OCHERASHVI..05		SELX	Σ^- nucleus ≈ 600 GeV
3519 ±1	16	[2] MATTSON	02	SELX	Σ^- nucleus ≈ 600 GeV

[1] OCHERASHVILI 05 claims "an excess of 5.62 events over ... 1.38 ± 0.13 events" for a significance of 4.8 σ in pD^+K^- events.

[2] MATTSON 02 claims "an excess of 15.9 events over an expected background of 6.1 ± 0.5 events, a statistical significance of 6.3 σ" in the $\Lambda_c^+ K^- \pi^+$ invariant-mass spectrum. The probability that the peak is a fluctuation increases from 1.0×10^{-6} to 1.1×10^{-4} when the number of bins searched is considered.

Ξ_{cc}^{+} MEAN LIFE

VALUE (10^{-15} s)	CL%	DOCUMENT ID		TECN	COMMENT
<33	90	MATTSON	02	SELX	Σ^- nucleus, ≈ 600 GeV

Ξ_{cc}^{+} DECAY MODES

	Mode
Γ_1	$\Lambda_c^+ K^- \pi^+$
Γ_2	pD^+K^-

$\Gamma(pD^+K^-)/\Gamma(\Lambda_c^+ K^- \pi^+)$ Γ_2/Γ_1

VALUE	EVTS	DOCUMENT ID	TECN	COMMENT
0.36±0.21	6	OCHERASHVI..05	SELX	Σ^- ≈ 600 GeV

Ξ_{cc}^{+} REFERENCES

KATO	14	PR D89 052003	Y. Kato *et al.*	(BELLE Collab.)
AAIJ	13CD	JHEP 1312 090	R. Aaij *et al.*	(LHCb Collab.)
AUBERT,B	06D	PR D74 011103	B. Aubert *et al.*	(BABAR Collab.)
CHISTOV	06	PRL 97 162001	R. Chistov *et al.*	(BELLE Collab.)
OCHERASHVI...05		PL B628 18	A. Ocherashvili *et al.*	(FNAL SELEX Collab.)
MATTSON	02	PRL 89 112001	M. Mattson *et al.*	(FNAL SELEX Collab.)

Ξ_{cc}^{++}

$I(J^P) = ?(?^?)$ Status: ***

A nerrow peak seen in 13 TeV pp collisions in $\Lambda_c^+ K^- 2\pi^+$ with a significance of 12 standard deviations. Supported by measurements at 8 TeV by the same collaboration.

Ξ_{cc}^{++} MASS

VALUE (MeV)	EVTS	DOCUMENT ID		TECN	COMMENT
3621.40±0.72±0.27±0.14	313	[1] AAIJ	17BC	LHCB	pp at 13 TeV

[1] The third error in AAIJ 17BC value is from the uncertainty of the Λ_c^+ mass. The width of the signal is 6.6 ± 0.8 MeV, consistent with the experimental resolution.

Ξ_{cc}^{++} DECAY MODES

	Mode	Fraction (Γ_i/Γ)
Γ_1	$\Lambda_c^+ K^- \pi^+ \pi^+$	seen

$\Gamma(\Lambda_c^+ K^- \pi^+ \pi^+)/\Gamma_{total}$ Γ_1/Γ

VALUE	DOCUMENT ID		TECN	COMMENT
seen	AAIJ	17BC	LHCB	pp at 13 TeV

Ξ_{cc}^{++} REFERENCES

AAIJ	17BC	PRL 119 112001	R. Aaij *et al.*	(LHCb Collab.)

BOTTOM BARYONS
($B = -1$)

$\Lambda_b^0 = udb$, $\Xi_b^0 = usb$, $\Xi_b^- = dsb$, $\Omega_b^- = ssb$

Λ_b^0

$I(J^P) = 0(\frac{1}{2}^+)$ Status: ***

In the quark model, a Λ_b^0 is an isospin-0 udb state. The lowest Λ_b^0 ought to have $J^P = 1/2^+$. None of I, J, or P have actually been measured.

Λ_b^0 MASS

$m_{\Lambda_b^0}$

VALUE (MeV)	EVTS	DOCUMENT ID		TECN	COMMENT
5619.60± 0.17 OUR AVERAGE					
5619.62± 0.16± 0.13		[1] AAIJ	17AM	LHCB	pp at 7, 8 TeV
5619.30± 0.34		[2] AAIJ	14AA	LHCB	pp at 7 TeV
5620.15± 0.31± 0.47		[3] AALTONEN	14B	CDF	$p\overline{p}$ at 1.96 TeV
5619.7 ± 0.7 ± 1.1		[3] AAD	13U	ATLS	pp at 7 TeV
5621 ± 4 ± 3		[4] ABE	97B	CDF	$p\overline{p}$ at 1.8 TeV
5668 ± 16 ± 8	4	[5] ABREU	96N	DLPH	$e^+e^- \to Z$
5614 ± 21 ± 4	4	[5] BUSKULIC	96L	ALEP	$e^+e^- \to Z$
• • • We do not use the following data for averages, fits, limits, etc. • • •					
5619.65± 0.17± 0.17		[6] AAIJ	16Y	LHCB	Repl. by AAIJ 17AM
5619.44± 0.13± 0.38		[3] AAIJ	13AV	LHCB	Repl. by AAIJ 17AM
5619.19± 0.70± 0.30		[3] AAIJ	12E	LHCB	Repl. by AAIJ 13AV
5619.7 ± 1.2 ± 1.2		[7] ACOSTA	06	CDF	Repl. by AALTONEN 14B
not seen		[8] ABE	93B	CDF	Repl. by ABE 97B
5640 ± 50 ±30	16	[9] ALBAJAR	91E	UA1	$p\overline{p}$ 630 GeV
5640 $^{+100}_{-210}$	52	BARI	91	SFM	$\Lambda_b^0 \to pD^0\pi^-$
5650 $^{+150}_{-200}$	90	BARI	91	SFM	$\Lambda_b^0 \to \Lambda_c^+\pi^+\pi^-\pi^-$

[1] Uses $\Lambda_b^0 \to \chi_{c1} p K^-$, $\Lambda_b^0 \to \chi_{c2} p K^-$, $\Lambda_b^0 \to J/\psi\Lambda$, $\Lambda_b^0 \to p\psi(2S) K^-$, $\Lambda_b^0 \to pJ/\psi\pi^+\pi^- K^-$, and $\Lambda_b^0 \to pJ/\psi K^-$ decays.

[2] Uses exclusively reconstructed final states $\Lambda_b^0 \to \Lambda_c^+ D_s^-$, $\Lambda_c^+ D^-$ and $\overline{B}^0 \to D^+ D_s^-$ decays. The uncertainty includes both statistical and systematic contributions.

[3] Uses $\Lambda_b^0 \to J/\psi\Lambda$ fully reconstructed decays.

[4] ABE 97B observed 38 events with a background of 18 ± 1.6 events in the mass range 5.60–5.65 GeV/c^2, a significance of > 3.4 standard deviations.

[5] Uses 4 fully reconstructed Λ_b events.

[6] Uses $\Lambda_b^0 \to p\psi(2S) K^-$, $\Lambda_b^0 \to pJ/\psi\pi^+\pi^- K^-$, and $\Lambda_b^0 \to pJ/\psi K^-$ decays.

[7] Uses exclusively reconstructed final states containing a $J/\psi \to \mu^+\mu^-$ decays.

[8] ABE 93B states that, based on the signal claimed by ALBAJAR 91E, CDF should have found 30 ± 23 $\Lambda_b^0 \to J/\psi(1S)\Lambda$ events. Instead, CDF found not more than 2 events.

[9] ALBAJAR 91E claims 16 ± 5 events above a background of 9 ± 1 events, a significance of about 5 standard deviations.

$m_{\Lambda_b^0} - m_{B^0}$

VALUE (MeV)	DOCUMENT ID		TECN	COMMENT
339.2±1.4±0.1	[1] ACOSTA	06	CDF	$p\overline{p}$ at 1.96 TeV

[1] Uses exclusively reconstructed final states containing $J/\psi \to \mu^+\mu^-$ decays.

$m_{\Lambda_b^0} - m_{B^+}$

VALUE (MeV)	DOCUMENT ID		TECN	COMMENT
339.72±0.28 OUR AVERAGE				
339.72±0.24±0.18	[1] AAIJ	14AA	LHCB	pp at 7 TeV
339.71±0.71±0.09	[2] AAIJ	12E	LHCB	pp at 7 TeV

[1] Uses exclusively reconstructed final states $\Lambda_b^0 \to \Lambda_c^+ D_s^-$, $\Lambda_c^+ D^-$ and $\overline{B}^0 \to D^+ D_s^-$ decays.

[2] Uses exclusively reconstructed final states containing $J/\psi \to \mu^+\mu^-$ decays.

Λ_b^0 MEAN LIFE

See b-baryon Admixture section for data on b-baryon mean life average over species of b-baryon particles.

"OUR EVALUATION" is an average using rescaled values of the data listed below. The average and rescaling were performed by the Heavy Flavor Averaging Group (HFLAV) and are described at http://www.slac.stanford.edu/xorg/hflav/. The averaging/rescaling procedure takes into account correlations between the measurements and asymmetric lifetime errors.

VALUE (10^{-12} s)	EVTS	DOCUMENT ID		TECN	COMMENT
1.470±0.010 OUR EVALUATION					
1.415±0.027±0.006		[1] AAIJ	14E	LHCB	pp at 7 TeV
1.479±0.009±0.010		[2] AAIJ	14U	LHCB	pp at 7, 8 TeV
1.565±0.035±0.020		[1] AALTONEN	14B	CDF	$p\overline{p}$ at 1.96 TeV
1.449±0.036±0.017		[1] AAD	13U	ATLS	pp at 7 TeV
1.503±0.052±0.031		[1] CHATRCHYAN	13AC	CMS	pp at 7 TeV
1.303±0.075±0.035		[1] ABAZOV	12U	D0	$p\overline{p}$ at 1.96 TeV
1.401±0.046±0.035		[3] AALTONEN	10B	CDF	$p\overline{p}$ at 1.96 TeV
• • • We do not use the following data for averages, fits, limits, etc. • • •					
1.482±0.018±0.012		[4] AAIJ	13BB	LHCB	Repl. by AAIJ 14U
1.537±0.045±0.014		[1] AALTONEN	11	CDF	Repl. by AALTONEN 14B
1.218 $^{+0.130}_{-0.115}$ ±0.042		[1] ABAZOV	07S	D0	Repl. by ABAZOV 12U
1.290 $^{+0.119}_{-0.110}$ $^{+0.087}_{-0.091}$		[5] ABAZOV	07U	D0	$p\overline{p}$ at 1.96 TeV
1.593 $^{+0.083}_{-0.078}$ ±0.033		[1] ABULENCIA	07A	CDF	Repl. by AALTONEN 11
1.22 $^{+0.22}_{-0.18}$ ±0.04		[1] ABAZOV	05C	D0	Repl. by ABAZOV 07S
1.11 $^{+0.19}_{-0.18}$ ±0.05		[6] ABREU	99W	DLPH	$e^+e^- \to Z$
1.29 $^{+0.24}_{-0.22}$ ±0.06		[6] ACKERSTAFF	98G	OPAL	$e^+e^- \to Z$
1.21 ±0.11		[6] BARATE	98D	ALEP	$e^+e^- \to Z$
1.32 ±0.15 ±0.07		[7] ABE	96M	CDF	$p\overline{p}$ at 1.8 TeV
1.19 $^{+0.21}_{-0.18}$ $^{+0.07}_{-0.08}$		ABREU	96D	DLPH	Repl. by ABREU 99W
1.14 $^{+0.22}_{-0.19}$ ±0.07	69	AKERS	95K	OPAL	Repl. by ACKERSTAFF 98G
1.02 $^{+0.23}_{-0.18}$ ±0.06	44	BUSKULIC	95L	ALEP	Repl. by BARATE 98D

[1] Measured mean life using fully reconstructed $\Lambda_b^0 \to J/\psi\Lambda$ decays.

[2] Used $\Lambda_b^0 \to J/\psi p K^-$ decays.

[3] Measured mean life using fully reconstructed $\Lambda_b^0 \to \Lambda_c^+\pi^-$ decays.

[4] Measured the lifetime ratio of decays $\Lambda_b^0 \to J/\psi p K^-$ to $B^0 \to J/\psi\pi^+ K^-$ to be 0.976 ± 0.012 ± 0.006 with $\tau_{B^0} = 1.519 \pm 0.007$ ps.

[5] Measured using semileptonic decays $\Lambda_b^0 \to \Lambda_c^+ \mu\nu X$ and $\Lambda_c^+ \to K_S^0 p$.

[6] Measured using $\Lambda_c \ell^-$ and $\Lambda \ell^+ \ell^-$.

[7] Excess $\Lambda_c \ell^-$, decay lengths.

$\tau_{\Lambda_b^0}/\tau_{\overline{\Lambda}_b^0}$

VALUE	DOCUMENT ID		TECN	COMMENT
0.940±0.035±0.006	[1] AAIJ	14E	LHCB	pp at 7 TeV

[1] Measured using $\Lambda_b^0 \to J/\psi\Lambda$ decays.

$\tau_{\Lambda_b^0}/\tau_{B^0}$ MEAN LIFE RATIO

$\tau_{\Lambda_b^0}/\tau_{B^0}$ (direct measurements)

"OUR EVALUATION" has been obtained by the Heavy Flavor Averaging Group (HFLAV) by including both B^0 and B^+ decays.

VALUE	DOCUMENT ID		TECN	COMMENT
0.964±0.007 OUR EVALUATION				
0.969±0.010 OUR AVERAGE Error includes scale factor of 1.6. See the ideogram below.				
0.929±0.018±0.004	[1] AAIJ	14E	LHCB	pp at 7 TeV
0.974±0.006±0.004	[2] AAIJ	14U	LHCB	pp at 7, 8 TeV
0.960±0.025±0.016	[3] AAD	13U	ATLS	pp at 7 TeV
0.864±0.052±0.033	[4,5] ABAZOV	12U	D0	$p\overline{p}$ at 1.96 TeV
1.020±0.030±0.008	[4] AALTONEN	11	CDF	$p\overline{p}$ at 1.96 TeV
• • • We do not use the following data for averages, fits, limits, etc. • • •				
0.976±0.012±0.006	[6] AAIJ	13BB	LHCB	Repl. by AAIJ 14U
0.811 $^{+0.096}_{-0.087}$ ±0.034	[4,5] ABAZOV	07S	D0	Repl. by ABAZOV 12U
1.041±0.057	[7] ABULENCIA	07A	CDF	Repl. by AALTONEN 11
0.87 $^{+0.17}_{-0.14}$ ±0.03	[7] ABAZOV	05C	D0	Repl. by ABAZOV 07S

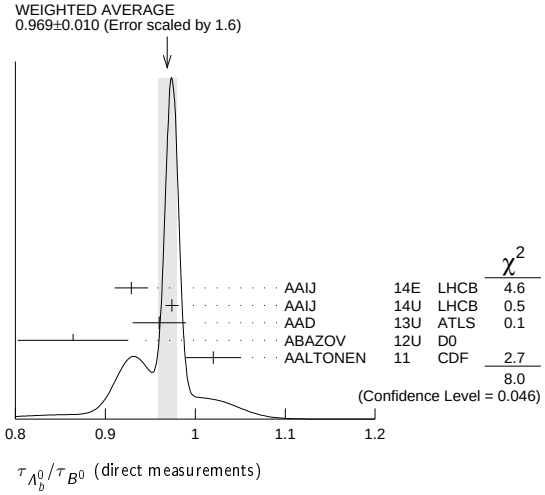

[1] Measured using $\Lambda_b^0 \to J/\psi\Lambda$ and $B^0 \to J/\psi K^{*0}$ decays.
[2] Used $\Lambda_b^0 \to J/\psi p K^-$ and $B^0 \to J/\psi K^*(892)^0$ decays.
[3] Measured with $\Lambda_b^0 \to J/\psi(\mu^+\mu^-)\,\Lambda^0(p\pi^-)$ decays.
[4] Uses fully reconstructed $\Lambda_b \to J/\psi\Lambda$ decays.
[5] Uses $B^0 \to J/\psi K_S^0$ decays for denominator.
[6] Measures $1/\tau_{\Lambda_b^0} - 1/\tau_{B^0}$ and uses $\tau_{B^0} = 1.519 \pm 0.007$ ps to extract lifetime ratio.
[7] Measured mean life ratio using fully reconstructed decays.

Λ_b^0 DECAY MODES

The branching fractions B(b-baryon $\to \Lambda\ell^-\overline{\nu}_\ell$ anything) and B($\Lambda_b^0 \to \Lambda_c^+\ell^-\overline{\nu}_\ell$ anything) are not pure measurements because the underlying measured products of these with B($b \to b$-baryon) were used to determine B($b \to b$-baryon), as described in the note "Production and Decay of b-Flavored Hadrons."

For inclusive branching fractions, *e.g.*, $\Lambda_b \to \overline{\Lambda}_c$ anything, the values usually are multiplicities, not branching fractions. They can be greater than one.

	Mode		Fraction (Γ_i/Γ)	Scale factor/ Confidence level
Γ_1	$J/\psi(1S)\Lambda \times$ B($b \to \Lambda_b^0$)		$(5.8 \pm 0.8) \times 10^{-5}$	
Γ_2	$J/\psi(1S)\Lambda$			
Γ_3	$\psi(2S)\Lambda$			
Γ_4	$pD^0\pi^-$		$(6.3 \pm 0.7) \times 10^{-4}$	
Γ_5	$\Lambda_c(2860)^+\pi^-$, $\Lambda_c^+ \to D^0 p$			
Γ_6	$\Lambda_c(2880)^+\pi^-$, $\Lambda_c^+ \to D^0 p$			
Γ_7	$\Lambda_c(2940)^+\pi^-$, $\Lambda_c^+ \to D^0 p$			
Γ_8	pD^0K^-		$(4.6 \pm 0.8) \times 10^{-5}$	
Γ_9	$pJ/\psi\pi^-$		$(2.6\ ^{+0.5}_{-0.4}) \times 10^{-5}$	
Γ_{10}	$p\pi^- J/\psi$, $J/\psi \to \mu^+\mu^-$		$(1.6 \pm 0.8) \times 10^{-6}$	
Γ_{11}	$pJ/\psi K^-$		$(3.2\ ^{+0.6}_{-0.5}) \times 10^{-4}$	
Γ_{12}	$P_c(4380)^+K^-$, $P_c \to pJ/\psi$	[a]	$(2.7 \pm 1.4) \times 10^{-5}$	
Γ_{13}	$P_c(4450)^+K^-$, $P_c \to pJ/\psi$	[a]	$(1.3 \pm 0.4) \times 10^{-5}$	
Γ_{14}	$\chi_{c1}(1P)pK^-$		$(7.6\ ^{+1.5}_{-1.3}) \times 10^{-5}$	
Γ_{15}	$\chi_{c2}(1P)pK^-$		$(7.9\ ^{+1.6}_{-1.4}) \times 10^{-5}$	
Γ_{16}	$pJ/\psi(1S)\pi^+\pi^-K^-$		$(6.6\ ^{+1.3}_{-1.1}) \times 10^{-5}$	
Γ_{17}	$p\psi(2S)K^-$		$(6.6\ ^{+1.2}_{-1.0}) \times 10^{-5}$	
Γ_{18}	$p\overline{K}^0\pi^-$		$(1.3 \pm 0.4) \times 10^{-5}$	
Γ_{19}	pK^-K^-		$< 3.5 \times 10^{-6}$	CL=90%
Γ_{20}	$\Lambda_c^+\pi^-$		$(4.9 \pm 0.4) \times 10^{-3}$	S=1.2
Γ_{21}	$\Lambda_c^+K^-$		$(3.59 \pm 0.30) \times 10^{-4}$	S=1.2
Γ_{22}	$\Lambda_c^+ a_1(1260)^-$		seen	
Γ_{23}	$\Lambda_c^+ D^-$		$(4.6 \pm 0.6) \times 10^{-4}$	
Γ_{24}	$\Lambda_c^+ D_s^-$		(1.10 ± 0.10) %	
Γ_{25}	$\Lambda_c^+\pi^+\pi^-\pi^-$		$(7.7 \pm 1.1) \times 10^{-3}$	S=1.1
Γ_{26}	$\Lambda_c(2595)^+\pi^-$, $\Lambda_c(2595)^+ \to \Lambda_c^+\pi^+\pi^-$		$(3.4 \pm 1.5) \times 10^{-4}$	
Γ_{27}	$\Lambda_c(2625)^+\pi^-$, $\Lambda_c(2625)^+ \to \Lambda_c^+\pi^+\pi^-$		$(3.3 \pm 1.3) \times 10^{-4}$	
Γ_{28}	$\Sigma_c(2455)^0\pi^+\pi^-$, $\Sigma_c^0 \to \Lambda_c^+\pi^-$		$(5.7 \pm 2.2) \times 10^{-4}$	
Γ_{29}	$\Sigma_c(2455)^{++}\pi^-\pi^-$, $\Sigma_c^{++} \to \Lambda_c^+\pi^+$		$(3.2 \pm 1.6) \times 10^{-4}$	
Γ_{30}	$\Lambda K^0 2\pi^+ 2\pi^-$			
Γ_{31}	$\Lambda_c^+\ell^-\overline{\nu}_\ell$ anything	[b]	(10.3 ± 2.1) %	
Γ_{32}	$\Lambda_c^+\ell^-\overline{\nu}_\ell$		$(6.2\ ^{+1.4}_{-1.3})$ %	
Γ_{33}	$\Lambda_c^+\pi^+\pi^-\ell^-\overline{\nu}_\ell$		(5.6 ± 3.1) %	
Γ_{34}	$\Lambda_c(2595)^+\ell^-\overline{\nu}_\ell$		$(7.9\ ^{+4.0}_{-3.5}) \times 10^{-3}$	
Γ_{35}	$\Lambda_c(2625)^+\ell^-\overline{\nu}_\ell$		$(1.3\ ^{+0.6}_{-0.5})$ %	
Γ_{36}	$\Sigma_c(2455)^0\pi^+\ell^-\overline{\nu}_\ell$			
Γ_{37}	$\Sigma_c(2455)^{++}\pi^-\ell^-\overline{\nu}_\ell$			
Γ_{38}	ph^-	[c]	$< 2.3 \times 10^{-5}$	CL=90%
Γ_{39}	$p\pi^-$		$(4.2 \pm 0.8) \times 10^{-6}$	
Γ_{40}	pK^-		$(5.1 \pm 0.9) \times 10^{-6}$	
Γ_{41}	pD_s^-		$< 4.8 \times 10^{-4}$	CL=90%
Γ_{42}	$p\mu^-\overline{\nu}_\mu$		$(4.1 \pm 1.0) \times 10^{-4}$	
Γ_{43}	$\Lambda\mu^+\mu^-$		$(1.08 \pm 0.28) \times 10^{-6}$	
Γ_{44}	$p\pi^-\mu^+\mu^-$		$(6.9 \pm 2.5) \times 10^{-8}$	
Γ_{45}	$\Lambda\gamma$		$< 1.3 \times 10^{-3}$	CL=90%
Γ_{46}	$\Lambda^0\eta$		$(9\ ^{+7}_{-5}) \times 10^{-6}$	
Γ_{47}	$\Lambda^0\eta'(958)$		$< 3.1 \times 10^{-6}$	CL=90%
Γ_{48}	$\Lambda\pi^+\pi^-$		$(4.6 \pm 1.9) \times 10^{-6}$	
Γ_{49}	$\Lambda K^+\pi^-$		$(5.7 \pm 1.2) \times 10^{-6}$	
Γ_{50}	ΛK^+K^-		$(1.61 \pm 0.23) \times 10^{-5}$	
Γ_{51}	$\Lambda^0\phi$		$(9.2 \pm 2.5) \times 10^{-6}$	
Γ_{52}	$p\pi^-\pi^+\pi^-$			
Γ_{53}	$pK^-K^+\pi^-$			

[a] P_c^+ is a pentaquark-charmonium state.
[b] Not a pure measurement. See note at head of Λ_b^0 Decay Modes.
[c] Here h^- means π^- or K^-.

CONSTRAINED FIT INFORMATION

An overall fit to 10 branching ratios uses 12 measurements and one constraint to determine 7 parameters. The overall fit has a $\chi^2 = 10.7$ for 6 degrees of freedom.

The following *off-diagonal* array elements are the correlation coefficients $\langle \delta x_i \delta x_j \rangle / (\delta x_i \cdot \delta x_j)$, in percent, from the fit to the branching fractions, $x_i \equiv \Gamma_i/\Gamma_{\text{total}}$. The fit constrains the x_i whose labels appear in this array to sum to one.

x_{21}	94				
x_{25}	50	47			
x_{32}	14	14	7		
x_{39}	0	0	0	0	
x_{40}	0	0	0	0	83
	x_{20}	x_{21}	x_{25}	x_{32}	x_{39}

Λ_b^0 BRANCHING RATIOS

$\Gamma(J/\psi(1S)\Lambda \times$ B($b \to \Lambda_b^0$)$)/\Gamma_{\text{total}}$ Γ_1/Γ

VALUE (units 10^{-5})	EVTS	DOCUMENT ID		TECN	COMMENT
5.8 ± 0.8 OUR AVERAGE					
$6.01 \pm 0.60 \pm 0.58 \pm 0.28$		[1] ABAZOV	11O	D0	$p\overline{p}$ at 1.96 TeV
$4.7 \pm 2.3 \pm 0.2$		[2] ABE	97B	CDF	$p\overline{p}$ at 1.8 TeV
• • • We do not use the following data for averages, fits, limits, etc. • • •					
$180 \pm 60 \pm 90$	16	ALBAJAR	91E	UA1	$p\overline{p}$ at 630 GeV

[1] ABAZOV 11O uses B($B^0 \to J/\psi K_S^0$) × B($b \to B^0$) $= (1.74 \pm 0.08) \times 10^{-4}$ to obtain the result. The $(\pm 0.08) \times 10^{-4}$ uncertainty of this product is listed as the last uncertainty of the measurement, $(\pm 0.28) \times 10^{-5}$.
[2] ABE 97B reports [B($\Lambda_b^0 \to J/\psi\Lambda$) × B($b \to \Lambda_b^0$)] / [B($B^0 \to J/\psi K_S^0$) × B($b \to B^0$)] $= 0.27 \pm 0.12 \pm 0.05$. We multiply by our best value B($B^0 \to J/\psi K_S^0$) × B($b \to B^0$) $= (1.74 \pm 0.08) \times 10^{-4}$. Our first error is their experiment error and our second error is the systematic error from using our best value.

$\Gamma(\psi(2S)\Lambda)/\Gamma(J/\psi(1S)\Lambda)$ Γ_3/Γ_2

VALUE	DOCUMENT ID		TECN	COMMENT
0.50 ± 0.03 ± 0.02	[1] AAD	15CH	ATLS	pp at 8 TeV

[1] AAD 15CH uses B($J/\psi \to \mu^+\mu^-$) $= (5.961 \pm 0.033) \times 10^{-2}$ (PDG 14). And B($\psi(2S) \to \mu^+\mu^-$) $= (7.89 \pm 0.17) \times 10^{-3}$ (PDG 14) is used assuming lepton universality.

$\Gamma(pD^0\pi^-)/\Gamma_{\text{total}}$ Γ_4/Γ

VALUE	EVTS	DOCUMENT ID		TECN	COMMENT
• • • We do not use the following data for averages, fits, limits, etc. • • •					
seen	52	BARI	91	SFM	$D^0 \to K^-\pi^+$
seen		BASILE	81	SFM	$D^0 \to K^-\pi^+$

$\Gamma(\Lambda_c(2860)^+\pi^-, \Lambda_c^+ \to D^0 p)/\Gamma(\Lambda_c(2880)^+\pi^-, \Lambda_c^+ \to D^0 p)$ Γ_5/Γ_6

VALUE	DOCUMENT ID		TECN	COMMENT
$4.54\ ^{+0.51}_{-0.39}\ ^{+0.21}_{-0.59}$	AAIJ	17S	LHCB	pp at 7, 8 TeV

$\Gamma(\Lambda_c(2940)^+\pi^-, \Lambda_c^+ \to D^0 p)/\Gamma(\Lambda_c(2880)^+\pi^-, \Lambda_c^+ \to D^0 p)$ Γ_7/Γ_6

VALUE	DOCUMENT ID		TECN	COMMENT
$0.83\ ^{+0.31}_{-0.10}\ ^{+0.18}_{-0.43}$	AAIJ	17S	LHCB	pp at 7, 8 TeV

$\Gamma(pD^0K^-)/\Gamma(pD^0\pi^-)$ Γ_8/Γ_4

VALUE (units 10^{-2})	DOCUMENT ID		TECN	COMMENT
$7.3 \pm 0.8\ ^{+0.5}_{-0.6}$	AAIJ	14H	LHCB	pp at 7 TeV

Baryon Particle Listings

Λ_b^0

$\Gamma(\chi_{c1}(1P)pK^-)/\Gamma(pJ/\psi K^-)$ Γ_{14}/Γ_{11}

VALUE	DOCUMENT ID		TECN	COMMENT
0.239±0.019±0.007	[1] AAIJ	17AM	LHCB	pp at 7, 8 TeV

[1] AAIJ 17AM reports 0.242 ± 0.014 ± 0.016 from a measurement of $[\Gamma(\Lambda_b^0 \to \chi_{c1}(1P)pK^-)/\Gamma(\Lambda_b^0 \to pJ/\psi K^-)] \times [B(\chi_{c1}(1P) \to \gamma J/\psi(1S))]$ assuming $B(\chi_{c1}(1P) \to \gamma J/\psi(1S)) = (33.9 \pm 1.2) \times 10^{-2}$, which we rescale to our best value $B(\chi_{c1}(1P) \to \gamma J/\psi(1S)) = (34.3 \pm 1.0) \times 10^{-2}$. Our first error is their experiment's error and our second error is the systematic error from using our best value.

$\Gamma(\chi_{c2}(1P)pK^-)/\Gamma(pJ/\psi K^-)$ Γ_{15}/Γ_{11}

VALUE	DOCUMENT ID		TECN	COMMENT
0.250±0.025±0.007	[1] AAIJ	17AM	LHCB	pp at 7, 8 TeV

[1] AAIJ 17AM reports 0.248 ± 0.02 ± 0.017 from a measurement of $[\Gamma(\Lambda_b^0 \to \chi_{c2}(1P)pK^-)/\Gamma(\Lambda_b^0 \to pJ/\psi K^-)] \times [B(\chi_{c2}(1P) \to \gamma J/\psi(1S))]$ assuming $B(\chi_{c2}(1P) \to \gamma J/\psi(1S)) = (19.2 \pm 0.7) \times 10^{-2}$, which we rescale to our best value $B(\chi_{c2}(1P) \to \gamma J/\psi(1S)) = (19.0 \pm 0.5) \times 10^{-2}$. Our first error is their experiment's error and our second error is the systematic error from using our best value.

$\Gamma(pJ/\psi\pi^-)/\Gamma(pJ/\psi K^-)$ Γ_9/Γ_{11}

VALUE (units 10^{-2})	DOCUMENT ID		TECN	COMMENT
8.24±0.25±0.42	AAIJ	14K	LHCB	pp at 7, 8 TeV

$\Gamma(pJ/\psi K^-)/\Gamma_{total}$ Γ_{11}/Γ

VALUE (units 10^{-4})	DOCUMENT ID		TECN	COMMENT
$3.17 \pm 0.04^{+0.57}_{-0.45}$	[1] AAIJ	16A	LHCB	pp at 7, 8 TeV

[1] AAIJ 16A reported the measurement of $(3.17 \pm 0.04 \pm 0.07 \pm 0.34^{+0.45}_{-0.28}) \times 10^{-4}$ where the first uncertainty is statistical, the second is systematic, the third is due to the branching fraction of $B^0 \to J/\psi K^*(892)^0$, and the fourth is due to the knowledge of f_{Λ_b}/f_d. We combined in quadrature second to fourth uncertainties to a total systematic uncertainty.

$\Gamma(P_c(4380)^+K^-,\ P_c \to pJ/\psi)/\Gamma_{total}$ Γ_{12}/Γ

P_c^+ is a pentaquark-charmonium state.

VALUE (units 10^{-5})	DOCUMENT ID		TECN	COMMENT
$2.66 \pm 0.22^{+1.41}_{-1.38}$	[1] AAIJ	16A	LHCB	pp at 7, 8 TeV

[1] AAIJ 16 total systematic includes the uncertainties on $f(P_c^+)$ and $B(\Lambda_b \to pJ/\psi K^-)$.

$\Gamma(P_c(4450)^+K^-,\ P_c \to pJ/\psi)/\Gamma_{total}$ Γ_{13}/Γ

P_c^+ is a pentaquark-charmonium state.

VALUE (units 10^{-5})	DOCUMENT ID		TECN	COMMENT
$1.30 \pm 0.16^{+0.42}_{-0.39}$	[1] AAIJ	16A	LHCB	pp at 7, 8 TeV

[1] AAIJ 16 total systematic includes the uncertainties on $f(P_c^+)$ and $B(\Lambda_b \to pJ/\psi K^-)$.

$\Gamma(pJ/\psi(1S)\pi^+\pi^-K^-)/\Gamma(pJ/\psi K^-)$ Γ_{16}/Γ_{11}

VALUE	DOCUMENT ID		TECN	COMMENT
0.2086±0.0096±0.0134	[1] AAIJ	16Y	LHCB	pp at 7, 8 TeV

[1] Excludes $\psi(2S) \to J/\psi\pi^+\pi^-$.

$\Gamma(p\psi(2S)K^-)/\Gamma(pJ/\psi K^-)$ Γ_{17}/Γ_{11}

VALUE	DOCUMENT ID		TECN	COMMENT
0.2070±0.0076±0.0059	[1] AAIJ	16Y	LHCB	pp at 7, 8 TeV

[1] AAIJ 16Y reports a measurement of 0.2070 ± 0.0076 ± 0.0046 ± 0.0037 where the third uncertainty is due to the knowledge of J/ψ and $\psi(2S)$ branching fractions. We have combined both systematic uncertainties in quadrature.

$\Gamma(p\overline{K}^0\pi^-)/\Gamma_{total}$ Γ_{18}/Γ

VALUE (units 10^{-5})	DOCUMENT ID		TECN	COMMENT
1.26±0.19±0.36	[1] AAIJ	14Q	LHCB	pp at 7 TeV

[1] Used the normalizing mode branching fraction value of $B(B^0 \to K^0\pi^+\pi^-) = (4.96 \pm 0.20) \times 10^{-5}$.

$\Gamma(pK^0K^-)/\Gamma_{total}$ Γ_{19}/Γ

VALUE	CL%	DOCUMENT ID	TECN	COMMENT
$<3.5 \times 10^{-6}$	90	AAIJ	14Q LHCB	pp at 7 TeV

$\Gamma(\Lambda_c^+\pi^-)/\Gamma_{total}$ Γ_{20}/Γ

VALUE (units 10^{-3})	EVTS	DOCUMENT ID		TECN	COMMENT
4.9 ±0.4 OUR FIT		Error includes scale factor of 1.2.			
4.9 ±0.5 OUR AVERAGE		Error includes scale factor of 1.5.			
$4.57^{+0.31}_{-0.30} \pm 0.23$		[1] AAIJ	14I	LHCB	pp at 7 TeV
$5.97 \pm 0.28 \pm 0.81$		[2] AAIJ	14Q	LHCB	pp at 7 TeV
8.8 ±2.8 ±1.5		[3] ABULENCIA	07B	CDF	$p\overline{p}$ at 1.96 TeV
• • • We do not use the following data for averages, fits, limits, etc. • • •					
seen	3	ABREU	96N	DLPH	$\Lambda_c^+ \to pK^-\pi^+$
seen	4	BUSKULIC	96L	ALEP	$\Lambda_c^+ \to pK^-\pi^+$, $p\overline{K}^0$, $\Lambda\pi^+\pi^+\pi^-$

[1] AAIJ 14I reports $(4.30 \pm 0.03^{+0.12}_{-0.11} \pm 0.26 \pm 0.21) \times 10^{-3}$ from a measurement of $[\Gamma(\Lambda_b^0 \to \Lambda_c^+\pi^-)/\Gamma_{total}] \times [B(B^0 \to D^-\pi^+)]$ assuming $B(B^0 \to D^-\pi^+) = (2.68 \pm 0.13) \times 10^{-3}$, which we rescale to our best value $B(B^0 \to D^-\pi^+) = (2.52 \pm 0.13) \times 10^{-3}$. Our first error is their experiment's error and our second error is the systematic error from using our best value. Uses information on f_{baryon}/f_d from measurement in semileptonic decays by the same authors.

[2] Obtained using the branching fraction of $\Lambda_c^+ \to pK^-\pi^+$ decay.

[3] The result is obtained from $(f_{baryon}/f_d)\ (B(\Lambda_b^0 \to \Lambda_c^+\pi^-)/B(\overline{B}^0 \to D^+\pi^-)) = 0.82 \pm 0.08 \pm 0.11 \pm 0.22$, assuming $f_{baryon}/f_d = 0.25 \pm 0.04$ and $B(\overline{B}^0 \to D^+\pi^-) = (2.68 \pm 0.13) \times 10^{-3}$.

$\Gamma(pD^0\pi^-)/\Gamma(\Lambda_c^+\pi^-)$ Γ_4/Γ_{20}

VALUE	DOCUMENT ID		TECN	COMMENT
0.129±0.007±0.007	[1] AAIJ	14H	LHCB	pp at 7 TeV

[1] AAIJ 14H reports $[\Gamma(\Lambda_b^0 \to pD^0\pi^-)/\Gamma(\Lambda_b^0 \to \Lambda_c^+\pi^-)] \times [B(D^0 \to K^-\pi^+)]\ /\ [B(\Lambda_c^+ \to pK^-\pi^+)] = (8.06 \pm 0.23 \pm 0.35) \times 10^{-2}$ which we multiply or divide by our best values $B(D^0 \to K^-\pi^+) = (3.89 \pm 0.04) \times 10^{-2}$, $B(\Lambda_c^+ \to pK^-\pi^+) = (6.23 \pm 0.33) \times 10^{-2}$. Our first error is their experiment's error and our second error is the systematic error from using our best values.

$\Gamma(\Lambda_c^+K^-)/\Gamma_{total}$ Γ_{21}/Γ

VALUE (units 10^{-4})	DOCUMENT ID		TECN	COMMENT
3.59±0.30 OUR FIT	Error includes scale factor of 1.2.			
3.55±0.44±0.50	[1] AAIJ	14Q	LHCB	pp at 7 TeV

[1] Obtained using the branching fraction of $\Lambda_c^+ \to pK^-\pi^+$ decay.

$\Gamma(\Lambda_c^+K^-)/\Gamma(\Lambda_c^+\pi^-)$ Γ_{21}/Γ_{20}

VALUE (units 10^{-2})	DOCUMENT ID		TECN	COMMENT
7.31±0.22 OUR FIT				
7.31±0.16±0.16	AAIJ	14H	LHCB	pp at 7 TeV

$\Gamma(\Lambda_c^+a_1(1260)^-)/\Gamma_{total}$ Γ_{22}/Γ

VALUE	EVTS	DOCUMENT ID		TECN	COMMENT
seen	1	ABREU	96N	DLPH	$\Lambda_c^+ \to pK^-\pi^+$, $a_1^- \to \rho^0\pi^- \to \pi^+\pi^-\pi^-$

$\Gamma(\Lambda_c^+D_s^-)/\Gamma_{total}$ Γ_{24}/Γ

VALUE (units 10^{-2})	DOCUMENT ID		TECN	COMMENT
1.1±0.1	[1] AAIJ	14AA	LHCB	pp at 7 TeV

[1] Uses $B(\overline{B}^0 \to D^+D_s^-) = (7.2 \pm 0.8) \times 10^{-3}$ and their measured $B(\Lambda_b^0 \to \Lambda_c^+\pi^-))/B(\overline{B}^0 \to D^+\pi^-)$ values.

$\Gamma(\Lambda_c^+D^-)/\Gamma(\Lambda_c^+D_s^-)$ Γ_{23}/Γ_{24}

VALUE	DOCUMENT ID		TECN	COMMENT
0.042±0.003±0.003	AAIJ	14AA	LHCB	pp at 7 TeV

$\Gamma(\Lambda_c^+\pi^+\pi^-\pi^-)/\Gamma_{total}$ Γ_{25}/Γ

VALUE (units 10^{-3})	EVTS	DOCUMENT ID		TECN	COMMENT
7.7±1.1 OUR FIT		Error includes scale factor of 1.1.			
$14.9^{+3.8}_{-3.2} \pm 1.2$		[1] AALTONEN	12A	CDF	$p\overline{p}$ at 1.96 TeV
• • • We do not use the following data for averages, fits, limits, etc. • • •					
seen	90	BARI	91	SFM	$\Lambda_c^+ \to pK^-\pi^+$

[1] AALTONEN 12A reports $[\Gamma(\Lambda_b^0 \to \Lambda_c^+\pi^+\pi^-\pi^-)/\Gamma_{total}]\ /\ [B(\Lambda_b^0 \to \Lambda_c^+\pi^-)] = 3.04 \pm 0.33^{+0.70}_{-0.55}$ which we multiply by our best value $B(\Lambda_b^0 \to \Lambda_c^+\pi^-) = (4.9 \pm 0.4) \times 10^{-3}$. Our first error is their experiment's error and our second error is the systematic error from using our best value.

$\Gamma(\Lambda_c^+\pi^+\pi^-\pi^-)/\Gamma(\Lambda_c^+\pi^-)$ Γ_{25}/Γ_{20}

VALUE	DOCUMENT ID		TECN	COMMENT
1.56±0.21 OUR FIT				
1.43±0.16±0.13	AAIJ	11E	LHCB	pp at 7 TeV

$\Gamma(\Lambda_c(2595)^+\pi^-, \Lambda_c(2595)^+ \to \Lambda_c^+\pi^+\pi^-)/\Gamma(\Lambda_c^+\pi^+\pi^-\pi^-)$ Γ_{26}/Γ_{25}

VALUE (units 10^{-2})	DOCUMENT ID		TECN	COMMENT
$4.4 \pm 1.7^{+0.6}_{-0.4}$	AAIJ	11E	LHCB	pp at 7 TeV

$\Gamma(\Lambda_c(2625)^+\pi^-, \Lambda_c(2625)^+ \to \Lambda_c^+\pi^+\pi^-)/\Gamma(\Lambda_c^+\pi^+\pi^-\pi^-)$ Γ_{27}/Γ_{25}

VALUE (units 10^{-2})	DOCUMENT ID		TECN	COMMENT
4.3±1.5±0.4	AAIJ	11E	LHCB	pp at 7 TeV

$\Gamma(\Sigma_c(2455)^0\pi^+\pi^-, \Sigma_c^0 \to \Lambda_c^+\pi^-)/\Gamma(\Lambda_c^+\pi^+\pi^-\pi^-)$ Γ_{28}/Γ_{25}

VALUE (units 10^{-2})	DOCUMENT ID		TECN	COMMENT
7.4±2.4±1.2	AAIJ	11E	LHCB	pp at 7 TeV

$\Gamma(\Sigma_c(2455)^{++}\pi^-\pi^-, \Sigma_c^{++} \to \Lambda_c^+\pi^+)/\Gamma(\Lambda_c^+\pi^+\pi^-\pi^-)$ Γ_{29}/Γ_{25}

VALUE (units 10^{-2})	DOCUMENT ID		TECN	COMMENT
4.2±1.8±0.7	AAIJ	11E	LHCB	pp at 7 TeV

$\Gamma(\Lambda K^0 2\pi^+ 2\pi^-)/\Gamma_{total}$ Γ_{30}/Γ

VALUE	EVTS	DOCUMENT ID		TECN	COMMENT
• • • We do not use the following data for averages, fits, limits, etc. • • •					
seen	4	[1] ARENTON	86	FMPS	$\Lambda K_S^0 2\pi^+ 2\pi^-$

[1] See the footnote to the ARENTON 86 mass value.

$\Gamma(\Lambda_c^+ \ell^- \overline{\nu}_\ell \text{anything})/\Gamma_{total}$ Γ_{31}/Γ

The values and averages in this section serve only to show what values result if one assumes our B($b \to$ b-baryon). They cannot be thought of as measurements since the underlying product branching fractions were also used to determine B($b \to$ b-baryon) as described in the note on "Production and Decay of b-Flavored Hadrons."

VALUE	EVTS	DOCUMENT ID		TECN	COMMENT
0.103±0.021 OUR AVERAGE					
0.097±0.018±0.013		[1] BARATE	98D	ALEP	$e^+e^- \to Z$
$0.13\ ^{+0.05}_{-0.04}\pm0.02$	29	[2] ABREU	95S	DLPH	$e^+e^- \to Z$
• • • We do not use the following data for averages, fits, limits, etc. • • •					
0.085±0.021±0.011	55	[3] BUSKULIC	95L	ALEP	Repl. by BARATE 98D
0.17 ±0.06 ±0.02	21	[4] BUSKULIC	92E	ALEP	$\Lambda_c^+ \to p K^- \pi^+$

[1] BARATE 98D reports $[\Gamma(\Lambda_b^0 \to \Lambda_c^+ \ell^- \overline{\nu}_\ell \text{anything})/\Gamma_{total}] \times [B(\overline{b} \to b\text{-baryon})] = 0.0086 \pm 0.0007 \pm 0.0014$ which we divide by our best value B($\overline{b} \to$ b-baryon) $= (8.9 \pm 1.2) \times 10^{-2}$. Our first error is their experiment's error and our second error is the systematic error from using our best value. Measured using $\Lambda_c \ell^-$ and $\Lambda \ell^+ \ell^-$.

[2] ABREU 95S reports $[\Gamma(\Lambda_b^0 \to \Lambda_c^+ \ell^- \overline{\nu}_\ell \text{anything})/\Gamma_{total}] \times [B(\overline{b} \to b\text{-baryon})] = 0.0118 \pm 0.0026\ ^{+0.0031}_{-0.0021}$ which we divide by our best value B($\overline{b} \to$ b-baryon) $= (8.9 \pm 1.2) \times 10^{-2}$. Our first error is their experiment's error and our second error is the systematic error from using our best value.

[3] BUSKULIC 95L reports $[\Gamma(\Lambda_b^0 \to \Lambda_c^+ \ell^- \overline{\nu}_\ell \text{anything})/\Gamma_{total}] \times [B(\overline{b} \to b\text{-baryon})] = 0.00755 \pm 0.0014 \pm 0.0012$ which we divide by our best value B($\overline{b} \to$ b-baryon) $= (8.9 \pm 1.2) \times 10^{-2}$. Our first error is their experiment's error and our second error is the systematic error from using our best value.

[4] BUSKULIC 92E reports $[\Gamma(\Lambda_b^0 \to \Lambda_c^+ \ell^- \overline{\nu}_\ell \text{anything})/\Gamma_{total}] \times [B(\overline{b} \to b\text{-baryon})] = 0.015 \pm 0.0035 \pm 0.0045$ which we divide by our best value B($\overline{b} \to$ b-baryon) $= (8.9 \pm 1.2) \times 10^{-2}$. Our first error is their experiment's error and our second error is the systematic error from using our best value. Superseded by BUSKULIC 95L.

$\Gamma(\Lambda_c^+ \ell^- \overline{\nu}_\ell)/\Gamma_{total}$ Γ_{32}/Γ

VALUE	DOCUMENT ID		TECN	COMMENT
$\mathbf{0.062^{+0.014}_{-0.013}}$ **OUR FIT**				
$\mathbf{0.050^{+0.011}_{-0.008}\pm0.016}$	[1] ABDALLAH	04A	DLPH	$e^+e^- \to Z^0$

[1] Derived from a combined likelihood and event rate fit to the distribution of the Isgur-Wise variable and using HQET. The slope of the form factor is measured to be $\rho^2 = 2.03 \pm 0.46^{+0.72}_{-1.00}$.

$\Gamma(\Lambda_c^+ \ell^- \overline{\nu}_\ell)/\Gamma(\Lambda_c^+ \pi^-)$ Γ_{32}/Γ_{20}

VALUE	DOCUMENT ID		TECN	COMMENT
$\mathbf{12.7^{+3.1}_{-2.7}}$ **OUR FIT**				
$\mathbf{16.6\pm3.0^{+2.8}_{-3.6}}$	AALTONEN	09E	CDF	$p\overline{p}$ at 1.96 TeV

$\Gamma(\Lambda_c^+ \pi^+ \pi^- \ell^- \overline{\nu}_\ell)/\Gamma_{total}$ Γ_{33}/Γ

VALUE	DOCUMENT ID		TECN	COMMENT
$\mathbf{0.056^{+0.031}_{-0.030}}$	[1] ABDALLAH	04A	DLPH	$e^+e^- \to Z^0$

[1] Derived from the fraction of $\Gamma(\Lambda_b^0 \to \Lambda_c^+ \ell^- \overline{\nu}_\ell)$ / ($\Gamma(\Lambda_b^0 \to \Lambda_c^+ \ell^- \overline{\nu}_\ell) + \Gamma(\Lambda_b^0 \to \Lambda_c^+ \pi^+ \pi^- \ell^- \overline{\nu}_\ell)$) $= 0.47^{+0.10+0.07}_{-0.08-0.06}$.

$\Gamma(\Lambda_c^+ \ell^- \overline{\nu}_\ell)/[\Gamma(\Lambda_c^+ \ell^- \overline{\nu}_\ell) + \Gamma(\Lambda_c^+ \pi^+ \pi^- \ell^- \overline{\nu}_\ell)]$ $\Gamma_{32}/(\Gamma_{32}+\Gamma_{33})$

VALUE	DOCUMENT ID		TECN	COMMENT
$\mathbf{0.47^{+0.10+0.07}_{-0.08-0.06}}$	ABDALLAH	04A	DLPH	$e^+e^- \to Z^0$

$\Gamma(\Lambda_c(2595)^+ \ell^- \overline{\nu}_\ell)/\Gamma(\Lambda_c^+ \ell^- \overline{\nu}_\ell)$ Γ_{34}/Γ_{32}

VALUE	DOCUMENT ID		TECN	COMMENT
$\mathbf{0.126\pm0.033^{+0.047}_{-0.038}}$	AALTONEN	09E	CDF	$p\overline{p}$ at 1.96 TeV

$\Gamma(\Lambda_c(2625)^+ \ell^- \overline{\nu}_\ell)/\Gamma(\Lambda_c^+ \ell^- \overline{\nu}_\ell)$ Γ_{35}/Γ_{32}

VALUE	DOCUMENT ID		TECN	COMMENT
$\mathbf{0.210\pm0.042^{+0.071}_{-0.050}}$	AALTONEN	09E	CDF	$p\overline{p}$ at 1.96 TeV

$[\frac{1}{2}\Gamma(\Sigma_c(2455)^0 \pi^+ \ell^- \overline{\nu}_\ell) + \frac{1}{2}\Gamma(\Sigma_c(2455)^{++} \pi^- \ell^- \overline{\nu}_\ell)]/\Gamma(\Lambda_c^+ \ell^- \overline{\nu}_\ell)$ $(\frac{1}{2}\Gamma_{36}+\frac{1}{2}\Gamma_{37})/\Gamma_{32}$

VALUE	DOCUMENT ID		TECN	COMMENT
$\mathbf{0.054\pm0.022^{+0.021}_{-0.018}}$	AALTONEN	09E	CDF	$p\overline{p}$ at 1.96 TeV

$\Gamma(ph^-)/\Gamma_{total}$ Γ_{38}/Γ

VALUE	CL%	DOCUMENT ID		TECN	COMMENT
$\mathbf{<2.3\times10^{-5}}$	90	[1] ACOSTA	05O	CDF	$p\overline{p}$ at 1.96 TeV

[1] Assumes f_Λ / $f_d = 0.25$, and equal momentum distribution for Λ_b and B mesons.

$\Gamma(p\pi^-)/\Gamma_{total}$ Γ_{39}/Γ

VALUE (units 10^{-6})	CL%	DOCUMENT ID		TECN	COMMENT
4.2±0.8 OUR FIT					
3.7±0.8±0.5		[1] AALTONEN	09C	CDF	$p\overline{p}$ at 1.96 TeV
• • • We do not use the following data for averages, fits, limits, etc. • • •					
<5.0	90	[2] BUSKULIC	96V	ALEP	$e^+e^- \to Z$

[1] AALTONEN 09C reports $[\Gamma(\Lambda_b^0 \to p\pi^-)/\Gamma_{total}]$ / $[B(B^0 \to K^+\pi^-)] \times [B(\overline{b} \to b\text{-baryon})]$ / $[B(\overline{b} \to B^0)] = 0.042 \pm 0.007 \pm 0.006$ which we multiply or divide by our best values B($B^0 \to K^+\pi^-$) $= (1.96 \pm 0.05) \times 10^{-5}$, B($\overline{b} \to$ b-baryon) $= (8.9 \pm 1.2) \times 10^{-2}$, B($\overline{b} \to B^0$) $= (40.5 \pm 0.6) \times 10^{-2}$. Our first error is their experiment's error and our second error is the systematic error from using our best values.

[2] BUSKULIC 96V assumes PDG 96 production fractions for B^0, B^+, B_s, b baryons.

$\Gamma(pK^-)/\Gamma_{total}$ Γ_{40}/Γ

VALUE (units 10^{-6})	CL%	DOCUMENT ID		TECN	COMMENT
5.1±0.9 OUR FIT					
5.9±1.1±0.8		[1] AALTONEN	09C	CDF	$p\overline{p}$ at 1.96 TeV
• • • We do not use the following data for averages, fits, limits, etc. • • •					
<360	90	[2] ADAM	96D	DLPH	$e^+e^- \to Z$
< 50	90	[3] BUSKULIC	96V	ALEP	$e^+e^- \to Z$

[1] AALTONEN 09C reports $[\Gamma(\Lambda_b^0 \to pK^-)/\Gamma_{total}]$ / $[B(B^0 \to K^+\pi^-)] \times [B(\overline{b} \to b\text{-baryon})]$ / $[B(\overline{b} \to B^0)] = 0.066 \pm 0.009 \pm 0.008$ which we multiply or divide by our best values B($B^0 \to K^+\pi^-$) $= (1.96 \pm 0.05) \times 10^{-5}$, B($\overline{b} \to$ b-baryon) $= (8.9 \pm 1.2) \times 10^{-2}$, B($\overline{b} \to B^0$) $= (40.5 \pm 0.6) \times 10^{-2}$. Our first error is their experiment's error and our second error is the systematic error from using our best values.

[2] ADAM 96D assumes $f_{B^0} = f_{B^-} = 0.39$ and $f_{B_s} = 0.12$.

[3] BUSKULIC 96V assumes PDG 96 production fractions for B^0, B^+, B_s, b baryons.

$\Gamma(p\pi^-)/\Gamma(pK^-)$ Γ_{39}/Γ_{40}

VALUE	DOCUMENT ID		TECN	COMMENT
0.84±0.09 OUR FIT				
0.86±0.08±0.05	AAIJ	12AR	LHCB	pp at 7 TeV

$\Gamma(pD_s^-)/\Gamma_{total}$ Γ_{41}/Γ

VALUE	CL%	DOCUMENT ID		TECN	COMMENT
$\mathbf{<4.8\times10^{-4}}$	90	AAIJ	14Q	LHCB	pp at 7 TeV

$\Gamma(p\mu^-\overline{\nu}_\mu)/\Gamma_{total}$ Γ_{42}/Γ

VALUE (units 10^{-4})	DOCUMENT ID		TECN	COMMENT
4.1±1.0	[1] AAIJ	15BG	LHCB	pp at 8 TeV

[1] The ratio of B($\Lambda_b^0 \to p\mu^-\overline{\nu}_\mu$) to B($\Lambda_b^0 \to \Lambda_c^+\mu^-\overline{\nu}_\mu$) is measured within a restricted q^2 region. Combined with theoretical calculations of the form factors and the previously measured value of $|V_{cb}|$, the first $|V_{ub}| = (3.27 \pm 0.15 \pm 0.16 \pm 0.06) \times 10^{-3}$ measurement from the Λ_b decay is obtained, consistent with the exclusively measured world averages.

$\Gamma(p\mu^-\overline{\nu}_\mu)/\Gamma(\Lambda_c^+ \ell^- \overline{\nu}_\ell)$ Γ_{42}/Γ_{32}

VALUE (units 10^{-2})	DOCUMENT ID		TECN	COMMENT
• • • We do not use the following data for averages, fits, limits, etc. • • •				
1.0±0.04±0.08	[1] AAIJ	15BG	LHCB	pp at 8 TeV

[1] This measurement is a ratio of $\Gamma(\Lambda_b^0 \to p\mu^-\overline{\nu}_\mu)[q^2 > 15\ \text{GeV}/c^2]$ to $\Gamma(\Lambda_b^0 \to \Lambda_c^+\mu^-\overline{\nu}_\mu)[q^2 > 7\ \text{GeV}/c^2]$ within a restricted q^2 region. Combined with theoretical calculations of the form factors and the previously measured value of $|V_{cb}|$, the first $|V_{ub}| = (3.27 \pm 0.15 \pm 0.16 \pm 0.06) \times 10^{-3}$ measurement from the Λ_b decay is obtained, consistent with the exclusively measured world averages.

$\Gamma(\Lambda\mu^+\mu^-)/\Gamma_{total}$ Γ_{43}/Γ

VALUE (units 10^{-7})	DOCUMENT ID		TECN	COMMENT
10.8±2.8 OUR AVERAGE				
9.6±1.6±2.5	[1] AAIJ	13AJ	LHCB	pp at 7 TeV
17.3±4.2±5.5	AALTONEN	11AI	CDF	$p\overline{p}$ at 1.96 TeV

[1] Uses $B(\Lambda_b^0 \to J/\psi\Lambda) = (6.2 \pm 1.4) \times 10^{-4}$. This measurement comes from the sum of the differential rates in q^2 regions excluding those corresponding to J/ψ and $\psi(2S)$ ([8.68,10.09] and [12.86, 14.18] GeV^2/c^4).

$\Gamma(p\pi^-\mu^+\mu^-)/\Gamma_{total}$ Γ_{44}/Γ

VALUE (units 10^{-8})	DOCUMENT ID		TECN	COMMENT
$\mathbf{6.9\pm1.9^{+1.7}_{-1.5}}$	[1] AAIJ	17P	LHCB	pp at 7, 8 TeV

[1] Excludes J/ψ and $\psi(2S)$ decays to $\mu^+\mu^-$.

$\Gamma(p\pi^-\mu^+\mu^-)/\Gamma(p\pi^- J/\psi,\ J/\psi \to \mu^+\mu^-)$ Γ_{44}/Γ_{10}

VALUE (units 10^{-2})	DOCUMENT ID		TECN	COMMENT
4.4±1.2±0.7	[1] AAIJ	17P	LHCB	pp at 7, 8 TeV

[1] The $p\pi^-\mu^+\mu^-$ mode excludes J/ψ and $\psi(2S)$ decays to $\mu^+\mu^-$.

Baryon Particle Listings

Λ_b^0

$\Gamma(\Lambda\gamma)/\Gamma_{\text{total}}$ Γ_{45}/Γ

VALUE	CL%	DOCUMENT ID		TECN	COMMENT
$<1.3\times10^{-3}$	90	ACOSTA	02G	CDF	$p\overline{p}$ at 1.8 TeV

$\Gamma(\Lambda^0\eta)/\Gamma_{\text{total}}$ Γ_{46}/Γ

VALUE (units 10^{-6})	DOCUMENT ID		TECN	COMMENT
$9^{+7}_{-5}\pm1$	[1] AAIJ	15AH	LHCB	pp at 7, 8 TeV

[1] AAIJ 15AH reports $[\Gamma(\Lambda_b^0\to\Lambda^0\eta)/\Gamma_{\text{total}}]$ / $[\mathrm{B}(B^0\to\eta' K^0)] = 0.142^{+0.11}_{-0.08}$ which we multiply by our best value $\mathrm{B}(B^0\to\eta' K^0) = (6.6\pm0.4)\times10^{-5}$. Our first error is their experiment's error and our second error is the systematic error from using our best value. The single uncertainty quoted with the original measurement combines in quadrature statistical and systematic uncertainties.

$\Gamma(\Lambda^0\eta'(958))/\Gamma_{\text{total}}$ Γ_{47}/Γ

VALUE	CL%	DOCUMENT ID		TECN	COMMENT
$<3.1\times10^{-6}$	90	[1] AAIJ	15AH	LHCB	pp at 7, 8 TeV

[1] AAIJ 15AH reports $[\Gamma(\Lambda_b^0\to\Lambda^0\eta'(958))/\Gamma_{\text{total}}]$ / $[\mathrm{B}(B^0\to\eta' K^0)] <$ 0.047 which we multiply by our best value $\mathrm{B}(B^0\to\eta' K^0) = 6.6\times10^{-5}$.

$\Gamma(\Lambda\pi^+\pi^-)/\Gamma(\Lambda_c^+\pi^-)$ Γ_{48}/Γ_{20}

VALUE (units 10^{-4})	DOCUMENT ID		TECN	COMMENT
$9.4\pm3.8\pm0.5$	[1] AAIJ	16W	LHCB	pp at 7, 8 TeV

[1] AAIJ 16W reports $[\Gamma(\Lambda_b^0\to\Lambda\pi^+\pi^-)/\Gamma(\Lambda_b^0\to\Lambda_c^+\pi^-)]$ / $[\mathrm{B}(\Lambda_c^+\to\Lambda\pi^+)] = (7.3\pm1.9\pm2.2)\times10^{-2}$ which we multiply by our best value $\mathrm{B}(\Lambda_c^+\to\Lambda\pi^+) = (1.29\pm0.07)\times10^{-2}$. Our first error is their experiment's error and our second error is the systematic error from using our best value.

$\Gamma(\Lambda K^+\pi^-)/\Gamma(\Lambda_c^+\pi^-)$ Γ_{49}/Γ_{20}

VALUE (units 10^{-4})	DOCUMENT ID		TECN	COMMENT
$11.5\pm2.3\pm0.6$	[1] AAIJ	16W	LHCB	pp at 7, 8 TeV

[1] AAIJ 16W reports $[\Gamma(\Lambda_b^0\to\Lambda K^+\pi^-)/\Gamma(\Lambda_b^0\to\Lambda_c^+\pi^-)]$ / $[\mathrm{B}(\Lambda_c^+\to\Lambda\pi^+)] = (8.9\pm1.2\pm1.3)\times10^{-2}$ which we multiply by our best value $\mathrm{B}(\Lambda_c^+\to\Lambda\pi^+) = (1.29\pm0.07)\times10^{-2}$. Our first error is their experiment's error and our second error is the systematic error from using our best value.

$\Gamma(\Lambda K^+K^-)/\Gamma(\Lambda_c^+\pi^-)$ Γ_{50}/Γ_{20}

VALUE (units 10^{-3})	DOCUMENT ID		TECN	COMMENT
$3.27\pm0.35^{+0.17}_{-0.18}$	[1] AAIJ	16W	LHCB	pp at 7, 8 TeV

[1] AAIJ 16W reports $[\Gamma(\Lambda_b^0\to\Lambda K^+K^-)/\Gamma(\Lambda_b^0\to\Lambda_c^+\pi^-)]$ / $[\mathrm{B}(\Lambda_c^+\to\Lambda\pi^+)] = (25.3\pm1.9\pm1.9)\times10^{-2}$ which we multiply by our best value $\mathrm{B}(\Lambda_c^+\to\Lambda\pi^+) = (1.29\pm0.07)\times10^{-2}$. Our first error is their experiment's error and our second error is the systematic error from using our best value.

$\Gamma(\Lambda^0\phi)/\Gamma_{\text{total}}$ Γ_{51}/Γ

VALUE (units 10^{-6})	DOCUMENT ID		TECN	COMMENT
$9.2\pm1.9\pm1.5$	[1] AAIJ	16J	LHCB	pp at 7, 8 TeV

[1] AAIJ 16J reports $[\Gamma(\Lambda_b^0\to\Lambda^0\phi)/\Gamma_{\text{total}}]$ / $[\mathrm{B}(B^0\to K^0\phi)] \times [\mathrm{B}(\overline{b}\to b\text{-baryon})]$ / $[\mathrm{B}(\overline{b}\to B^0)] = 0.275\pm0.055\pm0.020$ which we multiply or divide by our best values $\mathrm{B}(B^0\to K^0\phi) = (7.3\pm0.7)\times10^{-6}$, $\mathrm{B}(\overline{b}\to b\text{-baryon}) = (8.9\pm1.2)\times10^{-2}$, $\mathrm{B}(\overline{b}\to B^0) = (40.5\pm0.6)\times10^{-2}$. Our first error is their experiment's error and our second error is the systematic error from using our best values.

PARTIAL BRANCHING FRACTIONS IN $\Lambda_b\to\Lambda\mu^+\mu^-$

$\mathrm{B}(\Lambda_b\to\Lambda\mu^+\mu^-)$ ($q^2<2.0$ GeV$^2/c^4$)

VALUE (units 10^{-7})	DOCUMENT ID		TECN	COMMENT
0.71 ± 0.27 OUR AVERAGE				
$0.72^{+0.24}_{-0.22}\pm0.14$	[1] AAIJ	15AE	LHCB	pp at 7, 8 TeV
$0.15\pm2.01\pm0.05$	AALTONEN	11AI	CDF	$p\overline{p}$ at 1.96 TeV
• • • We do not use the following data for averages, fits, limits, etc. • • •				
$0.56\pm0.76\pm0.80$	[2] AAIJ	13AJ	LHCB	Repl. by AAIJ 15AE

[1] AAIJ 15AE measurement covers $0.1 < q^2 < 2.0$ GeV$^2/c^4$.
[2] Uses $\mathrm{B}(\Lambda_b^0\to J/\psi\Lambda) = (6.2\pm1.4)\times10^{-4}$.

$\mathrm{B}(\Lambda_b\to\Lambda\mu^+\mu^-)$ ($2.0<q^2<4.3$ GeV$^2/c^4$)

VALUE (units 10^{-7})	DOCUMENT ID		TECN	COMMENT
$0.28^{+0.28}_{-0.21}$ OUR AVERAGE				
$0.253^{+0.276}_{-0.207}\pm0.046$	[1] AAIJ	15AE	LHCB	pp at 7, 8 TeV
$1.8\ \pm1.7\ \pm0.6$	AALTONEN	11AI	CDF	$p\overline{p}$ at 1.96 TeV
• • • We do not use the following data for averages, fits, limits, etc. • • •				
$0.71\ \pm0.60\ \pm0.23$	[2] AAIJ	13AJ	LHCB	Repl. by AAIJ 15AE

[1] AAIJ 15AE measurement covers $2.0 < q^2 < 4.0$ GeV$^2/c^4$.
[2] Uses $\mathrm{B}(\Lambda_b^0\to J/\psi\Lambda) = (6.2\pm1.4)\times10^{-4}$.

$\mathrm{B}(\Lambda_b\to\Lambda\mu^+\mu^-)$ ($q^2<4.3$ GeV$^2/c^4$)

VALUE (units 10^{-7})	DOCUMENT ID		TECN	COMMENT
$2.7\pm2.5\pm0.9$	AALTONEN	11AI	CDF	$p\overline{p}$ at 1.96 TeV

$\mathrm{B}(\Lambda_b\to\Lambda\mu^+\mu^-)$ ($4.0<q^2<6.0$ GeV$^2/c^4$)

VALUE (units 10^{-7})	DOCUMENT ID		TECN	COMMENT
$0.04^{+0.18}_{-0.00}\pm0.02$	AAIJ	15AE	LHCB	pp at 7, 8 TeV

$\mathrm{B}(\Lambda_b\to\Lambda\mu^+\mu^-)$ ($1.0<q^2<6.0$ GeV$^2/c^4$)

VALUE (units 10^{-7})	DOCUMENT ID		TECN	COMMENT
$0.47^{+0.31}_{-0.27}$ OUR AVERAGE				
$0.45^{+0.30}_{-0.25}\pm0.10$	[1] AAIJ	15AE	LHCB	pp at 7 and 8 TeV
$1.3\ \pm2.1\ \pm0.4$	AALTONEN	11AI	CDF	$p\overline{p}$ at 1.96 TeV

[1] AAIJ 15AE measurement covers $1.1 < q^2 < 6.0$ GeV$^2/c^4$.

$\mathrm{B}(\Lambda_b\to\Lambda\mu^+\mu^-)$ ($6.0<q^2<8.0$ GeV$^2/c^4$)

VALUE (units 10^{-7})	DOCUMENT ID		TECN	COMMENT
$0.50^{+0.24}_{-0.22}\pm0.10$	AAIJ	15AE	LHCB	pp at 7, 8 TeV

$\mathrm{B}(\Lambda_b\to\Lambda\mu^+\mu^-)$ ($4.3<q^2<8.68$ GeV$^2/c^4$)

VALUE (units 10^{-7})	DOCUMENT ID		TECN	COMMENT
$0.5\ \pm0.7$ OUR AVERAGE				
$0.66\pm0.74\pm0.18$	[1] AAIJ	13AJ	LHCB	pp at 7 TeV
$-0.2\ \pm1.6\ \pm0.1$	AALTONEN	11AI	CDF	$p\overline{p}$ at 1.96 TeV

[1] Uses $\mathrm{B}(\Lambda_b^0\to J/\psi\Lambda) = (6.2\pm1.4)\times10^{-4}$.

$\mathrm{B}(\Lambda_b\to\Lambda\mu^+\mu^-)$ ($10.09<q^2<12.86$ GeV$^2/c^4$)

VALUE (units 10^{-7})	DOCUMENT ID		TECN	COMMENT
$2.2\ \pm0.6$ OUR AVERAGE				
$2.08^{+0.42}_{-0.39}\pm0.42$	[1] AAIJ	15AE	LHCB	pp at 7, 8 TeV
$3.0\ \pm1.5\ \pm1.0$	AALTONEN	11AI	CDF	$p\overline{p}$ at 1.96 TeV
• • • We do not use the following data for averages, fits, limits, etc. • • •				
$1.55\pm0.58\pm0.55$	[2] AAIJ	13AJ	LHCB	Repl. by AAIJ 15AE

[1] AAIJ 15AE measurement covers $11.0 < q^2 < 12.5$ GeV$^2/c^4$.
[2] Uses $\mathrm{B}(\Lambda_b^0\to J/\psi\Lambda) = (6.2\pm1.4)\times10^{-4}$.

$\mathrm{B}(\Lambda_b\to\Lambda\mu^+\mu^-)$ ($14.18<q^2<16.0$ GeV$^2/c^4$)

VALUE (units 10^{-7})	DOCUMENT ID		TECN	COMMENT
$1.7\ \pm0.5$ OUR AVERAGE Error includes scale factor of 1.1.				
$2.04^{+0.35}_{-0.33}\pm0.42$	[1] AAIJ	15AE	LHCB	pp at 7, 8 TeV
$1.0\ \pm0.7\ \pm0.3$	AALTONEN	11AI	CDF	$p\overline{p}$ at 1.96 TeV
• • • We do not use the following data for averages, fits, limits, etc. • • •				
$1.44\pm0.44\pm0.42$	[2] AAIJ	13AJ	LHCB	Repl. by AAIJ 15AE

[1] AAIJ 15AE measurement covers $15.0 < q^2 < 16.0$ GeV$^2/c^4$.
[2] Uses $\mathrm{B}(\Lambda_b^0\to J/\psi\Lambda) = (6.2\pm1.4)\times10^{-4}$.

$\mathrm{B}(\Lambda_b\to\Lambda\mu^+\mu^-)$ ($16.0<q^2$ GeV$^2/c^4$)

VALUE (units 10^{-7})	DOCUMENT ID		TECN	COMMENT
$7.0\ \pm1.9\ \pm2.2$	AALTONEN	11AI	CDF	$p\overline{p}$ at 1.96 TeV
• • • We do not use the following data for averages, fits, limits, etc. • • •				
$4.73\pm0.77\pm1.25$	[1,2] AAIJ	13AJ	LHCB	Repl. by AAIJ 15AE

[1] Uses $\mathrm{B}(\Lambda_b^0\to J/\psi\Lambda) = (6.2\pm1.4)\times10^{-4}$.
[2] Requires $16.00 < q^2 < 20.30$ GeV$^2/c^4$.

$\mathrm{B}(\Lambda_b\to\Lambda\mu^+\mu^-)$ ($18.0<q^2<20.0$ GeV$^2/c^4$)

VALUE (units 10^{-7})	DOCUMENT ID		TECN	COMMENT
$2.44\pm0.28\pm0.50$	AAIJ	15AE	LHCB	pp at 7, 8 TeV

$\mathrm{B}(\Lambda_b\to\Lambda\mu^+\mu^-)$ ($15.0<q^2<20.0$ GeV$^2/c^4$)

VALUE (units 10^{-7})	DOCUMENT ID		TECN	COMMENT
$6.00\pm0.45\pm1.25$	AAIJ	15AE	LHCB	pp at 7, 8 TeV

CP VIOLATION

A_{CP} is defined as

$$A_{CP} = \frac{B(\Lambda_b^0\to f) - B(\overline{\Lambda}_b^0\to\overline{f})}{B(\Lambda_b^0\to f) + B(\overline{\Lambda}_b^0\to\overline{f})},$$

the *CP*-violation asymmetry of exclusive Λ_b^0 and $\overline{\Lambda}_b^0$ decay.

$A_{CP}(\Lambda_b\to p\pi^-)$

VALUE	DOCUMENT ID		TECN	COMMENT
$0.06\pm0.07\pm0.03$	AALTONEN	14P	CDF	$p\overline{p}$ at 1.96 TeV
• • • We do not use the following data for averages, fits, limits, etc. • • •				
$0.03\pm0.17\pm0.05$	AALTONEN	11N	CDF	Repl. by AALTONEN 14P

$A_{CP}(\Lambda_b \to pK^-)$

VALUE	DOCUMENT ID		TECN	COMMENT
−0.10±0.08±0.04	AALTONEN	14P	CDF	$p\overline{p}$ at 1.96 TeV
• • • We do not use the following data for averages, fits, limits, etc. • • •				
0.37±0.17±0.03	AALTONEN	11N	CDF	Repl. by AALTONEN 14P

$A_{CP}(\Lambda_b \to p\overline{K}^0\pi^-)$

VALUE	DOCUMENT ID		TECN	COMMENT
0.22±0.13±0.03	AAIJ	14Q	LHCB	pp at 7 TeV

$\Delta A_{CP}(J/\psi p\pi^-/K^-) \equiv A_{CP}(J/\psi p\pi^-) - A_{CP}(J/\psi pK^-)$

VALUE (units 10^{-2})	DOCUMENT ID		TECN	COMMENT
5.7±2.4±1.2	AAIJ	14K	LHCB	pp at 7, 8 TeV

$A_{CP}(\Lambda_b \to \Lambda K^+\pi^-)$

VALUE	DOCUMENT ID		TECN	COMMENT
−0.53±0.23±0.11	[1] AAIJ	16W	LHCB	pp at 7, 8 TeV

[1] Measured relative to $\Lambda_b^0 \to \Lambda_c^+\pi^-$ decay.

$A_{CP}(\Lambda_b \to \Lambda K^+K^-)$

VALUE	DOCUMENT ID		TECN	COMMENT
−0.28±0.10±0.07	[1] AAIJ	16W	LHCB	pp at 7, 8 TeV

[1] Measured relative to $\Lambda_b^0 \to \Lambda_c^+\pi^-$ decay.

$\Delta A_{CP}(\Lambda_b^0 \to pK^-\mu^+\mu^-) \equiv A_{CP}(pK^-\mu^+\mu^-) - A_{CP}(pK^-J/\psi)$

VALUE (units 10^{-2})	DOCUMENT ID		TECN	COMMENT
−3.5±5.0±0.2	AAIJ	17T	LHCB	pp at 7, 8 TeV

CP AND *T* VIOLATION PARAMETERS

Measured values of the triple-product asymmetry parameters, odd under time-reversal, are defined as $A_{c(s)}(\Lambda/\phi) = (N^+_{c(s)} - N^-_{c(s)})$ / (sum) where $N^+_{c(s)}$, $N^-_{c(s)}$ are the number of Λ or ϕ candidates for which the cos(Φ) and sin(Φ) observables are positive and negative, respectively. Angles cos(Φ) and sin(Φ) are defined as in LEITNER 07.

$A_c(\Lambda)$

VALUE	DOCUMENT ID		TECN	COMMENT
−0.22±0.12±0.06	AAIJ	16J	LHCB	pp at 7, 8 TeV

$A_s(\Lambda)$

VALUE	DOCUMENT ID		TECN	COMMENT
0.13±0.12±0.05	AAIJ	16J	LHCB	pp at 7, 8 TeV

$A_c(\phi)$

VALUE	DOCUMENT ID		TECN	COMMENT
−0.01±0.12±0.03	AAIJ	16J	LHCB	pp at 7, 8 TeV

$A_s(\phi)$

VALUE	DOCUMENT ID		TECN	COMMENT
−0.07±0.12±0.01	AAIJ	16J	LHCB	pp at 7, 8 TeV

$a_P(\Lambda_b^0 \to p\pi^-\pi^+\pi^-)$

Observable calculated as average of the triple products for Λ_b^0 and $\overline{\Lambda}_b^0$, which is sensitive to parity violation.

VALUE (%)	DOCUMENT ID		TECN	COMMENT
−3.71±1.45±0.32	[1] AAIJ	17H	LHCB	pp at 7, 8 TeV

[1] Measured over full phase space of the decay.

$a_P(\Lambda_b^0 \to pK^-K^+\pi^-)$

Observable calculated as average of the triple products for Λ_b^0 and $\overline{\Lambda}_b^0$, which is sensitive to parity violation.

VALUE (%)	DOCUMENT ID		TECN	COMMENT
3.62±4.54±0.42	[1] AAIJ	17H	LHCB	pp at 7, 8 TeV

[1] Measured over full phase space of the decay.

$a_{CP}(\Lambda_b^0 \to p\pi^-\pi^+\pi^-)$

Observable calculated as half of the difference between triple products for Λ_b^0 and $\overline{\Lambda}_b^0$, which is sensitive to *CP* violation.

VALUE (%)	DOCUMENT ID		TECN	COMMENT
1.15±1.45±0.32	[1] AAIJ	17H	LHCB	pp at 7, 8 TeV

[1] Measured over full phase space of the decay.

$a_{CP}(\Lambda_b^0 \to pK^-K^+\pi^-)$

Observable calculated as half of the difference between triple products for Λ_b^0 and $\overline{\Lambda}_b^0$, which is sensitive to *CP* violation.

VALUE (%)	DOCUMENT ID		TECN	COMMENT
−0.93±4.54±0.42	[1] AAIJ	17H	LHCB	pp at 7, 8 TeV

[1] Measured over full phase space of the decay.

$a_P(\Lambda_b^0 \to pK^-\mu^+\mu^-)$

VALUE (%)	DOCUMENT ID		TECN	COMMENT
−4.8±5.0±0.7	AAIJ	17T	LHCB	pp at 7, 8 TeV

$a_{CP}(\Lambda_b^0 \to pK^-\mu^+\mu^-)$

VALUE (%)	DOCUMENT ID		TECN	COMMENT
1.2±5.0±0.7	AAIJ	17T	LHCB	pp at 7, 8 TeV

Λ_b^0 DECAY PARAMETERS

See the note on "Baryon Decay Parameters" in the neutron Listings.

α decay parameter for $\Lambda_b \to J/\psi\Lambda$

VALUE	DOCUMENT ID		TECN	COMMENT
0.18±0.13 OUR AVERAGE				
0.30±0.16±0.06	[1] AAD	14L	ATLS	pp at 7 TeV
0.05±0.17±0.07	[2] AAIJ	13AG	LHCB	pp at 7 TeV

[1] An angular analysis of $\Lambda_b \to J/\psi\Lambda$ decay is performed and magnitudes of all helicity amplitudes are also reported.

[2] An angular analysis of $\Lambda_b \to J/\psi\Lambda$ decay is performed and a Λ_b transverse production polarization of 0.06 ± 0.07 ± 0.02 is also reported.

$A^{\ell}_{FB}(\mu\mu)$ in $\Lambda_b \to \Lambda\mu^+\mu^-$

VALUE	DOCUMENT ID		TECN	COMMENT
−0.05±0.09±0.03	[1] AAIJ	15AE	LHCB	pp at 7, 8 TeV

[1] AAIJ 15AE measurement covers $15.0 < q^2 < 20.0$ GeV$^2/c^4$.

$A^{h}_{FB}(p\pi)$ in $\Lambda_b \to \Lambda(p\pi)\mu^+\mu^-$

VALUE	DOCUMENT ID		TECN	COMMENT
−0.29±0.07±0.03	[1] AAIJ	15AE	LHCB	pp at 7, 8 TeV

[1] AAIJ 15AE measurement covers $15.0 < q^2 < 20.0$ GeV$^2/c^4$.

$f_L(\mu\mu)$ longitudinal polarization fraction in $\Lambda_b \to \Lambda\mu^+\mu^-$

VALUE	DOCUMENT ID		TECN	COMMENT
$0.61^{+0.11}_{-0.14}$±0.03	[1] AAIJ	15AE	LHCB	pp at 7, 8 TeV

[1] AAIJ 15AE measurement covers $15.0 < q^2 < 20.0$ GeV$^2/c^4$.

FORWARD-BACKWARD ASYMMETRIES

The forward-backward assymmetry is defined as $A_{FB}(\Lambda_b^0)$ = [N(F) − N(B)] / [N(F) + N(B)], where the forward (F) direction corresponds to a particle (Λ_b^0 or $\overline{\Lambda}_b^0$) sharing valence quark flavors with a beam particle with the same sign of rapidity.

$A_{FB}(\Lambda_b^0 \to J/\psi\Lambda)$

VALUE	DOCUMENT ID		TECN	COMMENT
0.04±0.07±0.02	[1] ABAZOV	15I	D0	pp at 1.96 TeV

[1] The measured asymmetry integrated over rapidity y in the range of $0.1 < |y| < 2.0$.

$A_P(\Lambda_b^0)$

$A_P(\Lambda_b^0) = [\sigma(\Lambda_b^0) - \sigma(\overline{\Lambda}_b^0)] / [\sigma(\Lambda_b^0) + \sigma(\overline{\Lambda}_b^0)]$

VALUE (units 10^{-2})	DOCUMENT ID		TECN	COMMENT
2.4 ±1.6 OUR AVERAGE	Error includes scale factor of 1.1.			
−0.11±2.53±1.08	[1] AAIJ	17BF	LHCB	pp at 7 TeV
3.44±1.61±0.76	[1] AAIJ	17BF	LHCB	pp at 8 TeV

[1] Indirect determination in kinematic range $2 < p_T < 30$ GeV/c and $2.1 < \eta < 4.5$ from production asymmetries of B^+, B^0 and B_s^0.

Λ_b^0 REFERENCES

AAIJ	17AM PRL 119 062001	R. Aaij *et al.*	(LHCb Collab.)
AAIJ	17BF PL B774 139	R. Aaij *et al.*	(LHCb Collab.)
AAIJ	17H NATP 13 391	R. Aaij *et al.*	(LHCb Collab.)
AAIJ	17P JHEP 1704 029	R. Aaij *et al.*	(LHCb Collab.)
AAIJ	17S JHEP 1705 030	R. Aaij *et al.*	(LHCb Collab.)
AAIJ	17T JHEP 1706 108	R. Aaij *et al.*	(LHCb Collab.)
AAIJ	16 JHEP 1601 012	R. Aaij *et al.*	(LHCb Collab.)
AAIJ	16A CP C40 011001	R. Aaij *et al.*	(LHCb Collab.)
AAIJ	16J PL B759 282	R. Aaij *et al.*	(LHCb Collab.)
AAIJ	16W JHEP 1605 081	R. Aaij *et al.*	(LHCb Collab.)
AAIJ	16Y JHEP 1605 132	R. Aaij *et al.*	(LHCb Collab.)
AAD	15CH PL B751 63	G. Aad *et al.*	(ATLAS Collab.)
AAIJ	15AE JHEP 1506 115	R. Aaij *et al.*	(LHCb Collab.)
AAIJ	15AH JHEP 1509 006	R. Aaij *et al.*	(LHCb Collab.)
AAIJ	15BG NATP 11 743	R. Aaij *et al.*	(LHCb Collab.)
ABAZOV	15I PR D91 072008	V.M. Abazov *et al.*	(D0 Collab.)
AAD	14L PR D89 092009	G. Aad *et al.*	(ATLAS Collab.)
AAIJ	14AA PRL 112 202001	R. Aaij *et al.*	(LHCb Collab.)
AAIJ	14E JHEP 1404 114	R. Aaij *et al.*	(LHCb Collab.)
AAIJ	14H PR D89 032001	R. Aaij *et al.*	(LHCb Collab.)
AAIJ	14I JHEP 1408 143	R. Aaij *et al.*	(LHCb Collab.)
AAIJ	14K JHEP 1407 103	R. Aaij *et al.*	(LHCb Collab.)
AAIJ	14Q JHEP 1404 087	R. Aaij *et al.*	(LHCb Collab.)
AAIJ	14U PL B734 122	R. Aaij *et al.*	(LHCb Collab.)
AALTONEN	14B PR D89 072014	T. Aaltonen *et al.*	(CDF Collab.)
AALTONEN	14P PRL 113 242001	T. Aaltonen *et al.*	(CDF Collab.)
PDG	14 CP C38 070001	K. Olive *et al.*	(PDG Collab.)
AAD	13U PR D87 032002	G. Aad *et al.*	(ATLAS Collab.)
AAIJ	13AG PL B724 27	R. Aaij *et al.*	(LHCb Collab.)
AAIJ	13AJ PL B725 25	R. Aaij *et al.*	(LHCb Collab.)
AAIJ	13AV PRL 110 182001	R. Aaij *et al.*	(LHCb Collab.)
AAIJ	13BB PRL 111 102003	R. Aaij *et al.*	(LHCb Collab.)
CHATRCHYAN	13AC JHEP 1307 163	S. Chatrchyan *et al.*	(CMS Collab.)
AAIJ	12AR JHEP 1210 037	R. Aaij *et al.*	(LHCb Collab.)
AAIJ	12E PL B708 241	R. Aaij *et al.*	(LHCb Collab.)
AALTONEN	12A PR D85 032003	T. Aaltonen *et al.*	(CDF Collab.)
ABAZOV	12U PR D85 112003	V.M. Abazov *et al.*	(D0 Collab.)

AAIJ	11E	PR D84 092001	R. Aaij *et al.*	(LHCb Collab.)
Also		PR D85 039904 (errat.)	R. Aaij *et al.*	(LHCb Collab.)
AALTONEN	11	PRL 106 121804	T. Aaltonen *et al.*	(CDF Collab.)
AALTONEN	11AI	PRL 107 201802	T. Aaltonen *et al.*	(CDF Collab.)
AALTONEN	11N	PRL 106 181802	T. Aaltonen *et al.*	(CDF Collab.)
ABAZOV	11O	PR D84 031102	V.M. Abazov *et al.*	(D0 Collab.)
AALTONEN	10B	PRL 104 102002	T. Aaltonen *et al.*	(CDF Collab.)
AALTONEN	09C	PRL 103 031801	T. Aaltonen *et al.*	(CDF Collab.)
AALTONEN	09E	PR D79 032001	T. Aaltonen *et al.*	(CDF Collab.)
ABAZOV	07S	PRL 99 142001	V.M. Abazov *et al.*	(D0 Collab.)
ABAZOV	07U	PRL 99 182001	V.M. Abazov *et al.*	(D0 Collab.)
ABULENCIA	07A	PRL 98 122001	A. Abulencia *et al.*	(FNAL CDF Collab.)
ABULENCIA	07B	PRL 98 122002	A. Abulencia *et al.*	(FNAL CDF Collab.)
LEITNER	07	NPBPS 174 169	O. Leitner, Z.J. Ajaltouni	
ACOSTA	06	PRL 96 202001	D. Acosta *et al.*	(CDF Collab.)
ABAZOV	05C	PRL 94 102001	V.M. Abazov *et al.*	(D0 Collab.)
ACOSTA	05O	PR D72 051104	D. Acosta *et al.*	(CDF Collab.)
ABDALLAH	04A	PL B585 63	J. Abdallah *et al.*	(DELPHI Collab.)
ACOSTA	02G	PR D66 112002	D. Acosta *et al.*	(CDF Collab.)
ABREU	99W	EPJ C10 185	P. Abreu *et al.*	(DELPHI Collab.)
ACKERSTAFF	98G	PL B426 161	K. Ackerstaff *et al.*	(OPAL Collab.)
BARATE	98D	EPJ C2 197	R. Barate *et al.*	(ALEPH Collab.)
ABE	97B	PR D55 1142	F. Abe *et al.*	(CDF Collab.)
ABE	96M	PRL 77 1439	F. Abe *et al.*	(CDF Collab.)
ABREU	96D	ZPHY C71 199	P. Abreu *et al.*	(DELPHI Collab.)
ABREU	96N	PL B374 351	P. Abreu *et al.*	(DELPHI Collab.)
ADAM	96D	ZPHY C72 207	W. Adam *et al.*	(DELPHI Collab.)
BUSKULIC	96L	PL B380 442	D. Buskulic *et al.*	(ALEPH Collab.)
BUSKULIC	96V	PL B384 471	D. Buskulic *et al.*	(ALEPH Collab.)
PDG	96	PR D54 1	R. M. Barnett *et al.*	(PDG Collab.)
ABREU	95S	ZPHY C68 375	P. Abreu *et al.*	(DELPHI Collab.)
AKERS	95K	PL B353 402	R. Akers *et al.*	(OPAL Collab.)
BUSKULIC	95L	PL B357 685	D. Buskulic *et al.*	(ALEPH Collab.)
ABE	93B	PR D47 2639	F. Abe *et al.*	(CDF Collab.)
BUSKULIC	92E	PL B294 145	D. Buskulic *et al.*	(ALEPH Collab.)
ALBAJAR	91E	PL B273 540	C. Albajar *et al.*	(UA1 Collab.)
BARI	91	NC 104A 1787	G. Bari *et al.*	(CERN R422 Collab.)
ARENTON	86	NP B274 707	M.W. Arenton *et al.*	(ARIZ, NDAM, VAND)
BASILE	81	LNC 31 97	M. Basile *et al.*	(CERN R415 Collab.)

$\Lambda_b(5912)^0$

$J^P = \frac{1}{2}^-$ Status: ***

Quantum numbers are based on quark model expectations.

$\Lambda_b(5912)^0$ MASS

VALUE (MeV)	DOCUMENT ID		TECN	COMMENT
5912.20±0.13±0.17	[1,2] AAIJ	12AL	LHCB	pp at 7 TeV

[1] Observed in $\Lambda_b(5912)^0 \to \Lambda_b^0\pi^+\pi^-$ decays with 17.6 ± 4.8 candidates with a significance of 5.2 sigma.

[2] AAIJ 12AL measures $m(\Lambda_b(5912)^0) - m(\Lambda_b^0) = 292.60 \pm 0.12 \pm 0.04$ MeV. We have adjusted the measurement to our best value of $m(\Lambda_b^0) = 5619.60 \pm 0.17$ MeV. Our first error is their experiment's error and our second error is the systematic error from using our best values.

$\Lambda_b(5912)^0$ WIDTH

VALUE (MeV)	CL%	DOCUMENT ID	TECN	COMMENT
<0.66	90	AAIJ	12AL LHCB	pp at 7 TeV

$\Lambda_b(5912)^0$ DECAY MODES

	Mode	Fraction (Γ_i/Γ)
Γ_1	$\Lambda_b^0\pi^+\pi^-$	seen

$\Lambda_b(5912)^0$ BRANCHING RATIOS

$\Gamma(\Lambda_b^0\pi^+\pi^-)/\Gamma_{total}$ **Γ_1/Γ**

VALUE	DOCUMENT ID		TECN	COMMENT
seen	AAIJ	12AL	LHCB	pp at 7 TeV

$\Lambda_b(5912)^0$ REFERENCES

AAIJ	12AL	PRL 109 172003	R. Aaij *et al.*	(LHCb Collab.)

$\Lambda_b(5920)^0$

$J^P = \frac{3}{2}^-$ Status: ***

Quantum numbers are based on quark model expectations.

$\Lambda_b(5920)^0$ MASS

VALUE (MeV)	DOCUMENT ID		TECN	COMMENT
5919.92±0.19 OUR AVERAGE	Error includes scale factor of 1.1.			
5919.4 ±0.5 ±0.2	[1,2] AALTONEN	13V	CDF	$p\overline{p}$ at 1.96 TeV
5920.00±0.09±0.17	[3,4] AAIJ	12AL	LHCB	pp at 7 TeV

[1] Measured in $\Lambda_b(5920)^0 \to \Lambda_b^0\pi^+\pi^-$ decays with $17.3^{+5.3}_{-4.6}$ events, with a significance of 3.5 sigma.

[2] AALTONEN 13V measures $m(\Lambda_b(5920)^0) - m(\Lambda_b^0) - 2m(\pi) = 20.68 \pm 0.35 \pm 0.30$ MeV. We have adjusted the measurement to our best values of $m(\Lambda_b^0) = 5619.60 \pm 0.17$ MeV and $m(\pi) = 139.57061 \pm 0.00024$ MeV. Our first error is their experiment's error and our second error is the systematic error from using our best values.

[3] Observed in $\Lambda_b(5920)^0 \to \Lambda_b^0\pi^+\pi^-$ decays with 52.5 ± 8.1 candidates with a significance of 10.2 sigma.

[4] AAIJ 12AL measures $m(\Lambda_b(5920)^0) - m(\Lambda_b^0) = 300.40 \pm 0.08 \pm 0.04$ MeV. We have adjusted the measurement to our best value of $m(\Lambda_b^0) = 5619.60 \pm 0.17$ MeV. Our first error is their experiment's error and our second error is the systematic error from using our best values.

$\Lambda_b(5920)^0$ WIDTH

VALUE (MeV)	CL%	DOCUMENT ID	TECN	COMMENT
<0.63	90	AAIJ	12AL LHCB	pp at 7 TeV

$\Lambda_b(5920)^0$ DECAY MODES

	Mode	Fraction (Γ_i/Γ)
Γ_1	$\Lambda_b^0\pi^+\pi^-$	seen

$\Lambda_b(5920)^0$ BRANCHING RATIOS

$\Gamma(\Lambda_b^0\pi^+\pi^-)/\Gamma_{total}$ **Γ_1/Γ**

VALUE	DOCUMENT ID		TECN	COMMENT
seen	AAIJ	12AL	LHCB	pp at 7 TeV

$\Lambda_b(5920)^0$ REFERENCES

AALTONEN	13V	PR D88 071101	T. Aaltonen *et al.*	(CDF Collab.)
AAIJ	12AL	PRL 109 172003	R. Aaij *et al.*	(LHCb Collab.)

Σ_b

$I(J^P) = 1(\frac{1}{2}^+)$ Status: ***

I, *J*, *P* need confirmation.

In the quark model Σ_b^+, Σ_b^0, Σ_b^- are an isotriplet (*uub*, *udb*, *ddb*) state. The lowest Σ_b ought to have $J^P = 1/2^+$. None of *I*, *J*, or *P* have actually been measured.

Σ_b MASS

Σ_b^+ MASS

VALUE (MeV)	DOCUMENT ID		TECN	COMMENT
$5811.3^{+0.9}_{-0.8}\pm1.7$	[1] AALTONEN	12F	CDF	$p\overline{p}$ at 1.96 TeV
• • • We do not use the following data for averages, fits, limits, etc. • • •				
$5807.8^{+2.0}_{-2.2}\pm1.7$	[2] AALTONEN	07K	CDF	Repl. by AALTONEN 12F

Σ_b^- MASS

VALUE (MeV)	DOCUMENT ID		TECN	COMMENT
$5815.5^{+0.6}_{-0.5}\pm1.7$	[1] AALTONEN	12F	CDF	$p\overline{p}$ at 1.96 TeV
• • • We do not use the following data for averages, fits, limits, etc. • • •				
5815.2±1.0±1.7	[2] AALTONEN	07K	CDF	Repl. by AALTONEN 12F

$m_{\Sigma_b^+} - m_{\Sigma_b^-}$

VALUE (MeV)	DOCUMENT ID		TECN	COMMENT
$-4.2^{+1.1}_{-1.0}\pm0.1$	[1] AALTONEN	12F	CDF	$p\overline{p}$ at 1.96 TeV

[1] Measured using the fully reconstructed $\Lambda_b^0 \to \Lambda_c^+\pi^-$ and $\Lambda_c^+ \to K^-\pi^+$ decays.

[2] Observed four $\Lambda_b^0\pi^\pm$ resonances in the fully reconstructed decay mode $\Lambda_b^0 \to \Lambda_c^+\pi^-$, where $\Lambda_c^+ \to pK^-\pi^+$.

Σ_b WIDTH

Σ_b^+ WIDTH

VALUE (MeV)	DOCUMENT ID		TECN	COMMENT
$9.7^{+3.8}_{-2.8}{}^{+1.2}_{-1.1}$	[3] AALTONEN	12F	CDF	$p\overline{p}$ at 1.96 TeV

Σ_b^- WIDTH

VALUE (MeV)	DOCUMENT ID		TECN	COMMENT
$4.9^{+3.1}_{-2.1}\pm1.1$	[3] AALTONEN	12F	CDF	$p\overline{p}$ at 1.96 TeV

[3] Measured using the fully reconstructed $\Lambda_b^0 \to \Lambda_c^+\pi^-$ and $\Lambda_c^+ \to K^-\pi^+$ decays.

Σ_b DECAY MODES

	Mode	Fraction (Γ_i/Γ)
Γ_1	$\Lambda_b^0\pi$	dominant

Σ_b BRANCHING RATIOS

$\Gamma(\Lambda_b^0\pi)/\Gamma_{\text{total}}$ Γ_1/Γ

VALUE	DOCUMENT ID		TECN	COMMENT
dominant	AALTONEN	07K	CDF	$p\overline{p}$ at 1.96 TeV

Σ_b REFERENCES

AALTONEN	12F	PR D85 092011	T. Aaltonen *et al.*	(CDF Collab.)
AALTONEN	07K	PRL 99 202001	T. Aaltonen *et al.*	(CDF Collab.)

Σ_b^*

$I(J^P) = 1(\frac{3}{2}^+)$ Status: ***

I, J, P need confirmation.

I, J, P need confirmation. Quantum numbers shown are quark-model predictions.

Σ_b^* MASS

Σ_b^{*+} MASS

VALUE (MeV)	DOCUMENT ID		TECN	COMMENT
$\mathbf{5832.1 \pm 0.7^{+1.7}_{-1.8}}$	[1] AALTONEN	12F	CDF	$p\overline{p}$ at 1.96 TeV

Σ_b^{*-} MASS

VALUE (MeV)	DOCUMENT ID		TECN	COMMENT
$\mathbf{5835.1 \pm 0.6^{+1.7}_{-1.8}}$	[1] AALTONEN	12F	CDF	$p\overline{p}$ at 1.96 TeV

$m_{\Sigma_b^{*+}} - m_{\Sigma_b^{*-}}$

VALUE (MeV)	DOCUMENT ID		TECN	COMMENT
$\mathbf{-3.0^{+1.0}_{-0.9} \pm 0.1}$	[1] AALTONEN	12F	CDF	$p\overline{p}$ at 1.96 TeV

[1] Measured using the fully reconstructed $\Lambda_b^0 \to \Lambda_c^+\pi^-$ and $\Lambda_c^+ \to K^-\pi^+$ decays.

Σ_b^* WIDTH

Σ_b^{*+} WIDTH

VALUE (MeV)	DOCUMENT ID		TECN	COMMENT
$\mathbf{11.5^{+2.7+1.0}_{-2.2-1.5}}$	[2] AALTONEN	12F	CDF	$p\overline{p}$ at 1.96 TeV

Σ_b^{*-} WIDTH

VALUE (MeV)	DOCUMENT ID		TECN	COMMENT
$\mathbf{7.5^{+2.2+0.9}_{-1.8-1.4}}$	[2] AALTONEN	12F	CDF	$p\overline{p}$ at 1.96 TeV

[2] Measured using the fully reconstructed $\Lambda_b^0 \to \Lambda_c^+\pi^-$ and $\Lambda_c^+ \to K^-\pi^+$ decays.

$m_{\Sigma_b^*} - m_{\Sigma_b}$

VALUE (MeV)	DOCUMENT ID		TECN	COMMENT
$\mathbf{21.2^{+2.0+0.4}_{-1.9-0.3}}$	[3] AALTONEN	07K	CDF	$p\overline{p}$ at 1.96 TeV

[3] Observed four $\Lambda_b^0\pi^\pm$ resonances in the fully reconstructed decay mode $\Lambda_b^0 \to \Lambda_c^+\pi^-$, where $\Lambda_c^+ \to pK^-\pi^+$. Assumes $m_{\Sigma_b^{*+}} - m_{\Sigma_b^+} = m_{\Sigma_b^{*-}} - m_{\Sigma_b^-}$

Σ_b^* DECAY MODES

	Mode	Fraction (Γ_i/Γ)
Γ_1	$\Lambda_b^0\pi$	dominant

Σ_b^* BRANCHING RATIOS

$\Gamma(\Lambda_b^0\pi)/\Gamma_{\text{total}}$ Γ_1/Γ

VALUE	DOCUMENT ID		TECN	COMMENT
dominant	AALTONEN	07K	CDF	$p\overline{p}$ at 1.96 TeV

Σ_b^* REFERENCES

AALTONEN	12F	PR D85 092011	T. Aaltonen *et al.*	(CDF Collab.)
AALTONEN	07K	PRL 99 202001	T. Aaltonen *et al.*	(CDF Collab.)

Ξ_b^0, Ξ_b^-

$I(J^P) = \frac{1}{2}(\frac{1}{2}^+)$ Status: ***

I, J, P need confirmation.

In the quark model, Ξ_b^0 and Ξ_b^- are an isodoublet (*usb*, *dsb*) state; the lowest Ξ_b^0 and Ξ_b^- ought to have $J^P = 1/2^+$. None of *I*, *J*, or *P* have actually been measured.

Ξ_b MASSES

Ξ_b^- MASS

VALUE (MeV)	DOCUMENT ID		TECN	COMMENT
5797.0 ± 0.9 OUR AVERAGE	Error includes scale factor of 1.8. See the ideogram below.			
5797.72 ± 0.46 ± 0.31	[1] AAIJ	14BJ	LHCB	pp at 7, 8 TeV
5793.4 ± 1.8 ± 0.7	[2] AALTONEN	14B	CDF	$p\overline{p}$ at 1.96 TeV
5795.8 ± 0.9 ± 0.4	[3] AAIJ	13AV	LHCB	pp at 7 TeV
5774 ±11 ±15	[4] ABAZOV	07K	D0	$p\overline{p}$ at 1.96 TeV
• • • We do not use the following data for averages, fits, limits, etc. • • •				
5796.7 ± 5.1 ± 1.4	[5] AALTONEN	11X	CDF	Repl. by AALTONEN 14B
5790.9 ± 2.6 ± 0.8	[6] AALTONEN	09AP	CDF	Repl. by AALTONEN 14B
5792.9 ± 2.5 ± 1.7	[7] AALTONEN	07A	CDF	Repl. by AALTONEN 09AP

[1] Reconstructed in $\Xi_b^- \to \Xi_c^0\pi^-$, $\Xi_c^0 \to pK^-K^-\pi^+$ decays. Reference Λ_b^0 mass 5619.30 ± 0.34 MeV from AAIJ 14AA.

[2] Uses $\Xi_b^- \to J/\psi\Xi^-$ and $\Xi_c^0\pi^-$ decays.

[3] Measured in $\Xi_b^- \to J/\psi\Xi^-$ decays.

[4] Observed in $\Xi_b^- \to J/\psi\Xi^-$ decays with $15.2 \pm 4.4^{+1.9}_{-0.4}$ candidates, a significance of 5.5 sigma.

[5] Measured in $\Xi_b^- \to \Xi_c^0\pi^-$ with $25.8^{+5.5}_{-5.2}$ candidates.

[6] Measured in $\Xi_b^- \to J/\psi\Xi^-$ decays with 66^{+14}_{-9} candidates.

[7] Observed in $\Xi_b^- \to J/\psi\Xi^-$ decays with 17.5 ± 4.3 candidates, a significance of 7.7 sigma.

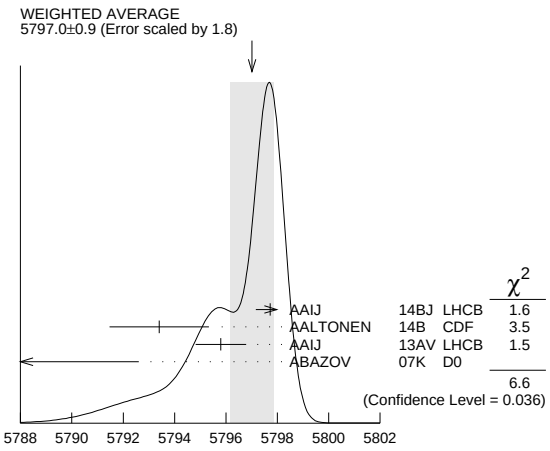

Ξ_b^0 MASS

VALUE (MeV)	DOCUMENT ID		TECN	COMMENT
5791.9 ±0.5 OUR AVERAGE				
5794.3 ±2.4 ±0.7	AAIJ	14H	LHCB	pp at 7 TeV
5791.80 ± 0.39 ± 0.31	[1] AAIJ	14Z	LHCB	pp at 7, 8 TeV
5788.7 ±4.3 ±1.4	[2] AALTONEN	14B	CDF	$p\overline{p}$ at 1.96 TeV
• • • We do not use the following data for averages, fits, limits, etc. • • •				
5787.8 ±5.0 ±1.3	[3] AALTONEN	11X	CDF	Repl. by AALTONEN 14B

[1] Uses $\Xi_b^0 \to \Xi_c^+\pi^-$ and $\Xi_c^+ \to pK^-\pi^+$ decays. The measurement comes from the mass difference of Ξ_b^0 and Λ_b^0.

[2] Uses $\Xi_b^0 \to \Xi_c^+\pi^-$ decays.

[3] Measured in $\Xi_b^0 \to \Xi_c^+\pi^-$ with $25.3^{+5.6}_{-5.4}$ candidates.

$m_{\Xi_b^-} - m_{\Lambda_b^0}$

VALUE (MeV)	DOCUMENT ID		TECN	COMMENT
177.5 ±0.5 OUR AVERAGE	Error includes scale factor of 1.6.			
177.73 ± 0.33 ± 0.14	[1] AAIJ	17BE	LHCB	pp at 7, 8 TeV
176.2 ±0.9 ±0.1	[2] AAIJ	13AV	LHCB	pp at 7 TeV
• • • We do not use the following data for averages, fits, limits, etc. • • •				
177.08 ± 0.47 ± 0.16	[3] AAIJ	17BE	LHCB	pp at 7, 8 TeV
178.36 ± 0.46 ± 0.16	[4,5] AAIJ	14BJ	LHCB	pp at 7, 8 TeV

[1] Combination of the original statistically independent measurements of AAIJ 14BE and AAIJ 17BJ taking into account correlation between systematic uncertainties.

[2] Reconstructed in $\Xi_b^- \to J/\psi\Xi^-$ decays.

[3] Reconstructed in $\Xi_b^- \to J/\psi\Lambda K^-$ decays. Reference decays $\Lambda_b^0 \to J/\psi\Lambda$ were used.

[4] Reconstructed in $\Xi_b^- \to \Xi_c^0\pi^-$, $\Xi_c^0 \to pK^-K^-\pi^+$ decays. Reference $\Lambda_b^0 \to \Lambda_c^+\pi^-$.

[5] Combined with AAIJ 17BE.

Baryon Particle Listings

Ξ_b^0, Ξ_b^-

$m_{\Xi_b^0} - m_{\Lambda_b^0}$

VALUE (MeV)	DOCUMENT ID		TECN	COMMENT
172.5 ±0.4 OUR AVERAGE				
174.8 ±2.4 ±0.5	AAIJ	14H	LHCB	pp at 7 TeV
172.44±0.39±0.17	[1] AAIJ	14Z	LHCB	pp at 7, 8 TeV

[1] Uses $\Xi_b^0 \to \Xi_c^+ \pi^-$ and $\Xi_c^+ \to p K^- \pi^+$ decays.

$m_{\Xi_b^-} - m_{\Xi_b^0}$

VALUE (MeV)	DOCUMENT ID		TECN	COMMENT
5.9 ±0.6 OUR AVERAGE				
5.92±0.60±0.23	[1] AAIJ	14BJ	LHCB	pp at 7, 8 TeV
3.1 ±5.6 ±1.3	[2] AALTONEN	11X	CDF	$p\overline{p}$ at 1.96 TeV

[1] Reconstructed in $\Xi_b^- \to \Xi_c^0 \pi^-$, $\Xi_c^0 \to p K^- K^- \pi^+$ decays. Uses $m(\Xi_b^0) - m(\Lambda_b^0) = 172.44 \pm 0.39 \pm 0.17$ MeV from AAIJ 14Z.
[2] Derived from measurements in $\Xi_b^0 \to \Xi_c^+ \pi^-$ and $\Xi_b^- \to J/\psi \Xi^-$ from AALTONEN 09AP taking correlated systematic uncertainties into account.

Ξ_b MEAN LIFE

"OUR EVALUATION" is an average using rescaled values of the data listed below. The average and rescaling were performed by the Heavy Flavor Averaging Group (HFLAV) and are described at http://www.slac.stanford.edu/xorg/hflav/. The averaging/rescaling procedure takes into account correlations between the measurements and asymmetric lifetime errors.

Ξ_b^- MEAN LIFE

VALUE (10^{-12} s)	DOCUMENT ID		TECN	COMMENT
1.571±0.040 OUR EVALUATION				
1.57 ±0.04 OUR AVERAGE Error includes scale factor of 1.1.				
1.599±0.041±0.022	[1] AAIJ	14BJ	LHCB	pp at 7, 8 TeV
1.55 $^{+0.10}_{-0.09}$ ±0.03	[2] AAIJ	14T	LHCB	pp at 7, 8 TeV
1.36 ±0.15 ±0.02	AALTONEN	14B	CDF	$p\overline{p}$ at 1.96 TeV
• • • We do not use the following data for averages, fits, limits, etc. • • •				
1.56 $^{+0.27}_{-0.25}$ ±0.02	[3] AALTONEN	09AP	CDF	Repl. by AALTONEN 14B

[1] Reconstructed in $\Xi_b^- \to \Xi_c^0 \pi^-$, $\Xi_c^0 \to p K^- K^- \pi^+$ decays. Reference Λ_b^0 lifetime $1.479 \pm 0.009 \pm 0.010$ ps from AAIJ 14U.
[2] Measured in $\Xi_b^- \to J/\psi \Xi^-$ decays.
[3] Measured in $\Xi_b^- \to J/\psi \Xi^-$ decays with 66^{+14}_{-9} candidates.

Ξ_b^0 MEAN LIFE

VALUE (10^{-12} s)	DOCUMENT ID		TECN	COMMENT
1.479±0.031 OUR EVALUATION				
1.477±0.026±0.019	[1] AAIJ	14Z	LHCB	pp at 7, 8 TeV

[1] Uses $\Xi_b^0 \to \Xi_c^+ \pi^-$ and $\Xi_c^+ \to p K^- \pi^+$ decays. The measurement comes from the value of relative lifetime of Ξ_b^0 to Λ_b^0.

Ξ_b MEAN LIFE

VALUE (10^{-12} s)	DOCUMENT ID		TECN	COMMENT
• • • We do not use the following data for averages, fits, limits, etc. • • •				
1.48 $^{+0.40}_{-0.31}$ ±0.12	[1] ABDALLAH	05C	DLPH	$e^+e^- \to Z^0$
1.35 $^{+0.37}_{-0.28}$ $^{+0.15}_{-0.17}$	[2] BUSKULIC	96T	ALEP	$e^+e^- \to Z$
1.5 $^{+0.7}_{-0.4}$ ±0.3	[3] ABREU	95V	DLPH	Repl. by ABDALLAH 05C

[1] Used the decay length of Ξ^- accompanied by a lepton of the same sign.
[2] Excess $\Xi^- \ell^-$, impact parameters.
[3] Excess $\Xi^- \ell^-$, decay lengths.

τ_{mix} (1/2π) times the oscillation period

VALUE (s)	DOCUMENT ID		TECN	COMMENT
$>13 \times 10^{-12}$	[1] AAIJ	17BH	LHCB	pp at 7, 8 TeV

[1] Uses Ξ_b^{*-} and $\Xi_b^{\prime -}$ decays to $\Xi_b^0 \pi^-$, where $\Xi_b^0 \to \Xi_c^+ \pi^-$, $\Xi_c^+ \to p K^- \pi^+$.

MEAN LIFE RATIOS

$\tau_{\Xi_b^-} / \tau_{\Lambda_b^0}$ mean life ratio

VALUE	DOCUMENT ID		TECN	COMMENT
1.089±0.026±0.011	[1] AAIJ	14BJ	LHCB	pp at 7, 8 TeV

[1] Reconstructed in $\Xi_b^- \to \Xi_c^0 \pi^-$, $\Xi_c^0 \to p K^- K^- \pi^+$ decays. Reference $\Lambda_b^0 \to \Lambda_c^+ \pi^-$.

$\tau_{\Xi_b^-} / \tau_{\Xi_b^0}$ mean life ratio

VALUE	DOCUMENT ID		TECN	COMMENT
1.083±0.032±0.016	[1] AAIJ	14BJ	LHCB	pp at 7, 8 TeV

[1] Reconstructed in $\Xi_b^- \to \Xi_c^0 \pi^-$, $\Xi_c^0 \to p K^- K^- \pi^+$ decays. Uses Ξ_b^0 measurements from AAIJ 14Z.

Ξ_b DECAY MODES

	Mode	Fraction (Γ_i/Γ)	Scale factor/ Confidence level
Γ_1	$\Xi^- \ell^- \overline{\nu}_\ell X \times B(\overline{b} \to \Xi_b)$	$(3.9 \pm 1.2) \times 10^{-4}$	S=1.4
Γ_2	$J/\psi \Xi^- \times B(b \to \Xi_b^-)$	$(1.02^{+0.26}_{-0.21}) \times 10^{-5}$	
Γ_3	$J/\psi \Lambda K^- \times B(b \to \Xi_b^-)$	$(2.5 \pm 0.4) \times 10^{-6}$	
Γ_4	$p D^0 K^- \times B(\overline{b} \to \Xi_b)$	$(1.8 \pm 0.6) \times 10^{-6}$	
Γ_5	$p \overline{K}^0 \pi^- \times B(\overline{b} \to \Xi_b)/B(\overline{b} \to B^0)$	$< 1.6 \times 10^{-6}$	CL=90%
Γ_6	$p K^0 K^- \times B(\overline{b} \to \Xi_b)/B(\overline{b} \to B^0)$	$< 1.1 \times 10^{-6}$	CL=90%
Γ_7	$p K^- K^- \times B(\overline{b} \to \Xi_b)$	$(3.6 \pm 0.8) \times 10^{-8}$	
Γ_8	$p K^- K^-$		
Γ_9	$p \pi^- \pi^-$		
Γ_{10}	$p K^- \pi^-$		
Γ_{11}	$\Lambda \pi^+ \pi^- \times B(b \to \Xi_b^0)/B(b \to \Lambda_b^0)$	$< 1.7 \times 10^{-6}$	CL=90%
Γ_{12}	$\Lambda K^- \pi^+ \times B(b \to \Xi_b^0)/B(b \to \Lambda_b^0)$	$< 8 \times 10^{-7}$	CL=90%
Γ_{13}	$\Lambda K^+ K^- \times B(b \to \Xi_b^0)/B(b \to \Lambda_b^0)$	$< 3 \times 10^{-7}$	CL=90%
Γ_{14}	$\Lambda_c^+ K^- \times B(\overline{b} \to \Xi_b)$	$(6 \pm 4) \times 10^{-7}$	
Γ_{15}	$\Lambda_b^0 \pi^- \times B(b \to \Xi_b^-)/B(b \to \Lambda_b^0)$	$(5.7 \pm 2.0) \times 10^{-4}$	

Ξ_b BRANCHING RATIOS

$\Gamma(\Xi^- \ell^- \overline{\nu}_\ell X \times B(\overline{b} \to \Xi_b))/\Gamma_{total}$ Γ_1/Γ

VALUE (units 10^{-4})	DOCUMENT ID		TECN	COMMENT
3.9±1.2 OUR AVERAGE Error includes scale factor of 1.4.				
3.0±1.0±0.3	ABDALLAH	05C	DLPH	$e^+e^- \to Z^0$
5.4±1.1±0.8	BUSKULIC	96T	ALEP	Excess $\Xi^- \ell^-$ over $\Xi^- \ell^+$
• • • We do not use the following data for averages, fits, limits, etc. • • •				
5.9±2.1±1.0	ABREU	95V	DLPH	Repl. by ABDALLAH 05C

$\Gamma(J/\psi \Xi^- \times B(b \to \Xi_b^-))/\Gamma_{total}$ Γ_2/Γ

VALUE (units 10^{-4})	DOCUMENT ID		TECN	COMMENT
0.102 $^{+0.026}_{-0.021}$ OUR AVERAGE				
0.098 $^{+0.023}_{-0.016}$ ±0.014	[1] AALTONEN	09AP	CDF	$p\overline{p}$ at 1.96 TeV
0.16 ±0.07 ±0.02	[2] ABAZOV	07K	D0	$p\overline{p}$ at 1.96 TeV

[1] AALTONEN 09AP reports $[\Gamma(\Xi_b \to J/\psi \Xi^- \times B(b \to \Xi_b^-))/\Gamma_{total}] / [B(\Lambda_b^0 \to J/\psi(1S) \Lambda \times B(b \to \Lambda_b^0))] = 0.167^{+0.037}_{-0.025} \pm 0.012$ which we multiply by our best value $B(\Lambda_b^0 \to J/\psi(1S) \Lambda \times B(b \to \Lambda_b^0)) = (5.8 \pm 0.8) \times 10^{-5}$. Our first error is their experiment's error and our second error is the systematic error from using our best value.
[2] ABAZOV 07K reports $[\Gamma(\Xi_b \to J/\psi \Xi^- \times B(b \to \Xi_b^-))/\Gamma_{total}] / [B(\Lambda_b^0 \to J/\psi(1S) \Lambda \times B(b \to \Lambda_b^0))] = 0.28 \pm 0.09^{+0.09}_{-0.08}$ which we multiply by our best value $B(\Lambda_b^0 \to J/\psi(1S) \Lambda \times B(b \to \Lambda_b^0)) = (5.8 \pm 0.8) \times 10^{-5}$. Our first error is their experiment's error and our second error is the systematic error from using our best value.

$\Gamma(J/\psi \Lambda K^- \times B(b \to \Xi_b^-))/\Gamma_{total}$ Γ_3/Γ

VALUE (10^{-6})	DOCUMENT ID		TECN	COMMENT
2.45±0.19±0.35	[1,2] AAIJ	17BE	LHCB	pp at 7 and 8 TeV

[1] AAIJ 17BE reports $[\Gamma(\Xi_b \to J/\psi \Lambda K^- \times B(b \to \Xi_b^-))/\Gamma_{total}] / [B(\Lambda_b^0 \to J/\psi(1S) \Lambda \times B(b \to \Lambda_b^0))] = (4.19 \pm 0.29 \pm 0.15) \times 10^{-2}$ which we multiply by our best value $B(\Lambda_b^0 \to J/\psi(1S) \Lambda \times B(b \to \Lambda_b^0)) = (5.8 \pm 0.8) \times 10^{-5}$. Our first error is their experiment's error and our second error is the systematic error from using our best value.
[2] Integrated over the b-baryon transverse momentum $p_T < 25$ GeV and rapidity $2.0 < y < 4.5$.

$\Gamma(p D^0 K^- \times B(\overline{b} \to \Xi_b))/\Gamma_{total}$ Γ_4/Γ

VALUE	DOCUMENT ID		TECN	COMMENT
(1.8±0.4±0.4) × 10^{-6}	[1] AAIJ	14H	LHCB	pp at 7 TeV

[1] AAIJ 14H reports $[\Gamma(\Xi_b \to p D^0 K^- \times B(\overline{b} \to \Xi_b))/\Gamma_{total}] / [B(\Lambda_b^0 \to p D^0 K^-)] = 0.44 \pm 0.09 \pm 0.06$ which we multiply by our best values $B(\overline{b} \to b\text{-baryon}) = (8.9 \pm 1.2) \times 10^{-2}$, $B(\Lambda_b^0 \to p D^0 K^-) = (4.6 \pm 0.8) \times 10^{-5}$. Our first error is their experiment's error and our second error is the systematic error from using our best values.

$\Gamma(p \overline{K}^0 \pi^- \times B(\overline{b} \to \Xi_b)/B(\overline{b} \to B^0))/\Gamma_{total}$ Γ_5/Γ

VALUE	CL%	DOCUMENT ID		TECN	COMMENT
< 1.6 × 10^{-6}	90	AAIJ	14Q	LHCB	pp at 7 TeV

$\Gamma(p K^0 K^- \times B(\overline{b} \to \Xi_b)/B(\overline{b} \to B^0))/\Gamma_{total}$ Γ_6/Γ

VALUE	CL%	DOCUMENT ID		TECN	COMMENT
< 1.1 × 10^{-6}	90	AAIJ	14Q	LHCB	pp at 7 TeV

$\Gamma(pK^-K^-\times B(\overline{b}\to\Xi_b))/\Gamma_{total}$ Γ_7/Γ

VALUE (units 10^{-8})	DOCUMENT ID		TECN	COMMENT
3.6±0.8±0.2	[1] AAIJ	17F	LHCB	pp at 7, 8 TeV

[1] AAIJ 17F reports $[\Gamma(\Xi_b\to pK^-K^-\times B(\overline{b}\to\Xi_b))/\Gamma_{total}]$ / $[B(B^+\to K^+K^-K^+)]$ / $[B(\overline{b}\to B^+)] = (2.65\pm0.35\pm0.47)\times10^{-3}$ which we multiply by our best values $B(B^+\to K^+K^-K^+) = (3.40\pm0.14)\times10^{-5}$, $B(\overline{b}\to B^+) = (40.5\pm0.6)\times10^{-2}$. Our first error is their experiment's error and our second error is the systematic error from using our best values.

$\Gamma(p\pi^-\pi^-)/\Gamma(pK^-K^-)$ Γ_9/Γ_8

VALUE	CL%	DOCUMENT ID		TECN	COMMENT
<0.56	90	[1] AAIJ	17F	LHCB	pp at 7, 8 TeV

[1] Measures the ratio as $0.28\pm0.16\pm0.13$.

$\Gamma(pK^-\pi^-)/\Gamma(pK^-K^-)$ Γ_{10}/Γ_8

VALUE	DOCUMENT ID		TECN	COMMENT
0.98±0.27±0.09	AAIJ	17F	LHCB	pp at 7, 8 TeV

$\Gamma(\Lambda\pi^+\pi^-\times B(b\to\Xi_b^0)/B(b\to\Lambda_b^0))/\Gamma_{total}$ Γ_{11}/Γ

VALUE	CL%	DOCUMENT ID		TECN	COMMENT
<1.7 × 10⁻⁶	90	AAIJ	16W	LHCB	pp at 7, 8 TeV

$\Gamma(\Lambda K^-\pi^+\times B(b\to\Xi_b^0)/B(b\to\Lambda_b^0))/\Gamma_{total}$ Γ_{12}/Γ

VALUE	CL%	DOCUMENT ID		TECN	COMMENT
<0.8 × 10⁻⁶	90	AAIJ	16W	LHCB	pp at 7, 8 TeV

$\Gamma(\Lambda K^+K^-\times B(b\to\Xi_b^0)/B(b\to\Lambda_b^0))/\Gamma_{total}$ Γ_{13}/Γ

VALUE	CL%	DOCUMENT ID		TECN	COMMENT
<0.3 × 10⁻⁶	90	AAIJ	16W	LHCB	pp at 7, 8 TeV

$\Gamma(\Lambda_c^+K^-\times B(\overline{b}\to\Xi_b))/\Gamma(pD^0K^-\times B(\overline{b}\to\Xi_b))$ Γ_{14}/Γ_4

VALUE	DOCUMENT ID		TECN	COMMENT
0.36±0.19±0.02	[1] AAIJ	14H	LHCB	pp at 7 TeV

[1] AAIJ 14H reports $[\Gamma(\Xi_b\to\Lambda_c^+K^-\times B(\overline{b}\to\Xi_b))/\Gamma(\Xi_b\to pD^0K^-\times B(\overline{b}\to\Xi_b))]\times[B(\Lambda_c^+\to pK^-\pi^+)]$ / $[B(D^0\to K^-\pi^+)] = 0.57\pm0.22\pm0.21$ which we multiply or divide by our best values $B(\Lambda_c^+\to pK^-\pi^+) = (6.23\pm0.33)\times10^{-2}$, $B(D^0\to K^-\pi^+) = (3.89\pm0.04)\times10^{-2}$. Our first error is their experiment's error and our second error is the systematic error from using our best values.

$\Gamma(\Lambda_b^0\pi^-\times B(b\to\Xi_b^-)/B(b\to\Lambda_b^0))/\Gamma_{total}$ Γ_{15}/Γ

VALUE (units 10^{-4})	DOCUMENT ID		TECN	COMMENT
$5.7\pm1.8^{+0.8}_{-0.9}$	[1] AAIJ	15BA	LHCB	pp at 7, 8 TeV

[1] A signal is reported with a significance of 3.2 standard deviations in the decay chain of $\Xi_b^-\to\Lambda_b^0\pi^-$, $\Lambda_b^0\to\Lambda_c^+\pi^-$, and $\Lambda_c^+\to pK^-\pi^+$.

Ξ_b REFERENCES

AAIJ	17BE	PL B772 265	R. Aaij *et al.*	(LHCb Collab.)
AAIJ	17BH	PRL 119 181807	R. Aaij *et al.*	(LHCb Collab.)
AAIJ	17BJ	PRL 119 232001	R. Aaij *et al.*	(LHCb Collab.)
AAIJ	17F	PRL 118 071801	R. Aaij *et al.*	(LHCb Collab.)
AAIJ	16W	JHEP 1605 081	R. Aaij *et al.*	(LHCb Collab.)
AAIJ	15BA	PRL 115 241801	R. Aaij *et al.*	(LHCb Collab.)
AAIJ	14AA	PRL 112 202001	R. Aaij *et al.*	(LHCb Collab.)
AAIJ	14BE	NP B888 169	R. Aaij *et al.*	(LHCb Collab.)
AAIJ	14BJ	PRL 113 242002	R. Aaij *et al.*	(LHCb Collab.)
AAIJ	14H	PR D89 032001	R. Aaij *et al.*	(LHCb Collab.)
AAIJ	14Q	JHEP 1404 087	R. Aaij *et al.*	(LHCb Collab.)
AAIJ	14T	PL B736 154	R. Aaij *et al.*	(LHCb Collab.)
AAIJ	14U	PL B734 122	R. Aaij *et al.*	(LHCb Collab.)
AAIJ	14Z	PRL 113 032001	R. Aaij *et al.*	(LHCb Collab.)
AALTONEN	14B	PR D89 072014	T. Aaltonen *et al.*	(CDF Collab.)
AAIJ	13AV	PRL 110 182001	R. Aaij *et al.*	(LHCb Collab.)
AALTONEN	11X	PRL 107 102001	T. Aaltonen *et al.*	(CDF Collab.)
AALTONEN	09AP	PR D80 072003	T. Aaltonen *et al.*	(CDF Collab.)
AALTONEN	07A	PRL 99 052002	T. Aaltonen *et al.*	(CDF Collab.)
ABAZOV	07K	PRL 99 052001	V.M. Abazov *et al.*	(D0 Collab.)
ABDALLAH	05C	EPJ C44 299	J. Abdallah *et al.*	(DELPHI Collab.)
BUSKULIC	96T	PL B384 449	D. Buskulic *et al.*	(ALEPH Collab.)
ABREU	95V	ZPHY C68 541	P. Abreu *et al.*	(DELPHI Collab.)

$\Xi_b'(5935)^-$ $J^P = \frac{1}{2}^+$ Status: ***

$\Xi_b'(5935)^-$ MASS

VALUE (MeV)	DOCUMENT ID		TECN	COMMENT
5935.02±0.02±0.05	[1] AAIJ	15H	LHCB	pp at 7, 8 TeV

[1] Not independent of the mass difference measurement below. Observed in $\Xi_b^0\pi^-$ channel with $\Xi_b^0\to\Xi_c^+\pi^-$ and $\Xi_c^+\to pK^-\pi^+$.

$m_{\Xi_b'(5935)^-} - m_{\Xi_b^0} - m_{\pi^-}$

VALUE (MeV)	DOCUMENT ID		TECN	COMMENT
3.653±0.018±0.006	[2] AAIJ	15H	LHCB	pp at 7, 8 TeV

[2] Observed in $\Xi_b^0\pi^-$ channel with $\Xi_b^0\to\Xi_c^+\pi^-$ and $\Xi_c^+\to pK^-\pi^+$.

$\Xi_b'(5935)^-$ WIDTH

VALUE (MeV)	CL%	DOCUMENT ID		TECN	COMMENT
<0.08	95	[3] AAIJ	15H	LHCB	pp at 7, 8 TeV

[3] Observed in $\Xi_b^0\pi^-$ channel with $\Xi_b^0\to\Xi_c^+\pi^-$ and $\Xi_c^+\to pK^-\pi^+$.

$\Xi_b'(5935)^-$ DECAY MODES

	Mode	Fraction (Γ_i/Γ)
Γ_1	$\Xi_b^0\pi^-\times B(\overline{b}\to\Xi_b'(5935)^-)/B(\overline{b}\to\Xi_b^0)$	(11.8±1.8) %

$\Xi_b'(5935)^-$ BRANCHING RATIOS

$\Gamma(\Xi_b^0\pi^-\times B(\overline{b}\to\Xi_b'(5935)^-)/B(\overline{b}\to\Xi_b^0))/\Gamma_{total}$ Γ_1/Γ

VALUE	DOCUMENT ID		TECN	COMMENT
0.118±0.017±0.007	[4] AAIJ	15H	LHCB	pp at 7, 8 TeV

[4] Observed in $\Xi_b^0\pi^-$ channel with $\Xi_b^0\to\Xi_c^+\pi^-$ and $\Xi_c^+\to pK^-\pi^+$.

$\Xi_b'(5935)^-$ REFERENCES

AAIJ	15H	PRL 114 062004	R. Aaij *et al.*	(LHCb Collab.)

$\Xi_b(5945)^0$ $J^P = \frac{3}{2}^+$ Status: ***

Quantum numbers are based on quark model expectations.

$\Xi_b(5945)^0$ MASS

VALUE (MeV)	DOCUMENT ID		TECN	COMMENT
5949.8±1.4 OUR AVERAGE				
5952.3±0.1±0.9	[1] AAIJ	16AE	LHCB	pp at 7, 8 TeV
5951.4±0.8±0.9	[2] CHATRCHYAN	12S	CMS	pp at 7 TeV, 5.3 fb^{-1}

[1] AAIJ 16AE measures $m(\Xi_b(5945)^0) - m(\Xi_b^-) - m(\pi^+) = 15.727\pm0.068\pm0.023$ MeV. We have adjusted the measurement to our best values of $m(\Xi_b^-) = 5797.0\pm0.9$ MeV, $m(\pi^+) = 139.57061\pm0.00024$ MeV. Our first error is their experiment's error and our second error is the systematic error from using our best values.

[2] CHATRCHYAN 12S measures $m(\Xi_b(5945)^0) - m(\Xi_b^-) - m(\pi^+) = 14.84\pm0.74\pm0.28$ MeV. We have adjusted the measurement to our best values of $m(\Xi_b^-) = 5797.0\pm0.9$ MeV, $m(\pi^+) = 139.57061\pm0.00024$ MeV. Our first error is their experiment's error and our second error is the systematic error from using our best values.

$\Xi_b(5945)^0$ WIDTH

VALUE (MeV)	DOCUMENT ID		TECN	COMMENT
0.90±0.16±0.08	[3] AAIJ	16AE	LHCB	pp at 7, 8 TeV
• • • We do not use the following data for averages, fits, limits, etc. • • •				
2.1 ±1.7	[4] CHATRCHYAN	12S	CMS	pp at 7 TeV, 5.3 fb^{-1}

[3] Measured using $\Xi_b(5945)^0\to\Xi_b^-\pi^+$, $\Xi_b^-\to\Xi_c^0\pi^-$, $\Xi_c^0\to pK^-K^-\pi^+$ decays.

[4] Systematic uncertainty not evaluated.

$\Xi_b(5945)^0$ DECAY MODES

	Mode	Fraction (Γ_i/Γ)
Γ_1	$\Xi_b^-\pi^+$	seen

$\Xi_b(5945)^0$ BRANCHING RATIOS

$\Gamma(\Xi_b^-\pi^+)/\Gamma_{total}$ Γ_1/Γ

VALUE	DOCUMENT ID		TECN	COMMENT
seen	AAIJ	16AE	ATLS	pp at 7, 8 TeV
seen	CHATRCHYAN	12S	CMS	pp at 7 TeV, 5.3 fb^{-1}

$\Xi_b(5945)^0$ REFERENCES

AAIJ	16AE	JHEP 1605 161	R. Aaij *et al.*	(LHCb Collab.)
CHATRCHYAN	12S	PRL 108 252002	S. Chatrchyan *et al.*	(CMS Collab.)

Baryon Particle Listings

$\Xi_b(5945)^0$, $\Xi_b(5955)^-$, Ω_b^-

$\Xi_b(5955)^-$

$J^P = \frac{3}{2}^+$ Status: ***

$\Xi_b(5955)^-$ MASS

VALUE (MeV)	DOCUMENT ID		TECN	COMMENT
5955.33±0.12±0.05	[1] AAIJ	15H	LHCB	pp at 7, 8 TeV

[1] Not independent of the mass difference measurement below. Observed in $\Xi_b^0\pi^-$ channel with $\Xi_b^0 \to \Xi_c^+\pi^-$ and $\Xi_c^+ \to pK^-\pi^+$.

$m_{\Xi_b(5955)^-} - m_{\Xi_b^0} - m_{\pi^-}$

VALUE (MeV)	DOCUMENT ID		TECN	COMMENT
23.96±0.12±0.06	[1] AAIJ	15H	LHCB	pp at 7, 8 TeV

[1] Observed in $\Xi_b^0\pi^-$ channel with $\Xi_b^0 \to \Xi_c^+\pi^-$ and $\Xi_c^+ \to pK^-\pi^+$.

$\Xi_b(5955)^-$ WIDTH

VALUE (MeV)	DOCUMENT ID		TECN	COMMENT
1.65±0.31±0.10	[1] AAIJ	15H	LHCB	pp at 7, 8 TeV

[1] Observed in $\Xi_b^0\pi^-$ channel with $\Xi_b^0 \to \Xi_c^+\pi^-$ and $\Xi_c^+ \to pK^-\pi^+$.

$\Xi_b(5955)^-$ DECAY MODES

	Mode	Fraction (Γ_i/Γ)
Γ_1	$\Xi_b^0\pi^- \times$ B($\overline{b} \to \Xi_b^*(5955)^-$)/B($\overline{b} \to \Xi_b^0$)	(20.7±3.5) %

$\Xi_b(5955)^-$ BRANCHING RATIOS

$\Gamma(\Xi_b^0\pi^- \times$ B($\overline{b} \to \Xi_b^*(5955)^-$)/B($\overline{b} \to \Xi_b^0$))/$\Gamma_{\text{total}}$ Γ_1/Γ

VALUE	DOCUMENT ID		TECN	COMMENT
0.207±0.032±0.015	[1] AAIJ	15H	LHCB	pp at 7, 8 TeV

[1] Observed in $\Xi_b^0\pi^-$ channel with $\Xi_b^0 \to \Xi_c^+\pi^-$ and $\Xi_c^+ \to pK^-\pi^+$.

$\Xi_b(5955)^-$ REFERENCES

AAIJ 15H PRL 114 062004 R. Aaij *et al.* (LHCb Collab.)

Ω_b^-

$I(J^P) = 0(\frac{1}{2}^+)$ Status: ***
I, J, P need confirmation.

In the quark model Ω_b^- is ssb ground state. None of its quantum numbers has been measured.

Ω_b^- MASS

VALUE (MeV)	DOCUMENT ID		TECN	COMMENT
6046.1± 1.7 OUR AVERAGE				
6045.1± 3.2± 0.8	[1] AAIJ	16O	LHCB	pp at 7, 8 TeV
6047.5± 3.8± 0.6	[2] AALTONEN	14B	CDF	$p\overline{p}$ at 1.96 TeV
6046.0± 2.2± 0.5	[3] AAIJ	13AV	LHCB	pp at 7 TeV
• • • We do not use the following data for averages, fits, limits, etc. • • •				
6054.4± 6.8± 0.9	[4] AALTONEN	09AP	CDF	Repl. by AALTONEN 14B
6165 ±10 ±13	[5] ABAZOV	08AL	D0	$p\overline{p}$ at 1.96 TeV

[1] Reconstructed in $\Omega_b^- \to \Omega_c^0\pi^-$, $\Omega_c^0 \to pK^-K^-\pi^+$ decays. Reference Ξ_b^- mass 5797.72 ± 0.6 MeV from AAIJ 14B.

[2] Uses $\Omega_b^- \to J/\psi\Omega^-$ and $\Omega_c^0\pi^-$ decays, with the first evidence for $\Omega_b^- \to \Omega_c^0\pi^-$ at 3.3 σ significance.

[3] Measured in $\Omega_b^- \to J/\psi\Omega^-$ with 19 ± 5 events.

[4] Observed in $\Omega_b^- \to J/\psi\Omega^-$ decays with 16^{+6}_{-4} candidates, a significance of 5.5 sigma from a combined mass-lifetime fit.

[5] Observed in $\Omega_b^- \to J/\psi\Omega^-$ decays with 17.8 ± 4.9 ± 0.8 candidates, a significance of 5.4 sigma.

$m_{\Omega_b^-} - m_{\Lambda_b^0}$

VALUE (MeV)	DOCUMENT ID		TECN	COMMENT
426.4±2.2±0.4	AAIJ	13AV	LHCB	pp at 7 TeV

$m_{\Omega_b^-} - m_{\Xi_b^-}$

VALUE (MeV)	DOCUMENT ID		TECN	COMMENT
247.3±3.2±0.5	[1] AAIJ	16O	LHCB	pp at 7, 8 TeV

[1] Uses $\Omega_b^- \to \Omega_c^0\pi^-$, $\Omega_c^0 \to pK^-K^-\pi^+$ and $\Xi_b^- \to \Xi_c^0\pi^-$, $\Xi_c^0 \to pK^-K^-\pi^+$ decays.

Ω_b MEAN LIFE

VALUE (10^{-12} s)	DOCUMENT ID		TECN	COMMENT
$1.64^{+0.18}_{-0.17}$ OUR EVALUATION				
$1.65^{+0.18}_{-0.16}$ OUR AVERAGE				
$1.78\pm0.26\pm0.05\pm0.06$	[1] AAIJ	16O	LHCB	pp at 7, 8 TeV
$1.54^{+0.26}_{-0.21}\pm0.05$	[2] AAIJ	14T	LHCB	pp at 7, 8 TeV
$1.66^{+0.53}_{-0.40}\pm0.02$	[2] AALTONEN	14B	CDF	$p\overline{p}$ at 1.96 TeV
• • • We do not use the following data for averages, fits, limits, etc. • • •				
$1.13^{+0.53}_{-0.40}\pm0.02$	[3] AALTONEN	09AP	CDF	Repl. by AALTONEN 14B

[1] Measured in $\Omega_b^- \to \Omega_c^0\pi^-$, $\Omega_c^0 \to pK^-K^-\pi^+$ decays relative to $\Xi_b^- \to \Xi_c^0\pi^-$, $\Xi_c^0 \to pK^-K^-\pi^+$ decays with reference Ξ_b^- mean life 1.599±0.06 ps from AAIJ 14B.

[2] Measured in $\Omega_b^- \to J/\psi\Omega^-$ decays.

[3] Observed in $\Omega_b^- \to J/\psi\Omega^-$ decays with 16^{+6}_{-4} candidates, a significance of 5.5 sigma from a combined mass-lifetime fit.

$\tau(\Omega_b^-)/\tau(\Xi_b^-)$ mean life ratio

VALUE	DOCUMENT ID		TECN	COMMENT
1.11±0.16±0.03	[1] AAIJ	16O	LHCB	pp at 7, 8 TeV

[1] Uses $\Omega_b^- \to \Omega_c^0\pi^-$, $\Omega_c^0 \to pK^-K^-\pi^+$ and $\Xi_b^- \to \Xi_c^0\pi^-$, $\Xi_c^0 \to pK^-K^-\pi^+$ decays.

Ω_b^- DECAY MODES

	Mode	Fraction (Γ_i/Γ)	Confidence level
Γ_1	$J/\psi\Omega^- \times$B($b \to \Omega_b$)	$(2.9^{+1.1}_{-0.8}) \times 10^{-6}$	
Γ_2	$pK^-K^- \times$B($\overline{b} \to \Omega_b$)	$< 2.5 \times 10^{-9}$	90%
Γ_3	$p\pi^-\pi^- \times$B($\overline{b} \to \Omega_b$)	$< 1.5 \times 10^{-8}$	90%
Γ_4	$pK^-\pi^- \times$B($\overline{b} \to \Omega_b$)	$< 7 \times 10^{-9}$	90%

Ω_b^- BRANCHING RATIOS

$\Gamma(J/\psi\Omega^- \times$B($b \to \Omega_b$))/$\Gamma_{\text{total}}$ Γ_1/Γ

VALUE (units 10^{-4})	DOCUMENT ID		TECN	COMMENT
$0.029^{+0.011}_{-0.008}$ OUR AVERAGE				
$0.026^{+0.010}_{-0.007}\pm0.004$	[1] AALTONEN	09AP	CDF	$p\overline{p}$ at 1.96 TeV
0.08 ±0.04 ±0.02	[2] ABAZOV	08AL	D0	$p\overline{p}$ at 1.96 TeV

[1] AALTONEN 09AP reports $[\Gamma(\Omega_b^- \to J/\psi\Omega^- \times B(b \to \Omega_b))/\Gamma_{\text{total}}] / [B(\Lambda_b^0 \to J/\psi(1S)\Lambda \times B(b \to \Lambda_b^0))] = 0.045^{+0.017}_{-0.012} \pm 0.004$ which we multiply by our best value $B(\Lambda_b^0 \to J/\psi(1S)\Lambda \times B(b \to \Lambda_b^0)) = (5.8 \pm 0.8) \times 10^{-5}$. Our first error is their experiment's error and our second error is the systematic error from using our best value.

[2] ABAZOV 08AL reports $[\Gamma(\Omega_b^- \to J/\psi\Omega^- \times B(b \to \Omega_b))/\Gamma_{\text{total}}] / [B(\Xi_b \to J/\psi\Xi^- \times B(b \to \Xi_b^-))] = 0.80 \pm 0.32^{+0.14}_{-0.22}$ which we multiply by our best value $B(\Xi_b \to J/\psi\Xi^- \times B(b \to \Xi_b^-)) = (1.02^{+0.26}_{-0.21}) \times 10^{-5}$. Our first error is their experiment's error and our second error is the systematic error from using our best value.

$\Gamma(pK^-K^- \times$B($\overline{b} \to \Omega_b$))/$\Gamma_{\text{total}}$ Γ_2/Γ

VALUE (units 10^{-5})	CL%	DOCUMENT ID		TECN	COMMENT
$< 2.5 \times 10^{-4}$	90	[1] AAIJ	17F	LHCB	pp at 7, 8 TeV

[1] AAIJ 17F reports $[\Gamma(\Omega_b^- \to pK^-K^- \times B(\overline{b} \to \Omega_b))/\Gamma_{\text{total}}] / [B(B^+ \to K^+K^-K^+)] / [B(\overline{b} \to B^+)] < 18 \times 10^{-5}$ which we multiply by our best values $B(B^+ \to K^+K^-K^+) = 3.40 \times 10^{-5}$, $B(\overline{b} \to B^+) = 40.5 \times 10^{-2}$.

$\Gamma(p\pi^-\pi^- \times$B($\overline{b} \to \Omega_b$))/$\Gamma_{\text{total}}$ Γ_3/Γ

VALUE (units 10^{-5})	CL%	DOCUMENT ID		TECN	COMMENT
$< 1.5 \times 10^{-3}$	90	[1] AAIJ	17F	LHCB	pp at 7, 8 TeV

[1] AAIJ 17F reports $[\Gamma(\Omega_b^- \to p\pi^-\pi^- \times B(\overline{b} \to \Omega_b))/\Gamma_{\text{total}}] / [B(B^+ \to K^+K^-K^+)] / [B(\overline{b} \to B^+)] < 109 \times 10^{-5}$ which we multiply by our best values $B(B^+ \to K^+K^-K^+) = 3.40 \times 10^{-5}$, $B(\overline{b} \to B^+) = 40.5 \times 10^{-2}$.

$\Gamma(pK^-\pi^- \times$B($\overline{b} \to \Omega_b$))/$\Gamma_{\text{total}}$ Γ_4/Γ

VALUE (units 10^{-5})	CL%	DOCUMENT ID		TECN	COMMENT
$< 7 \times 10^{-4}$	90	[1] AAIJ	17F	LHCB	pp at 7, 8 TeV

[1] AAIJ 17F reports $[\Gamma(\Omega_b^- \to pK^-\pi^- \times B(\overline{b} \to \Omega_b))/\Gamma_{\text{total}}] / [B(B^+ \to K^+K^-K^+)] / [B(\overline{b} \to B^+)] < 51 \times 10^{-5}$ which we multiply by our best values $B(B^+ \to K^+K^-K^+) = 3.40 \times 10^{-5}$, $B(\overline{b} \to B^+) = 40.5 \times 10^{-2}$.

Ω_b^- REFERENCES

AAIJ	17F	PRL 118 071801	R. Aaij *et al.*	(LHCb Collab.)
AAIJ	16O	PR D93 092007	R. Aaij *et al.*	(LHCb Collab.)
AAIJ	14B	PL B728 234	R. Aaij *et al.*	(LHCb Collab.)
AAIJ	14T	PL B736 154	R. Aaij *et al.*	(LHCb Collab.)
AALTONEN	14B	PR D89 072014	T. Aaltonen *et al.*	(CDF Collab.)
AAIJ	13AV	PRL 110 182001	R. Aaij *et al.*	(LHCb Collab.)
AALTONEN	09AP	PR D80 072003	T. Aaltonen *et al.*	(CDF Collab.)
ABAZOV	08AL	PRL 101 232002	V.M. Abazov *et al.*	(D0 Collab.)

b-baryon ADMIXTURE (Λ_b, Ξ_b, Σ_b, Ω_b)

b-baryon ADMIXTURE MEAN LIFE

Each measurement of the b-baryon mean life is an average over an admixture of various b baryons which decay weakly. Different techniques emphasize different admixtures of produced particles, which could result in a different b-baryon mean life. More b-baryon flavor specific channels are not included in the measurement.

VALUE (10^{-12} s)	EVTS	DOCUMENT ID		TECN	COMMENT
• • • We do not use the following data for averages, fits, limits, etc. • • •					
$1.218^{+0.130}_{-0.115}\pm0.042$		[1] ABAZOV	07S	D0	Repl. by ABAZOV 12U
$1.22\ ^{+0.22}_{-0.18}\pm0.04$		[1] ABAZOV	05C	D0	Repl. by ABAZOV 07S
$1.16\ \pm0.20\ \pm0.08$		[2] ABREU	99W	DLPH	$e^+e^-\to Z$
$1.19\ \pm0.14\ \pm0.07$		[3] ABREU	99W	DLPH	$e^+e^-\to Z$
$1.14\ \pm0.08\ \pm0.04$		[4] ABREU	99W	DLPH	$e^+e^-\to Z$
$1.11\ ^{+0.19}_{-0.18}\pm0.05$		[5] ABREU	99W	DLPH	$e^+e^-\to Z$
$1.29\ ^{+0.24}_{-0.22}\pm0.06$		[5] ACKERSTAFF	98G	OPAL	$e^+e^-\to Z$
$1.20\ \pm0.08\ \pm0.06$		[6] BARATE	98D	ALEP	$e^+e^-\to Z$
$1.21\ \pm0.11$		[5] BARATE	98D	ALEP	$e^+e^-\to Z$
$1.32\ \pm0.15\ \pm0.07$		[7] ABE	96M	CDF	$p\overline{p}$ at 1.8 TeV
$1.46\ ^{+0.22}_{-0.21}\ ^{+0.07}_{-0.09}$		ABREU	96D	DLPH	Repl. by ABREU 99W
$1.10\ ^{+0.19}_{-0.17}\pm0.09$		[5] ABREU	96D	DLPH	$e^+e^-\to Z$
$1.16\ \pm0.11\ \pm0.06$		[5] AKERS	96	OPAL	$e^+e^-\to Z$
$1.27\ ^{+0.35}_{-0.29}\pm0.09$		ABREU	95S	DLPH	Repl. by ABREU 99W
$1.05\ ^{+0.12}_{-0.11}\pm0.09$	290	BUSKULIC	95L	ALEP	Repl. by BARATE 98D
$1.04\ ^{+0.48}_{-0.38}\pm0.10$	11	[8] ABREU	93F	DLPH	Excess $\Lambda\mu^-$, decay lengths
$1.05\ ^{+0.23}_{-0.20}\pm0.08$	157	[9] AKERS	93	OPAL	Excess $\Lambda\ell^-$, decay lengths
$1.12\ ^{+0.32}_{-0.29}\pm0.16$	101	[10] BUSKULIC	92I	ALEP	Excess $\Lambda\ell^-$, impact parameters

[1] Measured mean life using fully reconstructed $\Lambda_b^0\to J/\psi\Lambda$ decays.
[2] Measured using $\Lambda\ell^-$ decay length.
[3] Measured using $p\ell^-$ decay length.
[4] This ABREU 99W result is the combined result of the $\Lambda\ell^-$, $p\ell^-$, and excess $\Lambda\mu^-$ impact parameter measurements.
[5] Measured using $\Lambda_c\ell^-$ and $\Lambda\ell^+\ell^-$.
[6] Measured using the excess of $\Lambda\ell^-$, lepton impact parameter.
[7] Measured using $\Lambda_c\ell^-$.
[8] ABREU 93F superseded by ABREU 96D.
[9] AKERS 93 superseded by AKERS 96.
[10] BUSKULIC 92I superseded by BUSKULIC 95L.

b-baryon ADMIXTURE DECAY MODES (Λ_b,Ξ_b,Σ_b,Ω_b)

These branching fractions are actually an average over weakly decaying b-baryons weighted by their production rates at the LHC, LEP, and Tevatron, branching ratios, and detection efficiencies. They scale with the b-baryon production fraction $B(b\to\ b\text{-baryon})$.

The branching fractions $B(b\text{-baryon}\to\ \Lambda\ell^-\overline{\nu}_\ell\text{anything})$ and $B(\Lambda_b^0\to\ \Lambda_c^+\ell^-\overline{\nu}_\ell\text{anything})$ are not pure measurements because the underlying measured products of these with $B(b\to\ b\text{-baryon})$ were used to determine $B(b\to\ b\text{-baryon})$, as described in the note "Production and Decay of b-Flavored Hadrons."

For inclusive branching fractions, *e.g.*, $B\to\ D^\pm$anything, the values usually are multiplicities, not branching fractions. They can be greater than one.

	Mode	Fraction (Γ_i/Γ)
Γ_1	$p\mu^-\overline{\nu}$anything	($5.5^{+\ 2.2}_{-\ 1.9}$) %
Γ_2	$p\ell\overline{\nu}_\ell$anything	(5.3± 1.1) %
Γ_3	$p$anything	(66 ±21) %
Γ_4	$\Lambda\ell^-\overline{\nu}_\ell$anything	(3.6± 0.6) %
Γ_5	$\Lambda\ell^+\nu_\ell$anything	(3.0± 0.8) %
Γ_6	Λanything	(37 ± 7) %
Γ_7	$\Xi^-\ell^-\overline{\nu}_\ell$anything	(6.2± 1.6) $\times10^{-3}$

b-baryon ADMIXTURE (Λ_b, Ξ_b, Σ_b, Ω_b) BRANCHING RATIOS

$\Gamma(p\mu^-\overline{\nu}$anything$)/\Gamma_{\text{total}}$ Γ_1/Γ

VALUE (%)	EVTS	DOCUMENT ID		TECN	COMMENT
$\mathbf{5.5^{+2.1}_{-1.7}\pm0.7}$	125	[11] ABREU	95S	DLPH	$e^+e^-\to Z$

[11] ABREU 95S reports $[\Gamma(b\text{-baryon}\to\ p\mu^-\overline{\nu}\text{anything})/\Gamma_{\text{total}}]\times[B(\overline{b}\to\ b\text{-baryon})] = 0.0049\pm0.0011^{+0.0015}_{-0.0011}$ which we divide by our best value $B(\overline{b}\to\ b\text{-baryon}) = (8.9\pm1.2)\times10^{-2}$. Our first error is their experiment's error and our second error is the systematic error from using our best value.

$\Gamma(p\ell\overline{\nu}_\ell$anything$)/\Gamma_{\text{total}}$ Γ_2/Γ

VALUE (%)	DOCUMENT ID		TECN	COMMENT
5.3±0.9±0.7	[12] BARATE	98V	ALEP	$e^+e^-\to Z$

[12] BARATE 98V reports $[\Gamma(b\text{-baryon}\to\ p\ell\overline{\nu}_\ell\text{anything})/\Gamma_{\text{total}}]\times[B(\overline{b}\to\ b\text{-baryon})] = (4.72\pm0.66\pm0.44)\times10^{-3}$ which we divide by our best value $B(\overline{b}\to\ b\text{-baryon}) = (8.9\pm1.2)\times10^{-2}$. Our first error is their experiment's error and our second error is the systematic error from using our best value.

$\Gamma(p\ell\overline{\nu}_\ell$anything$)/\Gamma(p$anything$)$ Γ_2/Γ_3

VALUE (%)	DOCUMENT ID		TECN	COMMENT
8.0±1.2±1.4	BARATE	98V	ALEP	$e^+e^-\to Z$

$\Gamma(\Lambda\ell^-\overline{\nu}_\ell$anything$)/\Gamma_{\text{total}}$ Γ_4/Γ

The values and averages in this section serve only to show what values result if one assumes our $B(b\to\ b\text{-baryon})$. They cannot be thought of as measurements since the underlying product branching fractions were also used to determine $B(b\to\ b\text{-baryon})$ as described in the note on "Production and Decay of b-Flavored Hadrons."

VALUE (%)	EVTS	DOCUMENT ID		TECN	COMMENT
3.6±0.6 OUR AVERAGE					
3.7±0.5±0.5		[13] BARATE	98D	ALEP	$e^+e^-\to Z$
3.3±0.4±0.4		[14] AKERS	96	OPAL	Excess of $\Lambda\ell^-$ over $\Lambda\ell^+$
3.4±0.8±0.5	262	[15] ABREU	95S	DLPH	Excess of $\Lambda\ell^-$ over $\Lambda\ell^+$
6.9±1.3±0.9	290	[16] BUSKULIC	95L	ALEP	Excess of $\Lambda\ell^-$ over $\Lambda\ell^+$
• • • We do not use the following data for averages, fits, limits, etc. • • •					
seen	157	[17] AKERS	93	OPAL	Excess of $\Lambda\ell^-$ over $\Lambda\ell^+$
7.9±2.3±1.1	101	[18] BUSKULIC	92I	ALEP	Excess of $\Lambda\ell^-$ over $\Lambda\ell^+$

[13] BARATE 98D reports $[\Gamma(b\text{-baryon}\to\ \Lambda\ell^-\overline{\nu}_\ell\text{anything})/\Gamma_{\text{total}}]\times[B(\overline{b}\to\ b\text{-baryon})] = 0.00326\pm0.00016\pm0.00039$ which we divide by our best value $B(\overline{b}\to\ b\text{-baryon}) = (8.9\pm1.2)\times10^{-2}$. Our first error is their experiment's error and our second error is the systematic error from using our best value. Measured using the excess of $\Lambda\ell^-$, lepton impact parameter.
[14] AKERS 96 reports $[\Gamma(b\text{-baryon}\to\ \Lambda\ell^-\overline{\nu}_\ell\text{anything})/\Gamma_{\text{total}}]\times[B(\overline{b}\to\ b\text{-baryon})] = 0.00291\pm0.00023\pm0.00025$ which we divide by our best value $B(\overline{b}\to\ b\text{-baryon}) = (8.9\pm1.2)\times10^{-2}$. Our first error is their experiment's error and our second error is the systematic error from using our best value.
[15] ABREU 95S reports $[\Gamma(b\text{-baryon}\to\ \Lambda\ell^-\overline{\nu}_\ell\text{anything})/\Gamma_{\text{total}}]\times[B(\overline{b}\to\ b\text{-baryon})] = 0.0030\pm0.0006\pm0.0004$ which we divide by our best value $B(\overline{b}\to\ b\text{-baryon}) = (8.9\pm1.2)\times10^{-2}$. Our first error is their experiment's error and our second error is the systematic error from using our best value.
[16] BUSKULIC 95L reports $[\Gamma(b\text{-baryon}\to\ \Lambda\ell^-\overline{\nu}_\ell\text{anything})/\Gamma_{\text{total}}]\times[B(\overline{b}\to\ b\text{-baryon})] = 0.0061\pm0.0006\pm0.0010$ which we divide by our best value $B(\overline{b}\to\ b\text{-baryon}) = (8.9\pm1.2)\times10^{-2}$. Our first error is their experiment's error and our second error is the systematic error from using our best value.
[17] AKERS 93 superseded by AKERS 96.
[18] BUSKULIC 92I reports $[\Gamma(b\text{-baryon}\to\ \Lambda\ell^-\overline{\nu}_\ell\text{anything})/\Gamma_{\text{total}}]\times[B(\overline{b}\to\ b\text{-baryon})] = 0.0070\pm0.0010\pm0.0018$ which we divide by our best value $B(\overline{b}\to\ b\text{-baryon}) = (8.9\pm1.2)\times10^{-2}$. Our first error is their experiment's error and our second error is the systematic error from using our best value. Superseded by BUSKULIC 95L.

$\Gamma(\Lambda\ell^+\nu_\ell$anything$)/\Gamma(\Lambda$anything$)$ Γ_5/Γ_6

VALUE (units 10^{-2})	DOCUMENT ID		TECN	COMMENT
8.0±1.2±0.8	ABBIENDI	99L	OPAL	$e^+e^-\to Z$
• • • We do not use the following data for averages, fits, limits, etc. • • •				
7.0±1.2±0.7	ACKERSTAFF	97N	OPAL	Repl. by ABBIENDI 99L

$\Gamma(\Lambda$anything$)/\Gamma_{\text{total}}$ Γ_6/Γ

VALUE (%)	DOCUMENT ID		TECN	COMMENT
37± 7 OUR AVERAGE				
39± 5±5	[19] ABBIENDI	99L	OPAL	$e^+e^-\to Z$
$25^{+14}_{-\ 9}\pm3$	[20] ABREU	95C	DLPH	$e^+e^-\to Z$
• • • We do not use the following data for averages, fits, limits, etc. • • •				
44± 7±6	[21] ACKERSTAFF	97N	OPAL	Repl. by ABBIENDI 99L

[19] ABBIENDI 99L reports $[\Gamma(b\text{-baryon}\to\ \Lambda\text{anything})/\Gamma_{\text{total}}]\times[B(\overline{b}\to\ b\text{-baryon})] = 0.035\pm0.0032\pm0.0035$ which we divide by our best value $B(\overline{b}\to\ b\text{-baryon}) = (8.9\pm1.2)\times10^{-2}$. Our first error is their experiment's error and our second error is the systematic error from using our best value.

[20] ABREU 95C reports $0.28^{+0.17}_{-0.12}$ from a measurement of $[\Gamma(b\text{-baryon} \to \Lambda\,\text{anything})/\Gamma_{\text{total}}] \times [B(\overline{b} \to b\text{-baryon})]$ assuming $B(\overline{b} \to b\text{-baryon}) = 0.08 \pm 0.02$, which we rescale to our best value $B(\overline{b} \to b\text{-baryon}) = (8.9 \pm 1.2) \times 10^{-2}$. Our first error is their experiment's error and our second error is the systematic error from using our best value.

[21] ACKERSTAFF 97N reports $[\Gamma(b\text{-baryon} \to \Lambda\,\text{anything})/\Gamma_{\text{total}}] \times [B(\overline{b} \to b\text{-baryon})] = 0.0393 \pm 0.0046 \pm 0.0037$ which we divide by our best value $B(\overline{b} \to b\text{-baryon}) = (8.9 \pm 1.2) \times 10^{-2}$. Our first error is their experiment's error and our second error is the systematic error from using our best value.

$\Gamma(\Xi^- \ell^- \overline{\nu}_\ell\,\text{anything})/\Gamma_{\text{total}}$ Γ_7/Γ

VALUE (units 10^{-3})	DOCUMENT ID		TECN	COMMENT
6.2±1.6 OUR AVERAGE				
6.1±1.5±0.8	[22] BUSKULIC	96T	ALEP	Excess $\Xi^- \ell^-$ over $\Xi^- \ell^+$
6.6±2.6±0.9	[23] ABREU	95V	DLPH	Excess $\Xi^- \ell^-$ over $\Xi^- \ell^+$

[22] BUSKULIC 96T reports $[\Gamma(b\text{-baryon} \to \Xi^- \ell^- \overline{\nu}_\ell\,\text{anything})/\Gamma_{\text{total}}] \times [B(\overline{b} \to b\text{-baryon})] = 0.00054 \pm 0.00011 \pm 0.00008$ which we divide by our best value $B(\overline{b} \to b\text{-baryon}) = (8.9 \pm 1.2) \times 10^{-2}$. Our first error is their experiment's error and our second error is the systematic error from using our best value.

[23] ABREU 95V reports $[\Gamma(b\text{-baryon} \to \Xi^- \ell^- \overline{\nu}_\ell\,\text{anything})/\Gamma_{\text{total}}] \times [B(\overline{b} \to b\text{-baryon})] = 0.00059 \pm 0.00021 \pm 0.0001$ which we divide by our best value $B(\overline{b} \to b\text{-baryon}) = (8.9 \pm 1.2) \times 10^{-2}$. Our first error is their experiment's error and our second error is the systematic error from using our best value.

b-baryon ADMIXTURE (Λ_b, Ξ_b, Σ_b, Ω_b) REFERENCES

ABAZOV	12U	PR D85 112003	V.M. Abazov *et al.*	(D0 Collab.)
ABAZOV	07S	PRL 99 142001	V.M. Abazov *et al.*	(D0 Collab.)
ABAZOV	05C	PRL 94 102001	V.M. Abazov *et al.*	(D0 Collab.)
ABBIENDI	99L	EPJ C9 1	G. Abbiendi *et al.*	(OPAL Collab.)
ABREU	99W	EPJ C10 185	P. Abreu *et al.*	(DELPHI Collab.)
ACKERSTAFF	98G	PL B426 161	K. Ackerstaff *et al.*	(OPAL Collab.)
BARATE	98D	EPJ C2 197	R. Barate *et al.*	(ALEPH Collab.)
BARATE	98V	EPJ C5 205	R. Barate *et al.*	(ALEPH Collab.)
ACKERSTAFF	97N	ZPHY C74 423	K. Ackerstaff *et al.*	(OPAL Collab.)
ABE	96M	PRL 77 1439	F. Abe *et al.*	(CDF Collab.)
ABREU	96D	ZPHY C71 199	P. Abreu *et al.*	(DELPHI Collab.)
AKERS	96	ZPHY C69 195	R. Akers *et al.*	(OPAL Collab.)
BUSKULIC	96T	PL B384 449	D. Buskulic *et al.*	(ALEPH Collab.)
ABREU	95C	PL B347 447	P. Abreu *et al.*	(DELPHI Collab.)
ABREU	95S	ZPHY C68 375	P. Abreu *et al.*	(DELPHI Collab.)
ABREU	95V	ZPHY C68 541	P. Abreu *et al.*	(DELPHI Collab.)
BUSKULIC	95L	PL B357 685	D. Buskulic *et al.*	(ALEPH Collab.)
ABREU	93F	PL B311 379	P. Abreu *et al.*	(DELPHI Collab.)
AKERS	93	PL B316 435	R. Akers *et al.*	(OPAL Collab.)
BUSKULIC	92I	PL B297 449	D. Buskulic *et al.*	(ALEPH Collab.)

EXOTIC BARYONS

See the related review(s):

Pentaquarks

$P_c(4380)^+$

Status: *

A resonance seen in $\Lambda_b^0 \to P_c^+ K^-$, then $P_c \to J/\psi p$, with a significance of 9 standard deviations. The $J/\psi p$ quark content is $uudc\overline{c}$, a pentaquark. See also the $P_c(4450)^+$. In the best amplitude fit, the two states have opposite parity, one having $J = 3/2$, the other $J = 5/2$.

Extraction of the pentaquark signals requires some understanding of the dominant $K^- p$ background. AAIJ 15P used a model-dependent approach. AAIJ 16AG reanalyzed the data making minimal assumptions about the $K^- p$ background, and thus confirmed the strong significance of the pentaquark signals.

$P_c(4380)^+$ MASS

VALUE (MeV)	DOCUMENT ID		TECN	COMMENT
4380±8±29	AAIJ	15P	LHCB	pp at 7, 8 TeV

$P_c(4380)^+$ WIDTH

VALUE (MeV)	DOCUMENT ID		TECN	COMMENT
205±18±86	AAIJ	15P	LHCB	pp at 7, 8 TeV

$P_c(4380)^+$ DECAY MODES

	Mode	Fraction (Γ_i/Γ)
Γ_1	$J/\psi p$	seen

$P_c(4380)^+$ BRANCHING RATIOS

$\Gamma(J/\psi p)/\Gamma_{total}$ Γ_1/Γ

VALUE	DOCUMENT ID		TECN	COMMENT
seen	AAIJ	15P	LHCB	pp at 7, 8 TeV

$P_c(4380)^+$ REFERENCES

AAIJ 16AG PRL 117 082002 R. Aaij *et al.* (LHCb Collab.)
AAIJ 15P PRL 115 072001 R. Aaij *et al.* (LHCb Collab.)

$P_c(4450)^+$

Status: *

A resonance seen in $\Lambda_b^0 \to P_c^+ K^-$, then $P_c \to J/\psi p$, with a significance of 12 standard deviations. The $J/\psi p$ quark content is $uudc\overline{c}$, a pentaquark. See also the $P_c(4380)^+$. In the best amplitude fit, the two states have opposite parity, one having $J = 3/2$, the other $J = 5/2$.

Extraction of the pentaquark signals requires some understanding of the dominant $K^- p$ background. AAIJ 15P used a model-dependent approach. AAIJ 16AG reanalyzed the data making minimal assumptions about the $K^- p$ background, and thus confirmed the strong significance of the pentaquark signals.

$P_c(4450)^+$ MASS

VALUE (MeV)	DOCUMENT ID		TECN	COMMENT
4449.8±1.7±2.5	AAIJ	15P	LHCB	pp at 7, 8 TeV

$P_c(4450)^+$ WIDTH

VALUE (MeV)	DOCUMENT ID		TECN	COMMENT
39±5±19	AAIJ	15P	LHCB	pp at 7, 8 TeV

$P_c(4450)^+$ DECAY MODES

	Mode	Fraction (Γ_i/Γ)
Γ_1	$J/\psi p$	seen

$P_c(4450)^+$ BRANCHING RATIOS

$\Gamma(J/\psi p)/\Gamma_{total}$ Γ_1/Γ

VALUE	DOCUMENT ID		TECN	COMMENT
seen	AAIJ	15P	LHCB	pp at 7, 8 TeV

$P_c(4450)^+$ REFERENCES

AAIJ 16AG PRL 117 082002 R. Aaij *et al.* (LHCb Collab.)
AAIJ 15P PRL 115 072001 R. Aaij *et al.* (LHCb Collab.)

MISCELLANEOUS SEARCHES

SEARCHES IN OTHER SECTIONS

Related Reviews in Volume 1

SEARCHES NOT IN OTHER SECTIONS

Magnetic Monopole Searches

See the related review(s):
Magnetic Monopoles

Monopole Production Cross Section — Accelerator Searches

X-SECT (cm^2)	MASS (GeV)	CHG (g)	ENERGY (GeV)	BEAM	DOCUMENT ID		TECN
$<2.5E-37$	200–6000	1	13000	pp	[1] ACHARYA	17	INDU
$<2E-37$	200–6000	2	13000	pp	[1] ACHARYA	17	INDU
$<4E-37$	200–5000	3	13000	pp	[1] ACHARYA	17	INDU
$<1.5E-36$	400–4000	4	13000	pp	[1] ACHARYA	17	INDU
$<7E-36$	1000–3000	5	13000	pp	[1] ACHARYA	17	INDU
$<5E-40$	200–2500	0.5–2.0	8000	pp	[2] AAD	16AB	ATLS
$<2E-37$	100–3500	1	8000	pp	[3] ACHARYA	16	INDU
$<2E-37$	100–3500	2	8000	pp	[3] ACHARYA	16	INDU
$<6E-37$	500–3000	3	8000	pp	[3] ACHARYA	16	INDU
$<7E-36$	1000–2000	4	8000	pp	[3] ACHARYA	16	INDU
$<1.6E-38$	200–1200	1	7000	pp	[4] AAD	12CS	ATLS
$<5E-38$	45–102	1	206	e^+e^-	[5] ABBIENDI	08	OPAL
$<0.2E-36$	200–700	1	1960	$p\overline{p}$	[6] ABULENCIA	06K	CNTR
$< 2.E-36$		1	300	e^+p	[7,8] AKTAS	05A	INDU
$< 0.2 E-36$		2	300	e^+p	[7,8] AKTAS	05A	INDU
$< 0.09E-36$		3	300	e^+p	[7,8] AKTAS	05A	INDU
$< 0.05E-36$		≥ 6	300	e^+p	[7,8] AKTAS	05A	INDU
$< 2.E-36$		1	300	e^+p	[7,9] AKTAS	05A	INDU
$< 0.2E-36$		2	300	e^+p	[7,9] AKTAS	05A	INDU
$< 0.07E-36$		3	300	e^+p	[7,9] AKTAS	05A	INDU
$< 0.06E-36$		≥ 6	300	e^+p	[7,9] AKTAS	05A	INDU
$< 0.6E-36$	>265	1	1800	$p\overline{p}$	[10] KALBFLEISCH	04	INDU
$< 0.2E-36$	>355	2	1800	$p\overline{p}$	[10] KALBFLEISCH	04	INDU
$< 0.07E-36$	>410	3	1800	$p\overline{p}$	[10] KALBFLEISCH	04	INDU
$< 0.2E-36$	>375	6	1800	$p\overline{p}$	[10] KALBFLEISCH	04	INDU
$< 0.7E-36$	>295	1	1800	$p\overline{p}$	[11,12] KALBFLEISCH	00	INDU
$< 7.8E-36$	>260	2	1800	$p\overline{p}$	[11,12] KALBFLEISCH	00	INDU
$< 2.3E-36$	>325	3	1800	$p\overline{p}$	[11,13] KALBFLEISCH	00	INDU
$< 0.11E-36$	>420	6	1800	$p\overline{p}$	[11,13] KALBFLEISCH	00	INDU
$<0.65E-33$	<3.3	≥ 2	11A	^{197}Au	[14,15] HE	97	
$<1.90E-33$	<8.1	≥ 2	160A	^{208}Pb	[14,15] HE	97	
$<3.E-37$	<45.0	1.0	88–94	e^+e^-	PINFOLD	93	PLAS
$<3.E-37$	<41.6	2.0	88–94	e^+e^-	PINFOLD	93	PLAS
$<7.E-35$	<44.9	0.2–1.0	89–93	e^+e^-	KINOSHITA	92	PLAS
$<2.E-34$	<850	≥ 0.5	1800	$p\overline{p}$	BERTANI	90	PLAS
$<1.2E-33$	<800	≥ 1	1800	$p\overline{p}$	PRICE	90	PLAS
$<1.E-37$	<29	1	50–61	e^+e^-	KINOSHITA	89	PLAS
$<1.E-37$	<18	2	50–61	e^+e^-	KINOSHITA	89	PLAS
$<1.E-38$	<17	<1	35	e^+e^-	BRAUNSCH...	88B	CNTR
$<8.E-37$	<24	1	50–52	e^+e^-	KINOSHITA	88	PLAS
$<1.3E-35$	<22	2	50–52	e^+e^-	KINOSHITA	88	PLAS
$<9.E-37$	<4	<0.15	10.6	e^+e^-	GENTILE	87	CLEO
$<3.E-32$	<800	≥ 1	1800	$p\overline{p}$	PRICE	87	PLAS
$<3.E-38$		<3	29	e^+e^-	FRYBERGER	84	PLAS
$<1.E-31$		1,3	540	$p\overline{p}$	AUBERT	83B	PLAS
$<4.E-38$	<10	<6	34	e^+e^-	MUSSET	83	PLAS
$<8.E-36$	<20		52	pp	[16] DELL	82	CNTR
$<9.E-37$	<30	<3	29	e^+e^-	KINOSHITA	82	PLAS
$<1.E-37$	<20	<24	63	pp	CARRIGAN	78	CNTR
$<1.E-37$	<30	<3	56	pp	HOFFMANN	78	PLAS
			62	pp	[16] DELL	76	SPRK
$<4.E-33$			300	p	[16] STEVENS	76B	SPRK
$<1.E-40$	<5	<2	70	p	[17] ZRELOV	76	CNTR
$<2.E-30$			300	n	[16] BURKE	75	OSPK
$<1.E-38$			8	ν	[18] CARRIGAN	75	HLBC
$<5.E-43$	<12	<10	400	p	EBERHARD	75B	INDU
$<2.E-36$	<30	<3	60	pp	GIACOMELLI	75	PLAS
$<5.E-42$	<13	<24	400	p	CARRIGAN	74	CNTR
$<6.E-42$	<12	<24	300	p	CARRIGAN	73	CNTR
$<2.E-36$		1	0.001	γ	[17] BARTLETT	72	CNTR
$<1.E-41$	<5		70	p	GUREVICH	72	EMUL
$<1.E-40$	<3	<2	28	p	AMALDI	63	EMUL
$<2.E-40$	<3	<2	30	p	PURCELL	63	CNTR
$<1.E-35$	<3	<4	28	p	FIDECARO	61	CNTR
$<2.E-35$	<1	1	6	p	BRADNER	59	EMUL

[1] The search was sensitive to monopoles which had stopped in aluminium trapping volumes. Monopoles with spins 0 and 1/2 were considered; mass-dependent spin 1/2 monopole limits are quoted here.
[2] AAD 16AB model-independent 95% CL limits estimated using a fiducial region of approximately constant acceptance. Limits are mass-dependent.
[3] ACHARYA 16 limits at 95% CL estimated using a Drell-Yan-like production mechanism for scalar monopoles.
[4] AAD 12CS searched for monopoles as highly ionising objects. The cross section limits are based on an assumed Drell Yan-like production process for spin 1/2 monopoles. The limits are mass- and scenario-dependent.
[5] ABBIENDI 08 assume production of spin 1/2 monopoles with effective charge $g\beta$ (n=1), via $e^+e^- \rightarrow \gamma^* \rightarrow M\overline{M}$, so that the cross section is proportional to $(1 + \cos^2\theta)$. There is no z information for such highly saturated tracks, so a parabolic track in the jet chamber is projected onto the xy plane. Charge per hit in the chamber produces a clean separation of signal and background.
[6] ABULENCIA 06K searches for high-ionizing signals in CDF central outer tracker and time-of-flight detector. For Drell-Yan $M\overline{M}$ production, the cross section limit implies $M > 360$ GeV at 95% CL.
[7] AKTAS 05A model-dependent limits as a function of monopole mass shown for arbitrary mass of 60 GeV. Based on search for stopped monopoles in the H1 Al beam pipe.
[8] AKTAS 05A limits with assumed elastic spin 0 monopole pair production.
[9] AKTAS 05A limits with assumed inelastic spin 1/2 monopole pair production.
[10] KALBFLEISCH 04 reports searches for stopped magnetic monopoles in Be, Al, and Pb samples obtained from discarded material from the upgrading of DØ and CDF. A large-aperture warm-bore cryogenic detector was used. The approach was an extension of the methods of KALBFLEISCH 00. Cross section results moderately model dependent; interpretation as a mass lower limit depends on possibly invalid perturbation expansion.
[11] KALBFLEISCH 00 used an induction method to search for stopped monopoles in pieces of the DØ (FNAL) beryllium beam pipe and in extensions to the drift chamber aluminum support cylinder. Results are model dependent.
[12] KALBFLEISCH 00 result is for aluminum.
[13] KALBFLEISCH 00 result is for beryllium.
[14] HE 97 used a lead target and barium phosphate glass detectors. Cross-section limits are well below those predicted via the Drell-Yan mechanism.
[15] This work has also been reinterpreted in the framework of monopole production via the thermal Schwinger process (GOULD 17); this gives rise to lower mass limits.
[16] Multipthoton events.
[17] Cherenkov radiation polarization.
[18] Re-examines CERN neutrino experiments.

Monopole Production — Other Accelerator Searches

MASS (GeV)	CHG (g)	SPIN	ENERGY (GeV)	BEAM	DOCUMENT ID		TECN
> 610	≥ 1	0	1800	$p\overline{p}$	[1] ABBOTT	98K	D0
> 870	≥ 1	1/2	1800	$p\overline{p}$	[1] ABBOTT	98K	D0
>1580	≥ 1	1	1800	$p\overline{p}$	[1] ABBOTT	98K	D0
> 510			88–94	e^+e^-	[2] ACCIARRI	95C	L3

[1] ABBOTT 98K search for heavy pointlike Dirac monopoles via central production of a pair of photons with high transverse energies.
[2] ACCIARRI 95C finds a limit $B(Z \rightarrow \gamma\gamma\gamma) < 0.8 \times 10^{-5}$ (which is possible via a monopole loop) at 95% CL and sets the mass limit via a cross section model.

Monopole Flux — Cosmic Ray Searches

"Caty" in the charge column indicates a search for monopole-catalyzed nucleon decay.

FLUX ($cm^{-2}sr^{-1}s^{-1}$)	MASS (GeV)	CHG (g)	COMMENTS ($\beta = v/c$)	EVTS	DOCUMENT ID		TECN
$<1.5E-18$		1	$\beta > 0.6$	0	[1] ALBERT	17	ANTR
$<2.5E-21$		1	$1E8 < \gamma < 1E13$	0	[2] AAB	16	AUGE
$<1.55E-18$			$\beta > 0.51$	0	[3] AARTSEN	16B	ICCB
$<1E-17$		Caty	$1E-3 < \beta < 1E-2$	0	[4] AARTSEN	14	ICCB
$<3E-18$		1	$\beta > 0.8$	0	[5] ABBASI	13	ICCB
$<1.3E-17$		1	$\beta > 0.625$	0	[6] ADRIAN-MAR...	12A	ANTR
$<6E-28$	$<1E17$	Caty	$1E-5 < \beta < 0.04$	0	[7] UENO	12	SKAM
$<1E-19$		**1**	**$\gamma > 1E10$**	0	[8] DETRIXHE	11	ANIT
$<3.8E-17$		1	$\beta > 0.76$	0	[5] ABBASI	10A	ICCB
$<1.3E-15$	$1E4<M<5E13$	1	$\beta > 0.05$	0	[9] BALESTRA	08	PLAS
$<0.65E-15$	$>5E13$	1	$\beta > 0.05$	0	[9] BALESTRA	08	PLAS
$<1E-18$		**1**	**$\gamma > 1$ E8**	0	[8] HOGAN	08	RICE
$<1.4E-16$		**1**	**$1.1E-4 < \beta < 1$**	0	[10] AMBROSIO	02B	MCRO
$<3E-16$		Caty	$1.1E-4 < \beta < 5E-3$	0	[11] AMBROSIO	02C	MCRO
$<1.5E-15$		1	$5E-3 < \beta < 0.99$	0	[12] AMBROSIO	02D	MCRO
$<1E-15$		1	1.1×10^{-4}–0.1	0	[13] AMBROSIO	97	MCRO
$<5.6E-15$		1	(0.18–3.0)E−3	0	[14] AHLEN	94	MCRO
$<2.7E-15$		Caty	$\beta \sim 1 \times 10^{-3}$	0	[15] BECKER-SZ...	94	IMB
$<8.7E-15$		1	$>2.E-3$	0	THRON	92	SOUD
$<4.4E-12$		1	all β	0	GARDNER	91	INDU
$<7.2E-13$		1	all β	0	HUBER	91	INDU
$<3.7E-15$	$>E12$	1	β=1.E−4	0	[16] ORITO	91	PLAS
$<3.2E-16$	$>E10$	1	$\beta > 0.05$	0	[16] ORITO	91	PLAS
$<3.2E-16$	$>E10$–E12	2, 3		0	[16] ORITO	91	PLAS
$<3.8E-13$		1	all β	0	BERMON	90	INDU
$<5.E-16$		Caty	$\beta < 1.E-3$	0	[15] BEZRUKOV	90	CHER
$<1.8E-14$		1	$\beta > 1.1E-4$	0	[17] BUCKLAND	90	HEPT
$<1E-18$			$3.E-4 < \beta < 1.5E-3$	0	[18] GHOSH	90	MICA
$<7.2E-13$		1	all β	0	HUBER	90	INDU
$<5.E-12$	$>E7$	1	$3.E-4 < \beta < 5.E-3$	0	BARISH	87	CNTR
$<1.E-13$		Caty	$1.E-5 < \beta < 1$	0	[15] BARTELT	87	SOUD
$<1.E-10$		1	all β	0	EBISU	87	INDU
$<2.E-13$			$1.E-4 < \beta < 6.E-4$	0	MASEK	87	HEPT
$<2.E-14$			$4.E-5 < \beta < 2.E-4$	0	NAKAMURA	87	PLAS
$<2.E-14$			$1.E-3 < \beta < 1$	0	NAKAMURA	87	PLAS
$<5.E-14$			$9.E-4 < \beta < 1.E-2$	0	SHEPKO	87	CNTR
$<2.E-13$			$4.E-4 < \beta < 1$	0	TSUKAMOTO	87	CNTR
$<5.E-14$		1	all β	1	[19] CAPLIN	86	INDU
$<5.E-12$		1		0	CROMAR	86	INDU
$<1.E-13$		1	$7.E-4 < \beta$	0	HARA	86	CNTR

Searches Particle Listings

Magnetic Monopole Searches

<7.E−11		1	all β	0	INCANDELA	86	INDU
<1.E−18			4.E−4 < β <1.E−3	0	[18] PRICE	86	MICA
<5.E−12		1		0	BERMON	85	INDU
<6.E−12		1		0	CAPLIN	85	INDU
<6.E−10		1		0	EBISU	85	INDU
<3.E−15		Caty	5.E−5 ≤ β ≤ 1.E−3	0	[15] KAJITA	85	KAMI
<2.E−21		Caty	β <1.E−3	0	[15,20] KAJITA	85	KAMI
<3.E−15		Caty	1.E−3 < β <1.E−1	0	[15] PARK	85B	CNTR
<5.E−12		1	1.E−4 < β <1	0	BATTISTONI	84	NUSX
<7.E−12		1		0	INCANDELA	84	INDU
<7.E−13		1	3.E−4 < β	0	[17] KAJINO	84	CNTR
<2.E−12		1	3.E−4 < β <1.E−1	0	KAJINO	84B	CNTR
<6.E−13		1	5.E−4 < β <1	0	KAWAGOE	84	CNTR
<2.E−14			1.E−3 < β	0	[15] KRISHNA...	84	CNTR
<4.E−13		1	6.E−4 < β <2.E−3	0	LISS	84	CNTR
<1.E−16			3.E−4 < β <1.E−3	0	[18] PRICE	84	MICA
<1.E−13		1	1.E−4 < β	0	PRICE	84B	PLAS
<4.E−13		1	6.E−4 < β <2.E−3	0	TARLE	84	CNTR
				7	[21] ANDERSON	83	EMUL
<4.E−13		1	1.E−2 < β <1.E−3	0	BARTELT	83B	CNTR
<1.E−12		1	7.E−3 < β <1	0	BARWICK	83	PLAS
<3.E−13		1	1.E−3 < β <4.E−1	0	BONARELLI	83	CNTR
<3.E−12		Caty	5.E−4 < β <5.E−2	0	[15] BOSETTI	83	CNTR
<4.E−11		1		0	CABRERA	83	INDU
<5.E−15		1	1.E−2 < β <1	0	DOKE	83	PLAS
<8.E−15		Caty	1.E−4 < β <1.E−1	0	[15] ERREDE	83	IMB
<5.E−12		1	1.E−4 < β <3.E−2	0	GROOM	83	CNTR
<2.E−12			6.E−4 < β <1	0	MASHIMO	83	CNTR
<1.E−13		1	β=3.E−3	0	ALEXEYEV	82	CNTR
<2.E−12		1	7.E−3 < β <6.E−1	0	BONARELLI	82	CNTR
6.E−10		1	all β	1	[22] CABRERA	82	INDU
<2.E−11			1.E−2 < β <1.E−1	0	MASHIMO	82	CNTR
<2.E−15			concentrator	0	BARTLETT	81	PLAS
<1.E−13	>1		1.E−3 < β	0	KINOSHITA	81B	PLAS
<5.E−11	<E17		3.E−4 < β <1.E−3	0	ULLMAN	81	CNTR
<2.E−11			concentrator	0	BARTLETT	78	PLAS
1.E−1	>200	2		1	[23] PRICE	75	PLAS
<2.E−13		>2		0	FLEISCHER	71	PLAS
<1.E−19		>2	obsidian, mica	0	FLEISCHER	69C	PLAS
<5.E−15	<15	<3	concentrator	0	CARITHERS	66	ELEC
<2.E−11		<1–3	concentrator	0	MALKUS	51	EMUL

[1] ALBERT 17 limits were estimated using a Cherenkov light in an array of optical modules under the Mediterranean Sea. The limits are for MM masses between 10^{10} and 10^{14} GeV. The limits are speed-dependent.

[2] AAB 16 search was made with a set of telescopes sampling the longitudinal profile of fluorescence light emitted by extensive air showers. Limits are speed dependent.

[3] AARTSEN 16B was based on a Cherenkov signature in an array of optical modules which were sunk in the Antarctic ice cap. Limits are speed-dependent.

[4] Beyond the monopole speed, the limits of AARTSEN 14 depend on the catalysis cross section (σ) which corresponds to the monopole radiating $\hat{l}$ times the light per track length compared to the Cherenkov light from a single electrically charged, relativistic particle. The values quoted here correspond to $\sigma = 1$ barn or $\hat{l} = 30$.

[5] ABBASI 13 and ABBASI 10A were based on a Cherenkov signature in an array of optical modules which were sunk in the Antarctic ice cap. Limits are speed-dependent.

[6] ADRIAN-MARTINEZ 12A measurements were based on a Cherenkov signature in an underwater telescope in the Western Mediterranean Sea. Limits are speed-dependent.

[7] The limits from UENO 12 depend on the monopole speed and are also sensitive to assumed values of monopole mass and the catalysis cross section.

[8] HOGAN 08 and DETRIXHE 11 limits on relativistic monopoles are based on nonobservation of radio Cherenkov signals at the South Pole. Limits are speed-dependent.

[9] BALESTRA 08 exposed of nuclear track detector modules totaling 400 m^2 for 4 years at the Chacaltaya Laboratory (5230 m) in search for intermediate-mass monopoles with $\beta >$ 0.05. The analysis is mainly based on three CR39 modules. For $M > 5 \times 10^{13}$ GeV there can be upward-going monopoles as well, hence the flux limit is half that obtained for less massive monopoles. Previous experiments (e.g. MACRO and OHYA (ORITO 91)) had set limits only for $M > 1 \times 10^{9}$ GeV.

[10] AMBROSIO 02B direct search final result for $m \geq 10^{17}$ GeV, based upon 4.2 to 9.5 years of running, depending upon the subsystem. Limit with CR39 track-etch detector extends the limit from $\beta = 4 \times 10^{-5}$ (3.1×10^{-16} cm^{-2} sr^{-1} s^{-1}) to $\beta = 1 \times 10^{-4}$ (2.1×10^{-16} cm^{-2} sr^{-1} s^{-1}). Limit curve in paper is piecewise continuous due to different detection techniques for different β ranges.

[11] AMBROSIO 02C limit for catalysis of nucleon decay with catalysis cross section of $\approx$ 1 mb. The flux limit increases by $\sim$ 3 at the higher β limit, and increases to 1×10^{-14} cm^{-2} sr^{-1} s^{-1} if the catalysis cross section is 0.01 mb. Based upon 71193 hr of data with the streamer detector, with an acceptance of 4250 m^2 sr.

[12] AMBROSIO 02D result for "more than two years of data." Ionization search using several subsystems. Limit curve as a function of β not given. Included in AMBROSIO 02B.

[13] AMBROSIO 97 global MACRO 90%CL is 0.78×10^{-15} at $\beta = 1.1 \times 10^{-4}$, goes through a minimum at 0.61×10^{-15} near $\beta = (1.1–2.7) \times 10^{-3}$, then rises to 0.84×10^{-15} at $\beta = 0.1$. The global limit in this region is below the Parker bound at 10^{-15}. Less stringent limits are established for $4 \times 10^{-5} < \beta < 1 \times 10^{-4}$. Limits set by various triggers and different subdetectors are given in the paper. All limits assume a catalysis cross section smaller than a few mb.

[14] AHLEN 94 limit for dyons extends down to β=0.9E−4 and a limit of 1.3E−14 extends to β = 0.8E−4. Also see comment by PRICE 94 and reply of BARISH 94. One loophole in the AHLEN 94 result is that in the case of monopoles catalyzing nucleon decay, relativistic particles could veto the events. See AMBROSIO 97 for additional results.

[15] Catalysis of nucleon decay; sensitive to assumed catalysis cross section.

[16] ORITO 91 limits are functions of velocity. Lowest limits are given here.

[17] Used DKMPR mechanism and Penning effect.

[18] Assumes monopole attaches fermion nucleus.

[19] Limit from combining data of CAPLIN 86, BERMON 85, INCANDELA 84, and CABRERA 83. For a discussion of controversy about CAPLIN 86 observed event, see GUY 87. Also see SCHOUTEN 87.

[20] Based on lack of high- energy solar neutrinos from catalysis in the sun.

[21] Anomalous long-range α (^{4}He) tracks.

[22] CABRERA 82 candidate event has single Dirac charge within ±5%.

[23] ALVAREZ 75, FLEISCHER 75, and FRIEDLANDER 75 explain as fragmenting nucleus. EBERHARD 75 and ROSS 76 discuss conflict with other experiments. HAGSTROM 77 reinterprets as antinucleus. PRICE 78 reassesses.

Monopole Flux — Astrophysics

FLUX ($cm^{-2} sr^{-1} s^{-1}$)	MASS (GeV)	CHG (g)	COMMENTS ($\beta = v/c$)	DOCUMENT ID		TECN
<1.3E−20			faint white dwarf	[1] FREESE	99	ASTR
<1.E−16	E17	1	galactic field	[2] ADAMS	93	COSM
<1.E−23			Jovian planets	[1] ARAFUNE	85	ASTR
<1.E−16	E15		solar trapping	BRACCI	85B	ASTR
<1.E−18		1		[1] HARVEY	84	COSM
<3.E−23			neutron stars	KOLB	84	ASTR
<7.E−22			pulsars	[1] FREESE	83B	ASTR
<1.E−18	<E18	1	intergalactic field	[1] REPHAELI	83	COSM
<1.E−23			neutron stars	[1] DIMOPOUL...	82	COSM
<5.E−22			neutron stars	[1] KOLB	82	COSM
<5.E−15	>E21		galactic halo	SALPETER	82	COSM
<1.E−12	E19	1	β=3.E−3	[3] TURNER	82	COSM
<1.E−16		1	galactic field	PARKER	70	COSM

[1] Catalysis of nucleon decay.

[2] ADAMS 93 limit based on "survival and growth of a small galactic seed field" is 10^{-16} ($m/10^{17}$ GeV) cm^{-2} s^{-1} sr^{-1}. Above 10^{17} GeV, limit 10^{-16} (10^{17} GeV/m) cm^{-2} s^{-1} sr^{-1} (from requirement that monopole density does not overclose the universe) is more stringent.

[3] Re-evaluates PARKER 70 limit for GUT monopoles.

Monopole Density — Matter Searches

DENSITY	CHG (g)	MATERIAL	DOCUMENT ID		TECN
<9.8E−5/gram	≥ 1	Polar rock	BENDTZ	13	INDU
<6.9E−6/gram	>1/3	Meteorites and other	JEON	95	INDU
<2.E−7/gram	>0.6	Fe ore	[1] EBISU	87	INDU
<4.6E−6/gram	> 0.5	deep schist	KOVALIK	86	INDU
<1.6E−6/gram	> 0.5	manganese nodules	[2] KOVALIK	86	INDU
<1.3E−6/gram	> 0.5	seawater	KOVALIK	86	INDU
>1.E+14/gram	>1/3	iron aerosols	MIKHAILOV	83	SPEC
<6.E−4/gram		air, seawater	CARRIGAN	76	CNTR
<5.E−1/gram	>0.04	11 materials	CABRERA	75	INDU
<2.E−4/gram	>0.05	moon rock	ROSS	73	INDU
<6.E−7/gram	<140	seawater	KOLM	71	CNTR
<1.E−2/gram	<120	manganese nodules	FLEISCHER	69	PLAS
<1.E−4/gram	>0	manganese	FLEISCHER	69B	PLAS
<2.E−3/gram	<1–3	magnetite, meteor	GOTO	63	EMUL
<2.E−2/gram		meteorite	PETUKHOV	63	CNTR

[1] Mass 1×10^{14}–1×10^{17} GeV.

[2] KOVALIK 86 examined 498 kg of schist from two sites which exhibited clear mineralogical evidence of having been buried at least 20 km deep and held below the Curie temperature.

Monopole Density — Astrophysics

DENSITY	CHG (g)	MATERIAL	DOCUMENT ID		TECN
<1.E−9/gram	1	sun, catalysis	[1] ARAFUNE	83	COSM
<6.E−33/nucl	1	moon wake	SCHATTEN	83	ELEC
<2.E−28/nucl		earth heat	CARRIGAN	80	COSM
<2.E−4/prot		42cm absorption	BRODERICK	79	COSM
<2.E−13/m^3		moon wake	SCHATTEN	70	ELEC

[1] Catalysis of nucleon decay.

REFERENCES FOR Magnetic Monopole Searches

ACHARYA	17	PRL 118 061801	B. Acharya *et al.*	(MoEDAL Collab.)
ALBERT	17	JHEP 1707 054	A. Albert *et al.*	(ANTARES Collab.)
GOULD	17	PRL 119 241601	O. Gould, A. Rajantie	
AAB	16	PR D94 082002	A. Aab *et al.*	(Pierre Auger Collab.)
AAD	16AB	PR D93 052009	G. Aad *et al.*	(ATLAS Collab.)
AARTSEN	16B	EPJ C76 133	M.G. Aartsen *et al.*	(IceCube Collab.)
ACHARYA	16	JHEP 1608 067	B. Acharya *et al.*	(MoEDAL Collab.)
AARTSEN	14	EPJ C74 2938	M.G. Aartsen *et al.*	(IceCube Collab.)
ABBASI	13	PR D87 022001	R. Abbasi *et al.*	(IceCube Collab.)
BENDTZ	13	PRL 110 121803	K. Bendtz *et al.*	
AAD	12CS	PRL 109 261803	G. Aad *et al.*	(ATLAS Collab.)
ADRIAN-MAR...	12A	ASP 35 634	S. Adrian-Martinez *et al.*	(ANTARES Collab.)
UENO	12	ASP 36 131	K. Ueno *et al.*	(Super-Kamiokande Collab.)
DETRIXHE	11	PR D83 023513	M. Detrixhe *et al.*	(ANITA Collab.)
ABBASI	10A	EPJ C69 361	R. Abbasi *et al.*	(IceCube Collab.)
ABBIENDI	08	PL B663 37	G. Abbiendi *et al.*	(OPAL Collab.)
BALESTRA	08	EPJ C55 57	S. Balestra *et al.*	(SLIM Collab.)
HOGAN	08	PR D78 075031	D.P. Hogan *et al.*	(KANS, NEBR, DELA)
ABULENCIA	06K	PRL 96 201801	A. Abulencia *et al.*	(CDF Collab.)
AKTAS	05A	EPJ C41 133	A. Aktas *et al.*	(H1 Collab.)
KALBFLEISCH	04	PR D69 052002	G.R. Kalbfleisch *et al.*	(OKLA)
AMBROSIO	02B	EPJ C25 511	M. Ambrosio *et al.*	(MACRO Collab.)
AMBROSIO	02C	EPJ C26 163	M. Ambrosio *et al.*	(MACRO Collab.)
AMBROSIO	02D	ASP 18 27	M. Ambrosio *et al.*	(MACRO Collab.)
KALBFLEISCH	00	PRL 85 5292	G.R. Kalbfleisch *et al.*	

FREESE	99	PR D59 063007	K. Freese, E. Krasteva	
ABBOTT	98K	PRL 81 524	B. Abbott *et al.*	(D0 Collab.)
AMBROSIO	97	PL B406 249	M. Ambrosio *et al.*	(MACRO Collab.)
HE	97	PRL 79 3134	Y.D. He	(UCB)
ACCIARRI	95C	PL B345 609	M. Acciarri *et al.*	(L3 Collab.)
JEON	95	PRL 75 1443	H. Jeon, M.J. Longo	(MICH)
Also		PRL 76 159 (erratum)	H. Jeon, M.J. Longo	
AHLEN	94	PRL 72 608	S.P. Ahlen *et al.*	(MACRO Collab.)
BARISH	94	PRL 73 1306	B.C. Barish, G. Giacomelli, J.T. Hong	(CIT+)
BECKER-SZ...	94	PR D49 2169	R.A. Becker-Szendy *et al.*	(IMB Collab.)
PRICE	94	PRL 73 1305	P.B. Price	(UCB)
ADAMS	93	PRL 70 2511	F.C. Adams *et al.*	(MICH, FNAL)
PINFOLD	93	PL B316 407	J.L. Pinfold *et al.*	(ALBE, HARV, MONT+)
KINOSHITA	92	PR D46 881	K. Kinoshita *et al.*	(HARV, BGNA, REHO)
THRON	92	PR D46 4846	J.L. Thron *et al.*	(SOUDAN-2 Collab.)
GARDNER	91	PR D44 622	R.D. Gardner *et al.*	(STAN)
HUBER	91	PR D44 636	M.E. Huber *et al.*	(STAN)
ORITO	91	PRL 66 1951	S. Orito *et al.*	(ICEPP, WASCR, NIHO, ICRR)
BERMON	90	PRL 64 839	S. Bermon *et al.*	(IBM, BNL)
BERTANI	90	EPL 12 613	M. Bertani *et al.*	(BGNA, INFN)
BEZRUKOV	90	SJNP 52 54	L.B. Bezrukov *et al.*	(INRM)
		Translated from YAF 52 86.		
BUCKLAND	90	PR D41 2726	K.N. Buckland *et al.*	(UCSD)
GHOSH	90	EPL 12 25	D.C. Ghosh, S. Chatterjea	(JADA)
HUBER	90	PRL 64 835	M.E. Huber *et al.*	(STAN)
PRICE	90	PRL 65 149	P.B. Price, J. Guiru, K. Kinoshita	(UCB, HARV)
KINOSHITA	89	PL B228 543	K. Kinoshita *et al.*	(HARV, TISA, KEK+)
BRAUNSCH...	88B	ZPHY C38 543	R. Braunschweig *et al.*	(TASSO Collab.)
KINOSHITA	88	PRL 60 1610	K. Kinoshita *et al.*	(HARV, TISA, KEK+)
BARISH	87	PR D36 2641	B.C. Barish, G. Liu, C. Lane	(CIT)
BARTELT	87	PR D36 1990	J.E. Bartelt *et al.*	(Soudan Collab.)
Also		PR D40 1701 (erratum)	J.E. Bartelt *et al.*	(Soudan Collab.)
EBISU	87	PR D36 3359	T. Ebisu, T. Watanabe	(KOBE)
Also		JP G11 883	T. Ebisu, T. Watanabe	(KOBE)
GENTILE	87	PR D35 1081	T. Gentile *et al.*	(CLEO Collab.)
GUY	87	NAT 325 463	J. Guy	(LOIC)
MASEK	87	PR D35 2758	G.E. Masek *et al.*	(UCSD)
NAKAMURA	87	PL B183 395	S. Nakamura *et al.*	(INUS, WASCR, NIHO)
PRICE	87	PRL 59 2523	P.B. Price, R. Guoxiao, K. Kinoshita	(UCB, HARV)
SCHOUTEN	87	JP E20 850	J.C. Schouten *et al.*	(LOIC)
SHEPKO	87	PR D35 2917	M.J. Shepko *et al.*	(TAMU)
TSUKAMOTO	87	EPL 3 39	T. Tsukamoto *et al.*	(ICRR)
CAPLIN	86	NAT 321 402	A.D. Caplin *et al.*	(LOIC)
Also		JP E20 850	J.C. Schouten *et al.*	(LOIC)
Also		NAT 325 463	J. Guy	(LOIC)
CROMAR	86	PRL 56 2561	M.W. Cromar, A.F. Clark, F.R. Fickett	(NBSB)
HARA	86	PRL 56 553	T. Hara *et al.*	(ICRR, KYOT, KEK, KOBE+)
INCANDELA	86	PR D34 2637	J. Incandela *et al.*	(CHIC, FNAL, MICH)
KOVALIK	86	PR A33 1183	J.M. Kovalik, J.L. Kirschvink	(CIT)
PRICE	86	PRL 56 1226	P.B. Price, M.H. Salamon	(UCB)
ARAFUNE	85	PR D32 2586	J. Arafune, M. Fukugita, S. Yanagita	(ICRR, KYOTU+)
BERMON	85	PRL 55 1850	S. Bermon *et al.*	(IBM)
BRACCI	85B	NP B258 726	L. Bracci, G. Fiorentini, G. Mezzorani	(PISA+)
Also		LNC 42 123	L. Bracci, G. Fiorentini	(PISA)
CAPLIN	85	NAT 317 234	A.D. Caplin *et al.*	(LOIC)
EBISU	85	JP G11 883	T. Ebisu, T. Watanabe	(KOBE)
KAJITA	85	JPSJ 54 4065	T. Kajita *et al.*	(ICRR, KEK, NIIG)
PARK	85B	NP B252 261	H.S. Park *et al.*	(IMB Collab.)
BATTISTONI	84	PL 133B 454	G. Battistoni *et al.*	(NUSEX Collab.)
FRYBERGER	84	PR D29 1524	D. Fryberger *et al.*	(SLAC, UCB)
HARVEY	84	NP B236 255	J.A. Harvey	(PRIN)
INCANDELA	84	PRL 53 2067	J. Incandela *et al.*	(CHIC, FNAL, MICH)
KAJINO	84	PRL 52 1373	F. Kajino *et al.*	(ICRR)
KAJINO	84B	JP G10 447	F. Kajino *et al.*	(ICRR)
KAWAGOE	84	LNC 41 315	K. Kawagoe *et al.*	(TOKY)
KOLB	84	APJ 286 702	E.W. Kolb, M.S. Turner	(FNAL, CHIC)
KRISHNA...	84	PL 142B 99	M.R. Krishnaswamy *et al.*	(TATA, OSKC+)
LISS	84	PR D30 884	T.M. Liss, S.P. Ahlen, G. Tarle	(UCB, IND+)
PRICE	84	PRL 52 1265	P.B. Price *et al.*	(ROMA, UCB, IND+)
PRICE	84B	PL 140B 112	P.B. Price	(CERN)
TARLE	84	PRL 52 90	G. Tarle, S.P. Ahlen, T.M. Liss	(UCB, MICH+)
ANDERSON	83	PR D28 2308	S.N. Anderson *et al.*	(WASH)
ARAFUNE	83	PL 133B 380	J. Arafune, M. Fukugita	(ICRR, KYOTU)
AUBERT	83B	PL 120B 465	B. Aubert *et al.*	(CERN, LAPP)
BARTELT	83B	PRL 50 655	J.E. Bartelt *et al.*	(MINN, ANL)
BARWICK	83	PR D28 2338	S.W. Barwick, K. Kinoshita, P.B. Price	(UCB)
BONARELLI	83	PL 126B 137	R. Bonarelli, P. Capiluppi, I. d'Antone	(BGNA)
BOSETTI	83	PL 133B 265	P.C. Bosetti *et al.*	(AACH3, HAWA, TOKY)
CABRERA	83	PRL 51 1933	B. Cabrera *et al.*	(STAN)
DOKE	83	PL 129B 370	T. Doke *et al.*	(WASU, RIKK, TTAM, RIKEN)
ERREDE	83	PRL 51 245	S.M. Errede *et al.*	(IMB Collab.)
FREESE	83B	PRL 51 1625	K. Freese, M.S. Turner, D.N. Schramm	(CHIC)
GROOM	83	PRL 50 573	D.E. Groom *et al.*	(UTAH, STAN)
MASHIMO	83	PL 128B 327	T. Mashimo *et al.*	(ICEPP)
MIKHAILOV	83	PL 130B 331	V.F. Mikhailov	(KAZA)
MUSSET	83	PL 128B 333	P. Musset, M. Price, E. Lohrmann	(CERN, HAMB)
REPHAELI	83	PL 121B 115	Y. Rephaeli, M.S. Turner	(CHIC)
SCHATTEN	83	PR D27 1525	K.H. Schatten	(NASA)
ALEXEYEV	82	LNC 35 413	E.N. Alekseev *et al.*	(INRM)
BONARELLI	82	PL 112B 100	R. Bonarelli *et al.*	(BGNA)
CABRERA	82	PRL 48 1378	B. Cabrera	(STAN)
DELL	82	NP B209 45	G.F. Dell *et al.*	(BNL, ADEL, ROMA)
DIMOPOUL...	82	PL 119B 320	S. Dimopoulos, J. Preskill, F. Wilczek	(HARV+)
KINOSHITA	82	PRL 48 77	K. Kinoshita, P.B. Price, D. Fryberger	(UCB+)
KOLB	82	PRL 49 1373	E.W. Kolb, S.A. Colgate, J.A. Harvey	(LASL, PRIN)
MASHIMO	82	JPSJ 51 3067	T. Mashimo, K. Kawagoe, M. Koshiba	(INUS)
SALPETER	82	PRL 49 1114	E.E. Salpeter, S.L. Shapiro, I. Wasserman	(CORN)
TURNER	82	PR D26 1296	M.S. Turner, E.N. Parker, T.J. Bogdan	(CHIC)
BARTLETT	81	PR D24 612	D.F. Bartlett *et al.*	(COLO, GESC)
KINOSHITA	81B	PR D24 1707	K. Kinoshita, P.B. Price	(UCB)
ULLMAN	81	PRL 47 289	J.D. Ullman	(LEHM, BNL)
CARRIGAN	80	NAT 288 348	R.A. Carrigan	(FNAL)
BRODERICK	79	PR D19 1046	J.J. Broderick *et al.*	(VPI)
BARTLETT	78	PR D18 2253	D.F. Bartlett, D. Soo, M.G. White	(COLO, PRIN)
CARRIGAN	78	PR D17 1754	R.A. Carrigan, B.P. Strauss, G. Giacomelli	(FNAL+)
HOFFMANN	78	LNC 23 357	H. Hoffmann *et al.*	(CERN, ROMA)
PRICE	78	PR D18 1382	P.B. Price *et al.*	(UCB, HOUS)
HAGSTROM	77	PRL 38 729	R. Hagstrom	(LBL)
CARRIGAN	76	PR D13 1823	R.A. Carrigan, F.A. Nezrick, B.P. Strauss	(FNAL)
DELL	76	LNC 15 269	G.F. Dell *et al.*	(CERN, BNL, ROMA, ADEL)
ROSS	76	LBL-4665	R.R. Ross	(LBL)
STEVENS	76B	PR D14 2207	D.M. Stevens *et al.*	(VPI, BNL)
ZRELOV	76	CZJP B26 1306	V.P. Zrelov *et al.*	(JINR)
ALVAREZ	75	LBL-4260	L.W. Alvarez	(LBL)
BURKE	75	PL 60B 113	D.L. Burke *et al.*	(MICH)
CABRERA	75	Thesis	B. Cabrera	(STAN)
CARRIGAN	75	NP B91 279	R.A. Carrigan, F.A. Nezrick	(FNAL)
Also		PR D3 56	R.A. Carrigan, F.A. Nezrick	(FNAL)
EBERHARD	75	PR D11 3099	P.H. Eberhard *et al.*	(LBL, MPIM)
EBERHARD	75B	LBL-4289	P.H. Eberhard	(LBL)
FLEISCHER	75	PRL 35 1412	R.L. Fleischer, R.N.F. Walker	(GESC, WUSL)
FRIEDLANDER	75	PRL 35 1167	M.W. Friedlander	(WUSL)
GIACOMELLI	75	NC 28A 21	G. Giacomelli *et al.*	(BGNA, CERN, SACL+)
PRICE	75	PRL 35 487	P.B. Price *et al.*	(UCB, HOUS)
CARRIGAN	74	PR D10 3867	R.A. Carrigan, F.A. Nezrick, B.P. Strauss	(FNAL)
CARRIGAN	73	PR D8 3717	R.A. Carrigan, F.A. Nezrick, B.P. Strauss	(FNAL)
ROSS	73	PR D8 698	R.R. Ross *et al.*	(LBL, SLAC)
Also		PR D4 3260	P.H. Eberhard *et al.*	(LBL, SLAC)
Also		SCI 167 701	L.W. Alvarez *et al.*	(LBL, SLAC)
BARTLETT	72	PR D6 1817	D.F. Bartlett, M.D. Lahana	(COLO)
GUREVICH	72	PL 38B 549	I.I. Gurevich *et al.*	(KIAE, NOVO, SERP)
Also		JETP 34 917	L.M. Barkov, I.I. Gurevich, M.S. Zolotorev	(KIAE+)
		Translated from ZETF 61 1721.		
Also		PL 31B 394	I.I. Gurevich *et al.*	(KIAE, NOVO, SERP)
FLEISCHER	71	PR D4 24	R.L. Fleischer *et al.*	(GESC)
KOLM	71	PR D4 1285	H.H. Kolm, F. Villa, A. Odian	(MIT, SLAC)
PARKER	70	APJ 160 383	E.N. Parker	(CHIC)
SCHATTEN	70	PR D1 2245	K.H. Schatten	(NASA)
FLEISCHER	69	PR 177 2029	R.L. Fleischer *et al.*	(GESC, FSU)
FLEISCHER	69B	PR 184 1393	R.L. Fleischer *et al.*	(GESC, UNCS, GSCO)
FLEISCHER	69C	PR 184 1398	R.L. Fleischer, P.B. Price, R.T. Woods	(GESC)
Also		JAP 41 958	R.L. Fleischer *et al.*	(GESC)
CARITHERS	66	PR 149 1070	W.C.J. Carithers, R.J. Stefanski, R.K. Adair	
AMALDI	63	NC 28 773	E. Amaldi *et al.*	(ROMA, UCSD, CERN)
GOTO	63	PR 132 387	E. Goto, H.H. Kolm, K.W. Ford	(TOKY, MIT, BRAN)
PETUKHOV	63	NP 49 87	V.A. Petukhov, M.N. Yakimenko	(LEBD)
PURCELL	63	PR 129 2326	E.M. Purcell *et al.*	(HARV, BNL)
FIDECARO	61	NC 22 657	M. Fidecaro, G. Finocchiaro, G. Giacomelli	(CERN)
BRADNER	59	PR 114 603	H. Bradner, W.M. Isbell	(LBL)
MALKUS	51	PR 83 899	W.V.R. Malkus	(CHIC)

OTHER RELATED PAPERS

GROOM	86	PRPL 140 323	D.E. Groom	(UTAH)
Review				

Supersymmetric Particle Searches

The exclusion of particle masses within a mass range (m_1, m_2) will be denoted with the notation "none m_1–m_2" in the VALUE column of the following Listings. The latest unpublished results are described in the "Supersymmetry: Experiment" review.

See the related review(s):

Supersymmetry, Part I (Theory)

Supersymmetry, Part II (Experiment)

CONTENTS:

Most of the results shown below, unless stated otherwise, are based on the Minimal Supersymmetric Standard Model (MSSM), as described in the Note on Supersymmetry. Unless otherwise indicated, this includes the assumption of common gaugino and scalar masses at the scale of Grand Unification (GUT), and use of the resulting relations in the spectrum and

decay branching ratios. Unless otherwise indicated, it is also assumed that R-parity (R) is conserved and that:

1) The $\widetilde{\chi}_1^0$ is the lighest supersymmetric particle (LSP)
2) $m_{\widetilde{f}_L} = m_{\widetilde{f}_R}$, where $\widetilde{f}_{L,R}$ refer to the scalar partners of left- and right-handed fermions.

Limits involving different assumptions are identified in the Comments or in the Footnotes. We summarize here the notations used in this Chapter to characterize some of the most common deviations from the MSSM (for further details, see the Note on Supersymmetry).

Theories with R-parity violation ($\not{R}$) are characterized by a superpotential of the form: $\lambda_{ijk} L_i L_j e_k^c + \lambda'_{ijk} L_i Q_j d_k^c + \lambda''_{ijk} u_i^c d_j^c d_k^c$, where i, j, k are generation indices. The presence of any of these couplings is often identified in the following by the symbols $LL\overline{E}$, $LQ\overline{D}$, and $\overline{U}\overline{D}\overline{D}$. Mass limits in the presence of $\not{R}$ will often refer to "direct" and "indirect" decays. Direct refers to $\not{R}$ decays of the particle in consideration. Indirect refers to cases where $\not{R}$ appears in the decays of the LSP. The LSP need not be the $\widetilde{\chi}_1^0$.

In several models, most notably in theories with so-called Gauge Mediated Supersymmetry Breaking (GMSB), the gravitino ($\widetilde{G}$) is the LSP. It is usually much lighter than any other massive particle in the spectrum, and $m_{\widetilde{G}}$ is then neglected in all decay processes involving gravitinos. In these scenarios, particles other than the neutralino are sometimes considered as the next-to-lighest supersymmetric particle (NLSP), and are assumed to decay to their even-R partner plus $\widetilde{G}$. If the lifetime is short enough for the decay to take place within the detector, $\widetilde{G}$ is assumed to be undetected and to give rise to missing energy ($\not{E}$) or missing transverse energy ($\not{E}_T$) signatures.

When needed, specific assumptions on the eigenstate content of $\widetilde{\chi}^0$ and $\widetilde{\chi}^\pm$ states are indicated, using the notation $\widetilde{\gamma}$ (photino), $\widetilde{H}$ (higgsino), $\widetilde{W}$ (wino), and $\widetilde{Z}$ (zino) to signal that the limit of pure states was used. The terms gaugino is also used, to generically indicate wino-like charginos and zino-like neutralinos.

In the listings we have made use of the following abbreviations for simplified models employed by the experimental collaborations in supersymmetry searches published in the past year.

Simplified Models Table

Tglu1A: gluino pair production with $\tilde{g} \to q\bar{q}\tilde{\chi}_1^0$.
Tglu1B: gluino pair production with $\tilde{g} \to qq'\tilde{\chi}_1^\pm$, $\tilde{\chi}_1^\pm \to W^\pm\tilde{\chi}_1^0$.
Tglu1C: gluino pair production with a 2/3 probability of having a $\tilde{g} \to qq'\tilde{\chi}_1^\pm$, $\tilde{\chi}_1^\pm \to W^\pm\tilde{\chi}_1^0$ decay and a 1/3 probability of having a $\tilde{g} \to qq\tilde{\chi}_2^0$, $\tilde{\chi}_2^0 \to Z^\pm\tilde{\chi}_1^0$ decay.
Tglu1D: gluino pair production with one gluino decaying to $q\bar{q}'\tilde{\chi}_1^\pm$ with $\tilde{\chi}_1^\pm \to W^\pm + \tilde{G}$, and the other gluino decaying to $q\bar{q}\tilde{\chi}_1^0$ with $\tilde{\chi}_1^0 \to \gamma + \tilde{G}$.
Tglu1E: gluino pair production with $\tilde{g} \to qq'\tilde{\chi}_1^\pm$, $\tilde{\chi}_1^\pm \to W^\pm\tilde{\chi}_2^0$ and $\tilde{\chi}_2^0 \to Z^\pm\tilde{\chi}_1^0$ where $m_{\tilde{\chi}_1^\pm} = (m_{\tilde{g}} + m_{\tilde{\chi}_1^0})/2$, $m_{\tilde{\chi}_2^0} = (m_{\tilde{\chi}_1^\pm} + m_{\tilde{\chi}_1^0})/2$.
Tglu1F: gluino pair production with $\tilde{g} \to qq'\tilde{\chi}_1^\pm$ or $\tilde{g} \to qq\tilde{\chi}_2^0$ with equal branching ratios, where $\tilde{\chi}_1^\pm$ decays through an intermediate scalar tau lepton or sneutrino to $\tau\nu\tilde{\chi}_1^0$ and where $\tilde{\chi}_2^0$ decays through an intermediate scalar tau lepton or sneutrino to $\tau^+\tau^-\tilde{\chi}_1^0$ or $\nu\bar{\nu}\tilde{\chi}_1^0$; the mass hierarchy is such that $m_{\chi_1^\pm} \sim m_{\tilde{\chi}_2^0} = (m_{\tilde{g}} + m_{\chi_1^0})/2$ and $m_{\tilde{\tau},\tilde{\nu}} = (m_{\tilde{\chi}_1^\pm} + m_{\tilde{\chi}_1^0})/2$.
Tglu1G: gluino pair production with $\tilde{g} \to q\bar{q}\tilde{\chi}_2^0$, and $\tilde{\chi}_2^0$ decaying through an intermediate slepton or sneutrino to $l^+l^-\tilde{\chi}_1^0$ or $\nu\bar{\nu}\tilde{\chi}_1^0$ where $m_{\tilde{\chi}_2^0} = (m_{\tilde{g}} + m_{\tilde{\chi}_1^0})/2$ and $m_{\tilde{\ell},\tilde{\nu}} = (m_{\tilde{\chi}_2^0} + m_{\tilde{\chi}_1^0})/2$.
Tglu1H: gluino pair production with $\tilde{g} \to q\bar{q}\tilde{\chi}_2^0$, and $\tilde{\chi}_2^0 \to \tilde{\chi}_1^0 Z^{0(*)}$.
Tglu2A: gluino pair production with $\tilde{g} \to b\bar{b}\tilde{\chi}_1^0$.
Tglu3A: gluino pair production with $\tilde{g} \to t\bar{t}\tilde{\chi}_1^0$.
Tglu3B: gluino pair production with $\tilde{g} \to t\bar{\tilde{t}}$ where $\tilde{t}$ decays exclusively to $t\tilde{\chi}_1^0$.
Tglu3C: gluino pair production with $\tilde{g} \to t\bar{\tilde{t}}$ where $\tilde{t}$ decays exclusively to $c\tilde{\chi}_1^0$.
Tglu3D: gluino pair production with $\tilde{g} \to t\bar{b}\tilde{\chi}_1^\pm$ with $\tilde{\chi}_1^\pm \to W^\pm\tilde{\chi}_1^0$.
Tglu3E: gluino pair production where the gluino decays 25% of the time through $\tilde{g} \to t\bar{t}\tilde{\chi}_1^0$, 25% of the time through $\tilde{g} \to b\bar{b}\tilde{\chi}_1^0$ and 50% of the time through $\tilde{g} \to t\bar{b}\tilde{\chi}_1^\pm$ with $\tilde{\chi}_1^\pm \to W^\pm\tilde{\chi}_1^0$
Tglu4A: gluino pair production with one gluino decaying to $q\bar{q}'\tilde{\chi}_1^\pm$ with $\tilde{\chi}_1^\pm \to W^\pm + \tilde{G}$, and the other gluino decaying to $q\bar{q}\tilde{\chi}_1^0$ with $\tilde{\chi}_1^0 \to \gamma + \tilde{G}$.
Tglu4B: gluino pair production with gluinos decaying to $q\bar{q}\tilde{\chi}_1^0$ and $\tilde{\chi}_1^0 \to \gamma + \tilde{G}$.
Tglu4C: gluino pair production with gluinos decaying to $\tilde{g} \to q\bar{q}\tilde{\chi}_1^0$ and $\tilde{\chi}_1^0 \to Z + \tilde{G}$.

Tsqk1: squark pair production with $\tilde{q} \to q\tilde{\chi}_1^0$.
Tsqk2: squark pair production with $\tilde{q} \to q\tilde{\chi}_2^0$ and $\tilde{\chi}_2^0 \to Z + \tilde{\chi}_1^0$.
Tsqk3: squark pair production with $\tilde{q} \to q'\tilde{\chi}_1^\pm$, $\tilde{\chi}_1^\pm \to W^\pm\tilde{\chi}_1^0$ (like Tglu1B but for squarks)
Tsqk4: squark pair production with squarks decaying to $q\tilde{\chi}_1^0$ and $\tilde{\chi}_1^0 \to \gamma + \tilde{G}$.
Tsqk4A: squark pair production with one squark decaying to $q\tilde{\chi}_1^\pm$ with $\tilde{\chi}_1^\pm \to W^\pm + \tilde{G}$, and the other squark decaying to $q\tilde{\chi}_1^0$ with $\tilde{\chi}_1^0 \to \gamma + \tilde{G}$.
Tsqk4B: squark pair production with squarks decaying to $q\tilde{\chi}_1^0$ and $\tilde{\chi}_1^0 \to \gamma + \tilde{G}$.

Tstop1: stop pair production with $\tilde{t} \to t\tilde{\chi}_1^0$.
Tstop2: stop pair production with $\tilde{t} \to b\tilde{\chi}_1^\pm$ with $\tilde{\chi}_1^\pm \to W^\pm\tilde{\chi}_1^0$.
Tstop3: stop pair production with the subsequent four-body decay $\tilde{t} \to bff'\tilde{\chi}_1^0$ where f represents a lepton or a quark.
Tstop4: stop pair production with $\tilde{t} \to c\tilde{\chi}_1^0$.
Tstop5: stop pair production with $\tilde{t} \to b\bar{\nu}\tilde{\tau}$ with $\tilde{\tau} \to \tau\tilde{G}$.
Tstop6: stop pair production with $\tilde{t} \to t + \tilde{\chi}_2^0$, where $\tilde{\chi}_2^0 \to Z + \tilde{\chi}_1^0$ or $H + \tilde{\chi}_1^0$ each with Br=50%.
Tstop7: stop pair production with $\tilde{t}_2 \to \tilde{t}_1 + H/Z$, where $\tilde{t}_1 \to t + \tilde{\chi}_1^0$.
Tstop8: stop pair production with equal probability of the stop decaying via $\tilde{t} \to t\tilde{\chi}_1^0$ or via $\tilde{t} \to b\tilde{\chi}_1^\pm$ with $\tilde{\chi}_1^\pm \to W^\pm\tilde{\chi}_1^0$.
Tstop9: stop pair production with equal probability of the stop decaying via $\tilde{t} \to c\tilde{\chi}_1^0$ or via the four-body decay $\tilde{t} \to bff'\tilde{\chi}_1^0$ where f represents a lepton or a quark.
Tstop10: stop pair production with $\tilde{t} \to b\tilde{\chi}_1^\pm$ and $\tilde{\chi}_1^\pm \to W^{\pm *}\tilde{\chi}_1^0 \to (f\bar{f}') + \tilde{\chi}_1^0$ with a virtual W-boson.
Tstop11: stop pair production with $\tilde{t} \to b\tilde{\chi}_1^\pm$ with $\tilde{\chi}_1^\pm$ decaying through an intermediate slepton to $l\nu\tilde{\chi}_1^0$
Tstop1RPV: stop pair production with $\tilde{t} \to \bar{b}\bar{s}$ via RPV coupling λ''_{323}.

Tsbot1: sbottom pair production with $\tilde{b} \to b\tilde{\chi}_1^0$.
Tsbot2: sbottom pair production with $\tilde{b} \to t\chi_1^-$, $\chi_1^- \to W^-\tilde{\chi}_1^0$.
Tsbot3: sbottom pair production with $\tilde{b} \to b\tilde{\chi}_2^0$, where one of the $\tilde{\chi}_2^0 \to Z^{(*)}\tilde{\chi}_1^0 \to f\bar{f}\tilde{\chi}_1^0$ and the other $\tilde{\chi}_2^0 \to \tilde{\ell}\ell^+ \to \ell^+\ell^-\tilde{\chi}_1^0$.

Tchi1chi1A: electroweak pair and associated production of nearly mass-degenerate charginos $\tilde{\chi}_1^\pm$ and neutralinos $\tilde{\chi}_1^0$, where $\tilde{\chi}_1^\pm$ decays to $\tilde{\chi}_1^0$ plus soft radiation, and where one of the $\tilde{\chi}_1^0$ decays to $\gamma + \tilde{G}$ while the other one decays to $Z/H + \tilde{G}$ (with equal probability).
Tchi1chi1B: electroweak pair production of charginos $\tilde{\chi}_1^\pm$, where $\tilde{\chi}_1^\pm$ decays through an intermediate slepton or sneutrino to $l\nu\tilde{\chi}_1^0$ and where the slepton or sneutrino mass is 5%, 25%, 50%, 75% and 95% of the $\tilde{\chi}_1^\pm$ mass.
Tchi1chi1C: electroweak pair production of charginos $\tilde{\chi}_1^\pm$, where $\tilde{\chi}_1^\pm$ decays through an intermediate slepton or sneutrino to $l\nu\tilde{\chi}_1^0$ and where $m_{\tilde{\ell},\tilde{\nu}} = (m_{\tilde{\chi}_1^\pm} + m_{\tilde{\chi}_1^0})/2$.

Tchi1n1A: electroweak associated production of mass-degenerate charginos $\tilde{\chi}_1^\pm$ and neutralinos $\tilde{\chi}_1^0$, where $\tilde{\chi}_1^\pm$ decays exclusively to $W^\pm + \tilde{G}$ and $\tilde{\chi}_1^0$ decays exclusively to $\gamma + \tilde{G}$.

Tchi1n2A: electroweak associated production of mass-degenerate charginos $\tilde{\chi}_1^\pm$ and neutralinos $\tilde{\chi}_2^0$, where $\tilde{\chi}_1^\pm$ decays through an intermediate slepton or sneutrino to $l\nu\tilde{\chi}_1^0$ and where $\tilde{\chi}_2^0$ decays through an intermediate slepton or sneutrino to $l^+l^-\tilde{\chi}_1^0$ or $\nu\bar{\nu}\tilde{\chi}_1^0$.

Tchi1n2B: electroweak associated production of mass-degenerate charginos $\tilde{\chi}_1^\pm$ and neutralinos $\tilde{\chi}_2^0$, where $\tilde{\chi}_1^\pm$ decays through an intermediate slepton or sneutrino to $l\nu\tilde{\chi}_1^0$ and where $chiz_2$ decays through an intermediate slepton or sneutrino to $l^+l^-\tilde{\chi}_1^0$ or $\nu\bar{\nu}\tilde{\chi}_1^0$ and where the slepton or sneutrino mass is 5%, 25%, 50%, 75% and 95% of the $\tilde{\chi}_1^\pm$ mass.

Tchi1n2C: electroweak associated production of mass-degenerate charginos $\tilde{\chi}_1^\pm$ and neutralinos $\tilde{\chi}_2^0$, where $\tilde{\chi}_1^\pm$ decays through an intermediate slepton or sneutrino to $l\nu\tilde{\chi}_1^0$ and where $chiz_2$ decays through an intermediate slepton or sneutrino to $l^+l^-\tilde{\chi}_1^0$ or $\nu\bar{\nu}\tilde{\chi}_1^0$ and where $m_{\tilde{\ell},\tilde{\nu}} = (m_{\tilde{\chi}_1^\pm} + m_{\tilde{\chi}_1^0})/2$.

Tchi1n2D: electroweak associated production of mass-degenerate charginos $\tilde{\chi}_1^\pm$ and neutralinos $\tilde{\chi}_2^0$, where $\tilde{\chi}_1^\pm$ decays through an intermediate scalar tau lepton or sneutrino to $\tau\nu\tilde{\chi}_1^0$ and where $chiz_2$ decays through an intermediate scalar tau lepton or sneutrino to $\tau^+\tau^-\tilde{\chi}_1^0$ or $\nu\bar{\nu}\tilde{\chi}_1^0$ and where $m_{\tilde{\tau},\tilde{\nu}} = (m_{\tilde{\chi}_1^\pm} + m_{\tilde{\chi}_1^0})/2$.

Tchi1n2E: electroweak associated production of mass-degenerate charginos $\tilde{\chi}_1^\pm$ and neutralinos $\tilde{\chi}_2^0$, where $\tilde{\chi}_1^\pm \to W^\pm + \tilde{\chi}_1^0$ and $\tilde{\chi}_2^0 \to H + \tilde{\chi}_1^0$.

Tn2n3A: electroweak associated production of mass-degenerate neutralinos $\tilde{\chi}_2^0$ and $\tilde{\chi}_3^0$, where $\tilde{\chi}_2^0$ and $\tilde{\chi}_3^0$ decay through intermediate sleptons to $l^+l^-\tilde{\chi}_1^0$ and where the slepton mass is 5%, 25%, 50%, 75% and 95% of the $\tilde{\chi}_2^0$ mass.

Tn2n3B: electroweak associated production of mass-degenerate neutralinos $\tilde{\chi}_2^0$ and $\tilde{\chi}_3^0$, where $\tilde{\chi}_2^0$ and $\tilde{\chi}_3^0$ decay through intermediate sleptons to $l^+l^-\tilde{\chi}_1^0$ and where $m_{\tilde{\ell}} = (m_{\tilde{\chi}_2^0} + m_{\tilde{\chi}_1^0})/2$.

$\tilde{\chi}_1^0$ (Lightest Neutralino) mass limit

$\tilde{\chi}_1^0$ is often assumed to be the lightest supersymmetric particle (LSP). See also the $\tilde{\chi}_2^0$, $\tilde{\chi}_3^0$, $\tilde{\chi}_4^0$ section below.

We have divided the $\tilde{\chi}_1^0$ listings below into five sections:

1) Accelerator limits for stable $\tilde{\chi}_1^0$,

2) Bounds on $\tilde{\chi}_1^0$ from dark matter searches,

3) $\tilde{\chi}_1^0 - p$ elastic cross section (spin-dependent, spin-independent interactions),

4) Other bounds on $\tilde{\chi}_1^0$ from astrophysics and cosmology, and

5) Unstable $\tilde{\chi}_1^0$ (Lightest Neutralino) mass limit.

Accelerator limits for stable $\tilde{\chi}_1^0$

Unless otherwise stated, results in this section assume spectra, production rates, decay modes, and branching ratios as evaluated in the MSSM, with gaugino and sfermion mass unification at the GUT scale. These papers generally study production of $\tilde{\chi}_i^0\tilde{\chi}_j^0$ ($i \geq 1$, $j \geq 2$), $\tilde{\chi}_1^+\tilde{\chi}_1^-$, and (in the case of hadronic collisions) $\tilde{\chi}_1^+\tilde{\chi}_2^0$ pairs. The mass limits on $\tilde{\chi}_1^0$ are either direct, or follow indirectly from the constraints set by the non-observation of $\tilde{\chi}_1^\pm$ and $\tilde{\chi}_2^0$ states on the gaugino and higgsino MSSM parameters M_2 and μ. In some cases, information is used from the nonobservation of slepton decays.

Obsolete limits obtained from e^+e^- collisions up to $\sqrt{s}$=184 GeV have been removed from this compilation and can be found in the 2000 Edition (The European Physical Journal **C15** 1 (2000)) of this Review. $\Delta m = m_{\tilde{\chi}_2^0} - m_{\tilde{\chi}_1^0}$.

VALUE (GeV)	CL%	DOCUMENT ID		TECN	COMMENT
		[1] DREINER	09	THEO	
>40	95	[2] ABBIENDI	04H	OPAL	all tanβ, Δm >5 GeV, m_0 >500 GeV, $A_0 = 0$
>42.4	95	[3] HEISTER	04	ALEP	all tanβ, all Δm, all m_0
>39.2	95	[4] ABDALLAH	03M	DLPH	all tanβ, $m_{\tilde{\nu}}$ >500 GeV
>46	95	[5] ABDALLAH	03M	DLPH	all tanβ, all Δm, all m_0
>32.5	95	[6] ACCIARRI	00D	L3	tan$\beta > 0.7$, $\Delta m > 3$ GeV, all m_0
• • • We do not use the following data for averages, fits, limits, etc. • • •					
		[7] AAD	14K	ATLS	

[1] DREINER 09 show that in the general MSSM with non-universal gaugino masses there exists no model-independent laboratory bound on the mass of the lightest neutralino. An essentially massless χ_1^0 is allowed by the experimental and observational data, imposing some constraints on other MSSM parameters, including M_2, μ and the slepton and squark masses.

[2] ABBIENDI 04H search for charginos and neutralinos in events with acoplanar leptons+jets and multi-jet final states in the 192–209 GeV data, combined with the results on leptonic final states from ABBIENDI 04. The results hold for a scan over the parameter space covering the region $0 < M_2 < 5000$ GeV, $-1000 < \mu < 1000$ GeV and tanβ from 1 to 40. This limit supersedes ABBIENDI 00H.

[3] HEISTER 04 data collected up to 209 GeV. Updates earlier analysis of selectrons from HEISTER 02E, includes a new analysis of charginos and neutralinos decaying into stau and uses results on charginos with initial state radiation from HEISTER 02J. The limit is based on the direct search for charginos and neutralinos, the constraints from the slepton search and the Higgs mass limits from HEISTER 02 using a top mass of 175 GeV, interpreted in a framework with universal gaugino and sfermion masses. Assuming the mixing in the stau sector to be negligible, the limit improves to 43.1 GeV. Under the assumption of MSUGRA with unification of the Higgs and sfermion masses, the limit improves to 50 GeV, and reaches 53 GeV for $A_0 = 0$. These limits include and update the results of BARATE 01.

[4] ABDALLAH 03M uses data from $\sqrt{s} = 192$–208 GeV. A limit on the mass of $\tilde{\chi}_1^0$ is derived from direct searches for neutralinos combined with the chargino search. Neutralinos are searched in the production of $\tilde{\chi}_1^0\tilde{\chi}_2^0$, $\tilde{\chi}_1^0\tilde{\chi}_3^0$, as well as $\tilde{\chi}_2^0\tilde{\chi}_3^0$ and $\tilde{\chi}_2^0\tilde{\chi}_4^0$ giving rise to cascade decays, and $\tilde{\chi}_1^0\tilde{\chi}_2^0$ and $\tilde{\chi}_1^0\tilde{\chi}_2^0$, followed by the decay $\tilde{\chi}_2^0 \to \tilde{\tau}\tau$. The results hold for the parameter space defined by values of $M_2 < 1$ TeV, $|\mu| \leq 2$ TeV with the $\tilde{\chi}_1^0$ as LSP. The limit is obtained for tan$\beta = 1$ and large m_0, where $\tilde{\chi}_2^0\tilde{\chi}_4^0$ and chargino pair production are important. If the constraint from Higgs searches is also imposed, the limit improves to 49.0 GeV in the $m_h^{\max}$ scenario with m_t=174.3 GeV. These limits update the results of ABREU 00J.

[5] ABDALLAH 03M uses data from $\sqrt{s}$ = 192–208 GeV. An indirect limit on the mass of $\tilde{\chi}_1^0$ is derived by constraining the MSSM parameter space by the results from direct searches for neutralinos (including cascade decays and $\tilde{\tau}\tau$ final states), for charginos (for all Δm_+) and for sleptons, stop and sbottom. The results hold for the full parameter space defined by values of $M_2 < 1$ TeV, $|\mu| \leq 2$ TeV with the $\tilde{\chi}_1^0$ as LSP. Constraints from the Higgs search in the $m_h^{\max}$ scenario assuming m_t=174.3 GeV are included. The limit is obtained for tan$\beta \geq 5$ when stau mixing leads to mass degeneracy between $\tilde{\tau}_1$ and $\tilde{\chi}_1^0$ and the limit is based on $\tilde{\chi}_2^0$ production followed by its decay to $\tilde{\tau}_1\tau$. In the pathological scenario where m_0 and $|\mu|$ are large, so that the $\tilde{\chi}_2^0$ production cross section is negligible, and where there is mixing in the stau sector but not in stop nor sbottom, the limit is based on charginos with soft decay products and an ISR photon. The limit then degrades to 39 GeV. See Figs. 40–42 for the dependence of the limit on tanβ and $m_{\tilde{\nu}}$. These limits update the results of ABREU 00W.

[6] ACCIARRI 00D data collected at $\sqrt{s}$=189 GeV. The results hold over the full parameter space defined by $0.7 \leq$ tan$\beta \leq 60$, $0 \leq M_2 \leq 2$ TeV, $m_0 \leq 500$ GeV, $|\mu| \leq 2$ TeV The minimum mass limit is reached for tanβ=1 and large m_0. The results of slepton searches from ACCIARRI 99W are used to help set constraints in the region of small m_0. The limit improves to 48 GeV for $m_0 \gtrsim 200$ GeV and tan$\beta \gtrsim 10$. See their Figs. 6–8 for the tanβ and m_0 dependence of the limits. Updates ACCIARRI 98F.

[7] AAD 14K sets limits on the χ-nucleon spin-dependent and spin-independent cross sections out to $m_\chi = 10$ TeV.

Bounds on $\tilde{\chi}_1^0$ from dark matter searches

These papers generally exclude regions in the $M_2 - \mu$ parameter plane assuming that $\tilde{\chi}_1^0$ is the dominant form of dark matter in the galactic halo. These limits are based on the lack of detection in laboratory experiments, telescopes, or by the absence of a signal in underground neutrino detectors. The latter signal is expected if $\tilde{\chi}_1^0$ accumulates in the Sun or the Earth and annihilates into high-energy ν's.

VALUE	DOCUMENT ID		TECN
• • • We do not use the following data for averages, fits, limits, etc. • • •			
	[1] AARTSEN	17	ICCB
	[2] AARTSEN	17A	ICCB
	[3] AARTSEN	17C	ICCB
	[4] ALBERT	17A	ANTR
	[5] ARCHAMBAU..	17	VRTS
	[6] AARTSEN	16D	ICCB
	[7] ABDALLAH	16	HESS
	[8] ABDALLAH	16A	HESS
	[9] ADRIAN-MAR..	16	ANTR
	[10] AHNEN	16	MGFL
	[11] AVRORIN	16	BAIK
	[12] CIRELLI	16	THEO
	[12] LEITE	16	THEO
	[13] ABRAMOWSKI	15	HESS
	[14] ACKERMANN	15	FLAT
	[15] ACKERMANN	15A	FLAT
	[16] ACKERMANN	15B	FLAT
	[17] BUCKLEY	15	THEO
	[18] CHOI	15	SKAM
	[19] ALEKSIC	14	MGIC
	[20] AVRORIN	14	BAIK
	[21] AARTSEN	13C	ICCB
	[22] ABRAMOWSKI	13	HESS
	[23] BERGSTROM	13	COSM
	[24] BOLIEV	13	BAKS

[23] JIN 13 ASTR
[23] KOPP 13 COSM
[25] ABBASI 12 ICCB
[26] ABRAMOWSKI 11 HESS
[27] ABDO 10 FLAT
[28] ACKERMANN 10 FLAT
[29] ACHTERBERG 06 AMND
[30] ACKERMANN 06 AMND
[31] DEBOER 06 RVUE
[32] DESAI 04 SKAM
[32] AMBROSIO 99 MCRO
[33] LOSECCO 95 RVUE
[34] MORI 93 KAMI
[35] BOTTINO 92 COSM
[36] BOTTINO 91 RVUE
[37] GELMINI 91 COSM
[38] KAMIONKOW.. 91 RVUE
[39] MORI 91B KAMI
[40] OLIVE 88 COSM

none 4–15 GeV

[1] AARTSEN 17 is based on data collected during 327 days of detector livetime with IceCube. They looked for interactions of ν's resulting from neutralino annihilations in the Earth over a background of atmospheric neutrinos and set 90% CL limits on the spin independent neutralino-proton cross section for neutralino masses in the range 10–10000 GeV.

[2] AARTSEN 17A is based on data collected during 532 days of livetime with the IceCube 86-string detector including the DeepCore sub-array. They looked for interactions of ν's from neutralino annihilations in the Sun over a background of atmospheric neutrinos and set 90% CL limits on the spin dependent neutralino-proton cross section for neutralino masses in the range 10–10000 GeV. This updates AARTSEN 16C.

[3] AARTSEN 17C is based on 1005 days of running with the IceCube detector. They set a limit on the annihilation cross section for dark matter with masses between 10–1000 GeV annihilating in the Galactic center assuming an NFW profile. The limit is of 1.2×10^{23} cm^{3}s^{-1} in the $\tau^+\tau^-$ channel. Supercedes AARTSEN 15E.

[4] ALBERT 17A is based on data from the ANTARES neutrino telescope. They looked for interactions of ν's from neutralino annihilations in the Milky Way galaxy over a background of atmospheric neutrinos and set 90% CL limits on the muon neutrino flux. They also obtain limits on the thermally averaged cross section for neutralino masses in the range 50 to 100,000 GeV. This updates ADRIAN-MARTINEZ 15.

[5] ARCHAMBAULT 17 performs a joint statistical analysis of four dwarf galaxies with VERITAS looking for gamma-ray emission from neutralino annihilation. They set limits on the neutralino annihilation cross section.

[6] AARTSEN 16D is based on 329 live days of running with the DeepCore subdetector of the IceCube detector. They set a limit of 10^{-23} cm^{3}s^{-1} on the annihilation cross section to $\nu\overline{\nu}$. This updates AARTSEN 15C.

[7] ABDALLAH 16 places constraints on the dark matter annihilation cross section for annihilations in the Galactic center for masses between 200 GeV to 70 TeV. This updates ABRAMOWSKI 15.

[8] ABDALLAH 16A place upper limits on the annihilation cross section with final states in the energy range of 0.1 to 2 TeV. This complements ABRAMOWSKI 13.

[9] ADRIAN-MARTINEZ 16 is based on data from the ANTARES neutrino telescope. They looked for interactions of ν's from neutralino annihilations in the Sun over a background of atmospheric neutrinos and set 90% CL limits on the muon neutrino flux. They also obtain limits on the spin dependent and spin independent neutralino-proton cross section for neutralino masses in the range 50 to 5,000 GeV. This updates ADRIAN-MARTINEZ 13.

[10] AHNEN 16 combines 158 hours of Segue 1 observations with MAGIC with 6 year observations of 15 dwarf satellite galaxies by Fermi-LAT to set limits on annihilation cross sections for dark matter masses between 10 GeV and 100 TeV.

[11] AVRORIN 16 is based on 2.76 years with Lake Baikal neutrino telescope. They derive 90% upper limits on the annihilation cross section from dark matter annihilations in the Galactic center.

[12] CIRELLI 16 and LEITE 16 derive bounds on the annihilation cross section from radio observations.

[13] ABRAMOWSKI 15 places constraints on the dark matter annihilation cross section for annihilations in the Galactic center for masses between 300 GeV to 10 TeV.

[14] ACKERMANN 15 is based on 5.8 years of data with Fermi-LAT and search for monochromatic gamma-rays in the energy range of 0.2–500 GeV from dark matter annihilations. This updates ACKERMANN 13A.

[15] ACKERMANN 15A is based on 50 months of data with Fermi-LAT and search for dark matter annihilation signals in the isotropic gamma-ray background as well as galactic subhalos in the energy range of a few GeV to a few tens of TeV.

[16] ACKERMANN 15B is based on 6 years of data with Fermi-LAT observations of Milky Way dwarf spheroidal galaxies. Set limits on the annihilation cross section from $m_\chi =$ 2 GeV to 10 TeV. This updates ACKERMANN 14.

[17] BUCKLEY 15 is based on 5 years of Fermi-LAT data searching for dark matter annihilation signals from Large Magellanic Cloud.

[18] CHOI 15 is based on 3903 days of SuperKamiokande data searching for neutrinos produced from dark matter annihilations in the sun. They place constraints on the dark matter-nucleon scattering cross section for dark matter masses between 4–200 GeV.

[19] ALEKSIC 14 is based on almost 160 hours of observations of Segue 1 satellite dwarf galaxy using the MAGIC telescopes between 2011 and 2013. Sets limits on the annihilation cross section out to $m_\chi = 10$ TeV.

[20] AVRORIN 14 is based on almost 2.76 years with Lake Baikal neutrino telescope. They derive 90% upper limits on the fluxes of muons and muon neutrinos from dark matter annihilations in the Sun.

[21] AARTSEN 13C is based on data collected during 339.8 effective days with the IceCube 59-string detector. They looked for interactions of ν_μ's from neutralino annihilations in nearby galaxies and galaxy clusters. They obtain limits on the neutralino annihilation cross section for neutralino masses in the range 30–100,000 GeV.

[22] ABRAMOWSKI 13 place upper limits on the annihilation cross section with $\gamma\gamma$ final states in the energy range of 0.5–25 TeV.

[23] BERGSTROM 13, JIN 13, and KOPP 13 derive limits on the mass and annihilation cross section using AMS-02 data. JIN 13 also sets a limit on the lifetime of the dark matter particle.

[24] BOLIEV 13 is based on data collected during 24.12 years of live time with the Bakson Underground Scintillator Telescope. They looked for interactions of ν_μ's from neutralino annihilations in the Sun over a background of atmospheric neutrinos and set 90% CL limits on the muon flux. They also obtain limits on the spin dependent and spin independent neutralino-proton cross section for neutralino masses in the range 10–1000 GeV.

[25] ABBASI 12 is based on data collected during 812 effective days with AMANDA II and 149 days of the IceCube 40-string detector combined with the data of ABBASI 09B. They looked for interactions of ν_μ's from neutralino annihilations in the Sun over a background of atmospheric neutrinos and set 90% CL limits on the muon flux. No excess is observed. They also obtain limits on the spin dependent neutralino-proton cross section for neutralino masses in the range 50–5000 GeV.

[26] ABRAMOWSKI 11 place upper limits on the annihilation cross section with $\gamma\gamma$ final states.

[27] ABDO 10 place upper limits on the annihilation cross section with $\gamma\gamma$ or $\mu^+\mu^-$ final states.

[28] ACKERMANN 10 place upper limits on the annihilation cross section with $b\overline{b}$ or $\mu^+\mu^-$ final states.

[29] ACHTERBERG 06 is based on data collected during 421.9 effective days with the AMANDA detector. They looked for interactions of ν_μs from the centre of the Earth over a background of atmospheric neutrinos and set 90 % CL limits on the muon flux. Their limit is compared with the muon flux expected from neutralino annihilations into W^+W^- and $b\overline{b}$ at the centre of the Earth for MSSM parameters compatible with the relic dark matter density, see their Fig. 7.

[30] ACKERMANN 06 is based on data collected during 143.7 days with the AMANDA-II detector. They looked for interactions of ν_μs from the Sun over a background of atmospheric neutrinos and set 90 % CL limits on the muon flux. Their limit is compared with the muon flux expected from neutralino annihilations into W^+W^- in the Sun for SUSY model parameters compatible with the relic dark matter density, see their Fig. 3.

[31] DEBOER 06 interpret an excess of diffuse Galactic gamma rays observed with the EGRET satellite as originating from π^0 decays from the annihilation of neutralinos into quark jets. They analyze the corresponding parameter space in a supergravity inspired MSSM model with radiative electroweak symmetry breaking, see their Fig. 3 for the preferred region in the $(m_0, m_{1/2})$ plane of a scenario with large tanβ.

[32] AMBROSIO 99 and DESAI 04 set new neutrino flux limits which can be used to limit the parameter space in supersymmetric models based on neutralino annihilation in the Sun and the Earth.

[33] LOSECCO 95 reanalyzed the IMB data and places lower limit on $m_{\widetilde{\chi}^0_1}$ of 18 GeV if the LSP is a photino and 10 GeV if the LSP is a higgsino based on LSP annihilation in the sun producing high-energy neutrinos and the limits on neutrino fluxes from the IMB detector.

[34] MORI 93 excludes some region in M_2–μ parameter space depending on tanβ and lightest scalar Higgs mass for neutralino dark matter $m_{\widetilde{\chi}^0} > m_W$, using limits on upgoing muons produced by energetic neutrinos from neutralino annihilation in the Sun and the Earth.

[35] BOTTINO 92 excludes some region M_2-μ parameter space assuming that the lightest neutralino is the dark matter, using upgoing muons at Kamiokande, direct searches by Ge detectors, and by LEP experiments. The analysis includes top radiative corrections on Higgs parameters and employs two different hypotheses for nucleon-Higgs coupling. Effects of rescaling in the local neutralino density according to the neutralino relic abundance are taken into account.

[36] BOTTINO 91 excluded a region in $M_2 - \mu$ plane using upgoing muon data from Kamioka experiment, assuming that the dark matter surrounding us is composed of neutralinos and that the Higgs boson is not too heavy.

[37] GELMINI 91 exclude a region in $M_2 - \mu$ plane using dark matter searches.

[38] KAMIONKOWSKI 91 excludes a region in the M_2–μ plane using IMB limit on upgoing muons originated by energetic neutrinos from neutralino annihilation in the sun, assuming that the dark matter is composed of neutralinos and that $m_{H^0_1} \lesssim 50$ GeV. See Fig. 8 in the paper.

[39] MORI 91B exclude a part of the region in the M_2–μ plane with $m_{\widetilde{\chi}^0_1} \lesssim 80$ GeV using a limit on upgoing muons originated by energetic neutrinos from neutralino annihilation in the earth, assuming that the dark matter surrounding us is composed of neutralinos and that $m_{H^0_1} \lesssim 80$ GeV.

[40] OLIVE 88 result assumes that photinos make up the dark matter in the galactic halo. Limit is based on annihilations in the sun and is due to an absence of high energy neutrinos detected in underground experiments. The limit is model dependent.

$\widetilde{\chi}^0_1$-p elastic cross section

Experimental results on the $\widetilde{\chi}^0_1$-p elastic cross section are evaluated at $m_{\widetilde{\chi}^0_1}$=100 GeV. The experimental results on the cross section are often mass dependent. Therefore, the mass and cross section results are also given where the limit is strongest, when appropriate. Results are quoted separately for spin-dependent interactions (based on an effective 4-Fermi Lagrangian of the form $\overline{\chi}\gamma^\mu\gamma^5\chi\overline{q}\gamma_\mu\gamma^5 q$) and spin-independent interactions ($\overline{\chi}\chi\overline{q}q$). For calculational details see GRIEST 88B, ELLIS 88D, BARBIERI 89C, DREES 93B, ARNOWITT 96, BERGSTROM 96, and BAER 97 in addition to the theory papers listed in the Tables. For a description of the theoretical assumptions and experimental techniques underlying most of the listed papers, see the review on "Dark matter" in this "Review of Particle Physics," and references therein. Most of the following papers use galactic halo and nuclear interaction assumptions from (LEWIN 96).

Spin-dependent interactions

VALUE (pb)	CL%	DOCUMENT ID		TECN	COMMENT
• • • We do not use the following data for averages, fits, limits, etc. • • •					
$< 8 \times 10^{-4}$	90	[1] AKERIB	17A	LUX	Xe
$< 5 \times 10^{-5}$	90	[2] AMOLE	17	PICO	C_3F_8
< 0.28	90	[3] BATTAT	17	DRFT	CS_2; CF_4
< 0.027	90	[4] BEHNKE	17	PICA	C_4F_{10}
$< 2 \times 10^{-3}$	90	[5] FU	17	PNDX	Xe
$< 5 \times 10^{-4}$	90	[6] AMOLE	16	PICO	CF_3I

$<$ 6.8	$\times 10^{-3}$	90	[7] APRILE	16B	X100 Xe
$<$ 6.3	$\times 10^{-3}$	90	[8] FELIZARDO	14	SMPL C_2ClF_5
$<$ 0.01		90	[9] AKIMOV	12	ZEP3 Xe
$<$ 7	$\times 10^{-3}$		[10] BEHNKE	12	COUP CF_3I
$<$ 8.5	$\times 10^{-3}$		[11] FELIZARDO	12	SMPL C_2ClF_5
$<$ 0.016		90	[12] KIM	12	KIMS CsI
5×10^{-10} to 10^{-5}		95	[13] BUCHMUEL...	11B	THEO
$<$ 1		90	[14] ANGLE	08A	XE10 Xe
$<$ 0.055			[15] BEDNYAKOV	08	HDMS Ge
$<$ 0.33		90	[16] BEHNKE	08	COUP CF_3I
$<$ 5			[17] AKERIB	06	CDMS Ge
$<$ 2			[18] SHIMIZU	06A	CNTR CaF_2
$<$ 0.4			[19] ALNER	05	NAIA NaI Spin Dep.
$<$ 2			[20] BARNABE-HE...	05	PICA C
2×10^{-11} to 1×10^{-4}			[21] ELLIS	04	THEO $\mu > 0$
$<$ 0.8			[22] AHMED	03	NAIA NaI Spin Dep.
$<$ 40			[23] TAKEDA	03	BOLO NaF Spin Dep.
$<$ 10			[24] ANGLOHER	02	CRES Saphire
8×10^{-7} to 2×10^{-5}			[25] ELLIS	01C	THEO $\tan\beta \leq 10$
$<$ 3.8			[26] BERNABEI	00D	DAMA Xe
$<$ 0.8			SPOONER	00	UKDM NaI
$<$ 4.8			[27] BELLI	99C	DAMA F
$<$100			[28] OOTANI	99	BOLO LiF
$<$ 0.6			BERNABEI	98C	DAMA Xe
$<$ 5			[27] BERNABEI	97	DAMA F

[1] The strongest limit is 5×10^{-4} pb at $m_\chi = 35$ GeV. The limit for scattering on neutrons is 3×10^{-5} pb at 100 GeV and is 1.6×10^{-5} pb at 35 GeV. This updates AKERIB 16A.

[2] The strongest limit is 3.4×10^{-5} pb at $m_\chi = 30$ GeV. This updates AMOLE 16A.

[3] Directional recoil detector. This updates DAW 12.

[4] This result updates ARCHAMBAULT 12. The strongest limit is 0.013 pb at $m_\chi = 20$ GeV.

[5] The strongest limit is 1.2×10^{-3} pb at 40 GeV. The limit for scattering on neutrons is 5×10^{-5} pb at 100 GeV and the strongest limit is 4.1×10^{-5} pb at 40 GeV.

[6] The strongest limit is 5×10^{-4} pb at $m_\chi = 80$ GeV.

[7] The strongest limit is 5.2×10^{-3} pb at 50 GeV. The limit for scattering on neutrons is 2.8×10^{-4} pb at 100 GeV and the strongest limit is 2.0×10^{-4} pb at 50 GeV. This updates APRILE 13.

[8] The strongest limit is 0.0043 pb and occurs at $m_\chi = 35$ GeV. FELIZARDO 14 also presents limits for the scattering on neutrons. At $m_\chi = 100$ GeV, the upper limit is 0.13 pb and the strongest limit is 0.066 pb at $m_\chi = 35$ GeV.

[9] This result updates LEBEDENKO 09A. The strongest limit is 8×10^{-3} pb at $m_\chi = 50$ GeV. Limit applies to the neutralino neutron elastic cross section.

[10] The strongest limit is 6×10^{-3} at $m_\chi = 60$ GeV.

[11] The strongest limit is 5.7×10^{-3} at $m_\chi = 35$ GeV.

[12] This result updates LEE 07A. The strongest limit is at $m_\chi = 80$ GeV.

[13] Predictions for the spin-dependent elastic cross section based on a frequentist approach to electroweak observables in the framework of $N = 1$ supergravity models with radiative breaking of the electroweak gauge symmetry.

[14] The strongest limit is 0.6 pb and occurs at m_χ= 30 GeV. The limit for scattering on neutrons is 0.01 pb at m_χ= 100 GeV, and the strongest limit is 0.0045 pb at m_χ= 30 GeV.

[15] Limit applies to neutron elastic cross section.

[16] The strongest upper limit is 0.25 pb and occurs at $m_\chi \simeq 40$ GeV.

[17] The strongest upper limit is 4 pb and occurs at $m_\chi \simeq 60$ GeV. The limit on the neutron spin-dependent elastic cross section is 0.07 pb. This latter limit is improved in AHMED 09, where a limit of 0.02 pb is obtained at $m_\chi = 100$ GeV. The strongest limit in AHMED 09 is 0.018 pb and occurs at $m_\chi = 60$ GeV.

[18] The strongest upper limit is 1.2 pb and occurs at $m_\chi \simeq 40$ GeV. The limit on the neutron spin-dependent cross section is 35 pb.

[19] The strongest upper limit is 0.35 pb and occurs at $m_\chi \simeq 60$ GeV.

[20] The strongest upper limit is 1.2 pb and occurs $m_\chi \simeq 30$ GeV.

[21] ELLIS 04 calculates the χp elastic scattering cross section in the framework of N=1 supergravity models with radiative breaking of the electroweak gauge symmetry, but without universal scalar masses. In the case of universal squark and slepton masses, but non-universal Higgs masses, the limit becomes 2×10^{-4}, see ELLIS 03E.

[22] The strongest upper limit is 0.75 pb and occurs at $m_\chi \approx 70$ GeV.

[23] The strongest upper limit is 30 pb and occurs at $m_\chi \approx 20$ GeV.

[24] The strongest upper limit is 8 pb and occurs at $m_\chi \simeq 30$ GeV.

[25] ELLIS 01C calculates the χ-p elastic scattering cross section in the framework of N=1 supergravity models with radiative breaking of the electroweak gauge symmetry. In models with nonuniversal Higgs masses, the upper limit to the cross section is 6×10^{-4}.

[26] The strongest upper limit is 3 pb and occurs at $m_\chi \simeq 60$ GeV. The limits are for inelastic scattering $X^0 + {}^{129}Xe \rightarrow X^0 + {}^{129}Xe^*$ (39.58 keV).

[27] The strongest upper limit is 4.4 pb and occurs at $m_\chi \simeq 60$ GeV.

[28] The strongest upper limit is about 35 pb and occurs at $m_\chi \simeq 15$ GeV.

Spin-independent interactions

VALUE (pb)	CL%	DOCUMENT ID		TECN	COMMENT
• • • We do not use the following data for averages, fits, limits, etc. • • •					
$<1.8\times10^{-10}$	90	[1] AKERIB	17	LUX	Xe
$<1.5\times10^{-10}$	90	[2] APRILE	17G	XE1T	Xe
$<1.4\times10^{-10}$	90	[3] CUI	17A	PNDX	Xe
$<3\times10^{-8}$	90	AMOLE	16	PICO	CF_3I
$<1.5\times10^{-9}$	90	[4] APRILE	16B	X100	Xe
$<6.1\times10^{-8}$	90	AGNES	15	DS50	Ar
$<2.2\times10^{-8}$	90	[5] AGNESE	15B	CDMS	Ge
$<1.5\times10^{-9}$	90	[6] AKERIB	14	LUX	Xe
10^{-11}–10^{-7}	95	[7] BUCHMUEL...	14A	THEO	
$<4.6\times10^{-6}$	90	[8] FELIZARDO	14	SMPL	C_2ClF_5
10^{-11}–10^{-8}	95	[9] ROSZKOWSKI	14	THEO	
$<2.2\times10^{-6}$	90	[10] AGNESE	13	CDMS	Si
$<5\times10^{-8}$	90	[11] AKIMOV	12	ZEP3	Xe
1.6×10^{-6}; 3.7×10^{-5}		[12] ANGLOHER	12	CRES	$CaWO_4$
3×10^{-12} to 3×10^{-9}	95	[13] BECHTLE	12	THEO	
$<1.6\times10^{-7}$		[14] BEHNKE	12	COUP	CF_3I
$<6.5\times10^{-6}$		[15] FELIZARDO	12	SMPL	C_2ClF_5
$<2.3\times10^{-7}$	90	[16] KIM	12	KIMS	CsI
$<3.3\times10^{-8}$	90	[17] AHMED	11A		Ge
$<4.4\times10^{-8}$	90	[18] ARMENGAUD	11	EDE2	Ge
$<7\times10^{-7}$	90	[19] ANGLOHER	09	CRES	$CaWO_4$
$<1\times10^{-7}$	90	[20] ANGLE	08	XE10	Xe
$<1\times10^{-6}$	90	BENETTI	08	WARP	Ar
$<7.5\times10^{-7}$	90	[21] ALNER	07A	ZEP2	Xe
$<2\times10^{-7}$		[22] AKERIB	06A	CDMS	Ge
$<90\times10^{-7}$		ALNER	05	NAIA	NaI Spin Indep.
$<12\times10^{-7}$		[23] ALNER	05A	ZEPL	
$<20\times10^{-7}$		[24] ANGLOHER	05	CRES	$CaWO_4$
$<14\times10^{-7}$		SANGLARD	05	EDEL	Ge
$<4\times10^{-7}$		[25] AKERIB	04	CDMS	Ge
2×10^{-11} to 1.5×10^{-7}	95	[26] BALTZ	04	THEO	
2×10^{-11} to 8×10^{-6}		[27,28] ELLIS	04	THEO	$\mu > 0$
$<5\times10^{-8}$		[29] PIERCE	04A	THEO	
$<2\times10^{-5}$		[30] AHMED	03	NAIA	NaI Spin Indep.
$<3\times10^{-6}$		[31] AKERIB	03	CDMS	Ge
2×10^{-13} to 2×10^{-7}		[32] BAER	03A	THEO	
$<1.4\times10^{-5}$		[33] KLAPDOR-K...	03	HDMS	Ge
$<6\times10^{-6}$		[34] ABRAMS	02	CDMS	Ge
$<1.4\times10^{-6}$		[35] BENOIT	02	EDEL	Ge
1×10^{-12} to 7×10^{-6}		[27] KIM	02B	THEO	
$<3\times10^{-5}$		[36] MORALES	02B	CSME	Ge
$<1\times10^{-5}$		[37] MORALES	02C	IGEX	Ge
$<1\times10^{-6}$		BALTZ	01	THEO	
$<3\times10^{-5}$		[38] BAUDIS	01	HDMS	Ge
$<4.5\times10^{-6}$		BENOIT	01	EDEL	Ge
$<7\times10^{-6}$		[39] BOTTINO	01	THEO	
$<1\times10^{-8}$		[40] CORSETTI	01	THEO	$\tan\beta \leq 25$
5×10^{-10} to 1.5×10^{-8}		[41] ELLIS	01C	THEO	$\tan\beta \leq 10$
$<4\times10^{-6}$		[40] GOMEZ	01	THEO	
2×10^{-10} to 1×10^{-7}		[40] LAHANAS	01	THEO	
$<3\times10^{-6}$		ABUSAIDI	00	CDMS	Ge, Si
$<6\times10^{-7}$		[42] ACCOMANDO	00	THEO	
		[43] BERNABEI	00	DAMA	NaI
2.5×10^{-9} to 3.5×10^{-8}		[44] FENG	00	THEO	$\tan\beta$=10
$<1.5\times10^{-5}$		MORALES	00	IGEX	Ge
$<4\times10^{-5}$		SPOONER	00	UKDM	NaI
$<7\times10^{-6}$		BAUDIS	99	HDMO	^{76}Ge
$<7\times10^{-6}$		BERNABEI	98C	DAMA	Xe

[1] The strongest limit is 1.1×10^{-10} at 50 GeV. This updates AKERIB 16.

[2] The strongest limit is 7.7×10^{-11} pb at $m_\chi = 35$ GeV.

[3] The strongest limit is 8.6×10^{-11} pb at 40 GeV. This updates TAN 16B.

[4] The strongest limit is 1.1×10^{-9} pb at 50 GeV. This updates APRILE 12.

[5] AGNESE 15B result updates AHMED 10 and AHMED 09. The strongest limit is 1.8×10^{-8} pb and occurs at $m_\chi = 60$ GeV.

[6] The strongest upper limit is 7.6×10^{-10} at $m_\chi = 33$ GeV.

[7] Predictions for the spin-independent elastic cross section based on a frequentist approach to electroweak observables in the framework of $N = 1$ supergravity models with radiative breaking of the electroweak gauge symmetry using the 20 fb^{-1} 8 TeV and the 5 fb^{-1} 7 TeV LHC data and the LUX data.

[8] The strongest limit is 3.6×10^{-6} pb and occurs at $m_\chi = 35$ GeV.

[9] Predictions for the spin-independent elastic cross section based on a Bayesian approach to electroweak observables in the framework of $N = 1$ supergravity models with radiative breaking of the electroweak gauge symmetry using the 20 fb^{-1} LHC data and LUX.

[10] AGNESE 13 presents 90% CL limits on the elastic cross section for masses in the range 7–100 GeV using the Si based detector. The strongest upper limit is 1.8×10^{-6} pb at $m_\chi = 50$ GeV. This limit is improved to 7×10^{-7} pb in AGNESE 13A.

[11] This result updates LEBEDENKO 09. The strongest limit is 3.9×10^{-8} pb at m_χ = 52 GeV.

[12] ANGLOHER 12 presents results of 730 kg days from the CRESST-II dark matter detector. They find two maxima in the likelihood function corresponding to best fit WIMP masses of 25.3 and 11.6 GeV with elastic cross sections of 1.6×10^{-6} and 3.7×10^{-5} pb respectively, see their Table 4. The statistical significance is more than 4σ.

[13] Predictions for the spin-independent elastic cross section based on a frequentist approach to electroweak observables in the framework of $N = 1$ supergravity models with radiative breaking of the electroweak gauge symmetry using the 5 fb^{-1} LHC data and XENON100.

[14] The strongest limit is 1.4×10^{-7} at $m_\chi = 60$ GeV.

[15] The strongest limit is 4.7×10^{-6} at $m_\chi = 35$ GeV.

[16] This result updates LEE 07A. The strongest limit is 2.1×10^{-7} at $m_\chi = 70$ GeV.

[17] AHMED 11A gives combined results from CDMS and EDELWEISS. The strongest limit is at $m_\chi = 90$ GeV.

[18] ARMENGAUD 11 updates result of ARMENGAUD 10. Strongest limit at $m_\chi = 85$ GeV.

[19] The strongest upper limit is 4.8×10^{-7} pb and occurs at $m_\chi = 50$ GeV.

[20] The strongest upper limit is 5.1×10^{-8} pb and occurs at $m_\chi \simeq 30$ GeV. The values quoted here are based on the analysis performed in ANGLE 08 with the update from SORENSEN 09.

[21] The strongest upper limit is 6.6×10^{-7} pb and occurs at $m_\chi \simeq 65$ GeV.

[22] AKERIB 06A updates the results of AKERIB 05. The strongest upper limit is 1.6×10^{-7} pb and occurs at $m_\chi \approx 60$ GeV.

[23] The strongest upper limit is also close to 1.0×10^{-6} pb and occurs at $m_\chi \simeq 70$ GeV. BENOIT 06 claim that the discrimination power of ZEPLIN-I measurement (ALNER 05A) is not reliable enough to obtain a limit better than 1×10^{-3} pb. However, SMITH 06 do not agree with the criticisms of BENOIT 06.

[24] The strongest upper limit is also close to 1.4×10^{-6} pb and occurs at $m_\chi \simeq 70$ GeV.

[25] AKERIB 04 is incompatible with BERNABEI 00 most likely value, under the assumption of standard WIMP-halo interactions. The strongest upper limit is 4×10^{-7} pb and occurs at $m_\chi \simeq 60$ GeV.

[26] Predictions for the spin-independent elastic cross section in the framework of $N = 1$ supergravity models with radiative breaking of the electroweak gauge symmetry.

[27] KIM 02 and ELLIS 04 calculate the χp elastic scattering cross section in the framework of N=1 supergravity models with radiative breaking of the electroweak gauge symmetry, but without universal scalar masses.

[28] In the case of universal squark and slepton masses, but non-universal Higgs masses, the limit becomes 2×10^{-6} (2×10^{-11} when constraint from the BNL $g-2$ experiment are included), see ELLIS 03E. ELLIS 05 display the sensitivity of the elastic scattering cross section to the π-Nucleon Σ term.

[29] PIERCE 04A calculates the χp elastic scattering cross section in the framework of models with very heavy scalar masses. See Fig. 2 of the paper.

[30] The strongest upper limit is 1.8×10^{-5} pb and occurs at $m_\chi \approx 80$ GeV.

[31] Under the assumption of standard WIMP-halo interactions, Akerib 03 is incompatible with BERNABEI 00 most likely value at the 99.98% CL. See Fig. 4.

[32] BAER 03A calculates the χp elastic scattering cross section in several models including the framework of N=1 supergravity models with radiative breaking of the electroweak gauge symmetry.

[33] The strongest upper limit is 7×10^{-6} pb and occurs at $m_\chi \simeq 30$ GeV.

[34] ABRAMS 02 is incompatible with the DAMA most likely value at the 99.9% CL. The strongest upper limit is 3×10^{-6} pb and occurs at $m_\chi \simeq 30$ GeV.

[35] BENOIT 02 excludes the central result of DAMA at the 99.8%CL.

[36] The strongest upper limit is 2×10^{-5} pb and occurs at $m_\chi \simeq 40$ GeV.

[37] The strongest upper limit is 7×10^{-6} pb and occurs at $m_\chi \simeq 46$ GeV.

[38] The strongest upper limit is 1.8×10^{-5} pb and occurs at $m_\chi \simeq 32$ GeV

[39] BOTTINO 01 calculates the χ-p elastic scattering cross section in the framework of the following supersymmetric models: N=1 supergravity with the radiative breaking of the electroweak gauge symmetry, N=1 supergravity with nonuniversal scalar masses and an effective MSSM model at the electroweak scale.

[40] Calculates the χ-p elastic scattering cross section in the framework of N=1 supergravity models with radiative breaking of the electroweak gauge symmetry.

[41] ELLIS 01C calculates the χ-p elastic scattering cross section in the framework of N=1 supergravity models with radiative breaking of the electroweak gauge symmetry. ELLIS 02B find a range 2×10^{-8}–1.5×10^{-7} at tanβ=50. In models with nonuniversal Higgs masses, the upper limit to the cross section is 4×10^{-7}.

[42] ACCOMANDO 00 calculate the χ-p elastic scattering cross section in the framework of minimal N=1 supergravity models with radiative breaking of the electroweak gauge symmetry. The limit is relaxed by at least an order of magnitude when models with nonuniversal scalar masses are considered. A subset of the authors in ARNOWITT 02 updated the limit to $< 9 \times 10^{-8}$ (tanβ < 55).

[43] BERNABEI 00 search for annual modulation of the WIMP signal. The data favor the hypothesis of annual modulation at 4σ and are consistent, for a particular model framework quoted there, with m_{χ^0}=44 $^{+12}_{-9}$ GeV and a spin-independent χ^0-proton cross section of $(5.4 \pm 1.0) \times 10^{-6}$ pb. See also BERNABEI 01 and BERNABEI 00C.

[44] FENG 00 calculate the χ-p elastic scattering cross section in the framework of N=1 supergravity models with radiative breaking of the electroweak gauge symmetry with a particular emphasis on focus point models. At tanβ=50, the range is 8×10^{-8}–4×10^{-7}.

Other bounds on $\tilde{\chi}_1^0$ from astrophysics and cosmology

Most of these papers generally exclude regions in the $M_2 - \mu$ parameter plane by requiring that the $\tilde{\chi}_1^0$ contribution to the overall cosmological density is less than some maximal value to avoid overclosure of the Universe. Those not based on the cosmological density are indicated. Many of these papers also include LEP and/or other bounds.

VALUE	DOCUMENT ID		TECN	COMMENT
>46 GeV	[1] ELLIS	00	RVUE	
• • • We do not use the following data for averages, fits, limits, etc. • • •				
	[2] BUCHMUEL...	14	COSM	
	[3] BUCHMUEL...	14A	COSM	
	[4] ROSZKOWSKI	14	COSM	
	[5] CABRERA	13	COSM	
	[6] ELLIS	13B	COSM	
	[5] STREGE	13	COSM	
	[2] AKULA	12	COSM	
	[2] ARBEY	12A	COSM	
	[2] BAER	12	COSM	
	[7] BALAZS	12	COSM	
	[8] BECHTLE	12	COSM	
	[9] BESKIDT	12	COSM	
> 18 GeV	[10] BOTTINO	12	COSM	
	[2] BUCHMUEL...	12	COSM	
	[2] CAO	12A	COSM	
	[2] ELLIS	12B	COSM	
	[11] FENG	12B	COSM	
	[2] KADASTIK	12	COSM	
	[7] STREGE	12	COSM	
	[12] BUCHMUEL...	11	COSM	
	[13] ROSZKOWSKI	11	COSM	
	[14] ELLIS	10	COSM	
	[15] BUCHMUEL...	09	COSM	
	[16] DREINER	09	THEO	
	[17] BUCHMUEL...	08	COSM	
	[13] ELLIS	08	COSM	
	[18] CALIBBI	07	COSM	
	[19] ELLIS	07	COSM	
	[20] ALLANACH	06	COSM	
	[21] DE-AUSTRI	06	COSM	
	[13] BAER	05	COSM	
	[22] BALTZ	04	COSM	
> 6 GeV	[10,23] BELANGER	04	THEO	
	[24] ELLIS	04B	COSM	
	[25] PIERCE	04A	COSM	
	[26] BAER	03	COSM	
> 6 GeV	[10] BOTTINO	03	COSM	
	[26] CHATTOPAD...	03	COSM	
	[27] ELLIS	03	COSM	
	[13] ELLIS	03B	COSM	
	[26] ELLIS	03C	COSM	
	[26] LAHANAS	03	COSM	
	[28] LAHANAS	02	COSM	
	[29] BARGER	01C	COSM	
	[30] ELLIS	01B	COSM	
	[27] BOEHM	00B	COSM	
	[31] FENG	00	COSM	
< 600 GeV	[32] ELLIS	98B	COSM	
	[33] EDSJO	97	COSM	Co-annihilation
	[34] BAER	96	COSM	
	[13] BEREZINSKY	95	COSM	
	[35] FALK	95	COSM	*CP*-violating phases
	[36] DREES	93	COSM	Minimal supergravity
	[37] FALK	93	COSM	Sfermion mixing
	[36] KELLEY	93	COSM	Minimal supergravity
	[38] MIZUTA	93	COSM	Co-annihilation
	[39] LOPEZ	92	COSM	Minimal supergravity, m_0=A=0
	[40] MCDONALD	92	COSM	
	[41] GRIEST	91	COSM	
	[42] NOJIRI	91	COSM	Minimal supergravity
	[43] OLIVE	91	COSM	
	[44] ROSZKOWSKI	91	COSM	
	[45] GRIEST	90	COSM	
	[43] OLIVE	89	COSM	
none 100 eV – 15 GeV	SREDNICKI	88	COSM	$\tilde{\gamma}$; $m_{\tilde{f}}$=100 GeV
none 100 eV–5 GeV	ELLIS	84	COSM	$\tilde{\gamma}$; for $m_{\tilde{f}}$=100 GeV
	GOLDBERG	83	COSM	$\tilde{\gamma}$
	[46] KRAUSS	83	COSM	$\tilde{\gamma}$
	VYSOTSKII	83	COSM	$\tilde{\gamma}$

[1] ELLIS 00 updates ELLIS 98. Uses LEP e^+e^- data at $\sqrt{s}$=202 and 204 GeV to improve bound on neutralino mass to 51 GeV when scalar mass universality is assumed and 46 GeV when Higgs mass universality is relaxed. Limits on tanβ improve to > 2.7 ($\mu > 0$), > 2.2 ($\mu < 0$) when scalar mass universality is assumed and > 1.9 (both signs of μ) when Higgs mass universality is relaxed.

[2] Implications of the LHC result on the Higgs mass and on the SUSY parameter space in the framework of $N = 1$ supergravity models with radiative breaking of the electroweak gauge symmetry.

[3] BUCHMUELLER 14A places constraints on the SUSY parameter space in the framework of $N = 1$ supergravity models with radiative breaking of the electroweak gauge symmetry using indirect experimental searches using the 20 fb^{-1} 8 TeV and the 5 fb^{-1} 7 TeV LHC and the LUX data.

[4] ROSZKOWSKI 14 places constraints on the SUSY parameter space in the framework of $N = 1$ supergravity models with radiative breaking of the electroweak gauge symmetry using Bayesian statistics and indirect experimental searches using the 20 fb^{-1} LHC and the LUX data.

[5] CABRERA 13 and STREGE 13 place constraints on the SUSY parameter space in the framework of $N = 1$ supergravity models with radiative breaking of the electroweak gauge symmetry with and without non-universal Higgs masses using the 5.8 fb^{-1}, $\sqrt{s} = 7$ TeV ATLAS supersymmetry searches and XENON100 results.

[6] ELLIS 13B place constraints on the SUSY parameter space in the framework of $N = 1$ supergravity models with radiative breaking of the electroweak gauge symmetry with and without Higgs mass universality. Models with universality below the GUT scale are also considered.

[7] BALAZS 12 and STREGE 12 place constraints on the SUSY parameter space in the framework of $N = 1$ supergravity models with radiative breaking of the electroweak gauge symmetry using the 1 fb^{-1} LHC supersymmetry searches, the 5 fb^{-1} Higgs mass constraints, both with $\sqrt{s} = 7$ TeV, and XENON100 results.

[8] BECHTLE 12 places constraints on the SUSY parameter space in the framework of $N = 1$ supergravity models with radiative breaking of the electroweak gauge symmetry using indirect experimental searches, using the 5 fb^{-1} LHC and XENON100 data.

[9] BESKIDT 12 places constraints on the SUSY parameter space in the framework of $N = 1$ supergravity models with radiative breaking of the electroweak gauge symmetry using indirect experimental searches, the 5 fb^{-1} LHC and the XENON100 data.

[10] BELANGER 04 and BOTTINO 12 (see also BOTTINO 03, BOTTINO 03A and BOTTINO 04) do not assume gaugino or scalar mass unification.

[11] FENG 12B places constraints on the SUSY parameter space in the framework of $N = 1$ supergravity models with radiative breaking of the electroweak gauge symmetry and large sfermion masses using the 1 fb^{-1} LHC supersymmetry searches, the 5 fb^{-1} LHC Higgs mass constraints both with $\sqrt{s} = 7$ TeV, and XENON100 results.

[12] BUCHMUELLER 11 places constraints on the SUSY parameter space in the framework of $N = 1$ supergravity models with radiative breaking of the electroweak gauge symmetry using indirect experimental searches and including supersymmetry breaking relations between A and B parameters.

[13] Places constraints on the SUSY parameter space in the framework of N=1 supergravity models with radiative breaking of the electroweak gauge symmetry but non-Universal Higgs masses.

[14] ELLIS 10 places constraints on the SUSY parameter space in the framework of $N = 1$ supergravity models with radiative breaking of the electroweak gauge symmetry with universality above the GUT scale.

[15] BUCHMUELLER 09 places constraints on the SUSY parameter space in the framework of $N = 1$ supergravity models with radiative breaking of the electroweak gauge symmetry using indirect experimental searches.

[16] DREINER 09 show that in the general MSSM with non-universal gaugino masses there exists no model-independent laboratory bound on the mass of the lightest neutralino. An essentially massless χ_1^0 is allowed by the experimental and observational data, imposing some constraints on other MSSM parameters, including M_2, μ and the slepton and squark masses.

[17] BUCHMUELLER 08 places constraints on the SUSY parameter space in the framework of $N = 1$ supergravity models with radiative breaking of the electroweak gauge symmetry using indirect experimental searches.

[18] CALIBBI 07 places constraints on the SUSY parameter space in the framework of $N = 1$ supergravity models with radiative breaking of the electroweak gauge symmetry with universality above the GUT scale including the effects of right-handed neutrinos.

[19] ELLIS 07 places constraints on the SUSY parameter space in the framework of $N = 1$ supergravity models with radiative breaking of the electroweak gauge symmetry with universality below the GUT scale.

[20] ALLANACH 06 places constraints on the SUSY parameter space in the framework of $N = 1$ supergravity models with radiative breaking of the electroweak gauge symmetry.

[21] DE-AUSTRI 06 places constraints on the SUSY parameter space in the framework of $N = 1$ supergravity models with radiative breaking of the electroweak gauge symmetry.

[22] BALTZ 04 places constraints on the SUSY parameter space in the framework of $N = 1$ supergravity models with radiative breaking of the electroweak gauge symmetry.

[23] Limit assumes a pseudo scalar mass < 200 GeV. For larger pseudo scalar masses, $m_\chi >$ 18(29) GeV for $\tan\beta = 50(10)$. Bounds from WMAP, $(g-2)_\mu$, $b \to s\gamma$, LEP.

[24] ELLIS 04B places constraints on the SUSY parameter space in the framework of N=1 supergravity models with radiative breaking of the electroweak gauge symmetry including supersymmetry breaking relations between A and B parameters. See also ELLIS 03D.

[25] PIERCE 04A places constraints on the SUSY parameter space in the framework of models with very heavy scalar masses.

[26] BAER 03, CHATTOPADHYAY 03, ELLIS 03C and LAHANAS 03 place constraints on the SUSY parameter space in the framework of N=1 supergravity models with radiative breaking of the electroweak gauge symmetry based on WMAP results for the cold dark matter density.

[27] BOEHM 00B and ELLIS 03 place constraints on the SUSY parameter space in the framework of minimal N=1 supergravity models with radiative breaking of the electroweak gauge symmetry. Includes the effect of χ-$\tilde{t}$ co-annihilations.

[28] LAHANAS 02 places constraints on the SUSY parameter space in the framework of minimal N=1 supergravity models with radiative breaking of the electroweak gauge symmetry. Focuses on the role of pseudo-scalar Higgs exchange.

[29] BARGER 01C use the cosmic relic density inferred from recent CMB measurements to constrain the parameter space in the framework of minimal N=1 supergravity models with radiative breaking of the electroweak gauge symmetry.

[30] ELLIS 01B places constraints on the SUSY parameter space in the framework of minimal N=1 supergravity models with radiative breaking of the electroweak gauge symmetry. Focuses on models with large $\tan\beta$.

[31] FENG 00 explores cosmologically allowed regions of MSSM parameter space with multi-TeV masses.

[32] ELLIS 98B assumes a universal scalar mass and radiative supersymmetry breaking with universal gaugino masses. The upper limit to the LSP mass is increased due to the inclusion of $\chi - \tilde{\tau}_R$ coannihilations.

[33] EDSJO 97 included all coannihilation processes between neutralinos and charginos for any neutralino mass and composition.

[34] Notes the location of the neutralino Z resonance and h resonance annihilation corridors in minimal supergravity models with radiative electroweak breaking.

[35] Mass of the bino (=LSP) is limited to $m_{\widetilde{B}} \lesssim 350$ GeV for $m_t = 174$ GeV.

[36] DREES 93, KELLEY 93 compute the cosmic relic density of the LSP in the framework of minimal N=1 supergravity models with radiative breaking of the electroweak gauge symmetry.

[37] FALK 93 relax the upper limit to the LSP mass by considering sfermion mixing in the MSSM.

[38] MIZUTA 93 include coannihilations to compute the relic density of Higgsino dark matter.

[39] LOPEZ 92 calculate the relic LSP density in a minimal SUSY GUT model.

[40] MCDONALD 92 calculate the relic LSP density in the MSSM including exact tree-level annihilation cross sections for all two-body final states.

[41] GRIEST 91 improve relic density calculations to account for coannihilations, pole effects, and threshold effects.

[42] NOJIRI 91 uses minimal supergravity mass relations between squarks and sleptons to narrow cosmologically allowed parameter space.

[43] Mass of the bino (=LSP) is limited to $m_{\widetilde{B}} \lesssim 350$ GeV for $m_t \leq 200$ GeV. Mass of the higgsino (=LSP) is limited to $m_{\widetilde{H}} \lesssim 1$ TeV for $m_t \leq 200$ GeV.

[44] ROSZKOWSKI 91 calculates LSP relic density in mixed gaugino/higgsino region.

[45] Mass of the bino (=LSP) is limited to $m_{\widetilde{B}} \lesssim 550$ GeV. Mass of the higgsino (=LSP) is limited to $m_{\widetilde{H}} \lesssim 3.2$ TeV.

[46] KRAUSS 83 finds $m_{\widetilde{\gamma}}$ not 30 eV to 2.5 GeV. KRAUSS 83 takes into account the gravitino decay. Find that limits depend strongly on reheated temperature. For example a new allowed region $m_{\widetilde{\gamma}} = 4$–20 MeV exists if $m_{\text{gravitino}} < 40$ TeV. See figure 2.

Unstable $\widetilde{\chi}_1^0$ (Lightest Neutralino) mass limit

Unless otherwise stated, results in this section assume spectra and production rates as evaluated in the MSSM. Unless otherwise stated, the goldstino or gravitino mass $m_{\widetilde{G}}$ is assumed to be negligible relative to all other masses. In the following, $\widetilde{G}$ is assumed to be undetected and to give rise to a missing energy ($\not{E}$) signature.

Some earlier papers are now obsolete and have been omitted. They were last listed in our PDG 14 edition: K. Olive, *et al.* (Particle Data Group), Chinese Physics **C38** 070001 (2014) (http://pdg.lbl.gov).

VALUE (GeV)	CL%	DOCUMENT ID		TECN	COMMENT
>380	95	[1] KHACHATRY...14L		CMS	$\widetilde{\chi}_1^0 \to Z\widetilde{G}$ simplified models,GMSB
• • • We do not use the following data for averages, fits, limits, etc. • • •					
		[2] AAIJ	17Z		displaced vertex with associated μ
		[3] KHACHATRY...16BX			$\geq 3\ell^{\pm}$, RPV, λ or λ' couplings, wino- or higgsino-like neutralinos
		[4] AAD	14BH	ATLS	$2\gamma + \not{E}_T$, GMSB, SPS8
		[5] AAD	13AP	ATLS	$2\gamma + \not{E}_T$, GMSB, SPS8
none 220–380	95	[6] AAD	13Q	ATLS	$\gamma + b + \not{E}_T$, higgsino-like neutralino, GMSB
		[7] AAD	13R	ATLS	$\widetilde{\chi}_1^0 \to \mu jj$, RPV, $\lambda'_{211} \neq 0$
		[8] AALTONEN	13I	CDF	$\widetilde{\chi}_1^0 \to \gamma\widetilde{G}$, $\not{E}_T$, GMSB
>220	95	[9] CHATRCHYAN	13AH	CMS	$\widetilde{\chi}_1^0 \to \gamma\widetilde{G}$, GMSB, SPS8, $c\tau <$ 500 mm
		[10] AAD	12CP	ATLS	$2\gamma + \not{E}_T$, GMSB
		[11] AAD	12CT	ATLS	$\geq 4\ell^{\pm}$, RPV
		[12] AAD	12R	ATLS	$\widetilde{\chi}_1^0 \to \mu jj$, RPV, $\lambda'_{211} \neq 0$
		[13] ABAZOV	12AD	D0	$\widetilde{\chi}_1^0\widetilde{\chi}_1^0 \to \gamma Z\widetilde{G}\widetilde{G}$, GMSB
		[14] CHATRCHYAN	12BK	CMS	$2\gamma + \not{E}_T$, GMSB
		[15] CHATRCHYAN	11B	CMS	$\widetilde{W}^0 \to \gamma\widetilde{G}$, $\widetilde{W}^{\pm} \to \ell^{\pm}\widetilde{G}$, GMSB
>149	95	[16] AALTONEN	10	CDF	$p\overline{p} \to \widetilde{\chi}\widetilde{\chi}$, $\widetilde{\chi}$=$\widetilde{\chi}_2^0$, $\widetilde{\chi}_1^{\pm}$, $\widetilde{\chi}_1^0 \to \gamma\widetilde{G}$, GMSB
>175	95	[17] ABAZOV	10P	D0	$\widetilde{\chi}_1^0 \to \gamma\widetilde{G}$, GMSB
>125	95	[18] ABAZOV	08F	D0	$p\overline{p} \to \widetilde{\chi}\widetilde{\chi}$, $\widetilde{\chi}$=$\widetilde{\chi}_2^0$, $\widetilde{\chi}_1^{\pm}$, $\widetilde{\chi}_1^0 \to \gamma\widetilde{G}$, GMSB
		[19] ABULENCIA	07H	CDF	RPV, $LL\overline{E}$
> 96.8	95	[20] ABBIENDI	06B	OPAL	$e^+e^- \to \widetilde{B}\widetilde{B}$, $(\widetilde{B} \to \widetilde{G}\gamma)$
		[21] ABDALLAH	05B	DLPH	$e^+e^- \to \widetilde{G}\widetilde{\chi}_1^0$, $(\widetilde{\chi}_1^0 \to \widetilde{G}\gamma)$
> 96	95	[22] ABDALLAH	05B	DLPH	$e^+e^- \to \widetilde{B}\widetilde{B}$, $(\widetilde{B} \to \widetilde{G}\gamma)$

[1] KHACHATRYAN 14L searched in 19.5 fb^{-1} of pp collisions at $\sqrt{s} = 8$ TeV for evidence of direct pair production of neutralinos with Higgs or Z-bosons in the decay chain, leading to HH, HZ and ZZ final states with missing transverse energy. The decays of 16–20. a Higgs boson to a b-quark pair, to a photon pair, and to final states with leptons are considered in conjunction with hadronic and leptonic decay modes of the Z and W bosons. No significant excesses over the expected SM backgrounds are observed. The results are interpreted in the context of GMSB simplified models where the decays $\widetilde{\chi}_1^0 \to H\widetilde{G}$ or $\widetilde{\chi}_1^0 \to Z\widetilde{G}$ take place either 100% or 50% of the time, see Figs. 16–20.

[2] AAIJ 17Z searched in 1 fb^{-1} of pp collisions at $\sqrt{s} = 7$ TeV and in 2 fb^{-1} of pp collisions at $\sqrt{s} = 8$ TeV for events containing a displaced vertex with one associated high transverse momentum μ. No excess is observed above the background expected from Standard Model processes. The results are used to set 95% C.L. upper limits on the cross section times branching fractions of pair-produced neutralinos decaying non-promptly into a muon and two quarks. Long-lived particles in a mass range 23–198 GeV are considered, see their Fig. 5 and Fig. 6.

[3] KHACHATRYAN 16BX searched in 19.5 fb^{-1} of pp collisions at $\sqrt{s} = 8$ TeV for events containing 3 or more leptons coming from the electroweak production of wino- or higgsino-like neutralinos, assuming non-zero R-parity-violating leptonic couplings λ_{122}, λ_{123}, and λ_{233} or semileptonic couplings λ'_{131}, λ'_{233}, λ'_{331}, and λ'_{333}. No excess over the expected background is observed and limits are derived on the neutralino mass, see Figs. 24 and 25.

[4] AAD 14BH searched in 20.3 fb^{-1} of pp collisions at $\sqrt{s} = 8$ TeV for events containing non-pointing photons in a diphoton plus missing transverse energy final state. No excess is observed above the background expected from Standard Model processes. The results are used to set 95% C.L. exclusion limits in the contact of gauge-mediated supersymmetric breaking models, with the lightest neutralino being the next-to-lightest supersymmetric particle and decaying with a lifetime in the range from 0.25 ns to about 100 ns into a photon and a gravitino. For limits on the NLSP lifetime versus Λ plane, for the SPS8 model, see their Fig. 7.

[5] AAD 13AP searched in 4.8 fb^{-1} of pp collisions at $\sqrt{s} = 7$ TeV for events containing non-pointing photons in a diphoton plus missing transverse energy final state. No excess is observed above the background expected from Standard Model processes. The results are used to set 95% C.L. exclusion limits in the context of gauge-mediated supersymmetric breaking models, with the lightest neutralino being the next-to-lightest supersymmetric particle and decaying with a lifetime in excess of 0.25 ns into a photon and a gravitino. For limits in the NLSP lifetime versus Λ plane, for the SPS8 model, see their Fig. 8.

[6] AAD 13Q searched in 4.7 fb^{-1} of pp collisions at $\sqrt{s} = 7$ TeV for events containing a high-p_T isolated photon, at least one jet identified as originating from a bottom quark, and high missing transverse momentum. Such signatures may originate from supersymmetric models with gauge-mediated supersymmetry breaking in events in which one of a pair of higgsino-like neutralinos decays into a photon and a gravitino while the other decays into a Higgs boson and a gravitino. No significant excess above the expected background was found and limits were set on the neutralino mass in a generalized GMSB model (GGM) with a higgsino-like neutralino NLSP, see their Fig. 4. Intermediate

neutralino masses between 220 and 380 GeV are excluded at 95% C.L, regardless of the squark and gluino masses, purely on the basis of the expected weak production.

[7] AAD 13R looked in 4.4 fb^{-1} of pp collisions at $\sqrt{s}$ = 7 TeV for events containing new, heavy particles that decay at a significant distance from their production point into a final state containing a high-momentum muon and charged hadrons. No excess over the expected background is observed and limits are placed on the production cross-section of neutralinos via squarks for various $m_{\widetilde{q}}$, $m_{\widetilde{\chi}^0_1}$ in an R-parity violating scenario with $\lambda'_{211} \neq 0$, as a function of the neutralino lifetime, see their Fig. 6.

[8] AALTONEN 13I searched in 6.3 fb^{-1} of $p\overline{p}$ collisions at $\sqrt{s}$ = 1.96 TeV for events containing $\not\!\!E_T$ and a delayed photon that arrives late in the detector relative to the time expected from prompt production. No evidence of delayed photon production is observed.

[9] CHATRCHYAN 13AH searched in 4.9 fb^{-1} of pp collisions at $\sqrt{s}$ = 7 TeV for events containing $\not\!\!E_T$ and a delayed photon that arrives late in the detector relative to the time expected from prompt production. No significant excess above the expected background was found and limits were set on the pair production of $\widetilde{\chi}^0_1$ depending on the neutralino proper decay length, see Fig. 8. Supersedes CHATRCHYAN 12BK.

[10] AAD 12CP searched in 4.8 fb^{-1} of pp collisions at $\sqrt{s}$ = 7 TeV for events with two photons and large $\not\!\!E_T$ due to $\widetilde{\chi}^0_1 \to \gamma\widetilde{G}$ decays in a GMSB framework. No significant excess above the expected background was found and limits were set on the neutralino mass in a generalized GMSB model (GGM) with a bino-like neutralino NLSP, see Figs. 6 and 7. The other sparticle masses were decoupled, tanβ = 2 and $c\tau_{NLSP}$ < 0.1 mm. Also, in the framework of the SPS8 model, limits are presented in Fig. 8.

[11] AAD 12CT searched in 4.7 fb^{-1} of pp collisions at $\sqrt{s}$ = 7 TeV for events containing four or more leptons (electrons or muons) and either moderate values of missing transverse momentum or large effective mass. No significant excess is found in the data. Limits are presented in a simplified model of R-parity violating supersymmetry in which charginos are pair-produced and then decay into a W-boson and a $\widetilde{\chi}^0_1$, which in turn decays through an RPV coupling into two charged leptons ($e^{\pm}e^{\mp}$ or $\mu^{\pm}\mu^{\mp}$) and a neutrino. In this model, limits are set on the neutralino mass as a function of the chargino mass, see Fig. 3a. Limits are also set in an R-parity violating mSUGRA model, see Fig. 3b.

[12] AAD 12R looked in 33 pb^{-1} of pp collisions at $\sqrt{s}$ = 7 TeV for events containing new, heavy particles that decay at a significant distance from their production point into a final state containing a high-momentum muon and charged hadrons. No excess over the expected background is observed and limits are placed on the production cross-section of neutralinos via squarks for various ($m_{\widetilde{q}}$, $m_{\widetilde{\chi}^0_1}$) in an R-parity violating scenario with $\lambda'_{211} \neq 0$, as a function of the neutralino lifetime, see their Fig. 8. Superseded by AAD 13R.

[13] ABAZOV 12AD looked in 6.2 fb^{-1} of pp collisions at $\sqrt{s}$ = 1.96 TeV for events with a photon, a Z-boson, and large $\not\!\!E_T$ in the final state. This topology corresponds to a GMSB model where pairs of neutralino NLSPs are either pair produced promptly or from decays of other supersymmetric particles and then decay to either $Z\widetilde{G}$ or $\gamma\widetilde{G}$. No significant excess over the SM expectation is observed and a limit at 95% C.L. on the cross section is derived as a function of the effective SUSY breaking scale Λ, see Fig. 3. Assuming N_{mes} = 2, M_{mes} = 3 Λ, tanβ = 3, μ = 0.75 M_1, and C_{grav} = 1, the model is excluded at 95% C.L. for values of Λ < 87 TeV.

[14] CHATRCHYAN 12BK searched in 2.23 fb^{-1} of pp collisions at $\sqrt{s}$ = 7 TeV for events with two photons and large $\not\!\!E_T$ due to $\widetilde{\chi}^0_1 \to \gamma\widetilde{G}$ decays in a GMSB framework. No significant excess above the expected background was found and limits were set on the pair production of $\widetilde{\chi}^0_1$ depending on the neutralino lifetime, see Fig. 6.

[15] CHATRCHYAN 11B looked in 35 pb^{-1} of pp collisions at $\sqrt{s}$=7 TeV for events with an isolated lepton (e or μ), a photon and $\not\!\!E_T$ which may arise in a generalized gauge mediated model from the decay of Wino-like NLSPs. No evidence for an excess over the expected background is observed. Limits are derived in the plane of squark/gluino mass versus Wino mass (see Fig. 4). Mass degeneracy of the produced squarks and gluinos is assumed.

[16] AALTONEN 10 searched in 2.6 fb^{-1} of $p\overline{p}$ collisions at $\sqrt{s}$ = 1.96 TeV for diphoton events with large $\not\!\!E_T$. They may originate from the production of $\widetilde{\chi}^{\pm}$ in pairs or associated to a $\widetilde{\chi}^0_2$, decaying into $\widetilde{\chi}^0_1$ which itself decays in GMSB to $\gamma\widetilde{G}$. There is no excess of events beyond expectation. An upper limit on the cross section is calculated in the GMSB model as a function of the $\widetilde{\chi}^0_1$ mass and lifetime, see their Fig. 2. A limit is derived on the $\widetilde{\chi}^0_1$ mass of 149 GeV for $\tau_{\widetilde{\chi}^0_1} \ll 1$ ns, which improves the results of previous searches.

[17] ABAZOV 10P looked in 6.3 fb^{-1} of $p\overline{p}$ collisions at $\sqrt{s}$ = 1.96 TeV for events with at least two isolated γs and large $\not\!\!E_T$. These could be the signature of $\widetilde{\chi}^0_2$ and $\widetilde{\chi}^{\pm}_1$ production, decaying to $\widetilde{\chi}^0_1$ and finally $\widetilde{\chi}^0_1 \to \gamma\widetilde{G}$ in a GMSB framework. No significant excess over the SM expectation is observed, and a limit at 95% C.L. on the cross section is derived for N_{mes} = 1, tanβ = 15 and μ > 0, see their Fig. 2. This allows them to set a limit on the effective SUSY breaking scale Λ > 124 TeV, from which the excluded $\widetilde{\chi}^0_1$ mass range is obtained.

[18] ABAZOV 08F looked in 1.1 fb^{-1} of $p\overline{p}$ collisions at $\sqrt{s}$ = 1.96 TeV for diphoton events with large $\not\!\!E_T$. They may originate from the production of $\widetilde{\chi}^{\pm}$ in pairs or associated to a $\widetilde{\chi}^0_2$, decaying to a $\widetilde{\chi}^0_1$ which itself decays promptly in GMSB to $\widetilde{\chi}^0_1 \to \gamma\widetilde{G}$. No significant excess was found compared to the background expectation. A limit is derived on the masses of SUSY particles in the GMSB framework for $M = 2\Lambda$, N = 1, tanβ = 15 and μ > 0, see Figure 2. It also excludes Λ < 91.5 TeV. Supersedes the results of ABAZOV 05A. Superseded by ABAZOV 10P.

[19] ABULENCIA 07H searched in 346 pb^{-1} of $p\overline{p}$ collisions at $\sqrt{s}$ = 1.96 TeV for events with at least three leptons (e or μ) from the decay of $\widetilde{\chi}^0_1$ via $LL\overline{E}$ couplings. The results are consistent with the hypothesis of no signal. Upper limits on the cross-section are extracted and a limit is derived in the framework of mSUGRA on the masses of $\widetilde{\chi}^0_1$ and $\widetilde{\chi}^{\pm}_1$, see e.g. their Fig. 3 and Tab. II.

[20] ABBIENDI 06B use 600 pb^{-1} of data from $\sqrt{s}$ = 189–209 GeV. They look for events with diphotons + $\not\!\!E$ final states originating from prompt decays of pair-produced neutralinos in a GMSB scenario with $\widetilde{\chi}^0_1$ NLSP. Limits on the cross-section are computed as a function of m($\widetilde{\chi}^0_1$), see their Fig. 14. The limit on the $\widetilde{\chi}^0_1$ mass is for a pure Bino state assuming a prompt decay, with lifetimes up to 10^{-9}s. Supersedes the results of ABBIENDI 04N.

[21] ABDALLAH 05B use data from $\sqrt{s}$ = 180–209 GeV. They look for events with single photons + $\not\!\!E$ final states. Limits are computed in the plane (m($\widetilde{G}$) , m($\widetilde{\chi}^0_1$)), shown in their Fig. 9b for a pure Bino state in the GMSB framework and in Fig. 9c for a no-scale supergravity model. Supersedes the results of ABREU 00Z.

[22] ABDALLAH 05B use data from $\sqrt{s}$ = 130–209 GeV. They look for events with diphotons + $\not\!\!E$ final states and single photons not pointing to the vertex, expected in GMSB when the $\widetilde{\chi}^0_1$ is the NLSP. Limits are computed in the plane (m($\widetilde{G}$), m($\widetilde{\chi}^0_1$)), see their Fig. 10. The lower limit is derived on the $\widetilde{\chi}^0_1$ mass for a pure Bino state assuming a prompt decay and $m_{\widetilde{e}_R} = m_{\widetilde{e}_L} = 2\, m_{\widetilde{\chi}^0_1}$. It improves to 100 GeV for $m_{\widetilde{e}_R} = m_{\widetilde{e}_L} = 1.1\, m_{\widetilde{\chi}^0_1}$. and the limit in the plane (m($\widetilde{\chi}^0_1$), m($\widetilde{e}_R$)) is shown in Fig. 10b. For long-lived neutralinos, cross-section limits are displayed in their Fig 11. Supersedes the results of ABREU 00Z.

$\widetilde{\chi}^0_2$, $\widetilde{\chi}^0_3$, $\widetilde{\chi}^0_4$ (Neutralinos) mass limits

Neutralinos are unknown mixtures of photinos, z-inos, and neutral higgsinos (the supersymmetric partners of photons and of Z and Higgs bosons). The limits here apply only to $\widetilde{\chi}^0_2$, $\widetilde{\chi}^0_3$, and $\widetilde{\chi}^0_4$. $\widetilde{\chi}^0_1$ is the lightest supersymmetric particle (LSP); see $\widetilde{\chi}^0_1$ Mass Limits. It is not possible to quote rigorous mass limits because they are extremely model dependent; i.e. they depend on branching ratios of various $\widetilde{\chi}^0$ decay modes, on the masses of decay products ($\widetilde{e}$, $\widetilde{\gamma}$, $\widetilde{q}$, $\widetilde{g}$), and on the $\widetilde{e}$ mass exchanged in $e^+e^- \to \widetilde{\chi}^0_i\widetilde{\chi}^0_j$. Limits arise either from direct searches, or from the MSSM constraints set on the gaugino and higgsino mass parameters M_2 and μ through searches for lighter charginos and neutralinos. Often limits are given as contour plots in the $m_{\widetilde{\chi}^0} - m_{\widetilde{e}}$ plane vs other parameters. When specific assumptions are made, e.g, the neutralino is a pure photino ($\widetilde{\gamma}$), pure z-ino ($\widetilde{Z}$), or pure neutral higgsino ($\widetilde{H}^0$), the neutralinos will be labelled as such.

Limits obtained from e^+e^- collisions at energies up to 136 GeV, as well as other limits from different techniques, are now superseded and have not been included in this compilation. They can be found in the 1998 Edition (The European Physical Journal **C3** 1 (1998)) of this Review. Some later papers are now obsolete and have been omitted. They were last listed in our PDG 14 edition: K. Olive, *et al.* (Particle Data Group), Chinese Physics **C38** 070001 (2014) (http://pdg.lbl.gov).

VALUE (GeV)	CL%	DOCUMENT ID		TECN	COMMENT
none 220–490	95	[1] SIRUNYAN	17AW	CMS	1ℓ+ 2 b-jets + $\not\!\!E_T$, Tchi1n2E, $m_{\widetilde{\chi}^0_1}$ = 0 GeV
>600	95	[2] AAD	16AA	ATLS	3/4ℓ + $\not\!\!E_T$, Tn2n3A, $m_{\widetilde{\chi}^0_1}$=0GeV
>670	95	[2] AAD	16AA	ATLS	3/4ℓ+$\not\!\!E_T$,Tn2n3B,$m_{\widetilde{\chi}^0_1}$ < 200GeV
>250	95	[3] AAD	15BA	ATLS	$m_{\widetilde{\chi}^{\pm}_1} = m_{\widetilde{\chi}^0_2}$, $m_{\widetilde{\chi}^0_1}$ = 0 GeV
>380	95	[4] AAD	14H	ATLS	$\widetilde{\chi}^{\pm}_1\widetilde{\chi}^0_2 \to \tau^{\pm}\nu\widetilde{\chi}^0_1\tau^{\pm}\tau^{\mp}\widetilde{\chi}^0_1$, simplified model, $m_{\widetilde{\chi}^{\pm}_1} = m_{\widetilde{\chi}^0_2}$, $m_{\widetilde{\chi}^0_1}$ = 0 GeV
>700	95	[4] AAD	14H	ATLS	$\widetilde{\chi}^{\pm}_1\widetilde{\chi}^0_2 \to \ell^{\pm}\nu\widetilde{\chi}^0_1\ell^{\pm}\ell^{\mp}\widetilde{\chi}^0_1$, simplified model, $m_{\widetilde{\chi}^{\pm}_1} = m_{\widetilde{\chi}^0_2}$, $m_{\widetilde{\chi}^0_1}$ = 0 GeV
>345	95	[4] AAD	14H	ATLS	$\widetilde{\chi}^{\pm}_1\widetilde{\chi}^0_2 \to W\widetilde{\chi}^0_1 Z\widetilde{\chi}^0_1$, simplified model, $m_{\widetilde{\chi}^{\pm}_1} = m_{\widetilde{\chi}^0_2}$, $m_{\widetilde{\chi}^0_1}$ = 0 GeV
>148	95	[4] AAD	14H	ATLS	$\widetilde{\chi}^{\pm}_1\widetilde{\chi}^0_2 \to W\widetilde{\chi}^0_1 H\widetilde{\chi}^0_1$, simplified model, $m_{\widetilde{\chi}^{\pm}_1} = m_{\widetilde{\chi}^0_2}$, $m_{\widetilde{\chi}^0_1}$ = 0 GeV
>620	95	[5] AAD	14X	ATLS	$\geq 4\ell^{\pm}$, $\widetilde{\chi}^0_{2,3} \to \ell^{\pm}\ell^{\mp}\widetilde{\chi}^0_1$, $m_{\widetilde{\chi}^0_1}$ = 0 GeV
		[6] AAD	13	ATLS	3$\ell^{\pm}$ + $\not\!\!E_T$, pMSSM, SMS
		[7] CHATRCHYAN	12BJ	CMS	$\geq 2\,\ell$, jets + $\not\!\!E_T$, $pp \to \widetilde{\chi}^{\pm}_1\widetilde{\chi}^0_2$
>116.0	95	[8] ABREU	00W	DLPH	$\widetilde{\chi}^0_4$, $1 \leq \tan\beta \leq 40$, all Δm, all m_0

• • • We do not use the following data for averages, fits, limits, etc. • • •

none 180–355	95	[9] AAD	14G	ATLS	$\widetilde{\chi}^{\pm}_1\widetilde{\chi}^0_2 \to W\widetilde{\chi}^0_1 Z\widetilde{\chi}^0_1$, simplified model, $m_{\widetilde{\chi}^{\pm}_1} = m_{\widetilde{\chi}^0_2}$, $m_{\widetilde{\chi}^0_1}$ = 0
		[10] KHACHATRY...14I		CMS	$\widetilde{\chi}^0_2 \to (Z,\ H)\widetilde{\chi}^0_1\,\widetilde{\ell}\ell$, simplified model
		[11] AAD	12AS	ATLS	3$\ell^{\pm}$ + $\not\!\!E_T$, pMSSM
		[12] AAD	12T	ATLS	$\ell^{\pm}\ell^{\pm}$ + $\not\!\!E_T$, $pp \to \widetilde{\chi}^{\pm}_1\widetilde{\chi}^0_2$

[1] SIRUNYAN 17AW searched in 35.9 fb^{-1} of pp collisions at $\sqrt{s}$ = 13 TeV for events with a charged lepton (electron or muon), two jets identified as originating from a b-quark, and large $\not\!\!E_T$. No significant excess above the Standard Model expectations is observed. Limits are set on the mass of the chargino and the next-to-lightest neutralino in the Tchi1n2E simplified model, see their Figure 6.

[2] AAD 16AA summarized and extended ATLAS searches for electroweak supersymmetry in final states containing several charged leptons, $\not\!\!E_T$, with or without hadronic jets, in 20 fb^{-1} of pp collisions at $\sqrt{s}$ = 8 TeV. The paper reports the results of new interpretations and statistical combinations of previously published analyses, as well as new analyses. Exclusion limits at 95% C.L. are set on mass-degenerate $\widetilde{\chi}^0_2$ and $\widetilde{\chi}^0_3$ masses in the Tn2n3A and Tn2n3B simplified models. See their Fig. 15.

[3] AAD 15BA searched in 20.3 fb^{-1} of pp collisions at $\sqrt{s}$ = 8 TeV for electroweak production of charginos and neutralinos decaying to a final state containing a W boson and a 125 GeV Higgs boson, plus missing transverse momentum. No excess beyond the Standard Model expectation is observed. Exclusion limits are derived in simplified models of direct chargino and next-to-lightest neutralino production, with the decays

$\tilde{\chi}_1^\pm \to W^\pm \tilde{\chi}_1^0$ and $\tilde{\chi}_2^0 \to H\tilde{\chi}_1^0$ having 100% branching fraction, see Fig. 8. A combination of the multiple final states for the Higgs decay yields the best limits (Fig. 8d).

[4] AAD 14H searched in 20.3 fb^{-1} of pp collisions at $\sqrt{s} = 8$ TeV for electroweak production of charginos and neutralinos decaying to a final sate with three leptons and missing transverse momentum. No excess beyond the Standard Model expectation is observed. Exclusion limits are derived in simplified models of direct chargino and next-to-lightest neutralino production, with decays to the lightest neutralino via either all three generations of leptons, staus only, gauge bosons, or Higgs bosons, see Fig. 7. An interpretation in the pMSSM is also given, see Fig. 8.

[5] AAD 14X searched in 20.3 fb^{-1} of pp collisions at $\sqrt{s} = 8$ TeV for events with at least four leptons (electrons, muons, taus) in the final state. No significant excess above the Standard Model expectations is observed. Limits are set on the neutralino mass in an R-parity conserving simplified model where the decay $\tilde{\chi}_{2,3}^0 \to \ell^\pm \ell^\mp \tilde{\chi}_1^0$ takes place with a branching ratio of 100%, see Fig. 10.

[6] AAD 13 searched in 4.7 fb^{-1} of pp collisions at $\sqrt{s} = 7$ TeV for charginos and neutralinos decaying to a final state with three leptons (e and μ) and missing transverse energy. No excess beyond the Standard Model expectation is observed. Exclusion limits are derived in the phenomenological MSSM, see Fig. 2 and 3, and in simplified models, see Fig. 4. For the simplified models with intermediate slepton decays, degenerate $\tilde{\chi}_1^\pm$ and $\tilde{\chi}_2^0$ masses up to 500 GeV are excluded at 95% C.L. for very large mass differences with the $\tilde{\chi}_1^0$. Supersedes AAD 12AS.

[7] CHATRCHYAN 12BJ searched in 4.98 fb^{-1} of pp collisions at $\sqrt{s} = 7$ TeV for direct electroweak production of charginos and neutralinos in events with at least two leptons, jets and missing transverse momentum. No significant excesses over the expected SM backgrounds are observed and 95% C.L. limits on the production cross section of $\tilde{\chi}_1^\pm \tilde{\chi}_2^0$ pair production were set in a number of simplified models, see Figs. 7 to 12. Most limits are for exactly 3 jets.

[8] ABREU 00W combines data collected at $\sqrt{s}$=189 GeV with results from lower energies. The mass limit is obtained by constraining the MSSM parameter space with gaugino and sfermion mass universality at the GUT scale, using the results of negative direct searches for neutralinos (including cascade decays and $\tilde{\tau}\tau$ final states) from ABREU 01, for charginos from ABREU 00J and ABREU 00T (for all Δm_+), and for charged sleptons from ABREU 01B. The results hold for the full parameter space defined by all values of M_2 and $|\mu| \leq 2$ TeV with the $\tilde{\chi}_1^0$ as LSP.

[9] AAD 14G searched in 20.3 fb^{-1} of pp collisions at $\sqrt{s} = 8$ TeV for electroweak production of chargino-neutralino pairs, decaying to a final sate with two leptons (e and μ) and missing transverse momentum. No excess beyond the Standard Model expectation is observed. Exclusion limits are derived in simplified models of chargino and next-to-lightest neutralino production, with decays to the lightest neutralino via gauge bosons, see Fig. 7. An interpretation in the pMSSM is also given, see Fig. 10.

[10] KHACHATRYAN 14I searched in 19.5 fb^{-1} of pp collisions at $\sqrt{s} = 8$ TeV for electroweak production of charginos and neutralinos decaying to a final state with three leptons (e or μ) and missing transverse momentum, or with a Z-boson, dijets and missing transverse momentum. No excess beyond the Standard Model expectation is observed. Exclusion limits are derived in simplified models, see Figs. 12–16.

[11] AAD 12AS searched in 2.06 fb^{-1} of pp collisions at $\sqrt{s} = 7$ TeV for charginos and neutralinos decaying to a final state with three leptons (e and μ) and missing transverse energy. No excess beyond the Standard Model expectation is observed. Exclusion limits are derived in the phenomenological MSSM, see Fig. 2 (top), and in simplified models, see Fig. 2 (bottom).

[12] AAD 12T looked in 1 fb^{-1} of pp collisions at $\sqrt{s} = 7$ TeV for the production of supersymmetric particles decaying into final states with missing transverse momentum and exactly two isolated leptons (e or μ). Same-sign dilepton events were separately studied. Additionally, in opposite-sign events, a search was made for an excess of same-flavor over different-flavor lepton pairs. No excess over the expected background is observed and limits are placed on the effective production cross section of opposite-sign dilepton events with $\not{E}_T > 250$ GeV and on same-sign dilepton events with $\not{E}_T > 100$ GeV. The latter limit is interpreted in a simplified electroweak gaugino production model.

$\tilde{\chi}_1^\pm$, $\tilde{\chi}_2^\pm$ (Charginos) mass limits

Charginos are unknown mixtures of w-inos and charged higgsinos (the supersymmetric partners of W and Higgs bosons). A lower mass limit for the lightest chargino ($\tilde{\chi}_1^\pm$) of approximately 45 GeV, independent of the field composition and of the decay mode, has been obtained by the LEP experiments from the analysis of the Z width and decays. These results, as well as other now superseded limits from e^+e^- collisions at energies below 136 GeV, and from hadronic collisions, can be found in the 1998 Edition (The European Physical Journal **C3** 1 (1998)) of this Review.

Unless otherwise stated, results in this section assume spectra, production rates, decay modes and branching ratios as evaluated in the MSSM, with gaugino and sfermion mass unification at the GUT scale. These papers generally study production of $\tilde{\chi}_1^0 \tilde{\chi}_2^0$, $\tilde{\chi}_1^+ \tilde{\chi}_1^-$ and (in the case of hadronic collisions) $\tilde{\chi}_1^\pm \tilde{\chi}_2^0$ pairs, including the effects of cascade decays. The mass limits on $\tilde{\chi}_1^\pm$ are either direct, or follow indirectly from the constraints set by the non-observation of $\tilde{\chi}_2^0$ states on the gaugino and higgsino MSSM parameters M_2 and μ. For generic values of the MSSM parameters, limits from high-energy e^+e^- collisions coincide with the highest value of the mass allowed by phase-space, namely $m_{\tilde{\chi}_1^\pm} \lesssim \sqrt{s}/2$. The still unpublished combination of the results of the four LEP collaborations from the 2000 run of LEP2 at $\sqrt{s}$ up to $\simeq 209$ GeV yields a lower mass limit of 103.5 GeV valid for general MSSM models. The limits become however weaker in certain regions of the MSSM parameter space where the detection efficiencies or production cross sections are suppressed. For example, this may happen when: (i) the mass differences $\Delta m_+ = m_{\tilde{\chi}_1^+} - m_{\tilde{\chi}_1^0}$ or $\Delta m_\nu = m_{\tilde{\chi}_1^+} - m_{\tilde{\nu}}$ are very small, and the detection efficiency is reduced; (ii) the electron sneutrino mass is small, and the $\tilde{\chi}_1^\pm$ production rate is suppressed due to a destructive interference between s and t channel exchange diagrams. The regions of MSSM parameter space where the following limits are valid are indicated in the comment lines or in the footnotes.

Some earlier papers are now obsolete and have been omitted. They were last listed in our PDG 14 edition: K. Olive, *et al.* (Particle Data Group), Chinese Physics **C38** 070001 (2014) (http://pdg.lbl.gov).

VALUE (GeV)	CL%	DOCUMENT ID		TECN	COMMENT
> 420	95	[1] KHACHATRY...17L		CMS	2 τ+$\not{E}_T$, Tchi1chi1C and $\tilde{\tau}$-only, $m_{\tilde{\chi}_1^0}$=0 GeV
none 220–490	95	[2] SIRUNYAN	17AW		1ℓ + 2b-jets + $\not{E}_T$, Tchi1n2E, $m_{\tilde{\chi}_1^0} = 0$ GeV
> 500	95	[3] AAD	16AA	ATLS	2$\ell^\pm$+$\not{E}_T$,Tchi1chi1B,$m_{\tilde{\chi}_1^0}$=0 GeV
> 220	95	[3] AAD	16AA	ATLS	2$\ell^\pm$+$\not{E}_T$, Tchi1chi1C, low Δm for $\tilde{\chi}_1^\pm$, $\tilde{\chi}_1^0$
> 700	95	[4] AAD	16AA	ATLS	3/4ℓ+$\not{E}_T$,Tchi1n2B, $m_{\tilde{\chi}_1^0}$=0 GeV
> 700	95	[4] AAD	16AA	ATLS	3/4ℓ+$\not{E}_T$, Tchi1n2C, $m_{\tilde{\ell}} = m_{\tilde{\chi}_1^0}$+ 0.5 (or 0.95) ($m_{\tilde{\chi}_1^\pm} - m_{\tilde{\chi}_1^0}$)
> 400	95	[4] AAD	16AA	ATLS	2 hadronic τ+$\not{E}_T$ & 3ℓ+$\not{E}_T$ combination,Tchi1n2D,$m_{\tilde{\chi}_1^0}$=0 GeV
> 540	95	[5] KHACHATRY...16R		CMS	$\geq 1\gamma + 1$ e or μ + $\not{E}_T$, Tchi1n1A
> 250	95	[6] AAD	15BA	ATLS	$m_{\tilde{\chi}_1^\pm} = m_{\tilde{\chi}_2^0}$, $m_{\tilde{\chi}_1^0} = 0$ GeV
> 590	95	[7] AAD	15CA	ATLS	$\geq 2\ \gamma + \not{E}_T$, GGM, bino-like NLSP, any NLSP mass
none 124–361	95	[7] AAD	15CA	ATLS	$\geq 1\ \gamma + e,\mu + \not{E}_T$, GGM, wino-like NLSP
> 700	95	[8] AAD	14H	ATLS	$\tilde{\chi}_1^\pm \tilde{\chi}_2^0 \to \ell^\pm \nu \tilde{\chi}_1^0 \ell^\pm \ell^\mp \tilde{\chi}_1^0$, simplified model, $m_{\tilde{\chi}_1^\pm} = m_{\tilde{\chi}_2^0}$, $m_{\tilde{\chi}_1^0} = 0$ GeV
> 345	95	[8] AAD	14H	ATLS	$\tilde{\chi}_1^\pm \tilde{\chi}_2^0 \to W\tilde{\chi}_1^0 Z\tilde{\chi}_1^0$, simplified model, $m_{\tilde{\chi}_1^\pm} = m_{\tilde{\chi}_2^0}$, $m_{\tilde{\chi}_1^0} = 0$ GeV
> 148	95	[8] AAD	14H	ATLS	$\tilde{\chi}_1^\pm \tilde{\chi}_2^0 \to W\tilde{\chi}_1^0 H\tilde{\chi}_1^0$, simplified model, $m_{\tilde{\chi}_1^\pm} = m_{\tilde{\chi}_2^0}$, $m_{\tilde{\chi}_1^0} = 0$ GeV
> 380	95	[8] AAD	14H	ATLS	$\tilde{\chi}_1^\pm \tilde{\chi}_2^0 \to \tau^\pm \nu \tilde{\chi}_1^0 \tau^\pm \tau^\mp \tilde{\chi}_1^0$, simplified model, $m_{\tilde{\chi}_1^\pm} = m_{\tilde{\chi}_2^0}$, $m_{\tilde{\chi}_1^0} = 0$ GeV
> 750	95	[9] AAD	14X	ATLS	RPV, $\geq 4\ell^\pm$, $\tilde{\chi}_1^\pm \to W^{(*)\pm}\tilde{\chi}_1^0$, $\tilde{\chi}_1^0 \to \ell^\pm \ell^\mp \nu$
> 210	95	[10] KHACHATRY...14L		CMS	$\tilde{\chi}_2^0 \to H\tilde{\chi}_1^0$ and $\tilde{\chi}_1^\pm \to W^\pm \tilde{\chi}_1^0$ simplified models, $m_{\tilde{\chi}_2^0} = m_{\tilde{\chi}_1^\pm}$, $m_{\tilde{\chi}_1^0} = 0$ GeV
		[11] AAD	13	ATLS	3$\ell^\pm$ + $\not{E}_T$, pMSSM, SMS
		[12] AAD	13B	ATLS	2$\ell^\pm$ + $\not{E}_T$, pMSSM, SMS
> 540	95	[13] AAD	12CT	ATLS	$\geq 4\ell^\pm$, RPV, $m_{\tilde{\chi}_1^0} > 300$ GeV
		[14] CHATRCHYAN	12BJ	CMS	$\geq 2\ \ell$, jets + $\not{E}_T$, $pp \to \tilde{\chi}_1^\pm \tilde{\chi}_2^0$
> 94	95	[15] ABDALLAH	03M	DLPH	$\tilde{\chi}_1^\pm$, $\tan\beta \leq 40$, $\Delta m_+ > 3$ GeV,all m_0
• • • We do not use the following data for averages, fits, limits, etc. • • •					
> 570	95	[16] KHACHATRY...16AA		CMS	$\geq 1\gamma$ + jets + $\not{E}_T$, Tchi1chi1A
> 680	95	[16] KHACHATRY...16AA		CMS	$\geq 1\gamma$ + jets + $\not{E}_T$, Tchi1n1A
> 710	95	[16] KHACHATRY...16AA		CMS	$\geq 1\gamma$ + jets + $\not{E}_T$, GGM, $\tilde{\chi}_2^0 \tilde{\chi}_1^\pm$ pair production, wino-like NLSP
>1000	95	[17] KHACHATRY...16R		CMS	$\geq 1\gamma + 1$ e or μ + $\not{E}_T$, Tglu1F, $m_{\tilde{\chi}_1^\pm} = m_{\tilde{\chi}_2^0} > 200$ GeV
> 307	95	[18] KHACHATRY...16Y		CMS	1 or 2 soft $\ell^\pm$+jets+$\not{E}_T$, Tchi1n2A, $m_{\tilde{\chi}_1^\pm} - m_{\tilde{\chi}_1^0}$=20 GeV
> 410	95	[19] AAD	14AV	ATLS	$\geq 2\ \tau + \not{E}_T$, direct $\tilde{\chi}_1^\pm \tilde{\chi}_2^0$, $\tilde{\chi}_1^\pm \tilde{\chi}_1^\mp$ production, $m_{\tilde{\chi}_2^0} = m_{\tilde{\chi}_1^\pm}$, $m_{\tilde{\chi}_1^0} = 0$ GeV
> 345	95	[20] AAD	14AV	ATLS	$\geq 2\ \tau + \not{E}_T$, direct $\tilde{\chi}_1^\pm \tilde{\chi}_1^\mp$ production, $m_{\tilde{\chi}_1^0} = 0$ GeV
none 100–105, 120–135, 145–160	95	[21] AAD	14G	ATLS	$\tilde{\chi}_1^\pm \tilde{\chi}_1^\mp \to W^+ \tilde{\chi}_1^0 W^- \tilde{\chi}_1^0$, simplified model, $m_{\tilde{\chi}_1^0} = 0$ GeV
none 140–465	95	[21] AAD	14G	ATLS	$\tilde{\chi}_1^\pm \tilde{\chi}_1^\mp \to \ell^+ \nu \tilde{\chi}_1^0 \ell^- \overline{\nu} \tilde{\chi}_1^0$, simplified model, $m_{\tilde{\chi}_1^0} = 0$ GeV
none 180–355	95	[21] AAD	14G	ATLS	$\tilde{\chi}_1^\pm \tilde{\chi}_2^0 \to W\tilde{\chi}_1^0 Z\tilde{\chi}_1^0$, simplified model, $m_{\tilde{\chi}_1^\pm} = m_{\tilde{\chi}_2^0}$, $m_{\tilde{\chi}_1^0} = 0$ GeV
> 168	95	[22] AALTONEN	14	CDF	3$\ell^\pm$+ $\not{E}_T$, $\tilde{\chi}_1^\pm \to \ell\nu\tilde{\chi}_1^0$, mSUGRA with m_0=60 GeV
		[23] KHACHATRY...14I		CMS	$\tilde{\chi}_1^\pm \to W\tilde{\chi}_1^0$, $\ell\tilde{\nu}$, $\tilde{\ell}\nu$, simplified model

		[24] AALTONEN	13Q	CDF	$\tilde{\chi}_1^\pm \to \tau X$, simplified gravity- and gauge-mediated models
		[25] AAD	12AS	ATLS	$3\ell^\pm + \not{E}_T$, pMSSM
		[26] AAD	12T	ATLS	$\ell^\pm\ell^\mp + \not{E}_T$, $\ell^\pm\ell^\pm + \not{E}_T$, $pp \to \tilde{\chi}_1^\pm \tilde{\chi}_2^0$
		[27] CHATRCHYAN	11B	CMS	$\widetilde{W}^0 \to \gamma\widetilde{G}$,$\widetilde{W}^\pm \to \ell^\pm\widetilde{G}$,GMSB
> 163	95	[28] CHATRCHYAN	11V	CMS	$\tan\beta$=3, m_0=60 GeV, A_0=0, μ >0

[1] KHACHATRYAN 17L searched in about 19 fb^{-1} of pp collisions at $\sqrt{s}$ = 8 TeV for events with two τ (at least one decaying hadronically) and $\not{E}_T$. In the Tchi1chi1C model, assuming decays via intermediate $\tilde{\tau}$ or $\tilde{\nu}_\tau$ with equivalent mass, the observed limits rule out $\tilde{\chi}_1^\pm$ masses up to 420 GeV for a massless $\tilde{\chi}_1^0$. See their Fig.5.

[2] SIRUNYAN 17AW searched in 35.9 fb^{-1} of pp collisions at $\sqrt{s}$ = 13 TeV for events with a charged lepton (electron or muon), two jets identified as originating from a b-quark, and large $\not{E}_T$. No significant excess above the Standard Model expectations is observed. Limits are set on the mass of the chargino and the next-to-lightest neutralino in the Tchi1n2E simplified model, see their Figure 6.

[3] AAD 16AA summarized and extended ATLAS searches for electroweak supersymmetry in final states containing several charged leptons, $\not{E}_T$, with or without hadronic jets, in 20 fb^{-1} of pp collisions at $\sqrt{s}$ = 8 TeV. The paper reports the results of new interpretations and statistical combinations of previously published analyses, as well as new analyses. Exclusion limits at 95% C.L. are set on the $\tilde{\chi}_1^\pm$ mass in the Tchi1chi1B and Tchi1chi1C simplified models. See their Fig. 13.

[4] AAD 16AA summarized and extended ATLAS searches for electroweak supersymmetry in final states containing several charged leptons, $\not{E}_T$, with or without hadronic jets, in 20 fb^{-1} of pp collisions at $\sqrt{s}$ = 8 TeV. The paper reports the results of new interpretations and statistical combinations of previously published analyses, as well as new analyses. Exclusion limits at 95% C.L. are set on mass-degenerate $\tilde{\chi}_1^\pm$ and $\tilde{\chi}_2^0$ masses in the Tchi1n2B, Tchi1n2C, and Tchi1n2D simplified models. See their Figs. 16, 17, and 18. Interpretations in phenomenological-MSSM, two-parameter Non Universal Higgs Masses (NUHM2), and gauge-mediated symmetry breaking (GMSB) models are also given in their Figs. 20, 21 and 22.

[5] KHACHATRYAN 16R searched in 19.7 fb^{-1} of pp collisions at $\sqrt{s}$ = 8 TeV for events with one or more photons, one electron or muon, and $\not{E}_T$. No significant excess above the Standard Model expectations is observed. Limits are set on wino masses in a general gauge-mediated SUSY breaking model (GGM), for a wino-like neutralino NLSP scenario, see Fig. 5. Limits are also set in the Tglu1D and Tchi1n1A simplified models, see Fig. 6. The Tchi1n1A limit is reduced to 340 GeV for a branching ratio reduced by the weak mixing angle.

[6] AAD 15BA searched in 20.3 fb^{-1} of pp collisions at $\sqrt{s}$ = 8 TeV for electroweak production of charginos and neutralinos decaying to a final state containing a W boson and a 125 GeV Higgs boson, plus missing transverse momentum. No excess beyond the Standard Model expectation is observed. Exclusion limits are derived in simplified models of direct chargino and next-to-lightest neutralino production, with the decays $\tilde{\chi}_1^\pm \to W^\pm\tilde{\chi}_1^0$ and $\tilde{\chi}_2^0 \to H\tilde{\chi}_1^0$ having 100% branching fraction, see Fig. 8. A combination of the multiple final states for the Higgs decay yields the best limits (Fig. 8d).

[7] AAD 15CA searched in 20.3 fb^{-1} of pp collisions at $\sqrt{s}$ = 8 TeV for events with one or more photons and $\not{E}_T$, with or without leptons (e, μ). No significant excess above the Standard Model expectations is observed. Limits are set on wino masses in the general gauge-mediated SUSY breaking model (GGM), for wino-like NLSP, see Fig. 9, 12

[8] AAD 14H searched in 20.3 fb^{-1} of pp collisions at $\sqrt{s}$ = 8 TeV for electroweak production of charginos and neutralinos decaying to a final sate with three leptons and missing transverse momentum. No excess beyond the Standard Model expectation is observed. Exclusion limits are derived in simplified models of direct chargino and next-to-lightest neutralino production, with decays to the lightest neutralino via either all three generations of leptons, staus only, gauge bosons, or Higgs bosons, see Fig. 7. An interpretation in the pMSSM is also given, see Fig. 8.

[9] AAD 14X searched in 20.3 fb^{-1} of pp collisions at $\sqrt{s}$ = 8 TeV for events with at least four leptons (electrons, muons, taus) in the final state. No significant excess above the Standard Model expectations is observed. Limits are set on the wino-like chargino mass in an R-parity violating simplified model where the decay $\tilde{\chi}_1^\pm \to W^{(*)}\pm\tilde{\chi}_1^0$, with $\tilde{\chi}_1^0 \to \ell^\pm\ell^\mp\nu$, takes place with a branching ratio of 100%, see Fig. 8.

[10] KHACHATRYAN 14L searched in 19.5 fb^{-1} of pp collisions at $\sqrt{s}$ = 8 TeV for evidence of chargino-neutralino $\tilde{\chi}_1^\pm\tilde{\chi}_2^0$ pair production with Higgs or W-bosons in the decay chain, leading to HW final states with missing transverse energy. The decays of a Higgs boson to a photon pair are considered in conjunction with hadronic and leptonic decay modes of the W bosons. No significant excesses over the expected SM backgrounds are observed. The results are interpreted in the context of simplified models where the decays $\tilde{\chi}_2^0 \to H\tilde{\chi}_1^0$ and $\tilde{\chi}_1^\pm \to W^\pm\tilde{\chi}_1^0$ take place 100% of the time, see Figs. 22–23.

[11] AAD 13 searched in 4.7 fb^{-1} of pp collisions at $\sqrt{s}$ = 7 TeV for charginos and neutralinos decaying to a final state with three leptons (e and μ) and missing transverse energy. No excess beyond the Standard Model expectation is observed. Exclusion limits are derived in the phenomenological MSSM, see Fig. 2 and 3, and in simplified models, see Fig. 4. For the simplified models with intermediate slepton decays, degenerate $\tilde{\chi}_1^\pm$ and $\tilde{\chi}_2^0$ masses up to 500 GeV are excluded at 95% C.L. for very large mass differences with the $\tilde{\chi}_1^0$. Supersedes AAD 12AS.

[12] AAD 13B searched in 4.7 fb^{-1} of pp collisions at $\sqrt{s}$ = 7 TeV for gauginos decaying to a final state with two leptons (e and μ) and missing transverse energy. No excess beyond the Standard Model expectation is observed. Limits are derived in a simplified model of wino-like chargino pair production, where the chargino always decays to the lightest neutralino via an intermediate on-shell charged slepton, see Fig. 2(b). Chargino masses between 110 and 340 GeV are excluded at 95% C.L. for $m_{\tilde{\chi}_1^0}$ = 10 GeV. Exclusion limits are also derived in the phenomenological MSSM, see Fig. 3.

[13] AAD 12CT searched in 4.7 fb^{-1} of pp collisions at $\sqrt{s}$ = 7 TeV for events containing four or more leptons (electrons or muons) and either moderate values of missing transverse momentum or large effective mass. No significant excess is found in the data. Limits are presented in a simplified model of R-parity violating supersymmetry in which charginos are pair-produced and then decay into a W-boson and a $\tilde{\chi}_1^0$, which in turn decays through an RPV coupling into two charged leptons ($e^\pm e^\mp$ or $e^\pm\mu^\mp$) and a neutrino. In this model, chargino masses up to 540 GeV are excluded at 95% C.L. for $m_{\tilde{\chi}_1^0}$ above 300 GeV, see Fig. 3a. The limit deteriorates for lighter $\tilde{\chi}_1^0$. Limits are also set in an R-parity violating mSUGRA model, see Fig. 3b.

[14] CHATRCHYAN 12BJ searched in 4.98 fb^{-1} of pp collisions at $\sqrt{s}$ = 7 TeV for direct electroweak production of charginos and neutralinos in events with at least two leptons, jets and missing transverse momentum. No significant excesses over the expected SM backgrounds are observed and 95% C.L. limits on the production cross section of $\tilde{\chi}_1^\pm\tilde{\chi}_2^0$ pair production were set in a number of simplified models, see Figs. 7 to 12.

[15] ABDALLAH 03M uses data from $\sqrt{s}$ = 192–208 GeV to obtain limits in the framework of the MSSM with gaugino and sfermion mass universality at the GUT scale. An indirect limit on the mass of charginos is derived by constraining the MSSM parameter space by the results from direct searches for neutralinos (including cascade decays), for charginos and for sleptons. These limits are valid for values of $M_2 < 1$ TeV, $|\mu| \leq 2$ TeV with the $\tilde{\chi}_1^0$ as LSP. Constraints from the Higgs search in the $m_h^{\max}$ scenario assuming m_t= 174.3 GeV are included. The quoted limit applies if there is no mixing in the third family or when $m_{\tilde{\tau}_1} - m_{\tilde{\chi}_1^0} > 6$ GeV. If mixing is included the limit degrades to 90 GeV. See Fig. 43 for the mass limits as a function of $\tan\beta$. These limits update the results of ABREU 00W.

[16] KHACHATRYAN 16AA searched in 7.4 fb^{-1} of pp collisions at $\sqrt{s}$ = 8 TeV for events with one or more photons, hadronic jets and $\not{E}_T$. No significant excess above the Standard Model expectations is observed. Limits are set on wino masses in the general gauge-mediated SUSY breaking model (GGM), for a wino-like neutralino NLSP scenario and with the wino mass fixed at 10 GeV above the bino mass, see Fig. 4. Limits are also set in the Tchi1chi1A and Tchi1n1A simplified models, see Fig. 3.

[17] KHACHATRYAN 16R searched in 19.7 fb^{-1} of pp collisions at $\sqrt{s}$ = 8 TeV for events with one or more photons, one electron or muon, and $\not{E}_T$. No significant excess above the Standard Model expectations is observed. Limits are also set in the Tglu1F simplified model, see Fig. 6.

[18] KHACHATRYAN 16Y searched in 19.7 fb^{-1} of pp collisions at $\sqrt{s}$ = 8 TeV for events with one or two soft isolated leptons, hadronic jets, and $\not{E}_T$. No significant excess above the Standard Model expectations is observed. Limits are set on the $\tilde{\chi}_1^\pm$ mass (which is degenerate with the $\tilde{\chi}_2^0$) in the Tchi1n2A simplified model, see Fig. 4.

[19] AAD 14AV searched in 20.3 fb^{-1} of pp collisions at $\sqrt{s}$ = 8 TeV for the direct production of charginos, neutralinos and staus in events containing at last two hadronically decaying τ-leptons, large missing transverse momentum and low jet activity. The quoted limit was derived for direct $\tilde{\chi}_1^\pm\tilde{\chi}_2^0$ and $\tilde{\chi}_1^\pm\tilde{\chi}_1^\mp$ production with $\tilde{\chi}_2^0 \to \tilde{\tau}\tau \to \tau\tau\tilde{\chi}_1^0$ and $\tilde{\chi}_1^\pm \to \tilde{\tau}\nu(\tilde{\nu}_\tau\tau) \to \tau\nu\tilde{\chi}_1^0$, $m_{\tilde{\chi}_2^0} = m_{\tilde{\chi}_1^\pm}$, $m_{\tilde{\tau}}$ = 0.5 ($m_{\tilde{\chi}_1^\pm} + m_{\tilde{\chi}_1^0}$), $m_{\tilde{\chi}_1^0}$ = 0 GeV. No excess over the expected SM background is observed. Exclusion limits are set in simplified models of $\tilde{\chi}_1^\pm\tilde{\chi}_1^\mp$ and $\tilde{\chi}_1^\pm\tilde{\chi}_2^0$ pair production, see their Figure 7. Upper limits on the cross section and signal strength for direct di-stau production are derived, see Figures 8 and 9. Also, limits are derived in a pMSSM model where the only light slepton is the $\tilde{\tau}_R$, see Figure 10.

[20] AAD 14AV searched in 20.3 fb^{-1} of pp collisions at $\sqrt{s}$ = 8 TeV for the direct production of charginos, neutralinos and staus in events containing at last two hadronically decaying τ-leptons, large missing transverse momentum and low jet activity. The quoted limit was derived for direct $\tilde{\chi}_1^\pm\tilde{\chi}_1^\mp$ production with $\tilde{\chi}_1^\pm \to \tilde{\tau}\nu(\tilde{\nu}_\tau\tau) \to \tau\nu\tilde{\chi}_1^0$, $m_{\tilde{\tau}}$ = 0.5 ($m_{\tilde{\chi}_1^\pm} + m_{\tilde{\chi}_1^0}$), $m_{\tilde{\chi}_1^0}$ = 0 GeV. No excess over the expected SM background is observed. Exclusion limits are set in simplified models of $\tilde{\chi}_1^\pm\tilde{\chi}_1^\mp$ and $\tilde{\chi}_1^\pm\tilde{\chi}_2^0$ pair production, see their Figure 7. Upper limits on the cross section and signal strength for direct di-stau production are derived, see Figures 8 and 9. Also, limits are derived in a pMSSM model where the only light slepton is the $\tilde{\tau}_R$, see Figure 10.

[21] AAD 14G searched in 20.3 fb^{-1} of pp collisions at $\sqrt{s}$ = 8 TeV for electroweak production of chargino pairs, or chargino-neutralino pairs, decaying to a final sate with two leptons (e and μ) and missing transverse momentum. No excess beyond the Standard Model expectation is observed. Exclusion limits are derived in simplified models of chargino pair production, with chargino decays to the lightest neutralino via either sleptons or gauge bosons, see Fig 5.; or in simplified models of chargino and next-to-lightest neutralino production, with decays to the lightest neutralino via gauge bosons, see Fig. 7. An interpretation in the pMSSM is also given, see Fig. 10.

[22] AALTONEN 14 searched in 5.8 fb^{-1} of $p\overline{p}$ collisions at $\sqrt{s}$ = 1.96 TeV for evidence of chargino and next-to-lightest neutralino associated production in final states consisting of three leptons (electrons, muons or taus) and large missing transverse momentum. The results are consistent with the Standard Model predictions within 1.85 σ. Limits on the chargino mass are derived in an mSUGRA model with m_0 = 60 GeV, $\tan\beta$ = 3, A_0 = 0 and μ >0, see their Fig. 2.

[23] KHACHATRYAN 14I searched in 19.5 fb^{-1} of pp collisions at $\sqrt{s}$ = 8 TeV for electroweak production of chargino pairs decaying to a final state with opposite-sign lepton pairs (e or μ) and missing transverse momentum. No excess beyond the Standard Model expectation is observed. Exclusion limits are derived in simplified models, see Fig. 18.

[24] AALTONEN 13Q searched in 6.0 fb^{-1} of $p\overline{p}$ collisions at $\sqrt{s}$ = 1.96 TeV for evidence of chargino-neutralino associated production in like-sign dilepton final states. One lepton is identified as the hadronic decay of a tau lepton, while the other is an electron or muon. Good agreement with the Standard Model predictions is observed and limits are set on the chargino-neutralino cross section for simplified gravity- and gauge-mediated models, see their Figs. 2 and 3.

[25] AAD 12AS searched in 2.06 fb^{-1} of pp collisions at $\sqrt{s}$ = 7 TeV for charginos and neutralinos decaying to a final state with three leptons (e and μ) and missing transverse energy. No excess beyond the Standard Model expectation is observed. Exclusion limits are derived in the phenomenological MSSM, see Fig. 2 (top), and in simplified models, see Fig. 2 (bottom).

[26] AAD 12T looked in 1 fb^{-1} of pp collisions at $\sqrt{s}$ = 7 TeV for the production of supersymmetric particles decaying into final states with missing transverse momentum and exactly two isolated leptons (e or μ). Opposite-sign and same-sign dilepton events were separately studied. Additionally, in opposite-sign events, a search was made for an excess of same-flavor over different-flavor lepton pairs. No excess over the expected background is observed and limits are placed on the effective production cross section of opposite-sign dilepton events with $\not{E}_T$ > 250 GeV and on same-sign dilepton events with $\not{E}_T$ > 100 GeV. The latter limit is interpreted in a simplified electroweak gaugino production model as a lower chargino mass limit.

[27] CHATRCHYAN 11B looked in 35 pb^{-1} of pp collisions at $\sqrt{s}$=7 TeV for events with an isolated lepton (e or μ), a photon and $\not{E}_T$ which may arise in a generalized gauge

mediated model from the decay of Wino-like NLSPs. No evidence for an excess over the expected background is observed. Limits are derived in the plane of squark/gluino mass versus Wino mass (see Fig. 4). Mass degeneracy of the produced squarks and gluinos is assumed.

[28] CHATRCHYAN 11V looked in 35 pb^{-1} of pp collisions at $\sqrt{s} = 7$ TeV for events with ≥ 3 isolated leptons (e, μ or τ), with or without jets and $\not{E}_T$. No evidence for an excess over the expected background is observed. Limits are derived in the CMSSM (m_0, $m_{1/2}$) plane for tan$\beta = 3$ (see Fig. 5).

Long-lived $\widetilde{\chi}^{\pm}$ (Chargino) mass limit

Limits on charginos which leave the detector before decaying.

VALUE (GeV)	CL%	DOCUMENT ID		TECN	COMMENT
>620	95	[1] AAD	15AE	ATLS	stable $\widetilde{\chi}^{\pm}$
>534	95	[2] AAD	15BM	ATLS	stable $\widetilde{\chi}^{\pm}$
>239	95	[2] AAD	15BM	ATLS	$\widetilde{\chi}^{\pm} \to \widetilde{\chi}^0_1 \pi^{\pm}$, lifetime 1 ns, $m_{\widetilde{\chi}^{\pm}} - m_{\widetilde{\chi}^0_1} = 0.14$ GeV
>482	95	[2] AAD	15BM	ATLS	$\widetilde{\chi}^{\pm} \to \widetilde{\chi}^0_1 \pi^{\pm}$, lifetime 15 ns, $m_{\widetilde{\chi}^{\pm}} - m_{\widetilde{\chi}^0_1} = 0.14$ GeV
>103	95	[3] AAD	13H	ATLS	long-lived $\widetilde{\chi}^{\pm} \to \widetilde{\chi}^0_1 \pi^{\pm}$, mAMSB, $\Delta m_{\widetilde{\chi}^0_1} = 160$ MeV
> 92	95	[4] AAD	12BJ	ATLS	long-lived $\widetilde{\chi}^{\pm} \to \pi^{\pm} \widetilde{\chi}^0_1$, mAMSB
>171	95	[5] ABAZOV	09M	D0	$\widetilde{H}$
>102	95	[6] ABBIENDI	03L	OPAL	$m_{\widetilde{\nu}}$ >500 GeV
none 2–93.0	95	[7] ABREU	00T	DLPH	$\widetilde{H}^{\pm}$ or $m_{\widetilde{\nu}} > m_{\widetilde{\chi}^{\pm}}$
• • • We do not use the following data for averages, fits, limits, etc. • • •					
>260	95	[8] KHACHATRY...15AB		CMS	$\widetilde{\chi}^{\pm}_1 \to \widetilde{\chi}^0_1 \pi^{\pm}$, $\tau_{\widetilde{\chi}^{\pm}_1}$=0.2ns, AMSB
>800	95	[9] KHACHATRY...15AO		CMS	long-lived $\widetilde{\chi}^{\pm}_1$, mAMSB, τ >100ns
>100	95	[9] KHACHATRY...15AO		CMS	long-lived $\widetilde{\chi}^{\pm}_1$, mAMSB, $\tau > 3$ ns
	95	[10] KHACHATRY...15W		CMS	long-lived $\widetilde{\chi}^0$, $\widetilde{q} \to q\widetilde{\chi}^0$, $\widetilde{\chi}^0 \to \ell^+\ell^-\nu$, RPV
>270	95	[11] AAD	13BD	ATLS	disappearing-track signature, AMSB
>278	95	[12] ABAZOV	13B	D0	long-lived $\widetilde{\chi}^{\pm}$, gaugino-like
>244	95	[12] ABAZOV	13B	D0	long-lived $\widetilde{\chi}^{\pm}$, higgsino-like

[1] AAD 15AE searched in 19.1 fb^{-1} of pp collisions at $\sqrt{s} = 8$ TeV for heavy long-lived charged particles, measured through their specific ionization energy loss in the ATLAS pixel detector or their time-of-flight in the ALTAS muon system. In the absence of an excess of events above the expected backgrounds, limits are set on stable charginos, see Fig. 10.

[2] AAD 15BM searched in 18.4 fb^{-1} of pp collisions at $\sqrt{s} = 8$ TeV for stable and metastable non-relativistic charged particles through their anomalous specific ionization energy loss in the ATLAS pixel detector. In absence of an excess of events above the expected backgrounds, limits are set on stable charginos (see Table 5) and on metastable charginos decaying to $\widetilde{\chi}^0_1 \pi^{\pm}$, see Fig. 11.

[3] AAD 13H searched in 4.7 fb^{-1} of pp collisions at $\sqrt{s} = 7$ TeV for direct electroweak production of long-lived charginos in the context of AMSB scenarios. The search is based on the signature of a high-momentum isolated track with few associated hits in the outer part of the tracking system, arising from a chargino decay into a neutralino and a low-momentum pion. The p_T spectrum of the tracks was found to be consistent with the SM expectations. Constraints on the lifetime and the production cross section were obtained, see Fig. 6. In the minimal AMSB framework with tan$\beta = 5$, and $\mu > 0$, a chargino having a mass below 103 (85) GeV for a chargino-neutralino mass splitting $\Delta m_{\widetilde{\chi}^0_1}$ of 160 (170) MeV is excluded at the 95% C.L. See Fig. 7 for more precise bounds.

[4] AAD 12BJ looked in 1.02 fb^{-1} of pp collisions at $\sqrt{s} = 7$ TeV for signatures of decaying charginos resulting in isolated tracks with few associated hits in the outer region of the tracking system. The p_T spectrum of the tracks was found to be consistent with the SM expectations. Constraints on the lifetime and the production cross section were obtained. In the minimal AMSB framework with $m_{3/2} < 32$ TeV, $m_0 < 1.5$ TeV, tan$\beta = 5$, and $\mu > 0$, a chargino having a mass below 92 GeV and a lifetime between 0.5 ns and 2 ns is excluded at the 95% C.L. See their Fig. 8 for more precise bounds.

[5] ABAZOV 09M searched in 1.1 fb^{-1} of $p\overline{p}$ collisions at $\sqrt{s} = 1.96$ TeV for events with direct production of a pair of charged massive stable particles identified by their TOF. The number of the observed events is consistent with the predicted background. The data are used to constrain the production cross section as a function of the $\widetilde{\chi}^{\pm}_1$ mass, see their Fig. 2. The quoted limit improves to 206 GeV for gaugino-like charginos.

[6] ABBIENDI 03L used e^+e^- data at $\sqrt{s} = 130$–209 GeV to select events with two high momentum tracks with anomalous dE/dx. The excluded cross section is compared to the theoretical expectation as a function of the heavy particle mass in their Fig. 3. The bounds are valid for colorless fermions with lifetime longer than 10^{-6} s. Supersedes the results from ACKERSTAFF 98P.

[7] ABREU 00T searches for the production of heavy stable charged particles, identified by their ionization or Cherenkov radiation, using data from $\sqrt{s}$= 130 to 189 GeV. These limits include and update the results of ABREU 98P.

[8] KHACHATRYAN 15AB searched in 19.5 fb^{-1} of pp collisions at $\sqrt{s} = 8$ TeV for events containing tracks with little or no associated calorimeter energy deposits and with missing hits in the outer layers of the tracking system (disappearing-track signature). Such disappearing tracks can result from the decay of charginos that are nearly mass degenerate with the lightest neutralino. The number of observed events is in agreement with the background expectation. Limits are set on the cross section of electroweak chargino production in terms of the chargino mass and mean proper lifetime, see Fig. 4. In the minimal AMSB model, a chargino mass below 260 GeV is excluded at 95% C.L., see their Fig. 5.

[9] KHACHATRYAN 15O searched in 18.8 fb^{-1} of pp collisions at $\sqrt{s} = 8$ TeV for evidence of long-lived charginos in the context of AMSB and pMSSM scenarios. The results are based on a previously published search for heavy stable charged particles at 7 and 8 TeV. In the minimal AMSB framework with tan$\beta = 5$ and $\mu \geq 0$, constraints on the chargino mass and lifetime were placed, see Fig. 5. Charginos with a mass below 800 (100) GeV are excluded at the 95% C.L. for lifetimes above 100 ns (3 ns). Constraints are also placed on the pMSSM parameter space, see Fig. 3.

[10] KHACHATRYAN 15W searched in up to 20.5 fb^{-1} of pp collisions at $\sqrt{s} = 8$ TeV for evidence of long-lived neutralinos produced through $\widetilde{q}$-pair production, with $\widetilde{q} \to q\widetilde{\chi}^0$ and $\widetilde{\chi}^0 \to \ell^+\ell^-\nu$ (RPV: λ_{121}, $\lambda_{122} \neq 0$). 95% C.L. exclusion limits on cross section times branching ratio are set as a function of mean proper decay length of the neutralino, see Figs. 6 and 9.

[11] AAD 13BD searched in 20.3 fb^{-1} of pp collisions at $\sqrt{s} = 8$ TeV for events containing tracks with no associated hits in the outer region of the tracking system resulting from the decay of charginos that are nearly mass degenerate with the lightest neutralino, as is often the case in AMSB scenarios. No significant excess above the background expectation is observed for candidate tracks with large transverse momentum. Constraints on chargino properties are obtained and in the minimal AMSB model, a chargino mass below 270 GeV is excluded at 95% C.L., see their Fig. 7.

[12] ABAZOV 13B looked in 6.3 fb^{-1} of $p\overline{p}$ collisions at $\sqrt{s} = 1.96$ TeV for charged massive long-lived particles in events with muon-like particles that have both speed and ionization energy loss inconsistent with muons produced in beam collisions. In the absence of an excess, limits are set at 95% C.L. on gaugino- and higgsino-like charginos, see their Table 20 and Fig. 23.

$\widetilde{\nu}$ (Sneutrino) mass limit

The limits may depend on the number, $N(\widetilde{\nu})$, of sneutrinos assumed to be degenerate in mass. Only $\widetilde{\nu}_L$ (not $\widetilde{\nu}_R$) is assumed to exist. It is possible that $\widetilde{\nu}$ could be the lightest supersymmetric particle (LSP).

We report here, but do not include in the Listings, the limits obtained from the fit of the final results obtained by the LEP Collaborations on the invisible width of the Z boson ($\Delta\Gamma_{\text{inv.}} < 2.0$ MeV, LEP-SLC 06): $m_{\widetilde{\nu}} > 43.7$ GeV ($N(\widetilde{\nu})$=1) and $m_{\widetilde{\nu}} > 44.7$ GeV ($N(\widetilde{\nu})$=3) .

Some earlier papers are now obsolete and have been omitted. They were last listed in our PDG 14 edition: K. Olive, *et al.* (Particle Data Group), Chinese Physics **C38** 070001 (2014) (http://pdg.lbl.gov).

VALUE (GeV)	CL%	DOCUMENT ID		TECN	COMMENT
>2300	95	[1] AABOUD	16P	ATLS	RPV, $\widetilde{\nu}_\tau \to e\mu$, $\lambda'_{311} = 0.11$
>2200	95	[1] AABOUD	16P	ATLS	RPV, $\widetilde{\nu}_\tau \to e\tau$, $\lambda'_{311} = 0.11$
>1900	95	[1] AABOUD	16P	ATLS	RPV, $\widetilde{\nu}_\tau \to \mu\tau$, $\lambda'_{311} = 0.11$
> 400	95	[2] AAD	14X	ATLS	RPV, $\geq 4\ell^{\pm}$, $\widetilde{\nu} \to \nu\widetilde{\chi}^0_1$, $\widetilde{\chi}^0_1 \to \ell^{\pm}\ell^{\mp}\nu$
		[3] AAD	11Z	ATLS	RPV, $\widetilde{\nu}_\tau \to e\mu$
> 94	95	[4] ABDALLAH	03M	DLPH	$1 \leq \tan\beta \leq 40$, $m_{\widetilde{e}_R} - m_{\widetilde{\chi}^0_1} >$10 GeV
> 84	95	[5] HEISTER	02N	ALEP	$\widetilde{\nu}_e$, any Δm
> 41	95	[6] DECAMP	92	ALEP	$\Gamma(Z \to$ invisible); $N(\widetilde{\nu})$=3, model independent
• • • We do not use the following data for averages, fits, limits, etc. • • •					
>1280	95	[7] KHACHATRY...16BE		CMS	RPV, $\widetilde{\nu}_\tau \to e\mu$, $\lambda_{132} = \lambda_{231} = \lambda'_{311} = 0.01$
>2300	95	[7] KHACHATRY...16BE		CMS	RPV, $\widetilde{\nu}_\tau \to e\mu$, $\lambda_{132} = \lambda_{231} =$ 0.07, $\lambda'_{311} = 0.11$
>2000	95	[8] AAD	15O	ATLS	RPV ($e\mu$), $\widetilde{\nu}_\tau$, $\lambda'_{311} = 0.11$, $\lambda_{i3k} = 0.07$
>1700	95	[8] AAD	15O	ATLS	RPV ($\tau\mu$, $e\tau$), $\widetilde{\nu}_\tau$, $\lambda'_{311} = 0.11$, $\lambda_{i3k} = 0.07$
		[9] AAD	13AI	ATLS	RPV, $\widetilde{\nu}_\tau \to e\mu$, $e\tau$, $\mu\tau$
		[10] AAD	11H	ATLS	RPV, $\widetilde{\nu}_\tau \to e\mu$
		[11] AALTONEN	10Z	CDF	RPV, $\widetilde{\nu}_\tau \to e\mu$, $e\tau$, $\mu\tau$
		[12] ABAZOV	10M	D0	RPV, $\widetilde{\nu}_\tau \to e\mu$
> 95	95	[13] ABDALLAH	04H	DLPH	AMSB, $\mu > 0$
> 37.1	95	[14] ADRIANI	93M	L3	$\Gamma(Z \to$ invisible); $N(\widetilde{\nu})$=1
> 36	95	ABREU	91F	DLPH	$\Gamma(Z \to$ invisible); $N(\widetilde{\nu})$=1
> 31.2	95	[15] ALEXANDER	91F	OPAL	$\Gamma(Z \to$ invisible); $N(\widetilde{\nu})$=1

[1] AABOUD 16P searched in 3.2 fb^{-1} of pp collisions at $\sqrt{s} = 13$ TeV for events with different flavour dilepton pairs ($e\mu$, $e\tau$, $\mu\tau$) from the production of $\widetilde{\nu}_\tau$ via an RPV λ'_{311} coupling and followed by a decay via $\lambda_{312} = \lambda_{321} = 0.07$ for $e + \mu$, via $\lambda_{313} = \lambda_{331} = 0.07$ for $e + \tau$ and via $\lambda_{323} = \lambda_{332} = 0.07$ for $\mu + \tau$. No evidence for a dilepton resonance over the SM expectation is observed, and limits are derived on $m_{\widetilde{\nu}}$ at 95% CL, see their Figs. 2(b), 3(b), 4(b), and Table 3.

[2] AAD 14X searched in 20.3 fb^{-1} of pp collisions at $\sqrt{s} = 8$ TeV for events with at least four leptons (electrons, muons, taus) in the final state. No significant excess above the Standard Model expectations is observed. Limits are set on the sneutrino mass in an R-parity violating simplified model where the decay $\widetilde{\nu} \to \nu\widetilde{\chi}^0_1$, with $\widetilde{\chi}^0_1 \to \ell^{\pm}\ell^{\mp}\nu$, takes place with a branching ratio of 100%, see Fig. 9.

[3] AAD 11Z looked in 1.07 fb^{-1} of pp collisions at $\sqrt{s} = 7$ TeV for events with one electron and one muon of opposite charge from the production of $\widetilde{\nu}_\tau$ via an RPV λ'_{311} coupling and followed by a decay via λ_{312} into $e + \mu$. No evidence for an (e, μ) resonance over the SM expectation is observed, and a limit is derived in the plane of λ'_{311} versus $m_{\widetilde{\nu}}$ for three values of λ_{312}, see their Fig. 2. Masses $m_{\widetilde{\nu}} < 1.32$ (1.45) TeV are excluded for $\lambda'_{311} = 0.10$ and $\lambda_{312} = 0.05$ ($\lambda'_{311} = 0.11$ and $\lambda_{312} = 0.07$).

[4] ABDALLAH 03M uses data from $\sqrt{s} = 192$–208 GeV to obtain limits in the framework of the MSSM with gaugino and sfermion mass universality at the GUT scale. An indirect limit on the mass is derived by constraining the MSSM parameter space by the results from direct searches for neutralinos (including cascade decays) and for sleptons. These limits are valid for values of $M_2 < 1$ TeV, $|\mu| \leq 1$ TeV with the $\widetilde{\chi}^0_1$ as LSP. The quoted limit is obtained when there is no mixing in the third family. See Fig. 43 for the mass limits as a function of tanβ. These limits update the results of ABREU 00W.

[5] HEISTER 02N derives a bound on $m_{\widetilde{\nu}_e}$ by exploiting the mass relation between the $\widetilde{\nu}_e$ and $\widetilde{e}$, based on the assumption of universal GUT scale gaugino and scalar masses $m_{1/2}$ and m_0 and the search described in the $\widetilde{e}$ section. In the MSUGRA framework with radiative electroweak symmetry breaking, the limit improves to $m_{\widetilde{\nu}_e}$ >130 GeV, assuming a trilinear coupling A_0=0 at the GUT scale. See Figs. 5 and 7 for the dependence of the limits on tanβ.

[6] DECAMP 92 limit is from $\Gamma(\text{invisible})/\Gamma(\ell\ell) = 5.91 \pm 0.15$ ($N_\nu = 2.97 \pm 0.07$).

[7] KHACHATRYAN 16BE searched in 19.7 fb^{-1} of pp collisions at $\sqrt{s}$ = 8 TeV for evidence of narrow resonances decaying into $e\mu$ final states. No significant excess above the Standard Model expectation is observed and 95% C.L. exclusions are placed on the cross section times branching ratio for the production of an R-parity-violating supersymmetric tau sneutrino, see their Fig. 3.

[8] AAD 15O searched in 20.3 fb^{-1} of pp collisions at $\sqrt{s}$ = 8 TeV for evidence of heavy particles decaying into $e\mu$, $e\tau$ or $\mu\tau$ final states. No significant excess above the Standard Model expectation is observed, and 95% C.L. exclusions are placed on the cross section times branching ratio for the production of an R-parity-violating supersymmetric tau sneutrino, applicable to any sneutrino flavour, see their Fig. 2.

[9] AAD 13AI searched in 4.6 fb^{-1} of pp collisions at $\sqrt{s}$ = 7 TeV for evidence of heavy particles decaying into $e\mu$, $e\tau$ or $\mu\tau$ final states. No significant excess above the Standard Model expectation is observed, and 95% C.L. exclusions are placed on the cross section times branching ratio for the production of an R-parity-violating supersymmetric tau sneutrino, see their Fig. 2. For couplings λ'_{311} = 0.10 and λ_{i3k} = 0.05, the lower limits on the $\widetilde{\nu}_\tau$ mass are 1610, 1110, 1100 GeV in the $e\mu$, $e\tau$, and $\mu\tau$ channels, respectively.

[10] AAD 11H looked in 35 pb^{-1} of pp collisions at $\sqrt{s}$ = 7 TeV for events with one electron and one muon of opposite charge from the production of $\widetilde{\nu}_\tau$ via an RPV λ'_{311} coupling and followed by a decay via λ_{312} into $e + \mu$. No evidence for an excess over the SM expectation is observed, and a limit is derived in the plane of λ'_{311} versus $m_{\widetilde{\nu}}$ for several values of λ_{312}, see their Fig. 2. Superseded by AAD 11Z.

[11] AALTONEN 10Z searched in 1 fb^{-1} of $p\overline{p}$ collisions at $\sqrt{s}$ = 1.96 TeV for events from the production $d\overline{d} \to \widetilde{\nu}_\tau$ with the subsequent decays $\widetilde{\nu}_\tau \to e\mu$, $\mu\tau$, $e\tau$ in the MSSM framework with RPV. Two isolated leptons of different flavor and opposite charges are required, with τs identified by their hadronic decay. No statistically significant excesses are observed over the SM background. Upper limits on λ'^2_{311} times the branching ratio are listed in their Table III for various $\widetilde{\nu}_\tau$ masses. Limits on the cross section times branching ratio for λ'_{311} = 0.10 and λ_{i3k} = 0.05, displayed in Fig. 2, are used to set limits on the $\widetilde{\nu}_\tau$ mass of 558 GeV for the $e\mu$, 441 GeV for the $\mu\tau$ and 442 GeV for the $e\tau$ channels.

[12] ABAZOV 10M looked in 5.3 fb^{-1} of $p\overline{p}$ collisions at $\sqrt{s}$ = 1.96 TeV for events with exactly one pair of high p_T isolated $e\mu$ and a veto against hard jets. No evidence for an excess over the SM expectation is observed, and a limit at 95% C.L. on the cross section times branching ratio is derived, see their Fig. 3. These limits are translated into limits on couplings as a function of $m_{\widetilde{\nu}_\tau}$ as shown on their Fig. 4. As an example, for $m_{\widetilde{\nu}_\tau}$ = 100 GeV and $\lambda_{312} \leq 0.07$, couplings $\lambda'_{311} > 7.7 \times 10^{-4}$ are excluded.

[13] ABDALLAH 04H use data from LEP 1 and $\sqrt{s}$ = 192–208 GeV. They re-use results or re-analyze the data from ABDALLAH 03M to put limits on the parameter space of anomaly-mediated supersymmetry breaking (AMSB), which is scanned in the region 1< $m_{3/2}$ <50 TeV, 0< m_0 <1000 GeV, 1.5<tanβ <35, both signs of μ. The constraints are obtained from the searches for mass degenerate chargino and neutralino, for SM-like and invisible Higgs, for leptonically decaying charginos and from the limit on non-SM Z width of 3.2 MeV. The limit is for m_t = 174.3 GeV (see Table 2 for other m_t values). The limit improves to 114 GeV for $\mu < 0$.

[14] ADRIANI 93M limit from $\Delta\Gamma(Z)$(invisible)< 16.2 MeV.

[15] ALEXANDER 91F limit is for one species of $\widetilde{\nu}$ and is derived from Γ(invisible, new)/$\Gamma(\ell\ell)$ < 0.38.

Charged sleptons

This section contains limits on charged scalar leptons ($\widetilde{\ell}$, with ℓ=e,μ,τ). Studies of width and decays of the Z boson (use is made here of $\Delta\Gamma_{\text{inv}} < 2.0$ MeV, LEP 00) conclusively rule out $m_{\widetilde{\ell}_R} < 40$ GeV (41 GeV for $\widetilde{\ell}_L$) , independently of decay modes, for each individual slepton. The limits improve to 43 GeV (43.5 GeV for $\widetilde{\ell}_L$) assuming all 3 flavors to be degenerate. Limits on higher mass sleptons depend on model assumptions and on the mass splitting Δm= $m_{\widetilde{\ell}} - m_{\widetilde{\chi}^0_1}$. The mass and composition of $\widetilde{\chi}^0_1$ may affect the selectron production rate in e^+e^- collisions through t-channel exchange diagrams. Production rates are also affected by the potentially large mixing angle of the lightest mass eigenstate $\widetilde{\ell}_1$=$\widetilde{\ell}_R$ sinθ_ℓ + $\widetilde{\ell}_L$ cosθ_ℓ. It is generally assumed that only $\widetilde{\tau}$ may have significant mixing. The coupling to the Z vanishes for θ_ℓ=0.82. In the high-energy limit of e^+e^- collisions the interference between γ and Z exchange leads to a minimal cross section for θ_ℓ=0.91, a value which is sometimes used in the following entries relative to data taken at LEP2. When limits on $m_{\widetilde{\ell}_R}$ are quoted, it is understood that limits on $m_{\widetilde{\ell}_L}$ are usually at least as strong.

Possibly open decays involving gauginos other than $\widetilde{\chi}^0_1$ will affect the detection efficiencies. Unless otherwise stated, the limits presented here result from the study of $\widetilde{\ell}^+\widetilde{\ell}^-$ production, with production rates and decay properties derived from the MSSM. Limits made obsolete by the recent analyses of e^+e^- collisions at high energies can be found in previous Editions of this Review.

For decays with final state gravitinos ($\widetilde{G}$), $m_{\widetilde{G}}$ is assumed to be negligible relative to all other masses.

R-parity conserving $\widetilde{e}$ (Selectron) mass limit

Some earlier papers are now obsolete and have been omitted. They were last listed in our PDG 14 edition: K. Olive, *et al.* (Particle Data Group), Chinese Physics **C38** 070001 (2014) (http://pdg.lbl.gov).

VALUE (GeV)	CL%	DOCUMENT ID		TECN	COMMENT
		[1] CHATRCHYAN 14R		CMS	$\geq 3\ell^\pm$, $\widetilde{\ell} \to \ell^\pm\tau^\mp\tau^\mp\widetilde{G}$ simplified model, GMSB, stau (N)NLSP scenario
		[2] AAD	13B	ATLS	$2\ell^\pm + \not{E}_T$, SMS, pMSSM
> 97.5		[3] ABBIENDI	04	OPAL	$\widetilde{e}_R$,$\Delta m > 11$ GeV, $\lvert\mu\rvert$ >100 GeV, tanβ=1.5
> 94.4		[4] ACHARD	04	L3	$\widetilde{e}_R$,$\Delta m > 10$ GeV, $\lvert\mu\rvert$ >200 GeV, tan$\beta \geq 2$
> 71.3		[4] ACHARD	04	L3	$\widetilde{e}_R$, all Δm
none 30–94	95	[5] ABDALLAH	03M	DLPH	Δm >15 GeV, $\widetilde{e}^\pm_R\widetilde{e}^\mp_R$
> 94	95	[6] ABDALLAH	03M	DLPH	$\widetilde{e}_R$,$1 \leq \tan\beta \leq 40$, Δm >10 GeV
> 95	95	[7] HEISTER	02E	ALEP	$\Delta m > 15$ GeV, $\widetilde{e}^+_R\widetilde{e}^-_R$
> 73	95	[8] HEISTER	02N	ALEP	$\widetilde{e}_R$, any Δm
>107	95	[8] HEISTER	02N	ALEP	$\widetilde{e}_L$, any Δm
• • • We do not use the following data for averages, fits, limits, etc. • • •					
none 90–325	95	[9] AAD	14G	ATLS	$\widetilde{\ell}\widetilde{\ell} \to \ell^+\widetilde{\chi}^0_1\ell^-\widetilde{\chi}^0_1$, simplified model, $m_{\widetilde{\ell}_L} = m_{\widetilde{\ell}_R}$, $m_{\widetilde{\chi}^0_1}$ = 0 GeV
		[10] KHACHATRY...14I		CMS	$\widetilde{\ell} \to \ell\widetilde{\chi}^0_1$, simplified model

[1] CHATRCHYAN 14R searched in 19.5 fb^{-1} of pp collisions at $\sqrt{s}$ = 8 TeV for events with at least three leptons (electrons, muons, taus) in the final state. No significant excess above the Standard Model expectations is observed. Limits are set on the slepton mass in a stau (N)NLSP simplified model (GMSB) where the decay $\widetilde{\ell} \to \ell^\pm\tau^\pm\tau^\mp\widetilde{G}$ takes place with a branching ratio of 100%, see Fig. 8.

[2] AAD 13B searched in 4.7 fb^{-1} of pp collisions at $\sqrt{s}$ = 7 TeV for sleptons decaying to a final state with two leptons (e and μ) and missing transverse energy. No excess beyond the Standard Model expectation is observed. Limits are derived in a simplified model of direct left-handed slepton pair production, where left-handed slepton masses between 85 and 195 GeV are excluded at 95% C.L. for $m_{\widetilde{\chi}^0_1}$ = 20 GeV. See also Fig. 2(a). Exclusion limits are also derived in the phenomenological MSSM, see Fig. 3.

[3] ABBIENDI 04 search for $\widetilde{e}_R\widetilde{e}_R$ production in acoplanar di-electron final states in the 183–208 GeV data. See Fig. 13 for the dependence of the limits on $m_{\widetilde{\chi}^0_1}$ and for the limit at tanβ=35 This limit supersedes ABBIENDI 00G.

[4] ACHARD 04 search for $\widetilde{e}_R\widetilde{e}_L$ and $\widetilde{e}_R\widetilde{e}_R$ production in single- and acoplanar di-electron final states in the 192–209 GeV data. Absolute limits on $m_{\widetilde{e}_R}$ are derived from a scan over the MSSM parameter space with universal GUT scale gaugino and scalar masses $m_{1/2}$ and m_0, $1 \leq \tan\beta \leq 60$ and $-2 \leq \mu \leq 2$ TeV. See Fig. 4 for the dependence of the limits on $m_{\widetilde{\chi}^0_1}$. This limit supersedes ACCIARRI 99W.

[5] ABDALLAH 03M looked for acoplanar dielectron $+\not{E}$ final states at $\sqrt{s}$ = 189–208 GeV. The limit assumes μ=$-$200 GeV and tanβ=1.5 in the calculation of the production cross section and B($\widetilde{e} \to e\widetilde{\chi}^0_1$). See Fig. 15 for limits in the ($m_{\widetilde{e}_R}$, $m_{\widetilde{\chi}^0_1}$) plane. These limits include and update the results of ABREU 01

[6] ABDALLAH 03M uses data from $\sqrt{s}$ = 192–208 GeV to obtain limits in the framework of the MSSM with gaugino and sfermion mass universality at the GUT scale. An indirect limit on the mass is derived by constraining the MSSM parameter space by the results from direct searches for neutralinos (including cascade decays) and for sleptons. These limits are valid for values of M_2 <1 TeV, $\lvert\mu\rvert \leq 1$ TeV with the $\widetilde{\chi}^0_1$ as LSP. The quoted limit is obtained when there is no mixing in the third family. See Fig. 43 for the mass limits as a function of tanβ. These limits update the results of ABREU 00W.

[7] HEISTER 02E looked for acoplanar dielectron + $\not{E}_T$ final states from e^+e^- interactions between 183 and 209 GeV. The mass limit assumes $\mu < -200$ GeV and tanβ=2 for the production cross section and B($\widetilde{e} \to e\widetilde{\chi}^0_1$)=1. See their Fig. 4 for the dependence of the limit on Δm. These limits include and update the results of BARATE 01.

[8] HEISTER 02N search for $\widetilde{e}_R\widetilde{e}_L$ and $\widetilde{e}_R\widetilde{e}_R$ production in single- and acoplanar di-electron final states in the 183–208 GeV data. Absolute limits on $m_{\widetilde{e}_R}$ are derived from a scan over the MSSM parameter space with universal GUT scale gaugino and scalar masses $m_{1/2}$ and m_0, $1 \leq \tan\beta \leq 50$ and $-10 \leq \mu \leq 10$ TeV. The region of small $\lvert\mu\rvert$, where cascade decays are important, is covered by a search for $\widetilde{\chi}^0_1\widetilde{\chi}^0_3$ in final states with leptons and possibly photons. Limits on $m_{\widetilde{e}_L}$ are derived by exploiting the mass relation between the $\widetilde{e}_L$ and $\widetilde{e}_R$, based on universal m_0 and $m_{1/2}$. When the constraint from the mass limit of the lightest Higgs from HEISTER 02 is included, the bounds improve to $m_{\widetilde{e}_R}$ >77(75) GeV and $m_{\widetilde{e}_L}$ >115(115) GeV for a top mass of 175(180) GeV. In the MSUGRA framework with radiative electroweak symmetry breaking, the limits improve further to $m_{\widetilde{e}_R}$ >95 GeV and $m_{\widetilde{e}_L}$ >152 GeV, assuming a trilinear coupling A_0=0 at the GUT scale. See Figs. 4, 5, 7 for the dependence of the limits on tanβ.

[9] AAD 14G searched in 20.3 fb^{-1} of pp collisions at $\sqrt{s}$ = 8 TeV for electroweak production of slepton pairs, decaying to a final sate with two leptons (e and μ) and missing transverse momentum. No excess beyond the Standard Model expectation is observed. Exclusion limits are derived in simplified models of slepton pair production, see Fig. 8. An interpretation in the pMSSM is also given, see Fig. 10.

[10] KHACHATRYAN 14I searched in 19.5 fb^{-1} of pp collisions at $\sqrt{s}$ = 8 TeV for electroweak production of slepton pairs decaying to a final state with opposite-sign lepton pairs (e or μ) and missing transverse momentum. No excess beyond the Standard Model expectation is observed. Exclusion limits are derived in simplified models, see Fig. 18.

R-partiy violating $\widetilde{e}$ (Selectron) mass limit

Some earlier papers are now obsolete and have been omitted. They were last listed in our PDG 14 edition: K. Olive, *et al.* (Particle Data Group), Chinese Physics **C38** 070001 (2014) (http://pdg.lbl.gov).

VALUE (GeV)	CL%	DOCUMENT ID		TECN	COMMENT
>410	95	[1] AAD	14X	ATLS	RPV, $\geq 4\ell^\pm$, $\widetilde{\ell} \to l\widetilde{\chi}^0_1$, $\widetilde{\chi}^0_1 \to \ell^\pm\ell^\mp\nu$

• • • We do not use the following data for averages, fits, limits, etc. • • •

> 89	95	[2] ABBIENDI	04F	OPAL	RPV, $\tilde{e}_L$	
> 92	95	[3] ABDALLAH	04M	DLPH	RPV, $\tilde{e}_R$, indirect, Δm >5 GeV	

[1] AAD 14X searched in 20.3 fb^{-1} of pp collisions at $\sqrt{s}$ = 8 TeV for events with at least four leptons (electrons, muons, taus) in the final state. No significant excess above the Standard Model expectations is observed. Limits are set on the slepton mass in an R-parity violating simplified model where the decay $\tilde{\ell} \to \ell\tilde{\chi}_1^0$, with $\tilde{\chi}_1^0 \to \ell^\pm\ell^\mp\nu$, takes place with a branching ratio of 100%, see Fig. 9.

[2] ABBIENDI 04F use data from $\sqrt{s}$ = 189–209 GeV. They derive limits on sparticle masses under the assumption of RPV with $LL\overline{E}$ or $LQ\overline{D}$ couplings. The results are valid for tanβ = 1.5, $\mu = -200$ GeV, with, in addition, $\Delta m > 5$ GeV for indirect decays via $LQ\overline{D}$. The limit quoted applies to direct decays via $LL\overline{E}$ or $LQ\overline{D}$ couplings. For indirect decays, the limits on the $\tilde{e}_R$ mass are respectively 99 and 92 GeV for $LL\overline{E}$ and $LQ\overline{D}$ couplings and $m_{\tilde{\chi}_1^0}$ = 10 GeV and degrade slightly for larger $\tilde{\chi}_1^0$ mass. Supersedes the results of ABBIENDI 00.

[3] ABDALLAH 04M use data from $\sqrt{s}$ = 192–208 GeV to derive limits on sparticle masses under the assumption of RPV with $LL\overline{E}$ or $\overline{UDD}$ couplings. The results are valid for $\mu = -200$ GeV, tanβ = 1.5, $\Delta m > 5$ GeV and assuming a BR of 1 for the given decay. The limit quoted is for indirect $\overline{UDD}$ decays using the neutralino constraint of 39.5 GeV for $LL\overline{E}$ and of 38.0 GeV for $\overline{UDD}$ couplings, also derived in ABDALLAH 04M. For indirect decays via $LL\overline{E}$ the limit improves to 95 GeV if the constraint from the neutralino is used and to 94 GeV if it is not used. For indirect decays via $\overline{UDD}$ couplings it remains unchanged when the neutralino constraint is not used. Supersedes the result of ABREU 00U.

R-parity conserving $\tilde{\mu}$ (Smuon) mass limit

VALUE (GeV)	CL%	DOCUMENT ID		TECN	COMMENT
		[1] CHATRCHYAN	14R	CMS	$\geq 3\ell^\pm$, $\tilde{\ell} \to \ell^\pm\tau^\mp\tau^\mp\tilde{G}$ simplified model, GMSB, stau (N)NLSP scenario
		[2] AAD	13B	ATLS	$2\ell^\pm + \not{E}_T$, SMS, pMSSM
>91.0		[3] ABBIENDI	04	OPAL	Δm >3 GeV, $\tilde{\mu}_R^+\tilde{\mu}_R^-$, $\lvert\mu\rvert$ >100 GeV, tanβ=1.5
>86.7		[4] ACHARD	04	L3	Δm >10 GeV, $\tilde{\mu}_R^+\tilde{\mu}_R^-$, $\lvert\mu\rvert$ >200 GeV, tan$\beta \geq 2$
none 30–88	95	[5] ABDALLAH	03M	DLPH	Δm >5 GeV, $\tilde{\mu}_R^+\tilde{\mu}_R^-$
>94	95	[6] ABDALLAH	03M	DLPH	$\tilde{\mu}_R$,1 $\leq$ tan$\beta \leq$ 40, Δm >10 GeV
>88	95	[7] HEISTER	02E	ALEP	$\Delta m > 15$ GeV, $\tilde{\mu}_R^+\tilde{\mu}_R^-$

• • • We do not use the following data for averages, fits, limits, etc. • • •

none 90–325	95	[8] AAD	14G	ATLS	$\tilde{\ell}\tilde{\ell} \to \ell^+\tilde{\chi}_1^0\ell^-\tilde{\chi}_1^0$, simplified model, $m_{\tilde{\ell}_L} = m_{\tilde{\ell}_R}$, $m_{\tilde{\chi}_1^0}$ = 0 GeV
		[9] KHACHATRY...	14I	CMS	$\tilde{\ell} \to \ell\tilde{\chi}_1^0$, simplified model
>80	95	[10] ABREU	00V	DLPH	$\tilde{\mu}_R\tilde{\mu}_R$ ($\tilde{\mu}_R \to \mu\tilde{G}$), $m_{\tilde{G}}$ >8 eV

[1] CHATRCHYAN 14R searched in 19.5 fb^{-1} of pp collisions at $\sqrt{s}$ = 8 TeV for events with at least three leptons (electrons, muons, taus) in the final state. No significant excess above the Standard Model expectations is observed. Limits are set on the slepton mass in a stau (N)NLSP simplified model (GMSB) where the decay $\tilde{\ell} \to \ell^\pm\tau^\pm\tau^\mp\tilde{G}$ takes place with a branching ratio of 100%, see Fig. 8.

[2] AAD 13B searched in 4.7 fb^{-1} of pp collisions at $\sqrt{s}$ = 7 TeV for sleptons decaying to a final state with two leptons (e and μ) and missing transverse energy. No excess beyond the Standard Model expectation is observed. Limits are derived in a simplified model of direct left-handed slepton pair production, where left-handed slepton masses between 85 and 195 GeV are excluded at 95% C.L. for $m_{\tilde{\chi}_1^0}$ = 20 GeV. See also Fig. 2(a). Exclusion limits are also derived in the phenomenological MSSM, see Fig. 3.

[3] ABBIENDI 04 search for $\tilde{\mu}_R\tilde{\mu}_R$ production in acoplanar di-muon final states in the 183–208 GeV data. See Fig. 14 for the dependence of the limits on $m_{\tilde{\chi}_1^0}$ and for the limit at tanβ=35. Under the assumption of 100% branching ratio for $\tilde{\mu}_R \to \mu\tilde{\chi}_1^0$, the limit improves to 94.0 GeV for $\Delta m > 4$ GeV. See Fig. 11 for the dependence of the limits on $m_{\tilde{\chi}_1^0}$ at several values of the branching ratio. This limit supersedes ABBIENDI 00G.

[4] ACHARD 04 search for $\tilde{\mu}_R\tilde{\mu}_R$ production in acoplanar di-muon final states in the 192–209 GeV data. Limits on $m_{\tilde{\mu}_R}$ are derived from a scan over the MSSM parameter space with universal GUT scale gaugino and scalar masses $m_{1/2}$ and m_0, $1 \leq$ tan$\beta \leq 60$ and $-2 \leq \mu \leq 2$ TeV. See Fig. 4 for the dependence of the limits on $m_{\tilde{\chi}_1^0}$. This limit supersedes ACCIARRI 99W.

[5] ABDALLAH 03M looked for acoplanar dimuon $+\not{E}$ final states at $\sqrt{s}$ = 189–208 GeV. The limit assumes B($\tilde{\mu} \to \mu\tilde{\chi}_1^0$) = 100%. See Fig. 16 for limits on the ($m_{\tilde{\mu}_R}$, $m_{\tilde{\chi}_1^0}$) plane. These limits include and update the results of ABREU 01.

[6] ABDALLAH 03M uses data from $\sqrt{s}$ = 192–208 GeV to obtain limits in the framework of the MSSM with gaugino and sfermion mass universality at the GUT scale. An indirect limit on the mass is derived by constraining the MSSM parameter space by the results from direct searches for neutralinos (including cascade decays) and for sleptons. These limits are valid for values of $M_2 < 1$ TeV, $\lvert\mu\rvert \leq 1$ TeV with the $\tilde{\chi}_1^0$ as LSP. The quoted limit is obtained when there is no mixing in the third family. See Fig. 43 for the mass limits as a function of tanβ. These limits update the results of ABREU 00W.

[7] HEISTER 02E looked for acoplanar dimuon + $\not{E}_T$ final states from e^+e^- interactions between 183 and 209 GeV. The mass limit assumes B($\tilde{\mu} \to \mu\tilde{\chi}_1^0$)=1. See their Fig. 4 for the dependence of the limit on Δm. These limits include and update the results of BARATE 01.

[8] AAD 14G searched in 20.3 fb^{-1} of pp collisions at $\sqrt{s}$ = 8 TeV for electroweak production of slepton pairs, decaying to a final sate with two leptons (e and μ) and missing transverse momentum. No excess beyond the Standard Model expectation is observed. Exclusion limits are derived in simplified models of slepton pair production, see Fig. 8. An interpretation in the pMSSM is also given, see Fig. 10.

[9] KHACHATRYAN 14I searched in 19.5 fb^{-1} of pp collisions at $\sqrt{s}$ = 8 TeV for electroweak production of slepton pairs decaying to a final state with opposite-sign lepton pairs (e or μ) and missing transverse momentum. No excess beyond the Standard Model expectation is observed. Exclusion limits are derived in simplified models, see Fig. 18.

[10] ABREU 00V use data from $\sqrt{s}$= 130–189 GeV to search for tracks with large impact parameter or visible decay vertices. Limits are obtained as function of $m_{\tilde{G}}$, after combining these results with the search for slepton pair production in the SUGRA framework from ABREU 01 to cover prompt decays and on stable particle searches from ABREU 00Q. For limits at different $m_{\tilde{G}}$, see their Fig. 12.

R-parity violating $\tilde{\mu}$ (Smuon) mass limit

VALUE (GeV)	CL%	DOCUMENT ID		TECN	COMMENT
>410	95	[1] AAD	14X	ATLS	RPV, $\geq 4\ell^\pm$, $\tilde{\ell} \to \ell\tilde{\chi}_1^0$, $\tilde{\chi}_1^0 \to \ell^\pm\ell^\mp\nu$

• • • We do not use the following data for averages, fits, limits, etc. • • •

> 87	95	[2] ABDALLAH	04M	DLPH	RPV, $\tilde{\mu}_R$, indirect, Δm >5 GeV
> 81	95	[3] HEISTER	03G	ALEP	RPV, $\tilde{\mu}_L$	

[1] AAD 14X searched in 20.3 fb^{-1} of pp collisions at $\sqrt{s}$ = 8 TeV for events with at least four leptons (electrons, muons, taus) in the final state. No significant excess above the Standard Model expectations is observed. Limits are set on the slepton mass in an R-parity violating simplified model where the decay $\tilde{\ell} \to \ell\tilde{\chi}_1^0$, with $\tilde{\chi}_1^0 \to \ell^\pm\ell^\mp\nu$, takes place with a branching ratio of 100%, see Fig. 9.

[2] ABDALLAH 04M use data from $\sqrt{s}$ = 192–208 GeV to derive limits on sparticle masses under the assumption of RPV with $LL\overline{E}$ or $\overline{UDD}$ couplings. The results are valid for $\mu = -200$ GeV, tanβ = 1.5, $\Delta m > 5$ GeV and assuming a BR of 1 for the given decay. The limit quoted is for indirect $\overline{UDD}$ decays using the neutralino constraint of 39.5 GeV for $LL\overline{E}$ and of 38.0 GeV for $\overline{UDD}$ couplings, also derived in ABDALLAH 04M. For indirect decays via $LL\overline{E}$ the limit improves to 90 GeV if the constraint from the neutralino is used and remains at 87 GeV if it is not used. For indirect decays via $\overline{UDD}$ couplings it degrades to 85 GeV when the neutralino constraint is not used. Supersedes the result of ABREU 00U.

[3] HEISTER 03G searches for the production of smuons in the case of RPV prompt decays with $LL\overline{E}$, $LQ\overline{D}$ or $\overline{UDD}$ couplings at $\sqrt{s}$ = 189–209 GeV. The search is performed for direct and indirect decays, assuming one coupling at a time to be non-zero. The limit holds for direct decays mediated by RPV $LQ\overline{D}$ couplings and improves to 90 GeV for indirect decays (for $\Delta m > 10$ GeV). Limits are also given for $LL\overline{E}$ direct ($m_{\tilde{\mu}R}$ > 87 GeV) and indirect decays ($m_{\tilde{\mu}R}$ > 96 GeV for $m(\tilde{\chi}_1^0) > 23$ GeV from BARATE 98S) and for $\overline{UDD}$ indirect decays ($m_{\tilde{\mu}R}$ > 85 GeV for $\Delta m > 10$ GeV). Supersedes the results from BARATE 01B.

R-parity conserving $\tilde{\tau}$ (Stau) mass limit

Some earlier papers are now obsolete and have been omitted. They were last listed in our PDG 14 edition: K. Olive, *et al.* (Particle Data Group), Chinese Physics **C38** 070001 (2014) (http://pdg.lbl.gov).

VALUE (GeV)	CL%	DOCUMENT ID		TECN	COMMENT
>85.2		[1] ABBIENDI	04	OPAL	$\Delta m > 6$ GeV, $\theta_\tau = \pi/2$, $\lvert\mu\rvert >$ 100 GeV, tanβ=1.5
>78.3		[2] ACHARD	04	L3	$\Delta m > 15$ GeV, $\theta_\tau = \pi/2$, $\lvert\mu\rvert$ >200 GeV, tan$\beta \geq 2$
>81.9	95	[3] ABDALLAH	03M	DLPH	Δm >15 GeV, all θ_τ
>79	95	[4] HEISTER	02E	ALEP	$\Delta m > 15$ GeV, $\theta_\tau = \pi/2$
>76	95	[4] HEISTER	02E	ALEP	$\Delta m > 15$ GeV, θ_τ=0.91

• • • We do not use the following data for averages, fits, limits, etc. • • •

	95	[5] KHACHATRY...	17L	CMS	2 $\tau + \not{E}_T$, $\tilde{\tau}_L \to \tau\tilde{\chi}_1^0$, $m_{\tilde{\chi}_1^0}$ = 0 GeV
none 109	95	[6] AAD	16AA	ATLS	2 hadronic $\tau + \not{E}_T$, $\tilde{\tau}_{R/L} \to \tau\tilde{\chi}_1^0$, $m_{\tilde{\chi}_1^0}$ = 0 GeV
		[7] AAD	12AF	ATLS	2τ + jets + $\not{E}_T$, GMSB
		[8] AAD	12AG	ATLS	$\geq 1\tau_h$ + jets + $\not{E}_T$, GMSB
		[9] AAD	12CM	ATLS	$\geq 1\tau$ + jets + $\not{E}_T$, GMSB
>87.4	95	[10] ABBIENDI	06B	OPAL	$\tilde{\tau}_R \to \tau\tilde{G}$, all $\tau(\tilde{\tau}_R)$
>68	95	[11] ABDALLAH	04H	DLPH	AMSB, $\mu > 0$
none m_τ– 26.3	95	[3] ABDALLAH	03M	DLPH	$\Delta m > m_\tau$, all θ_τ

[1] ABBIENDI 04 search for $\tilde{\tau}\tilde{\tau}$ production in acoplanar di-tau final states in the 183–208 GeV data. See Fig. 15 for the dependence of the limits on $m_{\tilde{\chi}_1^0}$ and for the limit at tanβ=35. Under the assumption of 100% branching ratio for $\tilde{\tau}_R \to \tau\tilde{\chi}_1^0$, the limit improves to 89.8 GeV for $\Delta m > 8$ GeV. See Fig. 12 for the dependence of the limits on $m_{\tilde{\chi}_1^0}$ at several values of the branching ratio and for their dependence on θ_τ. This limit supersedes ABBIENDI 00G.

[2] ACHARD 04 search for $\tilde{\tau}\tilde{\tau}$ production in acoplanar di-tau final states in the 192–209 GeV data. Limits on $m_{\tilde{\tau}_R}$ are derived from a scan over the MSSM parameter space with universal GUT scale gaugino and scalar masses $m_{1/2}$ and m_0, $1 \leq$ tan$\beta \leq 60$ and $-2 \leq \mu \leq 2$ TeV. See Fig. 4 for the dependence of the limits on $m_{\tilde{\chi}_1^0}$.

[3] ABDALLAH 03M looked for acoplanar ditaus $+\not{E}$ final states at $\sqrt{s}$ = 130–208 GeV. A dedicated search was made for low mass $\tilde{\tau}$s decoupling from the Z^0. The limit assumes B($\tilde{\tau} \to \tau\tilde{\chi}_1^0$) = 100%. See Fig. 20 for limits on the ($m_{\tilde{\tau}}$,$m_{\tilde{\chi}_1^0}$) plane and as function of the $\tilde{\chi}_1^0$ mass and of the branching ratio. The limit in the low-mass region improves to 29.6 and 31.1 GeV for $\tilde{\tau}_R$ and $\tilde{\tau}_L$, respectively, at $\Delta m > m_\tau$. The limit in the high-mass region improves to 84.7 GeV for $\tilde{\tau}_R$ and $\Delta m > 15$ GeV. These limits include and update the results of ABREU 01.

[4] HEISTER 02E looked for acoplanar ditau + $\not{E}_T$ final states from e^+e^- interactions between 183 and 209 GeV. The mass limit assumes B($\tilde{\tau} \to \tau\tilde{\chi}_1^0$)=1. See their Fig. 4 for the dependence of the limit on Δm. These limits include and update the results of BARATE 01.

[5] KHACHATRYAN 17L searched in about 19 fb^{-1} of pp collisions at $\sqrt{s}$ = 8 TeV for events with two τ (at least one decaying hadronically) and $\not{E}_T$. Results were interpreted to set constraints on the cross section for production of $\tilde{\tau}_L$ pairs for $m_{\tilde{\chi}^0_1}$=1 GeV. No mass constraints are set, see their Fig. 7.

[6] AAD 16AA summarized and extended ATLAS searches for electroweak supersymmetry in final states containing several charged leptons, $\not{E}_T$, with or without hadronic jets, in 20 fb^{-1} of pp collisions at $\sqrt{s}$ = 8 TeV. The paper reports 95% C.L. exclusion limits on the cross-section for production of $\tilde{\tau}_R$ and $\tilde{\tau}_L$ pairs for various $m_{\tilde{\chi}^0_1}$, using the 2 hadronic $\tau + \not{E}_T$ analysis. The $m_{\tilde{\tau}_{R/L}}$ = 109 GeV is excluded for $m_{\tilde{\chi}^0_1}$ = 0 GeV, with the constraints being stronger for $\tilde{\tau}_R$. See their Fig. 12.

[7] AAD 12AF searched in 2 fb^{-1} of pp collisions at $\sqrt{s}$ = 7 TeV for events with two tau leptons, jets and large $\not{E}_T$ in a GMSB framework. No significant excess above the expected background was found and an upper limit on the visible cross section for new phenomena is set. A 95% C.L. lower limit of 32 TeV on the mGMSB breaking scale Λ is set for M_{mess} = 250 TeV, N_S = 3, $\mu > 0$ and C_{grav} = 1, independent of tanβ.

[8] AAD 12AG searched in 2.05 fb^{-1} of pp collisions at $\sqrt{s}$ = 7 TeV for events with at least one hadronically decaying tau lepton, jets, and large $\not{E}_T$ in a GMSB framework. No significant excess above the expected background was found and an upper limit on the visible cross section for new phenomena is set. A 95% C.L. lower limit of 30 TeV on the mGMSB breaking scale Λ is set for M_{mess} = 250 TeV, N_S = 3, $\mu > 0$ and C_{grav} = 1, independent of tanβ. For large values of tanβ, the limit on Λ increases to 43 TeV.

[9] AAD 12CM searched in 4.7 fb^{-1} of pp collisions at $\sqrt{s}$=7 TeV for events with at least one tau lepton, zero or one additional light lepton (e/μ) jets, and large $\not{E}_T$ in a GMSB framework. No significant excess above the expected background was found and an upper limit on the visible cross section for new phenomena is set. A 95% C. L. lower limit of 54 TeV on the mGMSB breaking scale Λ is set for M_{mess} = 250 TeV, N_S = 3, $\mu > 0$ and C_{grav} = 1, for tan$\beta > 20$. Here the $\tilde{\tau}_1$ is the NLSP.

[10] ABBIENDI 06B use 600 pb^{-1} of data from $\sqrt{s}$ = 189–209 GeV. They look for events from pair-produced staus in a GMSB scenario with $\tilde{\tau}$ NLSP including prompt $\tilde{\tau}$ decays to ditaus + $\not{E}$ final states, large impact parameters, kinked tracks and heavy stable charged particles. Limits on the cross-section are computed as a function of m($\tilde{\tau}$) and the lifetime, see their Fig. 7. The limit is compared to the $\sigma \cdot BR^2$ from a scan over the GMSB parameter space.

[11] ABDALLAH 04H use data from LEP 1 and $\sqrt{s}$ = 192–208 GeV. They re-use results or re-analyze the data from ABDALLAH 03M to put limits on the parameter space of anomaly-mediated supersymmetry breaking (AMSB), which is scanned in the region 1< $m_{3/2}$ <50 TeV, 0< m_0 <1000 GeV, 1.5<tanβ <35, both signs of μ. The constraints are obtained from the searches for mass degenerate chargino and neutralino, for SM-like and invisible Higgs, for leptonically decaying charginos and from the limit on non-SM Z width of 3.2 MeV. The limit is for m_t = 174.3 GeV (see Table 2 for other m_t values). The limit improves to 75 GeV for $\mu < 0$.

R-parity violating $\tilde{\tau}$ (Stau) mass limit

Some earlier papers are now obsolete and have been omitted. They were last listed in our PDG 14 edition: K. Olive, *et al.* (Particle Data Group), Chinese Physics **C38** 070001 (2014) (http://pdg.lbl.gov).

VALUE (GeV)	CL%	DOCUMENT ID		TECN	COMMENT
• • • We do not use the following data for averages, fits, limits, etc. • • •					
>74	95	[1] ABBIENDI	04F	OPAL	RPV, $\tilde{\tau}_L$
>90	95	[2] ABDALLAH	04M	DLPH	RPV, $\tilde{\tau}_R$, indirect, Δm >5 GeV

[1] ABBIENDI 04F use data from $\sqrt{s}$ = 189–209 GeV. They derive limits on sparticle masses under the assumption of RPV with $LL\overline{E}$ or $LQ\overline{D}$ couplings. The results are valid for tanβ = 1.5, $\mu = -200$ GeV, with, in addition, $\Delta m > 5$ GeV for indirect decays via $LQ\overline{D}$. The limit quoted applies to direct decays with $LL\overline{E}$ couplings and improves to 75 GeV for $LQ\overline{D}$ couplings. The limit on the $\tilde{\tau}_R$ mass for indirect decays is 92 GeV for $LL\overline{E}$ couplings at $m_{\tilde{\chi}^0} = 10$ GeV and no exclusion is obtained for $LQ\overline{D}$ couplings. Supersedes the results of ABBIENDI 00.

[2] ABDALLAH 04M use data from $\sqrt{s}$ = 192–208 GeV to derive limits on sparticle masses under the assumption of RPV with $LL\overline{E}$ couplings. The results are valid for $\mu = -200$ GeV, tanβ = 1.5, $\Delta m > 5$ GeV and assuming a BR of 1 for the given decay. The limit quoted is for indirect decays using the neutralino constraint of 39.5 GeV, also derived in ABDALLAH 04M. For indirect decays via $LL\overline{E}$ the limit decreases to 86 GeV if the constraint from the neutralino is not used. Supersedes the result of ABREU 00U.

Long-lived $\tilde{\ell}$ (Slepton) mass limit

Limits on scalar leptons which leave detector before decaying. Limits from Z decays are independent of lepton flavor. Limits from continuum e^+e^- annihilation are also independent of flavor for smuons and staus. Selectron limits from e^+e^- collisions in the continuum depend on MSSM parameters because of the additional neutralino exchange contribution.

VALUE (GeV)	CL%	DOCUMENT ID		TECN	COMMENT
>490	95	[1] KHACHATRY...16BW		CMS	long-lived $\tilde{\tau}$ from inclusive production, mGMSB SPS line 7 scenario
>240	95	[1] KHACHATRY...16BW		CMS	long-lived $\tilde{\tau}$ from direct pair production, mGMSB SPS line 7 scenario
>440	95	[2] AAD	15AE	ATLS	mGMSB, M_{mess}= 250 TeV, N_5 = 3, $\mu > 0$, C_{grav} = 5000, tanβ = 10
>385	95	[2] AAD	15AE	ATLS	mGMSB, M_{mess}= 250 TeV, N_5 = 3, $\mu > 0$, C_{grav} = 5000, tanβ = 50
>286	95	[2] AAD	15AE	ATLS	direct $\tilde{\tau}$ production
none 124–309	95	[3] AAIJ	15BD	LHCB	long-lived $\tilde{\tau}$, mGMSB, SPS7
> 98	95	[4] ABBIENDI	03L	OPAL	$\tilde{\mu}_R$, $\tilde{\tau}_R$
none 2–87.5	95	[5] ABREU	00Q	DLPH	$\tilde{\mu}_R$, $\tilde{\tau}_R$
> 81.2	95	[6] ACCIARRI	99H	L3	$\tilde{\mu}_R$, $\tilde{\tau}_R$
> 81	95	[7] BARATE	98K	ALEP	$\tilde{\mu}_R$, $\tilde{\tau}_R$
• • • We do not use the following data for averages, fits, limits, etc. • • •					
>300	95	[8] AAD	13AA	ATLS	long-lived $\tilde{\tau}$, GMSB, tanβ = 5–20
		[9] ABAZOV	13B	D0	long-lived $\tilde{\tau}$, 100 <$m_{\tilde{\tau}}$ <300 GeV
>339	95	[10,11] CHATRCHYAN	13AB	CMS	long-lived $\tilde{\tau}$, direct $\tilde{\tau}_1$ pair prod., minimal GMSB, SPS line 7
>500	95	[10,12] CHATRCHYAN	13AB	CMS	long-lived $\tilde{\tau}$, $\tilde{\tau}_1$ from direct pair prod. and from decay of heavier SUSY particles, minimal GMSB, SPS line 7
>314	95	[13] CHATRCHYAN	12L	CMS	long-lived $\tilde{\tau}$, $\tilde{\tau}_1$ from decay of heavier SUSY particles, minimal GMSB, SPS line 7
>136	95	[14] AAD	11P	ATLS	stable $\tilde{\tau}$, GMSB scenario, tanβ=5

[1] KHACHATRYAN 16BW searched in 2.5 fb^{-1} of pp collisions at $\sqrt{s}$ = 13 TeV for events with heavy stable charged particles, identified by their anomalously high energy deposits in the silicon tracker and/or long time-of-flight measurements by the muon system. No evidence for an excess over the expected background is observed. Limits are derived for pair production of tau sleptons as a function of mass, depending on their direct or inclusive production in a minimal GMSB scenario along the Snowmass Points and Slopes (SPS) line 7, see Fig. 4 and Table 7.

[2] AAD 15AE searched in 19.1 fb^{-1} of pp collisions at $\sqrt{s}$ = 8 TeV for heavy long-lived charged particles, measured through their specific ionization energy loss in the ATLAS pixel detector or their time-of-flight in the ALTAS muon system. In the absence of an excess of events above the expected backgrounds, limits are set on stable $\tilde{\tau}$ sleptons in various scenarios, see Figs. 5-7.

[3] AAIJ 15BD searched in 3.0 fb^{-1} of pp collisions at $\sqrt{s}$ = 7 and 8 TeV for evidence of Drell-Yan pair production of long-lived $\tilde{\tau}$ particles. No evidence for such particles is observed and 95% C.L. upper limits on the cross section of $\tilde{\tau}$ pair production are derived, see Fig. 7. In the mGMSB, assuming the SPS7 benchmark scenario $\tilde{\tau}$ masses between 124 and 309 GeV are excluded at 95% C.L.

[4] ABBIENDI 03L used e^+e^- data at $\sqrt{s}$ = 130–209 GeV to select events with two high momentum tracks with anomalous dE/dx. The excluded cross section is compared to the theoretical expectation as a function of the heavy particle mass in their Fig. 3. The limit improves to 98.5 GeV for $\tilde{\mu}_L$ and $\tilde{\tau}_L$. The bounds are valid for colorless spin 0 particles with lifetimes longer than 10^{-6} s. Supersedes the results from ACKERSTAFF 98P.

[5] ABREU 00Q searches for the production of pairs of heavy, charged stable particles in e^+e^- annihilation at $\sqrt{s}$= 130–189 GeV. The upper bound improves to 88 GeV for $\tilde{\mu}_L$, $\tilde{\tau}_L$. These limits include and update the results of ABREU 98P.

[6] ACCIARRI 99H searched for production of pairs of back-to-back heavy charged particles at $\sqrt{s}$=130–183 GeV. The upper bound improves to 82.2 GeV for $\tilde{\mu}_L$, $\tilde{\tau}_L$.

[7] The BARATE 98K mass limit improves to 82 GeV for $\tilde{\mu}_L$,$\tilde{\tau}_L$. Data collected at $\sqrt{s}$=161–184 GeV.

[8] AAD 13AA searched in 4.7 fb^{-1} of pp collisions at $\sqrt{s}$ = 7 TeV for events containing long-lived massive particles in a GMSB framework. No significant excess above the expected background was found. A 95% C.L. lower limit of 300 GeV is placed on long-lived $\tilde{\tau}$'s in the GMSB model with M_{mess} = 250 TeV, N_S = 3, $\mu > 0$, for tanβ = 5–20. The lower limit on the GMSB breaking scale Λ was found to be 99–110 TeV, for tanβ values between 5 and 40, see Fig. 4 (top). Also, directly produced long-lived sleptons, or sleptons decaying to long-lived ones, are excluded at 95% C.L. up to a $\tilde{\tau}$ mass of 278 GeV for models with slepton splittings smaller than 50 GeV.

[9] ABAZOV 13B looked in 6.3 fb^{-1} of $p\overline{p}$ collisions at $\sqrt{s}$ = 1.96 TeV for charged massive long-lived particles in events with muon-like particles that have both speed and ionization energy loss inconsistent with muons produced in beam collisions. In the absence of an excess, limits are set at 95% C.L. on the production cross section of stau leptons in the mass range 100–300 GeV, see their Table 20 and Fig. 23.

[10] CHATRCHYAN 13AB looked in 5.0 fb^{-1} of pp collisions at $\sqrt{s}$ = 7 TeV and in 18.8 fb^{-1} of pp collisions at $\sqrt{s}$ = 8 TeV for events with heavy stable particles, identified by their anomalous dE/dx in the tracker or additionally requiring that it be identified as muon in the muon chambers, from pair production of $\tilde{\tau}_1$'s. No evidence for an excess over the expected background is observed. Supersedes CHATRCHYAN 12L.

[11] CHATRCHYAN 13AB limits are derived for pair production of $\tilde{\tau}_1$ as a function of mass in minimal GMSB scenarios along the Snowmass Points and Slopes (SPS) line 7 (see Fig. 8 and Table 7). The limit given here is valid for direct pair $\tilde{\tau}_1$ production.

[12] CHATRCHYAN 13AB limits are derived for the production of $\tilde{\tau}_1$ as a function of mass in minimal GMSB scenarios along the Snowmass Points and Slopes (SPS) line 7 (see Fig. 8 and Table 7). The limit given here is valid for the production of $\tilde{\tau}_1$ from both direct pair production and from the decay of heavier supersymmetric particles.

[13] CHATRCHYAN 12L looked in 5.0 fb^{-1} of pp collisions at $\sqrt{s}$ = 7 TeV for events with heavy stable particles, identified by their anomalous dE/dx in the tracker or additionally requiring that it be identified as muon in the muon chambers, from pair production of $\tilde{\tau}_1$'s. No evidence for an excess over the expected background is observed. Limits are derived for the production of $\tilde{\tau}_1$ as a function of mass in minimal GMSB scenarios along the Snowmass Points and Slopes (SPS) line 7 (see Fig. 3). The limit given here is valid for the production of $\tilde{\tau}_1$ in the decay of heavier supersymmetric particles.

[14] AAD 11P looked in 37 pb^{-1} of pp collisions at $\sqrt{s}$ = 7 TeV for events with two heavy stable particles, reconstructed in the Inner tracker and the Muon System and identified by their time of flight in the Muon System. No evidence for an excess over the SM expectation is observed. Limits on the mass are derived, see Fig. 3, for $\tilde{\tau}$ in a GMSB scenario and for sleptons produced by electroweak processes only, in which case the limit degrades to 110 GeV.

$\tilde{q}$ (Squark) mass limit

For $m_{\tilde{q}} > 60$–70 GeV, it is expected that squarks would undergo a cascade decay via a number of neutralinos and/or charginos rather than undergo a direct decay to photinos as assumed by some papers. Limits obtained when direct decay is assumed are usually higher than limits when cascade decays are included.

Limits from e^+e^- collisions depend on the mixing angle of the lightest mass eigenstate $\tilde{q}_1 = \tilde{q}_R \sin\theta_q + \tilde{q}_L \cos\theta_q$. It is usually assumed that only the sbottom and stop squarks have non-trivial mixing angles (see the stop and sbottom sections). Here, unless otherwise noted, squarks are always taken to be either left/right degenerate, or purely of left or right type. Data from Z decays have set squark mass limits above 40 GeV, in the

case of $\tilde{q} \to q\tilde{\chi}_1$ decays if $\Delta m = m_{\tilde{q}} - m_{\tilde{\chi}_1^0} \gtrsim 5$ GeV. For smaller values of Δm, current constraints on the invisible width of the Z ($\Delta\Gamma_{\rm inv} < 2.0$ MeV, LEP 00) exclude $m_{\tilde{u}_{L,R}} < 44$ GeV, $m_{\tilde{d}_R} < 33$ GeV, $m_{\tilde{d}_L} < 44$ GeV and, assuming all squarks degenerate, $m_{\tilde{q}} < 45$ GeV.

Some earlier papers are now obsolete and have been omitted. They were last listed in our PDG 14 edition: K. Olive, *et al.* (Particle Data Group), Chinese Physics **C38** 070001 (2014) (http://pdg.lbl.gov).

R-parity conserving $\tilde{q}$ (Squark) mass limit

VALUE (GeV)	CL%	DOCUMENT ID		TECN	COMMENT
>1450 (CL = 95%) OUR EVALUATION					CMSSM, tanβ=30, μ >0
>1550 (CL = 95%) OUR EVALUATION					Mass degenerate squarks
>1050 (CL = 95%) OUR EVALUATION					Single light squark bounds
>1220	95	[1] AABOUD	17AR	ATLS	1ℓ+jets+$\not{E}_T$, Tsqk3, $m_{\tilde{\chi}_1^0} = 0$ GeV
>1000	95	[2] AABOUD	17N	ATLS	2 same-flavour, opposite-sign ℓ + jets + $\not{E}_T$, Tsqk2, $m_{\tilde{\chi}_1^0} = 0$ GeV
>1150	95	[3] KHACHATRY...	17P	CMS	1 or more jets+$\not{E}_T$, Tsqk1, 4(flavor) x 2(isospin) = 8 mass degenerate states, $m_{\tilde{\chi}_1^0} = 0$ GeV
> 575	95	[3] KHACHATRY...	17P	CMS	1 or more jets+$\not{E}_T$, Tsqk1, one light flavor state, $m_{\tilde{\chi}_1^0} = 0$ GeV
>1370	95	[4] KHACHATRY...	17V	CMS	2 γ + $\not{E}_T$, GGM, Tsqk4, any NLSP mass
>1600	95	[5] SIRUNYAN	17AY	CMS	γ + jets+$\not{E}_T$, Tsqk4B, $m_{\tilde{\chi}_1^0} = 0$ GeV
>1370	95	[5] SIRUNYAN	17AY	CMS	γ + jets+$\not{E}_T$, Tsqk4A, $m_{\tilde{\chi}_1^0} = 0$ GeV
>1050	95	[6] SIRUNYAN	17AZ	CMS	$\geq$ 1 jets+$\not{E}_T$, Tsqk1, single light flavor state, $m_{\tilde{\chi}_1^0} = 0$ GeV
>1550	95	[6] SIRUNYAN	17AZ	CMS	$\geq$ 1 jets+$\not{E}_T$, Tsqk1, 4(flavor) x 2(isospin) = 8 degenerate mass states, $m_{\tilde{\chi}_1^0} = 0$ GeV
>1390	95	[7] SIRUNYAN	17P	CMS	jets+$\not{E}_T$, Tsqk1, 4(flavor) x 2(isospin) = 8 degenerate mass states, $m_{\tilde{\chi}_1^0} = 0$ GeV
> 950	95	[7] SIRUNYAN	17P	CMS	jets+$\not{E}_T$, Tsqk1, one light flavor state, $m_{\tilde{\chi}_1^0} = 0$ GeV
> 608	95	[8] AABOUD	16D	ATLS	$\geq$ 1 jet + $\not{E}_T$, Tsqk1, $m_{\tilde{q}} - m_{\tilde{\chi}_1^0} = 5$ GeV
>1030	95	[9] AABOUD	16N	ATLS	$\geq$ 2 jets + $\not{E}_T$, Tsqk1, $m_{\tilde{\chi}_1^0} = 0$ GeV
> 600	95	[10] KHACHATRY...	16BS	CMS	jets + $\not{E}_T$, Tsqk1, single light squark, $m_{\tilde{\chi}_1^0} = 0$ GeV
>1260	95	[10] KHACHATRY...	16BS	CMS	jets + $\not{E}_T$, Tsqk1, 8 degenerate light squarks, $m_{\tilde{\chi}_1^0} = 0$ GeV
> 850	95	[11] AAD	15BV	ATLS	jets + $\not{E}_T$, $\tilde{q} \to q\tilde{\chi}_1^0$, $m_{\tilde{\chi}_1^0} =$ 100 GeV
> 250	95	[12] AAD	15CS	ATLS	photon + $\not{E}_T$, $pp \to \tilde{q}\bar{\tilde{q}}^*\gamma$, $\tilde{q} \to q\tilde{\chi}_1^0$, $m_{\tilde{q}} - m_{\tilde{\chi}_1^0} = m_c$
> 490	95	[13] AAD	15K	ATLS	$\tilde{c} \to c\tilde{\chi}_1^0$, $m_{\tilde{\chi}_1^0} < 200$ GeV
> 875	95	[14] KHACHATRY...	15AF	CMS	$\tilde{q} \to q\tilde{\chi}_1^0$, simplified model, 8 degenerate light $\tilde{q}$, $m_{\tilde{\chi}_1^0} = 0$
> 520	95	[14] KHACHATRY...	15AF	CMS	$\tilde{q} \to q\tilde{\chi}_1^0$, simplified model, single light squark, $m_{\tilde{\chi}_1^0} = 0$
>1450	95	[14] KHACHATRY...	15AF	CMS	CMSSM, tanβ = 30, $A_0 = -2\max(m_0, m_{1/2})$, $\mu > 0$
> 850	95	[15] AAD	14AE	ATLS	jets + $\not{E}_T$, $\tilde{q} \to q\tilde{\chi}_1^0$ simplified model, mass degenerate first and second generation squarks, $m_{\tilde{\chi}_1^0} = 0$ GeV
> 440	95	[15] AAD	14AE	ATLS	jets + $\not{E}_T$, $\tilde{q} \to q\tilde{\chi}_1^0$ simplified model, single light-flavour squark, $m_{\tilde{\chi}_1^0} = 0$ GeV
>1700	95	[15] AAD	14AE	ATLS	jets + $\not{E}_T$, mSUGRA/CMSSM, $m_{\tilde{q}} = m_{\tilde{g}}$
> 800	95	[16] CHATRCHYAN	14AH	CMS	jets + $\not{E}_T$, $\tilde{q} \to q\tilde{\chi}_1^0$ simplified model, $m_{\tilde{\chi}_1^0} = 50$ GeV
> 780	95	[17] CHATRCHYAN	14I	CMS	multijets + $\not{E}_T$, $\tilde{q} \to q\tilde{\chi}_1^0$ simplified model, $m_{\tilde{\chi}_1^0} < 200$ GeV
>1360	95	[18] AAD	13L	ATLS	jets + $\not{E}_T$, CMSSM, $m_{\tilde{g}} = m_{\tilde{q}}$
>1200	95	[19] AAD	13Q	ATLS	γ+b+$\not{E}_T$,higgsino-like neutralino, $m_{\tilde{\chi}_1^0} > 220$ GeV, GMSB
		[20] CHATRCHYAN	13	CMS	$\ell^\pm\ell^\mp$ + jets + $\not{E}_T$, CMSSM
>1250	95	[21] CHATRCHYAN	13G	CMS	0,1,2, $\geq$ 3 b-jets + $\not{E}_T$, CMSSM, $m_{\tilde{q}} = m_{\tilde{g}}$
>1430	95	[22] CHATRCHYAN	13H	CMS	2γ + $\geq$ 4 jets + low $\not{E}_T$, stealth SUSY model
> 750	95	[23] CHATRCHYAN	13T	CMS	jets + $\not{E}_T$, $\tilde{q} \to q\tilde{\chi}_1^0$ simplified model, $m_{\tilde{\chi}_1^0} = 0$ GeV
> 820	95	[24] AAD	12AX	ATLS	ℓ +jets +$\not{E}_T$, CMSSM, $m_{\tilde{q}} = m_{\tilde{g}}$
>1200	95	[25] AAD	12CJ	ATLS	$\ell^\pm$+jets+$\not{E}_T$, CMSSM, $m_{\tilde{q}} = m_{\tilde{g}}$
> 870	95	[26] AAD	12CP	ATLS	2γ +$\not{E}_T$, GMSB, bino NLSP, $m_{\tilde{\chi}_1^0} > 50$ GeV
> 950	95	[27] AAD	12W	ATLS	jets + $\not{E}_T$, CMSSM, $m_{\tilde{q}} = m_{\tilde{g}}$
		[28] CHATRCHYAN	12	CMS	e, μ, jets, razor, CMSSM
> 760	95	[29] CHATRCHYAN	12AE	CMS	jets + $\not{E}_T$, $\tilde{q} \to q\tilde{\chi}_1^0$, $m_{\tilde{\chi}_1^0} <$ 200 GeV
>1110	95	[30] CHATRCHYAN	12AT	CMS	jets + $\not{E}_T$, CMSSM
>1180	95	[30] CHATRCHYAN	12AT	CMS	jets + $\not{E}_T$, CMSSM, $m_{\tilde{q}} = m_{\tilde{g}}$
• • • We do not use the following data for averages, fits, limits, etc. • • •					
> 300	95	[31] KHACHATRY...	16BT	CMS	19-parameter pMSSM model, global Bayesian analysis, flat prior
	95	[32] AAD	15AI	ATLS	$\ell^\pm$ + jets + $\not{E}_T$
>1650	95	[11] AAD	15BV	ATLS	jets + $\not{E}_T$, $m_{\tilde{g}} = m_{\tilde{q}}$, $m_{\tilde{\chi}_1^0} = 1$ GeV
> 790	95	[11] AAD	15BV	ATLS	jets + $\not{E}_T$, $\tilde{q} \to qW\tilde{\chi}_1^0$, $m_{\tilde{\chi}_1^0} =$ 100 GeV
> 820	95	[11] AAD	15BV	ATLS	2 or 3 leptons + jets, $\tilde{q}$ decays via sleptons, $m_{\tilde{\chi}_1^0} = 100$ GeV
> 850	95	[11] AAD	15BV	ATLS	τ, $\tilde{q}$ decays via staus, $m_{\tilde{\chi}_1^0} = 50$ GeV
> 700	95	[33] KHACHATRY...	15AR	CMS	$\tilde{q} \to q\tilde{\chi}_1^0$, $\tilde{\chi}_1^0 \to \tilde{S}g$, $\tilde{S} \to S\tilde{G}$, $S \to gg$, $m_{\tilde{S}} = 100$ GeV, $m_S = 90$ GeV
> 550	95	[33] KHACHATRY...	15AR	CMS	$\ell^\pm$, $\tilde{q} \to q\tilde{\chi}_1^\pm$, $\tilde{\chi}_1^\pm \to \tilde{S}W^\pm$, $\tilde{S} \to S\tilde{G}$, $S \to gg$, $m_{\tilde{S}} =$ 100 GeV, $m_S = 90$ GeV
>1500	95	[34] KHACHATRY...	15AZ	CMS	$\geq$ 2 γ, $\geq$ 1 jet, (Razor), bino-like NLSP, $m_{\tilde{\chi}_1^0} = 375$ GeV
>1000	95	[34] KHACHATRY...	15AZ	CMS	$\geq$ 1 γ, $\geq$ 2 jet, wino-like NLSP, $m_{\tilde{\chi}_1^0} = 375$ GeV
> 670	95	[35] AAD	14E	ATLS	$\ell^\pm\ell^\pm(\ell^\mp)$ + jets, $\tilde{q} \to q'\tilde{\chi}_1^\pm$, $\tilde{\chi}_1^\pm \to W^{(*)\pm}\tilde{\chi}_2^0$, $\tilde{\chi}_2^0 \to Z^{(*)}\tilde{\chi}_1^0$ simplified model, $m_{\tilde{\chi}_1^0} < 300$ GeV
> 780	95	[35] AAD	14E	ATLS	$\ell^\pm\ell^\pm(\ell^\mp)$ + jets, $\tilde{q} \to q'\tilde{\chi}_1^\pm/\tilde{\chi}_2^0$, $\tilde{\chi}_1^\pm \to \ell^\pm\nu\tilde{\chi}_1^0$, $\tilde{\chi}_2^0 \to \ell^\pm\ell^\mp(\nu\nu)\tilde{\chi}_1^0$ simplified model
> 700	95	[36] CHATRCHYAN	13AO	CMS	$\ell^\pm\ell^\mp$ + jets + $\not{E}_T$, CMSSM, $m_0 < 700$ GeV
>1350	95	[37] CHATRCHYAN	13AV	CMS	jets (+ leptons) + $\not{E}_T$, CMSSM, $m_{\tilde{g}} = m_{\tilde{q}}$
> 800	95	[38] CHATRCHYAN	13W	CMS	$\geq$ 1 photons + jets + $\not{E}_T$, GGM, wino-like NLSP, $m_{\tilde{\chi}_1^0} =$ 375 GeV
>1000	95	[38] CHATRCHYAN	13W	CMS	$\geq$ 2 photons + jets + $\not{E}_T$, GGM, bino-like NLSP, $m_{\tilde{\chi}_1^0} =$ 375 GeV
> 340	95	[39] DREINER	12A	THEO	$m_{\tilde{q}} \sim m_{\tilde{\chi}_1^0}$
> 650	95	[40] DREINER	12A	THEO	$m_{\tilde{q}} = m_{\tilde{g}} \sim m_{\tilde{\chi}_1^0}$

[1] AABOUD 17AR searched in 36.1 fb^{-1} of pp collisions at $\sqrt{s}$ = 13 TeV for events with one isolated lepton, at least two jets and large missing transverse momentum. No significant excess above the Standard Model expectations is observed. Limits up to 1.25 TeV are set on the 1st and 2nd generation squark masses in Tsqk3 simplified models, with $x = (m_{\tilde{\chi}_1^\pm} - m_{\tilde{\chi}_1^0}) / (m_{\tilde{q}} - m_{\tilde{\chi}_1^0}) = 1/2$. Similar limits are obtained for variable x and fixed neutralino mass, $m_{\tilde{\chi}_1^0} = 60$ GeV. See their Figure 13.

[2] AABOUD 17N searched in 14.7 fb^{-1} of pp collisions at $\sqrt{s}$ = 13 TeV for events with 2 same-flavour, opposite-sign leptons (electrons or muons), jets and large missing transverse momentum. The results are interpreted as 95% C.L. limits in Tsqk2 models, assuming $m_{\tilde{\chi}_1^0} = 0$ GeV and $m_{\tilde{\chi}_2^0} = 600$ GeV. See their Fig. 12 for exclusion limits as a function of $m_{\tilde{\chi}_2^0}$.

[3] KHACHATRYAN 17P searched in 2.3 fb^{-1} of pp collisions at $\sqrt{s}$ = 13 TeV for events with one or more jets and large $\not{E}_T$. No significant excess above the Standard Model expectations is observed. Limits are set on the gluino mass in the Tglu1A, Tglu2A, Tglu3A, Tglu3B, Tglu3C and Tglu3D simplified models, see their Figures 7 and 8. Limits are also set on the squark mass in the Tsqk1 simplified model, see their Fig. 7, and on the sbottom mass in the Tsbot1 simplified model, see Fig. 8. Finally, limits are set on the stop mass in the Tstop1, Tstop3, Tstop4, Tstop6 and Tstop7 simplified models, see Fig. 8.

[4] KHACHATRYAN 17V searched in 2.3 fb^{-1} of pp collisions at $\sqrt{s} = 13$ TeV for events with two photons and large $\not{E}_T$. No significant excess above the Standard Model expectations is observed. Limits are set on the gluino and squark mass in the context of general gauge mediation models Tglu4B and Tsqk4, see their Fig. 4.

[5] SIRUNYAN 17AY searched in 35.9 fb^{-1} of pp collisions at $\sqrt{s} = 13$ TeV for events with at least one photon, jets and large $\not{E}_T$. No significant excess above the Standard Model expectations is observed. Limits are set on the gluino mass in the Tglu4A and Tglu4B simplified models, and on the squark mass in the Tskq4A and Tsqk4B simplified models, see their Figure 6.

[6] SIRUNYAN 17AZ searched in 35.9 fb^{-1} of pp collisions at $\sqrt{s} = 13$ TeV for events with one or more jets and large $\not{E}_T$. No significant excess above the Standard Model expectations is observed. Limits are set on the gluino mass in the Tglu1A, Tglu2A, Tglu3A simplified models, see their Figures 6. Limits are also set on the squark mass in the Tsqk1 simplified model (for single light squark and for 8 degenerate light squarks), on the sbottom mass in the Tsbot1 simplified model and on the stop mass in the Tstop1 simplified model, see their Fig. 7. Finally, limits are set on the stop mass in the Tstop2, Tstop4 and Tstop8 simplified models, see Fig. 8.

[7] SIRUNYAN 17P searched in 35.9 fb^{-1} of pp collisions at $\sqrt{s} = 13$ TeV for events with multiple jets and large $\not{E}_T$. No significant excess above the Standard Model expectations is observed. Limits are set on the gluino mass in the Tglu1A, Tglu1C, Tglu2A, Tglu3A and Tglu3D simplified models, see their Fig. 12. Limits are also set on the squark mass in the Tsqk1 simplified model, on the stop mass in the Tstop1 simplified model, and on the sbottom mass in the Tsbot1 simplified model, see Fig. 13.

[8] AABOUD 16D searched in 3.2 fb^{-1} of pp collisions at $\sqrt{s} = 13$ TeV for events with an energetic jet and large missing transverse momentum. The results are interpreted as 95% C.L. limits on masses of first and second generation squarks decaying into a quark and the lightest neutralino in scenarios with $m_{\tilde{q}} - m_{\tilde{\chi}_1^0} < 25$ GeV. See their Fig. 6.

[9] AABOUD 16N searched in 3.2 fb^{-1} of pp collisions at $\sqrt{s} = 13$ TeV for events containing hadronic jets, large $\not{E}_T$, and no electrons or muons. No significant excess above the Standard Model expectations is observed. First- and second-generation squark masses below 1030 GeV are excluded at the 95% C.L. decaying to quarks and a massless lightest neutralino. See their Fig. 7a.

[10] KHACHATRYAN 16BS searched in 2.3 fb^{-1} of pp collisions at $\sqrt{s} = 13$ TeV for events with at least one energetic jet , no isolated leptons, and significant $\not{E}_T$, using the transverse mass variable M_{T2} to discriminate between signal and background processes. No significant excess above the Standard Model expectations is observed. Limits are set on the squark mass in the Tskq1 simplified model, both in the assumption of a single light squark and of 8 degenerate squarks, see Fig. 11 and Table 3.

[11] AAD 15BV summarized and extended ATLAS searches for gluinos and first- and second-generation squarks in final states containing jets and missing transverse momentum, with or without leptons or b-jets in the $\sqrt{s} = 8$ TeV data set collected in 2012. The paper reports the results of new interpretations and statistical combinations of previously published analyses, as well as new analyses. Exclusion limits at 95% C.L. are set on the squark mass in several R-parity conserving models. See their Figs. 9, 11, 18, 22, 24, 27, 28.

[12] AAD 15CS searched in 20.3 fb^{-1} of pp collisions at $\sqrt{s} = 8$ TeV for evidence of pair production of squarks, decaying into a quark and a neutralino, where a photon was radiated either from an initial-state quark, from an intermediate squark, or from a final-state quark. No evidence was found for an excess above the expected level of Standard Model background and a 95% C.L. exclusion limit was set on the squark mass as a function of the squark-neutralino mass difference, see Fig. 19.

[13] AAD 15K searched in 20.3 fb^{-1} of pp collisions at $\sqrt{s} = 8$ TeV for events containing at least two jets, where the two leading jets are each identified as originating from c-quarks, and large missing transverse momentum. No excess of events above the expected level of Standard Model background was found. Exclusion limits at 95% C.L. are set on the mass of superpartners of charm quarks ($\tilde{c}$). Assuming that the decay $\tilde{c} \to c\tilde{\chi}_1^0$ takes place 100% of the time, a scalar charm mass below 490 GeV is excluded for $m_{\tilde{\chi}_1^0} < 200$ GeV. For more details, see their Fig. 2.

[14] KHACHATRYAN 15AF searched in 19.5 fb^{-1} of pp collisions at $\sqrt{s} = 8$ TeV for events with at least two energetic jets and significant $\not{E}_T$, using the transverse mass variable M_{T2} to discriminate between signal and background processes. No significant excess above the Standard Model expectations is observed. Limits are set on the squark mass in simplified models where the decay $\tilde{q} \to q\tilde{\chi}_1^0$ takes place with a branching ratio of 100%, both for the case of a single light squark or 8 degenerate squarks, see Fig. 12. See also Table 5. Exclusions in the CMSSM, assuming $\tan\beta = 30$, $A_0 = -2$ max(m_0, $m_{1/2}$) and $\mu > 0$, are also presented, see Fig. 15.

[15] AAD 14AE searched in 20.3 fb^{-1} of pp collisions at $\sqrt{s} = 8$ TeV for strongly produced supersymmetric particles in events containing jets and large missing transverse momentum, and no electrons or muons. No excess over the expected SM background is observed. Exclusion limits are derived in simplified models containing squarks that decay via $\tilde{q} \to q\tilde{\chi}_1^0$, where either a single light state or two degenerate generations of squarks are assumed, see Fig. 10.

[16] CHATRCHYAN 14AH searched in 4.7 fb^{-1} of pp collisions at $\sqrt{s} = 7$ TeV for events with at least two energetic jets and significant $\not{E}_T$, using the razor variables (M_R and R^2) to discriminate between signal and background processes. No significant excess above the Standard Model expectations is observed. Limits are set on squark masses in simplified models where the decay $\tilde{q} \to q\tilde{\chi}_1^0$ takes place with a branching ratio of 100%, see Fig. 28. Exclusions in the CMSSM, assuming $\tan\beta = 10$, $A_0 = 0$ and $\mu > 0$, are also presented, see Fig. 26.

[17] CHATRCHYAN 14I searched in 19.5 fb^{-1} of pp collisions at $\sqrt{s} = 8$ TeV for events containing multijets and large $\not{E}_T$. No excess over the expected SM background is observed. Exclusion limits are derived in simplified models containing squarks that decay via $\tilde{q} \to q\tilde{\chi}_1^0$, where either a single light state or two degenerate generations of squarks are assumed, see Fig. 7a.

[18] AAD 13L searched in 4.7 fb^{-1} of pp collisions at $\sqrt{s} = 7$ TeV for the production of squarks and gluinos in events containing jets, missing transverse momentum and no high-p_T electrons or muons. No excess over the expected SM background is observed. In mSUGRA/CMSSM models with $\tan\beta = 10$, $A_0 = 0$ and $\mu > 0$, squarks and gluinos of equal mass are excluded for masses below 1360 GeV at 95% C.L. In a simplified model containing only squarks of the first two generations, a gluino octet and a massless neutralino, squark masses below 1320 GeV are excluded at 95% C.L. for gluino masses below 2 TeV. See Figures 10–15 for more precise bounds.

[19] AAD 13Q searched in 4.7 fb^{-1} of pp collisions at $\sqrt{s} = 7$ TeV for events containing a high-p_T isolated photon, at least one jet identified as originating from a bottom quark, and high missing transverse momentum. Such signatures may originate from supersymmetric models with gauge-mediated supersymmetry breaking in events in which one of a pair of higgsino-like neutralinos decays into a photon and a gravitino while the other decays into a Higgs boson and a gravitino. No significant excess above the expected background was found and limits were set on the squark mass as a function of the neutralino mass in a generalized GMSB model (GGM) with a higgsino-like neutralino NLSP, see their Fig. 4. For neutralino masses greater than 220 GeV, squark masses below 1020 GeV are excluded at 95% C.L.

[20] CHATRCHYAN 13 looked in 4.98 fb^{-1} of pp collisions at $\sqrt{s} = 7$ TeV for events with two opposite-sign leptons (e, μ, τ), jets and missing transverse energy. No excess beyond the Standard Model expectation is observed. Exclusion limits are derived in the mSUGRA/CMSSM model with $\tan\beta = 10$, $A_0 = 0$ and $\mu > 0$, see Fig. 6.

[21] CHATRCHYAN 13G searched in 4.98 fb^{-1} of pp collisions at $\sqrt{s} = 7$ TeV for the production of squarks and gluinos in events containing 0,1,2, ≥ 3 b-jets, missing transverse momentum and no electrons or muons. No excess over the expected SM background is observed. In mSUGRA/CMSSM models with $\tan\beta = 10$, $A_0 = 0$, and $\mu > 0$, squarks and gluinos of equal mass are excluded for masses below 1250 GeV at 95% C.L. Exclusions are also derived in various simplified models, see Fig. 7.

[22] CHATRCHYAN 13H searched in 4.96 fb^{-1} of pp collisions at $\sqrt{s} = 7$ TeV for events with two photons, ≥ 4 jets and low $\not{E}_T$ due to $\tilde{q} \to \gamma\tilde{\chi}_1^0$ decays in a stealth SUSY framework, where the $\tilde{\chi}_1^0$ decays through a singlino ($\tilde{S}$) intermediate state to $\gamma S\tilde{G}$, with the singlet state S decaying to two jets. No significant excess above the expected background was found and limits were set in a particular R-parity conserving stealth SUSY model. The model assumes $m_{\tilde{\chi}_1^0} = 0.5\ m_{\tilde{q}}$, $m_{\tilde{S}} = 100$ GeV and $m_S = 90$ GeV. Under these assumptions, squark masses less than 1430 GeV were excluded at the 95% C.L.

[23] CHATRCHYAN 13T searched in 11.7 fb^{-1} of pp collisions at $\sqrt{s} = 8$ TeV for events with at least two energetic jets and significant $\not{E}_T$, using the α_T variable to discriminate between processes with genuine and misreconstructed $\not{E}_T$. No significant excess above the Standard Model expectations is observed. Limits are set on squark masses in simplified models where the decay $\tilde{q} \to q\tilde{\chi}_1^0$ takes place with a branching ratio of 100%, assuming an eightfold degeneracy of the masses of the first two generation squarks, see Fig. 8 and Table 9. Also limits in the case of a single light squark are given.

[24] AAD 12AX searched in 1.04 fb^{-1} of pp collisions at $\sqrt{s} = 7$ TeV for supersymmetry in events containing jets, missing transverse momentum and one isolated electron or muon. No excess over the expected SM background is observed and model-independent limits are set on the cross section of new physics contributions to the signal regions. In mSUGRA/CMSSM models with $\tan\beta = 10$, $A_0 = 0$ and $\mu > 0$, squarks and gluinos of equal mass are excluded for masses below 820 GeV at 95% C.L. Limits are also set on simplified models for squark production and decay via an intermediate chargino and on supersymmetric models with bilinear R-parity violation. Supersedes AAD 11G.

[25] AAD 12CJ searched in 4.7 fb^{-1} of pp collisions at $\sqrt{s} = 7$ TeV for events containing one or more isolated leptons (electrons or muons), jets and $\not{E}_T$. The observations are in good agreement with the SM expectations and exclusion limits have been set in number of SUSY models. In the mSUGRA/CMSSM model with $\tan\beta = 10$, $A_0 = 0$, and $\mu > 0$, 95% C.L. exclusion limits have been derived for $m_{\tilde{q}} < 1200$ GeV, assuming equal squark and gluino masses. In minimal GMSB, values of the effective SUSY breaking scale $\Lambda <$ 50 TeV are excluded at 95% C.L. for $\tan\beta < 45$. Also exclusion limits in a number of simplified models have been presented, see Figs. 10 and 12.

[26] AAD 12CP searched in 4.8 fb^{-1} of pp collisions at $\sqrt{s} = 7$ TeV for events with two photons and large $\not{E}_T$ due to $\tilde{\chi}_1^0 \to \gamma\tilde{G}$ decays in a GMSB framework. No significant excess above the expected background was found and limits were set on the squark mass as a function of the neutralino mass in a generalized GMSB model (GGM) with a bino-like neutralino NLSP. The other sparticle masses were decoupled, $\tan\beta = 2$ and $c\tau_{NLSP} < 0.1$ mm. Also, in the framework of the SPS8 model, a 95% C.L. lower limit was set on the breaking scale Λ of 196 TeV.

[27] AAD 12W searched in 1.04 fb^{-1} of pp collisions at $\sqrt{s} = 7$ TeV for the production of squarks and gluinos in events containing jets, missing transverse momentum and no electrons or muons. No excess over the expected SM background is observed. In mSUGRA/CMSSM models with $\tan\beta = 10$, $A_0 = 0$ and $\mu > 0$, squarks and gluinos of equal mass are excluded for masses below 950 GeV at 95% C.L. In a simplified model containing only squarks of the first two generations, a gluino octet and a massless neutralino, squark masses below 875 GeV are excluded at 95% C.L.

[28] CHATRCHYAN 12 looked in 35 pb^{-1} of pp collisions at $\sqrt{s} = 7$ TeV for events with e and/or μ and/or jets, a large total transverse energy, and $\not{E}_T$. The event selection is based on the dimensionless razor variable R, related to the $\not{E}_T$ and M_R, an indicator of the heavy particle mass scale. No evidence for an excess over the expected background is observed. Limits are derived in the CMSSM (m_0, $m_{1/2}$) plane for $\tan\beta = 3$, 10 and 50 (see Fig. 7 and 8). Limits are also obtained for Simplified Model Spectra.

[29] CHATRCHYAN 12AE searched in 4.98 fb^{-1} of pp collisions at $\sqrt{s} = 7$ TeV for events with at least three jets and large missing transverse momentum. No significant excesses over the expected SM backgrounds are observed and 95% C.L. limits on the production cross section of squarks in a scenario where $\tilde{q} \to q\tilde{\chi}_1^0$ with a 100% branching ratio, see Fig. 3. For $m_{\tilde{\chi}_1^0} < 200$ GeV, values of $m_{\tilde{q}}$ below 760 GeV are excluded at 95% C.L. Also limits in the CMSSM are presented, see Fig. 2.

[30] CHATRCHYAN 12AT searched in 4.73 fb^{-1} of pp collisions at $\sqrt{s} = 7$ TeV for the production of squarks and gluinos in events containing jets, missing transverse momentum and no electrons or muons. No excess over the expected SM background is observed. In mSUGRA/CMSSM models with $\tan\beta = 10$, $A_0 = 0$ and $\mu > 0$, squarks with masses below 1110 GeV are excluded at 95% C.L. Squarks and gluinos of equal mass are excluded for masses below 1180 GeV at 95% C.L. Exclusions are also derived in various simplified models, see Fig. 6.

[31] KHACHATRYAN 16BT performed a global Bayesian analysis of a wide range of CMS results obtained with data samples corresponding to 5.0 fb^{-1} of pp collisions at $\sqrt{s} =$ 7 TeV and in 19.5 fb^{-1} of pp collisions at $\sqrt{s} = 8$ TeV. The set of searches considered, both individually and in combination, includes those with all-hadronic final states, same-sign and opposite-sign dileptons, and multi-lepton final states. An interpretation was given in a scan of the 19-parameter pMSSM. No scan points with a gluino mass less than 500 GeV survived and 98% of models with a squark mass less than 300 GeV were excluded.

[32] AAD 15AI searched in 20 fb^{-1} of pp collisions at $\sqrt{s} = 8$ TeV for events containing at least one isolated lepton (electron or muon), jets, and large missing transverse momentum. No excess of events above the expected level of Standard Model background was found. Exclusion limits at 95% C.L. are set on the squark masses in the CMSSM/mSUGRA, see Fig. 15, in the NUHMG, see Fig. 16, and in various simplified models, see Figs. 19–21.

[33] KHACHATRYAN 15AR searched in 19.7 of fb^{-1} of pp collisions at $\sqrt{s}$ = 8 TeV for events containing jets, either a charged lepton or a photon, and low missing transverse momentum. No significant excess above the Standard Model expectations is observed. Limits are set on the squark mass in a stealth SUSY model where the decays $\tilde{q} \to q\tilde{\chi}_1^{\pm}$, $\tilde{\chi}_1^{\pm} \to \tilde{S}W^{\pm}$, $\tilde{S} \to S\tilde{G}$ and $S \to gg$, with $m_{\tilde{S}}$ = 100 GeV and m_S = 90 GeV, take place with a branching ratio of 100%. See Fig. 6 for γ or Fig. 7 for $\ell^{\pm}$ analyses.

[34] KHACHATRYAN 15AZ searched in 19.7 fb^{-1} of pp collisions at $\sqrt{s}$ = 8 TeV for events with either at least one photon, hadronic jets and $\not{E}_T$ (single photon channel) or with at least two photons and at least one jet and using the razor variables. No significant excess above the Standard Model expectations is observed. Limits are set on gluino masses in the general gauge-mediated SUSY breaking model (GGM), for both a bino-like and wino-like neutralino NLSP scenario, see Fig. 8 and 9.

[35] AAD 14E searched in 20.3 fb^{-1} of pp collisions at $\sqrt{s}$ = 8 TeV for strongly produced supersymmetric particles in events containing jets and two same-sign leptons or three leptons. The search also utilises jets originating from b-quarks, missing transverse momentum and other variables. No excess over the expected SM background is observed. Exclusion limits are derived in simplified models containing gluinos and squarks, see Figures 5 and 6. In the $\tilde{q} \to q'\tilde{\chi}_1^{\pm}$, $\tilde{\chi}_1^{\pm} \to W^{(*)\pm}\tilde{\chi}_2^0$, $\tilde{\chi}_2^0 \to Z^{(*)}\tilde{\chi}_1^0$ simplified model, the following assumptions have been made: $m_{\tilde{\chi}_1^{\pm}} = 0.5\ m_{\tilde{\chi}_1^0} + m_{\tilde{g}}$, $m_{\tilde{\chi}_2^0} = 0.5\ (\ m_{\tilde{\chi}_1^0} + m_{\tilde{\chi}_1^{\pm}}\ )$. In the $\tilde{q} \to q'\tilde{\chi}_1^{\pm}$ or $\tilde{q} \to q'\tilde{\chi}_2^0$, $\tilde{\chi}_1^{\pm} \to \ell^{\pm}\nu\tilde{\chi}_1^0$ or $\tilde{\chi}_2^0 \to \ell^{\pm}\ell^{\mp}(\nu\nu)\tilde{\chi}_1^0$ simplified model, the following assumptions have been made: $m_{\tilde{\chi}_1^{\pm}} = m_{\tilde{\chi}_2^0} = 0.5\ (\ m_{\tilde{\chi}_1^0} + m_{\tilde{q}}\ )$, $m_{\tilde{\chi}_1^0} < 460$ GeV. Limits are also derived in the mSUGRA/CMSSM, bRPV and GMSB models, see their Fig. 8.

[36] CHATRCHYAN 13AO searched in 4.98 fb^{-1} of pp collisions at $\sqrt{s}$ = 7 TeV for events with two opposite-sign isolated leptons accompanied by hadronic jets and $\not{E}_T$. No significant excesses over the expected SM backgrounds are observed and 95% C.L. exclusion limits are derived in the mSUGRA/CMSSM model with tanβ = 10, A_0 = 0 and $\mu > 0$, see Fig. 8.

[37] CHATRCHYAN 13AV searched in 4.7 fb^{-1} of pp collisions at $\sqrt{s}$ = 7 TeV for new heavy particle pairs decaying into jets (possibly b-tagged), leptons and $\not{E}_T$ using the Razor variables. No significant excesses over the expected SM backgrounds are observed and 95% C.L. exclusion limits are derived in the mSUGRA/CMSSM model with tanβ = 10, A_0 = 0 and $\mu > 0$, see Fig. 3. The results are also interpreted in various simplified models, see Fig. 4.

[38] CHATRCHYAN 13W searched in 4.93 fb^{-1} of pp collisions at $\sqrt{s}$ = 7 TeV for events with one or more photons, hadronic jets and $\not{E}_T$. No significant excess above the Standard Model expectations is observed. Limits are set on squark masses in the general gauge-mediated SUSY breaking model (GGM), for both a wino-like and bino-like neutralino NLSP scenario, see Fig. 5.

[39] DREINER 12A reassesses constraints from CMS (at 7 TeV, $\sim$ 4.4 fb^{-1}) under the assumption that the fist and second generation squarks and the lightest SUSY particle are quasi-degenerate in mass (compressed spectrum).

[40] DREINER 12A reassesses constraints from CMS (at 7 TeV, $\sim$ 4.4 fb^{-1}) under the assumption that the first and second generation squarks, the gluino, and the lightest SUSY particle are quasi-degenerate in mass (compressed spectrum).

R-parity violating $\tilde{q}$ (Squark) mass limit

VALUE (GeV)	CL%	DOCUMENT ID		TECN	COMMENT
>1600	95	[1] KHACHATRY...16BX		CMS	RPV, $\tilde{q} \to q\tilde{\chi}_1^0$, $\tilde{\chi}_1^0 \to \ell\ell\nu$, λ_{121} or $\lambda_{122} \neq 0$, $m_{\tilde{g}}$ = 2400 GeV
>1000	95	[2] AAD	15CB	ATLS	RPV, jets, $\tilde{q} \to q\tilde{\chi}_1^0$, $\tilde{\chi}_1^0 \to \ell q q$, $m_{\tilde{\chi}_1^0}$ = 108 GeV and $2.5 < c\tau_{\tilde{\chi}_1^0} < 200$ mm
		[3] AAD	12AX	ATLS	ℓ +jets +$\not{E}_T$, CMSSM, $m_{\tilde{q}}$=$m_{\tilde{g}}$
		[4] CHATRCHYAN	12AL	CMS	RPV, $\geq 3\ell^{\pm}$

[1] KHACHATRYAN 16BX searched in 19.5 fb^{-1} of pp collisions at $\sqrt{s}$ = 8 TeV for events containing 4 leptons coming from R-parity-violating decays of $\tilde{\chi}_1^0 \to \ell\ell\nu$ with $\lambda_{121} \neq 0$ or $\lambda_{122} \neq 0$. No excess over the expected background is observed. Limits are derived on the gluino, squark and stop masses, see Fig. 23.

[2] AAD 15CB searched for events containing at least one long-lived particle that decays at a significant distance from its production point (displaced vertex, DV) into two leptons or into five or more charged particles in 20.3 fb^{-1} of pp collisions at $\sqrt{s}$ = 8 TeV. The dilepton signature is characterised by DV formed from at least two lepton candidates. Four different final states were considered for the multitrack signature, in which the DV must be accompanied by a high-transverse momentum muon or electron candidate that originates from the DV, jets or missing transverse momentum. No events were observed in any of the signal regions. Results were interpreted in SUSY scenarios involving R-parity violation, split supersymmetry, and gauge mediation. See their Fig. 14–20.

[3] AAD 12AX searched in 1.04 fb^{-1} of pp collisions at $\sqrt{s}$ = 7 TeV for supersymmetry in events containing jets, missing transverse momentum and one isolated electron or muon. No excess over the expected SM background is observed and model-independent limits are set on the cross section of new physics contributions to the signal regions. In mSUGRA/CMSSM models with tanβ = 10, A_0 = 0 and $\mu > 0$, squarks and gluinos of equal mass are excluded for masses below 820 GeV at 95% C.L. Limits are also set on simplified models for squark production and decay via an intermediate chargino and on supersymmetric models with bilinear R-parity violation. Supersedes AAD 11G.

[4] CHATRCHYAN 12AL looked in 4.98 fb^{-1} of pp collisions at $\sqrt{s}$ = 7 TeV for anomalous production of events with three or more isolated leptons. Limits on squark and gluino masses are set in RPV SUSY models with leptonic $LL\bar{E}$couplings, $\lambda_{123} > 0.05$, and hadronic $\overline{UDD}$ couplings, $\lambda''_{112} > 0.05$, see their Fig. 5. In the $\overline{UDD}$ case the leptons arise from supersymmetric cascade decays. A very specific supersymmetric spectrum is assumed. All decays are prompt.

Long-lived $\tilde{q}$ (Squark) mass limit

The following are bounds on long-lived scalar quarks, assumed to hadronise into hadrons with lifetime long enough to escape the detector prior to a possible decay. Limits may depend on the mixing angle of mass eigenstates: $\tilde{q}_1 = \tilde{q}_L \cos\theta_q + \tilde{q}_R \sin\theta_q$.

The coupling to the Z^0 boson vanishes for up-type squarks when θ_u=0.98, and for down type squarks when θ_d=1.17.

VALUE (GeV)	CL%	DOCUMENT ID		TECN	COMMENT
> 805	95	[1] AABOUD	16B	ATLS	$\tilde{b}$ R-hadrons
> 890	95	[2] AABOUD	16B	ATLS	$\tilde{t}$ R-hadrons
>1040	95	[3] KHACHATRY...16BW		CMS	$\tilde{t}$ R-hadrons, cloud interaction model
>1000	95	[3] KHACHATRY...16BW		CMS	$\tilde{t}$ R-hadrons, charge-suppressed interaction model
> 845	95	[4] AAD	15AE	ATLS	$\tilde{b}$ R-hadron, stable, Regge model
> 900	95	[4] AAD	15AE	ATLS	$\tilde{t}$ R-hadron, stable, Regge model
>1500	95	[4] AAD	15AE	ATLS	$\tilde{g}$ decaying to 300 GeV stable sleptons, LeptoSUSY model
> 751	95	[5] AAD	15BM	ATLS	$\tilde{b}$ R-hadron, stable, Regge model
> 766	95	[5] AAD	15BM	ATLS	$\tilde{t}$ R-hadron, stable, Regge model
> 525	95	[6] KHACHATRY...15AK		CMS	$\tilde{t}$ R-hadrons, 10 μs< τ <1000 s
> 470	95	[6] KHACHATRY...15AK		CMS	$\tilde{t}$ R-hadrons, 1 μs< τ <1000 s
• • • We do not use the following data for averages, fits, limits, etc. • • •					
> 683	95	[7] AAD	13AA	ATLS	$\tilde{t}$, R-hadrons, generic interaction model
> 612	95	[8] AAD	13AA	ATLS	$\tilde{b}$, R-hadrons, generic interaction model
> 344	95	[9] AAD	13BC	ATLS	R-hadrons, $\tilde{t} \to b\tilde{\chi}_1^0$, Regge model, lifetime between 10^{-5} and 10^3 s, $m_{\tilde{\chi}_1^0}$ = 100 GeV
> 379	95	[10] AAD	13BC	ATLS	R-hadrons, $\tilde{t} \to t\tilde{\chi}_1^0$, Regge model, lifetime between 10^{-5} and 10^3 s, $m_{\tilde{\chi}_1^0}$ = 100 GeV
> 935	95	[11] CHATRCHYAN	13AB	CMS	long-lived $\tilde{t}$ forming R-hadrons, cloud interaction model

[1] AABOUD 16B searched in 3.2 fb^{-1} of pp collisions at $\sqrt{s}$ = 13 TeV for long-lived R-hadrons using observables related to large ionization losses and slow propagation velocities, which are signatures of heavy charged particles traveling significantly slower than the speed of light. Exclusion limits at 95% C.L. are set on the long-lived sbottom masses exceeding 805 GeV. See their Fig. 5.

[2] AABOUD 16B searched in 3.2 fb^{-1} of pp collisions at $\sqrt{s}$ = 13 TeV for long-lived R-hadrons using observables related to large ionization losses and slow propagation velocities, which are signatures of heavy charged particles traveling significantly slower than the speed of light. Exclusion limits at 95% C.L. are set on the long-lived stop masses exceeding 890 GeV. See their Fig. 5.

[3] KHACHATRYAN 16BW searched in 2.5 fb^{-1} of pp collisions at $\sqrt{s}$ = 13 TeV for events with heavy stable charged particles, identified by their anomalously high energy deposits in the silicon tracker and/or long time-of-flight measurements by the muon system. No evidence for an excess over the expected background is observed. Limits are derived for pair production of top squarks as a function of mass, depending on the interaction model, see Fig. 4 and Table 7.

[4] AAD 15AE searched in 19.1 fb^{-1} of pp collisions at $\sqrt{s}$ = 8 TeV for heavy long-lived charged particles, measured through their specific ionization energy loss in the ATLAS pixel detector or their time-of-flight in the ALTAS muon system. In the absence of an excess of events above the expected backgrounds, limits are set R-hadrons in various scenarios, see Fig. 11. Limits are also set in LeptoSUSY models where the gluino decays to stable 300 GeV leptons, see Fig. 9.

[5] AAD 15BM searched in 18.4 fb^{-1} of pp collisions at $\sqrt{s}$ = 8 TeV for stable and metastable non-relativistic charged particles through their anomalous specific ionization energy loss in the ATLAS pixel detector. In absence of an excess of events above the expected backgrounds, limits are set on stable bottom and top squark R-hadrons, see Table 5.

[6] KHACHATRYAN 15AK looked in a data set corresponding to fb^{-1} of pp collisions at $\sqrt{s}$ = 8 TeV, and a search interval corresponding to 281 h of trigger lifetime, for long-lived particles that have stopped in the CMS detector. No evidence for an excess over the expected background in a cloud interaction model is observed. Assuming the decay $\tilde{t} \to t\tilde{\chi}_1^0$ and lifetimes between 1 μs and 1000 s, limits are derived on $\tilde{t}$ production as a function of $m_{\tilde{\chi}_1^0}$, see Figs. 4 and 7. The exclusions require that $m_{\tilde{\chi}_1^0}$ is kinematically consistent with the minimum values of the jet energy thresholds used.

[7] AAD 13AA searched in 4.7 fb^{-1} of pp collisions at $\sqrt{s}$ = 7 TeV for events containing colored long-lived particles that hadronize forming R-hadrons. No significant excess above the expected background was found. Long-lived R-hadrons containing a $\tilde{t}$ are excluded for masses up to 683 GeV at 95% C.L in a general interaction model. Also, limits independent of the fraction of R-hadrons that arrive charged in the muon system were derived, see Fig. 6.

[8] AAD 13AA searched in 4.7 fb^{-1} of pp collisions at $\sqrt{s}$ = 7 TeV for events containing colored long-lived particles that hadronize forming R-hadrons. No significant excess above the expected background was found. Long-lived R-hadrons containing a $\tilde{b}$ are excluded for masses up to 612 GeV at 95% C.L in a general interaction model. Also, limits independent of the fraction of R-hadrons that arrive charged in the muon system were derived, see Fig. 6.

[9] AAD 13BC searched in 5.0 fb^{-1} of pp collisions at $\sqrt{s}$ = 7 TeV and in 22.9 fb^{-1} of pp collisions at $\sqrt{s}$ = 8 TeV for bottom squark R-hadrons that have come to rest within the ATLAS calorimeter and decay at some later time to hadronic jets and a neutralino. In absence of an excess of events above the expected backgrounds, limits are set on sbottom masses for the decay $\tilde{b} \to b\tilde{\chi}_1^0$, for different lifetimes, and for a neutralino mass of 100 GeV, see their Table 6 and Fig 10.

[10] AAD 13BC searched in 5.0 fb^{-1} of pp collisions at $\sqrt{s}$ = 7 TeV and in 22.9 fb^{-1} of pp collisions at $\sqrt{s}$ = 8 TeV for bottom squark R-hadrons that have come to rest within the ATLAS calorimeter and decay at some later time to hadronic jets and a neutralino. In absence of an excess of events above the expected backgrounds, limits are set on stop masses for the decay $\tilde{t} \to t\tilde{\chi}_1^0$, for different lifetimes, and for a neutralino mass of 100 GeV, see their Table 6 and Fig 10.

[11] CHATRCHYAN 13AB looked in 5.0 fb^{-1} of pp collisions at $\sqrt{s}$ = 7 TeV and in 18.8 fb^{-1} of pp collisions at $\sqrt{s}$ = 8 TeV for events with heavy stable particles, identified by their anomalous dE/dx in the tracker or additionally requiring that it be identified as muon in the muon chambers, from pair production of $\tilde{t}_1$'s. No evidence for an excess over the expected background is observed. Limits are derived for pair production of stops as a function of mass in the cloud interaction model (see Fig. 8 and Table 6). In the charge-suppressed model, the limit decreases to 818 GeV.

$\tilde{b}$ (Sbottom) mass limit

Limits in e^+e^- depend on the mixing angle of the mass eigenstate $\tilde{b}_1 = \tilde{b}_L \cos\theta_b + \tilde{b}_R \sin\theta_b$. Coupling to the Z vanishes for $\theta_b \sim 1.17$. As a consequence, no absolute constraint in the mass region $\lesssim$40 GeV is available in the literature at this time from e^+e^- collisions. In the Listings below, we use $\Delta m = m_{\tilde{b}_1} - m_{\tilde{\chi}^0_1}$.

Some earlier papers are now obsolete and have been omitted. They were last listed in our PDG 14 edition: K. Olive, *et al.* (Particle Data Group), Chinese Physics **C38** 070001 (2014) (http://pdg.lbl.gov).

R-parity conserving $\tilde{b}$ (Sbottom) mass limit

VALUE (GeV)	CL%	DOCUMENT ID		TECN	COMMENT
>1230	95	[1] SIRUNYAN	18B	CMS	jets+$\not{E}_T$, Tsbot1, $m_{\tilde{\chi}^0_1}$ = 0 GeV
> 700	95	[2] AABOUD	17AJ	ATLS	same-sign $\ell^\pm\ell^\pm$ / 3 ℓ + jets + $\not{E}_T$, Tsbot2, $m_{\tilde{\chi}^0_1}$ = 0 GeV
> 950	95	[3] AABOUD	17AX	ATLS	2 b-jets+$\not{E}_T$, Tsbot1, $m_{\tilde{\chi}^0_1}$ = 0 GeV
> 880	95	[4] AABOUD	17AX	ATLS	2 b-jets + $\not{E}_T$, mixture Tsbot1 and Tsbot2 BR=50%, $m_{\tilde{\chi}^0_1}$ = 0 GeV, $m_{\tilde{\chi}^\pm_1} - m_{\tilde{\chi}^0_1}$ = 1 GeV
> 315	95	[5] KHACHATRY...17A		CMS	2 VBF jets + $\not{E}_T$, Tsbot1, $m_{\tilde{b}} - m_{\tilde{\chi}^0_1}$ = 5 GeV
> 450	95	[6] KHACHATRY...17AW		CMS	$\geq 3\ell^\pm$, 2 jets, Tsbot2, $m_{\tilde{\chi}^0_1}$ = 50 GeV, $m_{\tilde{\chi}^\pm_1}$ = 200 GeV
> 800	95	[7] KHACHATRY...17P		CMS	1 or more jets+$\not{E}_T$, Tsbot1, $m_{\tilde{\chi}^0_1}$ = 0 GeV
>1175	95	[8] SIRUNYAN	17AZ	CMS	$\geq$ 1 jets+$\not{E}_T$, Tsbot1, $m_{\tilde{\chi}^0_1}$ = 0 GeV
> 890	95	[9] SIRUNYAN	17K	CMS	jets+$\not{E}_T$, Tsbot1, $m_{\tilde{\chi}^0_1}$ = 0 GeV
> 810	95	[10] SIRUNYAN	17S	CMS	same-sign $\ell^\pm\ell^\pm$ + jets + $\not{E}_T$, Tsbot2, $m_{\tilde{\chi}^0_1}$ = 50 GeV, $m_{\tilde{\chi}^\pm_1}$ = 100 GeV
> 323	95	[11] AABOUD	16D	ATLS	$\geq$ 1 jet + $\not{E}_T$, Tsbot1, $m_{\tilde{b}_1} - m_{\tilde{\chi}^0_1}$ = 5 GeV
> 840	95	[12] AABOUD	16Q	ATLS	2 b-jets + $\not{E}_T$, Tsbot1, $m_{\tilde{\chi}^0_1}$ = 100 GeV
> 540	95	[13] AAD	16BB	ATLS	2 same-sign/3ℓ + jets + $\not{E}_T$, Tsbot2, $m_{\tilde{\chi}^0_1}$ < 55 GeV
> 680	95	[14] KHACHATRY...16BJ		CMS	same-sign $\ell^\pm\ell^\pm$, Tsbot2, $m_{\tilde{\chi}^\pm_1}$ < 550 GeV, $m_{\tilde{\chi}^0_1}$ = 50 GeV
> 500	95	[14] KHACHATRY...16BJ		CMS	same-sign $\ell^\pm\ell^\pm$, Tsbot2, $m_{\tilde{b}} - m_{\tilde{\chi}^\pm_1}$ <100 GeV, $m_{\tilde{\chi}^0_1}$=50 GeV
> 880	95	[15] KHACHATRY...16BS		CMS	jets + $\not{E}_T$, Tsbot1, $m_{\tilde{\chi}^0_1}$ = 0 GeV
> 550	95	[16] KHACHATRY...16BY		CMS	opposite-sign $\ell^\pm\ell^\pm$, Tsbot3, $m_{\tilde{\chi}^0_1}$ = 100 GeV
> 600	95	[17] AAD	15CJ	ATLS	$\tilde{b} \to b\tilde{\chi}^0_1$, $m_{\tilde{\chi}^0_1}$ < 250 GeV
> 440	95	[17] AAD	15CJ	ATLS	$\tilde{b} \to t\tilde{\chi}^\pm_1$, $\tilde{\chi}^\pm_1 \to W^{(*)}\tilde{\chi}^0_1$, $m_{\tilde{\chi}^0_1}$ = 60 GeV, $m_{\tilde{b}} - m_{\tilde{\chi}^\pm_1} < m_t$
none 300–650	95	[17] AAD	15CJ	ATLS	$\tilde{b} \to \tilde{b}b\tilde{\chi}^0_2$, $\tilde{\chi}^0_2 \to h\tilde{\chi}^0_1$, $m_{\tilde{\chi}^0_1}$ = 60 GeV, $m_{\tilde{\chi}^0_2}$ > 250 GeV
> 640	95	[18] KHACHATRY...15AF		CMS	$\tilde{b} \to b\tilde{\chi}^0_1$, $m_{\tilde{\chi}^0_1}$ = 0
> 650	95	[19] KHACHATRY...15AH		CMS	$\tilde{b} \to b\tilde{\chi}^0_1$, $m_{\tilde{\chi}^0_1}$ = 0
> 250	95	[19] KHACHATRY...15AH		CMS	$\tilde{b} \to b\tilde{\chi}^0_1$, $m_{\tilde{b}} - m_{\tilde{\chi}^0_1}$ < 10 GeV
> 570	95	[20] KHACHATRY...15I		CMS	$\tilde{b} \to t\tilde{\chi}^\pm_1$, $\tilde{\chi}^\pm_1 \to W^\pm\tilde{\chi}^0_1$, $m_{\tilde{\chi}^0_1}$ =50 GeV, 150<$m_{\tilde{\chi}^\pm_1}$ <300 GeV
> 255	95	[21] AAD	14T	ATLS	$\tilde{b}_1 \to b\tilde{\chi}^0_1$, $m_{\tilde{b}_1} - m_{\tilde{\chi}^0_1} \approx m_b$
> 400	95	[22] CHATRCHYAN	14AH	CMS	jets + $\not{E}_T$, $\tilde{b} \to b\tilde{\chi}^0_1$ simplified model, $m_{\tilde{\chi}^0_1}$ = 50 GeV
		[23] CHATRCHYAN	14R	CMS	$\geq 3\ell^\pm$, $\tilde{b} \to t\tilde{\chi}^\pm_1$, $\tilde{\chi}^\pm_1 \to W^\pm\tilde{\chi}^0_1$ simplified model, $m_{\tilde{\chi}^0_1}$ = 50 GeV

• • • We do not use the following data for averages, fits, limits, etc. • • •

		[24] KHACHATRY...15AD		CMS	$\ell^\pm\ell^\mp$ + jets + $\not{E}_T$, $\tilde{b} \to b\ell^\pm\ell^\mp\tilde{\chi}^0_1$
none 340–600	95	[25] AAD	14AX	ATLS	$\geq$ 3 b-jets + $\not{E}_T$, $\tilde{b} \to b\tilde{\chi}^0_2$ simplified model with $\tilde{\chi}^0_2 \to h\tilde{\chi}^0_1$, $m_{\tilde{\chi}^0_1}$=60 GeV, $m_{\tilde{\chi}^0_2}$=300 GeV
> 440	95	[26] AAD	14E	ATLS	$\ell^\pm\ell^\pm(\ell^\mp)$ + jets, $\tilde{b}_1 \to t\tilde{\chi}^\pm_1$ with $\tilde{\chi}^\pm_1 \to W^{(*)\pm}\tilde{\chi}^0_1$ simplified model, $m_{\tilde{\chi}^\pm_1} = 2\, m_{\tilde{\chi}^0_1}$
> 500	95	[27] CHATRCHYAN	14H	CMS	same-sign $\ell^\pm\ell^\pm$, $\tilde{b} \to t\tilde{\chi}^\pm_1$, $\tilde{\chi}^\pm_1 \to W^\pm\tilde{\chi}^0_1$ simplified model, $m_{\tilde{\chi}^\pm_1}$ = 2 GeV, $m_{\tilde{\chi}^0_1}$ = 100 GeV
> 620	95	[28] AAD	13AU	ATLS	2 b-jets + $\not{E}_T$, $\tilde{b}_1 \to b\tilde{\chi}^0_1$, $m_{\tilde{\chi}^0_1}$ < 120 GeV
> 550	95	[29] CHATRCHYAN	13AT	CMS	jets + $\not{E}_T$, $\tilde{b} \to b\tilde{\chi}^0_1$ simplified model, $m_{\tilde{\chi}^0_1}$= 50 GeV
> 600	95	[30] CHATRCHYAN	13T	CMS	jets + $\not{E}_T$, $\tilde{b} \to b\tilde{\chi}^0_1$ simplified model, $m_{\tilde{\chi}^0_1}$= 0 GeV
> 450	95	[31] CHATRCHYAN	13V	CMS	same-sign $\ell^\pm\ell^\pm$ + $\geq$ 2 b-jets, $\tilde{b} \to t\tilde{\chi}^\pm_1$, $\tilde{\chi}^\pm_1 \to W^\pm\tilde{\chi}^0_1$ simplified model, $m_{\tilde{\chi}^0_1}$ = 50 GeV
> 390		[32] AAD	12AN	ATLS	$\tilde{b}_1 \to b\tilde{\chi}^0_1$, simplified model, $m_{\tilde{\chi}^0_1}$ < 60 GeV
		[33] CHATRCHYAN	12AI	CMS	$\ell^\pm\ell^\pm$ + b-jets + $\not{E}_T$
> 410	95	[34] CHATRCHYAN	12BO	CMS	$\tilde{b}_1 \to b\tilde{\chi}^0_1$, simplified model, $m_{\tilde{\chi}^0_1}$ = 50 GeV
> 294	95	[35] AAD	11K	ATLS	stable b
		[36] AAD	11O	ATLS	$\tilde{g} \to \tilde{b}_1 b$, $\tilde{b}_1 \to b\tilde{\chi}^0_1$, $m_{\tilde{\chi}^0_1}$=60 GeV
		[37] CHATRCHYAN	11D	CMS	$\tilde{b},\tilde{t} \to b$
> 230	95	[38] AALTONEN	10R	CDF	$\tilde{b}_1 \to b\tilde{\chi}^0_1$, $m_{\tilde{\chi}^0_1}$ < 70 GeV
> 247	95	[39] ABAZOV	10L	D0	$\tilde{b}_1 \to b\tilde{\chi}^0_1$, $m_{\tilde{\chi}^0_1}$ = 0 GeV

[1] SIRUNYAN 18B searched in 35.9 fb^{-1} of pp collisions at $\sqrt{s}$ = 13 TeV for the pair production of third-generation squarks in events with jets and large $\not{E}_T$. No significant excess above the Standard Model expectations is observed. Limits are set on the sbottom mass in the Tsbot1 simplified model, see their Figure 5, and on the stop mass in the Tstop4 simplified model, see their Figure 6.

[2] AABOUD 17AJ searched in 36.1 fb^{-1} of pp collisions at $\sqrt{s}$ = 13 TeV for events with two same-sign or three leptons, jets and large missing transverse momentum. No significant excess above the Standard Model expectations is observed. Limits up to 700 GeV are set on the bottom squark mass in Tsbot2 simplified models assuming $m_{\tilde{\chi}^0_1}$ = 0 GeV. See their Figure 4(d).

[3] AABOUD 17AX searched in 36 fb^{-1} of pp collisions at $\sqrt{s}$ = 13 TeV for events containing two jets identified as originating from b-quarks and large missing transverse momentum. No excess of events above the expected level of Standard Model background was found. Exclusion limits at 95% C.L. are set on the masses of bottom squarks. In the Tsbot1 simplified model, a $\tilde{b}_1$ mass below 950 GeV is excluded for $m_{\tilde{\chi}^0_1}$ = 0 (<420) GeV. See their Fig. 7(a).

[4] AABOUD 17AX searched in 36 fb^{-1} of pp collisions at $\sqrt{s}$ = 13 TeV for events containing two jets identified as originating from b-quarks and large missing transverse momentum, with or without leptons. No excess of events above the expected level of Standard Model background was found. Exclusion limits at 95% C.L. are set on the masses of bottom squarks. Assuming 50% BR for Tsbot1 and Tsbot2 simplified models, a $\tilde{b}_1$ mass below 880 (860) GeV is excluded for $m_{\tilde{\chi}^0_1}$ = 0 (<250) GeV. See their Fig. 7(b).

[5] KHACHATRYAN 17A searched in 18.5 fb^{-1} of pp collisions at $\sqrt{s}$ = 8 TeV for events with two forward jets, produced through vector boson fusion, and missing transverse momentum. No significant excess above the Standard Model expectations is observed. A limit is set on sbottom masses in the Tsbot1 simplified model, see Fig. 3.

[6] KHACHATRYAN 17AW searched in 2.3 fb^{-1} of pp collisions at $\sqrt{s}$ = 13 TeV for events with at least three charged leptons, in any combination of electrons and muons, and significant $\not{E}_T$. No significant excess above the Standard Model expectations is observed. Limits are set on the gluino mass in the Tglu3A and Tglu1C simplified models, and on the sbottom mass in the Tsbot2 simplified model, see their Figure 4.

[7] KHACHATRYAN 17P searched in 2.3 fb^{-1} of pp collisions at $\sqrt{s}$ = 13 TeV for events with one or more jets and large $\not{E}_T$. No significant excess above the Standard Model expectations is observed. Limits are set on the gluino mass in the Tglu1A, Tglu2A, Tglu3A, Tglu3B, Tglu3C and Tglu3D simplified models, see their Figures 7 and 8. Limits are also set on the squark mass in the Tsqk1 simplified model, see their Fig. 7, and on the sbottom mass in the Tsbot1 simplified model, see Fig. 8. Finally, limits are set on the stop mass in the Tstop1, Tstop3, Tstop4, Tstop6 and Tstop7 simplified models, see Fig. 8.

[8] SIRUNYAN 17AZ searched in 35.9 fb^{-1} of pp collisions at $\sqrt{s}$ = 13 TeV for events with one or more jets and large $\not{E}_T$. No significant excess above the Standard Model expectations is observed. Limits are set on the gluino mass in the Tglu1A, Tglu2A, Tglu3A simplified models, see their Figures 6. Limits are also set on the squark mass in the Tsqk1 simplified model (for single light squark and for 8 degenerate light squarks), on the sbottom mass in the Tsbot1 simplified model and on the stop mass in the Tstop1 simplified model, see their Fig. 7. Finally, limits are set on the stop mass in the Tstop2, Tstop4 and Tstop8 simplified models, see Fig. 8.

[9] SIRUNYAN 17K searched in 2.3 fb^{-1} of pp collisions at $\sqrt{s} = 13$ TeV for direct production of stop or sbottom pairs in events with multiple jets and significant $\not{E}_T$. A second search also requires an isolated lepton and is combined with the all-hadronic search. No significant excess above the Standard Model expectations is observed. Limits are set on the stop mass in the Tstop1, Tstop8 and Tstop4 simplified models, see their Figures 7, 8 and 9 (for the Tstop4 limits, only the results of the all-hadronic search are used). Limits are also set on the sbottom mass in the Tsbot1 simplified model, see Fig. 10 (also here, only the results of the all-hadronic search are used).

[10] SIRUNYAN 17S searched in 35.9 fb^{-1} of pp collisions at $\sqrt{s} = 13$ TeV for events with two isolated same-sign leptons, jets, and large $\not{E}_T$. No significant excess above the Standard Model expectations is observed. Limits are set on the mass of the gluino mass in the Tglu3A, Tglu3B, Tglu3C, Tglu3D and Tglu1B simplified models, see their Figures 5 and 6, and on the sbottom mass in the Tsbot2 simplified model, see their Figure 6.

[11] AABOUD 16D searched in 3.2 fb^{-1} of pp collisions at $\sqrt{s} = 13$ TeV for events with an energetic jet and large missing transverse momentum. The results are interpreted as 95%C.L. limits on mass of sbottom decaying into a b-quark and the lightest neutralino in scenarios with $m_{\tilde{b}_1} - m_{\tilde{\chi}^0_1}$ between 5 and 20 GeV. See their Fig. 6.

[12] AABOUD 16Q searched in 3.2 fb^{-1} of pp collisions at $\sqrt{s} = 13$ TeV for events containing two jets identified as originating from b-quarks and large missing transverse momentum. No excess of events above the expected level of Standard Model background was found. Exclusion limits at 95% C.L. are set on the masses of third-generation squarks. Assuming that the decay $\tilde{b}_1 \to b\tilde{\chi}^0_1$ (Tsbot1) takes place 100% of the time, a $\tilde{b}_1$ mass below 840 (800) GeV is excluded for $m_{\tilde{\chi}^0_1} < 100$ (360) GeV. Differences in mass above 100 GeV between the $\tilde{b}_1$ and the $\tilde{\chi}^0_1$ are excluded up to a $\tilde{b}_1$ mass of 500 GeV. For more details, see their Fig. 4.

[13] AAD 16BB searched in 3.2 fb^{-1} of pp collisions at $\sqrt{s} = 13$ TeV for events with exactly two same-sign leptons or at least three leptons, multiple hadronic jets, b-jets, and $\not{E}_T$. No significant excess over the Standard Model expectation is found. Exclusion limits at 95% C.L. are set on the sbottom mass for the Tsbot2 model, assuming $m_{\tilde{\chi}^\pm_1} = m_{\tilde{\chi}^0_1} +$ 100 GeV. See their Fig. 4c.

[14] KHACHATRYAN 16BJ searched in 2.3 fb^{-1} of pp collisions at $\sqrt{s} = 13$ TeV for events with two isolated same-sign dileptons and jets in the final state. No significant excess above the Standard Model expectations is observed. Limits are set on the sbottom mass in the Tsbot2 simplified model, see Fig. 6.

[15] KHACHATRYAN 16BS searched in 2.3 fb^{-1} of pp collisions at $\sqrt{s} = 13$ TeV for events with at least one energetic jet , no isolated leptons, and significant $\not{E}_T$, using the transverse mass variable M_{T2} to discriminate between signal and background processes. No significant excess above the Standard Model expectations is observed. Limits are set on the sbottom mass in the Tsbot1 simplified model, see Fig. 11 and Table 3.

[16] KHACHATRYAN 16BY searched in 2.3 fb^{-1} of pp collisions at $\sqrt{s} = 13$ TeV for events with two opposite-sign, same-flavour leptons, jets, and missing transverse momentum. No significant excess above the Standard Model expectations is observed. Limits are set on the gluino mass in the Tglu4C simplified model, see Fig. 4, and on sbottom masses in the Tsbot3 simplified model, see Fig. 5.

[17] AAD 15CJ searched in 20 fb^{-1} of pp collisions at $\sqrt{s} = 8$ TeV for evidence of third generation squarks by combining a large number of searches covering various final states. Limits on the sbottom mass are shown, either assuming the $\tilde{b} \to b\tilde{\chi}^0_1$ decay, see Fig. 11, or assuming the $\tilde{b} \to t\tilde{\chi}^\pm_1$ decay, with $\tilde{\chi}^\pm_1 \to W^{(*)}\tilde{\chi}^0_1$, see Fig. 12a, or assuming the $\tilde{b} \to b\tilde{\chi}^0_2$ decay, with $\tilde{\chi}^0_2 \to h\tilde{\chi}^0_1$, see Fig. 12b. Interpretations in the pMSSM are also discussed, see Figures 13–15.

[18] KHACHATRYAN 15AF searched in 19.5 fb^{-1} of pp collisions at $\sqrt{s} = 8$ TeV for events with at least two energetic jets and significant $\not{E}_T$, using the transverse mass variable M_{T2} to discriminate between signal and background processes. No significant excess above the Standard Model expectations is observed. Limits are set on the sbottom mass in simplified models where the decay $\tilde{b} \to b\tilde{\chi}^0_1$ takes place with a branching ratio of 100%, see Fig. 12. See also Table 5. Exclusions in the CMSSM, assuming tan$\beta = 30$, $A_0 = -2$ max(m_0, $m_{1/2}$) and $\mu > 0$, are also presented, see Fig. 15.

[19] KHACHATRYAN 15AH searched in 19.4 or 19.7 fb^{-1} of pp collisions at $\sqrt{s} = 8$ TeV for events containing either a fully reconstructed top quark, or events containing dijets requiring one or both jets to originate from b-quarks, or events containing a mono-jet. No significant excess above the Standard Model expectations is observed. Limits are set on the sbottom mass in simplified models where the decay $\tilde{b} \to b\tilde{\chi}^0_1$ takes place with a branching ratio of 100%, see Fig. 12. Limits are also set in a simplified model where the decay $\tilde{b} \to c\tilde{\chi}^0_1$ takes place with a branching ratio of 100%, see Fig. 12.

[20] KHACHATRYAN 15I searched in 19.5 fb^{-1} of pp collisions at $\sqrt{s} = 8$ TeV for events in which b-jets and four W-bosons are produced. Five individual search channels are combined (fully hadronic, single lepton, same-sign dilepton, opposite-sign dilepton, multilepton). No significant excess above the Standard Model expectations is observed. Limits are set on the sbottom mass in a simplified model where the decay $\tilde{b} \to t\tilde{\chi}^\pm_1$, with $\tilde{\chi}^\pm_1 \to W^\pm\tilde{\chi}^0_1$, takes place with a branching ratio of 100%, see Fig. 7.

[21] AAD 14T searched in 20.3 fb^{-1} of pp collisions at $\sqrt{s} = 8$ TeV for monojet-like events. No excess of events above the expected level of Standard Model background was found. Exclusion limits at 95% C.L. are set on the masses of third-generation squarks in simplified models which assume that the decay $\tilde{b}_1 \to b\tilde{\chi}^0_1$ takes place 100% of the time, see Fig. 12.

[22] CHATRCHYAN 14AH searched in 4.7 fb^{-1} of pp collisions at $\sqrt{s} = 7$ TeV for events with at least two energetic jets and significant $\not{E}_T$, using the razor variables (M_R and R^2) to discriminate between signal and background processes. A second analysis requires at least one of the jets to be originating from a b-quark. No significant excess above the Standard Model expectations is observed. Limits are set on sbottom masses in simplified models where the decay $\tilde{b} \to b\tilde{\chi}^0_1$ takes place with a branching ratio of 100%, see Figs. 28 and 29. Exclusions in the CMSSM, assuming tan$\beta = 10$, $A_0 = 0$ and $\mu > 0$, are also presented, see Fig. 26.

[23] CHATRCHYAN 14R searched in 19.5 fb^{-1} of pp collisions at $\sqrt{s} = 8$ TeV for events with at least three leptons (electrons, muons, taus) in the final state. No significant excess above the Standard Model expectations is observed. Limits are set on the gluino mass in a simplified model where the decay $\tilde{b} \to t\tilde{\chi}^\pm_1$, with $\tilde{\chi}^\pm_1 \to W^\pm\tilde{\chi}^0_1$, takes place with a branching ratio of 100%, see Fig. 11.

[24] KHACHATRYAN 15AD searched in 19.4 fb^{-1} of pp collisions at $\sqrt{s} = 8$ TeV for events with two opposite-sign same flavor isolated leptons featuring either a kinematic edge, or a peak at the Z-boson mass, in the invariant mass spectrum. No evidence for a statistically significant excess over the expected SM backgrounds is observed and 95% C.L. exclusion limits are derived in a simplified model of sbottom pair production where the sbottom decays into a b-quark, two opposite-sign dileptons and a neutralino LSP, through an intermediate state containing either an off-shell Z-boson or a slepton, see Fig. 8.

[25] AAD 14AX searched in 20.1 fb^{-1} of pp collisions at $\sqrt{s} = 8$ TeV for the strong production of supersymmetric particles in events containing either zero or at last one high high-p_T lepton, large missing transverse momentum, high jet multiplicity and at least three jets identified as originating from b-quarks. No excess over the expected SM background is observed. Limits are derived in mSUGRA/CMSSM models with tan$\beta = 30$, $A_0 = -2\ m_0$ and $\mu > 0$, see their Fig. 14. Also, exclusion limits are set in simplified models containing scalar bottom quarks, where the decay $\tilde{b} \to b\tilde{\chi}^0_2$ and $\tilde{\chi}^0_2 \to h\tilde{\chi}^0_1$ takes place with a branching ratio of 100%, see their Figures 11.

[26] AAD 14E searched in 20.3 fb^{-1} of pp collisions at $\sqrt{s} = 8$ TeV for strongly produced supersymmetric particles in events containing jets and two same-sign leptons or three leptons. The search also utilises jets originating from b-quarks, missing transverse momentum and other variables. No excess over the expected SM background is observed. Exclusion limits are derived in simplified models containing bottom, see Fig. 7. Limits are also derived in the mSUGRA/CMSSM, bRPV and GMSB models, see their Fig. 8.

[27] CHATRCHYAN 14H searched in 19.5 fb^{-1} of pp collisions at $\sqrt{s} = 8$ TeV for events with two isolated same-sign dileptons and jets in the final state. No significant excess above the Standard Model expectations is observed. Limits are set on the sbottom mass in a simplified models where the decay $\tilde{b} \to t\tilde{\chi}^\pm_1$, $\tilde{\chi}^\pm_1 \to W^\pm\tilde{\chi}^0_1$ takes place with a branching ratio of 100%, with varying mass of the $\tilde{\chi}^\pm_1$, for $m_{\tilde{\chi}^0_1} = 50$ GeV, see Fig. 6.

[28] AAD 13AU searched in 20.1 fb^{-1} of pp collisions at $\sqrt{s} = 8$ TeV for events containing two jets identified as originating from b-quarks and large missing transverse momentum. No excess of events above the expected level of Standard Model background was found. Exclusion limits at 95% C.L. are set on the masses of third-generation squarks. Assuming that the decay $\tilde{b}_1 \to b\tilde{\chi}^0_1$ takes place 100% of the time, a $\tilde{b}_1$ mass below 620 GeV is excluded for $m_{\tilde{\chi}^0_1} < 120$ GeV. For more details, see their Fig. 5.

[29] CHATRCHYAN 13AT provides interpretations of various searches for supersymmetry by the CMS experiment based on 4.73–4.98 fb^{-1} of pp collisions at $\sqrt{s} = 7$ TeV in the framework of simplified models. Limits are set on the sbottom mass in a simplified models where sbottom quarks are pair-produced and the decay $\tilde{b} \to b\tilde{\chi}^0_1$ takes place with a branching ratio of 100%, see Fig. 4.

[30] CHATRCHYAN 13T searched in 11.7 fb^{-1} of pp collisions at $\sqrt{s} = 8$ TeV for events with at least two energetic jets and significant $\not{E}_T$, using the α_T variable to discriminate between processes with genuine and misreconstructed $\not{E}_T$. No significant excess above the Standard Model expectations is observed. Limits are set on sbottom masses in simplified models where the decay $\tilde{b} \to b\tilde{\chi}^0_1$ takes place with a branching ratio of 100%, see Fig. 8 and Table 9.

[31] CHATRCHYAN 13V searched in 10.5 fb^{-1} of pp collisions at $\sqrt{s} = 8$ TeV for events with two isolated same-sign dileptons and at least two b-jets in the final state. No significant excess above the Standard Model expectations is observed. Limits are set on the bottom mass in a simplified models where the decay $\tilde{b} \to t\tilde{\chi}^\pm_1$, $\tilde{\chi}^\pm_1 \to W^\pm\tilde{\chi}^0_1$ takes place with a branching ratio of 100%, with varying mass of the $\tilde{\chi}^\pm_1$, for $m_{\tilde{\chi}^0_1} = 50$ GeV, see Fig. 4.

[32] AAD 12AN searched in 2.05 fb^{-1} of pp collisions at $\sqrt{s} = 7$ TeV for scalar bottom quarks in events with large missing transverse momentum and two b-jets in the final state. The data are found to be consistent with the Standard Model expectations. Limits are set in an R-parity conserving minimal supersymmetric scenario, assuming B($\tilde{b}_1 \to b\tilde{\chi}^0_1$) = 100%, see their Fig. 2.

[33] CHATRCHYAN 12AI looked in 4.98 fb^{-1} of pp collisions at $\sqrt{s} = 7$ TeV for events with two same-sign leptons (e, μ), but not necessarily same flavor, at least 2 b-jets and missing transverse energy. No excess beyond the Standard Model expectation is observed. Exclusion limits are derived in a simplified model for sbottom pair production, where the sbottom decays through $\tilde{b}_1 \to t\tilde{\chi}_1 W$, see Fig. 8.

[34] CHATRCHYAN 12BO searched in 4.7 fb^{-1} of pp collisions at $\sqrt{s} = 7$ TeV for scalar bottom quarks in events with large missing transverse momentum and two b-jets in the final state. The data are found to be consistent with the Standard Model expectations. Limits are set in an R-parity conserving minimal supersymmetric scenario, assuming B($\tilde{b}_1 \to b\tilde{\chi}^0_1$) = 100%, see their Fig. 2.

[35] AAD 11K looked in 34 pb^{-1} of pp collisions at $\sqrt{s} = 7$ TeV for events with heavy stable particles, identified by their anomalous dE/dx in the tracker or time of flight in the tile calorimeter, from pair production of $\tilde{b}$. No evidence for an excess over the SM expectation is observed and limits on the mass are derived for pair production of sbottom, see Fig. 4.

[36] AAD 11O looked in 35 pb^{-1} of pp collisions at $\sqrt{s} = 7$ TeV for events with jets, of which at least one is a b-jet, and $\not{E}_T$. No excess above the Standard Model was found. Limits are derived in the ($m_{\tilde{g}}$, $m_{\tilde{b}_1}$) plane (see Fig. 2) under the assumption of 100% branching ratios and $\tilde{b}_1$ being the lightest squark. The quoted limit is valid for $m_{\tilde{b}_1} <$ 500 GeV. A similar approach for $\tilde{t}_1$ as the lightest squark with $\tilde{g} \to \tilde{t}_1 t$ and $\tilde{t}_1 \to b\tilde{\chi}^\pm_1$ with 100% branching ratios leads to a gluino mass limit of 520 GeV for $130 < m_{\tilde{t}_1} <$ 300 GeV. Limits are also derived in the CMSSM (m_0, $m_{1/2}$) plane for tan$\beta = 40$, see Fig. 4, and in scenarios based on the gauge group SO(10).

[37] CHATRCHYAN 11D looked in 35 pb^{-1} of pp collisions at $\sqrt{s} = 7$ TeV for events with ≥ 2 jets, at least one of which is b-tagged, and $\not{E}_T$, where the b-jets are decay products of $\tilde{t}$ or $\tilde{b}$. No evidence for an excess over the expected background is observed. Limits are derived in the CMSSM (m_0, $m_{1/2}$) plane for tan$\beta = 50$ (see Fig. 2).

[38] AALTONEN 10R searched in 2.65 fb^{-1} of $p\bar{p}$ collisions at $\sqrt{s} = 1.96$ TeV for events with $\not{E}_T$ and exactly two jets, at least one of which is b-tagged. The results are in agreement with the SM prediction, and a limit on the cross section of 0.1 pb is obtained for the range of masses $80 < m_{\tilde{b}_1} < 280$ GeV assuming that the sbottom decays exclusively to $b\tilde{\chi}^0_1$. The excluded mass region in the framework of conserved R_p is shown in a plane of ($m_{\tilde{b}_1}$, $m_{\tilde{\chi}^0_1}$), see their Fig.2.

[39] ABAZOV 10L looked in 5.2 fb^{-1} of $p\overline{p}$ collisions at $\sqrt{s}$ = 1.96 TeV for events with at least 2 b-jets and $\not{E}_T$ from the production of $\tilde{b}_1\tilde{b}_1$. No evidence for an excess over the SM expectation is observed, and a limit on the cross section is derived under the assumption of 100% branching ratio. The excluded mass region in the framework of conserved R_p is shown in a plane of ($m_{\tilde{b}_1}$,$m_{\tilde{\chi}^0_1}$), see their Fig. 3b. The exclusion also extends to $m_{\tilde{\chi}^0_1}$ = 110 GeV for 160< $m_{\tilde{b}_1}$ < 200 GeV.

R-parity violating $\tilde{b}$ (Sbottom) mass limit

VALUE (GeV)	CL%	DOCUMENT ID		TECN	COMMENT
>307	95	[1] KHACHATRY...16BX		CMS	RPV, $\tilde{b} \to t\,d$ or $t\,s$, λ''_{332} or λ''_{331} coupling

• • • We do not use the following data for averages, fits, limits, etc. • • •

[2] AAD	14E	ATLS	$\ell^\pm\ell^\pm(\ell^\mp)$ + jets, $\tilde{b}_1 \to t\tilde{\chi}^\pm_1$ with $\tilde{\chi}^\pm_1 \to W^{(*)\pm}\tilde{\chi}^0_1$ simplified model, $m_{\tilde{\chi}^\pm_1} = 2\, m_{\tilde{\chi}^0_1}$

[1] KHACHATRYAN 16BX searched in 19.5 fb^{-1} of pp collisions at $\sqrt{s}$ = 8 TeV for events containing 2 leptons coming from R-parity-violating decays of supersymmetric particles. No excess over the expected background is observed. Limits are derived on the sbottom mass, assuming the RPV $\tilde{b} \to t\,d$ or $\tilde{b} \to t\,s$ decay, see Fig. 15.

[2] AAD 14E searched in 20.3 fb^{-1} of pp collisions at $\sqrt{s}$ = 8 TeV for strongly produced supersymmetric particles in events containing jets and two same-sign leptons or three leptons. The search also utilises jets originating from b-quarks, missing transverse momentum and other variables. No excess over the expected SM background is observed. Exclusion limits are derived in simplified models containing bottom, see Fig. 7. Limits are also derived in the mSUGRA/CMSSM, bRPV and GMSB models, see their Fig. 8.

$\tilde{t}$ (Stop) mass limit

Limits depend on the decay mode. In e^+e^- collisions they also depend on the mixing angle of the mass eigenstate $\tilde{t}_1 = \tilde{t}_L\cos\theta_t + \tilde{t}_R\sin\theta_t$. The coupling to the Z vanishes when θ_t = 0.98. In the Listings below, we use $\Delta m \equiv m_{\tilde{t}_1} - m_{\tilde{\chi}^0_1}$ or $\Delta m \equiv m_{\tilde{t}_1} - m_{\tilde{\nu}}$, depending on relevant decay mode. See also bounds in "$\tilde{q}$ (Squark) MASS LIMIT."

Some earlier papers are now obsolete and have been omitted. They were last listed in our PDG 14 edition: K. Olive, *et al.* (Particle Data Group), Chinese Physics **C38** 070001 (2014) (http://pdg.lbl.gov).

R-parity conserving $\tilde{t}$ (Stop) mass limit

VALUE (GeV)	CL%	DOCUMENT ID		TECN	COMMENT
> 510	95	[1] SIRUNYAN	18B	CMS	jets+$\not{E}_T$, Tstop4, $m_{\tilde{t}} - m_{\tilde{\chi}^0_1}$ = 10 GeV
> 800	95	[2] SIRUNYAN	18C	CMS	$\ell^\pm\ell^\mp$ + b-jets + $\not{E}_T$, Tstop1, $m_{\tilde{\chi}^0_1}$ = 0
> 750	95	[2] SIRUNYAN	18C	CMS	$\ell^\pm\ell^\mp$ + b-jets + $\not{E}_T$, Tstop2, $m_{\tilde{\chi}^\pm_1} = (m_{\tilde{t}} + m_{\tilde{\chi}^0_1})/2$, $m_{\tilde{\chi}^0_1}$ = 0
>1050	95	[2] SIRUNYAN	18C	CMS	Combination of all-hadronic, 1 $\ell^\pm$ and $\ell^\pm\ell^\mp$ searches, Tstop1, $m_{\tilde{\chi}^0_1}$ = 0
>1000	95	[2] SIRUNYAN	18C	CMS	Combination of all-hadronic, 1 $\ell^\pm$ and $\ell^\pm\ell^\mp$ searches, Tstop2, $m_{\tilde{\chi}^\pm_1} = (m_{\tilde{t}} + m_{\tilde{\chi}^0_1})/2$, $m_{\tilde{\chi}^0_1}$ = 0
>1200	95	[2] SIRUNYAN	18C	CMS	$\ell^\pm\ell^\mp$ + b-jets + $\not{E}_T$, Tstop11, $m_{\tilde{\chi}^\pm_1}$ = 0.5 ($m_{\tilde{t}} + m_{\tilde{\chi}^0_1}$), $m_{\tilde{l}}$ = 0.5 $m_{\tilde{\chi}^\pm_1}$, $m_{\tilde{\chi}^0_1}$ = 0
>1300	95	[2] SIRUNYAN	18C	CMS	$\ell^\pm\ell^\mp$ + b-jets + $\not{E}_T$, Tstop11, $m_{\tilde{\chi}^\pm_1}$ = 0.5 ($m_{\tilde{t}} + m_{\tilde{\chi}^0_1}$), $m_{\tilde{l}}$ = 0.95 $m_{\tilde{\chi}^\pm_1}$, $m_{\tilde{\chi}^0_1}$ = 0
none 460–1060	95	[2] SIRUNYAN	18C	CMS	$\ell^\pm\ell^\mp$ + b-jets + $\not{E}_T$, Tstop11, $m_{\tilde{\chi}^\pm_1}$ = 0.5 ($m_{\tilde{t}} + m_{\tilde{\chi}^0_1}$), $m_{\tilde{l}}$ = 0.05 $m_{\tilde{\chi}^\pm_1}$, $m_{\tilde{\chi}^0_1}$ = 0
>1020	95	[3] SIRUNYAN	18D	CMS	top quark (hadronically decaying) + jets + $\not{E}_T$, Tstop1, $m_{\tilde{\chi}^0_1}$ = 0 GeV
> 700	95	[4] AABOUD	17AJ	ATLS	same-sign $\ell^\pm\ell^\pm$ / 3 ℓ + jets + $\not{E}_T$, Tstop11, $m_{\tilde{\chi}^0_2} = m_{\tilde{\chi}^0_1}$ + 100 GeV
> 880	95	[5] AABOUD	17AX	ATLS	b-jets+$\not{E}_T$, mixture Tstop1 and Tstop2 with BR=50%, $m_{\tilde{\chi}^0_1}$ = 0 GeV, $m_{\tilde{\chi}^\pm_1}$ - $m_{\tilde{\chi}^0_1}$ = 1 GeV
none 250–1000	95	[6] AABOUD	17AY	ATLS	jets+$\not{E}_T$, Tstop1, $m_{\tilde{\chi}^0_1}$ = 0 GeV
none 450–850	95	[7] AABOUD	17AY	ATLS	jets+$\not{E}_T$, mixture of Tstop1 and Tstop2 with BR=50%, $m_{\tilde{\chi}^\pm_1} - m_{\tilde{\chi}^0_1}$ = 1 GeV
> 720	95	[8] AABOUD	17BE	ATLS	$\ell^\pm\ell^\mp$ + $\not{E}_T$, Tstop1, $m_{\tilde{\chi}^0_1}$ = 0 GeV
> 400	95	[9] AABOUD	17BE	ATLS	$\ell^\pm\ell^\mp$ + $\not{E}_T$, Tstop3, $m_{\tilde{t}_1} - m_{\tilde{\chi}^0_1}$ = 40 GeV
> 430	95	[10] AABOUD	17BE	ATLS	$\ell^\pm\ell^\mp$ + $\not{E}_T$, Tstop1 (offshell t), $m_{\tilde{t}_1} - m_{\tilde{\chi}^0_1} \sim m_W$
> 700	95	[11] AABOUD	17BE	ATLS	$\ell^\pm\ell^\mp$ + $\not{E}_T$, Tstop2, $m_{\tilde{t}_1} - m_{\tilde{\chi}^\pm_1}$ = 10 GeV, $m_{\tilde{\chi}^0_1}$ = 0 GeV
> 750	95	[12] KHACHATRY...17		CMS	jets+$\not{E}_T$,Tstop1,$m_{\tilde{\chi}^0_1}$=100GeV
none 250–740	95	[13] KHACHATRY...17AD		CMS	jets+b-jets+$\not{E}_T$, Tstop1, $m_{\tilde{\chi}^0_1}$ = 0 GeV
> 610	95	[14] KHACHATRY...17AD		CMS	jets+b-jets+$\not{E}_T$, mixture Tstop1 and Tstop2 with BR=50%, $m_{\tilde{\chi}^0_1}$ = 60 GeV
> 590	95	[15] KHACHATRY...17P		CMS	1 or more jets+$\not{E}_T$, Tstop8, $m_{\tilde{\chi}^\pm_1} - m_{\tilde{\chi}^0_1}$ = 5 GeV, $m_{\tilde{\chi}^0_1}$ = 100 GeV
none 280–640	95	[15] KHACHATRY...17P		CMS	1 or more jets+$\not{E}_T$, Tstop1, $m_{\tilde{\chi}^0_1}$ = 0 GeV
> 350	95	[15] KHACHATRY...17P		CMS	1 or more jets+$\not{E}_T$, Tstop4, 10 GeV < $m_{\tilde{t}_1} - m_{\tilde{\chi}^0_1}$ < 80 GeV
> 280	95	[15] KHACHATRY...17P		CMS	1 or more jets+$\not{E}_T$, Tstop3, 10 GeV < $m_{\tilde{t}_1} - m_{\tilde{\chi}^0_1}$ < 80 GeV
> 320	95	[15] KHACHATRY...17P		CMS	1 or more jets+$\not{E}_T$, Tstop9, 10 GeV < $m_{\tilde{t}_1} - m_{\tilde{\chi}^0_1}$ < 80 GeV
> 240	95	[16] KHACHATRY...17S		CMS	jets+$\not{E}_T$, Tstop4, $m_{\tilde{t}} - m_{\tilde{\chi}^0_1}$ = 10 GeV
> 225	95	[17] KHACHATRY...17S		CMS	jets+$\not{E}_T$, Tstop3, $m_{\tilde{t}} - m_{\tilde{\chi}^0_1}$ = 10 GeV
> 325	95	[18] KHACHATRY...17S		CMS	jets+$\not{E}_T$, Tstop2, $m_{\tilde{\chi}^\pm_1}$ = 0.25 $m_{\tilde{t}}$ + 0.75 $m_{\tilde{\chi}^0_1}$, $m_{\tilde{\chi}^0_1}$ = 225 GeV
> 400	95	[19] KHACHATRY...17S		CMS	jets+$\not{E}_T$, Tstop2, $m_{\tilde{\chi}^\pm_1}$ = 0.75 $m_{\tilde{t}}$ + 0.25 $m_{\tilde{\chi}^0_1}$, $m_{\tilde{\chi}^0_1}$ = 0 GeV
> 500	95	[20] KHACHATRY...17S		CMS	jets+$\not{E}_T$, Tstop1, $m_{\tilde{\chi}^0_1}$ = 0 GeV
>1120	95	[21] SIRUNYAN	17AS	CMS	1ℓ+jets+$\not{E}_T$, Tstop1, $m_{\tilde{\chi}^0_1}$ = 0 GeV
>1000	95	[21] SIRUNYAN	17AS	CMS	1ℓ+jets+$\not{E}_T$, Tstop2, $m_{\tilde{\chi}^\pm_1} = (m_{\tilde{t}} + m_{\tilde{\chi}^0_1})/2$, $m_{\tilde{\chi}^0_1}$ = 0 GeV
> 980	95	[21] SIRUNYAN	17AS	CMS	1ℓ+jets+$\not{E}_T$, Tstop8, $m_{\tilde{\chi}^\pm_1} - m_{\tilde{\chi}^0_1}$ = 5 GeV, $m_{\tilde{\chi}^0_1}$ = 0 GeV
>1040	95	[22] SIRUNYAN	17AT	CMS	jets+$\not{E}_T$, Tstop1, $m_{\tilde{\chi}^0_1}$ = 0 GeV
> 750	95	[22] SIRUNYAN	17AT	CMS	jets+$\not{E}_T$, Tstop2, $m_{\tilde{\chi}^\pm_1} = (m_{\tilde{t}} + m_{\tilde{\chi}^0_1})/2$, $m_{\tilde{\chi}^0_1}$ = 0 GeV
> 940	95	[22] SIRUNYAN	17AT	CMS	jets+$\not{E}_T$, Tstop8, $m_{\tilde{\chi}^\pm_1} - m_{\tilde{\chi}^0_1}$ = 5 GeV, $m_{\tilde{\chi}^0_1}$ = 100 GeV
> 540	95	[22] SIRUNYAN	17AT	CMS	jets+$\not{E}_T$, Tstop3, 10 GeV < $m_{\tilde{t}_1} - m_{\tilde{\chi}^0_1}$ < 80 GeV
> 480	95	[22] SIRUNYAN	17AT	CMS	jets+$\not{E}_T$, Tstop4, 10 GeV < $m_{\tilde{t}_1} - m_{\tilde{\chi}^0_1}$ < 80 GeV
> 530	95	[22] SIRUNYAN	17AT	CMS	jets+$\not{E}_T$, Tstop10, $m_{\tilde{\chi}^\pm_1} = (m_{\tilde{t}} + m_{\tilde{\chi}^0_1})/2$, 10 GeV < $m_{\tilde{t}_1} - m_{\tilde{\chi}^0_1}$ < 80 GeV
>1070	95	[23] SIRUNYAN	17AZ	CMS	$\geq$ 1 jets+$\not{E}_T$, Tstop1, $m_{\tilde{\chi}^0_1}$ = 0 GeV
> 900	95	[23] SIRUNYAN	17AZ	CMS	$\geq$ 1 jets+$\not{E}_T$, Tstop2, $m_{\tilde{\chi}^\pm_1} = (m_{\tilde{t}} + m_{\tilde{\chi}^0_1})/2$, $m_{\tilde{\chi}^0_1}$ = 0 GeV
>1020	95	[23] SIRUNYAN	17AZ	CMS	$\geq$ 1jets+$\not{E}_T$, Tstop8, $m_{\tilde{\chi}^\pm_1} - m_{\tilde{\chi}^0_1}$ = 5 GeV, $m_{\tilde{\chi}^0_1}$ = 100 GeV
> 540	95	[23] SIRUNYAN	17AZ	CMS	$\geq$ 1 jets+$\not{E}_T$, Tstop4, 10 GeV < $m_{\tilde{t}_1} - m_{\tilde{\chi}^0_1}$ < 80 GeV
none 280–830	95	[24] SIRUNYAN	17K	CMS	0, 1 $\ell^\pm$+jets+$\not{E}_T$ (combination), Tstop1, $m_{\tilde{\chi}^0_1}$ = 0 GeV

> 700	95	[24] SIRUNYAN	17K	CMS	0, 1 $\ell^{\pm}$+jets+$\not{E}_T$ (combination), Tstop8, $m_{\widetilde{\chi}_1^{\pm}} - m_{\widetilde{\chi}_1^0}$ = 5 GeV, $m_{\widetilde{\chi}_1^0} = 100$ GeV
> 160	95	[24] SIRUNYAN	17K	CMS	jets+$\not{E}_T$, Tstop4, $10 < m_{\widetilde{t}} - m_{\widetilde{\chi}_1^0} < 80$ GeV
none 230–960	95	[25] SIRUNYAN	17P	CMS	jets+$\not{E}_T$, Tstop1, $m_{\widetilde{\chi}_1^0} = 0$ GeV
> 990	95	[25] SIRUNYAN	17P	CMS	jets+$\not{E}_T$, Tsbot1, $m_{\widetilde{\chi}_1^0} = 0$ GeV
> 323	95	[26] AABOUD	16D	ATLS	$\geq$ 1 jet + $\not{E}_T$, Tstop4, $m_{\widetilde{t}_1} - m_{\widetilde{\chi}_1^0} = 5$ GeV
none, 745–780	95	[27] AABOUD	16J	ATLS	1 $\ell^{\pm}$ + $\geq$ 4 jets + $\not{E}_T$, Tstop1, $m_{\widetilde{\chi}_1^0} = 0$ GeV
> 490–650	95	[28] AAD	16AY	ATLS	2ℓ (including hadronic τ) + $\not{E}_T$, Tstop5, 87 GeV$< m_{\widetilde{\tau}} < m_{\widetilde{t}_1}$
> 700	95	[29] KHACHATRY...	16AV	CMS	1 or 2 $\ell^{\pm}$+jets+b-jets+$\not{E}_T$, Tstop1, $m_{\widetilde{\chi}_1^0} < 250$ GeV
> 700	95	[29] KHACHATRY...	16AV	CMS	1 or 2 $\ell^{\pm}$+jets+b-jets $\not{E}_T$, Tstop2, $m_{\widetilde{\chi}_1^0} = 0$ GeV, $m_{\widetilde{\chi}_1^{\pm}} = 0.75\ m_{\widetilde{t}_1} + 0.25\ m_{\widetilde{\chi}_1^0}$
> 775	95	[30] KHACHATRY...	16BK	CMS	jets+$\not{E}_T$,Tstop1,$m_{\widetilde{\chi}_1^0} <$200GeV
> 620	95	[30] KHACHATRY...	16BK	CMS	jets+$\not{E}_T$, Tstop2, $m_{\widetilde{\chi}_1^0}$=0 GeV
> 800	95	[31] KHACHATRY...	16BS	CMS	jets+$\not{E}_T$, Tstop1, $m_{\widetilde{\chi}_1^0}$=0 GeV
> 316	95	[32] KHACHATRY...	16Y	CMS	1 or 2 soft $\ell^{\pm}$ + jets + $\not{E}_T$, Tstop3,$m_{\widetilde{t}} - m_{\widetilde{\chi}_1^0}$=25 GeV
> 250	95	[33] AAD	15CJ	ATLS	B($\widetilde{t} \to c\widetilde{\chi}_1^0$)+B($\widetilde{t} \to bff'\widetilde{\chi}_1^0$) = 1, $m_{\widetilde{t}} - m_{\widetilde{\chi}_1^0} = 10$ GeV
> 270	95	[33] AAD	15CJ	ATLS	$\widetilde{t} \to c\widetilde{\chi}_1^0$, $m_{\widetilde{t}} - m_{\widetilde{\chi}_1^0}$=80 GeV
none, 200–700	95	[33] AAD	15CJ	ATLS	$\widetilde{t} \to t\widetilde{\chi}_1^0$, $m_{\widetilde{\chi}_1^0} = 0$
> 500	95	[33] AAD	15CJ	ATLS	B($\widetilde{t} \to t\widetilde{\chi}_1^0$) + B($\widetilde{t} \to b\widetilde{\chi}_1^{\pm}$) = 1, $\widetilde{\chi}_1^{\pm} \to W^{(*)}\widetilde{\chi}_1^0$, $m_{\widetilde{\chi}_1^{\pm}} = 2m_{\widetilde{\chi}_1^0}$, $m_{\widetilde{\chi}_1^0} < 160$ GeV
> 600	95	[33] AAD	15CJ	ATLS	$\widetilde{t}_2 \to Z\widetilde{t}_1$, $m_{\widetilde{t}_1} - m_{\widetilde{\chi}_1^0} = 180$ GeV, $m_{\widetilde{\chi}_1^0} = 0$
> 600	95	[33] AAD	15CJ	ATLS	$\widetilde{t}_2 \to h\widetilde{t}_1$, $m_{\widetilde{t}_1} - m_{\widetilde{\chi}_1^0} = 180$ GeV, $m_{\widetilde{\chi}_1^0} = 0$
none, 172.5–191	95	[34] AAD	15J	ATLS	$\widetilde{t} \to t\widetilde{\chi}_1^0$, $m_{\widetilde{\chi}_1^0} = 1$ GeV
> 450	95	[35] KHACHATRY...	15AF	CMS	$\widetilde{t} \to t\widetilde{\chi}_1^0$, $m_{\widetilde{\chi}_1^0} = 0$, $m_{\widetilde{t}} > m_t + m_{\widetilde{\chi}_1^0}$
> 560	95	[36] KHACHATRY...	15AH	CMS	$\widetilde{t} \to t\widetilde{\chi}_1^0$, $m_{\widetilde{\chi}_1^0} = 0$, $m_{\widetilde{t}} > m_t + m_{\widetilde{\chi}_1^0}$
> 250	95	[37] KHACHATRY...	15AH	CMS	$\widetilde{t} \to c\widetilde{\chi}_1^0$, $m_{\widetilde{t}} - m_{\widetilde{\chi}_1^0} <$10 GeV
none, 200–350	95	[38] KHACHATRY...	15L	CMS	$\widetilde{t} \to qq$, RPV, $\lambda''_{312} \neq 0$
none, 200–385	95	[38] KHACHATRY...	15L	CMS	$\widetilde{t} \to qb$, RPV, $\lambda''_{323} \neq 0$
> 730	95	[39] KHACHATRY...	15X	CMS	$\widetilde{t} \to t\widetilde{\chi}_1^0$, $m_{\widetilde{\chi}_1^0} = 100$ GeV, $m_{\widetilde{t}} > m_t + m_{\widetilde{\chi}_1^0}$
none 400–645	95	[39] KHACHATRY...	15X	CMS	$\widetilde{t} \to t\widetilde{\chi}_1^0$ or $\widetilde{t} \to b\widetilde{\chi}_1^{\pm}$, $m_{\widetilde{\chi}_1^0}$ = 100 GeV, $m_{\widetilde{\chi}_1^{\pm}} - m_{\widetilde{\chi}_1^0}$ = 5 GeV
none 270–645	95	[40] AAD	14AJ	ATLS	$\geq$ 4 jets + $\not{E}_T$, $\widetilde{t}_1 \to t\widetilde{\chi}_1^0$, $m_{\widetilde{\chi}_1^0} < 30$ GeV
none 250–550	95	[40] AAD	14AJ	ATLS	$\geq$4 jets + $\not{E}_T$, B($\widetilde{t}_1 \to b\widetilde{\chi}_1^{\pm}$) = 50 %, $m_{\widetilde{\chi}_1^{\pm}} = 2\ m_{\widetilde{\chi}_1^0}$, $m_{\widetilde{\chi}_1^0} < 60$ GeV
none 210–640	95	[41] AAD	14BD	ATLS	$\ell^{\pm}$ + jets + $\not{E}_T$, $\widetilde{t}_1 \to t\widetilde{\chi}_1^0$, $m_{\widetilde{\chi}_1^0} = 0$ GeV
> 500	95	[41] AAD	14BD	ATLS	$\ell^{\pm}$ + jets + $\not{E}_T$, $\widetilde{t}_1 \to b\widetilde{\chi}_1^{\pm}$, $m_{\widetilde{\chi}_1^{\pm}} = 2\ m_{\widetilde{\chi}_1^0}$, 100 GeV$< m_{\widetilde{\chi}_1^0} <$ 150 GeV
none 150–445	95	[42] AAD	14F	ATLS	$\ell^{\pm}\ell^{\mp}$ final state, $\widetilde{t}_1 \to b\widetilde{\chi}_1^{\pm}$, $m_{\widetilde{t}_1} - m_{\widetilde{\chi}_1^{\pm}} = 10$ GeV, $m_{\widetilde{\chi}_1^0} = 1$ GeV
none 215–530	95	[42] AAD	14F	ATLS	$\ell^{\pm}\ell^{\mp}$ final state, $\widetilde{t}_1 \to t\widetilde{\chi}_1^0$, $m_{\widetilde{\chi}_1^0} = 1$ GeV
> 270	95	[43] AAD	14T	ATLS	$\widetilde{t}_1 \to c\widetilde{\chi}_1^0$, $m_{\widetilde{\chi}_1^0} = 200$ GeV
> 240	95	[43] AAD	14T	ATLS	$\widetilde{t}_1 \to c\widetilde{\chi}_1^0$,$m_{\widetilde{t}_1} - m_{\widetilde{\chi}_1^0} <$85 GeV
> 255	95	[43] AAD	14T	ATLS	$\widetilde{t}_1 \to bff'\widetilde{\chi}_1^0$, $m_{\widetilde{t}_1} - m_{\widetilde{\chi}_1^0} \approx m_b$
> 400	95	[44] CHATRCHYAN	14AH	CMS	jets + $\not{E}_T$, $\widetilde{t} \to t\widetilde{\chi}_1^0$ simplified model, $m_{\widetilde{\chi}_1^0} = 50$ GeV
		[45] CHATRCHYAN	14R	CMS	$\geq 3\ell^{\pm}$, $\widetilde{t} \to (b\widetilde{\chi}_1^{\pm}/t\widetilde{\chi}_1^0)$, $\widetilde{\chi}_1^{\pm} \to (qq'/\ell\nu)\widetilde{\chi}_1^0$, $\widetilde{\chi}_1^0 \to (H/Z)\widetilde{G}$, GMSB, natural higgsino NLSP scenario
> 740	95	[46] KHACHATRY...	14T	CMS	τ + b-jets, RPV, $L\overline{QD}$, $\lambda'_{333} \neq 0$, $\widetilde{t} \to \tau b$ simplified model
> 580	95	[46] KHACHATRY...	14T	CMS	τ + b-jets, RPV, $L\overline{QD}$, $\lambda'_{3jk} \neq 0$ ($j \neq 3$), $\widetilde{t} \to \widetilde{\chi}^{\pm} b$, $\widetilde{\chi}^{\pm} \to qq\tau^{\pm}$ simplified model

• • • We do not use the following data for averages, fits, limits, etc. • • •

> 850	95	[47] AABOUD	17AF	ATLS	2ℓ+jets+b-jets+$\not{E}_T$, Tstop6, $m_{\widetilde{\chi}_1^0} = 0$
> 800	95	[48] AABOUD	17AF	ATLS	2ℓ+jets+b-jets+$\not{E}_T$, Tstop7 with 100% decays via Z, $m_{\widetilde{\chi}_1^0} = 50$ GeV
> 880	95	[49] AABOUD	17AF	ATLS	2ℓ+jets+b-jets+$\not{E}_T$, Tstop7 with 100% decays via higgs, $m_{\widetilde{\chi}_1^0} = 50$ GeV
		[50] AABOUD	17AY	ATLS	jets+$\not{E}_T$, pMSSM-inspired
> 230		ROLBIECKI	15	THEO	WW xsection, $\widetilde{t}_1 \to bW\widetilde{\chi}_1^0$, $m_{\widetilde{t}_1} \simeq m_b + m_W + m_{\widetilde{\chi}_1^0}$
> 600	95	[51] AAD	14B	ATLS	Z+b $\not{E}_T$, $\widetilde{t}_2 \to Z\widetilde{t}_1$, $\widetilde{t}_1 \to t\widetilde{\chi}_1^0$, $m_{\widetilde{\chi}_1^0} < 200$ GeV
> 540	95	[51] AAD	14B	ATLS	Z+b $\not{E}_T$, $\widetilde{t}_1 \to t\widetilde{\chi}_1^0$, $\widetilde{\chi}_1^0 \to Z\widetilde{G}$, natural GMSB, 100 GeV $< m_{\widetilde{\chi}_1^0} < m_{\widetilde{t}_1} -$10 GeV
> 360	95	[52] CHATRCHYAN	14U	CMS	$\widetilde{t}_1 \to b\widetilde{\chi}_1^{\pm}$r, $\widetilde{\chi}_1^{\pm} \to ff'\widetilde{\chi}_1^0$, $\widetilde{\chi}_1^0 \to H\widetilde{G}$ simplified model, $m_{\widetilde{\chi}_1^{\pm}} - m_{\widetilde{\chi}_1^0} = 5$ GeV,GMSB
> 215	95	CZAKON	14		$\widetilde{t} \to t\chi_1^0$, $m_{\chi_1^0} < 10$ GeV
		[53] KHACHATRY...	14C	CMS	$\widetilde{t}_2 \to H\widetilde{t}_1$ or $\widetilde{t}_2 \to Z\widetilde{t}_1$ simplified model

[1] SIRUNYAN 18B searched in 35.9 fb^{-1} of pp collisions at $\sqrt{s} = 13$ TeV for the pair production of third-generation squarks in events with jets and large $\not{E}_T$. No significant excess above the Standard Model expectations is observed. Limits are set on the sbottom mass in the Tsbot1 simplified model, see their Figure 5, and on the stop mass in the Tstop4 simplified model, see their Figure 6.

[2] SIRUNYAN 18C searched in 35.9 fb^{-1} of pp collisions at $\sqrt{s} = 13$ TeV for the pair production of top squarks in events with two oppositely charged leptons (electrons or muons), jets identified as originating from a b-quark and large $\not{E}_T$. No significant excess above the Standard Model expectations is observed. Limits are set on the stop mass in the Tstop1, Tstop2 and Tstop11 simplified models, see their Figures 11 and 12. The Tstop1 and Tstop2 results are combined with complementary searches in the all-hadronic and single lepton channels, see their Figures 13 and 14.

[3] SIRUNYAN 18D searched in 35.9 fb^{-1} of pp collisions at $\sqrt{s} = 13$ TeV for events containing identified hadronically decaying top quarks, no leptons, and $\not{E}_T$. No significant excess above the Standard Model expectations is observed. Limits are set on the stop mass in the Tstop1 simplified model, see their Figure 8, and on the gluino mass in the Tglu3A, Tglu3B, Tglu3C and Tglu3E simplified models, see their Figure 9.

[4] AABOUD 17AJ searched in 36.1 fb^{-1} of pp collisions at $\sqrt{s} = 13$ TeV for events with two same-sign or three leptons, jets and large missing transverse momentum. No significant excess above the Standard Model expectations is observed. Limits up to 700 GeV are set on the top squark mass in Tstop11 simplified models, assuming $m_{\widetilde{\chi}_1^0} = m_{\widetilde{t}} - 275$ GeV and $m_{\widetilde{\chi}_2^0} = m_{\widetilde{\chi}_1^0} + 100$ GeV. See their Figure 4(e).

[5] AABOUD 17AX searched in 36 fb^{-1} of pp collisions at $\sqrt{s} = 13$ TeV for events containing two jets identified as originating from b-quarks and large missing transverse momentum, with or without leptons. No excess of events above the expected level of Standard Model background was found. Exclusion limits at 95% C.L. are set on the masses of top squarks. Assuming 50% BR for Tstop1 and Tstop2 simplified models, a $\widetilde{t}_1$ mass below 880 (860) GeV is excluded for $m_{\widetilde{\chi}_1^0} = 0$ (<250) GeV. See their Fig. 7(b).

[6] AABOUD 17AY searched in 36.1 fb^{-1} of pp collisions at $\sqrt{s} = 13$ TeV for events with at least four jets and large missing transverse momentum. No significant excess above the Standard Model expectations is observed. Limits in the range 250–1000 GeV are set on the top squark mass in Tstop1 simplified models. For the first time, additional constraints are set for the region $m_{\widetilde{t}_1} \sim m_t + m_{\widetilde{\chi}_1^0}$, with exclusion of the $\widetilde{t}_1$ mass range 235–590 GeV. See their Figure 8.

[7] AABOUD 17AY searched in 36.1 fb^{-1} of pp collisions at $\sqrt{s} = 13$ TeV for events with at least four jets and large missing transverse momentum. No significant excess above the Standard Model expectations is observed. Limits in the range 450-850 GeV are set on the top squark mass in a mixture of Tstop1 and Tstop2 simplified models with BR=50% and assuming $m_{\widetilde{\chi}_1^{\pm}} - m_{\widetilde{\chi}_1^0} = 1$ GeV and $m_{\chi_1^0} < 240$ GeV. Constraints are given for various values of the BR. See their Figure 9.

[8] AABOUD 17BE searched in 36.1 fb^{-1} of pp collisions at $\sqrt{s} = 13$ TeV for events with two opposite-charge leptons (electrons and muons) and large missing transverse momentum. No significant excess above the Standard Model expectations is observed. Limits up to 720 GeV are set on the top squark mass in Tstop1 simplified models, assuming massless neutralinos. See their Figure 9 (2-body area).

[9] AABOUD 17BE searched in 36.1 fb^{-1} of pp collisions at $\sqrt{s}$ = 13 TeV for events with two opposite-charge leptons (electrons and muons) and large missing transverse momentum. No significant excess above the Standard Model expectations is observed. Limits up to 400 GeV are set on the top squark mass in Tstop3 simplified models, assuming $m_{\tilde{t}_1} - m_{\tilde{\chi}^0_1}$ = 40 GeV. See their Figure 9 (4-body area).

[10] AABOUD 17BE searched in 36.1 fb^{-1} of pp collisions at $\sqrt{s}$ = 13 TeV for events with two opposite-charge leptons (electrons and muons) and large missing transverse momentum. No significant excess above the Standard Model expectations is observed. Limits up to 430 GeV are set on the top squark mass in Tstop1 simplified models where top quarks are offshell, assuming $m_{\tilde{t}_1} - m_{\tilde{\chi}^0_1}$ close to the W mass. See their Figure 9 (3-body area).

[11] AABOUD 17BE searched in 36.1 fb^{-1} of pp collisions at $\sqrt{s}$ = 13 TeV for events with two opposite-charge leptons (electrons and muons) and large missing transverse momentum. No significant excess above the Standard Model expectations is observed. Limits up to 700 GeV are set on the top squark mass in Tstop2 simplified models, assuming $m_{\tilde{t}_1} - m_{\tilde{\chi}^\pm_1}$ = 10 GeV and massless neutralinos. See their Figure 10.

[12] KHACHATRYAN 17 searched in 2.3 fb^{-1} of pp collisions at $\sqrt{s}$ = 13 TeV for events containing four or more jets, no more than one lepton, and missing transverse momentum, using the razor variables (M_R and R^2) to discriminate between signal and background processes. No evidence for an excess over the expected background is observed. Limits are derived on the stop mass in the Tstop1 simplified model, see Fig. 17.

[13] KHACHATRYAN 17AD searched in 2.3 fb^{-1} of pp collisions at $\sqrt{s}$ = 13 TeV for events containing at least four jets (including b-jets), missing transverse momentum and tagged top quarks. No evidence for an excess over the expected background is observed. Top squark masses in the range 250–740 GeV and neutralino masses up to 240 GeV are excluded at 95% C.L. See Fig. 12.

[14] KHACHATRYAN 17AD searched in 2.3 fb^{-1} of pp collisions at $\sqrt{s}$ = 13 TeV for events containing at least four jets (including b-jets), missing transverse momentum and tagged top quarks. No evidence for an excess over the expected background is observed. Limits are derived on the $\tilde{t}$ mass in simplified models that are a mixture of Tstop1 and Tstop2 with branching fractions 50% for each of the two decay modes: top squark masses of up to 610 GeV and neutralino masses up to 190 GeV are excluded at 95% C.L. The $\tilde{\chi}^\pm_1$ and the $\tilde{\chi}^0_1$ are assumed to be nearly degenerate in mass, with a 5 GeV difference between their masses. See Fig. 12.

[15] KHACHATRYAN 17P searched in 2.3 fb^{-1} of pp collisions at $\sqrt{s}$ = 13 TeV for events with one or more jets and large $\not{E}_T$. No significant excess above the Standard Model expectations is observed. Limits are set on the gluino mass in the Tglu1A, Tglu2A, Tglu3A, Tglu3B, Tglu3C and Tglu3D simplified models, see their Figures 7 and 8. Limits are also set on the squark mass in the Tsqk1 simplified model, see their Fig. 7, and on the sbottom mass in the Tsbot1 simplified model, see Fig. 8. Finally, limits are set on the stop mass in the Tstop1, Tstop3, Tstop4, Tstop6 and Tstop7 simplified models, see Fig. 8.

[16] KHACHATRYAN 17S searched in 18.5 fb^{-1} of pp collisions at $\sqrt{s}$ = 8 TeV for events containing multiple jets and missing transverse momentum, using the α_T variable to discriminate between signal and background processes. No evidence for an excess over the expected background is observed. Limits are derived on the stop mass in the Tstop4 model: for $\Delta m = m_{\tilde{t}} - m_{\tilde{\chi}^0_1}$ equal to 10 and 80 GeV, masses of stop below 240 and 260 GeV are excluded, respectively. See their Fig.3.

[17] KHACHATRYAN 17S searched in 18.5 fb^{-1} of pp collisions at $\sqrt{s}$ = 8 TeV for events containing multiple jets and missing transverse momentum, using the α_T variable to discriminate between signal and background processes. No evidence for an excess over the expected background is observed. Limits are derived on the stop mass in the Tstop3 model: for $\Delta m = m_{\tilde{t}} - m_{\tilde{\chi}^0_1}$ equal to 10 and 80 GeV, masses of stop below 225 and 130 GeV are excluded, respectively. See their Fig.3.

[18] KHACHATRYAN 17S searched in 18.5 fb^{-1} of pp collisions at $\sqrt{s}$ = 8 TeV for events containing multiple jets and missing transverse momentum, using the α_T variable to discriminate between signal and background processes. No evidence for an excess over the expected background is observed. Limits are derived on the stop mass in the Tstop2 model: assuming $m_{\tilde{\chi}^\pm_1} = 0.25\ m_{\tilde{t}} + 0.75\ m_{\tilde{\chi}^0_1}$, masses of stop up to 325 GeV and masses of the neutralino up to 225 GeV are excluded. See their Fig.3.

[19] KHACHATRYAN 17S searched in 18.5 fb^{-1} of pp collisions at $\sqrt{s}$ = 8 TeV for events containing multiple jets and missing transverse momentum, using the α_T variable to discriminate between signal and background processes. No evidence for an excess over the expected background is observed. Limits are derived on the stop mass in the Tstop2 model: assuming $m_{\tilde{\chi}^\pm_1} = 0.75\ m_{\tilde{t}} + 0.25\ m_{\tilde{\chi}^0_1}$, masses of stop up to 400 GeV are excluded for low neutralino masses. See their Fig.3.

[20] KHACHATRYAN 17S searched in 18.5 fb^{-1} of pp collisions at $\sqrt{s}$ = 8 TeV for events containing multiple jets and missing transverse momentum, using the α_T variable to discriminate between signal and background processes. No evidence for an excess over the expected background is observed. Limits are derived on the stop mass in the Tstop1 model: assuming masses of stop up to 500 GeV and masses of the neutralino up to 105 GeV are excluded. See their Fig.3.

[21] SIRUNYAN 17AS searched in 35.9 fb^{-1} of pp collisions at $\sqrt{s}$ = 13 TeV for events with a single lepton (electron or muon), jets, and large $\not{E}_T$. No significant excess above the Standard Model expectations is observed. Limits are set on the stop mass in the Tstop1, Tstop2 and Tstop8 simplified models, see their Figures 5, 6 and 7.

[22] SIRUNYAN 17AT searched in 35.9 fb^{-1} of pp collisions at $\sqrt{s}$ = 13 TeV for direct production of top squarks in events with jets and large $\not{E}_T$. No significant excess above the Standard Model expectations is observed. Limits are set on the stop mass in the Tstop1, Tstop2 , Tstop3, Tstop4, Tstop8 and Tstop10 simplified models, see their Figures 9 to 14.

[23] SIRUNYAN 17AZ searched in 35.9 fb^{-1} of pp collisions at $\sqrt{s}$ = 13 TeV for events with one or more jets and large $\not{E}_T$. No significant excess above the Standard Model expectations is observed. Limits are set on the gluino mass in the Tglu1A, Tglu2A, Tglu3A simplified models, see their Figures 6. Limits are also set on the squark mass in the Tsqk1 simplified model (for single light squark and for 8 degenerate light squarks), on the sbottom mass in the Tsbot1 simplified model and on the stop mass in the Tstop1 simplified model, see their Fig. 7. Finally, limits are set on the stop mass in the Tstop2, Tstop4 and Tstop8 simplified models, see Fig. 8.

[24] SIRUNYAN 17K searched in 2.3 fb^{-1} of pp collisions at $\sqrt{s}$ = 13 TeV for direct production of stop or sbottom pairs in events with multiple jets and significant $\not{E}_T$. A second search also requires an isolated lepton and is combined with the all-hadronic search. No significant excess above the Standard Model expectations is observed. Limits are set on the stop mass in the Tstop1, Tstop8 and Tstop4 simplified models, see their Figures 7, 8 and 9 (for the Tstop4 limits, only the results of the all-hadronic search are used). Limits are also set on the sbottom mass in the Tsbot1 simplified model, see Fig. 10 (also here, only the results of the all-hadronic search are used).

[25] SIRUNYAN 17P searched in 35.9 fb^{-1} of pp collisions at $\sqrt{s}$ = 13 TeV for events with multiple jets and large $\not{E}_T$. No significant excess above the Standard Model expectations is observed. Limits are set on the gluino mass in the Tglu1A, Tglu1C, Tglu2A, Tglu3A and Tglu3D simplified models, see their Fig. 12. Limits are also set on the squark mass in the Tsqk1 simplified model, on the stop mass in the Tstop1 simplified model, and on the sbottom mass in the Tsbot1 simplified model, see Fig. 13.

[26] AABOUD 16D searched in 3.2 fb^{-1} of pp collisions at $\sqrt{s}$ = 13 TeV in events with an energetic jet and large missing transverse momentum. The results are interpreted as 95% C.L. limits on mass of stop decaying into a charm-quark and the lightest neutralino in scenarios with $m_{\tilde{t}_1} - m_{\tilde{\chi}^0_1}$ between 5 and 20 GeV. See their Fig. 5.

[27] AABOUD 16J searched in 3.2 fb^{-1} of pp collisions at $\sqrt{s}$ = 13 TeV in final states with one isolated electron or muon, jets, and missing transverse momentum. For the direct stop pair production model where the stop decays via top and lightest neutralino, the results exclude at 95% C.L. stop masses between 745 GeV and 780 GeV for a massless $\tilde{\chi}^0_1$. See their Fig. 8.

[28] AAD 16AY searched in 20 fb^{-1} of pp collisions at $\sqrt{s}$ = 8 TeV for events with either two hadronically decaying tau leptons, one hadronically decaying tau and one light lepton, or two light leptons. No significant excess over the Standard Model expectation is found. Exclusion limits at 95% C.L. on the mass of top squarks decaying via $\tilde{\tau}$ to a nearly massless gravitino are placed depending on $m_{\tilde{\tau}}$ which is ranging from the 87 GeV LEP limit to $m_{\tilde{t}_1}$. See their Figs. 9 and 10.

[29] KHACHATRYAN 16AV searched in 19.7 fb^{-1} of pp collisions at $\sqrt{s}$ = 8 TeV for events with one or two isolated leptons, hadronic jets, b-jets and $\not{E}_T$. No significant excess above the Standard Model expectations is observed. Limits are set on the stop mass in the Tstop1 and Tstop2 simplified models, see Fig. 11.

[30] KHACHATRYAN 16BK searched in 18.9 fb^{-1} of pp collisions at $\sqrt{s}$ = 8 TeV for events with hadronic jets and $\not{E}_T$. No significant excess above the Standard Model expectations is observed. Limits are set on the stop mass in the Tstop1 and Tstop2 simplified models, see Fig. 16.

[31] KHACHATRYAN 16BS searched in 2.3 fb^{-1} of pp collisions at $\sqrt{s}$ = 13 TeV for events with at least one energetic jet , no isolated leptons, and significant $\not{E}_T$, using the transverse mass variable M_{T2} to discriminate between signal and background processes. No significant excess above the Standard Model expectations is observed. Limits are set on the stop mass in the Tstop1 simplified model, see Fig. 11 and Table 3.

[32] KHACHATRYAN 16Y searched in 19.7 fb^{-1} of pp collisions at $\sqrt{s}$ = 8 TeV for events with one or two soft isolated leptons, hadronic jets, and $\not{E}_T$. No significant excess above the Standard Model expectations is observed. Limits are set on the stop mass in the Tstop3 simplified model, see Fig. 3.

[33] AAD 15CJ searched in 20 fb^{-1} of pp collisions at $\sqrt{s}$ = 8 TeV for evidence of third generation squarks by combining a large number of searches covering various final states. Stop decays with and without charginos in the decay chain are considered and summaries of all ATLAS Run 1 searches for direct stop production can be found in Fig. 4 (no intermediate charginos) and Fig. 7 (intermediate charginos). Limits are set on stop masses in compressed mass regions regions, with $B(\tilde{t} \to c\tilde{\chi}^0_1) + B(\tilde{t} \to bff'\tilde{\chi}^0_1)$ = 1, see Fig. 5. Limits are also set on stop masses assuming that both the decay $\tilde{t} \to t\tilde{\chi}^0_1$ and $\tilde{t} \to b\tilde{\chi}^\pm_1$ are possible, with both their branching rations summing up to 1, assuming $\tilde{\chi}^\pm_1 \to W^{(*)}\tilde{\chi}^0_1$ and $m_{\tilde{\chi}^\pm_1} = 2\ m_{\tilde{\chi}^0_1}$, see Fig. 6. Limits on the mass of the next-to-lightest stop $\tilde{t}_2$, decaying either to $Z\tilde{t}_1$, $h\tilde{t}_1$ or $t\tilde{\chi}^0_1$, are also presented, see Figs. 9 and 10.Interpretations in the pMSSM are also discussed, see Figs 13–15.

[34] AAD 15J interpreted the measurement of spin correlations in $t\bar{t}$ production using 20.3 fb^{-1} of pp collisions at $\sqrt{s}$ = 8 TeV in exclusion limits on the pair production of light $\tilde{t}_1$ squarks with masses similar to the top quark mass. The $\tilde{t}_1$ is assumed to decay through $\tilde{t}_1 \to t\tilde{\chi}^0_1$ with predominantly right-handed top and a 100% branching ratio. The data are found to be consistent with the Standard Model expectations and masses between the top quark mass and 191 GeV are excluded, see their Fig. 2

[35] KHACHATRYAN 15AF searched in 19.5 fb^{-1} of pp collisions at $\sqrt{s}$ = 8 TeV for events with at least two energetic jets and significant $\not{E}_T$, using the transverse mass variable M_{T2} to discriminate between signal and background processes. No significant excess above the Standard Model expectations is observed. Limits are set on the stop mass in simplified models where the decay $\tilde{t} \to t\tilde{\chi}^0_1$ takes place with a branching ratio of 100%, see Fig. 12. See also Table 5. Exclusions in the CMSSM, assuming tanβ = 30, $A_0 = -2$ max(m_0, $m_{1/2}$) and $\mu > 0$, are also presented, see Fig. 15.

[36] KHACHATRYAN 15AH searched in 19.4 or 19.7 fb^{-1} of pp collisions at $\sqrt{s}$ = 8 TeV for events containing either a fully reconstructed top quark, or events containing dijets requiring one or both jets to originate from b-quarks, or events containing a mono-jet. No significant excess above the Standard Model expectations is observed. Limits are set on the stop mass in simplified models where the decay $\tilde{t} \to t\tilde{\chi}^0_1$ takes place with a branching ratio of 100%, see Fig. 9. Limits are also set in simplified models where the decays $\tilde{t} \to t\tilde{\chi}^0_1$ and $\tilde{t} \to b\tilde{\chi}^\pm_1$, with $m_{\tilde{\chi}^\pm_1}$ - $m_{\tilde{\chi}^0_1}$ = 5 GeV, each take place with a branching ratio of 50%, see Fig. 10, or with other fractions, see Fig. 11. Finally, limits are set in a simplified model where the decay $\tilde{t} \to c\tilde{\chi}^0_1$ takes place with a branching ratio of 100%, see Figs. 9, 10 and 11.

[37] KHACHATRYAN 15AH searched in 19.4 or 19.7 fb^{-1} of pp collisions at $\sqrt{s}$ = 8 TeV for events containing either a fully reconstructed top quark, or events containing dijets requiring one or both jets to originate from b-quarks, or events containing a mono-jet. No significant excess above the Standard Model expectations is observed. Limits are set on the stop mass in simplified models where the decay $\tilde{t} \to t\tilde{\chi}^0_1$ takes place with a branching ratio of 100%, see Fig. 9. Limits are also set in simplified models where the decays $\tilde{t} \to t\tilde{\chi}^0_1$ and $\tilde{t} \to b\tilde{\chi}^\pm_1$, with $m_{\tilde{\chi}^\pm_1} - m_{\tilde{\chi}^0_1}$ = 5 GeV, each take place with a branching ratio of 50%, see Fig. 10, or with other fractions, see Fig. 11. Finally, limits

are set in a simplified model where the decay $\tilde{t} \to c\tilde{\chi}_1^0$ takes place with a branching ratio of 100%, see Figs. 9, 10, and 11.

[38] KHACHATRYAN 15L searched in 19.4 fb^{-1} of pp collisions at $\sqrt{s} = 8$ TeV for pair production of heavy resonances decaying to pairs of jets in four jet events. No significant excess above the Standard Model expectations is observed. Limits are set on the stop mass in R-parity-violating supersymmetry models where $\tilde{t} \to qq$ ($\lambda''_{312} \neq 0$), see Fig. 6 (top) and $\tilde{t} \to qb$ ($\lambda''_{323} \neq 0$), see Fig. 6 (bottom).

[39] KHACHATRYAN 15X searched in 19.3 fb^{-1} of pp collisions at $\sqrt{s} = 8$ TeV for events with at least two energetic jets, at least one of which is required to originate from a b quark, possibly a lepton, and significant $\not{E}_T$, using the razor variables (M_R and R^2) to discriminate between signal and background processes. No significant excess above the Standard Model expectations is observed. Limits are set on the stop mass in simplified models where the decay $\tilde{t} \to t\tilde{\chi}_1^0$ and the decay $\tilde{t} \to b\tilde{\chi}_1^{\pm}$, with $m_{\tilde{\chi}_1^{\pm}} - m_{\tilde{\chi}_1^0} = 5$ GeV, take place with branching ratios varying between 0 and 100%, see Figs. 15, 16 and 17.

[40] AAD 14AJ searched in 20.1 fb^{-1} of pp collisions at $\sqrt{s} = 8$ TeV for events containing four or more jets and large missing transverse momentum. No excess of events above the expected level of Standard Model background was found. Exclusion limits at 95% C.L. are set on the masses of third-generation squarks in simplified models which either assume that the decay $\tilde{t}_1 \to t\tilde{\chi}_1^0$ takes place 100% of the time, see Fig. 8, or that this decay takes place 50% of the time, while the decay $\tilde{t}_1 \to b\tilde{\chi}_1^{\pm}$ takes place the other 50% of the time, see Fig. 9.

[41] AAD 14BD searched in 20 fb^{-1} of pp collisions at $\sqrt{s} = 8$ TeV for events containing one isolated lepton, jets and large missing transverse momentum. No excess of events above the expected level of Standard Model background was found. Exclusion limits at 95% C.L. are set on the masses of third-generation squarks in simplified models which either assume that the decay $\tilde{t}_1 \to t\tilde{\chi}_1^0$ takes place 100% of the time, see Fig. 15, or the decay $\tilde{t}_1 \to b\tilde{\chi}_1^{\pm}$ takes place 100% of the time, see Fig. 16–22. For the mixed decay scenario, see Fig. 23.

[42] AAD 14F searched in 20.3 fb^{-1} of pp collisions at $\sqrt{s} = 8$ TeV for events containing two leptons (e or μ), and possibly jets and missing transverse momentum. No excess of events above the expected level of Standard Model background was found. Exclusion limits at 95% C.L. are set on the masses of third-generation squarks in simplified models which either assume that the decay $\tilde{t}_1 \to b\tilde{\chi}_1^{\pm}$ takes place 100% of the time, see Figs. 14–17 and 20, or that the decay $\tilde{t}_1 \to t\tilde{\chi}_1^0$ takes place 100% of the time, see Figs. 18 and 19.

[43] AAD 14T searched in 20.3 fb^{-1} of pp collisions at $\sqrt{s} = 8$ TeV for monojet-like and c-tagged events. No excess of events above the expected level of Standard Model background was found. Exclusion limits at 95% C.L. are set on the masses of third-generation squarks in simplified models which assume that the decay $\tilde{t}_1 \to c\tilde{\chi}_1^0$ takes place 100% of the time, see Fig. 9 and 10. The results of the monojet-like analysis are also interpreted in terms of stop pair production in the four-body decay $\tilde{t}_1 \to bff'\tilde{\chi}_1^0$, see Fig. 11.

[44] CHATRCHYAN 14AH searched in 4.7 fb^{-1} of pp collisions at $\sqrt{s} = 7$ TeV for events with at least two energetic jets and significant $\not{E}_T$, using the razor variables (M_R and R^2) to discriminate between signal and background processes. A second analysis requires at least one of the jets to be originating from a b-quark. No significant excess above the Standard Model expectations is observed. Limits are set on sbottom masses in simplified models where the decay $\tilde{t} \to t\tilde{\chi}_1^0$ takes place with a branching ratio of 100%, see Figs. 28 and 29. Exclusions in the CMSSM, assuming $\tan\beta = 10$, $A_0 = 0$ and $\mu > 0$, are also presented, see Fig. 26.

[45] CHATRCHYAN 14R searched in 19.5 fb^{-1} of pp collisions at $\sqrt{s} = 8$ TeV for events with at least three leptons (electrons, muons, taus) in the final state. No significant excess above the Standard Model expectations is observed. Limits are set on the stop mass in a natural higgsino NLSP simplified model (GMSB) where the decay $\tilde{t} \to b\tilde{\chi}_1^{\pm}$, with $\tilde{\chi}_1^{\pm} \to (qq'/\ell\nu)H$, $Z\tilde{G}$, takes place with a branching ratio of 100% (the particles between brackets have a soft p_T spectrum), see Figs. 4–6.

[46] KHACHATRYAN 14T searched in 19.7 fb^{-1} of pp collisions at $\sqrt{s} = 8$ TeV for events with τ-leptons and b-quark jets, possibly with extra light-flavour jets. No excess above the Standard Model expectations is observed. Limits are set on stop masses in RPV SUSY models with $LQ\overline{D}$ couplings, in two simplified models. In the first model, the decay $\tilde{t} \to \tau b$ is considered, with $\lambda'_{333} \neq 0$, see Fig. 3. In the second model, the decay $\tilde{t} \to \tilde{\chi}^{\pm} b$, with the subsequent decay $\tilde{\chi}^{\pm} \to qq\tau^{\pm}$ is considered, with $\lambda'_{3jk} \neq 0$ and the mass splitting between the top squark and the charging chosen to be 100 GeV, see Fig. 4.

[47] AABOUD 17AF searched in 36 fb^{-1} of pp collisions at $\sqrt{s} = 13$ TeV for evidence of top squarks in events containing 2 leptons, jets, b-jets and $\not{E}_T$. In Tstop6 model, assuming $m_{\tilde{\chi}_1^0} = 0$ GeV, $\tilde{t}_1$ masses up to 850 GeV are excluded for $m_{\tilde{\chi}_2^0} > 200$ GeV.

[48] AABOUD 17AF searched in 36 fb^{-1} of pp collisions at $\sqrt{s} = 13$ TeV for evidence of $\tilde{t}_2$ in events containing 2 leptons, jets, b-jets and $\not{E}_T$. In Tstop7 model, assuming $m_{\tilde{\chi}_1^0} =$ 50 GeV and 100% decays via Z boson, $\tilde{t}_2$ masses up to 800 GeV are excluded. Exclusion limits are also shown as a function of the $\tilde{t}_2$ branching ratios in their Figure 7.

[49] AABOUD 17AF searched in 36 fb^{-1} of pp collisions at $\sqrt{s} = 13$ TeV for evidence of $\tilde{t}_2$ in events containing 2 leptons, jets, b-jets and $\not{E}_T$. In Tstop7 model, assuming $m_{\tilde{\chi}_1^0}$ = 50 GeV and 100% decays via higgs boson, $\tilde{t}_2$ masses up to 880 GeV are excluded. Exclusion limits are also shown as a function of the $\tilde{t}_2$ branching ratios in their Figure 7.

[50] AABOUD 17AY searched in 36.1 fb^{-1} of pp collisions at $\sqrt{s} = 13$ TeV for events with at least four jets and large missing transverse momentum. No significant excess above the Standard Model expectations is observed. Limits are set on the top squark mass assuming three pMSSM-inspired models. The first one, referred to as Higgsino LSP model, assumes $m_{\tilde{\chi}_1^{\pm}} - m_{\tilde{\chi}_1^0} = 5$ GeV and $m_{\tilde{\chi}_2^0} - m_{\tilde{\chi}_1^0} = 10$ GeV, with a mixture of decay modes as in Tstop1, Tstop2 and Tstop6. See their Figure 10. The second and third models are referred to as Wino NLSP and well-tempered pMSSM models, respectively. See their Figure 11 and Figure 12, and text for details on assumptions.

[51] AAD 14B searched in 20.3 fb^{-1} of pp collisions at $\sqrt{s} = 8$ TeV for events containing a Z boson, with or without additional leptons, plus jets originating from b-quarks and significant missing transverse momentum. No excess over the expected SM background is observed. Limits are derived in simplified models featuring $\tilde{t}_2$ production, with $\tilde{t}_2 \to Z\tilde{t}_1$, $\tilde{t}_1 \to t\tilde{\chi}_1^0$ with a 100% branching ratio, see Fig. 4, and in the framework of natural GMSB, see Fig. 6.

[52] CHATRCHYAN 14U searched in 19.7 fb^{-1} of pp collisions at $\sqrt{s} = 8$ TeV for evidence of direct pair production of top squarks, with Higgs bosons in the decay chain. The search is performed using a selection of events containing two Higgs bosons, each decaying to a photon pair, missing transverse energy and possibly b-quark jets. No significant excesses over the expected SM backgrounds are observed. The results are interpreted in the context of a "natural SUSY" simplified model where the decays $\tilde{t}_1 \to b\tilde{\chi}_1^{\pm}$, with $\tilde{\chi}_1^{\pm} \to ff'\tilde{\chi}_1^0$, and $\tilde{\chi}_1^0 \to H\tilde{G}$, all happen with 100% branching ratio, see Fig. 4.

[53] KHACHATRYAN 14C searched in 19.5 fb^{-1} of pp collisions at $\sqrt{s} = 8$ TeV for evidence of direct pair production of top squarks, with Higgs or Z-bosons in the decay chain. The search is performed using a selection of events containing leptons and b-quark jets. No significant excesses over the expected SM backgrounds are observed. The results are interpreted in the context of a simplified model with pair production of a heavier top-squark mass eigenstate $\tilde{t}_2$ decaying to a lighter top-squark eigenstate $\tilde{t}_1$ via either $\tilde{t}_2 \to H\tilde{t}_1$ or $\tilde{t}_2 \to Z\tilde{t}_1$, followed in both cases by $\tilde{t}_1 \to t\tilde{\chi}_1^0$. The interpretation is performed in the region where the mass difference between the $\tilde{t}_1$ and $\tilde{\chi}_1^0$ is approximately equal to the top-quark mass, which is not probed by searches for direct $\tilde{t}_1$ pair production, see Figs. 5 and 6. The analysis excludes top squarks with masses $m_{\tilde{t}_2} < 575$ GeV and $m_{\tilde{t}_1} < 400$ GeV at 95% C.L.

R-parity violating $\tilde{t}$ (Stop) mass limit

VALUE (GeV)	CL%	DOCUMENT ID		TECN	COMMENT
>1200	95	[1] AABOUD	17AI	ATLS	RPV, $\geq 1\ell + \geq 8$ jets, Tstop1 with $\tilde{\chi}_1^0 \to tbs$, λ''_{323} coupling, $m_{\tilde{\chi}_1^0}$=500 GeV
none, 100–315	95	[2] AAD	16AM	ATLS	2 large-radius jets, Tstop1RPV
• • • We do not use the following data for averages, fits, limits, etc. • • •					
> 890	95	[3] KHACHATRY...16AC		CMS	$e^+e^- + \geq 5$ jets; $\tilde{t} \to b\tilde{\chi}_1^{\pm}$; $\tilde{\chi}_1^{\pm} \to \ell^{\pm}jj$, RPV, λ'_{ijk}
>1000	95	[3] KHACHATRY...16AC		CMS	$\mu^+\mu^- + \geq 5$ jets; $\tilde{t} \to b\tilde{\chi}_1^{\pm}$; $\tilde{\chi}_1^{\pm} \to \ell^{\pm}jj$, RPV, λ'_{ijk}
> 950	95	[4] KHACHATRY...16BX		CMS	$\tilde{t} \to t\tilde{\chi}_1^0$, $\tilde{\chi}_1^0 \to \ell\ell\nu$, RPV, λ_{121} or $\lambda_{122} \neq 0$
> 790	95	[5] KHACHATRY...15E		CMS	$\tilde{t}_1 \to b\ell$, RPV, $c\tau = 2$ cm

[1] AABOUD 17AI searched in 36.1 fb^{-1} of pp collisions at $\sqrt{s} = 13$ TeV for events with one or more isolated lepton, at least eight jets, either zero or many b-jets, for evidence of R-parity violating decays of the top squark. No significant excess above the Standard Model expectations is observed. Limits up to 1.25 (1.10) TeV are set on the top squark mass in R-parity-violating supersymmetry models where $\tilde{t}_1$ decays for a bino LSP as: $\tilde{t} \to t\tilde{\chi}_1^0$ and for a higgsino LSP as $\tilde{t} \to t\tilde{\chi}_{1,2}^0/b\tilde{\chi}_1^+$. These is followed by the decays through the non-zero λ''_{323} coupling $\tilde{\chi}_{1,2}^0 \to tbs$, $\tilde{\chi}_1^{\pm} \to bbs$. See their Figure 10 and text for details on model assumptions.

[2] AAD 16AM searched in 17.4 fb^{-1} of pp collisions at $\sqrt{s} = 8$ TeV for events containing two large-radius hadronic jets. No deviation from the background prediction is observed. Top squarks with masses between 100 and 315 GeV are excluded at 95% C.L. in the hypothesis that they both decay via R-parity violating coupling λ''_{323} to b- and s-quarks. See their Fig. 10.

[3] KHACHATRYAN 16AC searched in 19.7 fb^{-1} of pp collisions at $\sqrt{s} = 8$ TeV for events with low missing transverse momentum, two oppositely charged electrons or muons, and at least five jets, at least one of which is a b-jet, for evidence of R-parity violating, charging-mediated decays of the top squark. No significant excess above the Standard Model expectations is observed. Limits are set on the stop mass in R-parity-violating supersymmetry models where $\tilde{t} \to b\tilde{\chi}_1^{\pm}$ with $\tilde{\chi}_1^{\pm} \to \ell^{\pm}jj$, $\lambda'_{ijk} \neq 0$ ($i,j,k \leq 2$), and with $m_{\tilde{t}} - m_{\tilde{\chi}_1^{\pm}} = 100$ GeV, see Fig. 3.

[4] KHACHATRYAN 16BX searched in 19.5 fb^{-1} of pp collisions at $\sqrt{s} = 8$ TeV for events containing 4 leptons coming from R-parity-violating decays of $\tilde{\chi}_1^0 \to \ell\ell\nu$ with $\lambda_{121} \neq 0$ or $\lambda_{122} \neq 0$. No excess over the expected background is observed. Limits are derived on the gluino, squark and stop masses, see Fig. 23.

[5] KHACHATRYAN 15E searched for long-lived particles decaying to leptons in 19.7 fb^{-1} of pp collisions at $\sqrt{s} = 8$ TeV. Events were selected with an electron and muon with opposite charges and each with transverse impact parameter values between 0.02 and 2 cm. Limits are set on SUSY benchmark models with pair production of top squarks decaying into an $e\mu$ final state via RPV interactions. See their Fig. 2

Heavy $\tilde{g}$ (Gluino) mass limit

For $m_{\tilde{g}} > 60$–70 GeV, it is expected that gluinos would undergo a cascade decay via a number of neutralinos and/or charginos rather than undergo a direct decay to photinos as assumed by some papers. Limits obtained when direct decay is assumed are usually higher than limits when cascade decays are included.

Some earlier papers are now obsolete and have been omitted. They were last listed in our PDG 14 edition: K. Olive, *et al.* (Particle Data Group), Chinese Physics **C38** 070001 (2014) (http://pdg.lbl.gov).

VALUE (GeV)	CL%	DOCUMENT ID		TECN	COMMENT
>2040	95	[1] SIRUNYAN	18D	CMS	top quark (hadronically decaying) + jets + $\not{E}_T$, Tglu3A, $m_{\tilde{\chi}_1^0}$ = 0 GeV
>1930	95	[1] SIRUNYAN	18D	CMS	top quark (hadronically decaying) + jets + $\not{E}_T$, Tglu3B, $m_{\tilde{t}_1} - m_{\tilde{\chi}_1^0} = 175$ GeV, $m_{\tilde{\chi}_1^0}$ = 200 GeV

>1690	95	[1] SIRUNYAN	18D	CMS	top quark (hadronically decaying) + jets + $\not{E}_T$, Tglu3C, $m_{\widetilde{t}_1} - m_{\widetilde{\chi}^0_1} = 20$ GeV, $m_{\widetilde{\chi}^0_1} = 0$ GeV
>1990	95	[1] SIRUNYAN	18D	CMS	top quark (hadronically decaying) + jets + $\not{E}_T$, Tglu3E, $m_{\widetilde{\chi}^\pm_1} = m_{\widetilde{\chi}^0_1} + 5$ GeV, $m_{\widetilde{\chi}^0_1} = 100$ GeV
>2100	95	[2] AABOUD	17AI	ATLS	RPV, $\geq 1\ell + \geq 8$ jets, Tglu3A and $\widetilde{\chi}^0_1 \to uds$, λ''_{112} coupling, $m_{\widetilde{\chi}^0_1}$=1000 GeV
>1650	95	[3] AABOUD	17AI	ATLS	RPV, $\geq 1\ell + \geq 8$ jets, $\widetilde{g} \to t\widetilde{t}$, $\widetilde{t} \to bs$, λ''_{323} coupling, $m_{\widetilde{t}}$=1000 GeV
>1800	95	[4] AABOUD	17AI	ATLS	RPV, $\geq 1\ell + \geq 8$ jets, Tglu1A and $\widetilde{\chi}^0_1 \to qql$, λ' coupling, $m_{\widetilde{\chi}^0_1}$=1000 GeV
>1750	95	[5] AABOUD	17AJ	ATLS	same-sign $\ell^\pm\ell^\pm$ / 3 ℓ + jets + $\not{E}_T$, Tglu3A, $m_{\widetilde{\chi}^0_1} = 100$ GeV
>1570	95	[6] AABOUD	17AJ	ATLS	same-sign $\ell^\pm\ell^\pm$ / 3 ℓ + jets + $\not{E}_T$, Tglu1E, $m_{\widetilde{\chi}^0_1} = 100$ GeV
>1860	95	[7] AABOUD	17AJ	ATLS	same-sign $\ell^\pm\ell^\pm$ / 3 ℓ + jets + $\not{E}_T$, Tglu1G, $m_{\widetilde{\chi}^0_1} = 200$ GeV
>1800	95	[8] AABOUD	17AJ	ATLS	RPV, same-sign $\ell^\pm\ell^\pm$ / 3 ℓ + jets + $\not{E}_T$, Tglu3A, λ''_{112} coupling, $m_{\widetilde{\chi}^0_1} = 50$ GeV
>1750	95	[9] AABOUD	17AJ	ATLS	RPV, same-sign $\ell^\pm\ell^\pm$ / 3 ℓ + jets + $\not{E}_T$, Tglu1A and $\widetilde{\chi}^0_1 \to qq\ell$, λ' coupling
>1450	95	[10] AABOUD	17AJ	ATLS	RPV, same-sign $\ell^\pm\ell^\pm$ / 3 ℓ + jets + $\not{E}_T$, $\widetilde{g} \to t\widetilde{t}_1$ and $\widetilde{t}_1 \to sd$, λ''_{321} coupling
>1450	95	[11] AABOUD	17AJ	ATLS	RPV, same-sign $\ell^\pm\ell^\pm$ / 3 ℓ + jets + $\not{E}_T$, $\widetilde{g} \to t\widetilde{t}_1$ and $\widetilde{t}_1 \to bd$, λ''_{313} coupling
> 400	95	[12] AABOUD	17AJ	ATLS	RPV, same-sign $\ell^\pm\ell^\pm$ / 3 ℓ + jets + $\not{E}_T$, $\widetilde{d}_R \to tb(ts)$, λ''_{313} (λ''_{321}) coupling
>2100	95	[13] AABOUD	17AR	ATLS	1ℓ+jets+$\not{E}_T$, Tglu1B, $m_{\widetilde{\chi}^0_1} = 0$ GeV
>1740	95	[14] AABOUD	17AR	ATLS	1ℓ+jets+$\not{E}_T$, Tglu1E, $m_{\widetilde{\chi}^0_1} = 0$ GeV
>1800	95	[15] AABOUD	17AY	ATLS	jets+$\not{E}_T$, Tglu3A, $m_{\widetilde{t}_1} - m_{\widetilde{\chi}^0_1} = 5$ GeV
>1800	95	[16] AABOUD	17AZ	ATLS	$\geq$ 7 jets+$\not{E}_T$, large R-jets and/or b-jets, Tglu1E, $m_{\widetilde{\chi}^0_1} = 100$ GeV
>1540	95	[17] AABOUD	17AZ	ATLS	$\geq$ 7 jets+$\not{E}_T$, large R-jets and/or b-jets, Tglu3A, $m_{\widetilde{\chi}^0_1} = 0$ GeV
none 625–1375	95	[18] AABOUD	17AZ	ATLS	RPV, $\geq$ 7 jets+$\not{E}_T$, large R-jets and/or b-jets, $\widetilde{g} \to t\widetilde{t}_1$ and $\widetilde{t}_1 \to bs$, λ''_{323} coupling
>1340	95	[19] AABOUD	17N	ATLS	2 same-flavor, opposite-sign ℓ + jets + $\not{E}_T$, Tglu1H, $m_{\widetilde{\chi}^0_1} = 0$ GeV
>1310	95	[20] AABOUD	17N	ATLS	2 same-flavor, opposite-sign ℓ + jets + $\not{E}_T$, Tglu1H, $m_{\widetilde{\chi}^0_2} = (m_{\widetilde{g}}+m_{\widetilde{\chi}^0_1})/2$, $m_{\widetilde{\chi}^0_1} < 400$ GeV
>1700	95	[21] AABOUD	17N	ATLS	2 same-flavor, opposite-sign ℓ + jets + $\not{E}_T$, Tglu1G, $m_{\widetilde{\chi}^0_1} \sim 1$ GeV
>1400	95	[22] KHACHATRY...17		CMS	jets+$\not{E}_T$,Tglu1A,$m_{\widetilde{\chi}^0_1}$=200GeV
>1650	95	[22] KHACHATRY...17		CMS	jets+$\not{E}_T$,Tglu2A,$m_{\widetilde{\chi}^0_1}$=200 GeV
>1600	95	[22] KHACHATRY...17		CMS	jets+$\not{E}_T$,Tglu3A,$m_{\widetilde{\chi}^0_1}$=200GeV
>1550	95	[23] KHACHATRY...17AD		CMS	jets+b-jets+$\not{E}_T$, Tglu3A, $m_{\widetilde{\chi}^0_1} = 0$ GeV
>1450	95	[24] KHACHATRY...17AD		CMS	jets+b-jets+$\not{E}_T$, Tglu3C, 200 < $m_{\widetilde{\chi}^0_1}$ < 400 GeV
>1570	95	[25] KHACHATRY...17AS		CMS	1ℓ, Tglu3A, $m_{\widetilde{\chi}^0_1} < 600$ GeV
>1500	95	[25] KHACHATRY...17AS		CMS	1ℓ, Tglu3A, $m_{\widetilde{\chi}^0_1} < 775$ GeV
>1400	95	[25] KHACHATRY...17AS		CMS	1ℓ, Tglu1B, $m_{\widetilde{\chi}^\pm_1} = (m_{\widetilde{g}} + m_{\widetilde{\chi}^0_1})/2$, $m_{\widetilde{\chi}^0_1} < 725$ GeV
none 1050–1350	95	[25] KHACHATRY...17AS		CMS	1ℓ, Tglu1B, $m_{\widetilde{\chi}^\pm_1} = (m_{\widetilde{g}} + m_{\widetilde{\chi}^0_1})/2$, $m_{\widetilde{\chi}^0_1} < 850$ GeV
>1175	95	[26] KHACHATRY...17AW		CMS	$\geq 3\ell^\pm$, 2 jets, Tglu3A, $m_{\widetilde{\chi}^0_1} = 0$ GeV
> 825	95	[26] KHACHATRY...17AW		CMS	$\geq 3\ell^\pm$, 2 jets, Tglu1C, $m_{\widetilde{\chi}^\pm_1} = (m_{\widetilde{g}} + m_{\widetilde{\chi}^0_1})/2$, $m_{\widetilde{\chi}^0_1} = 0$ GeV
>1350	95	[27] KHACHATRY...17P		CMS	1 or more jets+$\not{E}_T$, Tglu1A, $m_{\widetilde{\chi}^0_1} = 0$ GeV
>1545	95	[27] KHACHATRY...17P		CMS	1 or more jets+$\not{E}_T$, Tglu2A, $m_{\widetilde{\chi}^0_1} = 0$ GeV
>1120	95	[27] KHACHATRY...17P		CMS	1 or more jets+$\not{E}_T$, Tglu3A, $m_{\widetilde{\chi}^0_1} = 0$ GeV
>1300	95	[27] KHACHATRY...17P		CMS	1 or more jets+$\not{E}_T$, Tglu3D, $m_{\widetilde{\chi}^\pm_1} = m_{\widetilde{\chi}^0_1} + 5$ GeV, $m_{\widetilde{\chi}^0_1} = 100$ GeV
> 780	95	[27] KHACHATRY...17P		CMS	1 or more jets+$\not{E}_T$, Tglu3B, $m_{\widetilde{t}_1} - m_{\widetilde{\chi}^0_1} = 175$ GeV, $m_{\widetilde{\chi}^0_1} = 50$ GeV
> 790	95	[27] KHACHATRY...17P		CMS	1 or more jets+$\not{E}_T$, Tglu3C, $m_{\widetilde{t}_1} - m_{\widetilde{\chi}^0_1} = 20$ GeV, $m_{\widetilde{\chi}^0_1} = 0$ GeV
>1650	95	[28] KHACHATRY...17V		CMS	2 $\gamma + \not{E}_T$, GGM, Tglu4B, any NLSP mass
none 600–650	95	[29] KHACHATRY...17Y		CMS	$\widetilde{g} \to qqqq$, RPV, λ''_{212} coupling, $m_{\widetilde{q}} = 100$ GeV
none 600–1030	95	[29] KHACHATRY...17Y		CMS	$\widetilde{g} \to qqqq$, RPV, λ''_{212} coupling, $m_{\widetilde{q}} = 900$ GeV
none 600–650	95	[29] KHACHATRY...17Y		CMS	$\widetilde{g} \to qqqb$, RPV, λ''_{213} coupling, $m_{\widetilde{q}} = 100$ GeV
none 600–1080	95	[29] KHACHATRY...17Y		CMS	$\widetilde{g} \to qqqb$, RPV, λ''_{213} coupling, $m_{\widetilde{q}} = 900$ GeV
none 600–680	95	[29] KHACHATRY...17Y		CMS	$\widetilde{g} \to qqbb$, RPV, λ''_{212} coupling, $m_{\widetilde{q}} = 100$ GeV
none 600–1080	95	[29] KHACHATRY...17Y		CMS	$\widetilde{g} \to qqbb$, RPV, λ''_{212} coupling, $m_{\widetilde{q}} = 900$ GeV
none 600–650	95	[29] KHACHATRY...17Y		CMS	$\widetilde{g} \to qbbb$, RPV, λ''_{213} coupling, $m_{\widetilde{q}} = 100$ GeV
none 600–1100	95	[29] KHACHATRY...17Y		CMS	$\widetilde{g} \to qbbb$, RPV, λ''_{213} coupling, $m_{\widetilde{q}} = 900$ GeV
>1900	95	[30] SIRUNYAN	17AF	CMS	1ℓ+jets+b-jets+$\not{E}_T$, Tglu3A, $m_{\widetilde{\chi}^0_1} = 0$ GeV
>1600	95	[30] SIRUNYAN	17AF	CMS	1ℓ+jets+b-jets+$\not{E}_T$, Tglu3B, $m_{\widetilde{t}_1} - m_{\widetilde{\chi}^0_1} = 175$ GeV, $m_{\widetilde{\chi}^0_1} = 50$ GeV
>1800	95	[31] SIRUNYAN	17AY	CMS	γ + jets+$\not{E}_T$, Tglu4B, $m_{\widetilde{\chi}^0_1} = 0$ GeV
>1600	95	[31] SIRUNYAN	17AY	CMS	γ + jets+$\not{E}_T$, Tglu4A, $m_{\widetilde{\chi}^0_1} = 0$ GeV
>1860	95	[32] SIRUNYAN	17AZ	CMS	$\geq$ 1 jets + $\not{E}_T$, Tglu1A, $m_{\widetilde{\chi}^0_1} = 0$ GeV
>2025	95	[32] SIRUNYAN	17AZ	CMS	$\geq$ 1 jets+$\not{E}_T$, Tglu2A, $m_{\widetilde{\chi}^0_1} = 0$ GeV
>1900	95	[32] SIRUNYAN	17AZ	CMS	$\geq$ 1 jets+$\not{E}_T$, Tglu3A, $m_{\widetilde{\chi}^0_1} = 0$ GeV
>1825	95	[33] SIRUNYAN	17P	CMS	jets+$\not{E}_T$, Tglu1A, $m_{\widetilde{\chi}^0_1} = 0$ GeV
>1950	95	[33] SIRUNYAN	17P	CMS	jets+$\not{E}_T$, Tglu2A, $m_{\widetilde{\chi}^0_1} = 0$ GeV
>1960	95	[33] SIRUNYAN	17P	CMS	jets+$\not{E}_T$, Tglu3A, $m_{\widetilde{\chi}^0_1} = 0$ GeV
>1800	95	[33] SIRUNYAN	17P	CMS	jets+$\not{E}_T$, Tglu1C, $m_{\widetilde{\chi}^\pm_1} = m_{\widetilde{\chi}^0_2} = (m_{\widetilde{g}}+m_{\widetilde{\chi}^0_1})/2$, $m_{\widetilde{\chi}^0_1} = 0$ GeV
>1870	95	[33] SIRUNYAN	17P	CMS	jets+$\not{E}_T$, Tglu3D, $m_{\widetilde{\chi}^\pm_1} = m_{\widetilde{\chi}^0_1} + 5$ GeV, $m_{\widetilde{\chi}^0_1} = 1000$ GeV
>1520	95	[34] SIRUNYAN	17S	CMS	same-sign $\ell^\pm\ell^\pm$ + jets + $\not{E}_T$, Tglu3A, $m_{\widetilde{\chi}^0_1} = 0$ GeV
>1200	95	[34] SIRUNYAN	17S	CMS	same-sign $\ell^\pm\ell^\pm$ + jets + $\not{E}_T$, Tglu3D, $m_{\widetilde{\chi}^\pm_1} = m_{\widetilde{\chi}^0_1} + 5$ GeV, $m_{\widetilde{\chi}^0_1} = 100$ GeV
>1370	95	[34] SIRUNYAN	17S	CMS	same-sign $\ell^\pm\ell^\pm$ + jets + $\not{E}_T$, Tglu3B, $m_{\widetilde{t}_1} - m_{\widetilde{\chi}^0_1} = 175$ GeV, $m_{\widetilde{\chi}^0_1} = 50$ GeV
>1180	95	[34] SIRUNYAN	17S	CMS	same-sign $\ell^\pm\ell^\pm$ + jets + $\not{E}_T$, Tglu3C, $m_{\widetilde{t}_1} - m_{\widetilde{\chi}^0_1} = 20$ GeV, $m_{\widetilde{\chi}^0_1} = 0$ GeV
>1280	95	[34] SIRUNYAN	17S	CMS	same-sign $\ell^\pm\ell^\pm$ + jets + $\not{E}_T$, Tglu1B, $m_{\widetilde{\chi}^\pm_1} = (m_{\widetilde{g}} + m_{\widetilde{\chi}^0_1})/2$, $m_{\widetilde{\chi}^0_1} = 0$ GeV

>1300	95	[34] SIRUNYAN	17S	CMS	same-sign $\ell^\pm\ell^\pm$ + jets + $\not{E}_T$, Tglu1B, $m_{\widetilde{t}_1}-m_{\widetilde{\chi}^0_1}$ = 20 GeV, $m_{\widetilde{\chi}^0_1}$ = 100 GeV	
>1570	95	[35] AABOUD	16AC	ATLS	$\geq$ 2 jets + 1 or 2 τ + $\not{E}_T$, Tglu1F, $m_{\widetilde{\chi}^0_1}$ = 100 GeV	
>1460	95	[36] AABOUD	16J	ATLS	1 $\ell^\pm$ + $\geq$ 4 jets + $\not{E}_T$, Tglu3C, $m_{\widetilde{t}_1}-m_{\widetilde{\chi}^0_1}$ = 5 GeV	
>1650	95	[37] AABOUD	16M	ATLS	2 γ + $\not{E}_T$, Tglu1D, any NLSP mass	
>1510	95	[38] AABOUD	16N	ATLS	$\geq$ 4 jets + $\not{E}_T$, Tglu1A, $m_{\widetilde{\chi}^0_1}$ = 0 GeV	
>1500	95	[39] AABOUD	16N	ATLS	$\geq$ 4 jets + $\not{E}_T$, Tglu1B, $m_{\widetilde{\chi}^\pm_1}$ = $(m_{\widetilde{g}}+m_{\widetilde{\chi}^0_1})/2$, $m_{\widetilde{\chi}^0_1}$=200GeV	
>1780	95	[40] AAD	16AD	ATLS	0ℓ, $\geq$ 3 b-jets + $\not{E}_T$, Tglu2A, $m_{\widetilde{\chi}^0_1}$ < 800 GeV	
>1760	95	[41] AAD	16AD	ATLS	1ℓ, $\geq$ 3 b-jets + $\not{E}_T$, Tglu3A, $m_{\widetilde{\chi}^0_1}$ < 700 GeV	
>1300	95	[42] AAD	16BB	ATLS	2 same-sign/3ℓ + jets + $\not{E}_T$, Tglu1D, $m_{\widetilde{\chi}^0_1}$ < 600 GeV	
>1100	95	[42] AAD	16BB	ATLS	2 same-sign/3ℓ + jets + $\not{E}_T$, Tglu1E, $m_{\widetilde{\chi}^0_1}$ < 300 GeV	
>1200	95	[42] AAD	16BB	ATLS	2 same-sign /3ℓ + jets + $\not{E}_T$, Tglu3A, $m_{\widetilde{\chi}^0_1}$ < 600 GeV	
>1600		[43] AAD	16BG	ATLS	1ℓ, $\geq$ 4 jets, $\not{E}_T$, Tglu1B, $m_{\widetilde{\chi}^\pm_1}$= $(m_{\widetilde{g}}+m_{\widetilde{\chi}^0_1})/2$, $m_{\widetilde{\chi}^0_1}$= 100 GeV	
>1400	95	[44] AAD	16V	ATLS	$\geq$ 7 to $\geq$ 10 jets + $\not{E}_T$, Tglu1E, $m_{\widetilde{\chi}^0_1}$ < 200 GeV	
>1400	95	[44] AAD	16V	ATLS	$\geq$ 7 to $\geq$ 10 jets + $\not{E}_T$, pMSSM M_1 = 60 GeV, M_2 = 3 TeV, tanβ=10, μ < 0	
>1100	95	[45] KHACHATRY...16AM		CMS	boosted W+b, Tglu3C, $m_{\widetilde{t}_1}-m_{\widetilde{\chi}^0_1}$ <80GeV,$m_{\widetilde{\chi}^0_1}$ <400GeV	
> 700	95	[45] KHACHATRY...16AM		CMS	boosted W+b, Tglu3B, $m_{\widetilde{t}_1}-m_{\widetilde{\chi}^0_1}$=175 GeV, $m_{\widetilde{\chi}^0_1}$=0 GeV	
>1050	95	[46] KHACHATRY...16BJ		CMS	same-sign $\ell^\pm\ell^\pm$, Tglu3A, $m_{\widetilde{\chi}^0_1}$ < 800 GeV	
>1300	95	[46] KHACHATRY...16BJ		CMS	same-sign $\ell^\pm\ell^\pm$,Tglu3A,$m_{\widetilde{\chi}^0_1}$=0	
>1140	95	[46] KHACHATRY...16BJ		CMS	same-sign $\ell^\pm\ell^\pm$, Tglu3B, $m_{\widetilde{t}}-m_{\widetilde{\chi}^0_1}$ = 20 GeV, $m_{\widetilde{\chi}^0_1}$ = 0	
> 850	95	[46] KHACHATRY...16BJ		CMS	same-sign $\ell^\pm\ell^\pm$, Tglu3B, $m_{\widetilde{t}}-m_{\widetilde{\chi}^0_1}$=20 GeV,$m_{\widetilde{\chi}^0_1}$ <700 GeV	
> 950	95	[46] KHACHATRY...16BJ		CMS	same-sign $\ell^\pm\ell^\pm$, Tglu3D, $m_{\widetilde{\chi}^\pm_1}$ = $m_{\widetilde{\chi}^0_1}$ + 5 GeV	
>1100	95	[46] KHACHATRY...16BJ		CMS	same-sign $\ell^\pm\ell^\pm$,Tglu1B,$m_{\widetilde{\chi}^\pm_1}$= 0.5($m_{\widetilde{g}}$+$m_{\widetilde{\chi}^0_1}$),$m_{\widetilde{\chi}^0_1}$ <400GeV	
> 830	95	[46] KHACHATRY...16BJ		CMS	same-sign $\ell^\pm\ell^\pm$,Tglu1B,$m_{\widetilde{\chi}^\pm_1}$= 0.5($m_{\widetilde{g}}$+$m_{\widetilde{\chi}^0_1}$),$m_{\widetilde{\chi}^0_1}$ <700GeV	
>1300	95	[46] KHACHATRY...16BJ		CMS	same-sign $\ell^\pm\ell^\pm$, Tglu3B, $m_{\widetilde{t}}-m_{\widetilde{\chi}^0_1}=m_t$, $m_{\widetilde{\chi}^0_1}$ = 0	
>1050	95	[46] KHACHATRY...16BJ		CMS	same-sign $\ell^\pm\ell^\pm$, Tglu3B, $m_{\widetilde{t}}-m_{\widetilde{\chi}^0_1}=m_t$, $m_{\widetilde{\chi}^0_1}$ < 800 GeV	
>1725	95	[47] KHACHATRY...16BS		CMS	jets + $\not{E}_T$, Tglu1A, $m_{\widetilde{\chi}^0_1}$ = 0	
>1750	95	[47] KHACHATRY...16BS		CMS	jets + $\not{E}_T$, Tglu2A, $m_{\widetilde{\chi}^0_1}$ = 0	
>1550	95	[47] KHACHATRY...16BS		CMS	jets + $\not{E}_T$, Tglu3A, $m_{\widetilde{\chi}^0_1}$ = 0	
>1030	95	[48] KHACHATRY...16BX		CMS	$\widetilde{g}\rightarrow tbs$, RPV, λ''_{332} coupling	
>1280	95	[49] KHACHATRY...16BY		CMS	opposite-sign $\ell^\pm\ell^\pm$, Tglu4C, $m_{\widetilde{\chi}^0_1}$ = 1000 GeV	
>1030	95	[49] KHACHATRY...16BY		CMS	opposite-sign $\ell^\pm\ell^\pm$, Tglu4C, $m_{\widetilde{\chi}^0_1}$ = 0 GeV	
>1440	95	[50] KHACHATRY...16V		CMS	jets + $\not{E}_T$, Tglu1A, $m_{\widetilde{\chi}^0_1}$ = 0	
>1600	95	[50] KHACHATRY...16V		CMS	jets + $\not{E}_T$, Tglu2A, $m_{\widetilde{\chi}^0_1}$ = 0	
>1550	95	[50] KHACHATRY...16V		CMS	jets + $\not{E}_T$, Tglu3A, $m_{\widetilde{\chi}^0_1}$ = 0	
>1450	95	[50] KHACHATRY...16V		CMS	jets + $\not{E}_T$, Tglu1C, $m_{\widetilde{\chi}^0_1}$ = 0	
> 820	95	[51] AAD	15BG	ATLS	GGM, $\widetilde{g}\rightarrow q\bar{q}Z\widetilde{G}$, tan$\beta$ = 30, μ > 600 GeV	
> 850	95	[51] AAD	15BG	ATLS	GGM, $\widetilde{g}\rightarrow q\bar{q}Z\widetilde{G}$, tan$\beta$ = 1.5, μ > 450 GeV	
>1150	95	[52] AAD	15BV	ATLS	general RPC $\widetilde{g}$ decays, $m_{\widetilde{\chi}^0_1}$ < 100 GeV	
> 700	95	[53] AAD	15BX	ATLS	$\widetilde{g}\rightarrow X\widetilde{\chi}^0_1$, independent of $m_{\widetilde{\chi}^0_1}$	
>1290	95	[54] AAD	15CA	ATLS	$\geq$ 2 γ + $\not{E}_T$, GGM, bino-like NLSP, any NLSP mass	
>1260	95	[54] AAD	15CA	ATLS	$\geq$ 1 γ + b-jets + $\not{E}_T$, GGM, higgsino-bino admix. NLSP and μ <0, m(NLSP)>450 GeV	
>1140	95	[54] AAD	15CA	ATLS	$\geq$ 1 γ + jets + $\not{E}_T$, GGM, higgsino-bino admixture NLSP, all μ >0	
>1225	95	[55] KHACHATRY...15AF		CMS	$\widetilde{g}\rightarrow q\bar{q}\widetilde{\chi}^0_1$, $m_{\widetilde{\chi}^0_1}$ = 0	
>1300	95	[55] KHACHATRY...15AF		CMS	$\widetilde{g}\rightarrow b\bar{b}\widetilde{\chi}^0_1$, $m_{\widetilde{\chi}^0_1}$ = 0	
>1225	95	[55] KHACHATRY...15AF		CMS	$\widetilde{g}\rightarrow t\bar{t}\widetilde{\chi}^0_1$, $m_{\widetilde{\chi}^0_1}$ = 0	
>1550	95	[55] KHACHATRY...15AF		CMS	CMSSM, tanβ=30, $m_{\widetilde{g}}$=$m_{\widetilde{q}}$, A_0=$-2\max(m_0,m_{1/2})$, μ >0	
>1150	95	[55] KHACHATRY...15AF		CMS	CMSSM, tanβ=30, A_0=$-2\max(m_0,m_{1/2})$, μ >0	
>1280	95	[56] KHACHATRY...15I		CMS	$\widetilde{g}\rightarrow t\bar{t}\widetilde{\chi}^0_1$, $m_{\widetilde{\chi}^0_1}$ = 0	
>1310	95	[57] KHACHATRY...15X		CMS	$\widetilde{g}\rightarrow b\bar{b}\widetilde{\chi}^0_1$, $m_{\widetilde{\chi}^0_1}$ = 100 GeV	
>1175	95	[57] KHACHATRY...15X		CMS	$\widetilde{g}\rightarrow t\bar{t}\widetilde{\chi}^0_1$, $m_{\widetilde{\chi}^0_1}$ = 100 GeV	
>1330	95	[58] AAD	14AE	ATLS	jets + $\not{E}_T$, $\widetilde{g}\rightarrow q\bar{q}\widetilde{\chi}^0_1$ simplified model, $m_{\widetilde{\chi}^0_1}$ = 0 GeV	
>1700	95	[58] AAD	14AE	ATLS	jets + $\not{E}_T$, mSUGRA/CMSSM, $m_{\widetilde{q}}=m_{\widetilde{g}}$	
>1090	95	[59] AAD	14AG	ATLS	τ + jets + $\not{E}_T$, natural Gauge Mediation	
>1600	95	[59] AAD	14AG	ATLS	τ + jets + $\not{E}_T$, mGMSB, M_{messs} = 250 GeV, N_5 = 3, μ > 0, C_{grav} = 1	
>1350	95	[60] AAD	14X	ATLS	$\geq 4\ell^\pm$, $\widetilde{g}\rightarrow q\bar{q}\widetilde{\chi}^0_1$, $\widetilde{\chi}^0_1\rightarrow \ell^\pm\ell^\mp\nu$, RPV	
> 640	95	[61] AAD	14X	ATLS	$\geq 4\ell^\pm$, $\widetilde{g}\rightarrow q\bar{q}\widetilde{\chi}^0_1$, $\widetilde{\chi}^0_1\rightarrow \ell^\pm\ell^\mp\widetilde{G}$, tan$\beta$ = 30, GGM	
>1000	95	[62] CHATRCHYAN14AH		CMS	jets + $\not{E}_T$, $\widetilde{g}\rightarrow q\bar{q}\widetilde{\chi}^0_1$ simplified model, $m_{\widetilde{\chi}^0_1}$ = 50 GeV	
>1350	95	[62] CHATRCHYAN14AH		CMS	jets + $\not{E}_T$, CMSSM, $m_{\widetilde{g}}=m_{\widetilde{q}}$	
>1000	95	[63] CHATRCHYAN14AH		CMS	jets + $\not{E}_T$, $\widetilde{g}\rightarrow b\bar{b}\widetilde{\chi}^0_1$ simplified model, $m_{\widetilde{\chi}^0_1}$ = 50 GeV	
>1000	95	[64] CHATRCHYAN14AH		CMS	jets + $\not{E}_T$, $\widetilde{g}\rightarrow t\bar{t}\widetilde{\chi}^0_1$ simplified model, $m_{\widetilde{\chi}^0_1}$ = 50 GeV	
>1160	95	[65] CHATRCHYAN14I		CMS	jets + $\not{E}_T$, $\widetilde{g}\rightarrow q\bar{q}\widetilde{\chi}^0_1$ simplified model, $m_{\widetilde{\chi}^0_1}$ < 100 GeV	
>1130	95	[65] CHATRCHYAN14I		CMS	multijets + $\not{E}_T$, $\widetilde{g}\rightarrow t\bar{t}\widetilde{\chi}^0_1$ simplified model, $m_{\widetilde{\chi}^0_1}$ < 100 GeV	
>1210	95	[65] CHATRCHYAN14I		CMS	multijets + $\not{E}_T$, $\widetilde{g}\rightarrow q\bar{q}W/Z\widetilde{\chi}^0_1$ simplified model, $m_{\widetilde{\chi}^0_1}$ < 100 GeV	
>1260	95	[66] CHATRCHYAN14N		CMS	1$\ell^\pm$+ jets + $\geq$ 2b-jets, $\widetilde{g}\rightarrow t\bar{t}\chi^0_1$ simplified model, $m_{\chi^0_1}$=0 GeV, $m_{\widetilde{t}}>m_{\widetilde{g}}$	
> 650	95	[67] CHATRCHYAN14P		CMS	$\widetilde{g}\rightarrow jjj$, RPV	
none 200–835	95	[67] CHATRCHYAN14P		CMS	$\widetilde{g}\rightarrow bjj$, RPV	
		[68] CHATRCHYAN14R		CMS	$\geq 3\ell^\pm$, $(\widetilde{g}/\widetilde{q})\rightarrow q\ell^\pm\ell^\mp\widetilde{G}$ simplified model, GMSB, slepton co-NLSP scenario	
		[69] CHATRCHYAN14R		CMS	$\geq 3\ell^\pm$, $\widetilde{g}\rightarrow t\bar{t}\widetilde{\chi}^0_1$ simplified model	

• • • We do not use the following data for averages, fits, limits, etc. • • •

>1600	95	[70] AABOUD	17AZ	ATLS	$\geq$ 7 jets+$\not{E}_T$, large R-jets and/or b-jets, pMSSM, $m_{\widetilde{\chi}^\pm_1}$ = 200 GeV	
>1600	95	[71] KHACHATRY...16AY		CMS	1$\ell^\pm$ + jets + b-jets + $\not{E}_T$, Tglu3A, $m_{\widetilde{\chi}^0_1}$ = 0 GeV	
> 500	95	[72] KHACHATRY...16BT		CMS	19-parameter pMSSM model, global Bayesian analysis, flat prior	
>1400	95	[73] KHACHATRY...16BX		CMS	$\widetilde{g}\rightarrow qq\widetilde{\chi}^0_1$, $\widetilde{\chi}^0_1\rightarrow \ell\ell\nu$, RPV, λ_{121} or $\lambda_{122}\neq 0$, $m_{\widetilde{\chi}^0_1}$ > 400 GeV	
	95	[74] AAD	15AB	ATLS	$\widetilde{g}\rightarrow S\bar{g}$, $c\tau$ = 1 m, $\widetilde{S}\rightarrow S\bar{G}$ and $S\rightarrow gg$, BR = 100%	
	95	[75] AAD	15AI	ATLS	$\ell^\pm$ + jets + $\not{E}_T$	
>1600	95	[52] AAD	15BV	ATLS	pMSSM, M_1 = 60 GeV, $m_{\widetilde{q}}$ < 1500 GeV	
>1280	95	[52] AAD	15BV	ATLS	mSUGRA, m_0 > 2 TeV	
>1100	95	[52] AAD	15BV	ATLS	via $\widetilde{\tau}$, natural GMSB, all $m_{\widetilde{\tau}}$	
>1330	95	[52] AAD	15BV	ATLS	jets + $\not{E}_T$, $\widetilde{g}\rightarrow q\bar{q}\widetilde{\chi}^0_1$, $m_{\widetilde{\chi}^0_1}$ = 1 GeV	
>1500	95	[52] AAD	15BV	ATLS	jets + $\not{E}_T$, $\widetilde{g}\rightarrow \widetilde{q}q$, $\widetilde{q}\rightarrow q\widetilde{\chi}^0_1$, $m_{\widetilde{\chi}^0_1}$ = 1 GeV	

>1650	95	[52] AAD	15BV	ATLS	jets + $\not{E}_T$, $m_{\tilde{g}} = m_{\tilde{q}}$, $m_{\tilde{\chi}_1^0} = 1$ GeV
> 850	95	[52] AAD	15BV	ATLS	jets + $\not{E}_T$, $\tilde{g} \to g\tilde{\chi}_1^0$, $m_{\tilde{\chi}_1^0} <$ 550 GeV
>1270	95	[52] AAD	15BV	ATLS	jets + $\not{E}_T$, $\tilde{g} \to q\overline{q}W\tilde{\chi}_1^0$, $m_{\tilde{\chi}_1^0}$ = 100 GeV
>1150	95	[52] AAD	15BV	ATLS	jets + $\ell^{\pm}\ell^{\pm}$, $\tilde{g} \to q\overline{q}WZ\tilde{\chi}_1^0$, $m_{\tilde{\chi}_1^0} = 100$ GeV
>1320	95	[52] AAD	15BV	ATLS	jets + $\ell^{\pm}\ell^{\pm}$, $\tilde{g}$ decays via sleptons, $m_{\tilde{\chi}_1^0} = 100$ GeV
>1220	95	[52] AAD	15BV	ATLS	τ, $\tilde{q}$ decays via staus, $m_{\tilde{\chi}_1^0} = 100$ GeV
>1310	95	[52] AAD	15BV	ATLS	b-jets, $\tilde{g} \to t\overline{t}\tilde{\chi}_1^0$, $m_{\tilde{\chi}_1^0} < 400$ GeV
>1220	95	[52] AAD	15BV	ATLS	b-jets, $\tilde{g} \to \tilde{t}_1 t$ and $\tilde{t}_1 \to t\tilde{\chi}_1^0$, $m_{T_1} < 1000$ GeV
>1180	95	[52] AAD	15BV	ATLS	b-jets, $\tilde{g} \to \tilde{t}_1 t$ and $\tilde{t}_1 \to b\tilde{\chi}_1^{\pm}$, $m_{T_1} < 1000$ GeV, $m_{\tilde{\chi}_1^0} = 60$ GeV
>1260	95	[52] AAD	15BV	ATLS	b-jets, $\tilde{g} \to \tilde{t}_1 t$ and $\tilde{g} \to c\tilde{\chi}_1^0$
> 880	95	[52] AAD	15BV	ATLS	jets, $\tilde{g} \to \tilde{t}_1 t$ and $\tilde{t}_1 \to sb$, RPV, $400 < m_{\tilde{t}_1} < 1000$ GeV
>1200	95	[52] AAD	15BV	ATLS	b-jets, $\tilde{g} \to \tilde{b}_1 b$ and $\tilde{b}_1 \to b\tilde{\chi}_1^0$, $m_{\tilde{b}_1} < 1000$ GeV
>1250	95	[52] AAD	15BV	ATLS	b-jets, $\tilde{g} \to b\overline{b}\tilde{\chi}_1^0$, $m_{\tilde{\chi}_1^0} < 400$ GeV
none, 750–1250	95	[52] AAD	15BV	ATLS	b-jets, $\tilde{g}$ decay via offshell $\tilde{t}_1$ and $\tilde{b}_1$, $m_{\tilde{\chi}_1^0} < 500$ GeV
		[76] AAD	15CB	ATLS	ℓ, $\tilde{g} \to (e/\mu)qq$, RPV, benchmark gluino, neutralino masses
> 600	95	[76] AAD	15CB	ATLS	$\ell\ell/Z$, $\tilde{g} \to (ee/\mu\mu/e\mu)qq$, RPV, $m_{\tilde{\chi}_1^0} = 400$ GeV and $0.7 < c\tau_{\tilde{\chi}_1^0} < 3 \times 10^5$ mm
>1100	95	[76] AAD	15CB	ATLS	jets, $\tilde{g} \to qq\tilde{\chi}_1^0$, $\tilde{\chi}_1^0 \to Z\tilde{G}$, GGM, $m_{\tilde{\chi}_1^0} = 400$ GeV and $3 < c\tau_{\tilde{\chi}_1^0} < 500$ mm
>1400	95	[76] AAD	15CB	ATLS	jets or $\not{E}_T$, $\tilde{g} \to qq\tilde{\chi}_1^0$, Split SUSY, $m_{\tilde{\chi}_1^0} = 100$ GeV and $15 < c\tau < 300$ mm
>1500	95	[76] AAD	15CB	ATLS	$\not{E}_T$, $\tilde{g} \to qq\tilde{\chi}_1^0$, Split SUSY, $m_{\tilde{\chi}_1^0} = 100$ GeV and $20 < c\tau < 250$ mm
>1000	95	[77] AAD	15X	ATLS	≥ 10 jets, $\tilde{g} \to q\overline{q}\tilde{\chi}_1^0$, $\tilde{\chi}_1^0 \to qqq$ (RPV), $m_{\tilde{\chi}_1^0}$=500 GeV
> 917	95	[77] AAD	15X	ATLS	$\geq$ 6,7 jets, $\tilde{g} \to qq$, (light-quark, λ'' couplings, RPV)
> 929	95	[77] AAD	15X	ATLS	$\geq$ 6,7 jets, $\tilde{g} \to qqq$, (b-quark, λ'' couplings, RPV)
		[78] KHACHATRY...	15AD	CMS	$\ell^{\pm}\ell^{\mp}$ + jets + $\not{E}_T$, GMSB, $\tilde{g} \to q\overline{q}Z\tilde{G}$
>1300	95	[79] KHACHATRY...	15AZ	CMS	$\geq 2\ \gamma$, ≥ 1 jet, (Razor), bino-like NLSP, $m_{\tilde{\chi}_1^0} = 375$ GeV
> 800	95	[79] KHACHATRY...	15AZ	CMS	$\geq 1\ \gamma$, ≥ 2 jet, wino-like NLSP, $m_{\tilde{\chi}_1^0} = 375$ GeV
>1280	95	[80] AAD	14AX	ATLS	≥ 3 b-jets + $\not{E}_T$, CMSSM
>1250	95	[80] AAD	14AX	ATLS	≥ 3 b-jets + $\not{E}_T$, $\tilde{g} \to \tilde{b}_1 b\tilde{\chi}_1^0$ simplified model, $\tilde{b}_1 \to b\tilde{\chi}_1^0$, $m_{\tilde{\chi}_1^0} = 60$ GeV, $m_{\tilde{b}_1} < 900$ GeV
>1190	95	[80] AAD	14AX	ATLS	≥ 3 b-jets + $\not{E}_T$, $\tilde{g} \to \tilde{t}_1 t\tilde{\chi}_1^0$ simplified model, $\tilde{t}_1 \to t\tilde{\chi}_1^0$, $m_{\tilde{\chi}_1^0} = 60$ GeV, $m_{\tilde{t}_1} < 1000$ GeV
>1180	95	[80] AAD	14AX	ATLS	≥ 3 b-jets + $\not{E}_T$, $\tilde{g} \to \tilde{t}_1 t\tilde{\chi}_1^0$ simplified model, $\tilde{t}_1 \to b\tilde{\chi}_1^{\pm}$, $m_{\tilde{\chi}_1^{\pm}} = 2m_{\tilde{\chi}_1^0}$, $m_{\tilde{\chi}_1^0} = 60$ GeV, $m_{\tilde{t}_1} < 1000$ GeV
>1250	95	[80] AAD	14AX	ATLS	≥ 3 b-jets + $\not{E}_T$, $\tilde{g} \to b\overline{b}\tilde{\chi}_1^0$ simplified model, $m_{\tilde{\chi}_1^0} < 400$ GeV
>1340	95	[80] AAD	14AX	ATLS	≥ 3 b-jets + $\not{E}_T$, $\tilde{g} \to t\overline{t}\tilde{\chi}_1^0$ simplified model, $m_{\tilde{\chi}_1^0} < 400$ GeV
>1300	95	[80] AAD	14AX	ATLS	≥ 3 b-jets + $\not{E}_T$, $\tilde{g} \to t\overline{b}\tilde{\chi}_1^{\pm}$ simplified model, $\tilde{\chi}_1^{\pm} \to f f'\tilde{\chi}_1^0$, $m_{\tilde{\chi}_1^{\pm}} - m_{\tilde{\chi}_1^0} = 2$ GeV, $m_{\tilde{\chi}_1^0} < 300$ GeV
> 950	95	[81] AAD	14E	ATLS	$\ell^{\pm}\ell^{\pm}(\ell^{\mp})$ + jets, $\tilde{g} \to t\overline{t}\tilde{\chi}_1^0$ simplified model
>1000	95	[81] AAD	14E	ATLS	$\ell^{\pm}\ell^{\pm}(\ell^{\mp})$ + jets, $\tilde{g} \to t\tilde{t}_1$ with $\tilde{t}_1 \to b\tilde{\chi}_1^{\pm}$ simplified model, $m_{\tilde{t}_1} < 200$ GeV, $m_{\tilde{\chi}_1^{\pm}} = 118$ GeV, $m_{\tilde{\chi}_1^0} = 60$ GeV
> 640	95	[81] AAD	14E	ATLS	$\ell^{\pm}\ell^{\pm}(\ell^{\mp})$ + jets, $\tilde{g} \to t\tilde{t}_1$ with $\tilde{t}_1 \to c\tilde{\chi}_1^0$ simplified model, $m_{\tilde{t}_1} = m_{\tilde{\chi}_1^0} + 20$ GeV
> 850	95	[81] AAD	14E	ATLS	$\ell^{\pm}\ell^{\pm}(\ell^{\mp})$ + jets, $\tilde{g} \to t\tilde{t}_1$ with $\tilde{t}_1 \to bs$ simplified model, RPV
> 860	95	[81] AAD	14E	ATLS	$\ell^{\pm}\ell^{\pm}(\ell^{\mp})$ + jets, $\tilde{g} \to qq'\tilde{\chi}_1^{\pm}$, $\tilde{\chi}_1^{\pm} \to W^{(*)\pm}\tilde{\chi}_1^0$ simplified model, $m_{\tilde{\chi}_1^{\pm}} = 2\, m_{\tilde{\chi}_1^0}$, $m_{\tilde{\chi}_1^0} < 400$ GeV
>1040	95	[81] AAD	14E	ATLS	$\ell^{\pm}\ell^{\pm}(\ell^{\mp})$ + jets, $\tilde{g} \to qq'\tilde{\chi}_1^{\pm}$, $\tilde{\chi}_1^{\pm} \to W^{(*)\pm}\tilde{\chi}_2^0$, $\tilde{\chi}_2^0 \to Z^{(*)}\tilde{\chi}_1^0$ simplified model, $m_{\tilde{\chi}_1^0} < 520$ GeV
>1200	95	[81] AAD	14E	ATLS	$\ell^{\pm}\ell^{\pm}(\ell^{\mp})$ + jets, $\tilde{g} \to qq'\tilde{\chi}_1^{\pm}/\tilde{\chi}_2^0$, $\tilde{\chi}_1^{\pm} \to \ell^{\pm}\nu\tilde{\chi}_1^0$, $\tilde{\chi}_2^0 \to \ell^{\pm}\ell^{\mp}(\nu\nu)\tilde{\chi}_1^0$ simplified model
>1050	95	[82] CHATRCHYAN	14H	CMS	same-sign $\ell^{\pm}\ell^{\pm}$, $\tilde{g} \to t\overline{t}\tilde{\chi}_1^0$ simplified model, massless $\tilde{\chi}_1^0$
> 900	95	[83] CHATRCHYAN	14H	CMS	same-sign $\ell^{\pm}\ell^{\pm}$, $\tilde{g} \to qq'\tilde{\chi}_1^{\pm}$, $\tilde{\chi}_1^{\pm} \to W^{\pm}\tilde{\chi}_1^0$ simplified model, $m_{\tilde{\chi}_1^{\pm}} = 0.5\ m_{\tilde{g}}$, massless $\tilde{\chi}_1^0$
>1050	95	[84] CHATRCHYAN	14H	CMS	same-sign $\ell^{\pm}\ell^{\pm}$, $\tilde{g} \to b\overline{t}\tilde{\chi}_1^{\pm}$, $\tilde{\chi}_1^{\pm} \to W^{\pm}\tilde{\chi}_1^0$ simplified model, $m_{\tilde{\chi}_1^{\pm}} = 300$ GeV, $m_{\tilde{\chi}_1^0} = 50$ GeV
> 900	95	[85] CHATRCHYAN	14H		same-sign $\ell^{\pm}\ell^{\pm}$, $\tilde{g} \to tbs$ simplified model, RPV

[1] SIRUNYAN 18D searched in 35.9 fb^{-1} of pp collisions at $\sqrt{s} = 13$ TeV for events containing identified hadronically decaying top quarks, no leptons, and $\not{E}_T$. No significant excess above the Standard Model expectations is observed. Limits are set on the stop mass in the Tstop1 simplified model, see their Figure 8, and on the gluino mass in the Tglu3A, Tglu3B, Tglu3C and Tglu3E simplified models, see their Figure 9.

[2] AABOUD 17AI searched in 36.1 fb^{-1} of pp collisions at $\sqrt{s} = 13$ TeV for events with one or more isolated lepton, at least eight jets, either zero or many b-jets, for evidence of R-parity violating decays of the gluino. No significant excess above the Standard Model expectations is observed. Limits up to 2.1 TeV are set on the gluino mass in R-parity-violating supersymmetry models as Tglu3A with LSP decay through the non-zero λ''_{112} coupling as $\tilde{\chi}_1^0 \to uds$. See their Figure 9.

[3] AABOUD 17AI searched in 36.1 fb^{-1} of pp collisions at $\sqrt{s} = 13$ TeV for events with one or more isolated lepton, at least eight jets, either zero or many b-jets, for evidence of R-parity violating decays of the gluino. No significant excess above the Standard Model expectations is observed. Limits up to 1.65 TeV are set on the gluino mass in R-parity-violating supersymmetry models with $\tilde{g} \to t\tilde{t}$, $\tilde{t} \to bs$ through the non-zero λ''_{323} coupling. See their Figure 9.

[4] AABOUD 17AI searched in 36.1 fb^{-1} of pp collisions at $\sqrt{s} = 13$ TeV for events with one or more isolated lepton, at least eight jets, either zero or many b-jets, for evidence of R-parity violating decays of the gluino. No significant excess above the Standard Model expectations is observed. Limits up to 1.8 TeV are set on the gluino mass in R-parity-violating supersymmetry models as Tglu1A with the LSP decay through the non-zero λ' coupling as $\tilde{\chi}_1^0 \to qq\ell$. See their Figure 9.

[5] AABOUD 17AJ searched in 36.1 fb^{-1} of pp collisions at $\sqrt{s} = 13$ TeV for events with two same-sign or three leptons, jets and large missing transverse momentum. No significant excess above the Standard Model expectations is observed. Limits up to 1.75 TeV are set on the gluino mass in Tglu3A simplified models in case of off-shell top squarks and for $m_{\tilde{\chi}_1^0} = 100$ GeV. See their Figure 4(a).

[6] AABOUD 17AJ searched in 36.1 fb^{-1} of pp collisions at $\sqrt{s} = 13$ TeV for events with two same-sign or three leptons, jets and large missing transverse momentum. No significant excess above the Standard Model expectations is observed. Limits up to 1.57 TeV are set on the gluino mass in Tglu1E simplified models (2-step models) for $m_{\tilde{\chi}_1^0} = 100$ GeV. See their Figure 4(b).

[7] AABOUD 17AJ searched in 36.1 fb^{-1} of pp collisions at $\sqrt{s} = 13$ TeV for events with two same-sign or three leptons, jets and large missing transverse momentum. No significant excess above the Standard Model expectations is observed. Limits up to 1.86 TeV are set on the gluino mass in Tglu1G simplified models for $m_{\tilde{\chi}_1^0} = 200$ GeV. See their Figure 4(c).

[8] AABOUD 17AJ searched in 36.1 fb^{-1} of pp collisions at $\sqrt{s} = 13$ TeV for events with two same-sign or three leptons, jets and large missing transverse momentum. No significant excess above the Standard Model expectations is observed. Limits up to 1.8 TeV are set on the gluino mass in R-parity-violating supersymmetry models as Tglu3A with LSP decaying through the non-zero λ''_{112} coupling as $\tilde{\chi}^0_1 \to u\,d\,s$. See their Figure 5(d).

[9] AABOUD 17AJ searched in 36.1 fb^{-1} of pp collisions at $\sqrt{s} = 13$ TeV for events with two same-sign or three leptons, jets and large missing transverse momentum. No significant excess above the Standard Model expectations is observed. Limits up to 1.75 TeV are set on the gluino mass in R-parity-violating supersymmetry models as Tglu1A with LSP decaying through the non-zero λ' coupling as $\tilde{\chi}^0_1 \to q\,q\,\ell$. See their Figure 5(c).

[10] AABOUD 17AJ searched in 36.1 fb^{-1} of pp collisions at $\sqrt{s} = 13$ TeV for events with two same-sign or three leptons, jets and large missing transverse momentum. No significant excess above the Standard Model expectations is observed. Limits up to 1.45 TeV are set on the gluino mass in R-parity-violating supersymmetry models where $\tilde{g} \to t\,\tilde{t}_1$ and $\tilde{t}_1 \to s\,d$ through the non-zero λ''_{321} coupling. See their Figure 5(b).

[11] AABOUD 17AJ searched in 36.1 fb^{-1} of pp collisions at $\sqrt{s} = 13$ TeV for events with two same-sign or three leptons, jets and large missing transverse momentum. No significant excess above the Standard Model expectations is observed. Limits up to 1.45 TeV are set on the gluino mass in R-parity-violating supersymmetry models where $\tilde{g} \to t\,\tilde{t}_1$ and $\tilde{t}_1 \to b\,d$ through the non-zero λ''_{313} coupling. See their Figure 5(a).

[12] AABOUD 17AJ searched in 36.1 fb^{-1} of pp collisions at $\sqrt{s} = 13$ TeV for events with two same-sign or three leptons, jets and large missing transverse momentum. No significant excess above the Standard Model expectations is observed. Limits up to 400 GeV are set on the down type squark ($\tilde{d}_R$ mass in R-parity-violating supersymmetry models where $\tilde{d}_R \to t\,b$ through the non-zero λ''_{313} coupling or $\tilde{d}_R \to t\,s$ through the non-zero λ''_{321}. See their Figure 5(e) and 5(f).

[13] AABOUD 17AR searched in 36.1 fb^{-1} of pp collisions at $\sqrt{s} = 13$ TeV for events with one isolated lepton, at least two jets and large missing transverse momentum. No significant excess above the Standard Model expectations is observed. Limits up to 2.1 TeV are set on the gluino mass in Tglu1B simplified models, with $x = (m_{\tilde{\chi}^\pm_1} - m_{\tilde{\chi}^0_1}) / (m_{\tilde{g}} - m_{\tilde{\chi}^0_1}) = 1/2$. Similar limits are obtained for variable x and fixed neutralino mass, $m_{\tilde{\chi}^0_1} = 60$ GeV. See their Figure 13.

[14] AABOUD 17AR searched in 36.1 fb^{-1} of pp collisions at $\sqrt{s} = 13$ TeV for events with one isolated lepton, at least two jets and large missing transverse momentum. No significant excess above the Standard Model expectations is observed. Limits up to 1.74 TeV are set on the gluino mass in Tglu1E simplified model. Limits up to 1.7 TeV are also set on pMSSM models leading to similar signal event topologies. See their Figure 13.

[15] AABOUD 17AY searched in 36.1 fb^{-1} of pp collisions at $\sqrt{s} = 13$ TeV for events with at least four jets and large missing transverse momentum. No significant excess above the Standard Model expectations is observed. Limits up to 1.8 TeV are set on the gluino mass in Tglu3A simplified models assuming $m_{\tilde{t}_1} - m_{\tilde{\chi}^0_1} = 5$ GeV. See their Figure 13.

[16] AABOUD 17AZ searched in 36.1 fb^{-1} of pp collisions at $\sqrt{s} = 13$ TeV for events with at least seven jets and large missing transverse momentum. Selected events are further classified based on the presence of large R-jets or b-jets and no leptons. No significant excess above the Standard Model expectations is observed. Limits up to 1.8 TeV are set on the gluino mass in Tglu1E simplified models. See their Figure 6b.

[17] AABOUD 17AZ searched in 36.1 fb^{-1} of pp collisions at $\sqrt{s} = 13$ TeV for events with at least seven jets and large missing transverse momentum. Selected events are further classified based on the presence of large R-jets or b-jets and no leptons. No significant excess above the Standard Model expectations is observed. Limits up to 1.54 TeV are set on the gluino mass in Tglu3A simplified models. See their Figure 7a.

[18] AABOUD 17AZ searched in 36.1 fb^{-1} of pp collisions at $\sqrt{s} = 13$ TeV for events with at least seven jets and large missing transverse momentum. Selected events are further classified based on the presence of large R-jets or b-jets and no leptons. No significant excess above the Standard Model expectations is observed. Limits are set for R-parity violating decays of the gluino assuming $\tilde{g} \to t\,\tilde{t}_1$ and $\tilde{t}_1 \to b\,s$ through the non-zero λ''_{323} couplings. The range 625–1375 GeV is excluded for $m_{\tilde{t}_1} = 400$ GeV. See their Figure 7b.

[19] AABOUD 17N searched in 14.7 fb^{-1} of pp collisions at $\sqrt{s} = 13$ TeV in final states with 2 same-flavor, opposite-sign leptons (electrons or muons), jets and large missing transverse momentum. In Tglu1J models, gluino masses are excluded at 95% C.L. up to 1300 GeV for $m_{\tilde{\chi}^0_1} = 0$ GeV and $m_{\tilde{\chi}^0_2} = 1100$ GeV. See their Fig. 12 for exclusion limits as a function of $m_{\tilde{\chi}^0_2}$. Limits are also presented assuming $m_{\tilde{\chi}^0_2} = m_{\tilde{\chi}^0_1} + 100$ GeV, see their Fig. 13.

[20] AABOUD 17N searched in 14.7 fb^{-1} of pp collisions at $\sqrt{s} = 13$ TeV in final states with 2 same-flavor, opposite-sign leptons (electrons or muons), jets and large missing transverse momentum. In Tglu1H models, gluino masses are excluded at 95% C.L. up to 1310 GeV for $m_{\tilde{\chi}^0_1} < 400$ GeV and assuming $m_{\tilde{\chi}^0_2} = (m_{\tilde{g}} + m_{\tilde{\chi}^0_1})/2$. See their Fig. 15.

[21] AABOUD 17N searched in 14.7 fb^{-1} of pp collisions at $\sqrt{s} = 13$ TeV in final states with 2 same-flavor, opposite-sign leptons (electrons or muons), jets and large missing transverse momentum. In Tglu1G models, gluino masses are excluded at 95% C.L. up to 1700 GeV for small $m_{\tilde{\chi}^0_1}$. The results probe kinematic endpoints as small as $m_{\tilde{\chi}^0_2} - m_{\tilde{\chi}^0_1} = (m_{\tilde{g}} - m_{\tilde{\chi}^0_1})/2 = 50$ GeV. See their Fig. 14.

[22] KHACHATRYAN 17 searched in 2.3 fb^{-1} of pp collisions at $\sqrt{s} = 13$ TeV for events containing four or more jets, no more than one lepton, and missing transverse momentum, using the razor variables (M_R and R^2) to discriminate between signal and background processes. No evidence for an excess over the expected background is observed. Limits are derived on the gluino mass in the Tglu1A, Tglu2A and Tglu3A simplified models, see Figs. 16 and 17. Also, assuming gluinos decay only via three-body processes involving third-generation quarks plus a neutralino/chargino, and assuming $m_{\tilde{\chi}^\pm_1} = m_{\tilde{\chi}^0_1} + 5$ GeV, a branching ratio-independent limit on the gluino mass is given, see Fig. 16.

[23] KHACHATRYAN 17AD searched in 2.3 fb^{-1} of pp collisions at $\sqrt{s} = 13$ TeV for events containing at least four jets (including b-jets), missing transverse momentum and tagged top quarks. No evidence for an excess over the expected background is observed. Gluino masses up to 1550 GeV and neutralino masses up to 900 GeV are excluded at 95% C.L. See Fig. 13.

[24] KHACHATRYAN 17AD searched in 2.3 fb^{-1} of pp collisions at $\sqrt{s} = 13$ TeV for events containing at least four jets (including b-jets), missing transverse momentum and tagged top quarks. No evidence for an excess over the expected background is observed. Gluino masses up to 1450 GeV and neutralino masses up to 820 GeV are excluded at 95% C.L. See Fig. 13.

[25] KHACHATRYAN 17AS searched in 2.3 fb^{-1} of pp collisions at $\sqrt{s} = 13$ TeV for events with a single electron or muon and multiple jets. No significant excess above the Standard Model expectations is observed. Limits are set on the gluino mass in the Tglu3A and Tglu1B simplified models, see their Fig. 7.

[26] KHACHATRYAN 17AW searched in 2.3 fb^{-1} of pp collisions at $\sqrt{s} = 13$ TeV for events with at least three charged leptons, in any combination of electrons and muons, and significant $\not{E}_T$. No significant excess above the Standard Model expectations is observed. Limits are set on the gluino mass in the Tglu3A and Tglu1C simplified models, and on the sbottom mass in the Tsbot2 simplified model, see their Figure 4.

[27] KHACHATRYAN 17P searched in 2.3 fb^{-1} of pp collisions at $\sqrt{s} = 13$ TeV for events with one or more jets and large $\not{E}_T$. No significant excess above the Standard Model expectations is observed. Limits are set on the gluino mass in the Tglu1A, Tglu2A, Tglu3A, Tglu3B, Tglu3C and Tglu3D simplified models, see their Figures 7 and 8. Limits are also set on the squark mass in the Tsqk1 simplified model, see their Fig. 7, and on the sbottom mass in the Tsbot1 simplified model, see Fig. 8. Finally, limits are set on the stop mass in the Tstop1, Tstop3, Tstop4, Tstop6 and Tstop7 simplified models, see Fig. 8.

[28] KHACHATRYAN 17V searched in 2.3 fb^{-1} of pp collisions at $\sqrt{s} = 13$ TeV for events with two photons and large $\not{E}_T$. No significant excess above the Standard Model expectations is observed. Limits are set on the gluino and squark mass in the context of general gauge mediation models Tglu4B and Tsqk4, see their Fig. 4.

[29] KHACHATRYAN 17Y searched in 19.7 fb^{-1} of pp collisions at $\sqrt{s} = 8$ TeV for events containing at least 8 or 10 jets, possibly b-tagged, coming from R-parity-violating decays of supersymmetric particles. No excess over the expected background is observed. Limits are derived on the gluino mass, assuming various RPV decay modes, see Fig. 7.

[30] SIRUNYAN 17AF searched in 35.9 fb^{-1} of pp collisions at $\sqrt{s} = 13$ TeV for events with a single lepton (electron or muon), jets, including at least one jet originating from a b-quark, and large $\not{E}_T$. No significant excess above the Standard Model expectations is observed. Limits are set on the gluino mass in the Tglu3A and Tglu3B simplified models, see their Figure 2.

[31] SIRUNYAN 17AY searched in 35.9 fb^{-1} of pp collisions at $\sqrt{s} = 13$ TeV for events with at least one photon, jets and large $\not{E}_T$. No significant excess above the Standard Model expectations is observed. Limits are set on the gluino mass in the Tglu4A and Tglu4B simplified models, and on the squark mass in the Tskq4A and Tsqk4B simplified models, see their Figure 6.

[32] SIRUNYAN 17AZ searched in 35.9 fb^{-1} of pp collisions at $\sqrt{s} = 13$ TeV for events with one or more jets and large $\not{E}_T$. No significant excess above the Standard Model expectations is observed. Limits are set on the gluino mass in the Tglu1A, Tglu2A, Tglu3A simplified models, see their Figures 6. Limits are also set on the squark mass in the Tsqk1 simplified model (for single light squark and for 8 degenerate light squarks), on the sbottom mass in the Tsbot1 simplified model and on the stop mass in the Tstop1 simplified model, see their Fig. 7. Finally, limits are set on the stop mass in the Tstop2, Tstop4 and Tstop8 simplified models, see Fig. 8.

[33] SIRUNYAN 17P searched in 35.9 fb^{-1} of pp collisions at $\sqrt{s} = 13$ TeV for events with multiple jets and large $\not{E}_T$. No significant excess above the Standard Model expectations is observed. Limits are set on the gluino mass in the Tglu1A, Tglu1C, Tglu2A, Tglu3A and Tglu3D simplified models, see their Fig. 12. Limits are also set on the squark mass in the Tsqk1 simplified model, on the stop mass in the Tstop1 simplified model, and on the sbottom mass in the Tsbot1 simplified model, see Fig. 13.

[34] SIRUNYAN 17S searched in 35.9 fb^{-1} of pp collisions at $\sqrt{s} = 13$ TeV for events with two isolated same-sign leptons, jets, and large $\not{E}_T$. No significant excess above the Standard Model expectations is observed. Limits are set on the mass of the gluino mass in the Tglu3A, Tglu3B, Tglu3C, Tglu3D and Tglu1B simplified models, see their Figures 5 and 6, and on the sbottom mass in the Tsbot2 simplified model, see their Figure 6.

[35] AABOUD 16AC searched in 3.2 fb^{-1} of pp collisions at $\sqrt{s} = 13$ TeV in final states with hadronic jets, 1 or two hadronically decaying τ and $\not{E}_T$. In Tglu1F, gluino masses are excluded at 95% C.L. up to 1570 GeV for neutralino masses of 100 GeV or below. Neutralino masses up to 700 GeV are excluded for all gluino masses between 800 GeV and 1500 GeV, while the strongest neutralino-mass exclusion of 750 GeV is achieved for gluino masses around 1400 GeV. See their Fig. 8. Limits are also presented in the context of Gauge-Mediated Symmetry Breaking models: in this case, values of Λ below 92 TeV are excluded at the 95% CL, corresponding to gluino masses below 2000 GeV. See their Fig. 9.

[36] AABOUD 16J searched in 3.2 fb^{-1} of pp collisions at $\sqrt{s} = 13$ TeV in final states with one isolated electron or muon, hadronic jets, and $\not{E}_T$. Gluino-mediated pair production of stops with a nearly mass-degenerate stop and neutralino are targeted and gluino masses are excluded at 95% C.L. up to 1460 GeV. A 100% of stops decaying via charm + neutralino is assumed. The results are also valid in case of 4-body decays $\tilde{t}_1 \to f\,f'\,b\,\tilde{\chi}^0_1$. See their Fig. 8.

[37] AABOUD 16M searched in 3.2 fb^{-1} of pp collisions at $\sqrt{s} = 13$ TeV for events with two photons, hadronic jets and $\not{E}_T$. No significant excess above the Standard Model expectations is observed. Exclusion limits at 95% C.L. are set on gluino masses in the general gauge-mediated SUSY breaking model (GGM), for bino-like NLSP. See their Fig. 3.

[38] AABOUD 16N searched in 3.2 fb^{-1} of pp collisions at $\sqrt{s} = 13$ TeV for events containing hadronic jets, large $\not{E}_T$, and no electrons or muons. No significant excess above the Standard Model expectations is observed. Gluino masses below 1510 GeV are excluded at the 95% C.L. in a simplified model with only gluinos and the lightest neutralino. See their Fig. 7b.

[39] AABOUD 16N searched in 3.2 fb^{-1} of pp collisions at $\sqrt{s} = 13$ TeV for events containing hadronic jets, large $\not{E}_T$, and no electrons or muons. No significant excess above the Standard Model expectations is observed. Gluino masses below 1500 GeV are excluded at the 95% C.L. in a simplified model with gluinos decaying via an intermediate $\tilde{\chi}^\pm_1$ to two quarks, a W boson and a $\tilde{\chi}^0_1$, for $m_{\tilde{\chi}^0_1} = 200$ GeV. See their Fig 8.

[40] AAD 16AD searched in 3.2 fb^{-1} of pp collisions at $\sqrt{s} = 13$ TeV for events containing several energetic jets, of which at least three must be identified as b-jets, large $\not{E}_T$ and no electrons or muons. No significant excess above the Standard Model expectations is observed. For $\tilde{\chi}^0_1$ below 800 GeV, gluino masses below 1780 GeV are excluded at 95% C.L. for gluinos decaying via bottom squarks. See their Fig. 7a.

[41] AAD 16AD searched in 3.2 fb^{-1} of pp collisions at $\sqrt{s}$ = 13 TeV for events containing several energetic jets, of which at least three must be identified as b-jets, large $\not{E}_T$ and one electron or muon. Large-radius jets with a high mass are also used to identify highly boosted top quarks. No significant excess above the Standard Model expectations is observed. For $\tilde{\chi}_1^0$ below 700 GeV, gluino masses below 1760 GeV are excluded at 95% C.L. for gluinos decaying via top squarks. See their Fig. 7b.

[42] AAD 16BB searched in 3.2 fb^{-1} of pp collisions at $\sqrt{s}$ = 13 TeV for events with exactly two same-sign leptons or at least three leptons, multiple hadronic jets, b-jets, and $\not{E}_T$. No significant excess over the Standard Model expectation is found. Exclusion limits at 95% C.L. are set on the gluino mass in various simplified models (Tglu1D, Tglu1E, Tglu3A). See their Figs. 4.a, 4.b, and 4.d.

[43] AAD 16BG searched in 3.2 fb^{-1} of pp collisions at $\sqrt{s}$ = 13 TeV in final states with one isolated electron or muon, hadronic jets, and $\not{E}_T$. The data agree with the SM background expectation in the six signal selections defined in the search, and the largest deviation is a 2.1 standard deviation excess. Gluinos are excluded at 95% C.L. up to 1600 GeV assuming they decay via the lightest chargino to the lightest neutralino as in the model Tglu1B for $m_{\tilde{\chi}_1^0}$=100 GeV, assuming $m_{\tilde{\chi}_1^\pm}$=$(m_{\tilde{g}} + m_{\tilde{\chi}_1^0})/2$. See their Fig. 6.

[44] AAD 16V searched in 3.2 fb^{-1} of pp collisions at $\sqrt{s}$ = 13 TeV for events with $\not{E}_T$ various hadronic jet multiplicities from $\geq$ 7 to $\geq$ 10 and with various b-jet multiplicity requirements. No significant excess over the Standard Model expectation is found. Exclusion limits at 95% C.L. are set on the gluino mass in one simplified model (Tglu1E) and a pMSSM-inspired model. See their Fig. 5.

[45] KHACHATRYAN 16AM searched in 19.7 fb^{-1} of pp collisions at $\sqrt{s}$ = 8 TeV for events with highly boosted W-bosons and b-jets, using the razor variables (M_R and R^2) to discriminate between signal and background processes. No significant excess above the Standard Model expectations is observed. Limits are set on the gluino mass in the Tglu3C and Tglu3B simplified models, see Fig. 12.

[46] KHACHATRYAN 16BJ searched in 2.3 fb^{-1} of pp collisions at $\sqrt{s}$ = 13 TeV for events with two isolated same-sign dileptons and jets in the final state. No significant excess above the Standard Model expectations is observed. Limits are set on the gluino mass in the following simplified models: Tglu3A and Tglu3D, see Fig. 4, Tglu3B and Tglu3C, see Fig. 5, and Tglu1B, see Fig. 7.

[47] KHACHATRYAN 16BS searched in 2.3 fb^{-1} of pp collisions at $\sqrt{s}$ = 13 TeV for events with at least one energetic jet , no isolated leptons, and significant $\not{E}_T$, using the transverse mass variable M_{T2} to discriminate between signal and background processes. No significant excess above the Standard Model expectations is observed. Limits are set on the gluino mass in the Tglu1A, Tglu2A and Tglu3A simplified models, see Fig. 10 and Table 3.

[48] KHACHATRYAN 16BX searched in 19.5 fb^{-1} of pp collisions at $\sqrt{s}$ = 8 TeV for events containing 0 or 1 leptons and b-tagged jets, coming from R-parity-violating decays of supersymmetric particles. No excess over the expected background is observed. Limits are derived on the gluino mass, assuming the RPV $\tilde{g} \rightarrow t\,b\,s$ decay, see Fig. 7 and 10.

[49] KHACHATRYAN 16BY searched in 2.3 fb^{-1} of pp collisions at $\sqrt{s}$ = 13 TeV for events with two opposite-sign, same-flavour leptons, jets, and missing transverse momentum. No significant excess above the Standard Model expectations is observed. Limits are set on the gluino mass in the Tglu4C simplified model, see Fig. 4, and on sbottom masses in the Tsbot3 simplified model, see Fig. 5.

[50] KHACHATRYAN 16V searched in 2.3 fb^{-1} of pp collisions at $\sqrt{s}$ = 13 TeV for events with at least four energetic jets and significant $\not{E}_T$, no identified isolated electron or muon or charged track. No significant excess above the Standard Model expectations is observed. Limits are set on the gluino mass in the Tglu1A, Tglu1C, Tglu2A, and Tglu3A simplified models, see Fig. 8.

[51] AAD 15BG searched in 20.3 fb^{-1} of pp collisions at $\sqrt{s}$ = 8 TeV for events with jets, missing E_T, and two opposite-sign same flavor isolated leptons featuring either a kinematic edge, or a peak at the Z-boson mass, in the invariant mass spectrum. No evidence for a statistically significant excess over the expected SM backgrounds are observed and 95% C.L. exclusion limits are derived in a GGM simplified model of gluino pair production where the gluino decays into quarks, a Z-boson, and a massless gravitino LSP, see Fig. 12. Also, limits are set in simplified models with slepton /sneutrino intermediate states, see Fig. 13.

[52] AAD 15BV summarized and extended ATLAS searches for gluinos and first- and second-generation squarks in final states containing jets and missing transverse momentum, with or without leptons or b-jets in the $\sqrt{s}$ =8 TeV data set collected in 2012. The paper reports the results of new interpretations and statistical combinations of previously published analyses, as well as new analyses. Exclusion limits at 95% C.L. are set on the gluino mass in several R-parity conserving models, leading to a generalized constraint on gluino masses exceeding 1150 GeV for lightest supersymmetric particle masses below 100 GeV. See their Figs. 10, 19, 20, 21, 23, 25, 26, 29-37.

[53] AAD 15BX interpreted the results of a wide range of ATLAS direct searches for supersymmetry, during the first run of the LHC using the $\sqrt{s}$ =7 TeV and $\sqrt{s}$ = 8 TeV data set collected in 2012, within the wider framework of the phenomenological MSSM (pMSSM). The integrated luminosity was up to 20.3 fb^{-1}. From an initial random sampling of 500 million pMSSM points, generated from the 19-parameter pMSSM, a total of 310,327 model points with $\tilde{\chi}_1^0$ LSP were selected each of which satisfies constraints from previous collider searches, precision measurements, cold dark matter energy density measurements and direct dark matter searches. The impact of the ATLAS Run 1 searches on this space was presented, considering the fraction of model points surviving, after projection into two-dimensional spaces of sparticle masses. Good complementarity is observed between different ATLAS analyses, with almost all showing regions of unique sensitivity. ATLAS searches have good sensitivity at LSP mass below 800 GeV.

[54] AAD 15CA searched in 20.3 fb^{-1} of pp collisions at $\sqrt{s}$ = 8 TeV for events with one or more photons, hadronic jets or b-jets and $\not{E}_T$. No significant excess above the Standard Model expectations is observed. Limits are set on gluino masses in the general gauge-mediated SUSY breaking model (GGM), for bino-like or higgsino-bino admixtures NLSP, see Fig. 8, 10, 11

[55] KHACHATRYAN 15AF searched in 19.5 fb^{-1} of pp collisions at $\sqrt{s}$ = 8 TeV for events with at least two energetic jets and significant $\not{E}_T$, using the transverse mass variable M_{T2} to discriminate between signal and background processes. No significant excess above the Standard Model expectations is observed. Limits are set on the gluino mass in simplified models where the decay $\tilde{g} \rightarrow q\bar{q}\tilde{\chi}_1^0$ takes place with a branching ratio of 100%, see Fig. 13(a), or where the decay $\tilde{g} \rightarrow b\bar{b}\tilde{\chi}_1^0$ takes place with a branching ratio of 100%, see Fig. 13(b), or where the decay $\tilde{g} \rightarrow t\bar{t}\tilde{\chi}_1^0$ takes place with a branching ratio of 100%, see Fig. 13(c). See also Table 5. Exclusions in the CMSSM, assuming tanβ = 30, $A_0 = -2$ max(m_0, $m_{1/2}$) and $\mu > 0$, are also presented, see Fig. 15.

[56] KHACHATRYAN 15I searched in 19.5 fb^{-1} of pp collisions at $\sqrt{s}$ = 8 TeV for events in which b-jets and four W-bosons are produced. Five individual search channels are combined (fully hadronic, single lepton, same-sign dilepton, opposite-sign dilepton, multilepton). No significant excess above the Standard Model expectations is observed. Limits are set on the gluino mass in a simplified model where the decay $\tilde{g} \rightarrow t\bar{t}\tilde{\chi}_1^0$ takes place with a branching ratio of 100%, see Fig. 5. Also a simplified model with gluinos decaying into on-shell top squarks is considered, see Fig. 6.

[57] KHACHATRYAN 15X searched in 19.3fb^{-1} of pp collisions at $\sqrt{s}$ = 8 TeV for events with at least two energetic jets, at least one of which is required to originate from a b quark, and significant $\not{E}_T$, using the razor variables (M_R) and R^2) to discriminate between signal and background processes. No significant excess above the Standard Model expectations is observed. Limits are set on the gluino mass in simplified models where the decay $\tilde{g} \rightarrow b\bar{b}\tilde{\chi}_1^0$ and the decay $\tilde{g} \rightarrow t\bar{t}\tilde{\chi}_1^0$ take place with branching ratios varying between 0, 50 and 100%, see Figs. 13 and 14.

[58] AAD 14AE searched in 20.3 fb^{-1} of pp collisions at $\sqrt{s}$ = 8 TeV for strongly produced supersymmetric particles in events containing jets and large missing transverse momentum, and no electrons or muons. No excess over the expected SM background is observed. Exclusion limits are derived in simplified models containing gluinos and squarks, see Figures 5, 6 and 7. Limits are also derived in the mSUGRA/CMSSM with parameters tanβ = 30, $A_0 = -2\ m_0$ and $\mu > 0$, see their Fig. 8.

[59] AAD 14AG searched in 20.3 fb^{-1} of pp collisions at $\sqrt{s}$ = 8 TeV for events containing one hadronically decaying τ-lepton, zero or one additional light leptons (electrons or muons), jets and large missing transverse momentum. No excess of events above the expected level of Standard Model background was found. Exclusion limits at 95% C.L. are set in several SUSY scenarios. For an interpretation in the minimal GMSB model, see their Fig. 8. For an interpretation in the mSUGRA/CMSSM with parameters tanβ = 30, $A_0 = -2\ m_0$ and $\mu > 0$, see their Fig. 9. For an interpretation in the framework of natural Gauge Mediation, see Fig. 10. For an interpretation in the bRPV scenario, see their Fig. 11.

[60] AAD 14X searched in 20.3 fb^{-1} of pp collisions at $\sqrt{s}$ = 8 TeV for events with at least four leptons (electrons, muons, taus) in the final state. No significant excess above the Standard Model expectations is observed. Limits are set on the gluino mass in an R-parity violating simplified model where the decay $\tilde{g} \rightarrow q\bar{q}\tilde{\chi}_1^0$, with $\tilde{\chi}_1^0 \rightarrow \ell^\pm\ell^\mp\nu$, takes place with a branching ratio of 100%, see Fig. 8.

[61] AAD 14X searched in 20.3 fb^{-1} of pp collisions at $\sqrt{s}$ = 8 TeV for events with at least four leptons (electrons, muons, taus) in the final state. No significant excess above the Standard Model expectations is observed. Limits are set on the gluino mass in a general gauge-mediation model (GGM) where the decay $\tilde{g} \rightarrow q\bar{q}\tilde{\chi}_1^0$, with $\tilde{\chi}_1^0 \rightarrow \ell^\pm\ell^\mp\tilde{G}$, takes place with a branching ratio of 100%, for two choices of tanβ = 1.5 and 30, see Fig. 11. Also some constraints on the higgsino mass parameter μ are discussed.

[62] CHATRCHYAN 14AH searched in 4.7 fb^{-1} of pp collisions at $\sqrt{s}$ = 7 TeV for events with at least two energetic jets and significant $\not{E}_T$, using the razor variables (M_R and R^2) to discriminate between signal and background processes. No significant excess above the Standard Model expectations is observed. Limits are set on sbottom masses in simplified models where the decay $\tilde{g} \rightarrow q\bar{q}\tilde{\chi}_1^0$ takes place with a branching ratio of 100%, see Fig. 28. Exclusions in the CMSSM, assuming tanβ = 10, A_0 = 0 and $\mu > 0$, are also presented, see Fig. 26.

[63] CHATRCHYAN 14AH searched in 4.7 fb^{-1} of pp collisions at $\sqrt{s}$ = 7 TeV for events with at least two energetic jets and significant $\not{E}_T$, using the razor variables (M_R and R^2) to discriminate between signal and background processes. A second analysis requires at least one of the jets to be originating from a b-quark. No significant excess above the Standard Model expectations is observed. Limits are set on sbottom masses in simplified models where the decay $\tilde{g} \rightarrow b\bar{b}\tilde{\chi}_1^0$ takes place with a branching ratio of 100%, see Figs. 28 and 29. Exclusions in the CMSSM, assuming tanβ = 10, A_0 = 0 and $\mu > 0$, are also presented, see Fig. 26.

[64] CHATRCHYAN 14AH searched in 4.7 fb^{-1} of pp collisions at $\sqrt{s}$ = 7 TeV for events with at least two energetic jets and significant $\not{E}_T$, using the razor variables (M_R and R^2) to discriminate between signal and background processes. A second analysis requires at least one of the jets to be originating from a b-quark. No significant excess above the Standard Model expectations is observed. Limits are set on sbottom masses in simplified models where the decay $\tilde{g} \rightarrow t\bar{t}\tilde{\chi}_1^0$ takes place with a branching ratio of 100%, see Figs. 28 and 29. Exclusions in the CMSSM, assuming tanβ = 10, A_0 = 0 and $\mu >$0, are also presented, see Fig. 26.

[65] CHATRCHYAN 14I searched in 19.5 fb^{-1} of pp collisions at $\sqrt{s}$ = 8 TeV for events containing multijets and large $\not{E}_T$. No excess over the expected SM background is observed. Exclusion limits are derived in simplified models containing gluinos that decay via $\tilde{g} \rightarrow q\bar{q}\tilde{\chi}_1^0$ with a 100% branching ratio, see Fig. 7b, or via $\tilde{g} \rightarrow t\bar{t}\tilde{\chi}_1^0$ with a 100% branching ratio, see Fig. 7c, or via $\tilde{g} \rightarrow q\bar{q}W/Z\tilde{\chi}_1^0$, see Fig. 7d.

[66] CHATRCHYAN 14N searched in 19.3 fb^{-1} of pp collisions at $\sqrt{s}$ = 8 TeV for events containing a single isolated electron or muon and multiple jets, at least two of which are identified as originating from a b-quark. No significant excesses over the expected SM backgrounds are observed. The results are interpreted in three simplified models of gluino pair production with subsequent decay into virtual or on-shell top squarks, where each of the top squarks decays in turn into a top quark and a $\tilde{\chi}_1^0$, see Fig. 4. The models differ in which masses are allowed to vary.

[67] CHATRCHYAN 14P searched in 19.4 fb^{-1} of pp collisions at $\sqrt{s}$ = 8 TeV for three-jet resonances produced in the decay of a gluino in R-parity violating supersymmetric models. No excess over the expected SM background is observed. Assuming a 100% branching ratio for the gluino decay into three light-flavour jets, limits are set on the cross section of gluino pair production, see Fig. 7, and gluino masses below 650 GeV are excluded at 95% C.L. Assuming a 100% branching ratio for the gluino decaying to one b-quark jet and two light-flavour jets, gluino masses between 200 GeV and 835 GeV are excluded at 95% C L.

[68] CHATRCHYAN 14R searched in 19.5 fb^{-1} of pp collisions at $\sqrt{s}$ = 8 TeV for events with at least three leptons (electrons, muons, taus) in the final state. No significant excess above the Standard Model expectations is observed. Limits are set on the gluino mass in a slepton co-NLSP simplified model (GMSB) where the decay $\tilde{g} \rightarrow q\ell^\pm\ell^\mp\tilde{G}$ takes place with a branching ratio of 100%, see Fig. 8.

[69] CHATRCHYAN 14R searched in 19.5 fb^{-1} of pp collisions at $\sqrt{s}$ = 8 TeV for events with at least three leptons (electrons, muons, taus) in the final state. No significant excess above the Standard Model expectations is observed. Limits are set on the gluino mass in a simplified model where the decay $\tilde{g} \rightarrow t\bar{t}\tilde{\chi}_1^0$ takes place with a branching ratio of 100%, see Fig. 11.

[70] AABOUD 17AZ searched in 36.1 fb^{-1} of pp collisions at $\sqrt{s}$ = 13 TeV for events with at least seven jets and large missing transverse momentum. Selected events are further classified based on the presence of large R-jets or b-jets and no leptons. No significant excess above the Standard Model expectations is observed. Limits are set for pMSSM models with M_1 = 60 GeV, tan(β) = 10, μ < 0 varying the soft-breaking parameters M_3 and μ. Gluino masses up to 1600 GeV are excluded for $m_{\widetilde{\chi}_1^\pm}$ = 200 GeV. See their Figure 6a and text for details on the model.

[71] KHACHATRYAN 16AY searched in 2.3 fb^{-1} of pp collisions at $\sqrt{s}$ = 13 TeV for events with one isolated high transverse momentum lepton (e or μ), hadronic jets of which at least one is identified as coming from a b-quark, and large $\not{E}_T$. No significant excess above the Standard Model expectations is observed. Limits are set on the gluino mass in the Tglu3A simplified model, see Fig. 10, and in the Tglu3B model, see Fig. 11.

[72] KHACHATRYAN 16BT performed a global Bayesian analysis of a wide range of CMS results obtained with data samples corresponding to 5.0 fb^{-1} of pp collisions at $\sqrt{s}$ = 7 TeV and in 19.5 fb^{-1} of pp collisions at $\sqrt{s}$ = 8 TeV. The set of searches considered, both individually and in combination, includes those with all-hadronic final states, same-sign and opposite-sign dileptons, and multi-lepton final states. An interpretation was given in a scan of the 19-parameter pMSSM. No scan points with a gluino mass less than 500 GeV survived and 98% of models with a squark mass less than 300 GeV were excluded.

[73] KHACHATRYAN 16BX searched in 19.5 fb^{-1} of pp collisions at $\sqrt{s}$ = 8 TeV for events containing 4 leptons coming from R-parity-violating decays of $\widetilde{\chi}_1^0 \to \ell\ell\nu$ with $\lambda_{121} \neq 0$ or $\lambda_{122} \neq 0$. No excess over the expected background is observed. Limits are derived on the gluino, squark and stop masses, see Fig. 23.

[74] AAD 15AB searched for the decay of neutral, weakly interacting, long-lived particles in 20.3 fb^{-1} of pp collisions at $\sqrt{s}$ = 8 TeV. Signal events require at least two reconstructed vertices possibly originating from long-lived particles decaying to jets in the inner tracking detector and muon spectrometer. No significant excess of events over the expected background was found. Results were interpreted in Stealth SUSY benchmark models where a pair of gluinos decay to long-lived singlinos, $\widetilde{S}$, which in turn each decay to a low-mass gravitino and a pair of jets. The 95% confidence-level limits are set on the cross section × branching ratio for the decay $\widetilde{g} \to \widetilde{S}g$, as a function of the singlino proper lifetime ($c\tau$). See their Fig. 10(f)

[75] AAD 15AI searched in 20 fb^{-1} of pp collisions at $\sqrt{s}$ = 8 TeV for events containing at least one isolated lepton (electron or muon), jets, and large missing transverse momentum. No excess of events above the expected level of Standard Model background was found. Exclusion limits at 95% C.L. are set on the gluino mass in the CMSSM/mSUGRA, see Fig. 15, in the NUHMG, see Fig. 16, and in various simplified models, see Figs. 18–22.

[76] AAD 15CB searched for events containing at least one long-lived particle that decays at a significant distance from its production point (displaced vertex, DV) into two leptons or into five or more charged particles in 20.3 fb^{-1} of pp collisions at $\sqrt{s}$ = 8 TeV. The dilepton signature is characterised by DV formed from at least two lepton candidates. Four different final states were considered for the multitrak signature, in which the DV must be accompanied by a high-transverse momentum muon or electron candidate that originates from the DV, jets or missing transverse momentum. No events were observed in any of the signal regions. Results were interpreted in SUSY scenarios involving R-parity violation, split supersymmetry, and gauge mediation. See their Fig. 12–20.

[77] AAD 15X searched in 20.3 fb^{-1} of pp collisions at $\sqrt{s}$ = 8 TeV for events containing large number of jets, no requirements on missing transverse momentum and no isolated electrons or muons. The sensitivity of the search is enhanced by considering the number of b-tagged jets and the scalar sum of masses of large-radius jets in an event. No evidence was found for excesses above the expected level of Standard Model background. Exclusion limits at 95% C.L. are set on the gluino mass assuming the gluino decays to various quark flavors, and for various neutralino masses. See their Fig. 11–16.

[78] KHACHATRYAN 15AD searched in 19.4 fb^{-1} of pp collisions at $\sqrt{s}$ = 8 TeV for events with two opposite-sign same flavor isolated leptons featuring either a kinematic edge, or a peak at the Z-boson mass, in the invariant mass spectrum. No evidence for a statistically significant excess over the expected SM backgrounds is observed and 95% C.L. exclusion limits are derived in a simplified model of gluino pair production where the gluino decays into quarks, a Z-boson, and a massless gravitino LSP, see Fig. 9.

[79] KHACHATRYAN 15AZ searched in 19.7 fb^{-1} of pp collisions at $\sqrt{s}$ = 8 TeV for events with either at least one photon, hadronic jets and $\not{E}_T$ (single photon channel) or with at least two photons and at least one jet and using the razor variables. No significant excess above the Standard Model expectations is observed. Limits are set on gluino masses in the general gauge-mediated SUSY breaking model (GGM), for both a bino-like and wino-like neutralino NLSP scenario, see Fig. 8 and 9.

[80] AAD 14AX searched in 20.1 fb^{-1} of pp collisions at $\sqrt{s}$ = 8 TeV for the strong production of supersymmetric particles in events containing either zero or at last one high high-p_T lepton, large missing transverse momentum, high jet multiplicity and at least three jets identified as originating from b-quarks. No excess over the expected SM background is observed. Limits are derived in mSUGRA/CMSSM models with tanβ = 30, $A_0 = -2m_0$ and $\mu > 0$, see their Fig. 14. Also, exclusion limits in simplified models containing gluinos and scalar top and bottom quarks are set, see their Figures 12, 13.

[81] AAD 14E searched in 20.3 fb^{-1} of pp collisions at $\sqrt{s}$ = 8 TeV for strongly produced supersymmetric particles in events containing jets and two same-sign leptons or three leptons. The search also utilises jets originating from b-quarks, missing transverse momentum and other variables. No excess over the expected SM background is observed. Exclusion limits are derived in simplified models containing gluinos and squarks, see Figures 5 and 6. In the $\widetilde{g} \to qq'\widetilde{\chi}_1^\pm$, $\widetilde{\chi}_1^\pm \to W^{(*)\pm}\widetilde{\chi}_2^0$, $\widetilde{\chi}_2^0 \to Z^{(*)}\widetilde{\chi}_1^0$ simplified model, the following assumptions have been made: $m_{\widetilde{\chi}_1^\pm} = 0.5\ m_{\widetilde{\chi}_1^0} + m_{\widetilde{g}}$, $m_{\widetilde{\chi}_2^0} = 0.5\ (m_{\widetilde{\chi}_1^0} + m_{\widetilde{\chi}_1^\pm})$, $m_{\widetilde{\chi}_1^0} < 520$ GeV. In the $\widetilde{g} \to qq'\widetilde{\chi}_1^\pm$, $\widetilde{\chi}_1^\pm \to \ell^\pm\nu\widetilde{\chi}_1^0$ or $\widetilde{g} \to qq'\widetilde{\chi}_2^0$, $\widetilde{\chi}_2^0 \to \ell^\pm\ell^\mp(\nu\nu)\widetilde{\chi}_1^0$ simplified model, the following assumptions have been made: $m_{\widetilde{\chi}_1^\pm} = m_{\widetilde{\chi}_2^0} = 0.5\ (m_{\widetilde{\chi}_1^0} + m_{\widetilde{g}})$, $m_{\widetilde{\chi}_1^0} < 660$ GeV. Limits are also derived in the mSUGRA/CMSSM, bRPV and GMSB models, see their Fig. 8.

[82] CHATRCHYAN 14H searched in 19.5 fb^{-1} of pp collisions at $\sqrt{s}$ = 8 TeV for events with two isolated same-sign dileptons and jets in the final state. No significant excess above the Standard Model expectations is observed. Limits are set on the gluino mass in simplified models where the decay $\widetilde{g} \to t\overline{t}\widetilde{\chi}_1^0$ takes place with a branching ratio of 100%, or where the decay $\widetilde{g} \to \widetilde{t}\,t$, $\widetilde{t} \to t\widetilde{\chi}_1^0$ takes place with a branching ratio of 100%, with varying mass of the $\widetilde{\chi}_1^0$, or where the decay $\widetilde{g} \to \widetilde{b}\,b$, $\widetilde{b} \to t\widetilde{\chi}_1^\pm$, $\widetilde{\chi}_1^\pm \to W^\pm\widetilde{\chi}_1^0$ takes place with a branching ratio of 100%, with varying mass of the $\widetilde{\chi}_1^\pm$, see Fig. 5.

[83] CHATRCHYAN 14H searched in 19.5 fb^{-1} of pp collisions at $\sqrt{s}$ = 8 TeV for events with two isolated same-sign dileptons and jets in the final state. No significant excess above the Standard Model expectations is observed. Limits are set on the gluino mass in simplified models where the decay $\widetilde{g} \to qq'\widetilde{\chi}_1^\pm$, $\widetilde{\chi}_1^\pm \to W^\pm\widetilde{\chi}_1^0$ takes place with a branching ratio of 100%, with varying mass of the $\widetilde{\chi}_1^\pm$ and $\widetilde{\chi}_1^0$, see Fig. 7.

[84] CHATRCHYAN 14H searched in 19.5 fb^{-1} of pp collisions at $\sqrt{s}$ = 8 TeV for events with two isolated same-sign dileptons and jets in the final state. No significant excess above the Standard Model expectations is observed. Limits are set on the gluino mass in simplified models where the decay $\widetilde{g} \to b\overline{t}\widetilde{\chi}_1^\pm$, $\widetilde{\chi}_1^\pm \to W^\pm\widetilde{\chi}_1^0$ takes place with a branching ratio of 100%, for two choices of $m_{\widetilde{\chi}_1^\pm}$ and fixed $m_{\widetilde{\chi}_1^0}$, see Fig. 6.

[85] CHATRCHYAN 14H searched in 19.5 fb^{-1} of pp collisions at $\sqrt{s}$ = 8 TeV for events with two isolated same-sign dileptons and jets in the final state. No significant excess above the Standard Model expectations is observed. Limits are set on the gluino mass in simplified models where the R-parity violating decay $\widetilde{g} \to tbs$ takes place with a branching ratio of 100%, see Fig. 8.

Long-lived $\widetilde{g}$ (Gluino) mass limit

Limits on light gluinos ($m_{\widetilde{g}}$ < 5 GeV) were last listed in our PDG 14 edition: K. Olive, *et al.* (Particle Data Group), Chinese Physics **C38** 070001 (2014) (http://pdg.lbl.gov).

VALUE (GeV)	CL%	DOCUMENT ID		TECN	COMMENT
>1000	95	[1] KHACHATRY...17AR		CMS	long-lived $\widetilde{g}$, RPV, $\widetilde{g} \to t\overline{b}\overline{s}$, $c\tau$ = 0.3 mm
>1300	95	[1] KHACHATRY...17AR		CMS	long-lived $\widetilde{g}$, RPV, $\widetilde{g} \to t\overline{b}\overline{s}$, $c\tau$ = 1.0 mm
>1400	95	[1] KHACHATRY...17AR		CMS	long-lived $\widetilde{g}$, RPV, $\widetilde{g} \to t\overline{b}\overline{s}$, 2 mm < $c\tau$ < 30 mm
>1580	95	[2] AABOUD	16B	ATLS	long-lived R-hadrons
> 740–1590	95	[3] AABOUD	16C	ATLS	R-hadrons, Tglu1A, $\tau \geq$ 0.4 ns, $m_{\widetilde{\chi}_1^0}$ = 100 GeV
>1570	95	[3] AABOUD	16C	ATLS	R-hadrons, Tglu1A, stable
>1610	95	[4] KHACHATRY...16BW		CMS	long-lived $\widetilde{g}$ forming R-hadrons, f = 0.1, cloud interaction model
>1580	95	[4] KHACHATRY...16BW		CMS	long-lived $\widetilde{g}$ forming R-hadrons, f = 0.1, charge-suppressed interaction model
>1520	95	[4] KHACHATRY...16BW		CMS	long-lived $\widetilde{g}$ forming R-hadrons, f = 0.5, cloud interaction model
>1540	95	[4] KHACHATRY...16BW		CMS	long-lived $\widetilde{g}$ forming R-hadrons, f = 0.5, charge-suppressed interaction model
>1270	95	[5] AAD	15AE	ATLS	$\widetilde{g}$ R-hadron, generic R-hadron model
>1360	95	[5] AAD	15AE	ATLS	$\widetilde{g}$ decaying to 300 GeV stable sleptons, LeptoSUSY model
>1115	95	[6] AAD	15BM	ATLS	$\widetilde{g}$ R-hadron, stable
>1185	95	[6] AAD	15BM	ATLS	$\widetilde{g} \to (g/q\overline{q})\widetilde{\chi}_1^0$, lifetime 10 ns, $m_{\widetilde{\chi}_1^0}$ = 100 GeV
>1099	95	[6] AAD	15BM	ATLS	$\widetilde{g} \to (g/q\overline{q})\widetilde{\chi}_1^0$, lifetime 10 ns, $m_{\widetilde{g}} - m_{\widetilde{\chi}_1^0}$ = 100 GeV
>1182	95	[6] AAD	15BM	ATLS	$\widetilde{g} \to t\overline{t}\widetilde{\chi}_1^0$, lifetime 10 ns, $m_{\widetilde{\chi}_1^0}$ = 100 GeV
>1157	95	[6] AAD	15BM	ATLS	$\widetilde{g} \to t\overline{t}\widetilde{\chi}_1^0$, lifetime 10 ns, $m_{\widetilde{g}} - m_{\widetilde{\chi}_1^0}$ = 480 GeV
> 869	95	[6] AAD	15BM	ATLS	$\widetilde{g} \to (g/q\overline{q})\widetilde{\chi}_1^0$, lifetime 1 ns, $m_{\widetilde{\chi}_1^0}$ = 100 GeV
> 821	95	[6] AAD	15BM	ATLS	$\widetilde{g} \to (g/q\overline{q})\widetilde{\chi}_1^0$, lifetime 1 ns, $m_{\widetilde{g}} - m_{\widetilde{\chi}_1^0}$ = 100 GeV
> 836	95	[6] AAD	15BM	ATLS	$\widetilde{g} \to t\overline{t}\widetilde{\chi}_1^0$, lifetime 1 ns, $m_{\widetilde{\chi}_1^0}$ = 100 GeV
> 836	95	[6] AAD	15BM	ATLS	$\widetilde{g} \to t\overline{t}\widetilde{\chi}_1^0$, lifetime 10 ns, $m_{\widetilde{g}} - m_{\widetilde{\chi}_1^0}$ = 480 GeV
>1000	95	[7] KHACHATRY...15AK		CMS	$\widetilde{g}$ R-hadrons, 10 μs< τ <1000 s
> 880	95	[7] KHACHATRY...15AK		CMS	$\widetilde{g}$ R-hadrons, 1 μs< τ <1000 s
• • • We do not use the following data for averages, fits, limits, etc. • • •					
> 985	95	[8] AAD	13AA	ATLS	$\widetilde{g}$, R-hadrons, generic interaction model
> 832	95	[9] AAD	13BC	ATLS	R-hadrons, $\widetilde{g} \to g/q\overline{q}\widetilde{\chi}_1^0$, generic R-hadron model, lifetime between 10^{-5} and 10^3 s, $m_{\widetilde{\chi}_1^0}$ = 100 GeV
>1322	95	[10] CHATRCHYAN	13AB	CMS	long-lived $\widetilde{g}$ forming R-hadrons, f = 0.1, cloud interaction model
none 200–341	95	[11] AAD	12P	ATLS	long-lived $\widetilde{g} \to g\widetilde{\chi}_1^0$, $m_{\widetilde{\chi}_1^0}$ = 100 GeV
> 640	95	[12] CHATRCHYAN	12AN	CMS	long-lived $\widetilde{g} \to g\widetilde{\chi}_1^0$
>1098	95	[13] CHATRCHYAN	12L	CMS	long-lived $\widetilde{g}$ forming R-hadrons, f = 0.1

> 586	95	[14] AAD	11K	ATLS	stable $\tilde{g}$
> 544	95	[15] AAD	11P	ATLS	stable $\tilde{g}$, GMSB scenario, $\tan\beta$=5
> 370	95	[16] KHACHATRY...11		CMS	long lived $\tilde{g}$
> 398	95	[17] KHACHATRY...11C		CMS	stable $\tilde{g}$

[1] KHACHATRYAN 17AR searched in 17.6 fb^{-1} of pp collisions at $\sqrt{s}$ = 8 TeV for R-parity-violating SUSY in which long-lived neutralinos or gluinos decay into multijet final states. No significant excess above the Standard Model expectations is observed. Limits are set on the gluino mass for a range of mean proper decay lengths ($c\tau$), see their Fig. 7. The upper limits on the production cross section times branching ratio squared (Fig. 7) are also applicable to long-lived neutralinos.

[2] AABOUD 16B searched in 3.2 fb^{-1} of pp collisions at $\sqrt{s}$ = 13 TeV for long-lived R-hadrons using observables related to large ionization losses and slow propagation velocities, which are signatures of heavy charged particles traveling significantly slower than the speed of light. Exclusion limits at 95% C.L. are set on the long-lived gluino masses exceeding 1580 GeV. See their Fig. 5.

[3] AABOUD 16C searched in 3.2 fb^{-1} of pp collisions at $\sqrt{s}$ = 13 TeV for long-lived and stable R-hadrons identified by anomalous specific ionization energy loss in the ATLAS Pixel detector. Gluino R-hadrons with lifetimes above 0.4 ns are excluded at 95% C.L. with lower mass limit range between 740 GeV and 1590 GeV. In the case of stable R-hadrons, the lower mass limit is 1570 GeV. See their Figs. 5 and 6.

[4] KHACHATRYAN 16BW searched in 2.5 fb^{-1} of pp collisions at $\sqrt{s}$ = 13 TeV for events with heavy stable charged particles, identified by their anomalously high energy deposits in the silicon tracker and/or long time-of-flight measurements by the muon system. No evidence for an excess over the expected background is observed. Limits are derived for pair production of gluinos as a function of mass, depending on the interaction model and on the fraction f, of produced gluinos hadronizing into a $\tilde{g}$ - gluon state, see Fig. 4 and Table 7.

[5] AAD 15AE searched in 19.1 fb^{-1} of pp collisions at $\sqrt{s}$ = 8 TeV for heavy long-lived charged particles, measured through their specific ionization energy loss in the ATLAS pixel detector or their time-of-flight in the ALTAS muon system. In the absence of an excess of events above the expected backgrounds, limits are set R-hadrons in various scenarios, see Fig. 11. Limits are also set in LeptoSUSY models where the gluino decays to stable 300 GeV leptons, see Fig. 9.

[6] AAD 15BM searched in 18.4 fb^{-1} of pp collisions at $\sqrt{s}$ = 8 TeV for stable and metastable non-relativistic charged particles through their anomalous specific ionization energy loss in the ATLAS pixel detector. In absence of an excess of events above the expected backgrounds, limits are set within a generic R-hadron model, on stable gluino R-hadrons (see Table 5) and on metastable gluino R-hadrons decaying to $(g/q\overline{q})$ plus a light $\widetilde{\chi}_1^0$ (see Fig. 7) and decaying to $t\overline{t}$ plus a light $\widetilde{\chi}_1^0$ (see Fig. 9).

[7] KHACHATRYAN 15AK looked in a data set corresponding to 18.6 fb^{-1} of pp collisions at $\sqrt{s}$ = 8 TeV, and a search interval corresponding to 281 h of trigger lifetime, for long-lived particles that have stopped in the CMS detector. No evidence for an excess over the expected background in a cloud interaction model is observed. Assuming the decay $\tilde{g} \to g\widetilde{\chi}_1^0$ and lifetimes between 1 μs and 1000 s, limits are derived on $\tilde{g}$ production as a function of $m_{\widetilde{\chi}_1^0}$, see Figs. 4 and 6. The exclusions require that $m_{\widetilde{\chi}_1^0}$ is kinematically consistent with the minimum values of the jet energy thresholds used.

[8] AAD 13AA searched in 4.7 fb^{-1} of pp collisions at $\sqrt{s}$ = 7 TeV for events containing colored long-lived particles that hadronize forming R-hadrons. No significant excess above the expected background was found. Long-lived R-hadrons containing a $\tilde{g}$ are excluded for masses up to 985 GeV at 95% C.L in a general interaction model. Also, limits independent of the fraction of R-hadrons that arrive charged in the muon system were derived, see Fig. 6.

[9] AAD 13BC searched in 5.0 fb^{-1} of pp collisions at $\sqrt{s}$ = 7 TeV and in 22.9 fb^{-1} of pp collisions at $\sqrt{s}$ = 8 TeV for bottom squark R-hadrons that have come to rest within the ATLAS calorimeter and decay at some later time to hadronic jets and a neutralino. In absence of an excess of events above the expected backgrounds, limits are set on gluino masses for different decays, lifetimes, and neutralino masses, see their Table 6 and Fig. 10.

[10] CHATRCHYAN 13AB looked in 5.0 fb^{-1} of pp collisions at $\sqrt{s}$ = 7 TeV and in 18.8 fb^{-1} of pp collisions at $\sqrt{s}$ = 8 TeV for events with heavy stable particles, identified by their anomalous dE/dx in the tracker or additionally requiring that it be identified as muon in the muon chambers, from pair production of $\tilde{g}$'s. No evidence for an excess over the expected background is observed. Limits are derived for pair production of gluinos as a function of mass (see Fig. 8 and Table 5), depending on the fraction, f, of formation of $\tilde{g}-$g (R-gluonball) states. The quoted limit is for f = 0.1, while for f = 0.5 it degrades to 1276 GeV. In the conservative scenario where every hadronic interaction causes it to become neutral, the limit decreases to 928 GeV for f = 0.1.

[11] AAD 12P looked in 31 pb^{-1} of pp collisions at $\sqrt{s}$ = 7 TeV for events with pair production of long-lived gluinos. The hadronization of the gluinos leads to R-hadrons which may stop inside the detector and later decay via $\tilde{g} \to g\widetilde{\chi}_1^0$ during gaps between the proton bunches. No significant excess over the expected background is observed. From a counting experiment, a limit at 95% C.L. on the cross section as a function of $m_{\tilde{g}}$ is derived for $m_{\widetilde{\chi}_1^0}$ = 100 GeV, see Fig. 4. The limit is valid for lifetimes between 10^{-5} and 10^3 seconds and assumes the *Generic* matter interaction model for the production cross section.

[12] CHATRCHYAN 12AN looked in 4.0 fb^{-1} of pp collisions at $\sqrt{s}$ = 7 TeV for events with pair production of long-lived gluinos. The hadronization of the gluinos leads to R-hadrons which may stop inside the detector and later decay via $\tilde{g} \to g\widetilde{\chi}_1^0$ during gaps between the proton bunches. No significant excess over the expected background is observed. From a counting experiment, a limit at 95% C.L. on the cross section as a function of $m_{\tilde{g}}$ is derived, see Fig. 3. The mass limit is valid for lifetimes between 10^{-5} and 10^3 seconds, for what they call "the daughter gluon energy E_g >" 100 GeV and assuming the *cloud* interaction model for R-hadrons. Supersedes KHACHATRYAN 11.

[13] CHATRCHYAN 12L looked in 5.0 fb^{-1} of pp collisions at $\sqrt{s}$ = 7 TeV for events with heavy stable particles, identified by their anomalous dE/dx in the tracker or additionally requiring that it be identified as muon in the muon chambers, from pair production of $\tilde{g}$'s. No evidence for an excess over the expected background is observed. Limits are derived for pair production of gluinos as a function of mass (see Fig. 3), depending on the fraction, f, of formation of $\tilde{g}-$g (R-glueball) states. The quoted limit is for f = 0.1, while for f = 0.5 it degrades to 1046 GeV. In the conservative scenario where every hadronic interaction causes it to become neutral, the limit decreases to 928 GeV for f=0.1. Supersedes KHACHATRYAN 11C.

[14] AAD 11K looked in 34 pb^{-1} of pp collisions at $\sqrt{s}$ = 7 TeV for events with heavy stable particles, identified by their anomalous dE/dx in the tracker or time of flight in the tile calorimeter, from pair production of $\tilde{g}$. No evidence for an excess over the SM expectation is observed. Limits are derived for pair production of gluinos as a function of mass (see Fig. 4), for a fraction, f = 10%, of formation of $\tilde{g}-g$ (R-gluonball). If instead of a phase space driven approach for the hadronic scattering of the R-hadrons, a triple-Regge model or a bag-model is used, the limit degrades to 566 and 562 GeV, respectively.

[15] AAD 11P looked in 37 pb^{-1} of pp collisions at $\sqrt{s}$ = 7 TeV for events with heavy stable particles, reconstructed and identified by their time of flight in the Muon System. There is no requirement on their observation in the tracker to increase the sensitivity to cases where gluinos have a large fraction, f, of formation of neutral $\tilde{g}-g$ (R-gluonball). No evidence for an excess over the SM expectation is observed. Limits are derived as a function of mass (see Fig. 4), for f=0.1. For fractions f = 0.5 and 1.0 the limit degrades to 537 and 530 GeV, respectively.

[16] KHACHATRYAN 11 looked in 10 pb^{-1} of pp collisions at $\sqrt{s}$ = 7 TeV for events with pair production of long-lived gluinos. The hadronization of the gluinos leads to R-hadrons which may stop inside the detector and later decay via $\tilde{g} \to g\widetilde{\chi}_1^0$ during gaps between the proton bunches. No significant excess over the expected background is observed. From a counting experiment, a limit at 95% C.L. on the cross section times branching ratio is derived for $m_{\tilde{g}}-m_{\widetilde{\chi}_1^0} > 100$ GeV, see their Fig. 2. Assuming 100% branching ratio, lifetimes between 75 ns and 3×10^5 s are excluded for $m_{\tilde{g}}$ = 300 GeV. The $\tilde{g}$ mass exclusion is obtained with the same assumptions for lifetimes between 10 μs and 1000 s, but shows some dependence on the model for R-hadron interactions with matter, illustrated in Fig. 3. From a time-profile analysis, the mass exclusion is 382 GeV for a lifetime of 10 μs under the same assumptions as above.

[17] KHACHATRYAN 11C looked in 3.1 pb^{-1} of pp collisions at $\sqrt{s}$ = 7 TeV for events with heavy stable particles, identified by their anomalous dE/dx in the tracker or additionally requiring that it be identified as muon in the muon chambers, from pair production of $\tilde{g}$. No evidence for an excess over the expected background is observed. Limits are derived for pair production of gluinos as a function of mass (see Fig. 3), depending on the fraction, f, of formation of $\tilde{g}-g$ (R-gluonball). The quoted limit is for f=0.1, while for f=0.5 it degrades to 357 GeV. In the conservative scenario where every hadronic interaction causes it to become neutral, the limit decreases to 311 GeV for f=0.1.

Light $\widetilde{G}$ (Gravitino) mass limits from collider experiments

The following are bounds on light ($\ll$ 1 eV) gravitino indirectly inferred from its coupling to matter suppressed by the gravitino decay constant.

Unless otherwise stated, all limits assume that other supersymmetric particles besides the gravitino are too heavy to be produced. The gravitino is assumed to be undetected and to give rise to a missing energy ($\not{E}$) signature.

Some earlier papers are now obsolete and have been omitted. They were last listed in our PDG 14 edition: K. Olive, *et al.* (Particle Data Group), Chinese Physics **C38** 070001 (2014) (http://pdg.lbl.gov).

VALUE (eV)	CL%	DOCUMENT ID		TECN	COMMENT
• • • We do not use the following data for averages, fits, limits, etc. • • •					
> 3.5 $\times 10^{-4}$	95	[1] AAD	15BH	ATLS	jet + $\not{E}_T$, $pp \to (\tilde{q}/\tilde{g})\widetilde{G}$, $m_{\tilde{q}} = m_{\tilde{g}}$ = 500 GeV
> 3 $\times 10^{-4}$	95	[1] AAD	15BH	ATLS	jet + $\not{E}_T$, $pp \to (\tilde{q}/\tilde{g})\widetilde{G}$, $m_{\tilde{q}} = m_{\tilde{g}}$ = 1000 GeV
> 2 $\times 10^{-4}$	95	[1] AAD	15BH	ATLS	jet + $\not{E}_T$, $pp \to (\tilde{q}/\tilde{g})\widetilde{G}$, $m_{\tilde{q}} = m_{\tilde{g}}$ = 1500 GeV
> 1.09 $\times 10^{-5}$	95	[2] ABDALLAH	05B	DLPH	$e^+e^- \to \widetilde{G}\widetilde{G}\gamma$
> 1.35 $\times 10^{-5}$	95	[3] ACHARD	04E	L3	$e^+e^- \to \widetilde{G}\widetilde{G}\gamma$
> 1.3 $\times 10^{-5}$		[4] HEISTER	03C	ALEP	$e^+e^- \to \widetilde{G}\widetilde{G}\gamma$
>11.7 $\times 10^{-6}$	95	[5] ACOSTA	02H	CDF	$p\overline{p} \to \widetilde{G}\widetilde{G}\gamma$
> 8.7 $\times 10^{-6}$	95	[6] ABBIENDI,G	00D	OPAL	$e^+e^- \to \widetilde{G}\widetilde{G}\gamma$

[1] AAD 15BH searched in 20.3 fb^{-1} of pp collisions at $\sqrt{s}$ = 8 TeV for associated production of a light gravitino and a squark or gluino. The squark (gluino) is assumed to decay exclusively to a quark (gluon) and a gravitino. No evidence was found for an excess above the expected level of Standard Model background and 95% C.L. lower limits were set on the gravitino mass as a function of the squark/gluino mass, both in the case of degenerate and non-degenerate squark/gluino masses, see Figs. 14 and 15.

[2] ABDALLAH 05B use data from $\sqrt{s}$ = 180–208 GeV. They look for events with a single photon + $\not{E}$ final states from which a cross section limit of $\sigma < 0.18$ pb at 208 GeV is obtained, allowing a limit on the mass to be set. Supersedes the results of ABREU 00Z.

[3] ACHARD 04E use data from $\sqrt{s}$ = 189–209 GeV. They look for events with a single photon + $\not{E}$ final states from which a limit on the Gravitino mass is set corresponding to $\sqrt{F} > 238$ GeV. Supersedes the results of ACCIARRI 99R.

[4] HEISTER 03C use the data from $\sqrt{s}$ = 189–209 GeV to search for $\gamma\not{E}_T$ final states.

[5] ACOSTA 02H looked in 87 pb^{-1} of $p\overline{p}$ collisions at $\sqrt{s}$=1.8 TeV for events with a high-E_T photon and $\not{E}_T$. They compared the data with a GMSB model where the final state could arise from $q\overline{q} \to \widetilde{G}\,\widetilde{G}\,\gamma$. Since the cross section for this process scales as $1/|F|^4$, a limit at 95% CL is derived on $|F|^{1/2} > 221$ GeV. A model independent limit for the above topology is also given in the paper.

[6] ABBIENDI,G 00D searches for $\gamma\not{E}$ final states from $\sqrt{s}$=189 GeV.

Supersymmetry miscellaneous results

Results that do not appear under other headings or that make nonminimal assumptions.

Some earlier papers are now obsolete and have been omitted. They were last listed in our PDG 14 edition: K. Olive, *et al.* (Particle Data Group), Chinese Physics **C38** 070001 (2014) (http://pdg.lbl.gov).

VALUE	CL%	DOCUMENT ID		TECN	COMMENT
• • • We do not use the following data for averages, fits, limits, etc. • • •					
>65	95	[1] AABOUD	16AF	ATLS	selected ATLAS searches on EWK sector

none 0–2	95	[2] AAD	16AG	ATLS	dark photon, γ_d, in SUSY- and Higgs-portal models
		[3] AAD	13P	ATLS	dark γ, hidden valley
		[4] AALTONEN	12AB	CDF	hidden-valley Higgs
none 100–185	95	[5] AAD	11AA	ATLS	scalar gluons
		[6] CHATRCHYAN	11E	CMS	$\mu\mu$ resonances
		[7] ABAZOV	10N	D0	γ_D, hidden valley

[1] AABOUD 16AF uses a selection of searches by ATLAS for the electroweak production of SUSY particles studying resulting constraints on dark matter candidates. They use 20 fb^{-1} of pp collisions at $\sqrt{s} = 8$ TeV. A likelihood-driven scan of an effective model focusing on the gaugino-higgsino and Higgs sector of the pMSSM is performed. The ATLAS searches impact models where $m_{\tilde{\chi}_1^0} < 65$ GeV, excluding 86% of them. See their Figs. 2, 4, and 6.

[2] AAD 16AG searches for prompt lepton-jets using 20 fb^{-1} of pp collisions at $\sqrt{s} = 8$ TeV collected with the ATLAS detector. Lepton-jets are expected from decays of low-mass dark photons in SUSY-portal and Higgs-portal models. No significant excess of events is observed and 95% CL upper limits are computed on the production cross section times branching ratio for two prompt lepton-jets in models predicting 2 or 4 γ_d via SUSY-portal topologies, for γ_d mass values between 0 and 2 GeV. See their Figs 9 and 10. The results are also interpreted in terms of a 90% CL exclusion region in kinetic mixing and dark-photon mass parameter space. See their Fig. 13.

[3] AAD 13P searched in 5 fb^{-1} of pp collisions at $\sqrt{s} = 7$ TeV for single lepton-jets with at least four muons; pairs of lepton-jets, each with two or more muons; and pairs of lepton-jets with two or more electrons. All of these could be signatures of Hidden Valley supersymmetric models. No statistically significant deviations from the Standard Model expectations are found. 95% C.L. limits are placed on the production cross section times branching ratio of dark photons for several parameter sets of a Hidden Valley model.

[4] AALTONEN 12AB looked in 5.1 fb^{-1} of $p\overline{p}$ collisions at $\sqrt{s} = 1.96$ TeV for anomalous production of multiple low-energy leptons in association with a W or Z boson. Such events may occur in hidden valley models in which a supersymmetric Higgs boson is produced in association with a W or Z boson, with $H \rightarrow \tilde{\chi}_1^0\tilde{\chi}_1^0$ pair and with the $\tilde{\chi}_1^0$ further decaying into a dark photon (γ_D) and the unobservable lightest SUSY particle of the hidden sector. As the γ_D is expected to be light, it may decay into a lepton pair. No significant excess over the SM expectation is observed and a limit at 95% C.L. is set on the cross section for a benchmark model of supersymmetric hidden-valley Higgs production.

[5] AAD 11AA looked in 34 pb^{-1} of pp collisions at $\sqrt{s} = 7$ TeV for events with ≥ 4 jets originating from pair production of scalar gluons, each decaying to two gluons. No two-jet resonances are observed over the SM background. Limits are derived on the cross section times branching ratio (see Fig. 3). Assuming 100% branching ratio for the decay to two gluons, the quoted exclusion range is obtained, except for a 5 GeV mass window around 140 GeV.

[6] CHATRCHYAN 11E looked in 35 pb^{-1} of pp collisions at $\sqrt{s} = 7$ TeV for events with collimated μ pairs (leptonic jets) from the decay of hidden sector states. No evidence for new resonance production is found. Limits are derived and compared to various SUSY models (see Fig. 4) where the LSP, either the $\tilde{\chi}_1^0$ or a $\tilde{q}$, decays to dark sector particles.

[7] ABAZOV 10N looked in 5.8 fb^{-1} of $p\overline{p}$ collisions at $\sqrt{s} = 1.96$ TeV for events from hidden valley models in which a $\tilde{\chi}_1^0$ decays into a dark photon, γ_D, and the unobservable lightest SUSY particle of the hidden sector. As the γ_D is expected to be light, it may decay into a tightly collimated lepton pair, called lepton jet. They searched for events with $\not{E}_T$ and two isolated lepton jets observable by an opposite charged lepton pair ee, $e\mu$ or $\mu\mu$. No significant excess over the SM expectation is observed, and a limit at 95% C.L. on the cross section times branching ratio is derived, see their Table I. They also examined the invariant mass of the lepton jets for a narrow resonance, see their Fig. 4, but found no evidence for a signal.

REFERENCES FOR Supersymmetric Particle Searches

SIRUNYAN	18B	PL B778 263	A.M. Sirunyan *et al.*	(CMS Collab.)
SIRUNYAN	18C	PR D97 032009	A.M. Sirunyan *et al.*	(CMS Collab.)
SIRUNYAN	18D	PR D97 012007	A.M. Sirunyan *et al.*	(CMS Collab.)
AABOUD	17AF	JHEP 1708 006	M. Aaboud *et al.*	(ATLAS Collab.)
AABOUD	17AI	JHEP 1709 088	M. Aaboud *et al.*	(ATLAS Collab.)
AABOUD	17AJ	JHEP 1709 084	M. Aaboud *et al.*	(ATLAS Collab.)
AABOUD	17AR	PR D96 112010	M. Aaboud *et al.*	(ATLAS Collab.)
AABOUD	17AX	JHEP 1711 195	M. Aaboud *et al.*	(ATLAS Collab.)
AABOUD	17AY	JHEP 1712 085	M. Aaboud *et al.*	(ATLAS Collab.)
AABOUD	17AZ	JHEP 1712 034	M. Aaboud *et al.*	(ATLAS Collab.)
AABOUD	17BE	EPJ C77 898	M. Aaboud *et al.*	(ATLAS Collab.)
AABOUD	17N	EPJ C77 144	M. Aaboud *et al.*	(ATLAS Collab.)
AAIJ	17Z	EPJ C77 224	R. Aaij *et al.*	(LHCb Collab.)
AARTSEN	17	EPJ C77 82	M.G. Aartsen *et al.*	(IceCube Collab.)
AARTSEN	17A	EPJ C77 146	M.G. Aartsen *et al.*	(IceCube Collab.)
AARTSEN	17C	EPJ C77 627	M.G. Aartsen *et al.*	(IceCube Collab.)
AKERIB	17	PRL 118 021303	D.S. Akerib *et al.*	(LUX Collab.)
AKERIB	17A	PRL 118 251302	D.S. Akerib *et al.*	(LUX Collab.)
ALBERT	17A	PL B769 249	A. Albert *et al.*	(ANTARES Collab.)
AMOLE	17	PRL 118 251301	C. Amole *et al.*	(PICO Collab.)
APRILE	17G	PRL 119 181301	E. Aprile *et al.*	(XENON Collab.)
ARCHAMBAU...	17	PR D95 082001	S. Archambault *et al.*	(VERITAS Collab.)
BATTAT	17	ASP 91 65	J.B.R. Battat *et al.*	(DRIFT-IId Collab.)
BEHNKE	17	ASP 90 85	E. Behnke *et al.*	(PICASSO Collab.)
CUI	17A	PRL 119 181302	X. Cui *et al.*	(PandaX-II Collab.)
FU	17	PRL 118 071301	C. Fu *et al.*	(PandaX Collab.)
KHACHATRY...	17	PR D95 012003	V. Khachatryan *et al.*	(CMS Collab.)
KHACHATRY...	17A	PRL 118 021802	V. Khachatryan *et al.*	(CMS Collab.)
KHACHATRY...	17AD	PR D96 012004	V. Khachatryan *et al.*	(CMS Collab.)
KHACHATRY...	17AR	PR D95 012009	V. Khachatryan *et al.*	(CMS Collab.)
KHACHATRY...	17AS	PR D95 012011	V. Khachatryan *et al.*	(CMS Collab.)
KHACHATRY...	17AW	EPJ C77 635	V. Khachatryan *et al.*	(CMS Collab.)
KHACHATRY...	17L	JHEP 1704 018	V. Khachatryan *et al.*	(CMS Collab.)
KHACHATRY...	17P	EPJ C77 294	V. Khachatryan *et al.*	(CMS Collab.)
KHACHATRY...	17S	PL B767 403	V. Khachatryan *et al.*	(CMS Collab.)
KHACHATRY...	17V	PL B769 391	V. Khachatryan *et al.*	(CMS Collab.)
KHACHATRY...	17Y	PL B770 257	V. Khachatryan *et al.*	(CMS Collab.)
SIRUNYAN	17AF	PRL 119 151802	A.M. Sirunyan *et al.*	(CMS Collab.)
SIRUNYAN	17AS	JHEP 1710 019	A.M. Sirunyan *et al.*	(CMS Collab.)
SIRUNYAN	17AT	JHEP 1710 005	A.M. Sirunyan *et al.*	(CMS Collab.)
SIRUNYAN	17AW	JHEP 1711 029	A.M. Sirunyan *et al.*	(CMS Collab.)
SIRUNYAN	17AY	JHEP 1712 142	A.M. Sirunyan *et al.*	(CMS Collab.)
SIRUNYAN	17AZ	EPJ C77 710	A.M. Sirunyan *et al.*	(CMS Collab.)
SIRUNYAN	17K	EPJ C77 327	A.M. Sirunyan *et al.*	(CMS Collab.)
SIRUNYAN	17P	PR D96 032003	A.M. Sirunyan *et al.*	(CMS Collab.)
SIRUNYAN	17S	EPJ C77 578	A.M. Sirunyan *et al.*	(CMS Collab.)
AABOUD	16AC	EPJ C76 683	M. Aaboud *et al.*	(ATLAS Collab.)
AABOUD	16AF	JHEP 1609 175	M. Aaboud et al	(ATLAS Collab.)
AABOUD	16B	PL B760 647	M. Aaboud *et al.*	(ATLAS Collab.)
AABOUD	16C	PR D93 112015	M. Aaboud *et al.*	(ATLAS Collab.)
AABOUD	16D	PR D94 032005	M. Aaboud *et al.*	(ATLAS Collab.)
AABOUD	16J	PR D94 052009	M. Aaboud *et al.*	(ATLAS Collab.)
AABOUD	16M	EPJ C76 517	M. Aaboud *et al.*	(ATLAS Collab.)
AABOUD	16N	EPJ C76 392	M. Aaboud *et al.*	(ATLAS Collab.)
AABOUD	16P	EPJ C76 541	M. Aaboud *et al.*	(ATLAS Collab.)
AABOUD	16Q	EPJ C76 547	M. Aaboud *et al.*	(ATLAS Collab.)
AAD	16AA	PR D93 052002	G. Aad *et al.*	(ATLAS Collab.)
AAD	16AD	PR D94 032003	G. Aad *et al.*	(ATLAS Collab.)
AAD	16AG	JHEP 1602 062	G. Aad *et al.*	(ATLAS Collab.)
AAD	16AM	JHEP 1606 067	G. Aad *et al.*	(ATLAS Collab.)
AAD	16AY	EPJ C76 81	G. Aad *et al.*	(ATLAS Collab.)
AAD	16BB	EPJ C76 259	G. Aad *et al.*	(ATLAS Collab.)
AAD	16BG	EPJ C76 565	G. Aad *et al.*	(ATLAS Collab.)
AAD	16V	PL B757 334	G. Aad *et al.*	(ATLAS Collab.)
AARTSEN	16C	JCAP 1604 022	M.G. Aartsen *et al.*	(IceCube Collab.)
AARTSEN	16D	EPJ C76 531	M.G. Aartsen *et al.*	(IceCube Collab.)
ABDALLAH	16	PRL 117 111301	H. Abdallah *et al.*	(H.E.S.S. Collab.)
ABDALLAH	16A	PRL 117 151302	H. Abdallah *et al.*	(H.E.S.S. Collab.)
ADRIAN-MAR...	16	PL B759 69	S. Adrian-Martinez *et al.*	(ANTARES Collab.)
AHNEN	16	JCAP 1602 039	M.L. Ahnen *et al.*	(MAGIC and Fermi-LAT Collab.)
AKERIB	16	PRL 116 161301	D.S. Akerib *et al.*	(LUX Collab.)
AKERIB	16A	PRL 116 161302	D.S. Akerib *et al.*	(LUX Collab.)
AMOLE	16	PR D93 052014	C. Amole *et al.*	(PICO Collab.)
AMOLE	16A	PR D93 061101	C. Amole *et al.*	(PICO Collab.)
APRILE	16B	PR D94 122001	E. Aprile *et al.*	(XENON100 Collab.)
AVRORIN	16	ASP 81 12	A.D. Avrorin *et al.*	(BAIKAL Collab.)
CIRELLI	16	JCAP 1607 041	M. Cirelli, M. Taoso	(LPNHE, MADE)
KHACHATRY...	16AA	PL B759 479	V. Khachatryan *et al.*	(CMS Collab.)
KHACHATRY...	16AC	PL B760 178	V. Khachatryan *et al.*	(CMS Collab.)
KHACHATRY...	16AM	PR D93 092009	V. Khachatryan *et al.*	(CMS Collab.)
KHACHATRY...	16AV	JHEP 1607 027	V. Khachatryan *et al.*	(CMS Collab.)
KHACHATRY...	16AY	JHEP 1608 122	V. Khachatryan *et al.*	(CMS Collab.)
KHACHATRY...	16BE	EPJ C76 317	V. Khachatryan *et al.*	(CMS Collab.)
KHACHATRY...	16BJ	EPJ C76 439	V. Khachatryan *et al.*	(CMS Collab.)
KHACHATRY...	16BK	EPJ C76 460	V. Khachatryan *et al.*	(CMS Collab.)
KHACHATRY...	16BS	JHEP 1610 006	V. Khachatryan *et al.*	(CMS Collab.)
KHACHATRY...	16BT	JHEP 1610 129	V. Khachatryan *et al.*	(CMS Collab.)
KHACHATRY...	16BW	PR D94 112004	V. Khachatryan *et al.*	(CMS Collab.)
KHACHATRY...	16BX	PR D94 112009	V. Khachatryan *et al.*	(CMS Collab.)
KHACHATRY...	16BY	JHEP 1612 013	V. Khachatryan *et al.*	(CMS Collab.)
KHACHATRY...	16R	PL B757 6	V. Khachatryan *et al.*	(CMS Collab.)
KHACHATRY...	16V	PL B758 152	V. Khachatryan *et al.*	(CMS Collab.)
KHACHATRY...	16Y	PL B759 9	V. Khachatryan *et al.*	(CMS Collab.)
LEITE	16	JCAP 1611 021	N. Leite *et al.*	
TAN	16B	PRL 117 121303	A. Tan *et al.*	(PandaX Collab.)
AAD	15AB	PR D92 012010	G. Aad *et al.*	(ATLAS Collab.)
AAD	15AE	JHEP 1501 068	G. Aad *et al.*	(ATLAS Collab.)
AAD	15AI	JHEP 1504 116	G. Aad *et al.*	(ATLAS Collab.)
AAD	15BA	EPJ C75 208	G. Aad *et al.*	(ATLAS Collab.)
AAD	15BG	EPJ C75 318	G. Aad *et al.*	(ATLAS Collab.)
Also		EPJ C75 463	G. Aad *et al.*	(ATLAS Collab.)
AAD	15BH	EPJ C75 299	G. Aad *et al.*	(ATLAS Collab.)
Also		EPJ C75 408 (errat.)	G. Aad *et al.*	(ATLAS Collab.)
AAD	15BM	EPJ C75 407	G. Aad *et al.*	(ATLAS Collab.)
AAD	15BV	JHEP 1510 054	G. Aad *et al.*	(ATLAS Collab.)
AAD	15BX	JHEP 1510 134	G. Aad *et al.*	(ATLAS Collab.)
AAD	15CA	PR D92 072001	G. Aad *et al.*	(ATLAS Collab.)
AAD	15CB	PR D92 072004	G. Aad *et al.*	(ATLAS Collab.)
AAD	15CJ	EPJ C75 510	G. Aad	(ATLAS Collab.)
AAD	15CS	PR D91 012008	G. Aad *et al.*	(ATLAS Collab.)
Also		PR D92 059903 (errat.)	G. Aad *et al.*	(ATLAS Collab.)
AAD	15J	PRL 114 142001	G. Aad *et al.*	(ATLAS Collab.)
AAD	15K	PRL 114 161801	G. Aad *et al.*	(ATLAS Collab.)
AAD	15O	PRL 115 031801	G. Aad *et al.*	(ATLAS Collab.)
AAD	15X	PR D91 112016	G. Aad *et al.*	(ATLAS Collab.)
AAIJ	15BD	EPJ C75 595	R. Aaij *et al.*	(LHCb Collab.)
AARTSEN	15C	EPJ C75 20	M.G. Aartsen *et al.*	(IceCube Collab.)
AARTSEN	15E	EPJ C75 492	M.G. Aartsen *et al.*	(IceCube Collab.)
ABRAMOWSKI	15	PRL 114 081301	A. Abramowski *et al.*	(H.E.S.S. Collab.)
ACKERMANN	15	PR D91 122002	M. Ackermann *et al.*	(Fermi-LAT Collab.)
ACKERMANN	15A	JCAP 1509 008	M. Ackermann *et al.*	(Fermi-LAT Collab.)
ACKERMANN	15B	PRL 115 231301	M. Ackermann *et al.*	(Fermi-LAT Collab.)
ADRIAN-MAR...	15	JCAP 1510 068	S. Adrian-Martinez *et al.*	(ANTARES Collab.)
AGNES	15	PL B743 456	P. Agnes *et al.*	(DarkSide-50 Collab.)
AGNESE	15B	PR D92 072003	R. Agnese *et al.*	(SuperCDMS Collab.)
BUCKLEY	15	PR D91 102001	M.R. Buckley *et al.*	
CHOI	15	PRL 114 141301	K. Choi *et al.*	(Super-Kamiokande Collab.)
KHACHATRY...	15AB	JHEP 1501 096	V. Khachatryan *et al.*	(CMS Collab.)
KHACHATRY...	15AD	JHEP 1504 124	V. Khachatryan *et al.*	(CMS Collab.)
KHACHATRY...	15AF	JHEP 1505 078	V. Khachatryan *et al.*	(CMS Collab.)
KHACHATRY...	15AH	JHEP 1506 116	V. Khachatryan *et al.*	(CMS Collab.)
KHACHATRY...	15AK	EPJ C75 151	V. Khachatryan *et al.*	(CMS Collab.)
KHACHATRY...	15AO	EPJ C75 325	V. Khachatryan *et al.*	(CMS Collab.)
KHACHATRY...	15AR	PL B743 503	V. Khachatryan *et al.*	(CMS Collab.)
KHACHATRY...	15AZ	PR D92 072006	V. Khachatryan *et al.*	(CMS Collab.)
KHACHATRY...	15E	PRL 114 061801	V. Khachatryan *et al.*	(CMS Collab.)
KHACHATRY...	15I	PL B745 5	V. Khachatryan *et al.*	(CMS Collab.)
KHACHATRY...	15L	PL B747 98	V. Khachatryan *et al.*	(CMS Collab.)
KHACHATRY...	15O	PL B748 255	V. Khachatryan *et al.*	(CMS Collab.)
KHACHATRY...	15W	PR D91 052012	V. Khachatryan *et al.*	(CMS Collab.)
KHACHATRY...	15X	PR D91 052018	V. Khachatryan *et al.*	(CMS Collab.)
ROLBIECKI	15	PL B750 247	K. Rolbiecki, J. Tattersall	(MADE, HEID)
AAD	14AE	JHEP 1409 176	G. Aad *et al.*	(ATLAS Collab.)
AAD	14AG	JHEP 1409 103	G. Aad *et al.*	(ATLAS Collab.)
AAD	14AJ	JHEP 1409 015	G. Aad *et al.*	(ATLAS Collab.)
AAD	14AV	JHEP 1410 096	G. Aad *et al.*	(ATLAS Collab.)
AAD	14AX	JHEP 1410 024	G. Aad *et al.*	(ATLAS Collab.)
AAD	14B	EPJ C74 2883	G. Aad *et al.*	(ATLAS Collab.)
AAD	14BD	JHEP 1411 118	G. Aad *et al.*	(ATLAS Collab.)
AAD	14BH	PR D90 112005	G. Aad *et al.*	(ATLAS Collab.)
AAD	14E	JHEP 1406 035	G. Aad *et al.*	(ATLAS Collab.)
AAD	14F	JHEP 1406 124	G. Aad *et al.*	(ATLAS Collab.)
AAD	14G	JHEP 1405 071	G. Aad *et al.*	(ATLAS Collab.)
AAD	14H	JHEP 1404 169	G. Aad *et al.*	(ATLAS Collab.)
AAD	14K	PR D90 012004	G. Aad *et al.*	(ATLAS Collab.)
AAD	14T	PR D90 052008	G. Aad *et al.*	(ATLAS Collab.)
AAD	14X	PR D90 052001	G. Aad *et al.*	(ATLAS Collab.)
AALTONEN	14	PR D90 012011	T. Aaltonen *et al.*	(CDF Collab.)
ACKERMANN	14	PR D89 042001	M. Ackermann *et al.*	(Fermi-LAT Collab.)
AKERIB	14	PRL 112 091303	D.S. Akerib *et al.*	(LUX Collab.)
ALEKSIC	14	JCAP 1402 008	J. Aleksic *et al.*	(MAGIC Collab.)
AVRORIN	14	ASP 62 12	A.D. Avrorin *et al.*	(BAIKAL Collab.)
BUCHMUEL...	14	EPJ C74 2809	O. Buchmueller *et al.*	
BUCHMUEL...	14A	EPJ C74 2922	O. Buchmueller *et al.*	
CHATRCHYAN	14AH	PR D90 112001	S. Chatrchyan *et al.*	(CMS Collab.)
CHATRCHYAN	14H	JHEP 1401 163	S. Chatrchyan *et al.*	(CMS Collab.)
CHATRCHYAN	14I	JHEP 1406 055	S. Chatrchyan *et al.*	(CMS Collab.)

Searches Particle Listings

Supersymmetric Particle Searches

CHATRCHYAN 14N PL B733 328 S. Chatrchyan *et al.* (CMS Collab.)
CHATRCHYAN 14P PL B730 193 S. Chatrchyan *et al.* (CMS Collab.)
CHATRCHYAN 14R PR D90 032006 S. Chatrchyan *et al.* (CMS Collab.)
CHATRCHYAN 14U PRL 112 161802 S. Chatrchyan *et al.* (CMS Collab.)
CZAKON 14 PRL 113 201803 M. Czakon *et al.* (AACH, CAMB, UCB, LBL+)
FELIZARDO 14 PR D89 072013 M. Felizardo *et al.* (SIMPLE Collab.)
KHACHATRY... 14C PL B736 371 V. Khachatryan *et al.* (CMS Collab.)
KHACHATRY... 14I EPJ C74 3036 V. Khachatryan *et al.* (CMS Collab.)
KHACHATRY... 14L PR D90 092007 V. Khachatryan *et al.* (CMS Collab.)
KHACHATRY... 14T PL B739 229 V. Khachatryan *et al.* (CMS Collab.)
PDG 14 CP C38 070001 K. Olive *et al.* (PDG Collab.)
ROSZKOWSKI 14 JHEP 1408 067 L. Roszkowski, E.M. Sessolo, A.J. Williams (WINR)
AAD 13 PL B718 841 G. Aad *et al.* (ATLAS Collab.)
AAD 13AA PL B720 277 G. Aad *et al.* (ATLAS Collab.)
AAD 13AI PL B723 15 G. Aad *et al.* (ATLAS Collab.)
AAD 13AP PR D88 012001 G. Aad *et al.* (ATLAS Collab.)
AAD 13AU JHEP 1310 189 G. Aad *et al.* (ATLAS Collab.)
AAD 13B PL B718 879 G. Aad *et al.* (ATLAS Collab.)
AAD 13BC PR D88 112003 G. Aad *et al.* (ATLAS Collab.)
AAD 13BD PR D88 112006 G. Aad *et al.* (ATLAS Collab.)
AAD 13H JHEP 1301 131 G. Aad *et al.* (ATLAS Collab.)
AAD 13L PR D87 012008 G. Aad *et al.* (ATLAS Collab.)
AAD 13P PL B719 299 G. Aad *et al.* (ATLAS Collab.)
AAD 13Q PL B719 261 G. Aad *et al.* (ATLAS Collab.)
AAD 13R PL B719 280 G. Aad *et al.* (ATLAS Collab.)
AALTONEN 13I PR D88 031103 T. Aaltonen *et al.* (CDF Collab.)
AALTONEN 13Q PRL 110 201802 T. Aaltonen *et al.* (CDF Collab.)
AARTSEN 13C PR D88 122001 M.G. Aartsen *et al.* (IceCube Collab.)
ABAZOV 13B PR D87 052011 V.M. Abazov *et al.* (D0 Collab.)
ABRAMOWSKI 13 PRL 110 041301 A. Abramowski *et al.* (H.E.S.S. Collab.)
ACKERMANN 13A PR D88 082002 M. Ackermann *et al.* (Fermi-LAT Collab.)
ADRIAN-MAR... 13 JCAP 1311 032 S. Adrian-Martinez *et al.* (ANTARES Collab.)
AGNESE 13 PR D88 031104 R. Agnese *et al.* (CDMS Collab.)
AGNESE 13A PRL 111 251301 R. Agnese *et al.* (CDMS Collab.)
APRILE 13 PRL 111 021301 E. Aprile *et al.* (XENON100 Collab.)
BERGSTROM 13 PRL 111 171101 L. Bergstrom *et al.*
BOLIEV 13 JCAP 1309 019 M. Boliev *et al.*
CABRERA 13 JHEP 1307 182 M. Cabrera, J. Casas, R. de Austri
CHATRCHYAN 13 PL B718 815 S. Chatrchyan *et al.* (CMS Collab.)
CHATRCHYAN 13AB JHEP 1307 122 S. Chatrchyan *et al.* (CMS Collab.)
CHATRCHYAN 13AH PL B722 273 S. Chatrchyan *et al.* (CMS Collab.)
CHATRCHYAN 13AO PR D87 072001 S. Chatrchyan *et al.* (CMS Collab.)
CHATRCHYAN 13AT PR D88 052017 S. Chatrchyan *et al.* (CMS Collab.)
CHATRCHYAN 13AV PRL 111 081802 S. Chatrchyan *et al.* (CMS Collab.)
CHATRCHYAN 13G JHEP 1301 077 S. Chatrchyan *et al.* (CMS Collab.)
CHATRCHYAN 13H PL B719 42 S. Chatrchyan *et al.* (CMS Collab.)
CHATRCHYAN 13T EPJ C73 2568 S. Chatrchyan *et al.* (CMS Collab.)
CHATRCHYAN 13V JHEP 1303 037 S. Chatrchyan *et al.* (CMS Collab.)
Also JHEP 1307 041 (errat.) S. Chatrchyan *et al.* (CMS Collab.)
CHATRCHYAN 13W JHEP 1303 111 S. Chatrchyan *et al.* (CMS Collab.)
ELLIS 13B EPJ C73 2403 J. Ellis *et al.*
JIN 13 JCAP 1311 026 H.-B. Jin, Y.-L. Wu, Y.-F. Zhou
KOPP 13 PR D88 076013 J. Kopp
STREGE 13 JCAP 1304 013 C. Strege *et al.*
AAD 12AF PL B714 180 G. Aad *et al.* (ATLAS Collab.)
AAD 12AG PL B714 197 G. Aad *et al.* (ATLAS Collab.)
AAD 12AN PRL 108 181802 G. Aad *et al.* (ATLAS Collab.)
AAD 12AS PRL 108 261804 G. Aad *et al.* (ATLAS Collab.)
AAD 12AX PR D85 012006 G. Aad *et al.* (ATLAS Collab.)
Also PR D87 099903 (errat.) G. Aad *et al.* (ATLAS Collab.)
AAD 12BJ EPJ C72 1993 G. Aad *et al.* (ATLAS Collab.)
AAD 12CJ PR D86 092002 G. Aad *et al.* (ATLAS Collab.)
AAD 12CM EPJ C72 2215 G. Aad *et al.* (ATLAS Collab.)
AAD 12CP PL B718 411 G. Aad *et al.* (ATLAS Collab.)
AAD 12CT JHEP 1212 124 G. Aad *et al.* (ATLAS Collab.)
AAD 12P EPJ C72 1965 G. Aad *et al.* (ATLAS Collab.)
AAD 12R PL B707 478 G. Aad *et al.* (ATLAS Collab.)
AAD 12T PL B709 137 G. Aad *et al.* (ATLAS Collab.)
AAD 12W PL B710 67 G. Aad *et al.* (ATLAS Collab.)
AALTONEN 12AB PR D85 092001 T. Aaltonen *et al.* (CDF Collab.)
ABAZOV 12AD PR D86 071701 V.M. Abazov *et al.* (D0 Collab.)
ABBASI 12 PR D85 042002 R. Abbasi *et al.* (IceCube Collab.)
AKIMOV 12 PL B709 14 D.Yu. Akimov *et al.* (ZEPLIN-III Collab.)
AKULA 12 PR D85 075001 S. Akula *et al.* (NEAS, MICH)
ANGLOHER 12 EPJ C72 1971 G. Angloher *et al.* (CRESST-II Collab.)
APRILE 12 PRL 109 181301 E. Aprile *et al.* (XENON100 Collab.)
ARBEY 12A PL B708 162 A. Arbey *et al.*
ARCHAMBAU... 12 PL B711 153 S. Archambault *et al.* (PICASSO Collab.)
BAER 12 JHEP 1205 091 H. Baer, V. Barger, A. Mustafayev (OKLA, WISC+)
BALAZS 12 EPJ C73 2563 C. Balazs *et al.*
BECHTLE 12 JHEP 1206 098 P. Bechtle *et al.*
BEHNKE 12 PR D86 052001 E. Behnke *et al.* (COUPP Collab.)
Also PR D90 079902 (errat.) E. Behnke *et al.* (COUPP Collab.)
BESKIDT 12 EPJ C72 2166 C. Beskidt *et al.* (KARLE, JINR, ITEP)
BOTTINO 12 PR D85 095013 A. Bottino, N. Fornengo, S. Scopel (TORI, SOGA)
BUCHMUEL... 12 EPJ C72 2020 O. Buchmueller *et al.*
CAO 12A PL B710 665 J. Cao *et al.*
CHATRCHYAN 12 PR D85 012004 S. Chatrchyan *et al.* (CMS Collab.)
CHATRCHYAN 12AE PRL 109 171803 S. Chatrchyan *et al.* (CMS Collab.)
CHATRCHYAN 12AI JHEP 1208 110 S. Chatrchyan *et al.* (CMS Collab.)
CHATRCHYAN 12AL JHEP 1206 169 S. Chatrchyan *et al.* (CMS Collab.)
CHATRCHYAN 12AN JHEP 1208 026 S. Chatrchyan *et al.* (CMS Collab.)
CHATRCHYAN 12AT JHEP 1210 018 S. Chatrchyan *et al.* (CMS Collab.)
CHATRCHYAN 12BJ JHEP 1211 147 S. Chatrchyan *et al.* (CMS Collab.)
CHATRCHYAN 12BK JHEP 1211 172 S. Chatrchyan *et al.* (CMS Collab.)
CHATRCHYAN 12BO JHEP 1212 055 S. Chatrchyan *et al.* (CMS Collab.)
CHATRCHYAN 12L PL B713 408 S. Chatrchyan *et al.* (CMS Collab.)
DAW 12 ASP 35 397 E. Daw *et al.* (DRIFT-IId Collab.)
DREINER 12A EPL 99 61001 H.K. Dreiner, M. Kramer, J. Tattersall (BONN+)
ELLIS 12B EPJ C72 2005 J. Ellis, K. Olive
FELIZARDO 12 PRL 108 201302 M. Felizardo *et al.* (SIMPLE Collab.)
FENG 12B PR D85 075007 J. Feng, K. Matchev, D. Sanford
KADASTIK 12 JHEP 1205 061 M. Kadastik *et al.*
KIM 12 PRL 108 181301 S.C. Kim *et al.* (KIMS Collab.)
STREGE 12 JCAP 1203 030 C. Strege *et al.* (LOIC, AMST, MADU, GRAN+)
AAD 11AA EPJ C71 1828 G. Aad *et al.* (ATLAS Collab.)
AAD 11G PRL 106 131802 G. Aad *et al.* (ATLAS Collab.)
AAD 11H PRL 106 251801 G. Aad *et al.* (ATLAS Collab.)
AAD 11K PL B701 1 G. Aad *et al.* (ATLAS Collab.)
AAD 11O PL B701 398 G. Aad *et al.* (ATLAS Collab.)
AAD 11P PL B703 428 G. Aad *et al.* (ATLAS Collab.)
AAD 11Z EPJ C71 1809 G. Aad *et al.* (ATLAS Collab.)
ABRAMOWSKI 11 PRL 106 161301 A. Abramowski *et al.* (H.E.S.S. Collab.)
AHMED 11A PR D84 011102 Z. Ahmed *et al.* (CDMS and EDELWEISS Collabs.)
ARMENGAUD 11 PL B702 329 E. Armengaud *et al.* (EDELWEISS II Collab.)
BUCHMUEL... 11 EPJ C71 1583 O. Buchmueller *et al.*
BUCHMUEL... 11B EPJ C71 1722 O. Buchmueller *et al.*
CHATRCHYAN 11B JHEP 1106 093 S. Chatrchyan *et al.* (CMS Collab.)
CHATRCHYAN 11D JHEP 1107 113 S. Chatrchyan *et al.* (CMS Collab.)
CHATRCHYAN 11E JHEP 1107 098 S. Chatrchyan *et al.* (CMS Collab.)
CHATRCHYAN 11V PL B704 411 S. Chatrchyan *et al.* (CMS Collab.)
KHACHATRY... 11 PRL 106 011801 V. Khachatryan *et al.* (CMS Collab.)
KHACHATRY... 11C JHEP 1103 024 V. Khachatryan *et al.* (CMS Collab.)
ROSZKOWSKI 11 PR D83 015014 L. Roszkowski *et al.*
AALTONEN 10 PRL 104 011801 T. Aaltonen *et al.* (CDF Collab.)
AALTONEN 10R PRL 105 081802 T. Aaltonen *et al.* (CDF Collab.)
AALTONEN 10Z PRL 105 191801 T. Aaltonen *et al.* (CDF Collab.)
ABAZOV 10L PL B693 95 V.M. Abazov *et al.* (D0 Collab.)
ABAZOV 10M PRL 105 191802 V.M. Abazov *et al.* (D0 Collab.)
ABAZOV 10N PRL 105 211802 V.M. Abazov *et al.* (D0 Collab.)
ABAZOV 10P PRL 105 221802 V.M. Abazov *et al.* (D0 Collab.)
ABDO 10 JCAP 1004 014 A.A. Abdo *et al.* (Fermi-LAT Collab.)
ACKERMANN 10 JCAP 1005 025 M. Ackermann (Fermi-LAT Collab.)
AHMED 10 SCI 327 1619 Z. Ahmed *et al.* (CDMS II Collab.)
ARMENGAUD 10 PL B687 294 E. Armengaud *et al.* (EDELWEISS II Collab.)
ELLIS 10 EPJ C69 201 J. Ellis, A. Mustafayev, K. Olive
ABAZOV 09M PRL 102 161802 V.M. Abazov *et al.* (D0 Collab.)
ABBASI 09B PRL 102 201302 R. Abbasi *et al.* (IceCube Collab.)
AHMED 09 PRL 102 011301 Z. Ahmed *et al.* (CDMS Collab.)
ANGLOHER 09 ASP 31 270 G. Angloher *et al.* (CRESST Collab.)
BUCHMUEL... 09 EPJ C64 391 O. Buchmueller *et al.* (LOIC, FNAL, CERN+)
DREINER 09 EPJ C62 547 H. Dreiner *et al.*
LEBEDENKO 09 PR D80 052010 V.N. Lebedenko *et al.* (ZEPLIN-III Collab.)
LEBEDENKO 09A PRL 103 151302 V.N. Lebedenko *et al.* (ZEPLIN-III Collab.)
SORENSEN 09 NIM A601 339 P. Sorensen *et al.* (XENON10 Collab.)
ABAZOV 08F PL B659 856 V.M. Abazov *et al.* (D0 Collab.)
ANGLE 08 PRL 100 021303 J. Angle *et al.* (XENON10 Collab.)
ANGLE 08A PRL 101 091301 J. Angle *et al.* (XENON10 Collab.)
BEDNYAKOV 08 PAN 71 111 V.A. Bednyakov, H.P. Klapdor-Kleingrothaus, I.V. Krivosheina
Translated from YAF 71 112.
BEHNKE 08 SCI 319 933 E. Behnke (COUPP Collab.)
BENETTI 08 ASP 28 495 P. Benetti *et al.* (WARP Collab.)
BUCHMUEL... 08 JHEP 0809 117 O. Buchmueller *et al.*
ELLIS 08 PR D78 075012 J. Ellis, K. Olive, P. Sandick (CERN, MINN)
ABULENCIA 07H PRL 98 131804 A. Abulencia *et al.* (CDF Collab.)
ALNER 07A ASP 28 287 G.J. Alner *et al.* (ZEPLIN-II Collab.)
CALIBBI 07 JHEP 0709 081 L. Calibbi *et al.*
ELLIS 07 JHEP 0706 079 J. Ellis, K. Olive, P. Sandick (CERN, MINN)
LEE 07A PRL 99 091301 H.S. Lee *et al.* (KIMS Collab.)
ABBIENDI 06B EPJ C46 307 G. Abbiendi *et al.* (OPAL Collab.)
ACHTERBERG 06 ASP 26 129 A. Achterberg *et al.* (AMANDA Collab.)
ACKERMANN 06 ASP 24 459 M. Ackermann *et al.* (AMANDA Collab.)
AKERIB 06 PR D73 011102 D.S. Akerib *et al.* (CDMS Collab.)
AKERIB 06A PRL 96 011302 D.S. Akerib *et al.* (CDMS Collab.)
ALLANACH 06 PR D73 015013 B.C. Allanach *et al.*
BENOIT 06 PL B637 156 A. Benoit *et al.*
DE-AUSTRI 06 JHEP 0605 002 R.R. de Austri, R. Trotta, L. Roszkowski
DEBOER 06 PL B636 13 W. de Boer *et al.*
LEP-SLC 06 PRPL 427 257 ALEPH, DELPHI, L3, OPAL, SLD and working groups
SHIMIZU 06A PL B633 195 Y. Shimizu *et al.*
SMITH 06 PL B642 567 N.J.T. Smith, A.S. Murphy, T.J. Summer
ABAZOV 05A PRL 94 041801 V.M. Abazov *et al.* (D0 Collab.)
ABDALLAH 05B EPJ C38 395 J. Abdallah *et al.* (DELPHI Collab.)
AKERIB 05 PR D72 052009 D.S. Akerib *et al.* (CDMS Collab.)
ALNER 05 PL B616 17 G.J. Alner *et al.* (UK Dark Matter Collab.)
ALNER 05A ASP 23 444 G.J. Alner *et al.* (UK Dark Matter Collab.)
ANGLOHER 05 ASP 23 325 G. Angloher *et al.* (CRESST-II Collab.)
BAER 05 JHEP 0507 065 H. Baer *et al.* (FSU, MSU, HAWA)
BARNABE-HE...05 PL B624 186 M. Barnabe-Heider *et al.* (PICASSO Collab.)
ELLIS 05 PR D71 095007 J. Ellis *et al.*
SANGLARD 05 PR D71 122002 V. Sanglard *et al.* (EDELWEISS Collab.)
ABBIENDI 04 EPJ C32 453 G. Abbiendi *et al.* (OPAL Collab.)
ABBIENDI 04F EPJ C33 149 G. Abbiendi *et al.* (OPAL Collab.)
ABBIENDI 04H EPJ C35 1 G. Abbiendi *et al.* (OPAL Collab.)
ABBIENDI 04N PL B602 167 G. Abbiendi *et al.* (OPAL Collab.)
ABDALLAH 04H EPJ C34 145 J. Abdallah *et al.* (DELPHI Collab.)
ABDALLAH 04M EPJ C36 1 J. Abdallah *et al.* (DELPHI Collab.)
Also EPJ C37 129 (errat.) J. Abdallah *et al.* (DELPHI Collab.)
ACHARD 04 PL B580 37 P. Achard *et al.* (L3 Collab.)
ACHARD 04E PL B587 16 P. Achard *et al.* (L3 Collab.)
AKERIB 04 PRL 93 211301 D.S. Akerib *et al.* (CDMSII Collab.)
BALTZ 04 JHEP 0410 052 E. Baltz, P. Gondolo
BELANGER 04 JHEP 0403 012 G. Belanger *et al.*
BOTTINO 04 PR D69 037302 A. Bottino *et al.*
DESAI 04 PR D70 083523 S. Desai *et al.* (Super-Kamiokande Collab.)
ELLIS 04 PR D69 015005 J. Ellis *et al.*
ELLIS 04B PR D70 055005 J. Ellis *et al.*
HEISTER 04 PL B583 247 A. Heister *et al.* (ALEPH Collab.)
PIERCE 04A PR D70 075006 A. Pierce
ABBIENDI 03L PL B572 8 G. Abbiendi *et al.* (OPAL Collab.)
ABDALLAH 03M EPJ C31 421 J. Abdallah *et al.* (DELPHI Collab.)
AHMED 03 ASP 19 691 B. Ahmed *et al.* (UK Dark Matter Collab.)
AKERIB 03 PR D68 082002 D.S. Akerib *et al.* (CDMS Collab.)
BAER 03 JCAP 0305 006 H. Baer, C. Balazs
BAER 03A JCAP 0309 007 H. Baer *et al.*
BOTTINO 03 PR D68 043506 A. Bottino *et al.*
BOTTINO 03A PR D67 063519 A. Bottino, N. Fornengo, S. Scopel
CHATTOPAD... 03 PR D68 035005 U. Chattopadhyay, A. Corsetti, P. Nath
ELLIS 03 ASP 18 395 J. Ellis, K.A. Olive, Y. Santoso
ELLIS 03B NP B652 259 J. Ellis *et al.*
ELLIS 03C PL B565 176 J. Ellis *et al.*
ELLIS 03D PL B573 162 J. Ellis *et al.*
ELLIS 03E PR D67 123502 J. Ellis *et al.*
HEISTER 03C EPJ C28 1 A. Heister *et al.* (ALEPH Collab.)
HEISTER 03G EPJ C31 1 A. Heister *et al.* (ALEPH Collab.)
KLAPDOR-K... 03 ASP 18 525 H.V. Klapdor-Kleingrothaus *et al.*
LAHANAS 03 PL B568 55 A. Lahanas, D. Nanopoulos
TAKEDA 03 PL B572 145 A. Takeda *et al.*
ABRAMS 02 PR D66 122003 D. Abrams *et al.* (CDMS Collab.)
ACOSTA 02H PRL 89 281801 D. Acosta *et al.* (CDF Collab.)
ANGLOHER 02 ASP 18 43 G. Angloher *et al.* (CRESST Collab.)
ARNOWITT 02 hep-ph/0211417 R. Arnowitt, B. Dutta
BENOIT 02 PL B545 43 A. Benoit *et al.* (EDELWEISS Collab.)
ELLIS 02B PL B532 318 J. Ellis, A. Ferstl, K.A. Olive
HEISTER 02 PL B526 191 A. Heister *et al.* (ALEPH Collab.)
HEISTER 02E PL B526 206 A. Heister *et al.* (ALEPH Collab.)
HEISTER 02J PL B533 223 A. Heister *et al.* (ALEPH Collab.)
HEISTER 02N PL B544 73 A. Heister *et al.* (ALEPH Collab.)
KIM 02 PL B527 18 H.B. Kim *et al.*
KIM 02B JHEP 0212 034 Y.G. Kim *et al.*
LAHANAS 02 EPJ C23 185 A. Lahanas, V.C. Spanos
MORALES 02B ASP 16 325 A. Morales *et al.* (COSME Collab.)
MORALES 02C PL B532 8 A. Morales *et al.* (IGEX Collab.)
ABREU 01 EPJ C19 29 P. Abreu *et al.* (DELPHI Collab.)
ABREU 01B EPJ C19 201 P. Abreu *et al.* (DELPHI Collab.)
BALTZ 01 PR 86 5004 E. Baltz, P. Gondolo
BARATE 01 PL B499 67 R. Barate *et al.* (ALEPH Collab.)
BARATE 01B EPJ C19 415 R. Barate *et al.* (ALEPH Collab.)
BARGER 01C PL B518 117 V. Barger, C. Kao
BAUDIS 01 PR D63 022001 L. Baudis *et al.* (Heidelberg-Moscow Collab.)
BENOIT 01 PL B513 15 A. Benoit *et al.* (EDELWEISS Collab.)
BERNABEI 01 PL B509 197 R. Bernabei *et al.* (DAMA Collab.)
BOTTINO 01 PR D63 125003 A. Bottino *et al.*
CORSETTI 01 PR D64 125010 A. Corsetti, P. Nath

ELLIS 01B PL B510 236 J. Ellis *et al.*
ELLIS 01C PR D63 065016 J. Ellis, A. Ferstl, K.A. Olive
GOMEZ 01 PL B512 252 M.E. Gomez, J.D. Vergados
LAHANAS 01 PL B518 94 A. Lahanas, D.V. Nanopoulos, V. Spanos
ABBIENDI 00 EPJ C12 1 G. Abbiendi *et al.* (OPAL Collab.)
ABBIENDI 00G EPJ C14 51 G. Abbiendi *et al.* (OPAL Collab.)
ABBIENDI 00H EPJ C14 187 G. Abbiendi *et al.* (OPAL Collab.)
Also EPJ C16 707 (errat.) G. Abbiendi *et al.* (OPAL Collab.)
ABBIENDI,G 00D EPJ C18 253 G. Abbiendi *et al.* (OPAL Collab.)
ABREU 00J PL B479 129 P. Abreu *et al.* (DELPHI Collab.)
ABREU 00Q PL B478 65 P. Abreu *et al.* (DELPHI Collab.)
ABREU 00T PL B485 95 P. Abreu *et al.* (DELPHI Collab.)
ABREU 00U PL B487 36 P. Abreu *et al.* (DELPHI Collab.)
ABREU 00V EPJ C16 211 P. Abreu *et al.* (DELPHI Collab.)
ABREU 00W PL B489 38 P. Abreu *et al.* (DELPHI Collab.)
ABREU 00Z EPJ C17 53 P. Abreu *et al.* (DELPHI Collab.)
ABUSAIDI 00 PRL 84 5699 R. Abusaidi *et al.* (CDMS Collab.)
ACCIARRI 00D PL B472 420 M. Acciarri *et al.* (L3 Collab.)
ACCOMANDO 00 NP B585 124 E. Accomando *et al.*
BERNABEI 00 PL B480 23 R. Bernabei *et al.* (DAMA Collab.)
BERNABEI 00C EPJ C18 283 R. Bernabei *et al.* (DAMA Collab.)
BERNABEI 00D NJP 2 15 R. Bernabei *et al.* (DAMA Collab.)
BOEHM 00B PR D62 035012 C. Boehm, A. Djouadi, M. Drees
ELLIS 00 PR D62 075010 J. Ellis *et al.*
FENG 00 PL B482 388 J.L. Feng, K.T. Matchev, F. Wilczek
LEP 00 CERN-EP-2000-016 LEP Collabs. (ALEPH, DELPHI, L3, OPAL, SLD+)
MORALES 00 PL B489 268 A. Morales *et al.* (IGEX Collab.)
PDG 00 EPJ C15 1 D.E. Groom *et al.* (PDG Collab.)
SPOONER 00 PL B473 330 N.J.C. Spooner *et al.* (UK Dark Matter Col.)
ACCIARRI 99H PL B456 283 M. Acciarri *et al.* (L3 Collab.)
ACCIARRI 99R PL B470 268 M. Acciarri *et al.* (L3 Collab.)
ACCIARRI 99W PL B471 280 M. Acciarri *et al.* (L3 Collab.)
AMBROSIO 99 PR D60 082002 M. Ambrosio *et al.* (Macro Collab.)
BAUDIS 99 PR D59 022001 L. Baudis *et al.* (Heidelberg-Moscow Collab.)
BELLI 99C NP B563 97 P. Belli *et al.* (DAMA Collab.)
OOTANI 99 PL B461 371 W. Ootani *et al.*
ABREU 98P PL B444 491 P. Abreu *et al.* (DELPHI Collab.)
ACCIARRI 98F EPJ C4 207 M. Acciarri *et al.* (L3 Collab.)
ACKERSTAFF 98P PL B433 195 K. Ackerstaff *et al.* (OPAL Collab.)
BARATE 98K PL B433 176 R. Barate *et al.* (ALEPH Collab.)
BARATE 98S EPJ C4 433 R. Barate *et al.* (ALEPH Collab.)
BERNABEI 98C PL B436 379 R. Bernabei *et al.* (DAMA Collab.)
ELLIS 98 PR D58 095002 J. Ellis *et al.*
ELLIS 98B PL B444 367 J. Ellis, T. Falk, K. Olive
PDG 98 EPJ C3 1 C. Caso *et al.* (PDG Collab.)
BAER 97 PR D57 567 H. Baer, M. Brhlik
BERNABEI 97 ASP 7 73 R. Bernabei *et al.* (DAMA Collab.)
EDSJO 97 PR D56 1879 J. Edsjo, P. Gondolo
ARNOWITT 96 PR D54 2374 R. Arnowitt, P. Nath
BAER 96 PR D53 597 H. Baer, M. Brhlik
BERGSTROM 96 ASP 5 263 L. Bergstrom, P. Gondolo
LEWIN 96 ASP 6 87 J.D. Lewin, P.F. Smith
BEREZINSKY 95 ASP 5 1 V. Berezinsky *et al.*
FALK 95 PL B354 99 T. Falk, K.A. Olive, M. Srednicki (MINN, UCSB)
LOSECCO 95 PL B342 392 J.M. LoSecco (NDAM)
ADRIANI 93M PRPL 236 1 O. Adriani *et al.* (L3 Collab.)
DREES 93 PR D47 376 M. Drees, M.M. Nojiri (DESY, SLAC)
DREES 93B PR D48 3483 M. Drees, M.M. Nojiri
FALK 93 PL B318 354 T. Falk *et al.* (UCB, UCSB, MINN)
KELLEY 93 PR D47 2461 S. Kelley *et al.* (TAMU, ALAH)
MIZUTA 93 PL B298 120 S. Mizuta, M. Yamaguchi (TOHO)
MORI 93 PR D48 5505 M. Mori *et al.* (KEK, NIIG, TOKY, TOKA+)
BOTTINO 92 MPL A7 733 A. Bottino *et al.* (TORI, ZARA)
Also PL B265 57 A. Bottino *et al.* (TORI, INFN)
DECAMP 92 PRPL 216 253 D. Decamp *et al.* (ALEPH Collab.)
LOPEZ 92 NP B370 445 J.L. Lopez, D.V. Nanopoulos, K.J. Yuan (TAMU)
MCDONALD 92 PL B283 80 J. McDonald, K.A. Olive, M. Srednicki (LISB+)
ABREU 91F NP B367 511 P. Abreu *et al.* (DELPHI Collab.)
ALEXANDER 91F ZPHY C52 175 G. Alexander *et al.* (OPAL Collab.)
BOTTINO 91 PL B265 57 A. Bottino *et al.* (TORI, INFN)
GELMINI 91 NP B351 623 G.B. Gelmini, P. Gondolo, E. Roulet (UCLA, TRST)
GRIEST 91 PR D43 3191 K. Griest, D. Seckel
KAMIONKOW...91 PR D44 3021 M. Kamionkowski (CHIC, FNAL)
MORI 91B PL B270 89 M. Mori *et al.* (Kamiokande Collab.)
NOJIRI 91 PL B261 76 M.M. Nojiri (KEK)
OLIVE 91 NP B355 208 K.A. Olive, M. Srednicki (MINN, UCSB)
ROSZKOWSKI 91 PL B262 59 L. Roszkowski (CERN)
GRIEST 90 PR D41 3565 K. Griest, M. Kamionkowski, M.S. Turner (UCB+)
BARBIERI 89C NP B313 725 R. Barbieri, M. Frigeni, G. Giudice
OLIVE 89 PL B230 78 K.A. Olive, M. Srednicki (MINN, UCSB)
ELLIS 88D NP B307 883 J. Ellis, R. Flores
GRIEST 88B PR D38 2357 K. Griest
OLIVE 88 PL B205 553 K.A. Olive, M. Srednicki (MINN, UCSB)
SREDNICKI 88 NP B310 693 M. Srednicki, R. Watkins, K.A. Olive (MINN, UCSB)
ELLIS 84 NP B238 453 J. Ellis *et al.* (CERN)
GOLDBERG 83 PRL 50 1419 H. Goldberg (NEAS)
KRAUSS 83 NP B227 556 L.M. Krauss (HARV)
VYSOTSKII 83 SJNP 37 948 M.I. Vysotsky (ITEP)
Translated from YAF 37 1597.

Technicolor

See the related review(s):

Dynamical Electroweak Symmetry Breaking: Implications of the H^0

The latest unpublished results are described in "Dynamical Electroweak Symmetry Breaking" review.

MASS LIMITS for Resonances in Models of Dynamical Electroweak Symmetry Breaking

VALUE (GeV)	CL%	DOCUMENT ID		TECN	COMMENT
• • • We do not use the following data for averages, fits, limits, etc. • • •					
		[1] AAD	16W	ATLS	color octet vector resonance
>2400	95	[2] KHACHATRY...	16E	CMS	top-color Z'
		[3] AAD	15AB	ATLS	$h \to \pi_V \pi_V$
>1800	95	[4] AAD	15AO	ATLS	top-color Z'
		[5] AAD	15BB	ATLS	$pp \to \rho_T/a_{1T} \to WhorZh$
		[6] AAD	15Q	ATLS	$h \to \pi_V \pi_V$
		[7] AAIJ	15AN	LHCB	$h \to \pi_V \pi_V$
>1140	95	[8] KHACHATRY...	15C	CMS	$\rho_T \to WZ$
		[9] KHACHATRY...	15W	CMS	$H \to \pi_V \pi_V$
none 200–700, 750–890	95	[10] AAD	14AT	ATLS	$pp \to \omega_T \to Z\gamma$
none 275–960	95	[10] AAD	14AT	ATLS	$pp \to a_T \to W\gamma$
		[11] AAD	14V	ATLS	color singlet techni-vector
> 703		[12] AAD	13AN	ATLS	$pp \to a_T \to W\gamma$
> 494		[13] AAD	13AN	ATLS	$pp \to \omega_T \to Z\gamma$
none 500–1740	95	[14] AAD	13AQ	ATLS	top-color Z'
>1300	95	[15] CHATRCHYAN	13AP	CMS	top-color Z'
>2100	95	[14] CHATRCHYAN	13BM	CMS	top-color Z'
		[16] BAAK	12	RVUE	QCD-like technicolor
none 167–687	95	[17] CHATRCHYAN	12AF	CMS	$\rho_T \to WZ$
> 805	95	[14] AALTONEN	11AD	CDF	top-color Z'
> 805	95	[14] AALTONEN	11AE	CDF	top-color Z'
		[18] CHIVUKULA	11	RVUE	top-Higgs
		[19] CHIVUKULA	11A	RVUE	techini-π
		[20] AALTONEN	10I	CDF	$p\overline{p} \to \rho_T/\omega_T \to W\pi_T$
none 208–408	95	[21] ABAZOV	10A	D0	$\rho_T \to WZ$
		[22] ABAZOV	07I	D0	$p\overline{p} \to \rho_T/\omega_T \to W\pi_T$
> 280	95	[23] ABULENCIA	05A	CDF	$\rho_T \to e^+e^-, \mu^+\mu^-$
		[24] CHEKANOV	02B	ZEUS	color octet techni-π
> 207	95	[25] ABAZOV	01B	D0	$\rho_T \to e^+e^-$
none 90–206.7	95	[26] ABDALLAH	01	DLPH	$e^+e^- \to \rho_T$
		[27] AFFOLDER	00F	CDF	color-singlet techni-ρ, $\rho_T \to W\pi_T, 2\pi_T$
> 600	95	[28] AFFOLDER	00K	CDF	color-octet techni-ρ, $\rho_{T8} \to 2\pi_{LQ}$
none 350–440	95	[29] ABE	99F	CDF	color-octet techni-ρ, $\rho_{T8} \to \overline{b}b$
		[30] ABE	99N	CDF	techni-ω, $\omega_T \to \gamma\overline{b}b$
none 260–480	95	[31] ABE	97G	CDF	color-octet techni-ρ, $\rho_{T8} \to$ 2jets

[1] AAD 16W search for color octet vector resonance decaying to bB in pp collisions at $\sqrt{s}$ = 8 TeV. The vector like quark B is assumed to decay to bH. See their Fig.3 and Fig.4 for limits on $\sigma \cdot B$.

[2] KHACHATRYAN 16E search for top-color Z' decaying to $t\overline{t}$. The quoted limit is for $\Gamma_{Z'}/m_{Z'} = 0.012$. Also exclude $m_{Z'} < 2.9$ TeV for wider topcolor Z' with $\Gamma_{Z'}/m_{Z'}$ =0.1.

[3] AAD 15AB search for long-lived hidden valley π_V particles which are produced in pairs by the decay of a scalar boson. π_V is assumed to decay into dijets. See their Fig. 10 for the limit on σB.

[4] AAD 15AO search for top-color Z' decaying to $t\overline{t}$. The quoted limit is for $\Gamma_{Z'}/m_{Z'}$ = 0.012.

[5] AAD 15BB search for minimal walking technicolor (MWT) isotriplet vector and axial-vector resonances decaying to Wh or Zh. See their Fig. 3 for the exclusion limit in the MWT parameter space.

[6] AAD 15Q search for long-lived hidden valley π_V particles which are produced in pairs by the decay of scalar boson. π_V is assumed to decay into dijets. See their Fig. 5 and Fig. 6 for the limit on σB.

[7] AAIJ 15AN search for long-lived hidden valley π_V particles which are produced in pairs by the decay of scalar boson with a mass of 120GeV. π_V is assumed to decay into dijets. See their Fig. 4 for the limit on σB.

[8] KHACHATRYAN 15C search for a vector techni-resonance decaying to WZ. The limit assumes $M_{\pi_T} = (3/4)\ M_{\rho_T} - 25$ GeV. See their Fig.3 for the limit in $M_{\pi_T} - M_{\rho_T}$ plane of the low scale technicolor model.

[9] KHACHATRYAN 15W search for long-lived hidden valley π_V particles which are produced in pairs in the decay of heavy higgs boson H. π_V is assumed to decay into $\ell^+\ell^-$. See their Fig. 7 and Fig. 8 for the limits on σB.

[10] AAD 14AT search for techni-ω and techni-a resonances decaying to $V\gamma$ with $V = W(\to \ell\nu)$ or $Z(\to \ell^+\ell^-)$.

[11] AAD 14V search for vector techni-resonances decaying into electron or muon pairs in pp collisions at $\sqrt{s} = 8$ TeV. See their table IX for exclusion limits with various assumptions.

[12] AAD 13AN search for vector techni-resonance a_T decaying into $W\gamma$.

[13] AAD 13AN search for vector techni-resonance ω_T decaying into $Z\gamma$.

[14] Search for top-color Z' decaying to $t\overline{t}$. The quoted limit is for $\Gamma_{Z'}/m_{Z'} = 0.012$.

[15] CHATRCHYAN 13AP search for top-color leptophobic Z' decaying to $t\overline{t}$. The quoted limit is for $\Gamma_{Z'}/m_{Z'} = 0.012$.

[16] BAAK 12 give electroweak oblique parameter constraints on the QCD-like technicolor models. See their Fig. 28.

[17] CHATRCHYAN 12AF search for a vector techni-resonance decaying to WZ. The limit assumes $M_{\pi_T} = (3/4)\ M_{\rho_T} - 25$ GeV. See their Fig. 3 for the limit in $M_{\pi_T} - M_{\rho_T}$ plane of the low scale technicolor model.

[18] Using the LHC limit on the Higgs boson production cross section, CHIVUKULA 11 obtain a limit on the top-Higgs mass > 300 GeV at 95% CL assuming 150 GeV top-pion mass.

[19] Using the LHC limit on the Higgs boson production cross section, CHIVUKULA 11A obtain a limit on the techinipion mass ruling out the region 110 GeV $< m_P < 2m_t$. Existence of color techni-fermions, top-color mechanism, and $N_{TC} \geq 3$ are assumed.

[20] AALTONEN 10I search for the vector techni-resonances (ρ_T, ω_T) decaying into $W\pi_T$ with $W \to \ell\nu$ and $\pi_T \to b\overline{b}$, $b\overline{c}$, or $b\overline{u}$. See their Fig. 3 for the exclusion plot in $M_{\pi_T} - M_{\rho_T}$ plane.

[21] ABAZOV 10A search for a vector techni-resonance decaying into WZ. The limit assumes $M_{\rho_T} < M_{\pi_T} + M_W$.

[22] ABAZOV 07I search for the vector techni-resonances (ρ_T, ω_T) decaying into $W\pi_T$ with $W \to e\nu$ and $\pi_T \to b\overline{b}$ or $b\overline{c}$. See their Fig. 2 for the exclusion plot in $M_{\pi_T} - M_{\rho_T}$ plane.

[23] ABULENCIA 05A search for resonances decaying to electron or muon pairs in $p\overline{p}$ collisions. at $\sqrt{s} = 1.96$ TeV. The limit assumes Technicolor-scale mass parameters $M_V = M_A = 500$ GeV.

[24] CHEKANOV 02B search for color octet techni-π P decaying into dijets in ep collisions. See their Fig. 5 for the limit on $\sigma(ep \to eP X)\cdot B(P \to 2j)$.

[25] ABAZOV 01B searches for vector techni-resonances (ρ_T,ω_T) decaying to e^+e^-. The limit assumes $M_{\rho_T} = M_{\omega_T} < M_{\pi_T} + M_W$.

[26] The limit is independent of the π_T mass. See their Fig. 9 and Fig. 10 for the exclusion plot in the M_{ρ_T}–M_{π_T} plane. ABDALLAH 01 limit on the techni-pion mass is $M_{\pi_T} > 79.8$ GeV for N_D=2, assuming its point-like coupling to gauge bosons.

[27] AFFOLDER 00F search for ρ_T decaying into $W\pi_T$ or $\pi_T\pi_T$ with $W \to \ell\nu$ and $\pi_T \to \overline{b}b$, $\overline{b}c$. See Fig. 1 in the above Note on "Dynamical Electroweak Symmetry Breaking" for the exclusion plot in the M_{ρ_T}–M_{π_T} plane.

[28] AFFOLDER 00K search for the ρ_{T8} decaying into $\pi_{LQ}\pi_{LQ}$ with $\pi_{LQ} \to b\nu$. For $\pi_{LQ} \to c\nu$, the limit is $M_{\rho_{T8}} > 510$ GeV. See their Fig. 2 and Fig. 3 for the exclusion plot in the $M_{\rho_{T8}}$–$M_{\pi_{LQ}}$ plane.

[29] ABE 99F search for a new particle X decaying into $b\overline{b}$ in $p\overline{p}$ collisions at $E_{cm} = 1.8$ TeV. See Fig. 7 in the above Note on "Dynamical Electroweak Symmetry Breaking" for the upper limit on $\sigma(p\overline{p} \to X)\times B(X \to b\overline{b})$. ABE 99F also exclude top gluons of width $\Gamma = 0.3M$ in the mass interval $280 < M < 670$ GeV, of width $\Gamma = 0.5M$ in the mass interval $340 < M < 640$ GeV, and of width $\Gamma = 0.7M$ in the mass interval $375 < M < 560$ GeV.

[30] ABE 99N search for the techni-ω decaying into $\gamma\pi_T$. The technipion is assumed to decay $\pi_T \to b\overline{b}$. See Fig. 2 in the above Note on "Dynamical Electroweak Symmetry Breaking" for the exclusion plot in the M_{ω_T}–M_{π_T} plane.

[31] ABE 97G search for a new particle X decaying into dijets in $p\overline{p}$ collisions at $E_{cm} = 1.8$ TeV. See Fig. 5 in the above Note on "Dynamical Electroweak Symmetry Breaking" for the upper limit on $\sigma(p\overline{p} \to X)\times B(X \to 2j)$.

REFERENCES FOR Technicolor

AAD	16W	PL B758 249	G. Aad *et al.*	(ATLAS Collab.)
KHACHATRY...	16E	PR D93 012001	V. Khachatryan *et al.*	(CMS Collab.)
AAD	15AB	PR D92 012010	G. Aad *et al.*	(ATLAS Collab.)
AAD	15AO	JHEP 1508 148	G. Aad *et al.*	(ATLAS Collab.)
AAD	15BB	EPJ C75 263	G. Aad *et al.*	(ATLAS Collab.)
AAD	15Q	PL B743 15	G. Aad *et al.*	(ATLAS Collab.)
AAIJ	15AN	EPJ C75 152	R. Aaij *et al.*	(LHCb Collab.)
KHACHATRY...	15C	PL B740 83	V. Khachatryan *et al.*	(CMS Collab.)
KHACHATRY...	15W	PR D91 052012	V. Khachatryan *et al.*	(CMS Collab.)
AAD	14AT	PL B738 428	G. Aad *et al.*	(ATLAS Collab.)
AAD	14V	PR D90 052005	G. Aad *et al.*	(ATLAS Collab.)
AAD	13AN	PR D87 112003	G. Aad *et al.*	(ATLAS Collab.)
Also		PR D91 119901 (errat.)	G. Aad *et al.*	(ATLAS Collab.)
AAD	13AQ	PR D88 012004	G. Aad *et al.*	(ATLAS Collab.)
CHATRCHYAN	13AP	PR D87 072002	S. Chatrchyan *et al.*	(CMS Collab.)
CHATRCHYAN	13BM	PRL 111 211804	S. Chatrchyan *et al.*	(CMS Collab.)
Also		PRL 112 119903 (errat.)	S. Chatrchyan *et al.*	(CMS Collab.)
BAAK	12	EPJ C72 2003	M. Baak *et al.*	(Gfitter Group)
CHATRCHYAN	12AF	PRL 109 141801	S. Chatrchyan *et al.*	(CMS Collab.)
AALTONEN	11AD	PR D84 072003	T. Aaltonen *et al.*	(CDF Collab.)
AALTONEN	11AE	PR D84 072004	T. Aaltonen *et al.*	(CDF Collab.)
CHIVUKULA	11	PR D84 095022	R.S. Chivukula *et al.*	
CHIVUKULA	11A	PR D84 115025	R. S. Chivukula *et al.*	
AALTONEN	10I	PRL 104 111802	T. Aaltonen *et al.*	(CDF Collab.)
ABAZOV	10A	PRL 104 061801	V.M. Abazov *et al.*	(D0 Collab.)
ABAZOV	07I	PRL 98 221801	V.M. Abazov *et al.*	(D0 Collab.)
ABULENCIA	05A	PRL 95 252001	A. Abulencia *et al.*	(CDF Collab.)
CHEKANOV	02B	PL B531 9	S. Chekanov *et al.*	(ZEUS Collab.)
ABAZOV	01B	PRL 87 061802	V.M. Abazov *et al.*	(D0 Collab.)
ABDALLAH	01	EPJ C22 17	J. Abdallah *et al.*	(DELPHI Collab.)
AFFOLDER	00F	PRL 84 1110	T. Affolder *et al.*	(CDF Collab.)
AFFOLDER	00K	PRL 85 2056	T. Affolder *et al.*	(CDF Collab.)
ABE	99F	PRL 82 2038	F. Abe *et al.*	(CDF Collab.)
ABE	99N	PRL 83 3124	F. Abe *et al.*	(CDF Collab.)
ABE	97G	PR D55 5263	F. Abe *et al.*	(CDF Collab.)

Quark and Lepton Compositeness, Searches for

The latest unpublished results are described in the "Quark and Lepton Compositeness" review.

See the related review(s):

Searches for Quark and Lepton Compositeness

CONTENTS:

SCALE LIMITS for Contact Interactions: $\Lambda(eeee)$

Limits are for $\Lambda^{\pm}_{LL}$ only. For other cases, see each reference.

Λ^+_{LL}(TeV)	Λ^-_{LL}(TeV)	CL%	DOCUMENT ID		TECN	COMMENT
>8.3	**>10.3**	95	[1] BOURILKOV	01	RVUE	E_{cm} = 192–208 GeV
• • • We do not use the following data for averages, fits, limits, etc. • • •						
>4.5	>7.0	95	[2] SCHAEL	07A	ALEP	E_{cm} = 189–209 GeV
>5.3	>6.8	95	ABDALLAH	06C	DLPH	E_{cm} = 130–207 GeV
>4.7	>6.1	95	[3] ABBIENDI	04G	OPAL	E_{cm} = 130–207 GeV
>4.3	>4.9	95	ACCIARRI	00P	L3	E_{cm} = 130–189 GeV

[1] A combined analysis of the data from ALEPH, DELPHI, L3, and OPAL.
[2] SCHAEL 07A limits are from R_c, Q^{depl}_{FB}, and hadronic cross section measurements.
[3] ABBIENDI 04G limits are from $e^+e^- \to e^+e^-$ cross section at $\sqrt{s}$ = 130–207 GeV.

SCALE LIMITS for Contact Interactions: $\Lambda(ee\mu\mu)$

Limits are for $\Lambda^{\pm}_{LL}$ only. For other cases, see each reference.

Λ^+_{LL}(TeV)	Λ^-_{LL}(TeV)	CL%	DOCUMENT ID		TECN	COMMENT
>6.6	**>9.5**	95	[1] SCHAEL	07A	ALEP	E_{cm} = 189–209 GeV
> 8.5	>3.8	95	ACCIARRI	00P	L3	E_{cm} = 130–189 GeV
• • • We do not use the following data for averages, fits, limits, etc. • • •						
>7.3	>7.6	95	ABDALLAH	06C	DLPH	E_{cm} = 130–207 GeV
>8.1	>7.3	95	[2] ABBIENDI	04G	OPAL	E_{cm} = 130–207 GeV

[1] SCHAEL 07A limits are from R_c, Q^{depl}_{FB}, and hadronic cross section measurements.
[2] ABBIENDI 04G limits are from $e^+e^- \to \mu\mu$ cross section at $\sqrt{s}$ = 130–207 GeV.

SCALE LIMITS for Contact Interactions: $\Lambda(ee\tau\tau)$

Limits are for $\Lambda^{\pm}_{LL}$ only. For other cases, see each reference.

Λ^+_{LL}(TeV)	Λ^-_{LL}(TeV)	CL%	DOCUMENT ID		TECN	COMMENT
>7.9	>5.8	95	[1] SCHAEL	07A	ALEP	E_{cm} = 189–209 GeV
>7.9	>4.6	95	ABDALLAH	06C	DLPH	E_{cm} = 130–207 GeV
>4.9	**>7.2**	95	[2] ABBIENDI	04G	OPAL	E_{cm} = 130–207 GeV
• • • We do not use the following data for averages, fits, limits, etc. • • •						
>5.4	>4.7	95	ACCIARRI	00P	L3	E_{cm} = 130–189 GeV

[1] SCHAEL 07A limits are from R_c, Q^{depl}_{FB}, and hadronic cross section measurements.
[2] ABBIENDI 04G limits are from $e^+e^- \to \tau\tau$ cross section at $\sqrt{s}$ = 130–207 GeV.

SCALE LIMITS for Contact Interactions: $\Lambda(\ell\ell\ell\ell)$

Lepton universality assumed. Limits are for $\Lambda^{\pm}_{LL}$ only. For other cases, see each reference.

Λ^+_{LL}(TeV)	Λ^-_{LL}(TeV)	CL%	DOCUMENT ID		TECN	COMMENT
>7.9	**> 10.3**	95	[1] SCHAEL	07A	ALEP	E_{cm} = 189–209 GeV
>9.1	>8.2	95	ABDALLAH	06C	DLPH	E_{cm} = 130–207 GeV
• • • We do not use the following data for averages, fits, limits, etc. • • •						
>7.7	>9.5	95	[2] ABBIENDI	04G	OPAL	E_{cm} = 130–207 GeV
			[3] BABICH	03	RVUE	
>9.0	>5.2	95	ACCIARRI	00P	L3	E_{cm} = 130–189 GeV

[1] SCHAEL 07A limits are from R_c, Q^{depl}_{FB}, and hadronic cross section measurements.
[2] ABBIENDI 04G limits are from $e^+e^- \to \ell^+\ell^-$ cross section at $\sqrt{s}$ = 130–207 GeV.
[3] BABICH 03 obtain a bound -0.175 TeV$^{-2} < 1/\Lambda^2_{LL} < 0.095$ TeV^{-2} (95%CL) in a model independent analysis allowing all of Λ_{LL}, Λ_{LR}, Λ_{RL}, Λ_{RR} to coexist.

SCALE LIMITS for Contact Interactions: $\Lambda(eeqq)$

Limits are for $\Lambda^{\pm}_{LL}$ only. For other cases, see each reference.

Λ^+_{LL}(TeV)	Λ^-_{LL}(TeV)	CL%	DOCUMENT ID		TECN	COMMENT
>24	**>37**	95	[1] AABOUD	17AT	ATLS	$(eeqq)$
> 8.4	**>10.2**	95	[2] ABDALLAH	09	DLPH	$(eebb)$
> 9.4	**>5.6**	95	[3] SCHAEL	07A	ALEP	$(eecc)$
> 9.4	>4.9	95	[2] SCHAEL	07A	ALEP	$(eebb)$
>23.3	**>12.5**	95	[4] CHEUNG	01B	RVUE	$(eeuu)$
>11.1	**>26.4**	95	[4] CHEUNG	01B	RVUE	$(eedd)$

• • • We do not use the following data for averages, fits, limits, etc. • • •

>15.5	>19.5	95	[5] AABOUD	16U	ATLS	$(eeqq)$
>13.5	>18.3	95	[6] KHACHATRY...	15AE	CMS	$(eeqq)$
>16.4	>20.7	95	[7] AAD	14BE	ATLS	$(eeqq)$
> 9.5	>12.1	95	[8] AAD	13E	ATLS	$(eeqq)$
>10.1	>9.4	95	[9] AAD	12AB	ATLS	$(eeqq)$
> 4.2	>4.0	95	[10] AARON	11C	H1	$(eeqq)$
> 3.8	>3.8	95	[11] ABDALLAH	11	DLPH	$(eetc)$
>12.9	>7.2	95	[12] SCHAEL	07A	ALEP	$(eeqq)$
> 3.7	>5.9	95	[13] ABULENCIA	06L	CDF	$(eeqq)$

[1] AABOUD 17AT limits are from pp collisions at $\sqrt{s} = 13$ TeV. The quoted limit uses a uniform positive prior in $1/\Lambda^2$.
[2] ABDALLAH 09 and SCHAEL 07A limits are from R_b, A_{FB}^b.
[3] SCHAEL 07A limits are from R_c, Q_{FB}^{depl}, and hadronic cross section measurements.
[4] CHEUNG 01B is an update of BARGER 98E.
[5] AABOUD 16U limits are from pp collisions at $\sqrt{s} = 13$ TeV. The quoted limit uses a uniform positive prior in $1/\Lambda^2$.
[6] KHACHATRYAN 15AE limit is from e^+e^- mass distribution in pp collisions at $E_{cm} = 8$ TeV.
[7] AAD 14BE limits are from pp collisions at $\sqrt{s} = 8$ TeV. The quoted limit uses a uniform positive prior in $1/\Lambda^2$.
[8] AAD 13E limis are from e^+e^- mass distribution in pp collisions at $E_{cm} = 7$ TeV.
[9] AAD 12AB limis are from e^+e^- mass distribution in pp collisions at $E_{cm} = 7$ TeV.
[10] AARON 11C limits are from Q^2 spectrum measurements of $e^\pm p \to e^\pm X$.
[11] ABDALLAH 11 limit is from $e^+e^- \to t\bar{c}$ cross section. $\Lambda_{LL} = \Lambda_{LR} = \Lambda_{RL} = \Lambda_{RR}$ is assumed.
[12] SCHAEL 07A limit assumes quark flavor universality of the contact interactions.
[13] ABULENCIA 06L limits are from $p\overline{p}$ collisions at $\sqrt{s} = 1.96$ TeV.

SCALE LIMITS for Contact Interactions: $\Lambda(\mu\mu qq)$

Λ_{LL}^+(TeV)	Λ_{LL}^-(TeV)	CL%	DOCUMENT ID		TECN	COMMENT
>20	**>30**	95	[1] AABOUD	17AT	ATLS	$(\mu\mu qq)$

• • • We do not use the following data for averages, fits, limits, etc. • • •

>15.8	>21.8	95	[2] AABOUD	16U	ATLS	$(\mu\mu qq)$
>12.0	>15.2	95	[3] KHACHATRY...	15AE	CMS	$(\mu\mu qq)$
>12.5	>16.7	95	[4] AAD	14BE	ATLS	$(\mu\mu qq)$
> 9.6	>12.9	95	[5] AAD	13E	ATLS	$(\mu\mu qq)$ (isosinglet)
> 9.5	>13.1	95	[6] CHATRCHYAN	13K	CMS	$(\mu\mu qq)$ (isosinglet)
> 8.0	>7.0	95	[7] AAD	12AB	ATLS	$(\mu\mu qq)$ (isosinglet)

[1] AABOUD 17AT limits are from pp collisions at $\sqrt{s} = 13$ TeV. The quoted limit uses a uniform positive prior in $1/\Lambda^2$.
[2] AABOUD 16U limits are from pp collisions at $\sqrt{s} = 13$ TeV. The quoted limit uses a uniform positive prior in $1/\Lambda^2$.
[3] KHACHATRYAN 15AE limit is from $\mu^+\mu^-$ mass distribution in pp collisions at $E_{cm} = 8$ TeV.
[4] AAD 14BE limits are from pp collisions at $\sqrt{s} = 8$ TeV. The quoted limit uses a uniform positive prior in $1/\Lambda^2$.
[5] AAD 13E limis are from $\mu^+\mu^-$ mass distribution in pp collisions at $E_{cm} = 7$ TeV.
[6] CHATRCHYAN 13K limis are from $\mu^+\mu^-$ mass distribution in pp collisions at $E_{cm} = 7$ TeV.
[7] AAD 12AB limis are from $\mu^+\mu^-$ mass distribution in pp collisions at $E_{cm} = 7$ TeV.

SCALE LIMITS for Contact Interactions: $\Lambda(\ell\nu\ell\nu)$

VALUE (TeV)	CL%	DOCUMENT ID		TECN	COMMENT
>3.10	90	[1] JODIDIO	86	SPEC	$\Lambda_{LR}^\pm(\nu_\mu\nu_e\mu e)$

• • • We do not use the following data for averages, fits, limits, etc. • • •

>3.8	[2] DIAZCRUZ	94	RVUE	$\Lambda_{LL}^+(\tau\nu_\tau e\nu_e)$
>8.1	[2] DIAZCRUZ	94	RVUE	$\Lambda_{LL}^-(\tau\nu_\tau e\nu_e)$
>4.1	[3] DIAZCRUZ	94	RVUE	$\Lambda_{LL}^+(\tau\nu_\tau\mu\nu_\mu)$
>6.5	[3] DIAZCRUZ	94	RVUE	$\Lambda_{LL}^-(\tau\nu_\tau\mu\nu_\mu)$

[1] JODIDIO 86 limit is from $\mu^+ \to \overline{\nu}_\mu e^+\nu_e$. Chirality invariant interactions $L = (g^2/\Lambda^2)$ $[\eta_{LL}\ (\overline{\nu}_{\mu L}\gamma^\alpha\mu_L)\ (\overline{e}_L\gamma_\alpha\nu_{eL}) + \eta_{LR}\ (\overline{\nu}_{\mu L}\gamma^\alpha\nu_{eL}\ (\overline{e}_R\gamma_\alpha\mu_R)]$ with $g^2/4\pi = 1$ and $(\eta_{LL},\eta_{LR}) = (0,\pm1)$ are taken. No limits are given for $\Lambda_{LL}^\pm$ with $(\eta_{LL},\eta_{LR}) = (\pm1,0)$. For more general constraints with right-handed neutrinos and chirality nonconserving contact interactions, see their text.
[2] DIAZCRUZ 94 limits are from $\Gamma(\tau \to e\nu\nu)$ and assume flavor-dependent contact interactions with $\Lambda(\tau\nu_\tau e\nu_e) \ll \Lambda(\mu\nu_\mu e\nu_e)$.
[3] DIAZCRUZ 94 limits are from $\Gamma(\tau \to \mu\nu\nu)$ and assume flavor-dependent contact interactions with $\Lambda(\tau\nu_\tau\mu\nu_\mu) \ll \Lambda(\mu\nu_\mu e\nu_e)$.

SCALE LIMITS for Contact Interactions: $\Lambda(e\nu qq)$

VALUE (TeV)	CL%	DOCUMENT ID		TECN
>2.81	95	[1] AFFOLDER	01I	CDF

[1] AFFOLDER 00I bound is for a scalar interaction $\overline{q}_R\, q_L\, \overline{\nu} e_L$.

SCALE LIMITS for Contact Interactions: $\Lambda(qqqq)$

Λ_{LL}^+(TeV)	Λ_{LL}^-(TeV)	CL%	DOCUMENT ID		TECN	COMMENT
>13.1 none 17.4–29.5	**>21.8**	95	[1] AABOUD	17AK	ATLS	pp dijet angl.

• • • We do not use the following data for averages, fits, limits, etc. • • •

>11.5	>14.7	95	[2] SIRUNYAN	17F	CMS	pp dijet angl.
>12.0	>17.5	95	[3] AAD	16S	ATLS	pp dijet angl.
			[4] AAD	15AR	ATLS	$pp \to t\bar{t}t\bar{t}$
			[5] AAD	15BY	ATLS	$pp \to t\bar{t}t\bar{t}$
> 8.1	>12.0	95	[6] AAD	15L	ATLS	pp dijet angl.
> 9.0	>11.7	95	[7] KHACHATRY...	15J	CMS	pp dijet angl.
> 5		95	[8] FABBRICHESI	14	RVUE	$q\overline{q}t\bar{t}$

[1] AABOUD 17AK limit is from dijet angular distribution in pp collisions at $\sqrt{s} = 13$ TeV. u, d, and s quarks are assumed to be composite.
[2] SIRUNYAN 17F limit is from dijet angular cross sections in pp collisions at $E_{cm} = 13$ TeV. All quarks are assumed to be composite.
[3] AAD 16S limit is from dijet angular selections in pp collisions at $E_{cm} = 13$ TeV. u, d, and s quarks are assumed to be composite.
[4] AAD 15AR obtain limit on the t_R compositeness $2\pi/\Lambda_{RR}^2 < 6.6$ TeV^{-2} at 95% CL from the $t\bar{t}t\bar{t}$ production in the pp collisions at $E_{cm} = 8$ TeV.
[5] AAD 15BY obtain limit on the t_R compositeness $2\pi/\Lambda_{RR}^2 < 15.1$ TeV^{-2} at 95% CL from the $t\bar{t}t\bar{t}$ production in the pp collisions at $E_{cm} = 8$ TeV.
[6] AAD 15L limit is from dijet angular distribution in pp collisions at $E_{cm} = 8$ TeV. u, d, and s quarks are assumed to be composite.
[7] KHACHATRYAN 15J limit is from dijet angular distribution in pp collisions at $E_{cm} = 8$ TeV. u, d, s, c, and b quarks are assumed to be composite.
[8] FABBRICHESI 14 obtain bounds on chromoelectric and chromomagnetic form factors of the top-quark using $pp \to t\bar{t}$ and $p\overline{p} \to t\bar{t}$ cross sections. The quoted limit on the $q\overline{q}t\bar{t}$ contact interaction is derived from their bound on the chromoelectric form factor.

SCALE LIMITS for Contact Interactions: $\Lambda(\nu\nu qq)$

Limits are for $\Lambda_{LL}^\pm$ only. For other cases, see each reference.

Λ_{LL}^+(TeV)	Λ_{LL}^-(TeV)	CL%	DOCUMENT ID		TECN	COMMENT
>5.0	**>5.4**	95	[1] MCFARLAND	98	CCFR	νN scattering

[1] MCFARLAND 98 assumed a flavor universal interaction. Neutrinos were mostly of muon type.

MASS LIMITS for Excited e (e^*)

Most e^+e^- experiments assume one-photon or Z exchange. The limits from some e^+e^- experiments which depend on λ have assumed transition couplings which are chirality violating ($\eta_L = \eta_R$). However they can be interpreted as limits for chirality-conserving interactions after multiplying the coupling value λ by $\sqrt{2}$; see Note.

Excited leptons have the same quantum numbers as other ortholeptons. See also the searches for ortholeptons in the "Searches for Heavy Leptons" section.

Limits for Excited e (e^*) from Pair Production

These limits are obtained from $e^+e^- \to e^{*+}e^{*-}$ and thus rely only on the (electroweak) charge of e^*. Form factor effects are ignored unless noted. For the case of limits from Z decay, the e^* coupling is assumed to be of sequential type. Possible t channel contribution from transition magnetic coupling is neglected. All limits assume a dominant $e^* \to e\gamma$ decay except the limits from $\Gamma(Z)$.

For limits prior to 1987, see our 1992 edition (Physical Review **D45** S1 (1992)).

VALUE (GeV)	CL%	DOCUMENT ID		TECN	COMMENT
>103.2	95	[1] ABBIENDI	02G	OPAL	$e^+e^- \to e^*e^*$ Homodoublet type

• • • We do not use the following data for averages, fits, limits, etc. • • •

>102.8	95	[2] ACHARD	03B	L3	$e^+e^- \to e^*e^*$ Homodoublet type

[1] From e^+e^- collisions at $\sqrt{s} = 183$–209 GeV. $f = f'$ is assumed.
[2] From e^+e^- collisions at $\sqrt{s} = 189$–209 GeV. $f = f'$ is assumed. ACHARD 03B also obtain limit for $f = -f'$: $m_{e^*} > 96.6$ GeV.

Limits for Excited e (e^*) from Single Production

These limits are from $e^+e^- \to e^*e$, $W \to e^*\nu$, or $ep \to e^*X$ and depend on transition magnetic coupling between e and e^*. All limits assume $e^* \to e\gamma$ decay except as noted. Limits from LEP, UA2, and H1 are for chiral coupling, whereas all other limits are for nonchiral coupling, $\eta_L = \eta_R = 1$. In most papers, the limit is expressed in the form of an excluded region in the λ–m_{e^*} plane. See the original papers.

For limits prior to 1987, see our 1992 edition (Physical Review **D45** S1 (1992)).

VALUE (GeV)	CL%	DOCUMENT ID		TECN	COMMENT
>3000	95	[1] AAD	15AP	ATLS	$pp \to e^{(*)}e^*X$

• • • We do not use the following data for averages, fits, limits, etc. • • •

>2450	95	[2] KHACHATRY...	16AQ	CMS	$pp \to ee^*X$
>2200	95	[3] AAD	13BB	ATLS	$pp \to ee^*X$
>1900	95	[4] CHATRCHYAN	13AE	CMS	$pp \to ee^*X$
>1870	95	[5] AAD	12AZ	ATLS	$pp \to e^{(*)}e^*X$

[1] AAD 15AP search for e^* production in evens with three or more charged leptons in pp collisions at $\sqrt{s} = 8$ TeV. The quoted limit assumes $\Lambda = m_{e^*}$, $f = f' = 1$. The contact interaction is included in the e^* production and decay amplitudes.
[2] KHACHATRYAN 16AQ search for single e^* production in pp collisions at $\sqrt{s} = 8$ TeV. The limit above is from the $e^* \to e\gamma$ search channel assuming $f = f' = 1$, $m_{e^*} = \Lambda$. See their Table 7 for limits in other search channels or with different assumptions.

[3] AAD 13BB search for single e^* production in pp collisions with $e^* \to e\gamma$ decay. $f = f' = 1$, and e^* production via contact interaction with $\Lambda = m_{e^*}$ are assumed.

[4] CHATRCHYAN 13AE search for single e^* production in pp collisions with $e^* \to e\gamma$ decay. $f = f' = 1$, and e^* production via contact interaction with $\Lambda = m_{e^*}$ are assumed.

[5] AAD 12AZ search for e^* production via four-fermion contact interaction in pp collisions with $e^* \to e\gamma$ decay. The quoted limit assumes $\Lambda = m_{e^*}$. See their Fig. 8 for the exclusion plot in the mass-coupling plane.

Limits for Excited e (e^*) from $e^+e^- \to \gamma\gamma$

These limits are derived from indirect effects due to e^* exchange in the t channel and depend on transition magnetic coupling between e and e^*. All limits are for $\lambda_\gamma = 1$. All limits except ABE 89J and ACHARD 02D are for nonchiral coupling with $\eta_L = \eta_R = 1$. We choose the chiral coupling limit as the best limit and list it in the Summary Table.

For limits prior to 1987, see our 1992 edition (Physical Review **D45** S1 (1992)).

VALUE (GeV)	CL%	DOCUMENT ID		TECN	COMMENT
>356	95	[1] ABDALLAH	04N	DLPH	$\sqrt{s}$= 161–208 GeV
• • • We do not use the following data for averages, fits, limits, etc. • • •					
>310	95	ACHARD	02D	L3	$\sqrt{s}$= 192–209 GeV

[1] ABDALLAH 04N also obtain a limit on the excited electron mass with ee^* chiral coupling, $m_{e^*} > 295$ GeV at 95% CL.

Indirect Limits for Excited e (e^*)

These limits make use of loop effects involving e^* and are therefore subject to theoretical uncertainty.

VALUE (GeV)	DOCUMENT ID		TECN	COMMENT
• • • We do not use the following data for averages, fits, limits, etc. • • •				
	[1] DORENBOS...	89	CHRM	$\overline{\nu}_\mu e \to \overline{\nu}_\mu e$, $\nu_\mu e \to \nu_\mu e$
	[2] GRIFOLS	86	THEO	$\nu_\mu e \to \nu_\mu e$
	[3] RENARD	82	THEO	$g-2$ of electron

[1] DORENBOSCH 89 obtain the limit $\lambda_\gamma^2 \Lambda_{\rm cut}^2 / m_{e^*}^2 < 2.6$ (95% CL), where $\Lambda_{\rm cut}$ is the cutoff scale, based on the one-loop calculation by GRIFOLS 86. If one assumes that $\Lambda_{\rm cut} = 1$ TeV and $\lambda_\gamma = 1$, one obtains $m_{e^*} > 620$ GeV. However, one generally expects $\lambda_\gamma \approx m_{e^*}/\Lambda_{\rm cut}$ in composite models.

[2] GRIFOLS 86 uses $\nu_\mu e \to \nu_\mu e$ and $\overline{\nu}_\mu e \to \overline{\nu}_\mu e$ data from CHARM Collaboration to derive mass limits which depend on the scale of compositeness.

[3] RENARD 82 derived from $g-2$ data limits on mass and couplings of e^* and μ^*. See figures 2 and 3 of the paper.

MASS LIMITS for Excited μ (μ^*)

Limits for Excited μ (μ^*) from Pair Production

These limits are obtained from $e^+e^- \to \mu^{*+}\mu^{*-}$ and thus rely only on the (electroweak) charge of μ^*. Form factor effects are ignored unless noted. For the case of limits from Z decay, the μ^* coupling is assumed to be of sequential type. All limits assume a dominant $\mu^* \to \mu\gamma$ decay except the limits from $\Gamma(Z)$.

For limits prior to 1987, see our 1992 edition (Physical Review **D45** S1 (1992)).

VALUE (GeV)	CL%	DOCUMENT ID		TECN	COMMENT
>103.2	95	[1] ABBIENDI	02G	OPAL	$e^+e^- \to \mu^*\mu^*$ Homodoublet type
• • • We do not use the following data for averages, fits, limits, etc. • • •					
>102.8	95	[2] ACHARD	03B	L3	$e^+e^- \to \mu^*\mu^*$ Homodoublet type

[1] From e^+e^- collisions at $\sqrt{s} = 183$–209 GeV. $f = f'$ is assumed.

[2] From e^+e^- collisions at $\sqrt{s} = 189$–209 GeV. $f = f'$ is assumed. ACHARD 03B also obtain limit for $f = -f'$: $m_{\mu^*} > 96.6$ GeV.

Limits for Excited μ (μ^*) from Single Production

These limits are from $e^+e^- \to \mu^*\mu$ and depend on transition magnetic coupling between μ and μ^*. All limits assume $\mu^* \to \mu\gamma$ decay. Limits from LEP are for chiral coupling, whereas all other limits are for nonchiral coupling, $\eta_L = \eta_R = 1$. In most papers, the limit is expressed in the form of an excluded region in the λ–m_{μ^*} plane. See the original papers.

For limits prior to 1987, see our 1992 edition (Physical Review **D45** S1 (1992)).

VALUE (GeV)	CL%	DOCUMENT ID		TECN	COMMENT
>3000	95	[1] AAD	15AP	ATLS	$pp \to \mu^{(*)}\mu^* X$
• • • We do not use the following data for averages, fits, limits, etc. • • •					
>2800	95	[2] AAD	16BM	ATLS	$pp \to \mu\mu^* X$
>2470	95	[3] KHACHATRY...16AQ		CMS	$pp \to \mu\mu^* X$
>2200	95	[4] AAD	13BB	ATLS	$pp \to \mu\mu^* X$
>1900	95	[5] CHATRCHYAN	13AE	CMS	$pp \to \mu\mu^* X$
>1750	95	[6] AAD	12AZ	ATLS	$pp \to \mu^{(*)}\mu^* X$

[1] AAD 15AP search for μ^* production in evens with three or more charged leptons in pp collisions at $\sqrt{s} = 8$ TeV. The quoted limit assumes $\Lambda = m_{\mu^*}$, $f = f' = 1$. The contact interaction is included in the μ^* production and decay amplitudes.

[2] AAD 16BM search for μ^* production in $\mu\mu jj$ events in pp collisions at $\sqrt{s} = 8$ TeV. Both the production and decay are assumed to occur via a contact interaction with $\Lambda = m_{\mu^*}$.

[3] KHACHATRYAN 16AQ search for single μ^* production in pp collisions at $\sqrt{s} = 8$ TeV. The limit above is from the $\mu^* \to \mu\gamma$ search channel assuming $f = f' = 1$, $m_{\mu^*} = \Lambda$. See their Table 7 for limits in other search channels or with different assumptions.

[4] AAD 13BB search for single μ^* production in pp collisions with $\mu^* \to \mu\gamma$ decay. $f = f' = 1$, and μ^* production via contact interaction with $\Lambda = m_{\mu^*}$ are assumed.

[5] CHATRCHYAN 13AE search for single μ^* production in pp collisions with $\mu^* \to \mu\gamma$ decay. $f = f' = 1$, and μ^* production via contact interaction with $\Lambda = m_{\mu^*}$ are assumed.

[6] AAD 12AZ search for μ^* production via four-fermion contact interaction in pp collisions with $\mu^* \to \mu\gamma$ decay. The quoted limit assumes $\Lambda = m_{\mu^*}$. See their Fig. 8 for the exclusion plot in the mass-coupling plane.

Indirect Limits for Excited μ (μ^*)

These limits make use of loop effects involving μ^* and are therefore subject to theoretical uncertainty.

VALUE (GeV)	DOCUMENT ID		TECN	COMMENT
• • • We do not use the following data for averages, fits, limits, etc. • • •				
	[1] RENARD	82	THEO	$g-2$ of muon

[1] RENARD 82 derived from $g-2$ data limits on mass and couplings of e^* and μ^*. See figures 2 and 3 of the paper.

MASS LIMITS for Excited τ (τ^*)

Limits for Excited τ (τ^*) from Pair Production

These limits are obtained from $e^+e^- \to \tau^{*+}\tau^{*-}$ and thus rely only on the (electroweak) charge of τ^*. Form factor effects are ignored unless noted. For the case of limits from Z decay, the τ^* coupling is assumed to be of sequential type. All limits assume a dominant $\tau^* \to \tau\gamma$ decay except the limits from $\Gamma(Z)$.

For limits prior to 1987, see our 1992 edition (Physical Review **D45** S1 (1992)).

VALUE (GeV)	CL%	DOCUMENT ID		TECN	COMMENT
>103.2	95	[1] ABBIENDI	02G	OPAL	$e^+e^- \to \tau^*\tau^*$ Homodoublet type
• • • We do not use the following data for averages, fits, limits, etc. • • •					
>102.8	95	[2] ACHARD	03B	L3	$e^+e^- \to \tau^*\tau^*$ Homodoublet type

[1] From e^+e^- collisions at $\sqrt{s} = 183$–209 GeV. $f = f'$ is assumed.

[2] From e^+e^- collisions at $\sqrt{s} = 189$–209 GeV. $f = f'$ is assumed. ACHARD 03B also obtain limit for $f = -f'$: $m_{\tau^*} > 96.6$ GeV.

Limits for Excited τ (τ^*) from Single Production

These limits are from $e^+e^- \to \tau^*\tau$ and depend on transition magnetic coupling between τ and τ^*. All limits assume $\tau^* \to \tau\gamma$ decay. Limits from LEP are for chiral coupling, whereas all other limits are for nonchiral coupling, $\eta_L = \eta_R = 1$. In most papers, the limit is expressed in the form of an excluded region in the λ–m_{τ^*} plane. See the original papers.

VALUE (GeV)	CL%	DOCUMENT ID		TECN	COMMENT
>2500	95	[1] AAD	15AP	ATLS	$pp \to \tau^{(*)}\tau^* X$
• • • We do not use the following data for averages, fits, limits, etc. • • •					
> 180	95	[2] ACHARD	03B	L3	$e^+e^- \to \tau\tau^*$
> 185	95	[3] ABBIENDI	02G	OPAL	$e^+e^- \to \tau\tau^*$

[1] AAD 15AP search for τ^* production in events with three or more charged leptons in pp collisions at $\sqrt{s} = 8$ TeV. The quoted limit assumes $\Lambda = m_{\tau^*}$, $f = f' = 1$. The contact interaction is included in the τ^* production and decay amplitudes.

[2] ACHARD 03B result is from e^+e^- collisions at $\sqrt{s} = 189$–209 GeV. $f = f' = \Lambda/m_{\tau^*}$ is assumed. See their Fig. 4 for the exclusion plot in the mass-coupling plane.

[3] ABBIENDI 02G result is from e^+e^- collisions at $\sqrt{s} = 183$–209 GeV. $f = f' = \Lambda/m_{\tau^*}$ is assumed for τ^* coupling. See their Fig. 4c for the exclusion limit in the mass-coupling plane.

MASS LIMITS for Excited Neutrino (ν^*)

Limits for Excited ν (ν^*) from Pair Production

These limits are obtained from $e^+e^- \to \nu^*\nu^*$ and thus rely only on the (electroweak) charge of ν^*. Form factor effects are ignored unless noted. The ν^* coupling is assumed to be of sequential type unless otherwise noted. All limits assume a dominant $\nu^* \to \nu\gamma$ decay except the limits from $\Gamma(Z)$.

VALUE (GeV)	CL%	DOCUMENT ID		TECN	COMMENT
>1600	95	[1] AAD	15AP	ATLS	$pp \to \nu^*\nu^* X$
• • • We do not use the following data for averages, fits, limits, etc. • • •					
	[2] ABBIENDI	04N	OPAL		
> 102.6	95	[3] ACHARD	03B	L3	$e^+e^- \to \nu^*\nu^*$ Homodoublet type

[1] AAD 15AP search for ν^* pair production in evens with three or more charged leptons in pp collisions at $\sqrt{s} = 8$ TeV. The quoted limit assumes $\Lambda = m_{\nu^*}$, $f = f' = 1$. The contact interaction is included in the ν^* production and decay amplitudes.

[2] From e^+e^- collisions at $\sqrt{s} = 192$–209 GeV, ABBIENDI 04N obtain limit on $\sigma(e^+e^- \to \nu^*\nu^*)\,B^2(\nu^* \to \nu\gamma)$. See their Fig.2. The limit ranges from 20 to 45 fb for $m_{\nu^*} > 45$ GeV.

[3] From e^+e^- collisions at $\sqrt{s} = 189$–209 GeV. $f = -f'$ is assumed. ACHARD 03B also obtain limit for $f = f'$: $m_{\nu_e^*} > 101.7$ GeV, $m_{\nu_\mu^*} > 101.8$ GeV, and $m_{\nu_\tau^*} > 92.9$ GeV. See their Fig. 4 for the exclusion plot in the mass-coupling plane.

Limits for Excited ν (ν^*) from Single Production

These limits are from $e^+e^- \to \nu\nu^*$, $Z \to \nu\nu^*$, or $ep \to \nu^* X$ and depend on transition magnetic coupling between ν/e and ν^*. Assumptions about ν^* decay mode are given in footnotes.

VALUE (GeV)	CL%	DOCUMENT ID		TECN	COMMENT
>213	95	[1] AARON	08	H1	$ep \to \nu^* X$
• • • We do not use the following data for averages, fits, limits, etc. • • •					
>190	95	[2] ACHARD	03B	L3	$e^+e^- \to \nu\nu^*$
none 50–150	95	[3] ADLOFF	02	H1	$ep \to \nu^* X$
>158	95	[4] CHEKANOV	02D	ZEUS	$ep \to \nu^* X$

[1] AARON 08 search for single ν^* production in ep collisions with the decays $\nu^* \to \nu\gamma$, νZ, eW. The quoted limit assumes $f = -f' = \Lambda/m_{\nu^*}$. See their Fig. 3 and Fig. 4 for the exclusion plots in the mass-coupling plane.

[2] ACHARD 03B result is from e^+e^- collisions at $\sqrt{s}$ = 189–209 GeV. The quoted limit is for ν_e^*. $f = -f' = \Lambda/m_{\nu^*}$ is assumed. See their Fig. 4 for the exclusion plot in the mass-coupling plane.

[3] ADLOFF 02 search for single ν^* production in ep collisions with the decays $\nu^* \to \nu\gamma$, νZ, eW. The quoted limit assumes $f = -f' = \Lambda/m_{\nu^*}$. See their Fig. 1 for the exclusion plots in the mass-coupling plane.

[4] CHEKANOV 02D search for single ν^* production in ep collisions with the decays $\nu^* \to \nu\gamma$, νZ, eW. $f = -f' = \Lambda/m_{\nu^*}$ is assumed for the e^* coupling. CHEKANOV 02D also obtain limit for $f = f' = \Lambda/m_{\nu^*}$: m_{ν^*} >135 GeV. See their Fig. 5c and Fig. 5d for the exclusion plot in the mass-coupling plane.

MASS LIMITS for Excited q (q^*)

Limits for Excited q (q^*) from Pair Production

These limits are mostly obtained from $e^+e^- \to q^*\overline{q}^*$ and thus rely only on the (electroweak) charge of the q^*. Form factor effects are ignored unless noted. Assumptions about the q^* decay are given in the comments and footnotes.

VALUE (GeV)	CL%	DOCUMENT ID		TECN	COMMENT
>338	95	[1] AALTONEN	10H	CDF	$q^* \to tW^-$
• • • We do not use the following data for averages, fits, limits, etc. • • •					
		[2] BARATE	98U	ALEP	$Z \to q^*q^*$
> 45.6	95	[3] ADRIANI	93M	L3	u or d type, $Z \to q^*q^*$
> 41.7	95	[4] BARDADIN-...	92	RVUE	u-type, $\Gamma(Z)$
> 44.7	95	[4] BARDADIN-...	92	RVUE	d-type, $\Gamma(Z)$
> 40.6	95	[5] DECAMP	92	ALEP	u-type, $\Gamma(Z)$
> 44.2	95	[5] DECAMP	92	ALEP	d-type, $\Gamma(Z)$
> 45	95	[6] DECAMP	92	ALEP	u or d type, $Z \to q^*q^*$
> 45	95	[5] ABREU	91F	DLPH	u-type, $\Gamma(Z)$
> 45	95	[5] ABREU	91F	DLPH	d-type, $\Gamma(Z)$

[1] AALTONEN 10H obtain limits on the q^*q^* production cross section in $p\overline{p}$ collisions. See their Fig. 3.

[2] BARATE 98U obtain limits on the form factor. See their Fig. 16 for limits in mass-form factor plane.

[3] ADRIANI 93M limit is valid for B($q^* \to qg$)> 0.25 (0.17) for up (down) type.

[4] BARDADIN-OTWINOWSKA 92 limit based on $\Delta\Gamma(Z)$<36 MeV.

[5] These limits are independent of decay modes.

[6] Limit is for B($q^* \to qg$)+B($q^* \to q\gamma$)=1.

Limits for Excited q (q^*) from Single Production

These limits are from $e^+e^- \to q^*\overline{q}$, $p\overline{p} \to q^*X$, or $pp \to q^*X$ and depend on transition magnetic couplings between q and q^*. Assumptions about q^* decay mode are given in the footnotes and comments.

VALUE (GeV)	CL%	DOCUMENT ID		TECN	COMMENT
>6000	95	[1] AABOUD	17AK	ATLS	$pp \to q^*X$, $q^* \to qg$
• • • We do not use the following data for averages, fits, limits, etc. • • •					
none 600–5400	95	[2] KHACHATRY...	17W	CMS	$pp \to q^*X$, $q^* \to qg$
none 1100–2100	95	[3] AABOUD	16	ATLS	$pp \to b^*X$, $b^* \to bg$
>1500	95	[4] AAD	16AH	ATLS	$pp \to b^*X$, $b^* \to tW$
>4400	95	[5] AAD	16AI	ATLS	$pp \to q^*X$, $q^* \to q\gamma$
		[6] AAD	16AV	ATLS	$pp \to q^*X$, $q^* \to Wb$
>5200	95	[7] AAD	16S	ATLS	$pp \to q^*X$, $q^* \to qg$
>1390	95	[8] KHACHATRY...	16I	CMS	$pp \to b^*X$, $b^* \to tW$
>5000	95	[9] KHACHATRY...	16K	CMS	$pp \to q^*X$, $q^* \to qg$
none 500–1600	95	[10] KHACHATRY...	16L	CMS	$pp \to q^*X$, $q^* \to qg$
>4060	95	[11] AAD	15V	ATLS	$pp \to q^*X$, $q^* \to qg$
>3500	95	[12] KHACHATRY...	15V	CMS	$pp \to q^*X$, $q^* \to qg$
>3500	95	[13] AAD	14A	ATLS	$pp \to q^*X$, $q^* \to q\gamma$
>3200	95	[14] KHACHATRY...	14	CMS	$pp \to q^*X$, $q^* \to qW$
>2900	95	[15] KHACHATRY...	14	CMS	$pp \to q^*X$, $q^* \to qZ$
none 700–3500	95	[16] KHACHATRY...	14J	CMS	$pp \to q^*X$, $q^* \to q\gamma$
>2380	95	[17] CHATRCHYAN	13AJ	CMS	$pp \to q^*X$, $q^* \to qW$
>2150	95	[18] CHATRCHYAN	13AJ	CMS	$pp \to q^*X$, $q^* \to qZ$

[1] AABOUD 17AK assume $\Lambda = m_{q^*}$, $f_s = f = f' = 1$. The contact interactions are not included in q^* production and decay amplitudes. Only the decay of $q^* \to gu$ and $q^* \to gd$ is simulated as the benchmark signals in the analysis.

[2] KHACHATRYAN 17W assume $\Lambda = m_{q^*}$, $f_s = f = f' = 1$. The contact interactions are not included in q^* production and decay amplitudes.

[3] AABOUD 16 assume $\Lambda = m_{b^*}$, $f_s = f = f' = 1$. The contact interactions are not included in the b^* production and decay amplitudes.

[4] AAD 16AH search for b^* decaying to tW in pp collisions at $\sqrt{s}$ = 8 TeV. $f_g = f_L = f_R = 1$ are assumed. See their Fig. 12b for limits on $\sigma \cdot B$.

[5] AAD 16AI assume $\Lambda = m_{q^*}$, $f_s = f = f' = 1$.

[6] AAD 16AV search for single production of vector-like quarks decaying to Wb in pp collisions. See their Fig. 8 for the limits on couplings and mixings.

[7] AAD 16S assume $\Lambda = m_{q^*}$, $f_s = f = f' = 1$. The contact interactions are not included in q^* production and decay amplitudes.

[8] KHACHATRYAN 16I search for b^* decaying to tW in pp collisions at $\sqrt{s}$ = 8 TeV. $\kappa_L^b = g_L = 1$, $\kappa_R^b = g_R = 0$ are assumed. See their Fig. 8 for limits on $\sigma \cdot B$.

[9] KHACHATRYAN 16K assume $\Lambda = m_{q^*}$, $f_s = f = f' = 1$. The contact interactions are not included in q^* production and decay amplitudes.

[10] KHACHATRYAN 16L search for resonances decaying to dijets in pp collisions at $\sqrt{s}$ = 8 TeV using the data scouting technique which increases the sensitivity to the low mass resonances.

[11] AAD 15V assume $\Lambda = m_{q^*}$, $f_s = f = f' = 1$. The contact interactions are not included in q^* production and decay amplitudes.

[12] KHACHATRYAN 15V assume $\Lambda = m_{q^*}$, $f_s = f = f' = 1$. The contact interactions are not included in q^* production and decay amplitudes.

[13] AAD 14A assume $\Lambda = m_{q^*}$, $f_s = f = f' = 1$.

[14] KHACHATRYAN 14 use the hadronic decay of W, assuming $\Lambda = m_{q^*}$, f_s=f=f' = 1.

[15] KHACHATRYAN 14 use the hadronic decay of Z, assuming $\Lambda = m_{q^*}$, f_s=f=f' = 1.

[16] KHACHATRYAN 14J assume $f_s = f = f' = \Lambda$ / m_{q^*}.

[17] CHATRCHYAN 13AJ use the hadronic decay of W.

[18] CHATRCHYAN 13AJ use the hadronic decay of Z.

MASS LIMITS for Color Sextet Quarks (q_6)

VALUE (GeV)	CL%	DOCUMENT ID		TECN	COMMENT
>84	95	[1] ABE	89D	CDF	$p\overline{p} \to q_6\overline{q}_6$

[1] ABE 89D look for pair production of unit-charged particles which leave the detector before decaying. In the above limit the color sextet quark is assumed to fragment into a unit-charged or neutral hadron with equal probability and to have long enough lifetime not to decay within the detector. A limit of 121 GeV is obtained for a color decuplet.

MASS LIMITS for Color Octet Charged Leptons (ℓ_8)

$\lambda \equiv m_{\ell_8}/\Lambda$

VALUE (GeV)	CL%	DOCUMENT ID		TECN	COMMENT
>86	95	[1] ABE	89D	CDF	Stable ℓ_8: $p\overline{p} \to \ell_8\overline{\ell}_8$
• • • We do not use the following data for averages, fits, limits, etc. • • •					
		[2] ABT	93	H1	e_8: $ep \to e_8 X$

[1] ABE 89D look for pair production of unit-charged particles which leave the detector before decaying. In the above limit the color octet lepton is assumed to fragment into a unit-charged or neutral hadron with equal probability and to have long enough lifetime not to decay within the detector. The limit improves to 99 GeV if it always fragments into a unit-charged hadron.

[2] ABT 93 search for e_8 production via e-gluon fusion in ep collisions with $e_8 \to eg$. See their Fig. 3 for exclusion plot in the m_{e_8}–Λ plane for m_{e_8} = 35–220 GeV.

MASS LIMITS for Color Octet Neutrinos (ν_8)

$\lambda \equiv m_{\ell_8}/\Lambda$

VALUE (GeV)	CL%	DOCUMENT ID		TECN	COMMENT
>110	90	[1] BARGER	89	RVUE	ν_8: $p\overline{p} \to \nu_8\overline{\nu}_8$
• • • We do not use the following data for averages, fits, limits, etc. • • •					
none 3.8–29.8	95	[2] KIM	90	AMY	ν_8: $e^+e^- \to$ acoplanar jets
none 9–21.9	95	[3] BARTEL	87B	JADE	ν_8: $e^+e^- \to$ acoplanar jets

[1] BARGER 89 used ABE 89B limit for events with large missing transverse momentum. Two-body decay $\nu_8 \to \nu g$ is assumed.

[2] KIM 90 is at E_{cm} = 50–60.8 GeV. The same assumptions as in BARTEL 87B are used.

[3] BARTEL 87B is at E_{cm} = 46.3–46.78 GeV. The limit assumes the ν_8 pair production cross section to be eight times larger than that of the corresponding heavy neutrino pair production. This assumption is not valid in general for the weak couplings, and the limit can be sensitive to its $SU(2)_L \times U(1)_Y$ quantum numbers.

MASS LIMITS for W_8 (Color Octet W Boson)

VALUE (GeV)	DOCUMENT ID		TECN	COMMENT
• • • We do not use the following data for averages, fits, limits, etc. • • •				
	[1] ALBAJAR	89	UA1	$p\overline{p} \to W_8 X$, $W_8 \to Wg$

[1] ALBAJAR 89 give $\sigma(W_8 \to W + \text{jet})/\sigma(W) < 0.019$ (90% CL) for $m_{W_8} > 220$ GeV.

REFERENCES FOR Searches for Quark and Lepton Compositeness

AABOUD	17AK	PR D96 052004	M. Aaboud *et al.*	(ATLAS Collab.)
AABOUD	17AT	JHEP 1710 182	M. Aaboud *et al.*	(ATLAS Collab.)
KHACHATRY...	17W	PL B769 520	V. Khachatryan *et al.*	(CMS Collab.)
SIRUNYAN	17F	JHEP 1707 013	A.M. Sirunyan *et al.*	(CMS Collab.)
AABOUD	16	PL B759 229	M. Aaboud *et al.*	(ATLAS Collab.)
AABOUD	16U	PL B761 372	M. Aaboud *et al.*	(ATLAS Collab.)
AAD	16AH	JHEP 1602 110	G. Aad *et al.*	(ATLAS Collab.)
AAD	16AI	JHEP 1603 041	G. Aad *et al.*	(ATLAS Collab.)

Searches Particle Listings

Quark and Lepton Compositeness, Extra Dimensions

AAD 16AV EPJ C76 442 G. Aad *et al.* (ATLAS Collab.)
AAD 16BM NJP 18 073021 G. Aad *et al.* (ATLAS Collab.)
AAD 16S PL B754 302 G. Aad *et al.* (ATLAS Collab.)
KHACHATRY... 16AQ JHEP 1603 125 V. Khachatryan *et al.* (CMS Collab.)
KHACHATRY... 16I JHEP 1601 166 V. Khachatryan *et al.* (CMS Collab.)
KHACHATRY... 16K PRL 116 071801 V. Khachatryan *et al.* (CMS Collab.)
KHACHATRY... 16L PRL 117 031802 V. Khachatryan *et al.* (CMS Collab.)
AAD 15AP JHEP 1508 138 G. Aad *et al.* (ATLAS Collab.)
AAD 15AR JHEP 1508 105 G. Aad *et al.* (ATLAS Collab.)
AAD 15BY JHEP 1510 150 G. Aad *et al.* (ATLAS Collab.)
AAD 15L PRL 114 221802 G. Aad *et al.* (ATLAS Collab.)
AAD 15V PR D91 052007 G. Aad *et al.* (ATLAS Collab.)
KHACHATRY... 15AE JHEP 1504 025 V. Khachatryan *et al.* (CMS Collab.)
KHACHATRY... 15J PL B746 79 V. Khachatryan *et al.* (CMS Collab.)
KHACHATRY... 15V PR D91 052009 V. Khachatryan *et al.* (CMS Collab.)
AAD 14A PL B728 562 G. Aad *et al.* (ATLAS Collab.)
AAD 14BE EPJ C74 3134 G. Aad *et al.* (ATLAS Collab.)
FABBRICHESI 14 PR D89 074028 M. Fabbrichesi, M. Pinamonti, A. Tonero
KHACHATRY... 14 JHEP 1408 173 V. Khachatryan *et al.* (CMS Collab.)
KHACHATRY... 14J PL B738 274 V. Khachatryan *et al.* (CMS Collab.)
AAD 13BB NJP 15 093011 G. Aad *et al.* (ATLAS Collab.)
AAD 13E PR D87 015010 G. Aad *et al.* (ATLAS Collab.)
CHATRCHYAN 13AE PL B720 309 S. Chatrchyan *et al.* (CMS Collab.)
CHATRCHYAN 13AJ PL B723 280 S. Chatrchyan *et al.* (CMS Collab.)
CHATRCHYAN 13K PR D87 032001 S. Chatrchyan *et al.* (CMS Collab.)
AAD 12AB PL B712 40 G. Aad *et al.* (ATLAS Collab.)
AAD 12AZ PR D85 072003 G. Aad *et al.* (ATLAS Collab.)
AARON 11C PL B705 52 F. D. Aaron *et al.* (H1 Collab.)
ABDALLAH 11 EPJ C71 1555 J. Abdallah *et al.* (DELPHI Collab.)
AALTONEN 10H PRL 104 091801 T. Aaltonen *et al.* (CDF Collab.)
ABDALLAH 09 EPJ C60 1 J. Abdallah *et al.* (DELPHI Collab.)
AARON 08 PL B663 382 F.D. Aaron *et al.* (H1 Collab.)
SCHAEL 07A EPJ C49 411 S. Schael *et al.* (ALEPH Collab.)
ABDALLAH 06C EPJ C45 589 J. Abdallah *et al.* (DELPHI Collab.)
ABULENCIA 06L PRL 96 211801 A. Abulencia *et al.* (CDF Collab.)
ABBIENDI 04G EPJ C33 173 G. Abbiendi *et al.* (OPAL Collab.)
ABBIENDI 04N PL B602 167 G. Abbiendi *et al.* (OPAL Collab.)
ABDALLAH 04N EPJ C37 405 J. Abdallah *et al.* (DELPHI Collab.)
ACHARD 03B PL B568 23 P. Achard *et al.* (L3 Collab.)
BABICH 03 EPJ C29 103 A.A. Babich *et al.*
ABBIENDI 02G PL B544 57 G. Abbiendi *et al.* (OPAL Collab.)
ACHARD 02D PL B531 28 P. Achard *et al.* (L3 Collab.)
ADLOFF 02 PL B525 9 C. Adloff *et al.* (H1 Collab.)
CHEKANOV 02D PL B549 32 S. Chekanov *et al.* (ZEUS Collab.)
AFFOLDER 01I PRL 87 231803 T. Affolder *et al.* (CDF Collab.)
BOURILKOV 01 PR D64 071701 D. Bourilkov
CHEUNG 01B PL B517 167 K. Cheung
ACCIARRI 00P PL B489 81 M. Acciarri *et al.* (L3 Collab.)
AFFOLDER 00I PR D62 012004 T. Affolder *et al.* (CDF Collab.)
BARATE 98U EPJ C4 571 R. Barate *et al.* (ALEPH Collab.)
BARGER 98E PR D57 391 V. Barger *et al.*
MCFARLAND 98 EPJ C1 509 K.S. McFarland *et al.* (CCFR/NuTeV Collab.)
DIAZCRUZ 94 PR D49 2149 J.L. Diaz Cruz, O.A. Sampayo (CINV)
ABT 93 NP B396 3 I. Abt *et al.* (H1 Collab.)
ADRIANI 93M PRPL 236 1 O. Adriani *et al.* (L3 Collab.)
BARDADIN-... 92 ZPHY C55 163 M. Bardadin-Otwinowska (CLER)
DECAMP 92 PRPL 216 253 D. Decamp *et al.* (ALEPH Collab.)
PDG 92 PR D45 S1 K. Hikasa *et al.* (KEK, LBL, BOST+)
ABREU 91F NP B367 511 P. Abreu *et al.* (DELPHI Collab.)
KIM 90 PL B240 243 G.N. Kim *et al.* (AMY Collab.)
ABE 89B PRL 62 1825 F. Abe *et al.* (CDF Collab.)
ABE 89D PRL 63 1447 F. Abe *et al.* (CDF Collab.)
ABE 89J ZPHY C45 175 K. Abe *et al.* (VENUS Collab.)
ALBAJAR 89 ZPHY C44 15 C. Albajar *et al.* (UA1 Collab.)
BARGER 89 PL B220 464 V. Barger *et al.* (WISC, KEK)
DORENBOS... 89 ZPHY C41 567 J. Dorenbosch *et al.* (CHARM Collab.)
BARTEL 87B ZPHY C36 15 W. Bartel *et al.* (JADE Collab.)
GRIFOLS 86 PL 168B 264 J.A. Grifols, S. Peris (BARC)
JODIDIO 86 PR D34 1967 A. Jodidio *et al.* (LBL, NWES, TRIU)
Also PR D37 237 (erratum) A. Jodidio *et al.* (LBL, NWES, TRIU)
RENARD 82 PL 116B 264 F.M. Renard (CERN)

Extra Dimensions

For explanation of terms used and discussion of significant model dependence of following limits, see the "Extra Dimensions" review. Footnotes describe originally quoted limit. δ indicates the number of extra dimensions.

Limits not encoded here are summarized in the "Extra Dimensions" review, where the latest unpublished results are also described.

See the related review(s):
Extra Dimensions Searches

CONTENTS:

Limits on R from Deviations in Gravitational Force Law

This section includes limits on the size of extra dimensions from deviations in the Newtonian ($1/r^2$) gravitational force law at short distances. Deviations are parametrized by a gravitational potential of the form $V = -(G\ m\ m'/r)\ [1 + \alpha\ \exp(-r/R)]$. For δ toroidal extra dimensions of equal size, $\alpha = 8\delta/3$. Quoted bounds are for $\delta = 2$ unless otherwise noted.

VALUE (μm)	CL%	DOCUMENT ID		COMMENT
< 30	95	[1] KAPNER	07	Torsion pendulum
• • • We do not use the following data for averages, fits, limits, etc. • • •				
		[2] KLIMCHITSK...	17A	Torsion oscillator
		[3] XU	13	Nuclei properties
		[4] BEZERRA	11	Torsion oscillator
		[5] SUSHKOV	11	Torsion pendulum
		[6] BEZERRA	10	Microcantilever
		[7] MASUDA	09	Torsion pendulum
		[8] GERACI	08	Microcantilever
		[9] TRENKEL	08	Newton's constant
		[10] DECCA	07A	Torsion oscillator
< 47	95	[11] TU	07	Torsion pendulum
		[12] SMULLIN	05	Microcantilever
<130	95	[13] HOYLE	04	Torsion pendulum
		[14] CHIAVERINI	03	Microcantilever
$\lesssim$200	95	[15] LONG	03	Microcantilever
<190	95	[16] HOYLE	01	Torsion pendulum
		[17] HOSKINS	85	Torsion pendulum

[1] KAPNER 07 search for new forces, probing a range of $\alpha \simeq 10^{-3}$–10^{5} and length scales $R \simeq$ 10–1000 μm. For $\delta = 1$ the bound on R is 44 μm. For $\delta = 2$, the bound is expressed in terms of M_*, here translated to a bound on the radius. See their Fig. 6 for details on the bound.

[2] KLIMCHITSKAYA 17A uses an experiment that measures the difference of Casimir forces to obtain bounds on non-Newtonian forces with strengths $|\alpha| \simeq 10^{5}$–10^{17} and length scales $R = 0.03$–10 μm. See their Fig. 3. These constraints do not place limits on the size of extra flat dimensions.

[3] XU 13 obtain constraints on non-Newtonian forces with strengths $|\alpha| \simeq 10^{34}$–10^{36} and length scales $R \simeq$ 1–10 fm. See their Fig. 4 for more details. These constraints do not place limits on the size of extra flat dimensions.

[4] BEZERRA 11 obtain constraints on non-Newtonian forces with strengths $10^{11} \lesssim |\alpha| \lesssim 10^{18}$ and length scales $R =$ 30–1260 nm. See their Fig. 2 for more details. These constraints do not place limits on the size of extra flat dimensions.

[5] SUSHKOV 11 obtain improved limits on non-Newtonian forces with strengths $10^{7} \lesssim |\alpha| \lesssim 10^{11}$ and length scales 0.4 μm $< R <$ 4 μm (95% CL). See their Fig. 2. These bounds do not place limits on the size of extra flat dimensions. However, a model dependent bound of $M_* > 70$ TeV is obtained assuming gauge bosons that couple to baryon number also propagate in $(4 + \delta)$ dimensions.

[6] BEZERRA 10 obtain improved constraints on non-Newtonian forces with strengths $10^{19} \lesssim |\alpha| \lesssim 10^{29}$ and length scales $R =$ 1.6–14 nm (95% CL). See their Fig. 1. This bound does not place limits on the size of extra flat dimensions.

[7] MASUDA 09 obtain improved constraints on non-Newtonian forces with strengths $10^{9} \lesssim |\alpha| \lesssim 10^{11}$ and length scales $R =$ 1.0–2.9 μm (95% CL). See their Fig. 3. This bound does not place limits on the size of extra flat dimensions.

[8] GERACI 08 obtain improved constraints on non-Newtonian forces with strengths $|\alpha| >$ 14,000 and length scales $R =$ 5–15 μm. See their Fig. 9. This bound does not place limits on the size of extra flat dimensions.

[9] TRENKEL 08 uses two independent measurements of Newton's constant G to constrain new forces with strength $|\alpha| \simeq 10^{-4}$ and length scales $R =$ 0.02–1 m. See their Fig. 1. This bound does not place limits on the size of extra flat dimensions.

[10] DECCA 07A search for new forces and obtain bounds in the region with strengths $|\alpha| \simeq 10^{13}$–10^{18} and length scales $R =$ 20–86 nm. See their Fig. 6. This bound does not place limits on the size of extra flat dimensions.

[11] TU 07 search for new forces probing a range of $|\alpha| \simeq 10^{-1}$–10^{5} and length scales $R \simeq$ 20–1000 μm. For $\delta = 1$ the bound on R is 53 μm. See their Fig. 3 for details on the bound.

[12] SMULLIN 05 search for new forces, and obtain bounds in the region with strengths $\alpha \simeq 10^{3}$–10^{8} and length scales $R =$ 6–20 μm. See their Figs. 1 and 16 for details on the bound. This work does not place limits on the size of extra flat dimensions.

[13] HOYLE 04 search for new forces, probing α down to 10^{-2} and distances down to 10μm. Quoted bound on R is for $\delta = 2$. For $\delta = 1$, bound goes to 160 μm. See their Fig. 34 for details on the bound.

[14] CHIAVERINI 03 search for new forces, probing α above 10^{4} and λ down to 3μm, finding no signal. See their Fig. 4 for details on the bound. This bound does not place limits on the size of extra flat dimensions.

[15] LONG 03 search for new forces, probing α down to 3, and distances down to about 10μm. See their Fig. 4 for details on the bound.

[16] HOYLE 01 search for new forces, probing α down to 10^{-2} and distances down to 20μm. See their Fig. 4 for details on the bound. The quoted bound is for $\alpha \geq 3$.

[17] HOSKINS 85 search for new forces, probing distances down to 4 mm. See their Fig. 13 for details on the bound. This bound does not place limits on the size of extra flat dimensions.

Limits on R from On-Shell Production of Gravitons: $\delta = 2$

This section includes limits on on-shell production of gravitons in collider and astrophysical processes. Bounds quoted are on R, the assumed common radius of the flat extra dimensions, for $\delta = 2$ extra dimensions. Studies often quote bounds in terms of derived parameter; experiments are actually sensitive to the masses of the KK gravitons: $m_{\vec{n}} = |\vec{n}|/R$. See the Review on "Extra Dimensions" for details. Bounds are given in μm for $\delta = 2$.

VALUE (μm)	CL%	DOCUMENT ID		TECN	COMMENT
< 10.9	95	[1] AABOUD	16D	ATLS	$pp \to jG$
< 0.00016	95	[2] HANNESTAD	03		Neutron star heating
• • • We do not use the following data for averages, fits, limits, etc. • • •					
		[3] SIRUNYAN	17AQ	CMS	$pp \to \gamma G$
< 90	95	[4] AABOUD	16F	ATLS	$pp \to \gamma G$
		[5] KHACHATRY...	16N	CMS	$pp \to \gamma G$
< 17.2	95	[6] AAD	15BH	ATLS	$pp \to jG$
		[7] AAD	15CS	ATLS	$pp \to \gamma G$
< 15	95	[8] KHACHATRY...	15AL	CMS	$pp \to jG$
< 25	95	[9] AAD	13AD	ATLS	$pp \to jG$
< 127	95	[10] AAD	13C	ATLS	$pp \to \gamma G$
< 34.4	95	[11] AAD	13D	ATLS	$pp \to jj$
< 0.0087	95	[12] AJELLO	12	FLAT	Neutron star γ sources
< 23	95	[13] CHATRCHYAN	12AP	CMS	$pp \to jG$

< 92	95	[14] AAD	11S	ATLS	$pp \to jG$
< 72	95	[15] CHATRCHYAN	11U	CMS	$pp \to jG$
< 245	95	[16] AALTONEN	08AC	CDF	$p\overline{p} \to \gamma G, jG$
< 615	95	[17] ABAZOV	08S	D0	$p\overline{p} \to \gamma G$
< 0.916	95	[18] DAS	08		Supernova cooling
< 350	95	[19] ABULENCIA,A	06	CDF	$p\overline{p} \to jG$
< 270	95	[20] ABDALLAH	05B	DLPH	$e^+e^- \to \gamma G$
< 210	95	[21] ACHARD	04E	L3	$e^+e^- \to \gamma G$
< 480	95	[22] ACOSTA	04C	CDF	$\overline{p}p \to jG$
< 0.00038	95	[23] CASSE	04		Neutron star γ sources
< 610	95	[24] ABAZOV	03	D0	$\overline{p}p \to jG$
< 0.96	95	[25] HANNESTAD	03		Supernova cooling
< 0.096	95	[26] HANNESTAD	03		Diffuse γ background
< 0.051	95	[27] HANNESTAD	03		Neutron star γ sources
< 300	95	[28] HEISTER	03C	ALEP	$e^+e^- \to \gamma G$
		[29] FAIRBAIRN	01		Cosmology
< 0.66	95	[30] HANHART	01		Supernova cooling
		[31] CASSISI	00		Red giants
<1300	95	[32] ACCIARRI	99S	L3	$e^+e^- \to ZG$

[1] AABOUD 16D search for $pp \to jG$, using 3.2 fb^{-1} of data at $\sqrt{s} = 13$ TeV to place lower limits on M_D for two to six extra dimensions (see their Table X), from which this bound on R is derived.

[2] HANNESTAD 03 obtain a limit on R from the heating of old neutron stars by the surrounding cloud of trapped KK gravitons. Limits for all $\delta \leq 7$ are given in their Tables V and VI. These limits supersede those in HANNESTAD 02.

[3] SIRUNYAN 17AQ search for $pp \to \gamma G$, using 12.9 fb^{-1} of data at $\sqrt{s} = 13$ TeV to place limits on M_D for three to six extra dimensions (see their Table 3).

[4] AABOUD 16F search for $pp \to \gamma G$, using 3.2 fb^{-1} of data at $\sqrt{s} = 13$ TeV to place limits on M_D for two to six extra dimensions (see their Figure 9), from which this bound on R is derived.

[5] KHACHATRYAN 16N search for $pp \to \gamma G$, using 19.6 fb^{-1} of data at $\sqrt{s} = 8$ TeV to place limits on M_D for three to six extra dimensions (see their Table 5).

[6] AAD 15BH search for $pp \to jG$, using 20.3 fb^{-1} of data at $\sqrt{s} = 8$ TeV to place bounds on M_D for two to six extra dimensions, from which this bound on R is derived. See their Figure 9 for bounds on all $\delta \leq 6$.

[7] AAD 15CS search for $pp \to \gamma G$, using 20.3 fb^{-1} of data at $\sqrt{s} = 8$ TeV to place lower limits on M_D for two to six extra dimensions (see their Fig. 18).

[8] KHACHATRYAN 15AL search for $pp \to jG$, using 19.7 fb^{-1} of data at $\sqrt{s} = 8$ TeV to place bounds on M_D for two to six extra dimensions (see their Table 7), from which this bound on R is derived.

[9] AAD 13AD search for $pp \to jG$, using 4.7 fb^{-1} of data at $\sqrt{s} = 7$ TeV to place bounds on M_D for two to six extra dimensions, from which this bound on R is derived. See their Table 8 for bounds on all $\delta \leq 6$.

[10] AAD 13C search for $pp \to \gamma G$, using 4.6 fb^{-1} of data at $\sqrt{s} = 7$ TeV to place bounds on M_D for two to six extra dimensions, from which this bound on R is derived.

[11] AAD 13D search for the dijet decay of quantum black holes in 4.8 fb^{-1} of data produced in pp collisions at $\sqrt{s} = 7$ TeV to place bounds on M_D for two to seven extra dimensions, from which these bounds on R are derived. Limits on M_D for all $\delta \leq 7$ are given in their Table 3.

[12] AJELLO 12 obtain a limit on R from the gamma-ray emission of point γ sources that arise from the photon decay of KK gravitons which are gravitationally bound around neutron stars. Limits for all $\delta \leq 7$ are given in their Table 7.

[13] CHATRCHYAN 12AP search for $pp \to jG$, using 5.0 fb^{-1} of data at $\sqrt{s} = 7$ TeV to place bounds on M_D for two to six extra dimensions, from which this bound on R is derived. See their Table 7 for bounds on all $\delta \leq 6$.

[14] AAD 11S search for $pp \to jG$, using 33 pb^{-1} of data at $\sqrt{s} = 7$ TeV, to place bounds on M_D for two to four extra dimensions, from which these bounds on R are derived. See their Table 3 for bounds on all $\delta \leq 4$.

[15] CHATRCHYAN 11U search for $pp \to jG$, using 36 pb^{-1} of data at $\sqrt{s} = 7$ TeV, to place bounds on M_D for two to six extra dimensions, from which these bounds on R are derived. See their Table 3 for bounds on all $\delta \leq 6$.

[16] AALTONEN 08AC search for $p\overline{p} \to \gamma G$ and $p\overline{p} \to jG$ at $\sqrt{s} = 1.96$ TeV with 2.0 fb^{-1} and 1.1 fb^{-1} respectively, in order to place bounds on the fundamental scale and size of the extra dimensions. See their Table III for limits on all $\delta \leq 6$.

[17] ABAZOV 08S search for $p\overline{p} \to \gamma G$, using 1 fb^{-1} of data at $\sqrt{s} = 1.96$ TeV to place bounds on M_D for two to eight extra dimensions, from which these bounds on R are derived. See their paper for intermediate values of δ.

[18] DAS 08 obtain a limit on R from Kaluza-Klein graviton cooling of SN1987A due to plasmon-plasmon annihilation.

[19] ABULENCIA,A 06 search for $p\overline{p} \to jG$ using 368 pb^{-1} of data at $\sqrt{s} = 1.96$ TeV. See their Table II for bounds for all $\delta \leq 6$.

[20] ABDALLAH 05B search for $e^+e^- \to \gamma G$ at $\sqrt{s} = 180$–209 GeV to place bounds on the size of extra dimensions and the fundamental scale. Limits for all $\delta \leq 6$ are given in their Table 6. These limits supersede those in ABREU 00Z.

[21] ACHARD 04E search for $e^+e^- \to \gamma G$ at $\sqrt{s} = 189$–209 GeV to place bounds on the size of extra dimensions and the fundamental scale. See their Table 8 for limits with $\delta \leq 8$. These limits supersede those in ACCIARRI 99R.

[22] ACOSTA 04C search for $\overline{p}p \to jG$ at $\sqrt{s} = 1.8$ TeV to place bounds on the size of extra dimensions and the fundamental scale. See their paper for bounds on $\delta = 4, 6$.

[23] CASSE 04 obtain a limit on R from the gamma-ray emission of point γ sources that arises from the photon decay of gravitons around newly born neutron stars, applying the technique of HANNESTAD 03 to neutron stars in the galactic bulge. Limits for all $\delta \leq 7$ are given in their Table I.

[24] ABAZOV 03 search for $p\overline{p} \to jG$ at $\sqrt{s}$=1.8 TeV to place bounds on M_D for 2 to 7 extra dimensions, from which these bounds on R are derived. See their paper for bounds on intermediate values of δ. We quote results without the approximate NLO scaling introduced in the paper.

[25] HANNESTAD 03 obtain a limit on R from graviton cooling of supernova SN1987a. Limits for all $\delta \leq 7$ are given in their Tables V and VI.

[26] HANNESTAD 03 obtain a limit on R from gravitons emitted in supernovae and which subsequently decay, contaminating the diffuse cosmic γ background. Limits for all $\delta \leq 7$ are given in their Tables V and VI. These limits supersede those in HANNESTAD 02.

[27] HANNESTAD 03 obtain a limit on R from gravitons emitted in two recent supernovae and which subsequently decay, creating point γ sources. Limits for all $\delta \leq 7$ are given in their Tables V and VI. These limits are corrected in the published erratum.

[28] HEISTER 03C use the process $e^+e^- \to \gamma G$ at $\sqrt{s} = 189$–209 GeV to place bounds on the size of extra dimensions and the scale of gravity. See their Table4 for limits with $\delta \leq 6$ for derived limits on M_D.

[29] FAIRBAIRN 01 obtains bounds on R from over production of KK gravitons in the early universe. Bounds are quoted in paper in terms of fundamental scale of gravity. Bounds depend strongly on temperature of QCD phase transition and range from $R <$ 0.13 μm to 0.001 μm for δ=2; bounds for δ=3,4 can be derived from Table 1 in the paper.

[30] HANHART 01 obtain bounds on R from limits on graviton cooling of supernova SN 1987a using numerical simulations of proto-neutron star neutrino emission.

[31] CASSISI 00 obtain rough bounds on M_D (and thus R) from red giant cooling for δ=2,3. See their paper for details.

[32] ACCIARRI 99S search for $e^+e^- \to ZG$ at $\sqrt{s}$=189 GeV. Limits on the gravity scale are found in their Table 2, for $\delta \leq 4$.

Mass Limits on M_{TT}

This section includes limits on the cut-off mass scale, M_{TT}, of dimension-8 operators from KK graviton exchange in models of large extra dimensions. Ambiguities in the UV-divergent summation are absorbed into the parameter λ, which is taken to be $\lambda = \pm 1$ in the following analyses. Bounds for $\lambda = -1$ are shown in parenthesis after the bound for $\lambda = +1$, if appropriate. Different papers use slightly different definitions of the mass scale. The definition used here is related to another popular convention by $M_{TT}^4 = (2/\pi)\,\Lambda_T^4$, as discussed in the above Review on "Extra Dimensions."

VALUE (TeV)		CL%	DOCUMENT ID		TECN	COMMENT
> 8.4		95	[1] SIRUNYAN	17F	CMS	$pp \to$ dijet, ang. distrib.
>20.6	**(> 15.7)**	95	[2] GIUDICE	03	RVUE	Dim-6 operators
• • • We do not use the following data for averages, fits, limits, etc. • • •						
> 7.2		95	[3] AABOUD	17AP	ATLS	$pp \to \gamma\gamma$
> 3.7		95	[4] KHACHATRY...15AE		CMS	$pp \to e^+e^-,\ \mu^+\mu^-$
> 6.3		95	[5] KHACHATRY...15J		CMS	$pp \to$ dijet, ang. distrib.
> 3.8		95	[6] AAD	14BE	ATLS	$pp \to e^+e^-,\ \mu^+\mu^-$
> 2.94	(>2.52)	95	[7] AAD	13AS	ATLS	$pp \to \gamma\gamma$
> 3.2		95	[8] AAD	13E	ATLS	$pp \to e^+e^-, \mu^+\mu^-, \gamma\gamma$
> 2.66	(>2.27)	95	[9] AAD	12Y	ATLS	$pp \to \gamma\gamma$
			[10] BAAK	12	RVUE	Electroweak
> 2.86		95	[11] CHATRCHYAN	12J	CMS	$pp \to e^+e^-, \mu^+\mu^-$
> 2.84	(>2.41)	95	[12] CHATRCHYAN	12R	CMS	$pp \to \gamma\gamma$
> 0.90	(>0.92)	95	[13] AARON	11C	H1	$e^\pm p \to e^\pm X$
> 1.74	(>1.71)	95	[14] CHATRCHYAN	11A	CMS	$pp \to \gamma\gamma$
> 1.48		95	[15] ABAZOV	09AE	D0	$p\overline{p} \to$ dijet, ang. distrib.
> 1.45		95	[16] ABAZOV	09D	D0	$p\overline{p} \to e^+e^-, \gamma\gamma$
> 1.1	(> 1.0)	95	[17] SCHAEL	07A	ALEP	$e^+e^- \to e^+e^-$
> 0.898	(> 0.998)	95	[18] ABDALLAH	06C	DLPH	$e^+e^- \to \ell^+\ell^-$
> 0.853	(> 0.939)	95	[19] GERDES	06		$p\overline{p} \to e^+e^-, \gamma\gamma$
> 0.96	(> 0.93)	95	[20] ABAZOV	05V	D0	$p\overline{p} \to \mu^+\mu^-$
> 0.78	(> 0.79)	95	[21] CHEKANOV	04B	ZEUS	$e^\pm p \to e^\pm X$
> 0.805	(> 0.956)	95	[22] ABBIENDI	03D	OPAL	$e^+e^- \to \gamma\gamma$
> 0.7	(> 0.7)	95	[23] ACHARD	03D	L3	$e^+e^- \to ZZ$
> 0.82	(> 0.78)	95	[24] ADLOFF	03	H1	$e^\pm p \to e^\pm X$
> 1.28	(> 1.25)	95	[25] GIUDICE	03	RVUE	
> 0.80	(> 0.85)	95	[26] HEISTER	03C	ALEP	$e^+e^- \to \gamma\gamma$
> 0.84	(> 0.99)	95	[27] ACHARD	02D	L3	$e^+e^- \to \gamma\gamma$
> 1.2	(> 1.1)	95	[28] ABBOTT	01	D0	$p\overline{p} \to e^+e^-, \gamma\gamma$
> 0.60	(> 0.63)	95	[29] ABBIENDI	00R	OPAL	$e^+e^- \to \mu^+\mu^-$
> 0.63	(> 0.50)	95	[29] ABBIENDI	00R	OPAL	$e^+e^- \to \tau^+\tau^-$
> 0.68	(> 0.61)	95	[29] ABBIENDI	00R	OPAL	$e^+e^- \to \mu^+\mu^-, \tau^+\tau^-$
			[30] ABREU	00A	DLPH	$e^+e^- \to \gamma\gamma$
> 0.680	(> 0.542)	95	[31] ABREU	00S	DLPH	$e^+e^- \to \mu^+\mu^-, \tau^+\tau^-$
> 15–28		99.7	[32] CHANG	00B	RVUE	Electroweak
> 0.98		95	[33] CHEUNG	00	RVUE	$e^+e^- \to \gamma\gamma$
> 0.29–0.38		95	[34] GRAESSER	00	RVUE	$(g-2)_\mu$
> 0.50–1.1		95	[35] HAN	00	RVUE	Electroweak
> 2.0	(> 2.0)	95	[36] MATHEWS	00	RVUE	$\overline{p}p \to jj$
> 1.0	(> 1.1)	95	[37] MELE	00	RVUE	$e^+e^- \to VV$
			[38] ABBIENDI	99P	OPAL	
			[39] ACCIARRI	99M	L3	
			[40] ACCIARRI	99S	L3	
> 1.412	(> 1.077)	95	[41] BOURILKOV	99		$e^+e^- \to e^+e^-$

[1] SIRUNYAN 17F use dijet angular distributions in 2.6 fb^{-1} of data from pp collisions at $\sqrt{s} = 13$ TeV to place a lower bound on Λ_T, here converted to M_{TT}.

[2] GIUDICE 03 place bounds on Λ_6, the coefficient of the gravitationally-induced dimension-6 operator $(2\pi\lambda/\Lambda_6^2)(\sum \overline{f}\gamma_\mu\gamma^5 f)(\sum \overline{f}\gamma^\mu\gamma^5 f)$, using data from a variety of experiments. Results are quoted for $\lambda = \pm 1$ and are independent of δ.

[3] AABOUD 17AP use 36.7 fb^{-1} of data from pp collisions at $\sqrt{s} = 13$ TeV to place lower limits on M_{TT} (equivalent to their M_S).

[4] KHACHATRYAN 15AE use 20.6 (19.7) fb^{-1} of data from pp collisions at $\sqrt{s} = 8$ TeV in the dimuon (dielectron) channel to place a lower limit on Λ_T, here converted to M_{TT}.

[5] KHACHATRYAN 15J use dijet angular distributions in 19.7 fb^{-1} of data from pp collisions at $\sqrt{s} = 8$ TeV to place a lower bound on Λ_T, here converted to M_{TT}.

[6] AAD 14BE use 20 fb^{-1} of data from pp collisions at $\sqrt{s} = 8$ TeV in the dilepton channel to place lower limits on M_{TT} (equivalent to their M_S).

[7] AAD 13AS use 4.9 fb^{-1} of data from pp collisions at $\sqrt{s} = 7$ TeV to place lower limits on M_{TT} (equivalent to their M_S).

[8] AAD 13E use 4.9 and 5.0 fb^{-1} of data from pp collisions at $\sqrt{s}$ = 7 TeV in the dielectron and dimuon channels, respectively, to place lower limits on M_{TT} (equivalent to their M_S). The dielectron and dimuon channels are combined with previous results in the diphoton channel to set the best limit. Bounds on individual channels and different priors can be found in their Table VIII.

[9] AAD 12Y use 2.12 fb^{-1} of data from pp collisions at $\sqrt{s}$ = 7 TeV to place lower limits on M_{TT} (equivalent to their M_S).

[10] BAAK 12 use electroweak precision observables to place bounds on the ratio Λ_T/M_D as a function of M_D. See their Fig. 22 for constraints with a Higgs mass of 120 GeV.

[11] CHATRCHYAN 12J use approximately 2 fb^{-1} of data from pp collisions at $\sqrt{s}$ = 7 TeV in the dielectron and dimuon channels to place lower limits on Λ_T, here converted to M_{TT}.

[12] CHATRCHYAN 12R use 2.2 fb^{-1} of data from pp collisions at $\sqrt{s}$ = 7 TeV to place lower limits on M_{TT} (equivalent to their M_S).

[13] AARON 11C search for deviations in the differential cross section of $e^{\pm}p \rightarrow e^{\pm}X$ in 446 pb^{-1} of data taken at $\sqrt{s}$ = 301 and 319 GeV to place a bound on M_{TT}.

[14] CHATRCHYAN 11A use 36 pb^{-1} of data from pp collisions at $\sqrt{s}$ = 7 TeV to place lower limits on Λ_T, here converted to M_{TT}.

[15] ABAZOV 09AE use dijet angular distributions in 0.7 fb^{-1} of data from $p\overline{p}$ collisions at $\sqrt{s}$ = 1.96 TeV to place lower bounds on Λ_T (equivalent to their M_S), here converted to M_{TT}.

[16] ABAZOV 09D use 1.05 fb^{-1} of data from $p\overline{p}$ collisions at $\sqrt{s}$ = 1.96 TeV to place lower bounds on Λ_T (equivalent to their M_s), here converted to M_{TT}.

[17] SCHAEL 07A use e^+e^- collisions at $\sqrt{s}$ = 189–209 GeV to place lower limits on Λ_T, here converted to limits on M_{TT}.

[18] ABDALLAH 06C use e^+e^- collisions at $\sqrt{s} \sim$ 130–207 GeV to place lower limits on M_{TT}, which is equivalent to their definition of M_s. Bound shown includes all possible final state leptons, $\ell = e, \mu, \tau$. Bounds on individual leptonic final states can be found in their Table 31.

[19] GERDES 06 use 100 to 110 pb^{-1} of data from $p\overline{p}$ collisions at $\sqrt{s}$ = 1.8 TeV, as recorded by the CDF Collaboration during Run I of the Tevatron. Bound shown includes a K-factor of 1.3. Bounds on individual e^+e^- and $\gamma\gamma$ final states are found in their Table I.

[20] ABAZOV 05V use 246 pb^{-1} of data from $p\overline{p}$ collisions at $\sqrt{s}$ = 1.96 TeV to search for deviations in the differential cross section to $\mu^+\mu^-$ from graviton exchange.

[21] CHEKANOV 04B search for deviations in the differential cross section of $e^{\pm}p \rightarrow e^{\pm}X$ with 130 pb^{-1} of combined data and Q^2 values up to 40,000 GeV^2 to place a bound on M_{TT}.

[22] ABBIENDI 03D use e^+e^- collisions at $\sqrt{s}$=181–209 GeV to place bounds on the ultraviolet scale M_{TT}, which is equivalent to their definition of M_S.

[23] ACHARD 03D look for deviations in the cross section for $e^+e^- \rightarrow ZZ$ from $\sqrt{s}$ = 200–209 GeV to place a bound on M_{TT}.

[24] ADLOFF 03 search for deviations in the differential cross section of $e^{\pm}p \rightarrow e^{\pm}X$ at $\sqrt{s}$=301 and 319 GeV to place bounds on M_{TT}.

[25] GIUDICE 03 review existing experimental bounds on M_{TT} and derive a combined limit.

[26] HEISTER 03C use e^+e^- collisions at $\sqrt{s}$= 189–209 GeV to place bounds on the scale of dim-8 gravitational interactions. Their $M_s^{\pm}$ is equivalent to our M_{TT} with λ=$\pm$1.

[27] ACHARD 02 search for s-channel graviton exchange effects in $e^+e^- \rightarrow \gamma\gamma$ at E_{cm} = 192–209 GeV.

[28] ABBOTT 01 search for variations in differential cross sections to e^+e^- and $\gamma\gamma$ final states at the Tevatron.

[29] ABBIENDI 00R uses e^+e^- collisions at $\sqrt{s}$= 189 GeV.

[30] ABREU 00A search for s-channel graviton exchange effects in $e^+e^- \rightarrow \gamma\gamma$ at E_{cm}= 189–202 GeV.

[31] ABREU 00S uses e^+e^- collisions at $\sqrt{s}$=183 and 189 GeV. Bounds on μ and τ individual final states given in paper.

[32] CHANG 00B derive 3σ limit on M_{TT} of (28,19,15) TeV for δ=(2,4,6) respectively assuming the presence of a torsional coupling in the gravitational action. Highly model dependent.

[33] CHEUNG 00 obtains limits from anomalous diphoton production at OPAL due to graviton exchange. Original limit for δ=4. However, unknown UV theory renders δ dependence unreliable. Original paper works in HLZ convention.

[34] GRAESSER 00 obtains a bound from graviton contributions to $g-2$ of the muon through loops of 0.29 TeV for δ=2 and 0.38 TeV for δ=4,6. Limits scale as $\lambda^{1/2}$. However calculational scheme not well-defined without specification of high-scale theory. See the "Extra Dimensions Review."

[35] HAN 00 calculates corrections to gauge boson self-energies from KK graviton loops and constrain them using S and T. Bounds on M_{TT} range from 0.5 TeV (δ=6) to 1.1 TeV (δ=2); see text. Limits have strong dependence, $\lambda^{\delta+2}$, on unknown λ coefficient.

[36] MATHEWS 00 search for evidence of graviton exchange in CDF and DØ dijet production data. See their Table 2 for slightly stronger δ-dependent bounds. Limits expressed in terms of $\widetilde{M}_S^4 = M_{TT}^4/8$.

[37] MELE 00 obtains bound from KK graviton contributions to $e^+e^- \rightarrow VV$ (V=γ,W,Z) at LEP. Authors use Hewett conventions.

[38] ABBIENDI 99P search for s-channel graviton exchange effects in $e^+e^- \rightarrow \gamma\gamma$ at E_{cm}=189 GeV. The limits $G_+ > 660$ GeV and $G_- > 634$ GeV are obtained from combined E_{cm}=183 and 189 GeV data, where $G_{\pm}$ is a scale related to the fundamental gravity scale.

[39] ACCIARRI 99M search for the reaction $e^+e^- \rightarrow \gamma G$ and s-channel graviton exchange effects in $e^+e^- \rightarrow \gamma\gamma$, W^+W^-, ZZ, e^+e^-, $\mu^+\mu^-$, $\tau^+\tau^-$, $q\overline{q}$ at E_{cm}=183 GeV. Limits on the gravity scale are listed in their Tables 1 and 2.

[40] ACCIARRI 99S search for the reaction $e^+e^- \rightarrow ZG$ and s-channel graviton exchange effects in $e^+e^- \rightarrow \gamma\gamma$, W^+W^-, ZZ, e^+e^-, $\mu^+\mu^-$, $\tau^+\tau^-$, $q\overline{q}$ at E_{cm}=189 GeV. Limits on the gravity scale are listed in their Tables 1 and 2.

[41] BOURILKOV 99 performs global analysis of LEP data on e^+e^- collisions at $\sqrt{s}$=183 and 189 GeV. Bound is on Λ_T.

Limits on $1/R = M_c$

This section includes limits on $1/R = M_c$, the compactification scale in models with one TeV-sized extra dimension, due to exchange of Standard Model KK excitations. Bounds assume fermions are not in the bulk, unless stated otherwise. See the "Extra Dimensions" review for discussion of model dependence.

VALUE (TeV)	CL%	DOCUMENT ID		TECN	COMMENT
>4.16	95	[1] AAD	12CC	ATLS	$pp \rightarrow \ell\overline{\ell}$
>6.1		[2] BARBIERI	04	RVUE	Electroweak
• • • We do not use the following data for averages, fits, limits, etc. • • •					
>3.8	95	[3] ACCOMANDO	15	RVUE	Electroweak
>3.40	95	[4] KHACHATRY...15T		CMS	$pp \rightarrow \ell X$
		[5] CHATRCHYAN	13AQ	CMS	$pp \rightarrow \ell X$
>1.38	95	[6] CHATRCHYAN	13W	CMS	$pp \rightarrow \gamma\gamma$, δ=6, M_D=5 TeV
>0.715	95	[7] EDELHAUSER	13	RVUE	$pp \rightarrow \ell\overline{\ell} + X$
>1.40	95	[8] AAD	12CP	ATLS	$pp \rightarrow \gamma\gamma$, δ=6, M_D=5 TeV
>1.23	95	[9] AAD	12X	ATLS	$pp \rightarrow \gamma\gamma$, δ=6, M_D=5 TeV
>0.26	95	[10] ABAZOV	12M	D0	$p\overline{p} \rightarrow \mu\mu$
>0.75	95	[11] BAAK	12	RVUE	Electroweak
		[12] FLACKE	12	RVUE	Electroweak
>0.43	95	[13] NISHIWAKI	12	RVUE	$H \rightarrow WW, \gamma\gamma$
>0.729	95	[14] AAD	11F	ATLS	$pp \rightarrow \gamma\gamma$, δ=6, M_D=5 TeV
>0.961	95	[15] AAD	11X	ATLS	$pp \rightarrow \gamma\gamma$, δ=6, M_D=5 TeV
>0.477	95	[16] ABAZOV	10P	D0	$p\overline{p} \rightarrow \gamma\gamma$, δ=6, M_D=5 TeV
>1.59	95	[17] ABAZOV	09AE	D0	$p\overline{p} \rightarrow$ dijet, angular dist.
>0.6	95	[18] HAISCH	07	RVUE	$\overline{B} \rightarrow X_s\gamma$
>0.6	90	[19] GOGOLADZE	06	RVUE	Electroweak
>3.3	95	[20] CORNET	00	RVUE	Electroweak
> 3.3–3.8	95	[21] RIZZO	00	RVUE	Electroweak

[1] AAD 12CC use 4.9 and 5.0 fb^{-1} of data from pp collisions at $\sqrt{s}$ = 7 TeV in the dielectron and dimuon channels, respectively, to place a lower bound on the mass of the lightest KK Z/γ boson (equivalent to $1/R = M_c$). The limit quoted here assumes a flat prior corresponding to when the pure Z/γ KK cross section term dominates. See their Section 15 for more details.

[2] BARBIERI 04 use electroweak precision observables to place a lower bound on the compactification scale $1/R$. Both the gauge bosons and the Higgs boson are assumed to propagate in the bulk.

[3] ACCOMANDO 15 use electroweak precision observables to place a lower bound on the compactification scale $1/R$. See their Fig. 2 for the bound as a function of sinβ, which parametrizes the VEV contribution from brane and bulk Higgs fields. The quoted value is for the minimum bound which occurs at sinβ = 0.45.

[4] KHACHATRYAN 15T use 19.7 fb^{-1} of data from pp collisions at $\sqrt{s}$ = 8 TeV to place a lower bound on the compactification scale $1/R$.

[5] CHATRCHYAN 13AQ use 5.0 fb^{-1} of data from pp collisions at $\sqrt{s}$ = 7 TeV and a further 3.7 fb^{-1} of data at $\sqrt{s}$ = 8 TeV to place a lower bound on the compactification scale $1/R$, in models with universal extra dimensions and Standard Model fields propagating in the bulk. See their Fig. 5 for the bound as a function of the universal bulk fermion mass parameter μ.

[6] CHATRCHYAN 13W use diphoton events with large missing transverse momentum in 4.93 fb^{-1} of data produced from pp collisions at $\sqrt{s}$ = 7 TeV to place a lower bound on the compactification scale in a universal extra dimension model with gravitational decays. The bound assumes that the cutoff scale Λ, for the radiative corrections to the Kaluza-Klein masses, satisfies $\Lambda/M_c = 20$. The model parameters are chosen such that the decay $\gamma^* \rightarrow G\gamma$ occurs with an appreciable branching fraction.

[7] EDELHAUSER 13 use 19.6 and 20.6 fb^{-1} of data from pp collisions at $\sqrt{s}$ = 8 TeV analyzed by the CMS Collaboration in the dielectron and dimuon channels, respectively, to place a lower bound on the mass of the second lightest Kaluza-Klein Z/γ boson (converted to a limit on $1/R = M_c$). The bound assumes Standard Model fields propagating in the bulk and that the cutoff scale Λ, for the radiative corrections to the Kaluza-Klein masses, satisfies $\Lambda/M_c = 20$.

[8] AAD 12CP use diphoton events with large missing transverse momentum in 4.8 fb^{-1} of data produced from pp collisions at $\sqrt{s}$ = 7 TeV to place a lower bound on the compactification scale in a universal extra dimension model with gravitational decays. The bound assumes that the cutoff scale Λ, for the radiative corrections to the Kaluza-Klein masses, satisfies $\Lambda/M_c = 20$. The model parameters are chosen such that the decay $\gamma^* \rightarrow G\gamma$ occurs with an appreciable branching fraction.

[9] AAD 12X use diphoton events with large missing transverse momentum in 1.07 fb^{-1} of data produced from pp collisions at $\sqrt{s}$ = 7 TeV to place a lower bound on the compactification scale in a universal extra dimension model with gravitational decays. The bound assumes that the cutoff scale Λ, for the radiative corrections to the Kaluza-Klein masses, satisfies $\Lambda/M_c = 20$. The model parameters are chosen such that the decay $\gamma^* \rightarrow G\gamma$ occurs with an appreciable branching fraction.

[10] ABAZOV 12M use same-sign dimuon events in 7.3 fb^{-1} of data from $p\overline{p}$ collisions at $\sqrt{s}$ = 1.96 TeV to place a lower bound on the compactification scale $1/R$, in models with universal extra dimensions where all Standard Model fields propagate in the bulk.

[11] BAAK 12 use electroweak precision observables to place a lower bound on the compactification scale $1/R$, in models with universal extra dimensions and Standard Model fields propagating in the bulk. Bound assumes a 125 GeV Higgs mass. See their Fig. 25 for the bound as a function of the Higgs mass.

[12] FLACKE 12 use electroweak precision observables to place a lower bound on the compactification scale $1/R$, in models with universal extra dimensions and Standard Model fields propagating in the bulk. See their Fig. 1 for the bound as a function of the universal bulk fermion mass parameter μ.

[13] NISHIWAKI 12 use up to 2 fb^{-1} of data from the ATLAS and CMS experiments that constrains the production cross section of a Higgs-like particle to place a lower bound on the compactification scale $1/R$ in universal extra dimension models. The quoted bound assumes Standard Model fields propagating in the bulk and a 125 GeV Higgs mass. See their Fig. 1 for the bound as a function of the Higgs mass.

[14] AAD 11F use diphoton events with large missing transverse energy in 3.1 pb^{-1} of data produced from pp collisions at $\sqrt{s}$ = 7 TeV to place a lower bound on the compactification scale in a universal extra dimension model with gravitational decays. The bound assumes that the cutoff scale Λ, for the radiative corrections to the Kaluza-Klein masses,

satisfies $\Lambda/M_c = 20$. The model parameters are chosen such that the decay $\gamma^* \to G\gamma$ occurs with an appreciable branching fraction.

[15] AAD 11X use diphoton events with large missing transverse energy in 36 pb^{-1} of data produced from pp collisions at $\sqrt{s} = 7$ TeV to place a lower bound on the compactification scale in a universal extra dimension model with gravitational decays. The bound assumes that the cutoff scale Λ, for the radiative corrections to the Kaluza-Klein masses, satisfies $\Lambda/M_c = 20$. The model parameters are chosen such that the decay $\gamma^* \to G\gamma$ occurs with an appreciable branching fraction.

[16] ABAZOV 10P use diphoton events with large missing transverse energy in 6.3 fb^{-1} of data produced from $p\overline{p}$ collisions at $\sqrt{s} = 1.96$ TeV to place a lower bound on the compactification scale in a universal extra dimension model with gravitational decays. The bound assumes that the cutoff scale Λ, for the radiative corrections to the Kaluza-Klein masses, satisfies Λ/M_c=20. The model parameters are chosen such that the decay $\gamma^* \to G\gamma$ occurs with an appreciable branching fraction.

[17] ABAZOV 09AE use dijet angular distributions in 0.7 fb^{-1} of data from $p\overline{p}$ collisions at $\sqrt{s} = 1.96$ TeV to place a lower bound on the compactification scale.

[18] HAISCH 07 use inclusive $\overline{B}$-meson decays to place a Higgs mass independent bound on the compactification scale $1/R$ in the minimal universal extra dimension model.

[19] GOGOLADZE 06 use electroweak precision observables to place a lower bound on the compactification scale in models with universal extra dimensions. Bound assumes a 115 GeV Higgs mass. See their Fig. 3 for the bound as a function of the Higgs mass.

[20] CORNET 00 translates a bound on the coefficient of the 4-fermion operator $(\overline{\ell}\gamma_\mu\tau^a\ell)(\overline{\ell}\gamma^\mu\tau^a\ell)$ derived by Hagiwara and Matsumoto into a limit on the mass scale of KK W bosons.

[21] RIZZO 00 obtains limits from global electroweak fits in models with a Higgs in the bulk (3.8 TeV) or on the standard brane (3.3 TeV).

Limits on Kaluza-Klein Gravitons in Warped Extra Dimensions

This section places limits on the mass of the first Kaluza-Klein (KK) excitation of the graviton in the warped extra dimension model of Randall and Sundrum. Bounds in parenthesis assume Standard Model fields propagate in the bulk. Experimental bounds depend strongly on the warp parameter, k. See the "Extra Dimensions" review for a full discussion.

Here we list limits for the value of the warp parameter $k/\overline{M}_P = 0.1$.

VALUE (TeV)	CL%	DOCUMENT ID		TECN	COMMENT
>4.1	95	[1] AABOUD	17AP	ATLS	$pp \to G \to \gamma\gamma$
• • • We do not use the following data for averages, fits, limits, etc. • • •					
		[2] SIRUNYAN	18F	CMS	$pp \to G \to hh$
>3.11	95	[3] KHACHATRY...	17T	CMS	$pp \to G \to e^+e^-, \mu^+\mu^-$
>1.9	95	[4] KHACHATRY...	17W	CMS	$pp \to G \to jj$
		[5] SIRUNYAN	17AK	CMS	$pp \to G \to WW, ZZ$
		[6] AABOUD	16AE	ATLS	$pp \to G \to WW, ZZ$
		[7] AABOUD	16H	ATLS	$pp \to G \to \gamma\gamma$
		[8] AABOUD	16I	ATLS	$pp \to G \to hh$
		[9] AAD	16R	ATLS	$pp \to G \to WW, ZZ$
		[10] KHACHATRY...	16BQ	CMS	$pp \to G \to hh$
>3.3	95	[11] KHACHATRY...	16M	CMS	$pp \to G \to \gamma\gamma$
>2.66	95	[12] AAD	15AD	ATLS	$pp \to G \to \gamma\gamma$
		[13] AAD	15AU	ATLS	$pp \to G \to ZZ$
		[14] AAD	15AZ	ATLS	$pp \to G \to WW$
		[15] AAD	15BK	ATLS	$pp \to G \to hh$
		[16] AAD	15CT	ATLS	$pp \to G \to WW, ZZ$
>2.73	95	[17] KHACHATRY...	15AE	CMS	$pp \to e^+e^-, \mu^+\mu^-$
		[18] KHACHATRY...	15R	CMS	$pp \to G \to hh$
>2.68	95	[19] AAD	14V	ATLS	$pp \to G \to e^+e^-, \mu^+\mu^-$
		[20] KHACHATRY...	14A	CMS	$pp \to G \to WW, ZZ, WZ$
>1.23 (>0.84)	95	[21] AAD	13A	ATLS	$pp \to G \to WW$
>0.94 (>0.71)	95	[22] AAD	13AO	ATLS	$pp \to G \to WW$
>2.23	95	[23] AAD	13AS	ATLS	$pp \to \gamma\gamma, e^+e^-, \mu^+\mu^-$
>2.39	95	[24] CHATRCHYAN	13AF	CMS	$pp \to e^+e^-, \mu^+\mu^-$
		[25] CHATRCHYAN	13U	CMS	$pp \to G \to ZZ$
>0.845	95	[26] AAD	12AD	ATLS	$pp \to G \to ZZ$
>2.16	95	[27] AAD	12CC	ATLS	$pp \to G \to \ell\overline{\ell}$
>1.95	95	[28] AAD	12Y	ATLS	$pp \to \gamma\gamma, e^+e^-, \mu^+\mu^-$
		[29] AALTONEN	12V	CDF	$p\overline{p} \to G \to ZZ$
		[30] BAAK	12	RVUE	Electroweak
>1.84	95	[31] CHATRCHYAN	12R	CMS	$pp \to G \to \gamma\gamma$
>1.63	95	[32] AAD	11AD	ATLS	$pp \to G \to \ell\overline{\ell}$
		[33] AALTONEN	11G	CDF	$p\overline{p} \to G \to ZZ$
>1.058	95	[34] AALTONEN	11R	CDF	$p\overline{p} \to G \to e^+e^-, \gamma\gamma$
>0.754	95	[35] ABAZOV	11H	D0	$p\overline{p} \to G \to WW$
>1.079	95	[36] CHATRCHYAN	11	CMS	$pp \to G \to \ell\overline{\ell}$
>0.607		[37] AALTONEN	10N	CDF	$p\overline{p} \to G \to WW$
>1.05		[38] ABAZOV	10F	D0	$p\overline{p} \to G \to e^+e^-, \gamma\gamma$
		[39] AALTONEN	08S	CDF	$p\overline{p} \to G \to ZZ$
>0.90		[40] ABAZOV	08J	D0	$p\overline{p} \to G \to e^+e^-, \gamma\gamma$
		[41] AALTONEN	07G	CDF	$p\overline{p} \to G \to \gamma\gamma$
>0.889		[42] AALTONEN	07H	CDF	$p\overline{p} \to G \to e\overline{e}$
>0.785		[43] ABAZOV	05N	D0	$p\overline{p} \to G \to \ell\ell, \gamma\gamma$
>0.71		[44] ABULENCIA	05A	CDF	$p\overline{p} \to G \to \ell\overline{\ell}$

[1] AABOUD 17AP use 36.7 fb^{-1} of data from pp collisions at $\sqrt{s} = 13$ TeV in the diphoton channel to place a lower limit on the mass of the lightest KK graviton.

[2] SIRUNYAN 18F use 35.9 fb^{-1} of data from pp collisions at $\sqrt{s} = 13$ TeV to search for Higgs boson pair production in the $b\overline{b}\ell\nu\ell\nu$ final state. See their Figure 7 for limits on the cross section times branching fraction as a function of the KK graviton mass with a warp parameter value $k/\overline{M}_P = 0.1$.

[3] KHACHATRYAN 17T use 2.7 (2.9) fb^{-1} of data from pp collisions at $\sqrt{s} = 13$ TeV in the dielectron (dimuon) channel. This 13 TeV data is combined with 20 fb^{-1} of a previously analyzed set of 8 TeV data to place a lower bound on the mass of the lightest KK graviton. See their paper for the limit with warp parameter value $k/\overline{M}_P = 0.01$.

[4] KHACHATRYAN 17W use 12.9 fb^{-1} of data from pp collisions at $\sqrt{s} = 13$ TeV to place a lower bound on the mass of the lightest KK graviton. (The quoted bound is for a warp parameter value of $k/\overline{M}_P = 0.1$, although it was not disclosed in the publication.)

[5] SIRUNYAN 17AK use 19.7 fb^{-1} and up to 2.7 fb^{-1} of data from pp collisions at $\sqrt{s}$ = 8 TeV and 13 TeV, respectively, to place limits on the production cross section of a KK graviton resonance. See their Figure 3 for exclusion limits on the signal strength for $k/\overline{M}_P = 0.5$ and a mass range of 0.6 to 4.0 TeV .

[6] AABOUD 16AE use 3.2 fb^{-1} of data from pp collisions at $\sqrt{s} = 13$ TeV to place a lower bound on the mass of the lightest KK graviton. See their Figure 8 for the limit on the KK graviton mass as a function of the cross section times branching fraction for $k/\overline{M}_P = 1$.

[7] AABOUD 16H use 3.2 fb^{-1} of data from pp collisions at $\sqrt{s} = 13$ TeV in the diphoton channel to place a lower limit on the mass of the lightest KK graviton. See their Figure 11 for limits on the cross section times branching fraction as a function of the graviton mass with warp parameter values $k/\overline{M}_P$ between 0.01 and 0.3.

[8] AABOUD 16I use 3.2 fb^{-1} of data from pp collisions at $\sqrt{s} = 13$ TeV to search for Higgs boson pair production in the $b\overline{b}b\overline{b}$ final state. See their Figure 10 for limits on the cross section times branching fraction as a function of the KK graviton mass with warp parameter values $k/\overline{M}_P = 1.0$ and 2.0.

[9] AAD 16R use 20.3 fb^{-1} of data from pp collisions at $\sqrt{s} = 8$ TeV to place a lower bound on the mass of the lightest KK graviton. See their Figure 4 for the limit on the KK graviton mass as a function of the cross section times branching fraction.

[10] KHACHATRYAN 16BQ use 19.7 fb^{-1} of data from pp collisions at $\sqrt{s} = 8$ TeV to search for Higgs boson pair production in the $\gamma\gamma b\overline{b}$ final state. See their Figure 9 for limits on the cross section times branching fraction as a function of the KK graviton mass with a warp parameter value $k/\overline{M}_P = 0.2$.

[11] KHACHATRYAN 16M use 19.7 fb^{-1} and 3.3 fb^{-1} of data from pp collisions at $\sqrt{s}$ = 8 TeV and 13 TeV, respectively, in the diphoton channel to place a lower limit on the mass of the lightest KK graviton. See their paper for limits with other warp parameter values $k/\overline{M}_P = 0.01$ and 0.2.

[12] AAD 15AD use 20.3 fb^{-1} of data from pp collisions at $\sqrt{s} = 8$ TeV in the diphoton channel to place a lower limit on the mass of the lightest KK graviton. See their Table IV for limits with warp parameter values $k/\overline{M}_P$ between 0.01 and 0.1.

[13] AAD 15AU use 20 fb^{-1} of data from pp collisions at $\sqrt{s} = 8$ TeV to search for KK gravitons in a warped extra dimension decaying to ZZ dibosons. See their Figure 2 for limits on the KK graviton mass as a function of the cross section times branching fraction.

[14] AAD 15AZ use 20.3 fb^{-1} of data from pp collisions at $\sqrt{s} = 8$ TeV to place a lower bound on the mass of the lightest KK graviton. See their Figure 2 for limits on the KK graviton mass as a function of the cross section times branching ratio.

[15] AAD 15BK use 19.5 fb^{-1} of data from pp collisions at $\sqrt{s} = 8$ TeV to search for Higgs boson pair production in the $b\overline{b}b\overline{b}$ final state, and exclude masses of the lightest KK graviton. See their Table 9 for the excluded mass ranges with warp parameter values $k/\overline{M}_P = 1.0$, 1.5, and 2.0.

[16] AAD 15CT use 20.3 fb^{-1} of data from pp collisions at $\sqrt{s} = 8$ TeV to place a lower bound on the mass of the lightest KK graviton. See their Figures 6b and 6c for the limit on the KK graviton mass as a function of the cross section times branching fraction.

[17] KHACHATRYAN 15AE use 20.6 (19.7) fb^{-1} of data from pp collisions at $\sqrt{s} = 8$ TeV in the dimuon (dielectron) channel to place a lower bound on the mass of the lightest KK graviton.

[18] KHACHATRYAN 15R use 17.9 fb^{-1} of data from pp collisions at $\sqrt{s} = 8$ TeV to search for Higgs boson pair production in the $b\overline{b}b\overline{b}$ final state, and exclude a KK graviton with mass from 380 to 830 GeV.

[19] AAD 14V use 20 fb^{-1} of data from pp collisions at $\sqrt{s} = 8$ TeV in the dielectron and dimuon channels to place a lower bound on the mass of the lightest KK graviton.

[20] KHACHATRYAN 14A use 19.7 fb^{-1} of data from pp collisions at $\sqrt{s} = 8$ TeV to search for KK gravitons in a warped extra dimension decaying to dibosons. See their Figure 9 for limits on the cross section times branching fraction as a function of the KK graviton mass.

[21] AAD 13A use 4.7 fb^{-1} of data from pp collisions at $\sqrt{s} = 7$ TeV in the $\ell\nu\ell\nu$ channel, to place a lower bound on the mass of the lightest KK graviton.

[22] AAD 13AO use 4.7 fb^{-1} of data from pp collisions at $\sqrt{s} = 7$ TeV in the $\ell\nu jj$ channel, to place a lower bound on the mass of the lightest KK graviton.

[23] AAD 13AS use 4.9 fb^{-1} of data from pp collisions at $\sqrt{s} = 7$ TeV in the diphoton channel to place lower limits on the mass of the lightest KK graviton. The diphoton channel is combined with previous results in the dielectron and dimuon channels to set the best limit. See their Table 2 for warp parameter values $k/\overline{M}_P$ between 0.01 and 0.1.

[24] CHATRCHYAN 13AF use 5.3 and 4.1 fb^{-1} of data from pp collisions at $\sqrt{s} = 7$ TeV and 8 TeV, respectively, in the dielectron and dimuon channels, to place a lower bound on the mass of the lightest KK graviton.

[25] CHATRCHYAN 13U use 5 fb^{-1} of data from pp collisions at $\sqrt{s} = 7$ TeV to search for KK gravitons in a warped extra dimension decaying to ZZ dibosons. See their Figure 5 for limits on the lightest KK graviton mass as a function of $k/\overline{M}_P$.

[26] AAD 12AD use 1.02 fb^{-1} of data from pp collisions at $\sqrt{s} = 7$ TeV to search for KK gravitons in a warped extra dimension decaying to ZZ dibosons in the $lljj$ and $llll$ channels (ℓ=e, μ). The limit is quoted for the combined $lljj + llll$ channels. See their Figure 5 for limits on the cross section $\sigma(G \to ZZ)$ as a function of the graviton mass.

[27] AAD 12CC use 4.9 and 5.0 fb^{-1} of data from pp collisions at $\sqrt{s} = 7$ TeV in the dielectron and dimuon channels, respectively, to place a lower bound on the mass of the lightest KK graviton. See their Figure 5 for limits on the lightest KK graviton mass as a function of $k/\overline{M}_P$.

[28] AAD 12Y use 2.12 fb^{-1} of data from pp collisions at $\sqrt{s} = 7$ TeV in the diphoton channel to place lower limits on the mass of the lightest KK graviton. The diphoton channel is combined with previous results in the dielectron and dimuon channels to set the best limit. See their Table 3 for warp parameter values $k/\overline{M}_P$ between 0.01 and 0.1.

[29] AALTONEN 12V use 6 fb^{-1} of data from $p\overline{p}$ collisions at $\sqrt{s} = 1.96$ TeV to search for KK gravitons in a warped extra dimension decaying to ZZ dibosons in the $lljj$ and $llll$ channels (ℓ=e, μ). It provides improved limits over the previous analysis in AALTONEN 11G. See their Figure 16 for limits from all channels combined on the cross section times branching ratio $\sigma(p\overline{p} \to G^* \to ZZ)$ as a function of the graviton mass.

[30] BAAK 12 use electroweak precision observables to place a lower bound on the compactification scale $k\,e^{-\pi kR}$, assuming Standard Model fields propagate in the bulk and the Higgs is confined to the IR brane. See their Fig. 27 for more details.

[31] CHATRCHYAN 12R use 2.2 fb^{-1} of data from pp collisions at $\sqrt{s}$ = 7 TeV in the diphoton channel to place lower limits on the mass of the lightest KK graviton. See their Table III for warp parameter values $k/\overline{M}_P$ between 0.01 and 0.1.

[32] AAD 11AD use 1.08 and 1.21 fb^{-1} of data from pp collisions at $\sqrt{s}$ = 7 TeV in the dielectron and dimuon channels, respectively, to place a lower bound on the mass of the lightest graviton. For warp parameter values $k/\overline{M}_P$ between 0.01 to 0.1 the lower limit on the mass of the lightest graviton is between 0.71 and 1.63 TeV. See their Table IV for more details.

[33] AALTONEN 11G use 2.5–2.9 fb^{-1} of data from $p\overline{p}$ collisions at $\sqrt{s}$ = 1.96 TeV to search for KK gravitons in a warped extra dimension decaying to ZZ dibosons via the $eeee$, $ee\mu\mu$, $\mu\mu\mu\mu$, $eejj$, and $\mu\mu jj$ channels. See their Fig. 20 for limits on the cross section $\sigma(G \rightarrow ZZ)$ as a function of the graviton mass.

[34] AALTONEN 11R uses 5.7 fb^{-1} of data from $p\overline{p}$ collisions at $\sqrt{s}$ = 1.96 TeV in the dielectron channel to place a lower bound on the mass of the lightest graviton. It provides combined limits with the diphoton channel analysis of AALTONEN 11U. For warp parameter values $k/\overline{M}_P$ between 0.01 to 0.1 the lower limit on the mass of the lightest graviton is between 612 and 1058 GeV. See their Table I for more details.

[35] ABAZOV 11H use 5.4 fb^{-1} of data from $p\overline{p}$ collisions at $\sqrt{s}$ = 1.96 TeV to place a lower bound on the mass of the lightest graviton. Their 95% C.L. exclusion limit does not include masses less than 300 GeV.

[36] CHATRCHYAN 11 use 35 and 40 pb^{-1} of data from pp collisions at $\sqrt{s}$ = 7 TeV in the dielectron and dimuon channels, respectively, to place a lower bound on the mass of the lightest graviton. For a warp parameter value $k/\overline{M}_P$ = 0.05, the lower limit on the mass of the lightest graviton is 0.855 TeV.

[37] AALTONEN 10N use 2.9 fb^{-1} of data from $p\overline{p}$ collisions at $\sqrt{s}$ = 1.96 TeV to place a lower bound on the mass of the lightest graviton.

[38] ABAZOV 10F use 5.4 fb^{-1} of data from $p\overline{p}$ collisions at $\sqrt{s}$ = 1.96 TeV to place a lower bound on the mass of the lightest graviton. For warp parameter values of $k/\overline{M}_P$ between 0.01 and 0.1 the lower limit on the mass of the lightest graviton is between 560 and 1050 GeV. See their Fig. 3 for more details.

[39] AALTONEN 08S use $p\overline{p}$ collisions at $\sqrt{s}$ = 1.96 TeV to search for KK gravitons in warped extra dimensions. They search for graviton resonances decaying to four electrons via two Z bosons using 1.1 fb^{-1} of data. See their Fig. 8 for limits on $\sigma \cdot$ B$(G \rightarrow ZZ)$ versus the graviton mass.

[40] ABAZOV 08J use $p\overline{p}$ collisions at $\sqrt{s}$ = 1.96 TeV to search for KK gravitons in warped extra dimensions. They search for graviton resonances decaying to electrons and photons using 1 fb^{-1} of data. For warp parameter values of $k/\overline{M}_P$ between 0.01 and 0.1 the lower limit on the mass of the lightest excitation is between 300 and 900 GeV. See their Fig. 4 for more details.

[41] AALTONEN 07G use $p\overline{p}$ collisions at $\sqrt{s}$ = 1.96 TeV to search for KK gravitons in warped extra dimensions. They search for graviton resonances decaying to photons using 1.2 fb^{-1} of data. For warp parameter values of $k/\overline{M}_P$ = 0.1, 0.05, and 0.01 the bounds on the graviton mass are 850, 694, and 230 GeV, respectively. See their Fig. 3 for more details. See also AALTONEN 07H.

[42] AALTONEN 07H use $p\overline{p}$ collisions at $\sqrt{s}$ = 1.96 TeV to search for KK gravitons in warped extra dimensions. They search for graviton resonances decaying to electrons using 1.3 fb^{-1} of data. For a warp parameter value of $k/\overline{M}_P$ = 0.1 the bound on the graviton mass is 807 GeV. See their Fig. 4 for more details. A combined analysis with the diphoton data of AALTONEN 07G yields for $k/\overline{M}_P$ = 0.1 a graviton mass lower bound of 889 GeV.

[43] ABAZOV 05N use $p\overline{p}$ collisions at $\sqrt{s}$ = 1.96 TeV to search for KK gravitons in warped extra dimensions. They search for graviton resonances decaying to muons, electrons or photons, using 260 pb^{-1} of data. For warp parameter values of $k/\overline{M}_P$ = 0.1, 0.05, and 0.01, the bounds on the graviton mass are 785, 650 and 250 GeV respectively. See their Fig. 3 for more details.

[44] ABULENCIA 05A use $p\overline{p}$ collisions at $\sqrt{s}$ = 1.96 TeV to search for KK gravitons in warped extra dimensions. They search for graviton resonances decaying to muons or electrons, using 200 pb^{-1} of data. For warp parameter values of $k/\overline{M}_P$ = 0.1, 0.05, and 0.01, the bounds on the graviton mass are 710, 510 and 170 GeV respectively.

Limits on Kaluza-Klein Gluons in Warped Extra Dimensions

This section places limits on the mass of the first Kaluza-Klein (KK) excitation of the gluon in warped extra dimension models with Standard Model fields propagating in the bulk. Bounds are given for a specific benchmark model with Γ/m = 15.3% where Γ is the width and m the mass of the KK gluon. See the "Extra Dimensions" review for more discussion.

VALUE (TeV)	CL%	DOCUMENT ID		TECN	COMMENT
>2.5	95	[1] CHATRCHYAN	13BM	CMS	$g_{KK} \rightarrow t\overline{t}$
• • • We do not use the following data for averages, fits, limits, etc. • • •					
>2.07	95	[2] AAD	13AQ	ATLS	$g_{KK} \rightarrow t\overline{t} \rightarrow \ell j$
		[3] CHEN	13A		$\overline{B} \rightarrow X_s\gamma$
>1.5	95	[4] AAD	12BV	ATLS	$g_{KK} \rightarrow t\overline{t} \rightarrow \ell j$

[1] CHATRCHYAN 13BM use 19.7 fb^{-1} of data from pp collisions at $\sqrt{s}$ = 8 TeV. Bound is for a width of approximately 15–20% of the KK gluon mass.

[2] AAD 13AQ use 4.7 fb^{-1} of data from pp collisions at $\sqrt{s}$ = 7 TeV.

[3] CHEN 13A place limits on the KK mass scale for a specific warped model with custodial symmetry and bulk fermions. See their Figures 4 and 5.

[4] AAD 12BV use 2.05 fb^{-1} of data from pp collisions at $\sqrt{s}$ = 7 TeV.

REFERENCES FOR Extra Dimensions

SIRUNYAN	18F	JHEP 1801 054	A.M. Sirunyan *et al.*	(CMS Collab.)
AABOUD	17AP	PL B775 105	M. Aaboud *et al.*	(ATLAS Collab.)
KHACHATRY...	17T	PL B768 57	V. Khachatryan *et al.*	(CMS Collab.)
KHACHATRY...	17W	PL B769 520	V. Khachatryan *et al.*	(CMS Collab.)
KLIMCHITSK...	17A	PR D95 123013	G.L. Klimchitskaya, V.M. Mostepanenko	
SIRUNYAN	17AK	PL B774 533	A.M. Sirunyan *et al.*	(CMS Collab.)
SIRUNYAN	17AQ	JHEP 1710 073	A.M. Sirunyan *et al.*	(CMS Collab.)
SIRUNYAN	17F	JHEP 1707 013	A.M. Sirunyan *et al.*	(CMS Collab.)
AABOUD	16AE	JHEP 1609 173	M. Aaboud *et al.*	(ATLAS Collab.)
AABOUD	16D	PR D94 032005	M. Aaboud *et al.*	(ATLAS Collab.)
AABOUD	16F	JHEP 1606 059	M. Aaboud *et al.*	(ATLAS Collab.)
AABOUD	16H	JHEP 1609 001	M. Aaboud *et al.*	(ATLAS Collab.)
AABOUD	16I	PR D94 052002	M. Aaboud *et al.*	(ATLAS Collab.)
AAD	16R	PL B755 285	G. Aad *et al.*	(ATLAS Collab.)
KHACHATRY...	16BQ	PR D94 052012	V. Khachatryan *et al.*	(CMS Collab.)
KHACHATRY...	16M	PRL 117 051802	V. Khachatryan *et al.*	(CMS Collab.)
KHACHATRY...	16N	PL B755 102	V. Khachatryan *et al.*	(CMS Collab.)
AAD	15AD	PR D92 032004	G. Aad *et al.*	(ATLAS Collab.)
AAD	15AU	EPJ C75 69	G. Aad *et al.*	(ATLAS Collab.)
AAD	15AZ	EPJ C75 209	G. Aad *et al.*	(ATLAS Collab.)
Also		EPJ C75 370 (errat.)	G. Aad *et al.*	(ATLAS Collab.)
AAD	15BH	EPJ C75 299	G. Aad *et al.*	(ATLAS Collab.)
Also		EPJ C75 408 (errat.)	G. Aad *et al.*	(ATLAS Collab.)
AAD	15BK	EPJ C75 412	G. Aad *et al.*	(ATLAS Collab.)
AAD	15CS	PR D91 012008	G. Aad *et al.*	(ATLAS Collab.)
Also		PR D92 059903 (errat.)	G. Aad *et al.*	(ATLAS Collab.)
AAD	15CT	JHEP 1512 055	G. Aad *et al.*	(ATLAS Collab.)
ACCOMANDO	15	MPL A30 1540010	E. Accomando	(SHMP)
KHACHATRY...	15AE	JHEP 1504 025	V. Khachatryan *et al.*	(CMS Collab.)
KHACHATRY...	15AL	EPJ C75 235	V. Khachatryan *et al.*	(CMS Collab.)
KHACHATRY...	15J	PL B746 79	V. Khachatryan *et al.*	(CMS Collab.)
KHACHATRY...	15R	PL B749 560	V. Khachatryan *et al.*	(CMS Collab.)
KHACHATRY...	15T	PR D91 092005	V. Khachatryan *et al.*	(CMS Collab.)
AAD	14BE	EPJ C74 3134	G. Aad *et al.*	(ATLAS Collab.)
AAD	14V	PR D90 052005	G. Aad *et al.*	(ATLAS Collab.)
KHACHATRY...	14A	JHEP 1408 174	V. Khachatryan *et al.*	(CMS Collab.)
AAD	13A	PL B718 860	G. Aad *et al.*	(ATLAS Collab.)
AAD	13AD	JHEP 1304 075	G. Aad *et al.*	(ATLAS Collab.)
AAD	13AO	PR D87 112006	G. Aad *et al.*	(ATLAS Collab.)
AAD	13AQ	PR D88 012004	G. Aad *et al.*	(ATLAS Collab.)
AAD	13AS	NJP 15 043007	G. Aad *et al.*	(ATLAS Collab.)
AAD	13C	PRL 110 011802	G. Aad *et al.*	(ATLAS Collab.)
AAD	13D	JHEP 1301 029	G. Aad *et al.*	(ATLAS Collab.)
AAD	13E	PR D87 015010	G. Aad *et al.*	(ATLAS Collab.)
CHATRCHYAN	13AF	PL B720 63	S. Chatrchyan *et al.*	(CMS Collab.)
CHATRCHYAN	13AQ	PR D87 072005	S. Chatrchyan *et al.*	(CMS Collab.)
CHATRCHYAN	13BM	PRL 111 211804	S. Chatrchyan *et al.*	(CMS Collab.)
Also		PRL 112 119903 (errat.)	S. Chatrchyan *et al.*	(CMS Collab.)
CHATRCHYAN	13U	JHEP 1302 036	S. Chatrchyan *et al.*	(CMS Collab.)
CHATRCHYAN	13W	JHEP 1303 111	S. Chatrchyan *et al.*	(CMS Collab.)
CHEN	13A	CP C37 063102	J-B. Chen *et al.*	(DALI)
EDELHAUSER	13	JHEP 1308 091	L. Edelhauser, T. Flacke, M. Kramer	(AACH, KAIST)
XU	13	JP G40 035107	J. Xu *et al.*	
AAD	12AD	PL B712 331	G. Aad *et al.*	(ATLAS Collab.)
AAD	12BV	JHEP 1209 041	G. Aad *et al.*	(ATLAS Collab.)
AAD	12CC	JHEP 1211 138	G. Aad *et al.*	(ATLAS Collab.)
AAD	12CP	PL B718 411	G. Aad *et al.*	(ATLAS Collab.)
AAD	12X	PL B710 519	G. Aad *et al.*	(ATLAS Collab.)
AAD	12Y	PL B710 538	G. Aad *et al.*	(ATLAS Collab.)
AALTONEN	12V	PR D85 012008	T. Aaltonen *et al.*	(CDF Collab.)
ABAZOV	12M	PRL 108 131802	V.M. Abazov *et al.*	(D0 Collab.)
AJELLO	12	JCAP 1202 012	M. Ajello *et al.*	(Fermi-LAT Collab.)
BAAK	12	EPJ C72 2003	M. Baak *et al.*	(Gfitter Group)
CHATRCHYAN	12AP	JHEP 1209 094	S. Chatrchyan *et al.*	(CMS Collab.)
CHATRCHYAN	12J	PL B711 15	S. Chatrchyan *et al.*	(CMS Collab.)
CHATRCHYAN	12R	PRL 108 111801	S. Chatrchyan *et al.*	(CMS Collab.)
FLACKE	12	PR D85 126007	T. Flacke, C. Pasold	(WURZ)
NISHIWAKI	12	PL B707 506	K. Nishiwaki *et al.*	(KOBE, OSAK)
AAD	11AD	PRL 107 272002	G. Aad *et al.*	(ATLAS Collab.)
AAD	11F	PRL 106 121803	G. Aad *et al.*	(ATLAS Collab.)
AAD	11S	PL B705 294	G. Aad *et al.*	(ATLAS Collab.)
AAD	11X	EPJ C71 1744	G. Aad *et al.*	(ATLAS Collab.)
AALTONEN	11G	PR D83 112008	T. Aaltonen *et al.*	(CDF Collab.)
AALTONEN	11R	PRL 107 051801	T. Aaltonen *et al.*	(CDF Collab.)
AALTONEN	11U	PR D83 011102	T. Aaltonen *et al.*	(CDF Collab.)
AARON	11C	PL B705 52	F. D. Aaron *et al.*	(H1 Collab.)
ABAZOV	11H	PRL 107 011801	V.M. Abazov *et al.*	(D0 Collab.)
BEZERRA	11	PR D83 075004	V.B. Bezerra *et al.*	
CHATRCHYAN	11	JHEP 1105 093	S. Chatrchyan *et al.*	(CMS Collab.)
CHATRCHYAN	11A	JHEP 1105 085	S. Chatrchyan *et al.*	(CMS Collab.)
CHATRCHYAN	11U	PRL 107 201804	S. Chatychyan *et al.*	(CMS Collab.)
SUSHKOV	11	PRL 107 171101	A.O. Sushkov *et al.*	
AALTONEN	10N	PRL 104 241801	T. Aaltonen *et al.*	(CDF Collab.)
ABAZOV	10F	PRL 104 241802	V.M. Abazov *et al.*	(D0 Collab.)
ABAZOV	10P	PRL 105 221802	V.M. Abazov *et al.*	(D0 Collab.)
BEZERRA	10	PR D81 055003	V.B. Bezerra *et al.*	
ABAZOV	09AE	PRL 103 191803	V.M. Abazov *et al.*	(D0 Collab.)
ABAZOV	09D	PRL 102 051601	V.M. Abazov *et al.*	(D0 Collab.)
MASUDA	09	PRL 102 171101	M. Masuda, M. Sasaki	(ICRR)
AALTONEN	08AC	PRL 101 181602	T. Aaltonen *et al.*	(CDF Collab.)
AALTONEN	08S	PR D78 012008	T. Aaltonen *et al.*	(CDF Collab.)
ABAZOV	08J	PRL 100 091802	V.M. Abazov *et al.*	(D0 Collab.)
ABAZOV	08S	PRL 101 011601	V.M. Abazov *et al.*	(D0 Collab.)
DAS	08	PR D78 063011	P.K. Das, V.H.S. Kumar, P.K. Suresh	
GERACI	08	PR D78 022002	A.A. Geraci *et al.*	(STAN)
TRENKEL	08	PR D77 122001	C. Trenkel	
AALTONEN	07G	PRL 99 171801	T. Aaltonen *et al.*	(CDF Collab.)
AALTONEN	07H	PRL 99 171802	T. Aaltonen *et al.*	(CDF Collab.)
DECCA	07A	EPJ C51 963	R.S. Decca *et al.*	
HAISCH	07	PR D76 034014	U. Haisch, A. Weiler	
KAPNER	07	PRL 98 021101	D.J. Kapner *et al.*	
SCHAEL	07A	EPJ C49 411	S. Schael *et al.*	(ALEPH Collab.)
TU	07	PRL 98 201101	L.-C. Tu *et al.*	
ABDALLAH	06C	EPJ C45 589	J. Abdallah *et al.*	(DELPHI Collab.)
ABULENCIA,A	06	PRL 97 171802	A. Abulencia *et al.*	(CDF Collab.)
GERDES	06	PR D73 112008	D. Gerdes *et al.*	
GOGOLADZE	06	PR D74 093012	I. Gogoladze, C. Macesanu	
ABAZOV	05N	PRL 95 091801	V.M. Abazov *et al.*	(D0 Collab.)
ABAZOV	05V	PRL 95 161602	V.M. Abazov *et al.*	(D0 Collab.)
ABDALLAH	05B	EPJ C38 395	J. Abdallah *et al.*	(DELPHI Collab.)
ABULENCIA	05A	PRL 95 252001	A. Abulencia *et al.*	(CDF Collab.)
SMULLIN	05	PR D72 122001	S.J. Smullin *et al.*	
ACHARD	04E	PL B587 16	P. Achard *et al.*	(L3 Collab.)
ACOSTA	04C	PRL 92 121802	D. Acosta *et al.*	(CDF Collab.)
BARBIERI	04	NP B703 127	R. Barbieri *et al.*	
CASSE	04	PRL 92 111102	M. Casse *et al.*	
CHEKANOV	04B	PL B591 23	S. Chekanov *et al.*	(ZEUS Collab.)
HOYLE	04	PR D70 042004	C.D. Hoyle *et al.*	(WASH)
ABAZOV	03	PRL 90 251802	V.M. Abazov *et al.*	(D0 Collab.)
ABBIENDI	03D	EPJ C26 331	G. Abbiendi *et al.*	(OPAL Collab.)
ACHARD	03D	PL B572 133	P. Achard *et al.*	(L3 Collab.)
ADLOFF	03	PL B568 35	C. Adloff *et al.*	(H1 Collab.)
CHIAVERINI	03	PRL 90 151101	J. Chiaverini *et al.*	
GIUDICE	03	NP B663 377	G.F. Giudice, A. Strumia	
HANNESTAD	03	PR D67 125008	S. Hannestad, G.G. Raffelt	
Also		PR D69 029901(errat.)	S. Hannestad, G.G. Raffelt	
HEISTER	03C	EPJ C28 1	A. Heister *et al.*	(ALEPH Collab.)
LONG	03	Nature 421 922	J.C. Long *et al.*	
ACHARD	02	PL B524 65	P. Achard *et al.*	(L3 Collab.)
ACHARD	02D	PL B531 28	P. Achard *et al.*	(L3 Collab.)
HANNESTAD	02	PRL 88 071301	S. Hannestad, G. Raffelt	
ABBOTT	01	PRL 86 1156	B. Abbott *et al.*	(D0 Collab.)
FAIRBAIRN	01	PL B508 335	M. Fairbairn	

HANHART	01	PL B509 1	C. Hanhart *et al.*	
HOYLE	01	PRL 86 1418	C.D. Hoyle *et al.*	
ABBIENDI	00R	EPJ C13 553	G. Abbiendi *et al.*	(OPAL Collab.)
ABREU	00A	PL B491 67	P. Abreu *et al.*	(DELPHI Collab.)
ABREU	00S	PL B485 45	P. Abreu *et al.*	(DELPHI Collab.)
ABREU	00Z	EPJ C17 53	P. Abreu *et al.*	(DELPHI Collab.)
CASSISI	00	PL B481 323	S. Cassisi *et al.*	
CHANG	00B	PRL 85 3765	L.N. Chang *et al.*	
CHEUNG	00	PR D61 015005	K. Cheung	
CORNET	00	PR D61 037701	F. Cornet, M. Relano, J. Rico	
GRAESSER	00	PR D61 074019	M.L. Graesser	
HAN	00	PR D62 125018	T. Han, D. Marfatia, R.-J. Zhang	
MATHEWS	00	JHEP 0007 008	P. Mathews, S. Raychaudhuri, K. Sridhar	
MELE	00	PR D61 117901	S. Mele, E. Sanchez	
RIZZO	00	PR D61 016007	T.G. Rizzo, J.D. Wells	
ABBIENDI	99P	PL B465 303	G. Abbiendi *et al.*	(OPAL Collab.)
ACCIARRI	99M	PL B464 135	M. Acciarri *et al.*	(L3 Collab.)
ACCIARRI	99R	PL B470 268	M. Acciarri *et al.*	(L3 Collab.)
ACCIARRI	99S	PL B470 281	M. Acciarri *et al.*	(L3 Collab.)
BOURILKOV	99	JHEP 9908 006	D. Bourilkov	
HOSKINS	85	PR D32 3084	J.K. Hoskins *et al.*	

WIMP and Dark Matter Searches

OMITTED FROM SUMMARY TABLE

We omit papers on CHAMP's, millicharged particles, and other exotic particles.

GALACTIC WIMP SEARCHES

These limits are for weakly-interacting stable particles that may constitute the invisible mass in the galaxy. Unless otherwise noted, a local mass density of 0.3 GeV/cm^3 is assumed; see each paper for velocity distribution assumptions. In the papers the limit is given as a function of the X^0 mass. Here we list limits only for typical mass values of 20 GeV, 100 GeV, and 1 TeV. Specific limits on supersymmetric dark matter particles may be found in the Supersymmetry section.

Limits for Spin-Independent Cross Section of Dark Matter Particle (X^0) on Nucleon

Isoscalar coupling is assumed to extract the limits from those on X^0–nuclei cross section.

For m_{X^0} = 20 GeV

For limits from X^0 annihilation in the Sun, the assumed annihilation final state is shown in parenthesis in the comment.

VALUE (pb)	CL%	DOCUMENT ID		TECN	COMMENT
• • • We do not use the following data for averages, fits, limits, etc. • • •					
$<5 \times 10^{-6}$	95	[1] AGNESE	18	CDMS	Ge
$<2 \times 10^{-6}$	90	[2] AARTSEN	17	ICCB	ν, earth
$<1 \times 10^{4}$	90	[3] ANGLOHER	17A	CRES	χp
$<1 \times 10^{-3}$	90	[4] BARBOSA-D...	17	ICCB	NaI
$<7.3 \times 10^{-7}$	90	AGNES	16	DS50	Ar
$<1 \times 10^{-5}$	90	[5] AGNESE	16	CDMS	Ge
$<2 \times 10^{-4}$	90	[6] AGUILAR-AR...	16	DMIC	Si CCDs
$<4 \times 10^{-5}$	90	[7] ANGLOHER	16	CRES	$CaWO_4$
$<2 \times 10^{-6}$	90	[8] APRILE	16	X100	Xe
$<9.4 \times 10^{-8}$	90	[9] ARMENGAUD	16	EDE3	Ge
$<1.0 \times 10^{-7}$	90	[10] HEHN	16	EDE3	Ge
$<4 \times 10^{-6}$	90	[11] ZHAO	16	CDEX	Ge
$<1 \times 10^{-5}$	90	AGNES	15	DS50	Ar
$<1.5 \times 10^{-6}$	90	[12] AGNESE	15A	CDM2	Ge
$<1.5 \times 10^{-7}$	90	[13] AGNESE	15B	CDM2	Ge
$<2 \times 10^{-6}$	90	[14] AMOLE	15	PICO	C_3F_8
$<1.2 \times 10^{-5}$	90	CHOI	15	SKAM	H, solar ν ($b\overline{b}$)
$<1.19 \times 10^{-6}$	90	CHOI	15	SKAM	H, solar ν ($\tau^+\tau^-$)
$<2 \times 10^{-8}$	90	[15] XIAO	15	PNDX	Xe
$<2.0 \times 10^{-7}$	90	[16] AGNESE	14	SCDM	Ge
$<3.7 \times 10^{-5}$	90	[17] AGNESE	14A	SCDM	Ge
$<1 \times 10^{-9}$	90	[18] AKERIB	14	LUX	Xe
$<2 \times 10^{-6}$	90	[19] ANGLOHER	14	CRES	$CaWO_4$
$<5 \times 10^{-6}$	90	FELIZARDO	14	SMPL	C_2ClF_5
$<8 \times 10^{-6}$	90	[20] LEE	14A	KIMS	CsI
$<2 \times 10^{-4}$	90	[21] LIU	14A	CDEX	Ge
$<1 \times 10^{-5}$	90	[22] YUE	14	CDEX	Ge
$<1.08 \times 10^{-4}$	90	[23] AARTSEN	13	ICCB	H, solar ν ($\tau^+\tau^-$)
$<1.5 \times 10^{-5}$	90	[24] ABE	13B	XMAS	Xe
$<3.1 \times 10^{-6}$	90	[25] AGNESE	13	CDM2	Si
$<3.4 \times 10^{-6}$	90	[26] AGNESE	13A	CDM2	Si
$<2.2 \times 10^{-6}$	90	[27] AGNESE	13A	CDM2	Si
		[28] BERNABEI	13A	DAMA	NaI modulation
$<5 \times 10^{-5}$	90	[29] LI	13B	TEXO	Ge
		[30] ZHAO	13	CDEX	Ge
$<1.2 \times 10^{-7}$	90	AKIMOV	12	ZEP3	Xe
		[31] ANGLOHER	12	CRES	$CaWO_4$
$<8 \times 10^{-6}$	90	[32] ANGLOHER	12	CRES	$CaWO_4$
$<7 \times 10^{-9}$	90	[33] APRILE	12	X100	Xe
		[34] ARCHAMBAU...	12	PICA	F (C_4F_{10})
$<7 \times 10^{-7}$	90	[35] ARMENGAUD	12	EDE2	Ge
		[36] BARRETO	12	DMIC	CCD
$<2 \times 10^{-6}$	90	BEHNKE	12	COUP	CF_3I
$<7 \times 10^{-6}$		[37] FELIZARDO	12	SMPL	C_2ClF_5
$<1.5 \times 10^{-6}$	90	KIM	12	KIMS	CsI
$<5 \times 10^{-5}$	90	[38] AALSETH	11	CGNT	Ge
		[39] AALSETH	11A	CGNT	Ge
$<5 \times 10^{-7}$	90	[40] AHMED	11	CDM2	Ge, inelastic
$<2.7 \times 10^{-7}$	90	[41] AHMED	11A	RVUE	Ge
		[42] AHMED	11B	CDM2	Ge, low threshold
$<3 \times 10^{-6}$	90	[43] ANGLE	11	XE10	Xe
$<7 \times 10^{-8}$	90	[44] APRILE	11	X100	Xe
		[45] APRILE	11A	X100	Xe, inelastic
$<2 \times 10^{-8}$	90	[33] APRILE	11B	X100	Xe
		[46] HORN	11	ZEP3	Xe
$<2 \times 10^{-7}$	90	AHMED	10	CDM2	Ge
$<1 \times 10^{-5}$	90	[47] AKERIB	10	CDM2	Si, Ge, low threshold
$<1 \times 10^{-7}$	90	APRILE	10	X100	Xe
$<2 \times 10^{-6}$	90	ARMENGAUD	10	EDE2	Ge
$<4 \times 10^{-5}$	90	FELIZARDO	10	SMPL	C_2ClF_3
$<1.5 \times 10^{-7}$	90	[48] AHMED	09	CDM2	Ge
$<2 \times 10^{-4}$	90	[49] LIN	09	TEXO	Ge
		[50] AALSETH	08	CGNT	Ge

[1] AGNESE 18 give limits for $\sigma^{SI}(p_\chi)$ for m(WIMP) between 1.5 and 20 GeV using CDMSlite mode data.

[2] AARTSEN 17 obtain $\sigma(\mathrm{SI}) < 6 \times 10^{-6}$ pb for m(wimp) = 20 GeV from ν from earth.

[3] ANGLOHER 17A find $\sigma^{SI}(\chi p) < 10^4$ pb for m(WIMP) = 0.2 GeV.

[4] BARBOSA-DE-SOUZA 17 search for annual modulation of WIMP scatter on NaI using an exposure of 61 kg yr of DM-Ice17 for recoil energy in the 4–20 keV range (DAMA found modulation for recoil energy < 5 keV). No modulation seen. Sensitivity insufficient to distinguish DAMA signal from null.

[5] AGNESE 16 CDMSlite excludes low mass WIMPs 1.6–5.5 GeV and SI scattering cross section depending on m(WIMP); see Fig. 4.

[6] AGUILAR-AREVALO 16 search low mass 1–10 GeV WIMP scatter on Si CCDs; set limits Fig. 11.

[7] ANGLOHER 16 requires SI WIMP-nucleon cross section $< 9 \times 10^{-3}$ pb for m(WIMP) = 1 GeV on $CaWO_4$ target.

[8] APRILE 16 search low mass WIMP SI scatter on Xe; exclude $\sigma > 1.4 \times 10^{-5}$ pb for m(WIMP) = 6 GeV.

[9] ARMENGAUD 16 require SI WIMP-p cross section $< 4.3 \times 10^{-4}$ pb for m(WIMP) = 5 GeV on Ge target.

[10] HEHN 16 search for low mass WIMPs via SI scatter on Ge target; $\sigma(\mathrm{SI}) < 5.8 \times 10^{-4}$ pb for m(WIMP) = 5 GeV, Fig. 6.

[11] ZHAO 16 require SI scatter $< 4 \times 10^{-6}$ pb for m(WIMP) = 20 GeV using Ge target; limits also on SD scatter, see Fig. 19.

[12] AGNESE 15A reanalyse AHMED 11B low threshold data. See their Fig. 12 (left) for improved limits extending down to 5 GeV.

[13] AGNESE 15B reanalyse AHMED 10 data.

[14] See their Fig. 7 for limits extending down to 4 GeV.

[15] See their Fig. 13 for limits extending down to 5 GeV.

[16] This limit value is provided by the authors. See their Fig. 4 for limits extending down to $m_{X^0} = 3.5$ GeV.

[17] This limit value is provided by the authors. AGNESE 14A result is from CDMSlite mode operation with enhanced sensitivity to low mass m_{X^0}. See their Fig. 3 for limits extending down to $m_{X^0} = 3.5$ GeV (see also Fig. 4 in AGNESE 14).

[18] See their Fig. 5 for limits extending down to $m_{X^0} = 5.5$ GeV.

[19] See their Fig. 5 for limits extending down to $m_{X^0} = 1$ GeV.

[20] See their Fig. 5 for limits extending down to $m_{X^0} = 5$ GeV.

[21] LIU 14A result is based on prototype CDEX-0 detector. See their Fig. 13 for limits extending down to $m_{X^0} = 2$ GeV.

[22] See their Fig. 4 for limits extending down to $m_{X^0} = 4.5$ GeV.

[23] AARTSEN 13 search for neutrinos from the Sun arising from the pair annihilation of X^0 trapped by the sun in data taken between June 2010 and May 2011.

[24] See their Fig. 8 for limits extending down to $m_{X^0} = 7$ GeV.

[25] This limit value is provided by the authors. AGNESE 13 use data taken between Oct. 2006 and July 2007. See their Fig. 4 for limits extending down to $m_{X^0} = 7$ GeV.

[26] This limit value is provided by the authors. AGNESE 13A use data taken between July 2007 and Sep. 2008. Three candidate events are seen. Assuming these events are real, the best fit parameters are $m_{X^0} = 8.6$ GeV and $\sigma = 1.9 \times 10^{-5}$ pb.

[27] This limit value is provided by the authors. Limit from combined data of AGNESE 13 and AGNESE 13A. See their Fig. 4 for limits extending down to $m_{X^0} = 5.5$ GeV.

[28] BERNABEI 13A search for annual modulation of counting rate in the 2–6 keV recoil energy interval, in a 14 yr live time exposure of 1.33 t yr. Find a modulation of 0.0112 ± 0.0012 counts/(day kg keV) with 9.3 sigma C.L. Find period and phase in agreement with expectations from DM particles.

[29] See their Fig. 4 for limits extending down to $m_{X^0} = 4$ GeV.

[30] See their Fig. 5 for limits for $m_{X^0} = 4$–12 GeV.

[31] ANGLOHER 12 observe excess events above the expected background which are consistent with X^0 with mass $\sim$ 25 GeV (or 12 GeV) and spin-independent X^0-nucleon cross section of 2×10^{-6} pb (or 4×10^{-5} pb).

[32] Reanalysis of ANGLOHER 09 data with all three nuclides. See also BROWN 12.

[33] See also APRILE 14A.

[34] See their Fig. 7 for cross section limits for m_{X^0} between 4 and 12 GeV.

[35] See their Fig. 4 for limits extending down to $m_{X^0} = 7$ GeV.

[36] See their Fig. 13 for cross section limits for m_{X^0} between 1.2 and 10 GeV.

[37] See also DAHL 12 for a criticism.

[38] See their Fig. 4 for limits extending to $m_{X^0} = 3.5$ GeV.

[39] AALSETH 11A find indications of annual modulation of the data, the energy spectrum being compatible with X^0 mass around 8 GeV. See also AALSETH 13.
[40] AHMED 11 search for X^0 inelastic scattering. See their Fig. 8–10 for limits. The inelastic cross section reduces to the elastic cross section at the limit of zero mass splitting (Fig. 8, left).
[41] AHMED 11A combine CDMS II and EDELWEISS data.
[42] AHMED 11B give limits on spin-independent X^0-nucleon cross section for m_{X^0} = 4–12 GeV in the range 10^{-3}–10^{-5} pb. See their Fig. 3.
[43] See their Fig. 3 for limits down to m_{X^0} = 4 GeV.
[44] APRILE 11 reanalyze APRILE 10 data.
[45] APRILE 11A search for X^0 inelastic scattering. See their Fig. 2 and 3 for limits. See also APRILE 14A.
[46] HORN 11 perform detector calibration by neutrons. Earlier results are only marginally affected.
[47] See their Fig. 10 and 12 for limits extending to X^0 mass of 1 GeV.
[48] Superseded by AHMED 10.
[49] See their Fig. 6(a) for cross section limits for m_{X^0} extending down to 2 GeV.
[50] See their Fig. 2 for cross section limits for m_{X^0} between 4 and 10 GeV.

For m_{X^0} = 100 GeV

For limits from X^0 annihilation in the Sun, the assumed annihilation final state is shown in parenthesis in the comment.

VALUE (pb)	CL%	DOCUMENT ID		TECN	COMMENT
• • • We do not use the following data for averages, fits, limits, etc. • • •					
$<1 \times 10^{-8}$	90	[1] AGNESE	18A	CDMS	$\sigma^{SI}(\chi p)$
$<1.7 \times 10^{-10}$	90	[2] AKERIB	17	LUX	Xe
$<1.2 \times 10^{-10}$	90	[3] APRILE	17G	XE1T	Xe
$<1.2 \times 10^{-10}$	90	[4] CUI	17A	PNDX	Xe
$<2.0 \times 10^{-8}$	90	AGNES	16	DS50	Ar
$<1 \times 10^{-9}$	90	[5] AKERIB	16	LUX	Xe
$<1 \times 10^{-9}$	90	[6] APRILE	16B	X100	Xe
$<2 \times 10^{-8}$	90	[7] TAN	16	PNDX	Xe
$<4 \times 10^{-10}$	90	[8] TAN	16B	PNDX	Xe
$<6 \times 10^{-8}$	90	AGNES	15	DS50	Ar
$<4 \times 10^{-8}$	90	[9] AGNESE	15B	CDM2	Ge
$<7.13 \times 10^{-6}$	90	CHOI	15	SKAM	H, solar ν ($b\overline{b}$)
$<6.26 \times 10^{-7}$	90	CHOI	15	SKAM	H, solar ν (W^+W^-)
$<2.76 \times 10^{-7}$	90	CHOI	15	SKAM	H, solar ν ($\tau^+\tau^-$)
$<1.5 \times 10^{-8}$	90	XIAO	15	PNDX	Xe
$<1 \times 10^{-9}$	90	AKERIB	14	LUX	Xe
$<4.0 \times 10^{-6}$	90	[10] AVRORIN	14	BAIK	H, solar ν (W^+W^-)
$<1.0 \times 10^{-4}$	90	[10] AVRORIN	14	BAIK	H, solar ν ($b\overline{b}$)
$<1.6 \times 10^{-6}$	90	[10] AVRORIN	14	BAIK	H, solar ν ($\tau^+\tau^-$)
$<5 \times 10^{-6}$	90	FELIZARDO	14	SMPL	C_2ClF_5
$<6.01 \times 10^{-7}$	90	[11] AARTSEN	13	ICCB	H, solar ν (W^+W^-)
$<3.30 \times 10^{-5}$	90	[11] AARTSEN	13	ICCB	H, solar ν ($b\overline{b}$)
$<1.9 \times 10^{-6}$	90	[12] ADRIAN-MAR..13		ANTR	H, solar ν (W^+W^-)
$<1.2 \times 10^{-4}$	90	[12] ADRIAN-MAR..13		ANTR	H, solar ν ($b\overline{b}$)
$<7.6 \times 10^{-7}$	90	[12] ADRIAN-MAR..13		ANTR	H, solar ν ($\tau^+\tau^-$)
$<2 \times 10^{-6}$	90	[13] AGNESE	13	CDM2	Si
$<1.6 \times 10^{-6}$	90	[14] BOLIEV	13	BAKS	H, solar ν (W^+W^-)
$<1.9 \times 10^{-5}$	90	[14] BOLIEV	13	BAKS	H, solar ν ($b\overline{b}$)
$<7.1 \times 10^{-7}$	90	[14] BOLIEV	13	BAKS	H, solar ν ($\tau^+\tau^-$)
$<1.67 \times 10^{-6}$	90	[15] ABBASI	12	ICCB	H, solar ν (W^+W^-)
$<1.07 \times 10^{-4}$	90	[15] ABBASI	12	ICCB	H, solar ν ($b\overline{b}$)
$<4 \times 10^{-8}$	90	AKIMOV	12	ZEP3	Xe
$<1.4 \times 10^{-6}$	90	[16] ANGLOHER	12	CRES	$CaWO_4$
$<3 \times 10^{-9}$	90	[17] APRILE	12	X100	Xe
$<3 \times 10^{-7}$	90	BEHNKE	12	COUP	CF_3I
$<7 \times 10^{-6}$		FELIZARDO	12	SMPL	C_2ClF_5
$<2.5 \times 10^{-7}$	90	[18] KIM	12	KIMS	CsI
$<2 \times 10^{-4}$	90	AALSETH	11	CGNT	Ge
		[19] AHMED	11	CDM2	Ge, inelastic
$<3.3 \times 10^{-8}$	90	[20] AHMED	11A	RVUE	Ge
		[21] AJELLO	11	FLAT	
$<3 \times 10^{-8}$	90	[22] APRILE	11	X100	Xe
		[23] APRILE	11A	X100	Xe, inelastic
$<1 \times 10^{-8}$	90	[17] APRILE	11B	X100	Xe
$<5 \times 10^{-8}$	90	[24] ARMENGAUD	11	EDE2	Ge
		[25] HORN	11	ZEP3	Xe
$<4 \times 10^{-8}$	90	AHMED	10	CDM2	Ge
$<9 \times 10^{-6}$	90	AKERIB	10	CDM2	Si, Ge, low threshold
		[26] AKIMOV	10	ZEP3	Xe, inelastic
$<5 \times 10^{-8}$	90	APRILE	10	X100	Xe
$<1 \times 10^{-7}$	90	ARMENGAUD	10	EDE2	Ge
$<3 \times 10^{-5}$	90	FELIZARDO	10	SMPL	C_2ClF_3
$<5 \times 10^{-8}$	90	[27] AHMED	09	CDM2	Ge
		[28] ANGLE	09	XE10	Xe, inelastic
$<3 \times 10^{-4}$	90	LIN	09	TEXO	Ge
		[29] GIULIANI	05	RVUE	

[1] AGNESE 18A set limit $\sigma^{SI}(\chi p) < 10^{-8}$ pb for m(WIMP) = 100 GeV.
[2] AKERIB 17 exclude SI cross section $> 1.7 \times 10^{-10}$ pb for m(WIMP) = 100 GeV. Uses complete LUX data set.
[3] APRILE 17G set limit $\sigma^{SI}(\chi p) < 1.2\ 10^{-10}$ pb for m(WIMP) = 100 GeV using 1 ton fiducial mass Xe TPC. Exposure is 34.2 live days.
[4] CUI 17A require $\sigma^{SI}(\chi p) < 1.2 \times 10^{-10}$ pb for m(WIMP) = 100 GeV using 54 ton-day exposure of Xe.
[5] AKERIB 16 re-analysis of 2013 data exclude SI cross section $> 1 \times 10^{-9}$ pb for m(WIMP) = 100 GeV on Xe target.
[6] APRILE 16B combined 447 live days using Xe target exclude σ(SI) $> 1.1 \times 10^{-9}$ pb for m(WIMP) = 50 GeV.
[7] TAN 16 search for WIMP scatter off Xe target; see SI exclusion plot Fig. 6.
[8] TAN 16B search for WIMP-p scatter off Xe target; see Fig. 5 for SI exclusion.
[9] AGNESE 15B reanalyse AHMED 10 data.
[10] AVRORIN 14 search for neutrinos from the Sun arising from the pair annihilation of X^0 trapped by the Sun in data taken between 1998 and 2003. See their Table 1 for limits assuming annihilation into neutrino pairs.
[11] AARTSEN 13 search for neutrinos from the Sun arising from the pair annihilation of X^0 trapped by the sun in data taken between June 2010 and May 2011.
[12] ADRIAN-MARTINEZ 13 search for neutrinos from the Sun arising from the pair annihilation of X^0 trapped by the sun in data taken between Jan. 2007 and Dec. 2008.
[13] AGNESE 13 use data taken between Oct. 2006 and July 2007.
[14] BOLIEV 13 search for neutrinos from the Sun arising from the pair annihilation of X^0 trapped by the sun in data taken from 1978 to 2009. See also SUVOROVA 13 for an older analysis of the same data.
[15] ABBASI 12 search for neutrinos from the Sun arising from the pair annihilation of X^0 trapped by the Sun. The amount of X^0 depends on the X^0-proton cross section.
[16] Reanalysis of ANGLOHER 09 data with all three nuclides. See also BROWN 12.
[17] See also APRILE 14A.
[18] See their Fig. 6 for a limit on inelastically scattering X^0 for m_{X^0} = 70 GeV.
[19] AHMED 11 search for X^0 inelastic scattering. See their Fig. 8–10 for limits.
[20] AHMED 11A combine CDMS and EDELWEISS data.
[21] AJELLO 11 search for $e^{\pm}$ flux from X^0 annihilations in the Sun. Models in which X^0 annihilates into an intermediate long-lived weakly interacting particles or X^0 scatters inelastically are constrained. See their Fig. 6–8 for limits.
[22] APRILE 11 reanalyze APRILE 10 data.
[23] APRILE 11A search for X^0 inelastic scattering. See their Fig. 2 and 3 for limits. See also APRILE 14A.
[24] Supersedes ARMENGAUD 10. A limit on inelastic cross section is also given.
[25] HORN 11 perform detector calibration by neutrons. Earlier results are only marginally affected.
[26] AKIMOV 10 give cross section limits for inelastically scattering dark matter. See their Fig. 4.
[27] Superseded by AHMED 10.
[28] ANGLE 09 search for X^0 inelastic scattering. See their Fig. 4 for limits.
[29] GIULIANI 05 analyzes the spin-independent X^0-nucleon cross section limits with both isoscalar and isovector couplings. See their Fig. 3 and 4 for limits on the couplings.

For m_{X^0} = 1 TeV

For limits from X^0 annihilation in the Sun, the assumed annihilation final state is shown in parenthesis in the comment.

VALUE (pb)	CL%	DOCUMENT ID		TECN	COMMENT
• • • We do not use the following data for averages, fits, limits, etc. • • •					
<0.3	90	[1] CHEN	17E	PNDX	$\chi N \to \chi^* \to \chi\gamma$
$<8.6 \times 10^{-8}$	90	AGNES	16	DS50	Ar
$<2 \times 10^{-7}$	90	AGNES	15	DS50	Ar
$<2 \times 10^{-7}$	90	[2] AGNESE	15B	CDM2	Ge
$<1 \times 10^{-8}$	90	AKERIB	14	LUX	Xe
$<2.2 \times 10^{-6}$	90	[3] AVRORIN	14	BAIK	H, solar ν (W^+W^-)
$<5.5 \times 10^{-5}$	90	[3] AVRORIN	14	BAIK	H, solar ν ($b\overline{b}$)
$<6.8 \times 10^{-7}$	90	[3] AVRORIN	14	BAIK	H, solar ν ($\tau^+\tau^-$)
$<3.46 \times 10^{-7}$	90	[4] AARTSEN	13	ICCB	H, solar ν (W^+W^-)
$<7.75 \times 10^{-6}$	90	[4] AARTSEN	13	ICCB	H, solar ν ($b\overline{b}$)
$<6.9 \times 10^{-7}$	90	[5] ADRIAN-MAR..13		ANTR	H, solar ν (W^+W^-)
$<1.5 \times 10^{-5}$	90	[5] ADRIAN-MAR..13		ANTR	H, solar ν ($b\overline{b}$)
$<1.8 \times 10^{-7}$	90	[5] ADRIAN-MAR..13		ANTR	H, solar ν ($\tau^+\tau^-$)
$<4.3 \times 10^{-6}$	90	[6] BOLIEV	13	BAKS	H, solar ν (W^+W^-)
$<3.4 \times 10^{-5}$	90	[6] BOLIEV	13	BAKS	H, solar ν ($b\overline{b}$)
$<1.2 \times 10^{-6}$	90	[6] BOLIEV	13	BAKS	H, solar ν ($\tau^+\tau^-$)
$<2.12 \times 10^{-7}$	90	[7] ABBASI	12	ICCB	H, solar ν (W^+W^-)
$<6.56 \times 10^{-6}$	90	[7] ABBASI	12	ICCB	H, solar ν ($b\overline{b}$)
$<4 \times 10^{-7}$	90	AKIMOV	12	ZEP3	Xe
$<1.1 \times 10^{-5}$	90	[8] ANGLOHER	12	CRES	$CaWO_4$
$<2 \times 10^{-8}$	90	[9] APRILE	12	X100	Xe
$<2 \times 10^{-6}$	90	BEHNKE	12	COUP	CF_3I
$<4 \times 10^{-6}$		FELIZARDO	12	SMPL	C_2ClF_5
$<1.5 \times 10^{-6}$	90	KIM	12	KIMS	CsI
		[10] AHMED	11	CDM2	Ge, inelastic
$<1.5 \times 10^{-7}$	90	[11] AHMED	11A	RVUE	Ge
$<2 \times 10^{-7}$	90	[12] APRILE	11	X100	Xe
$<8 \times 10^{-8}$	90	[9] APRILE	11B	X100	Xe
$<2 \times 10^{-7}$	90	[13] ARMENGAUD	11	EDE2	Ge
		[14] HORN	11	ZEP3	Xe
$<2 \times 10^{-7}$	90	AHMED	10	CDM2	Ge
$<4 \times 10^{-7}$	90	APRILE	10	X100	Xe
$<6 \times 10^{-7}$	90	ARMENGAUD	10	EDE2	Ge
$<3.5 \times 10^{-7}$	90	[15] AHMED	09	CDM2	Ge

[1] CHEN 17E search for inelastic WIMP scatter on Xe; require $\sigma^{SI}(\chi N) < 0.3$ pb for m(χ) = 1 TeV and (mass difference) = 300 keV.
[2] AGNESE 15B reanalyse AHMED 10 data.
[3] AVRORIN 14 search for neutrinos from the Sun arising from the pair annihilation of X^0 trapped by the Sun in data taken between 1998 and 2003. See their Table 1 for limits assuming annihilation into neutrino pairs.

[4] AARTSEN 13 search for neutrinos from the Sun arising from the pair annihilation of X^0 trapped by the sun in data taken between June 2010 and May 2011.
[5] ADRIAN-MARTINEZ 13 search for neutrinos from the Sun arising from the pair annihilation of X^0 trapped by the sun in data taken between Jan. 2007 and Dec. 2008.
[6] BOLIEV 13 search for neutrinos from the Sun arising from the pair annihilation of X^0 trapped by the sun in data taken from 1978 to 2009. See also SUVOROVA 13 for an older analysis of the same data.
[7] ABBASI 12 search for neutrinos from the Sun arising from the pair annihilation of X^0 trapped by the Sun. The amount of X^0 depends on the X^0-proton cross section.
[8] Reanalysis of ANGLOHER 09 data with all three nuclides. See also BROWN 12.
[9] See also APRILE 14A.
[10] AHMED 11 search for X^0 inelastic scattering. See their Fig. 8–10 for limits.
[11] AHMED 11A combine CDMS and EDELWEISS data.
[12] APRILE 11 reanalyze APRILE 10 data.
[13] Supersedes ARMENGAUD 10. A limit on inelastic cross section is also given.
[14] HORN 11 perform detector calibration by neutrons. Earlier results are only marginally affected.
[15] Superseded by AHMED 10.

Limits for Spin-Dependent Cross Section of Dark Matter Particle (X^0) on Proton

For m_{X^0} = 20 GeV

For limits from X^0 annihilation in the Sun, the assumed annihilation final state is shown in parenthesis in the comment.

VALUE (pb)	CL%	DOCUMENT ID		TECN	COMMENT
• • • We do not use the following data for averages, fits, limits, etc. • • •					
< 30	95	[1] AGNESE	18	CDMS	Ge
$< 1.32 \times 10^{-2}$	90	[2] BEHNKE	17	PICA	C_4F_{10}
$< 5 \times 10^{-4}$	90	[3] AMOLE	16A	PICO	C_3F_8
$< 2 \times 10^{-6}$	90	[4] KHACHATRY...	16AJ	CMS	8 TeV $pp \to Z+\not{E}_T$; $Z \to \ell\overline{\ell}$
$< 1.2 \times 10^{-3}$	90	AMOLE	15	PICO	C_3F_8
$< 1.43 \times 10^{-3}$	90	CHOI	15	SKAM	H, solar ν ($b\overline{b}$)
$< 1.42 \times 10^{-4}$	90	CHOI	15	SKAM	H, solar ν ($\tau^+\tau^-$)
$< 5 \times 10^{-3}$	90	FELIZARDO	14	SMPL	C_2ClF_5
$< 1.29 \times 10^{-2}$	90	[5] AARTSEN	13	ICCB	H, solar ν ($\tau^+\tau^-$)
$< 3.17 \times 10^{-2}$	90	[6] APRILE	13	X100	Xe
$< 3 \times 10^{-2}$	90	ARCHAMBAU..	12	PICA	F (C_4F_{10})
$< 6 \times 10^{-2}$	90	BEHNKE	12	COUP	CF_3I
< 20	90	DAW	12	DRFT	F (CF_4)
$< 7 \times 10^{-3}$		FELIZARDO	12	SMPL	C_2ClF_5
< 0.15	90	KIM	12	KIMS	CsI
$< 1 \times 10^5$	90	[7] AHLEN	11	DMTP	F (CF_4)
< 0.1	90	[7] BEHNKE	11	COUP	CF_3I
$< 1.5 \times 10^{-2}$	90	[8] TANAKA	11	SKAM	H, solar ν ($b\overline{b}$)
< 0.2	90	ARCHAMBAU..	09	PICA	F
< 4	90	LEBEDENKO	09A	ZEP3	Xe
< 0.6	90	ANGLE	08A	XE10	Xe
<100	90	ALNER	07	ZEP2	Xe
< 1	90	LEE	07A	KIMS	CsI
< 20	90	[9] AKERIB	06	CDMS	^{73}Ge, ^{29}Si
< 2	90	SHIMIZU	06A	CNTR	F (CaF_2)
< 0.5	90	ALNER	05	NAIA	NaI
< 1.5	90	BARNABE-HE..	05	PICA	F (C_4F_{10})
< 1.5	90	GIRARD	05	SMPL	F (C_2ClF_5)
< 35	90	MIUCHI	03	BOLO	LiF
< 30	90	TAKEDA	03	BOLO	NaF

[1] AGNESE 18 give limits for $\sigma^{SD}(p\chi)$ for m(WIMP) between 1.5 and 20 GeV using CDMSlite mode data.
[2] BEHNKE 17 show final Picasso results based on 231.4 kg d exposure at SNOLab for WIMP scatter on C_4F_{10} search via superheated droplet; require $\sigma(\text{SD}) < 1.32 \times 10^{-2}$ pb for m(WIMP) = 20 GeV.
[3] AMOLE 16A require SD WIMP-p scattering $< 5 \times 10^{-4}$ pb for m(WIMP) = 20 GeV; bubbles from C_3F_8 target.
[4] KHACHATRYAN 16AJ require SD WIMP-p $< 2 \times 10^{-6}$ pb for m(WIMP) = 20 GeV from $pp \to Z + \not{E}_T$; $Z \to \ell\overline{\ell}$ signal.
[5] AARTSEN 13 search for neutrinos from the Sun arising from the pair annihilation of X^0 trapped by the sun in data taken between June 2010 and May 2011.
[6] The value has been provided by the authors. APRILE 13 note that the proton limits on Xe are highly sensitive to the theoretical model used. See also APRILE 14A.
[7] Use a direction-sensitive detector.
[8] TANAKA 11 search for neutrinos from the Sun arising from the pair annihilation of X^0 trapped by the Sun. The amount of X^0 depends on the X^0-proton cross section.
[9] See also AKERIB 05.

For m_{X^0} = 100 GeV

For limits from X^0 annihilation in the Sun, the assumed annihilation final state is shown in parenthesis in the comment.

VALUE (pb)	CL%	DOCUMENT ID		TECN	COMMENT
• • • We do not use the following data for averages, fits, limits, etc. • • •					
$< 5 \times 10^{-5}$	90	[1] AMOLE	17	PICO	C_3F_8
$< 3.3 \times 10^{-2}$	90	[2] APRILE	17A	X100	Xe inelastic
$< 2.8 \times 10^{-1}$	90	[3] BATTAT	17	DRFT	CS_2
$< 2 \times 10^{-3}$	90	[4] FU	17	PNDX	Xe
$< 0.553–0.019$	95	[5] AABOUD	16D	ATLS	$pp \to j + \not{E}_T$
$< 1 \times 10^{-5}$	90	[6] AABOUD	16F	ATLS	$pp \to \gamma + \not{E}_T$
$< 1 \times 10^{-4}$	90	[7] AARTSEN	16C	ICCB	solar ν (W^+W^-)
$< 2 \times 10^{-4}$	90	[8] ADRIAN-MAR..	16	ANTR	solar ν (WW, $b\overline{b}$, $\tau\overline{\tau}$)
$< 3 \times 10^{-3}$	90	[9] AKERIB	16A	LUX	Xe
$< 5 \times 10^{-4}$	90	[10] AMOLE	16	PICO	CF_3I
$< 1.5 \times 10^{-3}$	90	AMOLE	15	PICO	C_3F_8
$< 3.19 \times 10^{-3}$	90	CHOI	15	SKAM	H, solar ν ($b\overline{b}$)
$< 2.80 \times 10^{-4}$	90	CHOI	15	SKAM	H, solar ν (W^+W^-)
$< 1.24 \times 10^{-4}$	90	CHOI	15	SKAM	H, solar ν ($\tau^+\tau^-$)
$< 8 \times 10^2$	90	[11] NAKAMURA	15	NAGE	CF_4
$< 1.7 \times 10^{-3}$	90	[12] AVRORIN	14	BAIK	H, solar ν (W^+W^-)
$< 4.5 \times 10^{-2}$	90	[12] AVRORIN	14	BAIK	H, solar ν ($b\overline{b}$)
$< 7.1 \times 10^{-4}$	90	[12] AVRORIN	14	BAIK	H, solar ν ($\tau^+\tau^-$)
$< 6 \times 10^{-3}$	90	FELIZARDO	14	SMPL	C_2ClF_5
$< 2.68 \times 10^{-4}$	90	[13] AARTSEN	13	ICCB	H, solar ν (W^+W^-)
$< 1.47 \times 10^{-2}$	90	[13] AARTSEN	13	ICCB	H, solar ν ($b\overline{b}$)
$< 8.5 \times 10^{-4}$	90	[14] ADRIAN-MAR..	13	ANTR	H, solar ν (W^+W^-)
$< 5.5 \times 10^{-2}$	90	[14] ADRIAN-MAR..	13	ANTR	H, solar ν ($b\overline{b}$)
$< 3.4 \times 10^{-4}$	90	[14] ADRIAN-MAR..	13	ANTR	H, solar ν ($\tau^+\tau^-$)
$< 1.00 \times 10^{-2}$	90	[15] APRILE	13	X100	Xe
$< 7.1 \times 10^{-4}$	90	[16] BOLIEV	13	BAKS	H, solar ν (W^+W^-)
$< 8.4 \times 10^{-3}$	90	[16] BOLIEV	13	BAKS	H, solar ν ($b\overline{b}$)
$< 3.1 \times 10^{-4}$	90	[16] BOLIEV	13	BAKS	H, solar ν ($\tau^+\tau^-$)
$< 7.07 \times 10^{-4}$	90	[17] ABBASI	12	ICCB	H, solar ν (W^+W^-)
$< 4.53 \times 10^{-2}$	90	[17] ABBASI	12	ICCB	H, solar ν ($b\overline{b}$)
$< 7 \times 10^{-2}$	90	ARCHAMBAU..	12	PICA	F (C_4F_{10})
$< 1 \times 10^{-2}$	90	BEHNKE	12	COUP	CF_3I
< 1.8	90	DAW	12	DRFT	F (CF_4)
$< 9 \times 10^{-3}$		FELIZARDO	12	SMPL	C_2ClF_5
$< 2 \times 10^{-2}$	90	KIM	12	KIMS	CsI
$< 2 \times 10^3$	90	[11] AHLEN	11	DMTP	F (CF_4)
$< 7 \times 10^{-2}$	90	BEHNKE	11	COUP	CF_3I
$< 2.7 \times 10^{-4}$	90	[18] TANAKA	11	SKAM	H, solar ν (W^+W^-)
$< 4.5 \times 10^{-3}$	90	[18] TANAKA	11	SKAM	H, solar ν ($b\overline{b}$)
		[19] FELIZARDO	10	SMPL	C_2ClF_3
$< 6 \times 10^3$	90	[11] MIUCHI	10	NAGE	CF_4
< 0.4	90	ARCHAMBAU..	09	PICA	F
< 0.8	90	LEBEDENKO	09A	ZEP3	Xe
< 1.0	90	ANGLE	08A	XE10	Xe
< 15	90	ALNER	07	ZEP2	Xe
< 0.2	90	LEE	07A	KIMS	CsI
$< 1 \times 10^4$	90	[11] MIUCHI	07	NAGE	F (CF_4)
< 5	90	[20] AKERIB	06	CDMS	^{73}Ge, ^{29}Si
< 2	90	SHIMIZU	06A	CNTR	F (CaF_2)
< 0.3	90	ALNER	05	NAIA	NaI
< 2	90	BARNABE-HE..	05	PICA	F (C_4F_{10})
<100	90	BENOIT	05	EDEL	^{73}Ge
< 1.5	90	GIRARD	05	SMPL	F (C_2ClF_5)
< 0.7		[21] GIULIANI	05A	RVUE	
		[22] GIULIANI	04	RVUE	
		[23] GIULIANI	04A	RVUE	
< 35	90	MIUCHI	03	BOLO	LiF
< 40	90	TAKEDA	03	BOLO	NaF

[1] AMOLE 17 require $\sigma(\text{WIMP-}p)^{SD} < 5 \times 10^{-5}$ pb for m(WIMP) = 100 GeV using PICO-60 1167 kg-days exposure at SNOLab.
[2] APRILE 17A require require $\sigma(\text{WIMP-}p)(\text{inelastic})^{SD} < 3.3 \times 10^{-2}$ pb for m(WIMP) = 100 GeV, based on 7640 kg day exposure at LNGS.
[3] BATTAT 17 use directional detection of CS_2 ions to require $\sigma(\text{SD}) < 2.8 \times 10^{-1}$ pb for 100 GeV WIMP with a 55 days exposure at the Boulby Underground Science Facility.
[4] FU 17 from a 33000 kg d exposure at CJPL, PANDAX II derive for m(DM) = 100 GeV, $\sigma(\text{WIMP-p})^{SD} < 2 \times 10^{-3}$ pb and $\sigma(\text{WIMP-n})^{SD} < 6 \times 10^{-5}$ pb.
[5] AABOUD 16D use ATLAS 13 TeV 3.2 fb^{-1} of data to search for monojet plus missing E_T; agree with SM rates; present limits on large extra dimensions, compressed SUSY spectra and wimp pair production.
[6] AABOUD 16F search for monophoton plus missing E_T events at ATLAS with 13 Tev and 3.2 fb^{-1}; signal agrees with SM background; place limits on SD WIMP-proton scattering vs. mediator mass and large extra dimension models.
[7] AARTSEN 16C search for high energy νs from WIMP annihilation in solar core; limits set on SD WIMP-p scattering (Fig. 8).
[8] ADRIAN-MARTINEZ 16 search for WIMP annihilation into νs from solar core; exclude SD cross section $<$ few 10^{-4} depending on m(WIMP).
[9] AKERIB 16A using 2013 data exclude SD WIMP-proton scattering $> 3 \times 10^{-3}$ pb for m(WIMP) = 100 GeV.
[10] AMOLE 16 use bubble technique on CF_3I target to exclude SD WIMP-p scattering $> 5 \times 10^{-4}$ pb for m(WIMP) = 100 GeV.
[11] Use a direction-sensitive detector.
[12] AVRORIN 14 search for neutrinos from the Sun arising from the pair annihilation of X^0 trapped by the Sun in data taken between 1998 and 2003. See their Table 1 for limits assuming annihilation into neutrino pairs.
[13] AARTSEN 13 search for neutrinos from the Sun arising from the pair annihilation of X^0 trapped by the sun in data taken between June 2010 and May 2011.
[14] ADRIAN-MARTINEZ 13 search for neutrinos from the Sun arising from the pair annihilation of X^0 trapped by the sun in data taken between Jan. 2007 and Dec. 2008.
[15] The value has been provided by the authors. APRILE 13 note that the proton limits on Xe are highly sensitive to the theoretical model used. See also APRILE 14A.
[16] BOLIEV 13 search for neutrinos from the Sun arising from the pair annihilation of X^0 trapped by the sun in data taken from 1978 to 2009. See also SUVOROVA 13 for an older analysis of the same data.

[17] ABBASI 12 search for neutrinos from the Sun arising from the pair annihilation of X^0 trapped by the Sun. The amount of X^0 depends on the X^0-proton cross section.
[18] TANAKA 11 search for neutrinos from the Sun arising from the pair annihilation of X^0 trapped by the Sun. The amount of X^0 depends on the X^0-proton cross section.
[19] See their Fig. 3 for limits on spin-dependent proton couplings for X^0 mass of 50 GeV.
[20] See also AKERIB 05.
[21] GIULIANI 05A analyze available data and give combined limits.
[22] GIULIANI 04 reanalyze COLLAR 00 data and give limits for spin-dependent X^0-proton coupling.
[23] GIULIANI 04A give limits for spin-dependent X^0-proton couplings from existing data.

For m_{X^0} = 1 TeV

For limits from X^0 annihilation in the Sun, the assumed annihilation final state is shown in parenthesis in the comment.

VALUE (pb)	CL%	DOCUMENT ID		TECN	COMMENT
• • • We do not use the following data for averages, fits, limits, etc. • • •					
$< 2.05 \times 10^{-5}$	90	[1] AARTSEN	17A	ICCB	ν, sun
		[2] ADRIAN-MAR..	16B	ANTR	solar μ from WIMP annih.
$< 1 \times 10^{-2}$	90	AMOLE	15	PICO	C_3F_8
$< 1.5 \times 10^{3}$	90	NAKAMURA	15	NAGE	CF_4
$< 2.7 \times 10^{-3}$	90	[3] AVRORIN	14	BAIK	H, solar ν (W^+W^-)
$< 6.9 \times 10^{-2}$	90	[3] AVRORIN	14	BAIK	H, solar ν ($b\overline{b}$)
$< 8.4 \times 10^{-4}$	90	[3] AVRORIN	14	BAIK	H, solar ν ($\tau^+\tau^-$)
$< 4.48 \times 10^{-4}$	90	[4] AARTSEN	13	ICCB	H, solar ν (W^+W^-)
$< 1.00 \times 10^{-2}$	90	[4] AARTSEN	13	ICCB	H, solar ν ($b\overline{b}$)
$< 8.9 \times 10^{-4}$	90	[5] ADRIAN-MAR..	13	ANTR	H, solar ν (W^+W^-)
$< 2.0 \times 10^{-2}$	90	[5] ADRIAN-MAR..	13	ANTR	H, solar ν ($b\overline{b}$)
$< 2.3 \times 10^{-4}$	90	[5] ADRIAN-MAR..	13	ANTR	H, solar ν ($\tau^+\tau^-$)
$< 7.57 \times 10^{-2}$	90	[6] APRILE	13	X100	Xe
$< 5.4 \times 10^{-3}$	90	[7] BOLIEV	13	BAKS	H, solar ν (W^+W^-)
$< 4.2 \times 10^{-2}$	90	[7] BOLIEV	13	BAKS	H, solar ν ($b\overline{b}$)
$< 1.5 \times 10^{-3}$	90	[7] BOLIEV	13	BAKS	H, solar ν ($\tau^+\tau^-$)
$< 2.50 \times 10^{-4}$	90	[8] ABBASI	12	ICCB	H, solar ν (W^+W^-)
$< 7.86 \times 10^{-3}$	90	[8] ABBASI	12	ICCB	H, solar ν ($b\overline{b}$)
$< 8 \times 10^{-2}$	90	BEHNKE	12	COUP	CF_3I
< 8	90	DAW	12	DRFT	F (CF_4)
$< 6 \times 10^{-2}$		FELIZARDO	12	SMPL	C_2ClF_5
$< 8 \times 10^{-2}$	90	KIM	12	KIMS	CsI
$< 8 \times 10^{3}$	90	[9] AHLEN	11	DMTP	F (CF_4)
< 0.4	90	BEHNKE	11	COUP	CF_3I
$< 2 \times 10^{-3}$	90	[10] TANAKA	11	SKAM	H, solar ν ($b\overline{b}$)
$< 2 \times 10^{-2}$	90	[10] TANAKA	11	SKAM	H, solar ν (W^+W^-)
$< 1 \times 10^{-3}$	90	[11] ABBASI	10	ICCB	KK dark matter
$< 2 \times 10^{4}$	90	[9] MIUCHI	10	NAGE	CF_4
$< 8.7 \times 10^{-4}$	90	ABBASI	09B	ICCB	H, solar ν (W^+W^-)
$< 2.2 \times 10^{-2}$	90	ABBASI	09B	ICCB	H, solar ν ($b\overline{b}$)
< 3	90	ARCHAMBAU..	09	PICA	F
< 6	90	LEBEDENKO	09A	ZEP3	Xe
< 9	90	ANGLE	08A	XE10	Xe
<100	90	ALNER	07	ZEP2	Xe
< 0.8	90	LEE	07A	KIMS	CsI
$< 4 \times 10^{4}$	90	[9] MIUCHI	07	NAGE	F (CF_4)
< 30	90	[12] AKERIB	06	CDMS	^{73}Ge, ^{29}Si
< 1.5	90	ALNER	05	NAIA	NaI
< 15	90	BARNABE-HE..	05	PICA	F (C_4F_{10})
<600	90	BENOIT	05	EDEL	^{73}Ge
< 10	90	GIRARD	05	SMPL	F (C_2ClF_5)
<260	90	MIUCHI	03	BOLO	LiF
<150	90	TAKEDA	03	BOLO	NaF

[1] AARTSEN 17A search for neutrinos from solar WIMP annihilation into $\tau^+\tau^-$ in 532 days of live time.
[2] ADRIAN-MARTINEZ 16B search for secluded DM via WIMP annihilation in solar core into light mediator which later decays to μ or νs; limits presented in Figures 3 and 4.
[3] AVRORIN 14 search for neutrinos from the Sun arising from the pair annihilation of X^0 trapped by the Sun in data taken between 1998 and 2003. See their Table 1 for limits assuming annihilation into neutrino pairs.
[4] AARTSEN 13 search for neutrinos from the Sun arising from the pair annihilation of X^0 trapped by the sun in data taken between June 2010 and May 2011.
[5] ADRIAN-MARTINEZ 13 search for neutrinos from the Sun arising from the pair annihilation of X^0 trapped by the sun in data taken between Jan. 2007 and Dec. 2008.
[6] The value has been provided by the authors. APRILE 13 note that the proton limits on Xe are highly sensitive to the theoretical model used. See also APRILE 14A.
[7] BOLIEV 13 search for neutrinos from the Sun arising from the pair annihilation of X^0 trapped by the sun in data taken from 1978 to 2009. See also SUVOROVA 13 for an older analysis of the same data.
[8] ABBASI 12 search for neutrinos from the Sun arising from the pair annihilation of X^0 trapped by the Sun. The amount of X^0 depends on the X^0-proton cross section.
[9] Use a direction-sensitive detector.
[10] TANAKA 11 search for neutrinos from the Sun arising from the pair annihilation of X^0 trapped by the Sun. The amount of X^0 depends on the X^0-proton cross section.
[11] ABBASI 10 search for ν_μ from annihilations of Kaluza-Klein photon dark matter in the Sun.
[12] See also AKERIB 05.

Limits for Spin-Dependent Cross Section of Dark Matter Particle (X^0) on Neutron

For m_{X^0} = 20 GeV

VALUE (pb)	CL%	DOCUMENT ID		TECN	COMMENT
• • • We do not use the following data for averages, fits, limits, etc. • • •					
< 1.5	95	[1] AGNESE	18	CDMS	Ge
< 0.09	90	FELIZARDO	14	SMPL	C_2ClF_5
< 8	90	[2] UCHIDA	14	XMAS	^{129}Xe, inelastic
$< 1.13 \times 10^{-3}$	90	[3] APRILE	13	X100	Xe
< 0.02	90	AKIMOV	12	ZEP3	Xe
		[4] AHMED	11B	CDM2	Ge, low threshold
< 0.06	90	AHMED	09	CDM2	Ge
< 0.04	90	LEBEDENKO	09A	ZEP3	Xe
< 50		[5] LIN	09	TEXO	Ge
$< 6 \times 10^{-3}$	90	ANGLE	08A	XE10	Xe
< 0.5	90	ALNER	07	ZEP2	Xe
< 25	90	LEE	07A	KIMS	CsI
< 0.3	90	[6] AKERIB	06	CDMS	^{73}Ge, ^{29}Si
< 30	90	SHIMIZU	06A	CNTR	F (CaF_2)
< 60	90	ALNER	05	NAIA	NaI
< 20	90	BARNABE-HE..	05	PICA	F (C_4F_{10})
< 10	90	BENOIT	05	EDEL	^{73}Ge
< 4	90	KLAPDOR-K...	05	HDMS	^{73}Ge (enriched)
<600	90	TAKEDA	03	BOLO	NaF

[1] AGNESE 18 give limits for $\sigma^{SD}(n\chi)$ for m(WIMP) between 1.5 and 20 GeV using CDMSlite mode data.
[2] Derived limit from search for inelastic scattering $X^0 + {}^{129}\text{Xe} \rightarrow X^0 + {}^{129}\text{Xe}^*(39.58$ keV).
[3] The value has been provided by the authors. See also APRILE 14A.
[4] AHMED 11B give limits on spin-dependent X^0-neutron cross section for m_{X^0} = 4–12 GeV in the range 10^{-3}–10 pb. See their Fig. 3.
[5] See their Fig. 6(b) for cross section limits for m_{X^0} extending down to 2 GeV.
[6] See also AKERIB 05.

For m_{X^0} = 100 GeV

VALUE (pb)	CL%	DOCUMENT ID		TECN	COMMENT
• • • We do not use the following data for averages, fits, limits, etc. • • •					
$< 2.5 \times 10^{-5}$	90	[1] AKERIB	17A	LUX	Xe
< 0.1	90	FELIZARDO	14	SMPL	C_2ClF_5
< 0.05	90	[2] UCHIDA	14	XMAS	^{129}Xe, inelastic
$< 4.68 \times 10^{-4}$	90	[3] APRILE	13	X100	Xe
< 0.01	90	AKIMOV	12	ZEP3	Xe
		[4] FELIZARDO	10	SMPL	C_2ClF_3
< 0.02	90	AHMED	09	CDM2	Ge
< 0.01	90	LEBEDENKO	09A	ZEP3	Xe
<100	90	LIN	09	TEXO	Ge
< 0.01	90	ANGLE	08A	XE10	Xe
< 0.05	90	[5] BEDNYAKOV	08	RVUE	Ge
< 0.08	90	ALNER	07	ZEP2	Xe
< 6	90	LEE	07A	KIMS	CsI
< 0.07	90	[6] AKERIB	06	CDMS	^{73}Ge, ^{29}Si
< 30	90	SHIMIZU	06A	CNTR	F (CaF_2)
< 10	90	ALNER	05	NAIA	NaI
< 30	90	BARNABE-HE..	05	PICA	F (C_4F_{10})
< 0.7	90	BENOIT	05	EDEL	^{73}Ge
< 0.2		[7] GIULIANI	05A	RVUE	
< 1.5	90	KLAPDOR-K...	05	HDMS	^{73}Ge (enriched)
		[8] GIULIANI	04	RVUE	
		[9] GIULIANI	04A	RVUE	
		[10] MIUCHI	03	BOLO	LiF
<800	90	TAKEDA	03	BOLO	NaF

[1] AKERIB 17A require $\sigma(\chi p)_{SD} < 7 \times 10^{-4}$ pb for m(χ) = 100 GeV using 129.5 kg yr exposure.
[2] Derived limit from search for inelastic scattering $X^0 + {}^{129}\text{Xe}^* \rightarrow X^0 + {}^{129}\text{Xe}^*(39.58$ keV).
[3] The value has been provided by the authors. See also APRILE 14A.
[4] See their Fig. 3 for limits on spin-dependent neutron couplings for X^0 mass of 50 GeV.
[5] BEDNYAKOV 08 reanalyze KLAPDOR-KLEINGROTHAUS 05 and BAUDIS 01 data.
[6] See also AKERIB 05.
[7] GIULIANI 05A analyze available data and give combined limits.
[8] GIULIANI 04 reanalyze COLLAR 00 data and give limits for spin-dependent X^0-neutron coupling.
[9] GIULIANI 04A give limits for spin-dependent X^0-neutron couplings from existing data.
[10] MIUCHI 03 give model-independent limit for spin-dependent X^0-proton and neutron cross sections. See their Fig. 5.

For m_{X^0} = 1 TeV

VALUE (pb)	CL%	DOCUMENT ID		TECN	COMMENT
• • • We do not use the following data for averages, fits, limits, etc. • • •					
< 0.07	90	FELIZARDO	14	SMPL	C_2ClF_5
< 0.2	90	[1] UCHIDA	14	XMAS	^{129}Xe, inelastic
$< 3.64 \times 10^{-3}$	90	[2] APRILE	13	X100	Xe
< 0.08	90	AKIMOV	12	ZEP3	Xe
< 0.2	90	AHMED	09	CDM2	Ge
< 0.1	90	LEBEDENKO	09A	ZEP3	Xe

< 0.1		90	ANGLE	08A	XE10	Xe
< 0.25		90	[3] BEDNYAKOV	08	RVUE	Ge
< 0.6		90	ALNER	07	ZEP2	Xe
< 30		90	LEE	07A	KIMS	CsI
< 0.5		90	[4] AKERIB	06	CDMS	^{73}Ge, ^{29}Si
< 40		90	ALNER	05	NAIA	NaI
<200		90	BARNABE-HE...	05	PICA	F (C_4F_{10})
< 4		90	BENOIT	05	EDEL	^{73}Ge
< 10		90	KLAPDOR-K...	05	HDMS	^{73}Ge (enriched)
< 4	$\times 10^3$	90	TAKEDA	03	BOLO	NaF

[1] Derived limit from search for inelastic scattering $X^0 + {}^{129}Xe^* \rightarrow X^0 + {}^{129}Xe^*$(39.58 keV).
[2] The value has been provided by the authors. See also APRILE 14A.
[3] BEDNYAKOV 08 reanalyze KLAPDOR-KLEINGROTHAUS 05 and BAUDIS 01 data.
[4] See also AKERIB 05.

Cross-Section Limits for Dark Matter Particles (X^0) on Nuclei

For m_{X^0} = 20 GeV

VALUE (nb)		CL%	DOCUMENT ID		TECN	COMMENT
• • • We do not use the following data for averages, fits, limits, etc. • • •						
< 0.03		90	[1] UCHIDA	14	XMAS	^{129}Xe, inelastic
< 0.08		90	[2] ANGLOHER	02	CRES	Al
			[3] BENOIT	00	EDEL	Ge
< 0.04		95	[4] KLIMENKO	98	CNTR	^{73}Ge, inel.
< 0.8			ALESSAND...	96	CNTR	O
< 6			ALESSAND...	96	CNTR	Te
< 0.02		90	[5] BELLI	96	CNTR	^{129}Xe, inel.
			[6] BELLI	96C	CNTR	^{129}Xe
< 4	$\times 10^{-3}$	90	[7] BERNABEI	96	CNTR	Na
< 0.3		90	[7] BERNABEI	96	CNTR	I
< 0.2		95	[8] SARSA	96	CNTR	Na
< 0.015		90	[9] SMITH	96	CNTR	Na
< 0.05		95	[10] GARCIA	95	CNTR	Natural Ge
< 0.1		95	QUENBY	95	CNTR	Na
<90		90	[11] SNOWDEN-...	95	MICA	^{16}O
< 4	$\times 10^3$	90	[11] SNOWDEN-...	95	MICA	^{39}K
< 0.7		90	BACCI	92	CNTR	Na
< 0.12		90	[12] REUSSER	91	CNTR	Natural Ge
< 0.06		95	CALDWELL	88	CNTR	Natural Ge

[1] UCHIDA 14 limit is for inelastic scattering $X^0 + {}^{129}Xe^* \rightarrow X^0 + {}^{129}Xe^*$ (39.58 keV).
[2] ANGLOHER 02 limit is for spin-dependent WIMP-Aluminum cross section.
[3] BENOIT 00 find four event categories in Ge detectors and suggest that low-energy surface nuclear recoils can explain anomalous events reported by UKDMC and Saclay NaI experiments.
[4] KLIMENKO 98 limit is for inelastic scattering $X^0\,{}^{73}Ge \rightarrow X^0\,{}^{73}Ge^*$ (13.26 keV).
[5] BELLI 96 limit for inelastic scattering $X^0\,{}^{129}Xe \rightarrow X^0\,{}^{129}Xe^*$(39.58 keV).
[6] BELLI 96C use background subtraction and obtain $\sigma < 150$ pb (< 1.5 fb) (90% CL) for spin-dependent (independent) X^0-proton cross section. The confidence level is from R. Bernabei, private communication, May 20, 1999.
[7] BERNABEI 96 use pulse shape discrimination to enhance the possible signal. The limit here is from R. Bernabei, private communication, September 19, 1997.
[8] SARSA 96 search for annual modulation of WIMP signal. See SARSA 97 for details of the analysis. The limit here is from M.L. Sarsa, private communication, May 26, 1997.
[9] SMITH 96 use pulse shape discrimination to enhance the possible signal. A dark matter density of 0.4 GeV cm^{-3} is assumed.
[10] GARCIA 95 limit is from the event rate. A weaker limit is obtained from searches for diurnal and annual modulation.
[11] SNOWDEN-IFFT 95 look for recoil tracks in an ancient mica crystal. Similar limits are also given for ^{27}Al and ^{28}Si. See COLLAR 96 and SNOWDEN-IFFT 96 for discussion on potential backgrounds.
[12] REUSSER 91 limit here is changed from published (0.04) after reanalysis by authors. J.L. Vuilleumier, private communication, March 29, 1996.

For m_{X^0} = 100 GeV

VALUE (nb)		CL%	DOCUMENT ID		TECN	COMMENT
• • • We do not use the following data for averages, fits, limits, etc. • • •						
< 3	$\times 10^{-3}$	90	[1] UCHIDA	14	XMAS	^{129}Xe, inelastic
< 0.3		90	[2] ANGLOHER	02	CRES	Al
			[3] BELLI	02	RVUE	
			[4] BERNABEI	02C	DAMA	
			[5] GREEN	02	RVUE	
			[6] ULLIO	01	RVUE	
			[7] BENOIT	00	EDEL	Ge
< 4	$\times 10^{-3}$	90	[8] BERNABEI	00D		^{129}Xe, inel.
			[9] AMBROSIO	99	MCRO	
			[10] BRHLIK	99	RVUE	
< 8	$\times 10^{-3}$	95	[11] KLIMENKO	98	CNTR	^{73}Ge, inel.
< 0.08		95	[12] KLIMENKO	98	CNTR	^{73}Ge, inel.
< 4			ALESSAND...	96	CNTR	O
<25			ALESSAND...	96	CNTR	Te
< 6	$\times 10^{-3}$	90	[13] BELLI	96	CNTR	^{129}Xe, inel.
			[14] BELLI	96C	CNTR	^{129}Xe
< 1	$\times 10^{-3}$	90	[15] BERNABEI	96	CNTR	Na
< 0.3		90	[15] BERNABEI	96	CNTR	I
< 0.7		95	[16] SARSA	96	CNTR	Na
< 0.03		90	[17] SMITH	96	CNTR	Na
< 0.8		90	[17] SMITH	96	CNTR	I
< 0.35		95	[18] GARCIA	95	CNTR	Natural Ge
< 0.6		95	QUENBY	95	CNTR	Na
< 3		95	QUENBY	95	CNTR	I
< 1.5	$\times 10^2$	90	[19] SNOWDEN-...	95	MICA	^{16}O
< 4	$\times 10^2$	90	[19] SNOWDEN-...	95	MICA	^{39}K
< 0.08		90	[20] BECK	94	CNTR	^{76}Ge
< 2.5		90	BACCI	92	CNTR	Na
< 3		90	BACCI	92	CNTR	I
< 0.9		90	[21] REUSSER	91	CNTR	Natural Ge
< 0.7		95	CALDWELL	88	CNTR	Natural Ge

[1] UCHIDA 14 limit is for inelastic scattering $X^0 + {}^{129}Xe^* \rightarrow X^0 + {}^{129}Xe^*$(39.58 keV).
[2] ANGLOHER 02 limit is for spin-dependent WIMP-Aluminum cross section.
[3] BELLI 02 discuss dependence of the extracted WIMP cross section on the assumptions of the galactic halo structure.
[4] BERNABEI 02C analyze the DAMA data in the scenario in which X^0 scatters into a slightly heavier state as discussed by SMITH 01.
[5] GREEN 02 discusses dependence of extracted WIMP cross section limits on the assumptions of the galactic halo structure.
[6] ULLIO 01 disfavor the possibility that the BERNABEI 99 signal is due to spin-dependent WIMP coupling.
[7] BENOIT 00 find four event categories in Ge detectors and suggest that low-energy surface nuclear recoils can explain anomalous events reported by UKDMC and Saclay NaI experiments.
[8] BERNABEI 00D limit is for inelastic scattering $X^0{}^{129}Xe \rightarrow X^0{}^{129}Xe$ (39.58 keV).
[9] AMBROSIO 99 search for upgoing muon events induced by neutrinos originating from WIMP annihilations in the Sun and Earth.
[10] BRHLIK 99 discuss the effect of astrophysical uncertainties on the WIMP interpretation of the BERNABEI 99 signal.
[11] KLIMENKO 98 limit is for inelastic scattering $X^0\,{}^{73}Ge \rightarrow X^0\,{}^{73}Ge^*$ (13.26 keV).
[12] KLIMENKO 98 limit is for inelastic scattering $X^0\,{}^{73}Ge \rightarrow X^0\,{}^{73}Ge^*$ (66.73 keV).
[13] BELLI 96 limit for inelastic scattering $X^0\,{}^{129}Xe \rightarrow X^0\,{}^{129}Xe^*$(39.58 keV).
[14] BELLI 96C use background subtraction and obtain $\sigma < 0.35$ pb (< 0.15 fb) (90% CL) for spin-dependent (independent) X^0-proton cross section. The confidence level is from R. Bernabei, private communication, May 20, 1999.
[15] BERNABEI 96 use pulse shape discrimination to enhance the possible signal. The limit here is from R. Bernabei, private communication, September 19, 1997.
[16] SARSA 96 search for annual modulation of WIMP signal. See SARSA 97 for details of the analysis. The limit here is from M.L. Sarsa, private communication, May 26, 1997.
[17] SMITH 96 use pulse shape discrimination to enhance the possible signal. A dark matter density of 0.4 GeV cm^{-3} is assumed.
[18] GARCIA 95 limit is from the event rate. A weaker limit is obtained from searches for diurnal and annual modulation.
[19] SNOWDEN-IFFT 95 look for recoil tracks in an ancient mica crystal. Similar limits are also given for ^{27}Al and ^{28}Si. See COLLAR 96 and SNOWDEN-IFFT 96 for discussion on potential backgrounds.
[20] BECK 94 uses enriched ^{76}Ge (86% purity).
[21] REUSSER 91 limit here is changed from published (0.3) after reanalysis by authors. J.L. Vuilleumier, private communication, March 29, 1996.

For m_{X^0} = 1 TeV

VALUE (nb)		CL%	DOCUMENT ID		TECN	COMMENT
• • • We do not use the following data for averages, fits, limits, etc. • • •						
< 0.03		90	[1] UCHIDA	14	XMAS	^{129}Xe, inelastic
< 3		90	[2] ANGLOHER	02	CRES	Al
			[3] BENOIT	00	EDEL	Ge
			[4] BERNABEI	99D	CNTR	SIMP
			[5] DERBIN	99	CNTR	SIMP
< 0.06		95	[6] KLIMENKO	98	CNTR	^{73}Ge, inel.
< 0.4		95	[7] KLIMENKO	98	CNTR	^{73}Ge, inel.
< 40			ALESSAND...	96	CNTR	O
<700			ALESSAND...	96	CNTR	Te
< 0.05		90	[8] BELLI	96	CNTR	^{129}Xe, inel.
< 1.5		90	[9] BELLI	96	CNTR	^{129}Xe, inel.
			[10] BELLI	96C	CNTR	^{129}Xe
< 0.01		90	[11] BERNABEI	96	CNTR	Na
< 9		90	[11] BERNABEI	96	CNTR	I
< 7		95	[12] SARSA	96	CNTR	Na
< 0.3		90	[13] SMITH	96	CNTR	Na
< 6		90	[13] SMITH	96	CNTR	I
< 6		95	[14] GARCIA	95	CNTR	Natural Ge
< 8		95	QUENBY	95	CNTR	Na
< 50		95	QUENBY	95	CNTR	I
<700		90	[15] SNOWDEN-...	95	MICA	^{16}O
< 1	$\times 10^3$	90	[15] SNOWDEN-...	95	MICA	^{39}K
< 0.8		90	[16] BECK	94	CNTR	^{76}Ge
< 30		90	BACCI	92	CNTR	Na
< 30		90	BACCI	92	CNTR	I
< 15		90	[17] REUSSER	91	CNTR	Natural Ge
< 6		95	CALDWELL	88	CNTR	Natural Ge

[1] UCHIDA 14 limit is for inelastic scattering $X^0 + {}^{129}Xe^* \rightarrow X^0 + {}^{129}Xe^*$ (39.58 keV).
[2] ANGLOHER 02 limit is for spin-dependent WIMP-Aluminum cross section.
[3] BENOIT 00 find four event categories in Ge detectors and suggest that low-energy surface nuclear recoils can explain anomalous events reported by UKDMC and Saclay NaI experiments.

[4] BERNABEI 99D search for SIMPs (Strongly Interacting Massive Particles) in the mass range 10^3–10^{16} GeV. See their Fig. 3 for cross-section limits.
[5] DERBIN 99 search for SIMPs (Strongly Interacting Massive Particles) in the mass range 10^2–10^{14} GeV. See their Fig. 3 for cross-section limits.
[6] KLIMENKO 98 limit is for inelastic scattering $X^0\,{}^{73}\mathrm{Ge} \rightarrow X^0\,{}^{73}\mathrm{Ge}^*$ (13.26 keV).
[7] KLIMENKO 98 limit is for inelastic scattering $X^0\,{}^{73}\mathrm{Ge} \rightarrow X^0\,{}^{73}\mathrm{Ge}^*$ (66.73 keV).
[8] BELLI 96 limit for inelastic scattering $X^0\,{}^{129}\mathrm{Xe} \rightarrow X^0\,{}^{129}\mathrm{Xe}^*$(39.58 keV).
[9] BELLI 96 limit for inelastic scattering $X^0\,{}^{129}\mathrm{Xe} \rightarrow X^0\,{}^{129}\mathrm{Xe}^*$(236.14 keV).
[10] BELLI 96C use background subtraction and obtain $\sigma < 0.7$ pb (< 0.7 fb) (90% CL) for spin-dependent (independent) X^0-proton cross section. The confidence level is from R. Bernabei, private communication, May 20, 1999.
[11] BERNABEI 96 use pulse shape discrimination to enhance the possible signal. The limit here is from R. Bernabei, private communication, September 19, 1997.
[12] SARSA 96 search for annual modulation of WIMP signal. See SARSA 97 for details of the analysis. The limit here is from M.L. Sarsa, private communication, May 26, 1997.
[13] SMITH 96 use pulse shape discrimination to enhance the possible signal. A dark matter density of 0.4 GeV cm^{-3} is assumed.
[14] GARCIA 95 limit is from the event rate. A weaker limit is obtained from searches for diurnal and annual modulation.
[15] SNOWDEN-IFFT 95 look for recoil tracks in an ancient mica crystal. Similar limits are also given for ^{27}Al and ^{28}Si. See COLLAR 96 and SNOWDEN-IFFT 96 for discussion on potential backgrounds.
[16] BECK 94 uses enriched ^{76}Ge (86% purity).
[17] REUSSER 91 limit here is changed from published (5) after reanalysis by authors. J.L. Vuilleumier, private communication, March 29, 1996.

Miscellaneous Results from Underground Dark Matter Searches

VALUE	CL%	DOCUMENT ID		TECN	COMMENT
• • • We do not use the following data for averages, fits, limits, etc. • • •					
$<1\times10^{-12}$	90	[1] AGUILAR-AR...17		DMIC	γ' on Si
		[2] APRILE	17	X100	Xe
		[3] APRILE	17D	X100	Xe
		[4] APRILE	17H	X100	keV bosonic DM search
		[5] APRILE	17K	X100	$\chi N \rightarrow \chi^* \rightarrow \chi\gamma$
$<4\times10^{-3}$	90	[6] ANGLOHER	16A	CRES	$CaWO_4$
		[7] APRILE	15	X100	Event rate modulation
		[8] APRILE	15A	X100	Electron scattering

[1] AGUILAR-AREVALO 17 search for hidden photon DM scatter on Si target CCD; limit kinetic mixing $\kappa < 1\times10^{-12}$ for m = 10 eV.
[2] APRILE 17 search for WIMP-e annual modulation signal for recoil energy in the 2.0–5.8 keV interval using 4 years data with Xe. No significant effect seen.
[3] APRILE 17D set limits on 14 WIMP-nucleon different interaction operators. No deviations found using 225 live days in the 6.6–240 keV recoil energy range.
[4] APRILE 17H search for keV bosonic DM via $e\chi \rightarrow e$, looking for electronic recoils with 224.6 live days of data and 34 kg of LXe. Limits set on $\chi e e$ coupling for m(χ) = 8–125 keV.
[5] APRILE 17K search for magnetic inelastic DM via $\chi N \rightarrow \chi^* \rightarrow \chi\gamma$. Limits set in DM magnetic moment vs. mass splitting plane for two DM masses corresponding to the DAMA/LIBRA best fit values.
[6] ANGLOHER 16A require q^2 dependent scattering $< 8\times10^{-3}$ pb for asymmetric DM m(WIMP) = 3 GeV on $CaWO_4$ target. It uses a local dark matter density of 0.38 GeV/cm^3.
[7] APRILE 15 search for periodic variation of electronic recoil event rate in the data between Feb. 2011 and Mar. 2012. No significant modulation is found for periods up to 500 days.
[8] APRILE 15A search for X^0 scattering off electrons. See their Fig. 4 for limits on cross section through axial-vector coupling for m_{X^0} between 0.6 GeV and 1 TeV. For m_{X^0} = 2 GeV, $\sigma < 60$ pb (90%CL) is obtained.

X^0 Annihilation Cross Section

Limits are on σv for X^0 pair annihilation at threshold.

VALUE (cm^{3}s^{-1})	CL%	DOCUMENT ID		TECN	COMMENT
• • • We do not use the following data for averages, fits, limits, etc. • • •					
$<1.2\times10^{-23}$	95	[1] AARTSEN	17C	ICCB	$\chi\chi \rightarrow$ neutrinos
$<5\times10^{-25}$	90	[2] ALBERT	17A	ANTR	ν, Milky Way
$<1.32\times10^{-25}$	95	[3] ARCHAMBAU..17		VRTS	γ dwarf galaxies
$<7\times10^{-21}$	90	[4] AVRORIN	17	BAIK	cosmic ν
$<1\times10^{-28}$		[5] BOUDAUD	17		MeV DM to e^+e^-
		[6] AARTSEN	16D	ICCB	ν, galactic center
$<6\times10^{-26}$	95	[7] ABDALLAH	16	HESS	Central Galactic Halo
$<1\times10^{-27}$	95	[8] ABDALLAH	16A	HESS	WIMP+WIMP $\rightarrow \gamma\gamma$; galactic center
$<3\times10^{-26}$	95	[9] AHNEN	16	MGFL	Satellite galaxy, m(WIMP)=100 GeV
$<1.9\times10^{-21}$	90	[10] AVRORIN	16	BAIK	νs from galactic center
$<3\times10^{-26}$	95	[11] CAPUTO	16	FLAT	small Magellanic cloud
$<1\times10^{-25}$	95	[12] FORNASA	16	FLAT	Fermi-LAT γ-ray anisotropy
$<5\times10^{-27}$		[13] LEITE	16		WIMP, radio
$<2\times10^{-26}$	95	[14] LI	16	FLAT	dwarf galaxies
$<1\times10^{-25}$	95	[15] LI	16A	FLAT	Fermi-LAT; M31
$<1\times10^{-26}$		[16] LIANG	16	FLAT	Fermi-LAT, gamma line
$<1\times10^{-25}$	95	[17] LU	16	FLAT	Fermi-LAT and AMS-02
$<1\times10^{-23}$	95	[18] SHIRASAKI	16	FLAT	extra galactic
		[19] AARTSEN	15C	ICCB	ν, Galactic halo
		[20] AARTSEN	15E	ICCB	ν, Galactic center
		[21] ABRAMOWSKI	15	HESS	Galactic center
		[22] ACKERMANN	15	FLAT	monochromatic γ
		[23] ACKERMANN	15A	FLAT	isotropic γ background
		[24] ACKERMANN	15B	FLAT	Satellite galaxy
		[25] ADRIAN-MAR..15		ANTR	ν, Galactic center
$<2.90\times10^{-26}$	95	[26,27] ACKERMANN	14	FLAT	Satellite galaxy, m = 10 GeV
$<1.84\times10^{-25}$	95	[26,28] ACKERMANN	14	FLAT	Satellite galaxy, m = 100 GeV
$<1.75\times10^{-24}$	95	[26,28] ACKERMANN	14	FLAT	Satellite galaxy, m = 1 TeV
$<4.52\times10^{-24}$	95	[29] ALEKSIC	14	MGIC	Segue 1, m = 1.35 TeV
		[30] AARTSEN	13C	ICCB	Galaxies
		[31] ABRAMOWSKI	13	HESS	Central Galactic Halo
		[32] ACKERMANN	13A	FLAT	Galaxy
		[33] ABRAMOWSKI	12	HESS	Fornax Cluster
		[34] ACKERMANN	12	FLAT	Galaxy
		[35] ACKERMANN	12	FLAT	Galaxy
		[36] ALIU	12	VRTS	Segue 1
$<1\times10^{-22}$	90	[37] ABBASI	11C	ICCB	Galactic halo, m=1 TeV
$<3\times10^{-25}$	95	[38] ABRAMOWSKI	11	HESS	Near Galactic center, m=1 TeV
$<1\times10^{-26}$	95	[39] ACKERMANN	11	FLAT	Satellite galaxy, m=10 GeV
$<1\times10^{-25}$	95	[39] ACKERMANN	11	FLAT	Satellite galaxy, m=100 GeV
$<1\times10^{-24}$	95	[39] ACKERMANN	11	FLAT	Satellite galaxy, m=1 TeV

[1] AARTSEN 17C use 1005 days of IceCube data to search for $\chi\chi \rightarrow$ neutrinos via various annihilation channels. Limits set.
[2] ALBERT 17A maximum sensitivity to thermally averaged annihilation cross-section is for m(WIMP) = 10^5 GeV, where they require via $\tau\tau$ channel, $\langle\sigma\cdot v\rangle < 5\times10^{-25}$ cm^3/s assuming NFW halo profile, $\langle\sigma\cdot v\rangle < 2\times10^{-24}$ cm^3/s assuming McMillan profile, $\langle\sigma\cdot v\rangle < 1.2\times10^{-23}$ cm^3/s assuming Burkert profile.
[3] ARCHAMBAULT 17 set limits for WIMP mass between 100 GeV and 1 TeV on $\langle\sigma\cdot v\rangle$ for W^+W^-, ZZ, $b\overline{b}$, $s\overline{s}$, $u\overline{u}$, $d\overline{d}$, $t\overline{t}$, e^+e^-, gg, $c\overline{c}$, hh, $\gamma\gamma$, $\mu^+\mu^-$,$\tau^+\tau^-$ annihilation channels.
[4] AVRORIN 17 find upper limits for the annhilation cross section in various channels for DM particle mass between 30 GeV and 10 TeV. Strongest upper limits coming from the two neutrino channel require $\langle\sigma\cdot v\rangle < 6\times10^{-20}$ cm^3/s in dwarf galaxies and $\langle\sigma\cdot v\rangle < 7\times10^{-21}$ cm^3/s in LMC for 5 TeV WIMP mass.
[5] BOUDAUD 17 use data from the spacecraft Voyager 1, beyond the heliopause, and from AMS02 on $\chi\chi \rightarrow e^+e^-$ to require $\langle\sigma\cdot v\rangle < 1.\times10^{-28}$ cm^3/s for m(χ) = 10 MeV.
[6] AARTSEN 16D search for GeV νs from WIMP annihilation in galaxy; limits set on $\langle\sigma\cdot v\rangle$ in Fig. 6, 7.
[7] ABDALLAH 16 require $\langle\sigma\cdot v\rangle < 6\times10^{-26}$ cm^3/s for m(WIMP) = 1.5 TeV from 254 hours observation (WW channel) and $< 2\times10^{-26}$ cm^3/s for m(WIMP) = 1.0 TeV in $\tau^+\tau^-$ channel.
[8] ABDALLAH 16A search for line spectra from WIMP + WIMP $\rightarrow \gamma\gamma$ in 18 hr HESS data; rule out previous 130 GeV WIMP hint from Fermi-LAT data.
[9] AHNEN 16 require $\langle\sigma\cdot v\rangle < 3\times10^{-26}$ cm^3/s for m(WIMP) = 100 GeV (WW channel).
[10] AVRORIN 16 require $\langle s.v\rangle < 1.91\times10^{-21}$ cm^3/s from WIMP annihilation to νs via WW channel for m(WIMP) = 1 TeV.
[11] CAPUTO 16 place limits on WIMPs from annihilation to gamma rays in Small Magellanic Cloud using Fermi-LaT data: $\langle\sigma\cdot v\rangle < 3\times10^{-26}$cm^3/s for m(WIMP) = 10 GeV.
[12] FORNASA 16 use anisotropies in the γ-ray diffuse emission detected by Fermi-LAT to bound $\langle\sigma\cdot v\rangle < 10^{-25}$cm^3/s for m(WIMP) = 100 GeV in $b\overline{b}$ channel: see Fig. 28. The limit is driven by dark-matter subhalos in the Milky Way and it refers to their Most Constraining Scenario.
[13] LEITE 16 constrain WIMP annihilation via search for radio emissions from Smith cloud; $\langle\sigma\cdot v\rangle < 5\times10^{-27}$cm^3/s in ee channel for m(WIMP) = 5 GeV.
[14] LI 16 re-analyze Fermi-LAT data on 8 dwarf spheroidals; set limit $\langle\sigma\cdot v\rangle < 2\times10^{-26}$ cm^3/s for m(WIMP) = 100 GeV in $b\overline{b}$ mode with substructures included.
[15] LI 16A constrain $\langle\sigma\cdot v\rangle < 10^{-25}$cm^3/s in $b\overline{b}$ channel for m(WIMP) = 100 GeV using Fermi-LAT data from M31; see Fig. 6.
[16] LIANG 16 search dwarf spheroidal galaxies, Large Magellanic Cloud, and Small Magellanic Cloud for γ-line in Fermi-LAT data.
[17] LU 16 re-analyze Fermi-LAT and AMS-02 data; require $\langle\sigma\cdot v\rangle < 10^{-25}$cm^3/s for m_m(WIMP) = 1 TeV in $b\overline{b}$ channel .
[18] SHIRASAKI 16 re-anayze Fermi-LAT extra-galactic data; require $\langle\sigma\cdot v\rangle < 10^{-23}$cm^3/s for m(WIMP) = 1 TeV in $b\overline{b}$ channel; see Fig. 8.
[19] AARTSEN 15C search for neutrinos from X^0 annihilation in the Galactic halo. See their Figs. 16 and 17, and Table 5 for limits on $\sigma\cdot$v for X^0 mass between 100 GeV and 100 TeV.
[20] AARTSEN 15E search for neutrinos from X^0 annihilation in the Galactic center. See their Figs. 7 and 9, and Table 3 for limits on $\sigma\cdot$v for X^0 mass between 30 GeV and 10 TeV.
[21] ABRAMOWSKI 15 search for γ from X^0 annihilation in the Galactic center. See their Fig. 4 for limits on $\sigma\cdot$v for X^0 mass between 250 GeV and 10 TeV.
[22] ACKERMANN 15 search for monochromatic γ from X^0 annihilation in the Galactic halo. See their Fig. 8 and Tables 2–4 for limits on $\sigma\cdot$v for X^0 mass between 0.2 GeV and 500 GeV.
[23] ACKERMANN 15A search for γ from X^0 annihilation (both Galactic and extragalactic) in the isotropic γ background. See their Fig. 7 for limits on $\sigma\cdot$v for X^0 mass between 10 GeV and 30 TeV.
[24] ACKERMANN 15B search for γ from X^0 annihilation in 15 dwarf spheroidal satellite galaxies of the Milky Way. See their Figs. 1 and 2 for limits on $\sigma\cdot$v for X^0 mass between 2 GeV and 10 TeV.
[25] ADRIAN-MARTINEZ 15 search for neutrinos from X^0 annihilation in the Galactic center. See their Figs. 10 and 11 and Tables 1 and 2 for limits on $\sigma\cdot$v for X^0 mass between 25 GeV and 10 TeV.
[26] ACKERMANN 14 search for γ from X^0 annihilation in 25 dwarf spheroidal satellite galaxies of the Milky Way. See their Tables II–VII for limits assuming annihilation into e^+e^-, $\mu^+\mu^-$, $\tau^+\tau^-$, $u\overline{u}$, $b\overline{b}$, and W^+W^-, for X^0 mass ranging from 2 GeV to 10 TeV.
[27] Limit assuming X^0 pair annihilation into $b\overline{b}$.
[28] Limit assuming X^0 pair annihilation into W^+W^-.
[29] ALEKSIC 14 search for γ from X^0 annihilation in the dwarf spheroidal galaxy Segue 1. The listed limit assumes annihilation into W^+W^-. See their Figs. 6, 7, and 16 for

limits on $\sigma \cdot v$ for annihilation channels $\mu^+\mu^-$, $\tau^+\tau^-$, $b\overline{b}$, $t\overline{t}$, $\gamma\gamma$, γZ, W^+W^-, ZZ for X^0 mass between 10^2 and 10^4 GeV.

[30] AARTSEN 13C search for neutrinos from X^0 annihilation in nearby galaxies and galaxy clusters. See their Figs. 5–7 for limits on $\sigma \cdot v$ for $X^0X^0 \to \nu\overline{\nu}$, $\mu^+\mu^-$, $\tau^+\tau^-$, and W^+W^- for X^0 mass between 300 GeV and 100 TeV.

[31] ABRAMOWSKI 13 search for monochromatic γ from X^0 annihilation in the Milky Way halo in the central region. Limit on $\sigma \cdot v$ between 10^{-28} and 10^{-25} cm^3 s^{-1} (95% CL) is obtained for X^0 mass between 500 GeV and 20 TeV for $X^0X^0 \to \gamma\gamma$. X^0 density distribution in the Galaxy by Einasto is assumed. See their Fig. 4.

[32] ACKERMANN 13A search for monochromatic γ from X^0 annihilation in the Milky Way. Limit on $\sigma \cdot v$ for the process $X^0X^0 \to \gamma\gamma$ in the range 10^{-29}–10^{-27} cm^3 s^{-1} (95% CL) is obtained for X^0 mass between 5 and 300 GeV. The limit depends slightly on the assumed density profile of X^0 in the Galaxy. See their Tables VII–X and Fig.10. Supersedes ACKERMANN 12.

[33] ABRAMOWSKI 12 search for γ's from X^0 annihilation in the Fornax galaxy cluster. See their Fig. 7 for limits on $\sigma \cdot v$ for X^0 mass between 0.1 and 100 TeV for the annihilation channels $\tau^+\tau^-$, $b\overline{b}$, and W^+W^-.

[34] ACKERMANN 12 search for monochromatic γ from X^0 annihilation in the Milky Way. Limit on $\sigma \cdot v$ in the range 10^{-28}–10^{-26} cm^{3}s^{-1} (95% CL) is obtained for X^0 mass between 7 and 200 GeV if X^0 annihilates into $\gamma\gamma$. The limit depends slightly on the assumed density profile of X^0 in the Galaxy. See their Table III and Fig. 15.

[35] ACKERMANN 12 search for γ from X^0 annihilation in the Milky Way in the diffuse γ background. Limit on $\sigma \cdot v$ of 10^{-24} cm^{3}s^{-1} or larger is obtained for X^0 mass between 5 GeV and 10 TeV for various annihilation channels including W^+W^-, $b\overline{b}$, gg, e^+e^-, $\mu^+\mu^-$, $\tau^+\tau^-$. The limit depends slightly on the assumed density profile of X^0 in the Galaxy. See their Figs. 17–20.

[36] ALIU 12 search for γ's from X^0 annihilation in the dwarf spheroidal galaxy Segue 1. Limit on $\sigma \cdot v$ in the range 10^{-24}–10^{-20} cm^{3}s^{-1} (95% CL) is obtained for X^0 mass between 10 GeV and 2 TeV for annihilation channels e^+e^-, $\mu^+\mu^-$, $\tau^+\tau^-$, $b\overline{b}$, and W^+W^-. See their Fig. 3.

[37] ABBASI 11C search for ν_μ from X^0 annihilation in the outer halo of the Milky Way. The limit assumes annihilation into $\nu\nu$. See their Fig. 9 for limits with other annihilation channels.

[38] ABRAMOWSKI 11 search for γ from X^0 annihilation near the Galactic center. The limit assumes Einasto DM density profile.

[39] ACKERMANN 11 search for γ from X^0 annihilation in ten dwarf spheroidal satellite galaxies of the Milky Way. The limit for $m = 10$ GeV assumes annihilation into $b\overline{b}$, the others W^+W^-. See their Fig. 2 for limits with other final states. See also GERINGER-SAMETH 11 for a different analysis of the same data.

Dark Matter Particle (X^0) Production in Hadron Collisions

Searches for X^0 production in association with observable particles (γ, jets, ...) in high energy hadron collisions. If a specific form of effective interaction Lagrangian is assumed, the limits may be translated into limits on X^0-nucleon scattering cross section.

VALUE	DOCUMENT ID		TECN	COMMENT
• • • We do not use the following data for averages, fits, limits, etc. • • •				
	[1] AABOUD	18	ATLS	$pp \to Z\chi\chi$; $Z \to \ell\ell$
	[2] AABOUD	18A	ATLS	$pp \to t\overline{t}\,\not{E}_T$; $pp \to b\overline{b}\,\not{E}_T$
	[3] AABOUD	18I	ATLS	jet(s) + $\not{E}_T$
	[4] SIRUNYAN	18C	CMS	$pp \to t\overline{t}\,\not{E}_T$
	[5] AABOUD	17A	ATLS	pp ($H \to b\overline{b}$ + WIMP pair)
	[6] AABOUD	17AM	ATLS	$pp \to Z' \to Ah \to h(b\overline{b}) + \not{E}_T$
	[7] AABOUD	17AQ	ATLS	$pp \to h(\gamma\gamma) + \not{E}_T$
	[8] AABOUD	17BD	ATLS	$pp \to$ jet(s) + $\not{E}_T$
	[9] AABOUD	17R	ATLS	$pp \to \gamma\not{E}_T$
	[10] AGUILAR-AR...	17A	MBNE	$pN \to \chi\chi X$; $\chi N \to \chi N$
	[11] BANERJEE	17	NA64	$eN \to eN\gamma'$
	[12] KHACHATRY...	17A	CMS	forward jets + $\not{E}_T$
	[13] KHACHATRY...	17F	CMS	$H \to$ invisibles
	[14] SIRUNYAN	17	CMS	$Z + \not{E}_T$
	[15] SIRUNYAN	17AP	CMS	$pp \to Z' \to Ah \to h$+MET
	[16] SIRUNYAN	17AQ	CMS	$pp \to \gamma$+MET
	[17] SIRUNYAN	17BB	CMS	$pp \to t\overline{t}$+$\not{E}_T$; $pp \to b\overline{b}$+$\not{E}_T$
	[18] SIRUNYAN	17G	CMS	$pp \to j + \not{E}_T$
	[19] SIRUNYAN	17U	CMS	$pp \to Z\chi\chi$; $Z \to \ell\overline{\ell}$
	[20] AABOUD	16AD	ATLS	(W or $Z \to$ jets) + $\not{E}_T$
	[21] AAD	16AF	ATLS	$VV \to$ forward jets +$\not{E}_T$
	[22] AAD	16AG	ATLS	ℓ + jets
	[23] AAD	16M	ATLS	$pp \to H + \not{E}_T$, $H \to b\overline{b}$
	[24] KHACHATRY...	16BZ	CMS	jet(s) + $\not{E}_T$
	[25] KHACHATRY...	16CA	CMS	jets + $\not{E}_T$
	[26] KHACHATRY...	16N	CMS	$pp \to \gamma + \not{E}_T$
	[27] AAD	15AS	ATLS	b ($\overline{b}$) + $\not{E}_T$, $t\overline{t}$ + $\not{E}_T$
	[28] AAD	15BH	ATLS	jet + $\not{E}_T$
	[29] AAD	15CF	ATLS	$H^0 + \not{E}_T$
	[30] AAD	15CS	ATLS	$\gamma + \not{E}_T$
	[31] KHACHATRY...	15AG	CMS	$t\overline{t} + \not{E}_T$
	[32] KHACHATRY...	15AL	CMS	jet + $\not{E}_T$
	[33] KHACHATRY...	15T	CMS	$\ell + \not{E}_T$
	[34] AAD	14AI	ATLS	$W + \not{E}_T$
	[35] AAD	14BK	ATLS	W, $Z + \not{E}_T$
	[36] AAD	14K	ATLS	$Z + \not{E}_T$
	[37] AAD	14O	ATLS	$Z + \not{E}_T$
	[38] AAD	13AD	ATLS	jet + $\not{E}_T$
	[39] AAD	13C	ATLS	$\gamma + \not{E}_T$
	[40] AALTONEN	12K	CDF	$t + \not{E}_T$
	[41] AALTONEN	12M	CDF	jet + $\not{E}_T$
	[42] CHATRCHYAN	12AP	CMS	jet + $\not{E}_T$
	[43] CHATRCHYAN	12T	CMS	$\gamma + \not{E}_T$

[1] AABOUD 18 search for $pp \to Z + \not{E}_T$ with $Z \to \ell\ell$ at 13 TeV with 36.1 fb^{-1} of data. Limits set for simplified models.

[2] AABOUD 18A search for $pp \to t\overline{t}\,\not{E}_T$ or $pp \to b\overline{b}\,\not{E}_T$ at 13 TeV, 36.1 fb^{-1} of data. Limits set for simplified models.

[3] AABOUD 18I search for $pp \to j + \not{E}_T$ at 13 TeV with 36.1 fb^{-1} of data. Limits set for simplified models with pair-produced weakly interacting dark-matter candidates.

[4] SIRUNYAN 18C search for new physics in $pp \to$ final states with two oppositely charged leptons at 13 TeV with 35.9 fb^{-1}. Limits placed on m(mediator) and top squark for various simplified models.

[5] AABOUD 17A search for $H \to b\overline{b} + \not{E}_T$. See Fig. 4b for limits set on VB mediator vs WIMP mass.

[6] AABOUD 17AM search for $pp \to Z' \to Ah \to h(b\overline{b}) + \not{E}_T$ at 13 TeV. Limits set in m(Z') vs. m(A) plane and on the visible cross section of $h(b\overline{b}) + \not{E}_T$ events in bins of $\not{E}_T$.

[7] AABOUD 17AQ search for WIMP in $pp \to h(\gamma\gamma) + \not{E}_T$ in 36.1 fb^{-1} of data. Limits on the visible cross section are also provided. Model dependent limits on spin independent DM - Nucleon cross-section are also presented, which are more stringent than those from direct searches for DM mass smaller than 2.5 GeV .

[8] AABOUD 17BD search for $pp \to$ jet(s) + $\not{E}_T$ at 13 TeV with 3.2 fb^{-1} of data. Limits set for simplified models. Observables corrected for detector effects can be used to constrain other models.

[9] AABOUD 17R, for an axial vector mediator in the s-channel, excludes m(mediator) $<$ 750–1200 GeV for m(DM) $<$ 230–480 GeV, depending on the couplings.

[10] AGUILAR-AREVALO 17A search for DM produced in 8 GeV proton collisions with steel beam dump followed by DM-nucleon scattering in MiniBooNE detector. Limit placed on DM cross section parameter $Y < 2 \times 10^{-8}$ for $\alpha_D = 0.5$ and for $0.01 < m(\text{DM}) < 0.3$ GeV.

[11] BANERJEE 17 search for dark photon invisible decay via eN scattering; exclude m(γ') $<$ 100 MeV as an explanation of (g_μ−2) muon anomaly.

[12] KHACHATRYAN 17A search for WIMPs in forward jets + $\not{E}_T$ channel with 18.5 fb^{-1} at 8 TeV; limits set in effective theory model, Fig. 3.

[13] KHACHATRYAN 17F search for $H \to$ invisibles in pp collisions at 7, 8, and 13 TeV; place limits on Higgs portal DM.

[14] SIRUNYAN 17 search for $pp \to Z + \not{E}_T$ with 2.3 fb^{-1} at 13 TeV; no signal seen; limits placed on WIMPs and unparticles.

[15] SIRUNYAN 17AP search for $pp \to Z' \to Ah \to h$+MET with $h \to b\overline{b}$ or $\gamma\gamma$ and $A \to \chi\chi$ with 2.3 fb^{-1} at 13 TeV. Limits set in m(Z') vs. m(A) plane.

[16] SIRUNYAN 17AQ search for $pp \to \gamma$+MET at 13 TeV with 12.9 fb^{-1}. Limits derived for simplified DM models, effective electroweak-DM interaction and Extra Dimensions models.

[17] SIRUNYAN 17BB search for WIMPs via $pp \to t\overline{t}$+$\not{E}_T$, $pp \to b\overline{b}$+$\not{E}_T$ at 13 TeV with 2.2 fb^{-1}. Limits derived for various simplified models.

[18] SIRUNYAN 17G search for $pp \to j + \not{E}_T$ with 12.9 fb^{-1} at 13 TeV; limits placed on WIMP mass/mediators in DM simplified models.

[19] SIRUNYAN 17U search for WIMPs/unparticles via $pp \to Z\chi\chi$, $Z \to \ell\overline{\ell}$ at 13 TeV with 2.3 fb^{-1}. Limits derived for various simplified models.

[20] AABOUD 16AD place limits on $VVXX$ effective theory via search for hadronic W or Z plus WIMP pair production. See Fig. 5.

[21] AAD 16AF search for $VV \to (H \to$ WIMP pair) + forward jets with 20.3 fb^{-1} at 8 TeV; set limits in Higgs portal model, Fig. 8 .

[22] AAD 16AG search for lepton jets with 20.3 fb^{-1} of data at 8 TeV; Fig. 13 excludes dark photons around 0.1–1 GeV for kinetic mixing 10^{-6}–10^{-2}.

[23] AAD 16M search with 20.3 fb^{-1} of data at 8 TeV pp collisions; limits placed on EFT model (Fig. 7) and simplified Z' model (Fig. 6).

[24] KHACHATRYAN 16BZ search for jet(s) + $\not{E}_T$ in 19.7 fb^{-1} at 8 TeV; limits set for variety of simplified models.

[25] KHACHATRYAN 16CA search for WIMPs via jet(s) + $\not{E}_T$ using razor variable; require mediator scale $>$ 1 TeV for various effective theories.

[26] KHACHATRYAN 16N search for γ + WIMPs in 19.6 fb^{-1} at 8 TeV; limits set on SI and SD WIMP-p scattering in Fig. 3.

[27] AAD 15AS search for events with one or more bottom quark and missing E_T, and also events with a top quark pair and missing E_T in pp collisions at $E_{cm} = 8$ TeV with $L = 20.3$ fb^{-1}. See their Figs. 5 and 6 for translated limits on X^0-nucleon cross section for $m = 1$–700 GeV.

[28] AAD 15BH search for events with a jet and missing E_T in pp collisions at $E_{cm} = 8$ TeV with $L = 20.3$ fb^{-1}. See their Fig. 12 for translated limits on X^0-nucleon cross section for $m = 1$–1200 GeV.

[29] AAD 15CF search for events with a H^0 ($\to \gamma\gamma$) and missing E_T in pp collisions at $E_{cm} = 8$ TeV with $L = 20.3$ fb^{-1}. See paper for limits on the strength of some contact interactions containing X^0 and the Higgs fields.

[30] AAD 15CS search for events with a photon and missing E_T in pp collisions at $E_{cm} = 8$ TeV with $L = 20.3$ fb^{-1}. See their Fig. 13 (see also erratum) for translated limits on X^0-nucleon cross section for $m = 1$–1000 GeV.

[31] KHACHATRYAN 15AG search for events with a top quark pair and missing E_T in pp collisions at $E_{cm} = 8$ TeV with $L = 19.7$ fb^{-1}. See their Fig. 8 for translated limits on X^0-nucleon cross section for $m = 1$–200 GeV.

[32] KHACHATRYAN 15AL search for events with a jet and missing E_T in pp collisions at $E_{cm} = 8$ TeV with $L = 19.7$ fb^{-1}. See their Fig. 5 and Tables 4–6 for translated limits on X^0-nucleon cross section for $m = 1$–1000 GeV.

[33] KHACHATRYAN 15T search for events with a lepton and missing E_T in pp collisions at $E_{cm} = 8$ TeV with $L = 19.7$ fb^{-1}. See their Fig. 17 for translated limits on X^0-proton cross section for $m = 1$–1000 GeV.

[34] AAD 14AI search for events with a W and missing E_T in pp collisions at $E_{cm} = 8$ TeV with $L = 20.3$ fb^{-1}. See their Fig. 4 for translated limits on X^0–nucleon cross section for $m = 1$–1500 GeV.

Searches Particle Listings

WIMP and Dark Matter Searches

[35] AAD 14BK search for hadronically decaying W, Z in association with $\not{E}_T$ in 20.3 fb^{-1} at 8 TeV pp collisions. Fig. 5 presents exclusion results for SI and SD scattering cross section. In addition, cross section limits on the anomalous production of W or Z bosons with large missing transverse momentum are also set in two fiducial regions.

[36] AAD 14K search for events with a Z and missing E_T in pp collisions at E_{cm} = 8 TeV with L = 20.3 fb^{-1}. See their Fig. 5 and 6 for translated limits on X^0–nucleon cross section for m = 1–10^3 GeV.

[37] AAD 14O search for ZH^0 production with H^0 decaying to invisible final states. See their Fig. 4 for translated limits on X^0–nucleon cross section for m = 1–60 GeV in Higgs-portal X^0 scenario.

[38] AAD 13AD search for events with a jet and missing E_T in pp collisions at E_{cm} = 7 TeV with L = 4.7 fb^{-1}. See their Figs. 5 and 6 for translated limits on X^0–nucleon cross section for m = 1–1300 GeV.

[39] AAD 13C search for events with a photon and missing E_T in pp collisions at E_{cm} = 7 TeV with L = 4.6 fb^{-1}. See their Fig. 3 for translated limits on X^0–nucleon cross section for m = 1–1000 GeV.

[40] AALTONEN 12K search for events with a top quark and missing E_T in $p\overline{p}$ collisions at E_{cm} = 1.96 TeV with L = 7.7 fb^{-1}. Upper limits on $\sigma(tX^0)$ in the range 0.4–2 pb (95% CL) is given for m_{X^0} = 0–150 GeV.

[41] AALTONEN 12M search for events with a jet and missing E_T in $p\overline{p}$ collisions at E_{cm} = 1.96 TeV with L = 6.7 fb^{-1}. Upper limits on the cross section in the range 2–10 pb (90% CL) is given for m_{X^0} = 1–300 GeV. See their Fig. 2 for translated limits on X^0–nucleon cross section.

[42] CHATRCHYAN 12AP search for events with a jet and missing E_T in pp collisions at E_{cm} = 7 TeV with L = 5.0 fb^{-1}. See their Fig. 4 for translated limits on X^0–nucleon cross section for m_{X^0} = 0.1–1000 GeV.

[43] CHATRCHYAN 12T search for events with a photon and missing E_T in pp collisions at E_{cm} = 7 TeV with L = 5.0 fb^{-1}. Upper limits on the cross section in the range 13–15 fb (90% CL) is given for m_{X^0} = 1–1000 GeV. See their Fig. 2 for translated limits on X^0–nucleon cross section.

REFERENCES FOR WIMP and Dark Matter Searches

AABOUD	18	PL B776 318	M. Aaboud *et al.*	(ATLAS Collab.)
AABOUD	18A	EPJ C78 18	M. Aaboud *et al.*	(ATLAS Collab.)
AABOUD	18I	JHEP 1801 126	M. Aaboud *et al.*	(ATLAS Collab.)
AGNESE	18	PR D97 022002	R. Agnese *et al.*	(SuperCDMS Collab.)
AGNESE	18A	PRL 120 061802	R. Agnese *et al.*	(SuperCDMS Collab.)
SIRUNYAN	18C	PR D97 032009	A.M. Sirunyan *et al.*	(CMS Collab.)
AABOUD	17A	PL B765 11	M. Aaboud *et al.*	(ATLAS Collab.)
AABOUD	17AM	PRL 119 181804	M. Aaboud *et al.*	(ATLAS Collab.)
AABOUD	17AQ	PR D96 112004	M. Aaboud *et al.*	(ATLAS Collab.)
AABOUD	17BD	EPJ C77 765	M. Aaboud *et al.*	(ATLAS Collab.)
AABOUD	17R	EPJ C77 393	M. Aaboud *et al.*	(ATLAS Collab.)
AARTSEN	17	EPJ C77 82	M.G. Aartsen *et al.*	(IceCube Collab.)
AARTSEN	17A	EPJ C77 146	M.G. Aartsen *et al.*	(IceCube Collab.)
AARTSEN	17C	EPJ C77 627	M.G. Aartsen *et al.*	(IceCube Collab.)
AGUILAR-AR...	17	PRL 118 141803	A.A. Aguilar-Arevalo *et al.*	(DAMIC Collab.)
AGUILAR-AR...	17A	PRL 118 221803	A.A. Aguilar-Arevalo *et al.*	(MiniBooNE Collab.)
AKERIB	17	PRL 118 021303	D.S. Akerib *et al.*	(LUX Collab.)
AKERIB	17A	PRL 118 251302	D.S. Akerib *et al.*	(LUX Collab.)
ALBERT	17A	PL B769 249	A. Albert *et al.*	(ANTARES Collab.)
AMOLE	17	PRL 118 251301	C. Amole *et al.*	(PICO Collab.)
ANGLOHER	17A	EPJ C77 637	G. Angloher *et al.*	(CRESST Collab.)
APRILE	17	PRL 118 101101	E. Aprile *et al.*	(XENON100 Collab.)
APRILE	17A	PR D96 022008	E. Aprile *et al.*	(XENON100 Collab.)
APRILE	17D	PR D96 042004	E. Aprile *et al.*	(XENON100 Collab.)
APRILE	17G	PRL 119 181301	E. Aprile *et al.*	(XENON Collab.)
APRILE	17H	PR D96 122002	E. Aprile *et al.*	(XENON100 Collab.)
APRILE	17K	JCAP 1710 039	E. Aprile *et al.*	(XENON100 Collab.)
ARCHAMBAU...	17	PR D95 082001	S. Archambault *et al.*	(VERITAS Collab.)
AVRORIN	17	JETP 125 80	A.D. Avrorin *et al.*	(BAIKAL Collab.)
BANERJEE	17	PRL 118 011802	D. Banerjee *et al.*	(NA64 Collab.)
BARBOSA-D...	17	PR D95 032006	E. Barbosa de Souza *et al.*	(DM17 Collab.)
BATTAT	17	ASP 91 65	J.B.R. Battat *et al.*	(DRIFT-IId Collab.)
BEHNKE	17	ASP 90 85	E. Behnke *et al.*	(PICASSO Collab.)
BOUDAUD	17	PRL 119 021103	M. Boudaud, J. Lavalle, P. Salati	
CHEN	17E	PR D96 102007	X. Chen *et al.*	(PandaX-II Collab.)
CUI	17A	PRL 119 181302	X. Cui *et al.*	(PandaX-II Collab.)
FU	17	PRL 118 071301	C. Fu *et al.*	(PandaX Collab.)
KHACHATRY...	17A	PRL 118 021802	V. Khachatryan *et al.*	(CMS Collab.)
KHACHATRY...	17F	JHEP 1702 135	V. Khachatryan *et al.*	(CMS Collab.)
SIRUNYAN	17	JHEP 1703 061	A.M. Sirunyan *et al.*	(CMS Collab.)
SIRUNYAN	17AP	JHEP 1710 180	A.M. Sirunyan *et al.*	(CMS Collab.)
SIRUNYAN	17AQ	JHEP 1710 073	A.M. Sirunyan *et al.*	(CMS Collab.)
SIRUNYAN	17BB	EPJ C77 845	A.M. Sirunyan *et al.*	(CMS Collab.)
SIRUNYAN	17G	JHEP 1707 014	A.M. Sirunyan *et al.*	(CMS Collab.)
SIRUNYAN	17U	JHEP 1709 106	A.M. Sirunyan *et al.*	(CMS Collab.)
AABOUD	16AD	PL B763 251	M. Aaboud *et al.*	(ATLAS Collab.)
AABOUD	16D	PR D94 032005	M. Aaboud *et al.*	(ATLAS Collab.)
AABOUD	16F	JHEP 1606 059	M. Aaboud *et al.*	(ATLAS Collab.)
AAD	16AF	JHEP 1601 172	G. Aad *et al.*	(ATLAS Collab.)
AAD	16AG	JHEP 1602 062	G. Aad *et al.*	(ATLAS Collab.)
AAD	16M	PR D93 072007	G. Aad *et al.*	(ATLAS Collab.)
AARTSEN	16C	JCAP 1604 022	M.G. Aartsen *et al.*	(IceCube Collab.)
AARTSEN	16D	EPJ C76 531	M.G. Aartsen *et al.*	(IceCube Collab.)
ABDALLAH	16	PRL 117 111301	H. Abdallah *et al.*	(H.E.S.S. Collab.)
ABDALLAH	16A	PRL 117 151302	H. Abdallah *et al.*	(H.E.S.S. Collab.)
ADRIAN-MAR...	16	PL B759 69	S. Adrian-Martinez *et al.*	(ANTARES Collab.)
ADRIAN-MAR...	16B	JCAP 1605 016	S. Adrian-Martinez *et al.*	(ANTARES Collab.)
AGNES	16	PR D93 081101	P. Agnes *et al.*	(DarkSide-50 Collab.)
AGNESE	16	PRL 116 071301	R. Agnese *et al.*	(SuperCDMS Collab.)
AGUILAR-AR...	16	PR D94 082006	A.A. Aguilar-Arevalo *et al.*	(DAMIC Collab.)
AHNEN	16	JCAP 1602 039	M.L. Ahnen *et al.*	(MAGIC and Fermi-LAT Collab.)
AKERIB	16	PRL 116 161301	D.S. Akerib *et al.*	(LUX Collab.)
AKERIB	16A	PRL 116 161302	D.S. Akerib *et al.*	(LUX Collab.)
AMOLE	16	PR D93 052014	C. Amole *et al.*	(PICO Collab.)
AMOLE	16A	PR D93 061101	C. Amole *et al.*	(PICO Collab.)
ANGLOHER	16	EPJ C76 25	G. Angloher *et al.*	(CRESST-II Collab.)
ANGLOHER	16A	PRL 117 021303	G. Angloher *et al.*	(CRESST-II Collab.)
APRILE	16	PR D94 092001	E. Aprile *et al.*	(XENON100 Collab.)
APRILE	16B	PR D94 122001	E. Aprile *et al.*	(XENON100 Collab.)
ARMENGAUD	16	JCAP 1605 019	E. Armengaud *et al.*	(EDELWEISS-III Collab.)
AVRORIN	16	ASP 81 12	A.D. Avrorin *et al.*	(BAIKAL Collab.)
CAPUTO	16	PR D93 062004	R. Caputo *et al.*	
FORNASA	16	PR D94 123005	M. Fornasa *et al.*	(Fermi-LAT Collab.)
HEHN	16	EPJ C76 548	L. Hehn *et al.*	(EDELWEISS-III Collab.)
KHACHATRY...	16AJ	PR D93 052011	V. Khachatryan *et al.*	(CMS Collab.)
KHACHATRY...	16BZ	JHEP 1612 083	V. Khachatryan *et al.*	(CMS Collab.)
Also		JHEP 1708 035 (errat.)	V. Khachatryan *et al.*	(CMS Collab.)
KHACHATRY...	16CA	JHEP 1612 088	V. Khachatryan *et al.*	(CMS Collab.)
KHACHATRY...	16N	PL B755 102	V. Khachatryan *et al.*	(CMS Collab.)
LEITE	16	JCAP 1611 021	N. Leite *et al.*	
LI	16	PR D93 043518	S. Li *et al.*	
LI	16A	JCAP 1612 028	Z. Li *et al.*	
LIANG	16	PR D94 103502	Y.-F. Liang *et al.*	
LU	16	PR D93 103517	B-Q. Lu, H-S. Zong	
SHIRASAKI	16	PR D94 063522	M. Shirasaki *et al.*	
TAN	16	PR D93 122009	T.H. Tan *et al.*	(PandaX Collab.)
TAN	16B	PRL 117 121303	A. Tan *et al.*	(PandaX Collab.)
ZHAO	16	PR D93 092003	W. Zhao *et al.*	(CDEX Collab.)
AAD	15AS	EPJ C75 92	G. Aad *et al.*	(ATLAS Collab.)
AAD	15BH	EPJ C75 299	G. Aad *et al.*	(ATLAS Collab.)
Also		EPJ C75 408 (errat.)	G. Aad *et al.*	(ATLAS Collab.)
AAD	15CF	PRL 115 131801	G. Aad *et al.*	(ATLAS Collab.)
AAD	15CS	PR D91 012008	G. Aad *et al.*	(ATLAS Collab.)
Also		PR D92 059903 (errat.)	G. Aad *et al.*	(ATLAS Collab.)
AARTSEN	15C	EPJ C75 20	M.G. Aartsen *et al.*	(IceCube Collab.)
AARTSEN	15E	EPJ C75 492	M.G. Aartsen *et al.*	(IceCube Collab.)
ABRAMOWSKI	15	PRL 114 081301	A. Abramowski *et al.*	(H.E.S.S. Collab.)
ACKERMANN	15	PR D91 122002	M. Ackermann *et al.*	(Fermi-LAT Collab.)
ACKERMANN	15A	JCAP 1509 008	M. Ackermann *et al.*	(Fermi-LAT Collab.)
ACKERMANN	15B	PRL 115 231301	M. Ackermann *et al.*	(Fermi-LAT Collab.)
ADRIAN-MAR...	15	JCAP 1510 068	S. Adrian-Martinez *et al.*	(ANTARES Collab.)
AGNES	15	PL B743 456	P. Agnes *et al.*	(DarkSide-50 Collab.)
AGNESE	15A	PR D91 052021	R. Agnese *et al.*	(SuperCDMS Collab.)
AGNESE	15B	PR D92 072003	R. Agnese *et al.*	(SuperCDMS Collab.)
AMOLE	15	PRL 114 231302	C. Amole *et al.*	(PICO Collab.)
APRILE	15	PRL 115 091302	E. Aprile *et al.*	(XENON Collab.)
APRILE	15A	SCI 349 851	E. Aprile *et al.*	(XENON Collab.)
CHOI	15	PRL 114 141301	K. Choi *et al.*	(Super-Kamiokande Collab.)
KHACHATRY...	15AG	JHEP 1506 121	V. Khachatryan *et al.*	(CMS Collab.)
KHACHATRY...	15AL	EPJ C75 235	V. Khachatryan *et al.*	(CMS Collab.)
KHACHATRY...	15T	PR D91 092005	V. Khachatryan *et al.*	(CMS Collab.)
NAKAMURA	15	PTEP 2015 4 043F01	K. Nakamura *et al.*	(NEWAGE Collab.)
XIAO	15	PR D92 052004	X. Xiao *et al.*	(PandaX Collab.)
AAD	14AI	JHEP 1409 037	G. Aad *et al.*	(ATLAS Collab.)
AAD	14BK	PRL 112 041802	G. Aad *et al.*	(ATLAS Collab.)
AAD	14K	PR D90 012004	G. Aad *et al.*	(ATLAS Collab.)
AAD	14O	PRL 112 201802	G. Aad *et al.*	(ATLAS Collab.)
ACKERMANN	14	PR D89 042001	M. Ackermann *et al.*	(Fermi-LAT Collab.)
AGNESE	14	PRL 112 241302	R. Agnese *et al.*	(SuperCDMS Collab.)
AGNESE	14A	PRL 112 041302	R. Agnese *et al.*	(SuperCDMS Collab.)
AKERIB	14	PRL 112 091303	D.S. Akerib *et al.*	(LUX Collab.)
ALEKSIC	14	JCAP 1402 008	J. Aleksic *et al.*	(MAGIC Collab.)
ANGLOHER	14	EPJ C74 3184	G. Angloher *et al.*	(CRESST-II Collab.)
APRILE	14A	ASP 54 11	E. Aprile *et al.*	(XENON100 Collab.)
AVRORIN	14	ASP 62 12	A.D. Avrorin *et al.*	(BAIKAL Collab.)
FELIZARDO	14	PR D89 072013	M. Felizardo *et al.*	(SIMPLE Collab.)
LEE	14A	PR D90 052006	H.S. Lee *et al.*	(KIMS Collab.)
LIU	14A	PR D90 032003	S.K. Liu *et al.*	(CDEX Collab.)
UCHIDA	14	PTEP 2014 063C01	H. Uchida *et al.*	(XMASS Collab.)
YUE	14	PR D90 091701	Q. Yue *et al.*	(CDEX Collab.)
AAD	13AD	JHEP 1304 075	G. Aad *et al.*	(ATLAS Collab.)
AAD	13C	PRL 110 011802	G. Aad *et al.*	(ATLAS Collab.)
AALSETH	13	PR D88 012002	C.E. Aalseth *et al.*	(CoGeNT Collab.)
AARTSEN	13	PRL 110 131302	M.G. Aartsen *et al.*	(IceCube Collab.)
AARTSEN	13C	PR D88 122001	M.G. Aartsen *et al.*	(IceCube Collab.)
ABE	13B	PL B719 78	K. Abe *et al.*	(XMASS Collab.)
ABRAMOWSKI	13	PRL 110 041301	A. Abramowski *et al.*	(H.E.S.S. Collab.)
ACKERMANN	13A	PR D88 082002	M. Ackermann *et al.*	(Fermi-LAT Collab.)
ADRIAN-MAR...	13	JCAP 1311 032	S. Adrian-Martinez *et al.*	(ANTARES Collab.)
AGNESE	13	PR D88 031104	R. Agnese *et al.*	(CDMS Collab.)
AGNESE	13A	PRL 111 251301	R. Agnese *et al.*	(CDMS Collab.)
APRILE	13	PRL 111 021301	E. Aprile *et al.*	(XENON100 Collab.)
BERNABEI	13A	EPJ C73 2648	R. Bernabei *et al.*	(DAMA Collab.)
BOLIEV	13	JCAP 1309 019	M. Boliev *et al.*	
LI	13B	PRL 110 261301	H.B. Li *et al.*	(TEXONO Collab.)
SUVOROVA	13	PAN 76 1367 Translated from YAF 76 1433.	O.V. Suvorova *et al.*	(INRM)
ZHAO	13	PR D88 052004	W. Zhao *et al.*	(CDEX Collab.)
AALTONEN	12K	PRL 108 201802	T. Aaltonen *et al.*	(CDF Collab.)
AALTONEN	12M	PRL 108 211804	T. Aaltonen *et al.*	(CDF Collab.)
ABBASI	12	PR D85 042002	R. Abbasi *et al.*	(IceCube Collab.)
ABRAMOWSKI	12	APJ 750 123	A. Abramowski *et al.*	(H.E.S.S. Collab.)
ACKERMANN	12	PR D86 022002	M. Ackermann *et al.*	(Fermi-LAT Collab.)
AKIMOV	12	PL B709 14	D.Yu. Akimov *et al.*	(ZEPLIN-III Collab.)
ALIU	12	PR D85 062001	E. Aliu *et al.*	(VERITAS Collab.)
ANGLOHER	12	EPJ C72 1971	G. Angloher *et al.*	(CRESST-II Collab.)
APRILE	12	PRL 109 181301	E. Aprile *et al.*	(XENON100 Collab.)
ARCHAMBAU...	12	PL B711 153	S. Archambault *et al.*	(PICASSO Collab.)
ARMENGAUD	12	PR D86 051701	E. Armengaud *et al.*	(EDELWEISS Collab.)
BARRETO	12	PL B711 264	J. Barreto *et al.*	(DAMIC Collab.)
BEHNKE	12	PR D86 052001	E. Behnke *et al.*	(COUPP Collab.)
Also		PR D90 079902 (errat.)	E. Behnke *et al.*	(COUPP Collab.)
BROWN	12	PR D85 021301	A. Brown *et al.*	(OXF)
CHATRCHYAN	12AP	JHEP 1209 094	S. Chatrchyan *et al.*	(CMS Collab.)
CHATRCHYAN	12T	PRL 108 261803	S. Chatrchyan *et al.*	(CMS Collab.)
DAHL	12	PRL 108 259001	C.E. Dahl, J. Hall, W.H. Lippincott	(CHIC, FNAL)
DAW	12	ASP 35 397	E. Daw *et al.*	(DRIFT-IId Collab.)
FELIZARDO	12	PRL 108 201302	M. Felizardo *et al.*	(SIMPLE Collab.)
KIM	12	PRL 108 181301	S.C. Kim *et al.*	(KIMS Collab.)
AALSETH	11	PRL 106 131301	C.E. Aalseth *et al.*	(CoGeNT Collab.)
AALSETH	11A	PRL 107 141301	C.E. Aalseth *et al.*	(CoGeNT Collab.)
ABBASI	11C	PR D84 022004	R. Abbasi *et al.*	(IceCube Collab.)
ABRAMOWSKI	11	PRL 106 161301	A. Abramowski *et al.*	(H.E.S.S. Collab.)
ACKERMANN	11	PRL 107 241302	M. Ackermann *et al.*	(Fermi-LAT Collab.)
AHLEN	11	PL B695 124	S. Ahlen *et al.*	(DMTPC Collab.)
AHMED	11	PR D83 112002	Z. Ahmed *et al.*	(CDMS Collab.)
AHMED	11A	PR D84 011102	Z. Ahmed *et al.*	(CDMS and EDELWEISS Collabs.)
AHMED	11B	PRL 106 131302	Z. Ahmed *et al.*	(CDMS Collab.)
AJELLO	11	PR D84 032007	M. Ajello *et al.*	(Fermi-LAT Collab.)
ANGLE	11	PRL 107 051301	J. Angle *et al.*	(XENON10 Collab.)
Also		PRL 110 249901 (errat.)	J. Angle *et al.*	(XENON10 Collab.)
APRILE	11	PR D84 052003	E. Aprile *et al.*	(XENON100 Collab.)
APRILE	11A	PR D84 061101	E. Aprile *et al.*	(XENON100 Collab.)
APRILE	11B	PRL 107 131302	E. Aprile *et al.*	(XENON100 Collab.)
ARMENGAUD	11	PL B702 329	E. Armengaud *et al.*	(EDELWEISS II Collab.)
BEHNKE	11	PRL 106 021303	E. Behnke *et al.*	(COUPP Collab.)
GERINGER-SA...	11	PRL 107 241303	A. Geringer-Sameth, S.M. Koushiappas	
HORN	11	PL B705 471	M. Horn *et al.*	(ZEPLIN-III Collab.)
TANAKA	11	APJ 742 78	T. Tanaka *et al.*	(Super-Kamiokande Collab.)
ABBASI	10	PR D81 057101	R. Abbasi *et al.*	(IceCube Collab.)
AHMED	10	SCI 327 1619	Z. Ahmed *et al.*	(CDMS II Collab.)
AKERIB	10	PR D82 122004	D.S. Akerib *et al.*	(CDMS-II Collab.)
AKIMOV	10	PL B692 180	D.Yu. Akimov *et al.*	(ZEPLIN-III Collab.)
APRILE	10	PRL 105 131302	E. Aprile *et al.*	(XENON100 Collab.)
ARMENGAUD	10	PL B687 294	E. Armengaud *et al.*	(EDELWEISS II Collab.)
FELIZARDO	10	PRL 105 211301	M. Felizardo *et al.*	(The SIMPLE Collab.)
MIUCHI	10	PL B686 11	K. Miuchi *et al.*	(NEWAGE Collab.)

ABBASI	09B	PRL 102 201302	R. Abbasi *et al.*	(IceCube Collab.)
AHMED	09	PRL 102 011301	Z. Ahmed *et al.*	(CDMS Collab.)
ANGLE	09	PR D80 115005	J. Angle *et al.*	(XENON10 Collab.)
ANGLOHER	09	ASP 31 270	G. Angloher *et al.*	(CRESST Collab.)
ARCHAMBAU...	09	PL B682 185	S. Archambault *et al.*	(PICASSO Collab.)
LEBEDENKO	09A	PRL 103 151302	V.N. Lebedenko *et al.*	(ZEPLIN-III Collab.)
LIN	09	PR D79 061101	S.T. Lin *et al.*	(TEXONO Collab.)
AALSETH	08	PRL 101 251301	C.E. Aalseth *et al.*	(CoGeNT Collab.)
Also		PRL 102 109903 (errat.)	C.E. Aalseth *et al.*	(CoGeNT Collab.)
ANGLE	08A	PRL 101 091301	J. Angle *et al.*	(XENON10 Collab.)
BEDNYAKOV	08	PAN 71 111	V.A. Bednyakov, H.P. Klapdor-Kleingrothaus, I.V. Krivosheina	
		Translated from YAF 71 112.		
ALNER	07	PL B653 161	G.J. Alner *et al.*	(ZEPLIN-II Collab.)
LEE	07A	PRL 99 091301	H.S. Lee *et al.*	(KIMS Collab.)
MIUCHI	07	PL B654 58	K. Miuchi *et al.*	
AKERIB	06	PR D73 011102	D.S. Akerib *et al.*	(CDMS Collab.)
SHIMIZU	06A	PL B633 195	Y. Shimizu *et al.*	
AKERIB	05	PR D72 052009	D.S. Akerib *et al.*	(CDMS Collab.)
ALNER	05	PL B616 17	G.J. Alner *et al.*	(UK Dark Matter Collab.)
BARNABE-HE...	05	PL B624 186	M. Barnabe-Heider *et al.*	(PICASSO Collab.)
BENOIT	05	PL B616 25	A. Benoit *et al.*	(EDELWEISS Collab.)
GIRARD	05	PL B621 233	T.A. Girard *et al.*	(SIMPLE Collab.)
GIULIANI	05	PRL 95 101301	F. Giuliani	
GIULIANI	05A	PR D71 123503	F. Giuliani, T.A. Girard	
KLAPDOR-K...	05	PL B609 226	H.V. Klapdor-Kleingrothaus, I.V. Krivosheina, C. Tomei	
GIULIANI	04	PL B588 151	F. Giuliani, T.A. Girard	
GIULIANI	04A	PRL 93 161301	F. Giuliani	
MIUCHI	03	ASP 19 135	K. Miuchi *et al.*	
TAKEDA	03	PL B572 145	A. Takeda *et al.*	
ANGLOHER	02	ASP 18 43	G. Angloher *et al.*	(CRESST Collab.)
BELLI	02	PR D66 043503	P. Belli *et al.*	
BERNABEI	02C	EPJ C23 61	R. Bernabei *et al.*	(DAMA Collab.)
GREEN	02	PR D66 083003	A.M. Green	
BAUDIS	01	PR D63 022001	L. Baudis *et al.*	(Heidelberg-Moscow Collab.)
SMITH	01	PR D64 043502	D. Smith, N. Weiner	
ULLIO	01	JHEP 0107 044	P. Ullio, M. Kamionkowski, P. Vogel	
BENOIT	00	PL B479 8	A. Benoit *et al.*	(EDELWEISS Collab.)
BERNABEI	00D	NJP 2 15	R. Bernabei *et al.*	(DAMA Collab.)
COLLAR	00	PRL 85 3083	J.I. Collar *et al.*	(SIMPLE Collab.)
AMBROSIO	99	PR D60 082002	M. Ambrosio *et al.*	(Macro Collab.)
BERNABEI	99	PL B450 448	R. Bernabei *et al.*	(DAMA Collab.)
BERNABEI	99D	PRL 83 4918	R. Bernabei *et al.*	(DAMA Collab.)
BRHLIK	99	PL B464 303	M. Brhlik, L. Roszkowski	
DERBIN	99	PAN 62 1886	A.V. Derbin *et al.*	
		Translated from YAF 62 2034.		
KLIMENKO	98	JETPL 67 875	A.A. Klimenko *et al.*	
		Translated from ZETFP 67 835.		
SARSA	97	PR D56 1856	M.L. Sarsa *et al.*	(ZARA)
ALESSAND...	96	PL B384 316	A. Alessandrello *et al.*	(MILA, MILAI, SASSO)
BELLI	96	PL B387 222	P. Belli *et al.*	(DAMA Collab.)
Also		PL B389 783 (erratum)	P. Belli *et al.*	(DAMA Collab.)
BELLI	96C	NC C19 537	P. Belli *et al.*	(DAMA Collab.)
BERNABEI	96	PL B389 757	R. Bernabei *et al.*	(DAMA Collab.)
COLLAR	96	PRL 76 331	J.I. Collar	(SCUC)
SARSA	96	PL B386 458	M.L. Sarsa *et al.*	(ZARA)
Also		PR D56 1856	M.L. Sarsa *et al.*	(ZARA)
SMITH	96	PL B379 299	P.F. Smith *et al.*	(RAL, SHEF, LOIC+)
SNOWDEN-...	96	PRL 76 332	D.P. Snowden-Ifft, E.S. Freeman, P.B. Price	(UCB)
GARCIA	95	PR D51 1458	E. Garcia *et al.*	(ZARA, SCUC, PNL)
QUENBY	95	PL B351 70	J.J. Quenby *et al.*	(LOIC, RAL, SHEF+)
SNOWDEN-...	95	PRL 74 4133	D.P. Snowden-Ifft, E.S. Freeman, P.B. Price	(UCB)
Also		PRL 76 331	J.I. Collar	(SCUC)
Also		PRL 76 332	D.P. Snowden-Ifft, E.S. Freeman, P.B. Price	(UCB)
BECK	94	PL B336 141	M. Beck *et al.*	(MPIH, KIAE, SASSO)
BACCI	92	PL B293 460	C. Bacci *et al.*	(Beijing-Roma-Saclay Collab.)
REUSSER	91	PL B255 143	D. Reusser *et al.*	(NEUC, CIT, PSI)
CALDWELL	88	PRL 61 510	D.O. Caldwell *et al.*	(UCSB, UCB, LBL)

Other Particle Searches

OMITTED FROM SUMMARY TABLE

OTHER PARTICLE SEARCHES

Revised February 2018 by K. Hikasa (Tohoku University).

We collect here those searches which do not appear in any other search categories. These are listed in the following order:

- Concentration of stable particles in matter
- General new physics searches
- Limits on jet-jet resonance in hadron collisions
- Limits on neutral particle production at accelerators
- Limits on charged particles in e^+e^- collisions
- Limits on charged particles in hadron reactions
- Limits on charged particles in cosmic rays
- Searches for quantum black hole production

Note that searches appear in separate sections elsewhere for Higgs bosons (and technipions), other heavy bosons (including W_R, W', Z', leptoquarks, axigluons), axions (including pseudo-Goldstone bosons, Majorons, familons), WIMPs, heavy leptons, heavy neutrinos, free quarks, monopoles, supersymmetric particles, and compositeness.

We no longer list for limits on tachyons and centauros. See our 1994 edition for these limits.

CONCENTRATION OF STABLE PARTICLES IN MATTER

Concentration of Heavy (Charge +1) Stable Particles in Matter

VALUE	CL%	DOCUMENT ID		TECN	COMMENT
• • • We do not use the following data for averages, fits, limits, etc. • • •					
$<4\times10^{-17}$	95	[1] YAMAGATA	93	SPEC	Deep sea water, M=5–1600m_p
$<6\times10^{-15}$	95	[2] VERKERK	92	SPEC	Water, M= 10^5 to 3×10^7 GeV
$<7\times10^{-15}$	95	[2] VERKERK	92	SPEC	Water, M= 10^4, 6×10^7 GeV
$<9\times10^{-15}$	95	[2] VERKERK	92	SPEC	Water, M= 10^8 GeV
$<3\times10^{-23}$	90	[3] HEMMICK	90	SPEC	Water, $M=1000m_p$
$<2\times10^{-21}$	90	[3] HEMMICK	90	SPEC	Water, $M=5000m_p$
$<3\times10^{-20}$	90	[3] HEMMICK	90	SPEC	Water, $M=10000m_p$
$<1.\times10^{-29}$		SMITH	82B	SPEC	Water, M=30–400m_p
$<2.\times10^{-28}$		SMITH	82B	SPEC	Water, M=12–1000m_p
$<1.\times10^{-14}$		SMITH	82B	SPEC	Water, $M>1000\ m_p$
$<(0.2\text{–}1.)\times10^{-21}$		SMITH	79	SPEC	Water, M=6–350 m_p

[1] YAMAGATA 93 used deep sea water at 4000 m since the concentration is enhanced in deep sea due to gravity.

[2] VERKERK 92 looked for heavy isotopes in sea water and put a bound on concentration of stable charged massive particle in sea water. The above bound can be translated into into a bound on charged dark matter particle (5×10^6 GeV), assuming the local density, ρ=0.3 GeV/cm^3, and the mean velocity $\langle v\rangle$=300 km/s.

[3] See HEMMICK 90 Fig. 7 for other masses 100–10000 m_p.

Concentration of Heavy Stable Particles Bound to Nuclei

VALUE	CL%	DOCUMENT ID		TECN	COMMENT
• • • We do not use the following data for averages, fits, limits, etc. • • •					
$<1.2\times10^{-11}$	95	[1] JAVORSEK	01	SPEC	Au, M= 3 GeV
$<6.9\times10^{-10}$	95	[1] JAVORSEK	01	SPEC	Au, M= 144 GeV
$<1\ \times10^{-11}$	95	[2] JAVORSEK	01B	SPEC	Au, M= 188 GeV
$<1\ \times10^{-8}$	95	[2] JAVORSEK	01B	SPEC	Au, M= 1669 GeV
$<6\ \times10^{-9}$	95	[2] JAVORSEK	01B	SPEC	Fe, M= 188 GeV
$<1\ \times10^{-8}$	95	[2] JAVORSEK	01B	SPEC	Fe, M= 647 GeV
$<4\ \times10^{-20}$	90	[3] HEMMICK	90	SPEC	C, $M=100m_p$
$<8\ \times10^{-20}$	90	[3] HEMMICK	90	SPEC	C, $M=1000m_p$
$<2\ \times10^{-16}$	90	[3] HEMMICK	90	SPEC	C, $M=10000m_p$
$<6\ \times10^{-13}$	90	[3] HEMMICK	90	SPEC	Li, $M=1000m_p$
$<1\ \times10^{-11}$	90	[3] HEMMICK	90	SPEC	Be, $M=1000m_p$
$<6\ \times10^{-14}$	90	[3] HEMMICK	90	SPEC	B, $M=1000m_p$
$<4\ \times10^{-17}$	90	[3] HEMMICK	90	SPEC	O, $M=1000m_p$
$<4\ \times10^{-15}$	90	[3] HEMMICK	90	SPEC	F, $M=1000m_p$
$<1.5\times10^{-13}$/nucleon	68	[4] NORMAN	89	SPEC	^{206}PbX^-
$<1.2\times10^{-12}$/nucleon	68	[4] NORMAN	87	SPEC	^{56,58}FeX^-

[1] JAVORSEK 01 search for (neutral) SIMPs (strongly interacting massive particles) bound to Au nuclei. Here M is the effective SIMP mass.

[2] JAVORSEK 01B search for (neutral) SIMPs (strongly interacting massive particles) bound to Au and Fe nuclei from various origins with exposures on the earth's surface, in a satellite, heavy ion collisions, etc. Here M is the mass of the anomalous nucleus. See also JAVORSEK 02.

[3] See HEMMICK 90 Fig. 7 for other masses 100–10000 m_p.

[4] Bound valid up to $m_{X^-}\sim100$ TeV.

GENERAL NEW PHYSICS SEARCHES

This subsection lists some of the search experiments which look for general signatures characteristic of new physics, independent of the framework of a specific model.

The observed events are compatible with Standard Model expectation, unless noted otherwise.

VALUE	DOCUMENT ID		TECN	COMMENT
• • • We do not use the following data for averages, fits, limits, etc. • • •				
	[1] AAD	15AT	ATLS	$t+\not{E}_T$
	[2] KHACHATRY...	15F	CMS	$t+\not{E}_T$
	[3] AALTONEN	14J	CDF	W + 2 jets
	[4] AAD	13A	ATLS	$WW\to\ell\nu\ell'\nu$
	[5] AAD	13C	ATLS	$\gamma+\not{E}_T$
	[6] AALTONEN	13I	CDF	Delayed $\gamma+\not{E}_T$
	[7] CHATRCHYAN	13	CMS	$\ell^+\ell^-$ + jets + $\not{E}_T$
	[8] AAD	12C	ATLS	$t\bar{t}+\not{E}_T$
	[9] AALTONEN	12M	CDF	jet + $\not{E}_T$
	[10] CHATRCHYAN	12AP	CMS	jet + $\not{E}_T$
	[11] CHATRCHYAN	12Q	CMS	Z + jets + $\not{E}_T$
	[12] CHATRCHYAN	12T	CMS	$\gamma+\not{E}_T$
	[13] AAD	11S	ATLS	jet + $\not{E}_T$
	[14] AALTONEN	11AF	CDF	$\ell^\pm\ell^\pm$
	[15] CHATRCHYAN	11C	CMS	$\ell^+\ell^-$ + jets + $\not{E}_T$
	[16] CHATRCHYAN	11U	CMS	jet + $\not{E}_T$
	[17] AALTONEN	10AF	CDF	$\gamma\gamma+\ell$, $\not{E}_T$

[18] AALTONEN 09AF CDF $\ell\gamma b\,\not{E}_T$
[19] AALTONEN 09G CDF $\ell\ell\ell\,\not{E}_T$

[1] AAD 15AT search for events with a top quark and mssing E_T in pp collisions at E_{cm} = 8 TeV with L = 20.3 fb^{-1}.
[2] KHACHATRYAN 15F search for events with a top quark and mssing E_T in pp collisions at E_{cm} = 8 TeV with L = 19.7 fb^{-1}.
[3] AALTONEN 14J examine events with a W and two jets in $p\overline{p}$ collisions at E_{cm} = 1.96 TeV with L = 8.9 fb^{-1}. Invariant mass distributions of the two jets are consistent with the Standard Model expectation.
[4] AAD 13A search for resonant WW production in pp collisions at E_{cm} = 7 TeV with L = 4.7 fb^{-1}.
[5] AAD 13C search for events with a photon and missing $\not{E}_T$ in pp collisions at E_{cm} = 7 TeV with L = 4.6 fb^{-1}.
[6] AALTONEN 13I search for events with a photon and missing E_T, where the photon is detected after the expected timing, in $p\overline{p}$ collisions at E_{cm} = 1.96 TeV with L = 6.3 fb^{-1}. The data are consistent with the Standard Model expectation.
[7] CHATRCHYAN 13 search for events with an opposite-sign lepton pair, jets, and missing E_T in pp collisions at E_{cm} = 7 TeV with L = 4.98 fb^{-1}.
[8] AAD 12C search for events with a $t\overline{t}$ pair and missing $\not{E}_T$ in pp collisions at E_{cm} = 7 TeV with L = 1.04 fb^{-1}.
[9] AALTONEN 12M search for events with a jet and missing E_T in $p\overline{p}$ collisions at E_{cm} = 1.96 TeV with L = 6.7 fb^{-1}.
[10] CHATRCHYAN 12AP search for events with a jet and missing E_T in pp collisions at E_{cm} = 7 TeV with L = 5.0 fb^{-1}.
[11] CHATRCHYAN 12Q search for events with a Z, jets, and missing $\not{E}_T$ in pp collisions at E_{cm} = 7 TeV with L = 4.98 fb^{-1}.
[12] CHATRCHYAN 12T search for events with a photon and missing $\not{E}_T$ in pp collisions at E_{cm} = 7 TeV with L = 5.0 fb^{-1}.
[13] AAD 11S search for events with one jet and missing E_T in pp collisions at E_{cm} = 7 TeV with L = 33 pb^{-1}.
[14] AALTONEN 11AF search for high-p_T like-sign dileptons in $p\overline{p}$ collisions at E_{cm} = 1.96 TeV with L = 6.1 fb^{-1}.
[15] CHATRCHYAN 11C search for events with an opposite-sign lepton pair, jets, and missing E_T in pp collisions at E_{cm} = 7 TeV with L = 34 pb^{-1}.
[16] CHATRCHYAN 11U search for events with one jet and missing E_T in pp collisions at E_{cm} = 7 TeV with L = 36 pb^{-1}.
[17] AALTONEN 10AF search for $\gamma\gamma$ events with e, μ, τ, or missing E_T in $p\overline{p}$ collisions at E_{cm} = 1.96 TeV with L = 1.1–2.0 fb^{-1}.
[18] AALTONEN 09AF search for $\ell\gamma b$ events with missing E_T in $p\overline{p}$ collisions at E_{cm} = 1.96 TeV with L = 1.9 fb^{-1}. The observed events are compatible with Standard Model expectation including $t\overline{t}\gamma$ production.
[19] AALTONEN 09G search for $\mu\mu\mu$ and $\mu\mu e$ events with missing E_T in $p\overline{p}$ collisions at E_{cm} = 1.96 TeV with L = 976 pb^{-1}.

LIMITS ON JET-JET RESONANCES

Heavy Particle Production Cross Section

Limits are for a particle decaying to two hadronic jets.

Units(pb)	CL%	Mass(GeV)	DOCUMENT ID		TECN	COMMENT
• • • We do not use the following data for averages, fits, limits, etc. • • •						
			[1] KHACHATRY...17W	CMS		$pp \to jj$ resonance
			[2] KHACHATRY...17Y	CMS		$pp \to$ (8–10) $j+\not{E}_T$
			[3] SIRUNYAN	17F	CMS	$pp \to jj$ angular distribution
			[4] AABOUD	16	ATLS	$pp \to b$ + jet
			[5] AAD	16N	ATLS	$pp \to$ 3 high E_T jets
			[6] AAD	16S	ATLS	$pp \to jj$ resonance
			[7] KHACHATRY...16K	CMS		$pp \to jj$ resonance
			[8] KHACHATRY...16L	CMS		$pp \to jj$ resonance
			[9] AAD	13D	ATLS	7 TeV $pp \to 2$ jets
			[10] AALTONEN	13R	CDF	1.96 TeV $p\overline{p} \to 4$ jets
			[11] CHATRCHYAN	13A	CMS	7 TeV $pp \to 2$ jets
			[12] CHATRCHYAN	13A	CMS	7 TeV $pp \to b\overline{b}X$
			[13] AAD	12S	ATLS	7 TeV $pp \to 2$ jets
			[14] CHATRCHYAN	12BL	CMS	7 TeV $pp \to t\overline{t}X$
			[15] AAD	11AG	ATLS	7 TeV $pp \to 2$ jets
			[16] AALTONEN	11M	CDF	1.96 TeV $p\overline{p} \to W+2$ jets
			[17] ABAZOV	11I	D0	1.96 TeV $p\overline{p} \to W+2$ jets
			[18] AAD	10	ATLS	7 TeV $pp \to 2$ jets
			[19] KHACHATRY...10		CMS	7 TeV $pp \to 2$ jets
			[20] ABE	99F	CDF	1.8 TeV $p\overline{p} \to b\overline{b}+$ anything
			[21] ABE	97G	CDF	1.8 TeV $p\overline{p} \to 2$ jets
<2603	95	200	[22] ABE	93G	CDF	1.8 TeV $p\overline{p} \to 2$ jets
< 44	95	400	[22] ABE	93G	CDF	1.8 TeV $p\overline{p} \to 2$ jets
< 7	95	600	[22] ABE	93G	CDF	1.8 TeV $p\overline{p} \to 2$ jets

[1] KHACHATRYAN 17W search for dijet resonance in 12.9 fb^{-1} data at 13 TeV; see Fig. 2 for limits on axigluons, diquarks, dark matter mediators etc.
[2] KHACHATRYAN 17Y search for $pp \to$ (8–10) j in 19.7 fb^{-1} at 8 TeV. No signal seen. Limits set on colorons, axigluons, RPV, and SUSY.
[3] SIRUNYAN 17F measure $pp \to jj$ angular distribution in 2.6 fb^{-1} at 13 TeV; limits set on LEDs and quantum black holes.
[4] AABOUD 16 search for resonant dijets including one or two b-jets with 3.2 fb^{-1} at 13 TeV; exclude excited b^* quark from 1.1–2.1 TeV; exclude leptophilic Z' with SM couplings from 1.1–1.5 TeV.
[5] AAD 16N search for ≥ 3 jets with 3.6 fb^{-1} at 13 TeV; limits placed on micro black holes (Fig. 10) and string balls (Fig. 11).
[6] AAD 16S search for high mass jet-jet resonance with 3.6 fb^{-1} at 13 TeV; exclude portions of excited quarks, W', Z' and contact interaction parameter space.
[7] KHACHATRYAN 16K search for dijet resonance in 2.4 fb^{-1} data at 13 TeV; see Fig. 3 for limits on axigluons, diquarks etc.
[8] KHACHATRYAN 16L use data scouting technique to search for jj resonance on 18.8 fb^{-1} of data at 8 TeV. Limits on the coupling of a leptophobic Z' to quarks are set, improving on the results by other experiments in the mass range between 500–800 GeV.
[9] AAD 13D search for dijet resonances in pp collisions at E_{cm} = 7 TeV with L = 4.8 fb^{-1}. The observed events are compatible with Standard Model expectation. See their Fig. 6 and Table 2 for limits on resonance cross section in the range m = 1.0–4.0 TeV.
[10] AALTONEN 13R search for production of a pair of jet-jet resonances in $p\overline{p}$ collisions at E_{cm} = 1.96 TeV with L = 6.6 fb^{-1}. See their Fig. 5 and Tables I, II for cross section limits.
[11] CHATRCHYAN 13A search for qq, qg, and gg resonances in pp collisions at E_{cm} = 7 TeV with L = 4.8 fb^{-1}. See their Fig. 3 and Table 1 for limits on resonance cross section in the range m = 1.0–4.3 TeV.
[12] CHATRCHYAN 13A search for $b\overline{b}$ resonances in pp collisions at E_{cm} = 7 TeV with L = 4.8 fb^{-1}. See their Fig. 8 and Table 4 for limits on resonance cross section in the range m = 1.0–4.0 TeV.
[13] AAD 12S search for dijet resonances in pp collisions at E_{cm} = 7 TeV with L = 1.0 fb^{-1}. See their Fig. 3 and Table 2 for limits on resonance cross section in the range m = 0.9–4.0 TeV.
[14] CHATRCHYAN 12BL search for $t\overline{t}$ resonances in pp collisions at E_{cm} = 7 TeV with L = 4.4 fb^{-1}. See their Fig. 4 for limits on resonance cross section in the range m = 0.5–3.0 TeV.
[15] AAD 11AG search for dijet resonances in pp collisions at E_{cm} = 7 TeV with L = 36 pb^{-1}. Limits on number of events for m = 0.6–4 TeV are given in their Table 3.
[16] AALTONEN 11M find a peak in two jet invariant mass distribution around 140 GeV in W + 2 jet events in $p\overline{p}$ collisions at E_{cm} = 1.96 TeV with L = 4.3 fb^{-1}.
[17] ABAZOV 11I search for two-jet resonances in W + 2 jet events in $p\overline{p}$ collisions at E_{cm} = 1.96 TeV with L = 4.3 fb^{-1} and give limits $\sigma <$ (2.6–1.3) pb (95% CL) for m = 110–170 GeV. The result is incompatible with AALTONEN 11M.
[18] AAD 10 search for narrow dijet resonances in pp collisions at E_{cm} = 7 TeV with L = 315 nb^{-1}. Limits on the cross section in the range 10–10^3 pb is given for m = 0.3–1.7 TeV.
[19] KHACHATRYAN 10 search for narrow dijet resonances in pp collisions at E_{cm} = 7 TeV with L = 2.9 pb^{-1}. Limits on the cross section in the range 1–300 pb is given for m = 0.5–2.6 TeV separately in the final states qq, qg, and gg.
[20] ABE 99F search for narrow $b\overline{b}$ resonances in $p\overline{p}$ collisions at E_{cm}=1.8 TeV. Limits on $\sigma(p\overline{p} \to X+$ anything$)\times$B($X \to b\overline{b}$) in the range 3–10^3 pb (95%CL) are given for m_X=200–750 GeV. See their Table I.
[21] ABE 97G search for narrow dijet resonances in $p\overline{p}$ collisions with 106 pb^{-1} of data at E_{cm} = 1.8 TeV. Limits on $\sigma(p\overline{p} \to X+$ anything$)\cdot$B($X \to jj$) in the range 10^4–10^{-1} pb (95%CL) are given for dijet mass m=200–1150 GeV with both jets having $|\eta| < 2.0$ and the dijet system having $|\cos\theta^*| < 0.67$. See their Table I for the list of limits. Supersedes ABE 93G.
[22] ABE 93G give cross section times branching ratio into light (d, u, s, c, b) quarks for Γ = 0.02 M. Their Table II gives limits for M = 200–900 GeV and Γ = (0.02–0.2) M.

LIMITS ON NEUTRAL PARTICLE PRODUCTION

Production Cross Section of Radiatively-Decaying Neutral Particle

VALUE (pb)	CL%	DOCUMENT ID		TECN	COMMENT
• • • We do not use the following data for averages, fits, limits, etc. • • •					
		[1] KHACHATRY...17D	CMS		$Z\gamma$ resonance
<0.0008	95	[2] AAD	16AI	ATLS	$pp \to \gamma$ + jet
		[3] KHACHATRY...16M	CMS		$pp \to \gamma\gamma$ resonance
<(0.043–0.17)	95	[4] ABBIENDI	00D	OPAL	$e^+e^- \to X^0Y^0$, $X^0 \to Y^0\gamma$
<(0.05–0.8)	95	[5] ABBIENDI	00D	OPAL	$e^+e^- \to X^0X^0$, $X^0 \to Y^0\gamma$
<(2.5–0.5)	95	[6] ACKERSTAFF	97B	OPAL	$e^+e^- \to X^0Y^0$, $X^0 \to Y^0\gamma$
<(1.6–0.9)	95	[7] ACKERSTAFF	97B	OPAL	$e^+e^- \to X^0X^0$, $X^0 \to Y^0\gamma$

[1] KHACHATRYAN 17D search for new scalar resonance decaying to $Z\gamma$ with $Z \to e^+e^-$, $\mu^+\mu^-$ in pp collisions at 8 and 13 TeV; no signal seen.
[2] AAD 16AI search for excited quarks (EQ) and quantum black holes (QBH) in 3.2 fb^{-1} at 13 TeV of data; exclude EQ below 4.4 TeV and QBH below 3.8 (6.2) TeV for RS1 (ADD) models. The visible cross section limit was obtained for 5 TeV resonance with σ_G/M_G = 2%.
[3] KHACHATRYAN 16M search for $\gamma\gamma$ resonance using 19.7 fb^{-1} at 8 TeV and 3.3 fb^{-1} at 13 Tev; slight excess at 750 GeV noted; limit set on RS graviton.
[4] ABBIENDI 00D associated production limit is for m_{X^0}= 90–188 GeV, m_{Y^0}=0 at E_{cm}=189 GeV. See also their Fig. 9.
[5] ABBIENDI 00D pair production limit is for m_{X^0} = 45–94 GeV, m_{Y^0}=0 at E_{cm}=189 GeV. See also their Fig. 12.
[6] ACKERSTAFF 97B associated production limit is for m_{X^0} = 80–160 GeV, m_{Y^0}=0 from 10.0 pb^{-1} at E_{cm} = 161 GeV. See their Fig. 3(a).
[7] ACKERSTAFF 97B pair production limit is for m_{X^0} = 40–80 GeV, m_{Y^0}=0 from 10.0 pb^{-1} at E_{cm} = 161 GeV. See their Fig. 3(b).

Heavy Particle Production Cross Section

VALUE (cm^2/N)	CL%	DOCUMENT ID		TECN	COMMENT
• • • We do not use the following data for averages, fits, limits, etc. • • •					
		[1] AABOUD	17B	ATLS	WH, ZH resonance
		[2] AAIJ	17BR	LHCB	$pp \to \pi_V\pi_V$, $\pi_V \to jj$

		[3] AAD	16O	ATLS	ℓ + (ℓs or jets)
		[4] AAD	16R	ATLS	WW, WZ, ZZ resonance
		[5] LEES	15E	BABR	e^+e^- collisions
		[6] ADAMS	97B	KTEV	m= 1.2–5 GeV
$< 10^{-36}$–10^{-33}	90	[7] GALLAS	95	TOF	m= 0.5–20 GeV
$<(4$–$0.3)\times10^{-31}$	95	[8] AKESSON	91	CNTR	m = 0–5 GeV
$<2\times10^{-36}$	90	[9] BADIER	86	BDMP	$\tau = (0.05$–$1.)\times10^{-8}$ s
$<2.5\times10^{-35}$		[10] GUSTAFSON	76	CNTR	$\tau > 10^{-7}$ s

[1] AABOUD 17B exclude m(W', Z') < 1.49–2.31 TeV depending on the couplings and W'/Z' degeneracy assumptions via WH, ZH search in pp collisions at 13 TeV with 3.2 fb^{-1} of data.

[2] AAIJ 17BR search for long-lived hidden valley pions from Higgs decay. Limits are set on the signal strength as a function of the mass and lifetime of the long-lived particle in their Fig. 4 and Tab. 4.

[3] AAD 16O search for high E_T ℓ + (ℓs or jets) with 3.2 fb^{-1} at 13 TeV; exclude micro black holes mass < 8 TeV (Fig. 3) for models with two extra dimensions.

[4] AAD 16R search for WW, WZ, ZZ resonance in 20.3 fb^{-1} at 8 TeV data; limits placed on massive RS graviton (Fig. 4).

[5] LEES 15E search for long-lived neutral particles produced in e^+e^- collisions in the Upsilon region, which decays into e^+e^-, $\mu^+\mu^-$, $e^\pm\mu^\mp$, $\pi^+\pi^-$, K^+K^-, or $\pi^\pm K^\mp$. See their Fig. 2 for cross section limits.

[6] ADAMS 97B search for a hadron-like neutral particle produced in pN interactions, which decays into a ρ^0 and a weakly interacting massive particle. Upper limits are given for the ratio to K_L production for the mass range 1.2–5 GeV and lifetime 10^{-9}–10^{-4} s. See also our Light Gluino Section.

[7] GALLAS 95 limit is for a weakly interacting neutral particle produced in 800 GeV/c pN interactions decaying with a lifetime of 10^{-4}–10^{-8} s. See their Figs. 8 and 9. Similar limits are obtained for a stable particle with interaction cross section 10^{-29}–10^{-33} cm^2. See Fig. 10.

[8] AKESSON 91 limit is from weakly interacting neutral long-lived particles produced in pN reaction at 450 GeV/c performed at CERN SPS. Bourquin-Gaillard formula is used as the production model. The above limit is for $\tau > 10^{-7}$ s. For $\tau > 10^{-9}$ s, $\sigma < 10^{-30}$ cm^{-2}/nucleon is obtained.

[9] BADIER 86 looked for long-lived particles at 300 GeV π^- beam dump. The limit applies for nonstrongly interacting neutral or charged particles with mass >2 GeV. The limit applies for particle modes, $\mu^+\pi^-$, $\mu^+\mu^-$, $\pi^+\pi^-$X, $\pi^+\pi^-\pi^\pm$ etc. See their figure 5 for the contours of limits in the mass-τ plane for each mode.

[10] GUSTAFSON 76 is a 300 GeV FNAL experiment looking for heavy (m >2 GeV) long-lived neutral hadrons in the M4 neutral beam. The above typical value is for m = 3 GeV and assumes an interaction cross section of 1 mb. Values as a function of mass and interaction cross section are given in figure 2.

Production of New Penetrating Non-ν Like States in Beam Dump

VALUE	DOCUMENT ID		TECN	COMMENT
• • • We do not use the following data for averages, fits, limits, etc. • • •				
	[1] LOSECCO	81	CALO	28 GeV protons

[1] No excess neutral-current events leads to σ(production) × σ(interaction)×acceptance $< 2.26\times10^{-71}$ cm^4/nucleon^2 (CL = 90%) for light neutrals. Acceptance depends on models (0.1 to 4. × 10^{-4}).

LIMITS ON CHARGED PARTICLES IN e^+e^-

Heavy Particle Production Cross Section in e^+e^-

Ratio to $\sigma(e^+e^-\to\mu^+\mu^-)$ unless noted. See also entries in Free Quark Search and Magnetic Monopole Searches.

VALUE	CL%	DOCUMENT ID		TECN	COMMENT
• • • We do not use the following data for averages, fits, limits, etc. • • •					
$<1\times10^{-3}$	90	[1] ABLIKIM	17AA	BES3	$e^+e^-\to\ell\overline{\ell}\gamma$
		[2] ACKERSTAFF	98P	OPAL	Q=1,2/3, m=45–89.5 GeV
		[3] ABREU	97D	DLPH	Q=1,2/3, m=45–84 GeV
		[4] BARATE	97K	ALEP	Q=1, m=45–85 GeV
$<2\times10^{-5}$	95	[5] AKERS	95R	OPAL	Q=1, m= 5–45 GeV
$<1\times10^{-5}$	95	[5] AKERS	95R	OPAL	Q=2, m= 5–45 GeV
$<2\times10^{-3}$	90	[6] BUSKULIC	93C	ALEP	Q=1, m=32–72 GeV
$<(10^{-2}$–1)	95	[7] ADACHI	90C	TOPZ	Q=1, m=1–16, 18–27 GeV
$<7\times10^{-2}$	90	[8] ADACHI	90E	TOPZ	Q = 1, m = 5–25 GeV
$<1.6\times10^{-2}$	95	[9] KINOSHITA	82	PLAS	Q=3–180, m <14.5 GeV
$<5.0\times10^{-2}$	90	[10] BARTEL	80	JADE	Q=(3,4,5)/3 2–12 GeV

[1] ABLIKIM 17AA search for dark photon $A\to\ell\overline{\ell}$ at 3.773 GeV with 2.93 fb^{-1}. Limits are set in ϵ vs m(A) plane.

[2] ACKERSTAFF 98P search for pair production of long-lived charged particles at E_{cm} between 130 and 183 GeV and give limits σ <(0.05–0.2) pb (95%CL) for spin-0 and spin-1/2 particles with m=45–89.5 GeV, charge 1 and 2/3. The limit is translated to the cross section at E_{cm}=183 GeV with the s dependence described in the paper. See their Figs. 2–4.

[3] ABREU 97D search for pair production of long-lived particles and give limits σ <(0.4–2.3) pb (95%CL) for various center-of-mass energies E_{cm}=130–136, 161, and 172 GeV, assuming an almost flat production distribution in cosθ.

[4] BARATE 97K search for pair production of long-lived charged particles at E_{cm} = 130, 136, 161, and 172 GeV and give limits σ <(0.2–0.4) pb (95%CL) for spin-0 and spin-1/2 particles with m=45–85 GeV. The limit is translated to the cross section at E_{cm}=172 GeV with the E_{cm} dependence described in the paper. See their Figs. 2 and 3 for limits on J = 1/2 and J = 0 cases.

[5] AKERS 95R is a CERN-LEP experiment with $W_{cm}\sim m_Z$. The limit is for the production of a stable particle in multihadron events normalized to $\sigma(e^+e^-\to$ hadrons). Constant phase space distribution is assumed. See their Fig. 3 for bounds for $Q=\pm2/3$, $\pm4/3$.

[6] BUSKULIC 93C is a CERN-LEP experiment with $W_{cm} = m_Z$. The limit is for a pair or single production of heavy particles with unusual ionization loss in TPC. See their Fig. 5 and Table 1.

[7] ADACHI 90C is a KEK-TRISTAN experiment with W_{cm} = 52–60 GeV. The limit is for pair production of a scalar or spin-1/2 particle. See Figs. 3 and 4.

[8] ADACHI 90E is KEK-TRISTAN experiment with W_{cm} = 52–61.4 GeV. The above limit is for inclusive production cross section normalized to $\sigma(e^+e^-\to\mu^+\mu^-)\cdot\beta(3-\beta^2)/2$, where $\beta=(1-4m^2/W_{cm}^2)^{1/2}$. See the paper for the assumption about the production mechanism.

[9] KINOSHITA 82 is SLAC PEP experiment at W_{cm} = 29 GeV using lexan and ^{39}Cr plastic sheets sensitive to highly ionizing particles.

[10] BARTEL 80 is DESY-PETRA experiment with W_{cm} = 27–35 GeV. Above limit is for inclusive pair production and ranges between 1. × 10^{-1} and 1. × 10^{-2} depending on mass and production momentum distributions. (See their figures 9, 10, 11).

Branching Fraction of Z^0 to a Pair of Stable Charged Heavy Fermions

VALUE	CL%	DOCUMENT ID		TECN	COMMENT
• • • We do not use the following data for averages, fits, limits, etc. • • •					
$<5\times10^{-6}$	95	[1] AKERS	95R	OPAL	m= 40.4–45.6 GeV
$<1\times10^{-3}$	95	AKRAWY	90O	OPAL	m = 29–40 GeV

[1] AKERS 95R give the 95% CL limit $\sigma(X\overline{X})/\sigma(\mu\mu) < 1.8\times10^{-4}$ for the pair production of singly- or doubly-charged stable particles. The limit applies for the mass range 40.4–45.6 GeV for $X^\pm$ and < 45.6 GeV for $X^{\pm\pm}$. See the paper for bounds for $Q=\pm2/3$, $\pm4/3$.

LIMITS ON CHARGED PARTICLES IN HADRONIC REACTIONS

MASS LIMITS for Long-Lived Charged Heavy Fermions

Limits are for spin 1/2 particles with no color and SU(2)$_L$ charge. The electric charge Q of the particle (in the unit of e) is therefore equal to its weak hypercharge. Pair production by Drell-Yan like γ and Z exchange is assumed to derive the limits.

VALUE (GeV)	CL%	DOCUMENT ID		TECN	COMMENT
• • • We do not use the following data for averages, fits, limits, etc. • • •					
>660	95	[1] AAD	15BJ	ATLS	$\|Q\|$ = 2
>200	95	[2] CHATRCHYAN	13AB	CMS	$\|Q\|$ = 1/3
>480	95	[2] CHATRCHYAN	13AB	CMS	$\|Q\|$ = 2/3
>574	95	[2] CHATRCHYAN	13AB	CMS	$\|Q\|$ = 1
>685	95	[2] CHATRCHYAN	13AB	CMS	$\|Q\|$ = 2
>140	95	[3] CHATRCHYAN	13AR	CMS	$\|Q\|$ = 1/3
>310	95	[3] CHATRCHYAN	13AR	CMS	$\|Q\|$ = 2/3

[1] AAD 15BJ use 20.3 fb^{-1} of pp collisions at E_{cm} = 8 TeV. See paper for limits for $|Q|$ = 3, 4, 5, 6.

[2] CHATRCHYAN 13AB use 5.0 fb^{-1} of pp collisions at E_{cm} = 7 TeV and 18.8 fb^{-1} at E_{cm} = 8 TeV. See paper for limits for $|Q|$ = 3, 4,..., 8.

[3] CHATRCHYAN 13AR use 5.0 fb^{-1} of pp collisions at E_{cm} = 7 TeV.

Heavy Particle Production Cross Section

VALUE (nb)	CL%	DOCUMENT ID		TECN	COMMENT
• • • We do not use the following data for averages, fits, limits, etc. • • •					
		[1] AABOUD	17D	ATLS	anomalous $WWjj$, $WZjj$
		[2] AABOUD	17L	ATLS	m>870 GeV, $Z(\to\nu\nu)tX$
		[3] SIRUNYAN	17B	CMS	tH
		[4] SIRUNYAN	17C	CMS	Z + (t or b)
		[5] SIRUNYAN	17J	CMS	$X_{5/3}\to tW$
		[6] AAIJ	15BD	LHCB	m=124–309 GeV
		[7] AAD	13AH	ATLS	$\|q\|$=(2–6)e, m=50–600 GeV
$<1.2\times10^{-3}$	95	[8] AAD	11I	ATLS	$\|q\|$=10e, m=0.2–1 TeV
$<1.0\times10^{-5}$	95	[9,10] AALTONEN	09Z	CDF	m>100 GeV, noncolored
$<4.8\times10^{-5}$	95	[9,11] AALTONEN	09Z	CDF	m>100 GeV, colored
<0.31–0.04×10^{-3}	95	[12] ABAZOV	09M	D0	pair production
<0.19	95	[13] AKTAS	04C	H1	m=3–10 GeV
<0.05	95	[14] ABE	92J	CDF	m=50–200 GeV
<30–130		[15] CARROLL	78	SPEC	m=2–2.5 GeV
<100		[16] LEIPUNER	73	CNTR	m=3–11 GeV

[1] AABOUD 17D search for $WWjj$, $WZjj$ in pp collisions at 8 TeV with 3.2 fb^{-1}; set limits on anomalous couplings.

[2] AABOUD 17L search for the pair production of heavy vector-like T quarks in the $Z(\to\nu\nu)tX$ final state.

[3] SIRUNYAN 17B search for vector-like quark $pp\to TX\to tHX$ in 2.3 fb^{-1} at 13 TeV; no signal seen; limits placed.

[4] SIRUNYAN 17C search for vector-like quark $pp\to TX\to Z$ + (t or b) in 2.3 fb^{-1} at 13 TeV; no signal seen; limits placed.

[5] SIRUNYAN 17J search for $pp\to X_{5/3}X_{5/3}\to tWtW$ with 2.3 fb^{-1} at 13 TeV. No signal seen: m(X) > 1020 (990) GeV for RH (LH) new charge 5/3 quark.

[6] AAIJ 15BD search for production of long-lived particles in pp collisions at E_{cm} = 7 and 8 TeV. See their Table 6 for cross section limits.

[7] AAD 13AH search for production of long-lived particles with |q|=(2–6)e in pp collisions at E_{cm} = 7 TeV with 4.4 fb^{-1}. See their Fig. 8 for cross section limits.

[8] AAD 11I search for production of highly ionizing massive particles in pp collisions at E_{cm} = 7 TeV with L = 3.1 pb^{-1}. See their Table 5 for similar limits for |q| = 6e and 17e, Table 6 for limits on pair production cross section.

[9] AALTONEN 09Z search for long-lived charged particles in $p\overline{p}$ collisions at E_{cm} = 1.96 TeV with L = 1.0 fb^{-1}. The limits are on production cross section for a particle of mass above 100 GeV in the region $|\eta|\lesssim0.7$, p_T > 40 GeV, and 0.4 < β < 1.0.

[10] Limit for weakly interacting charge-1 particle.

[11] Limit for up-quark like particle.

[12] ABAZOV 09M search for pair production of long-lived charged particles in $p\overline{p}$ collisions at E_{cm} = 1.96 TeV with L = 1.1 fb^{-1}. Limit on the cross section of (0.31–0.04) pb (95% CL) is given for the mass range of 60–300 GeV, assuming the kinematics of stau pair production.
[13] AKTAS 04C look for charged particle photoproduction at HERA with mean c.m. energy of 200 GeV.
[14] ABE 92J look for pair production of unit-charged particles which leave detector before decaying. Limit shown here is for m=50 GeV. See their Fig. 5 for different charges and stronger limits for higher mass.
[15] CARROLL 78 look for neutral, $S = -2$ dihyperon resonance in $pp \rightarrow 2K^+X$. Cross section varies within above limits over mass range and p_{lab} = 5.1–5.9 GeV/c.
[16] LEIPUNER 73 is an NAL 300 GeV p experiment. Would have detected particles with lifetime greater than 200 ns.

Heavy Particle Production Differential Cross Section

VALUE (cm^{2}sr^{-1}GeV^{-1})	CL%	DOCUMENT ID		TECN	CHG	COMMENT
• • • We do not use the following data for averages, fits, limits, etc. • • •						
$<2.6\times10^{-36}$	90	[1] BALDIN	76	CNTR	−	Q= 1, m=2.1–9.4 GeV
$<2.2\times10^{-33}$	90	[2] ALBROW	75	SPEC	±	Q= ±1, m=4–15 GeV
$<1.1\times10^{-33}$	90	[2] ALBROW	75	SPEC	±	Q= ±2, m=6–27 GeV
$<8.\times10^{-35}$	90	[3] JOVANOV...	75	CNTR	±	m=15–26 GeV
$<1.5\times10^{-34}$	90	[3] JOVANOV...	75	CNTR	±	Q= ±2, m=3–10 GeV
$<6.\times10^{-35}$	90	[3] JOVANOV...	75	CNTR	±	Q= ±2, m=10–26 GeV
$<1.\times10^{-31}$	90	[4] APPEL	74	CNTR	±	m=3.2–7.2 GeV
$<5.8\times10^{-34}$	90	[5] ALPER	73	SPEC	±	m=1.5–24 GeV
$<1.2\times10^{-35}$	90	[6] ANTIPOV	71B	CNTR	−	Q=−, m=2.2–2.8
$<2.4\times10^{-35}$	90	[7] ANTIPOV	71C	CNTR	−	Q=−, m=1.2–1.7, 2.1–4
$<2.4\times10^{-35}$	90	BINON	69	CNTR	−	Q=−, m=1–1.8 GeV
$<1.5\times10^{-36}$		[8] DORFAN	65	CNTR		Be target m=3–7 GeV
$<3.0\times10^{-36}$		[8] DORFAN	65	CNTR		Fe target m=3–7 GeV

[1] BALDIN 76 is a 70 GeV Serpukhov experiment. Value is per Al nucleus at $\theta = 0$. For other charges in range −0.5 to −3.0, CL = 90% limit is $(2.6\times10^{-36})/|(\text{charge})|$ for mass range (2.1–9.4 GeV) × $|(\text{charge})|$. Assumes stable particle interacting with matter as do antiprotons.
[2] ALBROW 75 is a CERN ISR experiment with E_{cm} = 53 GeV. θ = 40 mr. See figure 5 for mass ranges up to 35 GeV.
[3] JOVANOVICH 75 is a CERN ISR 26+26 and 15+15 GeV pp experiment. Figure 4 covers ranges Q = 1/3 to 2 and m = 3 to 26 GeV. Value is per GeV momentum.
[4] APPEL 74 is NAL 300 GeV pW experiment. Studies forward production of heavy (up to 24 GeV) charged particles with momenta 24–200 GeV (−charge) and 40–150 GeV (+charge). Above typical value is for 75 GeV and is per GeV momentum per nucleon.
[5] ALPER 73 is CERN ISR 26+26 GeV pp experiment. p >0.9 GeV, 0.2 < β <0.65.
[6] ANTIPOV 71B is from same 70 GeV p experiment as ANTIPOV 71C and BINON 69.
[7] ANTIPOV 71C limit inferred from flux ratio. 70 GeV p experiment.
[8] DORFAN 65 is a 30 GeV/c p experiment at BNL. Units are per GeV momentum per nucleus.

Long-Lived Heavy Particle Invariant Cross Section

VALUE (cm^2/GeV^2/N)	CL%	DOCUMENT ID		TECN	CHG	COMMENT
• • • We do not use the following data for averages, fits, limits, etc. • • •						
<5–700×10^{-35}	90	[1] BERNSTEIN	88	CNTR		
<5–700×10^{-37}	90	[1] BERNSTEIN	88	CNTR		
$<2.5\times10^{-36}$	90	[2] THRON	85	CNTR	−	Q= 1, m=4–12 GeV
$<1.\times10^{-35}$	90	[2] THRON	85	CNTR	+	Q= 1, m=4–12 GeV
$<6.\times10^{-33}$	90	[3] ARMITAGE	79	SPEC		m=1.87 GeV
$<1.5\times10^{-33}$	90	[3] ARMITAGE	79	SPEC		m=1.5–3.0 GeV
		[4] BOZZOLI	79	CNTR	±	Q = (2/3, 1, 4/3, 2)
$<1.1\times10^{-37}$	90	[5] CUTTS	78	CNTR		m=4–10 GeV
$<3.0\times10^{-37}$	90	[6] VIDAL	78	CNTR		m=4.5–6 GeV

[1] BERNSTEIN 88 limits apply at x = 0.2 and p_T = 0. Mass and lifetime dependence of limits are shown in the regions: m = 1.5–7.5 GeV and $\tau = 10^{-8}$–2×10^{-6} s. First number is for hadrons; second is for weakly interacting particles.
[2] THRON 85 is FNAL 400 GeV proton experiment. Mass determined from measured velocity and momentum. Limits are for $\tau > 3\times10^{-9}$ s.
[3] ARMITAGE 79 is CERN-ISR experiment at E_{cm} = 53 GeV. Value is for x = 0.1 and p_T = 0.15. Observed particles at m = 1.87 GeV are found all consistent with being antideuterons.
[4] BOZZOLI 79 is CERN-SPS 200 GeV pN experiment. Looks for particle with τ larger than 10^{-8} s. See their figure 11–18 for production cross-section upper limits vs mass.
[5] CUTTS 78 is pBe experiment at FNAL sensitive to particles of $\tau > 5\times10^{-8}$ s. Value is for −0.3 <x <0 and p_T = 0.175.
[6] VIDAL 78 is FNAL 400 GeV proton experiment. Value is for x = 0 and p_T = 0. Puts lifetime limit of $< 5\times10^{-8}$ s on particle in this mass range.

Long-Lived Heavy Particle Production (σ(Heavy Particle) / $\sigma(\pi)$)

VALUE	EVTS	DOCUMENT ID		TECN	CHG	COMMENT
• • • We do not use the following data for averages, fits, limits, etc. • • •						
$<10^{-8}$		[1] NAKAMURA	89	SPEC	±	Q= (−5/3,±2)
	0	[2] BUSSIERE	80	CNTR	±	Q= (2/3,1,4/3,2)

[1] NAKAMURA 89 is KEK experiment with 12 GeV protons on Pt target. The limit applies for mass $\lesssim$ 1.6 GeV and lifetime $\gtrsim 10^{-7}$ s.
[2] BUSSIERE 80 is CERN-SPS experiment with 200–240 GeV protons on Be and Al target. See their figures 6 and 7 for cross-section ratio vs mass.

Production and Capture of Long-Lived Massive Particles

VALUE (10^{-36} cm^2)	DOCUMENT ID		TECN	COMMENT
• • • We do not use the following data for averages, fits, limits, etc. • • •				
<20 to 800	[1] ALEKSEEV	76	ELEC	τ=5 ms to 1 day
<200 to 2000	[1] ALEKSEEV	76B	ELEC	τ=100 ms to 1 day
<1.4 to 9	[2] FRANKEL	75	CNTR	τ=50 ms to 10 hours
<0.1 to 9	[3] FRANKEL	74	CNTR	τ=1 to 1000 hours

[1] ALEKSEEV 76 and ALEKSEEV 76B are 61–70 GeV p Serpukhov experiment. Cross section is per Pb nucleus.
[2] FRANKEL 75 is extension of FRANKEL 74.
[3] FRANKEL 74 looks for particles produced in thick Al targets by 300–400 GeV/c protons.

Long-Lived Particle Search at Hadron Collisions

Limits are for cross section times branching ratio.

VALUE (pb/nucleon)	CL%	DOCUMENT ID		TECN	COMMENT
• • • We do not use the following data for averages, fits, limits, etc. • • •					
		[1] AAIJ	16AR	LHCB	$H \rightarrow XX$ long-lived particles
		[2] KHACHATRY...	16BW	CMS	direct production: HSCPs
<2	90	[3] BADIER	86	BDMP	$\tau = (0.05–1.)\times10^{-8}$s

[1] AAIJ 16AR search for long lived particles from $H \rightarrow XX$ with displaced X decay vertex using 0.62 fb^{-1} at 7 TeV; limits set in Fig. 7.
[2] KHACHATRYAN 16BW search for heavy stable charged particles via ToF with 2.5 fb^{-1} at 13 TeV; require stable m(gluinoball) > 1610 GeV.
[3] BADIER 86 looked for long-lived particles at 300 GeV π^- beam dump. The limit applies for nonstrongly interacting neutral or charged particles with mass >2 GeV. The limit applies for particle modes, $\mu^+\pi^-$, $\mu^+\mu^-$, $\pi^+\pi^-$X, $\pi^+\pi^-\pi^\pm$ etc. See their figure 5 for the contours of limits in the mass-τ plane for each mode.

Long-Lived Heavy Particle Cross Section

VALUE (pb/sr)	CL%	DOCUMENT ID		TECN	COMMENT
• • • We do not use the following data for averages, fits, limits, etc. • • •					
<34	95	[1] RAM	94	SPEC	$1015<m_{X^{++}}<1085$ MeV
<75	95	[1] RAM	94	SPEC	$920<m_{X^{++}}<1025$ MeV

[1] RAM 94 search for a long-lived doubly-charged fermion X^{++} with mass between m_N and m_N+m_π and baryon number +1 in the reaction $pp \rightarrow X^{++}n$. No candidate is found. The limit is for the cross section at 15° scattering angle at 460 MeV incident energy and applies for $\tau(X^{++}) \gg 0.1\,\mu$s.

LIMITS ON CHARGED PARTICLES IN COSMIC RAYS

Heavy Particle Flux in Cosmic Rays

VALUE (cm^{-2}sr^{-1}s^{-1})		CL%	EVTS	DOCUMENT ID		TECN	CHG	COMMENT
• • • We do not use the following data for averages, fits, limits, etc. • • •								
< 1	$\times10^{-8}$	90	0	[1] AGNESE	15	CDM2		Q = 1/6
~ 6	$\times10^{-9}$		2	[2] SAITO	90			$Q \simeq$ 14, $m \simeq 370m_p$
< 1.4	$\times10^{-12}$	90	0	[3] MINCER	85	CALO		$m \geq$ 1 TeV
				[4] SAKUYAMA	83B	PLAS		$m \sim$ 1 TeV
< 1.7	$\times10^{-11}$	99	0	[5] BHAT	82	CC		
< 1.	$\times10^{-9}$	90	0	[6] MARINI	82	CNTR	±	Q= 1, $m \sim 4.5m_p$
2.	$\times10^{-9}$		3	[7] YOCK	81	SPRK	±	Q= 1, $m \sim 4.5m_p$
			3	[7] YOCK	81	SPRK		Fractionally charged
3.0	$\times10^{-9}$		3	[8] YOCK	80	SPRK		$m \sim 4.5\ m_p$
(4 ±1)	$\times10^{-11}$		3	GOODMAN	79	ELEC		$m \geq$ 5 GeV
< 1.3	$\times10^{-9}$	90		[9] BHAT	78	CNTR	±	m >1 GeV
< 1.0	$\times10^{-9}$		0	BRIATORE	76	ELEC		
< 7.	$\times10^{-10}$	90	0	YOCK	75	ELEC	±	Q >7e or < −7e
> 6.	$\times10^{-9}$		5	[10] YOCK	74	CNTR		m >6 GeV
< 3.0	$\times10^{-8}$		0	DARDO	72	CNTR		
< 1.5	$\times10^{-9}$		0	TONWAR	72	CNTR		m >10 GeV
< 3.0	$\times10^{-10}$		0	BJORNBOE	68	CNTR		m >5 GeV
< 5.0	$\times10^{-11}$	90	0	JONES	67	ELEC		m=5–15 GeV

[1] See AGNESE 15 Fig. 6 for limits extending down to Q = 1/200.
[2] SAITO 90 candidates carry about 450 MeV/nucleon. Cannot be accounted for by conventional backgrounds. Consistent with strange quark matter hypothesis.
[3] MINCER 85 is high statistics study of calorimeter signals delayed by 20–200 ns. Calibration with AGS beam shows they can be accounted for by rare fluctuations in signals from low-energy hadrons in the shower. Claim that previous delayed signals including BJORNBOE 68, DARDO 72, BHAT 82, SAKUYAMA 83B below may be due to this fake effect.
[4] SAKUYAMA 83B analyzed 6000 extended air shower events. Increase of delayed particles and change of lateral distribution above 10^{17} eV may indicate production of very heavy parent at top of atmosphere.
[5] BHAT 82 observed 12 events with delay > 2.×10^{-8} s and with more than 40 particles. 1 eV has good hadron shower. However all events are delayed in only one of two detectors in cloud chamber, and could not be due to strongly interacting massive particle.
[6] MARINI 82 applied PEP-counter for TOF. Above limit is for velocity = 0.54 of light. Limit is inconsistent with YOCK 80 YOCK 81 events if isotropic dependence on zenith angle is assumed.
[7] YOCK 81 saw another 3 events with $Q = \pm1$ and m about $4.5m_p$ as well as 2 events with $m > 5.3m_p$, $Q = \pm0.75 \pm 0.05$ and $m > 2.8m_p$, $Q = \pm0.70 \pm 0.05$ and 1 event with $m = (9.3 \pm 3.)m_p$, $Q = \pm0.89 \pm 0.06$ as possible heavy candidates.

[8] YOCK 80 events are with charge exactly or approximately equal to unity.
[9] BHAT 78 is at Kolar gold fields. Limit is for $\tau > 10^{-6}$ s.
[10] YOCK 74 events could be tritons.

Superheavy Particle (Quark Matter) Flux in Cosmic Rays

VALUE ($cm^{-2}sr^{-1}s^{-1}$)	CL%	DOCUMENT ID		TECN	COMMENT
• • • We do not use the following data for averages, fits, limits, etc. • • •					
		[1] ADRIANI	15	PMLA	$4 < m < 1.2 \times 10^5$ m_p
$<5 \times 10^{-16}$	90	[2] AMBROSIO	00B	MCRO	$m > 5 \times 10^{14}$ GeV
$<1.8 \times 10^{-12}$	90	[3] ASTONE	93	CNTR	$m \geq 1.5 \times 10^{-13}$gram
$<1.1 \times 10^{-14}$	90	[4] AHLEN	92	MCRO	$10^{-10} < m < 0.1$ gram
$<2.2 \times 10^{-14}$	90	[5] NAKAMURA	91	PLAS	$m > 10^{11}$ GeV
$<6.4 \times 10^{-16}$	90	[6] ORITO	91	PLAS	$m > 10^{12}$ GeV
$<2.0 \times 10^{-11}$	90	[7] LIU	88	BOLO	$m > 1.5 \times 10^{-13}$ gram
$<4.7 \times 10^{-12}$	90	[8] BARISH	87	CNTR	$1.4 \times 10^8 < m < 10^{12}$ GeV
$<3.2 \times 10^{-11}$	90	[9] NAKAMURA	85	CNTR	$m > 1.5 \times 10^{-13}$gram
$<3.5 \times 10^{-11}$	90	[10] ULLMAN	81	CNTR	Planck-mass 10^{19}GeV
$<7. \times 10^{-11}$	90	[10] ULLMAN	81	CNTR	$m \leq 10^{16}$ GeV

[1] ADRIANI 15 search for relatively light quark matter with charge $Z = 1$–8. See their Figs. 2 and 3 for flux upper limits.
[2] AMBROSIO 00B searched for quark matter ("nuclearites") in the velocity range $(10^{-5}$–1) c. The listed limit is for 2×10^{-3} c.
[3] ASTONE 93 searched for quark matter ("nuclearites") in the velocity range $(10^{-3}$–1) c. Their Table 1 gives a compilation of searches for nuclearites.
[4] AHLEN 92 searched for quark matter ("nuclearites"). The bound applies to velocity $< 2.5 \times 10^{-3}$ c. See their Fig. 3 for other velocity/c and heavier mass range.
[5] NAKAMURA 91 searched for quark matter in the velocity range $(4 \times 10^{-5}$–1) c.
[6] ORITO 91 searched for quark matter. The limit is for the velocity range $(10^{-4}$–$10^{-3})$ c.
[7] LIU 88 searched for quark matter ("nuclearites") in the velocity range $(2.5 \times 10^{-3}$–1)c. A less stringent limit of 5.8×10^{-11} applies for (1–2.5) $\times 10^{-3}c$.
[8] BARISH 87 searched for quark matter ("nuclearites") in the velocity range $(2.7 \times 10^{-4}$–$5 \times 10^{-3})c$.
[9] NAKAMURA 85 at KEK searched for quark-matter. These might be lumps of strange quark matter with roughly equal numbers of u, d, s quarks. These lumps or nuclearites were assumed to have velocity of $(10^{-4}$–$10^{-3})$ c.
[10] ULLMAN 81 is sensitive for heavy slow singly charge particle reaching earth with vertical velocity 100–350 km/s.

Highly Ionizing Particle Flux

VALUE ($m^{-2}yr^{-1}$)	CL%	EVTS	DOCUMENT ID		TECN	COMMENT
• • • We do not use the following data for averages, fits, limits, etc. • • •						
<0.4	95	0	KINOSHITA	81B	PLAS	Z/β 30–100

SEARCHES FOR BLACK HOLE PRODUCTION

VALUE	DOCUMENT ID		TECN	COMMENT
• • • We do not use the following data for averages, fits, limits, etc. • • •				
not seen	[1] AABOUD	16P	ATLS	13 TeV $pp \to e\mu, e\tau, \mu\tau$
	[2] AAD	15AN	ATLS	8 TeV $pp \to$ multijets
	[3] AAD	14A	ATLS	8 TeV $pp \to \gamma +$ jet
	[4] AAD	14AL	ATLS	8 TeV $pp \to \ell +$ jet
	[5] AAD	14C	ATLS	8 TeV $pp \to \ell +$ (ℓ or jets)
	[6] AAD	13D	ATLS	7 TeV $pp \to 2$ jets
	[7] CHATRCHYAN	13A	CMS	7 TeV $pp \to 2$ jets
	[8] CHATRCHYAN	13AD	CMS	8 TeV $pp \to$ multijets
	[9] AAD	12AK	ATLS	7 TeV $pp \to \ell +$ (ℓ or jets)
	[10] CHATRCHYAN	12W	CMS	7 TeV $pp \to$ multijets
	[11] AAD	11AG	ATLS	7 TeV $pp \to 2$ jets

[1] AABOUD 16P set limits on quantum BH production in n = 6 ADD or n = 1 RS models.
[2] AAD 15AN search for black hole or string ball formation followed by its decay to multijet final states, in pp collisions at $E_{cm} = 8$ TeV with $L = 20.3$ fb^{-1}. See their Figs. 6–8 for limits.
[3] AAD 14A search for quantum black hole formation followed by its decay to a γ and a jet, in pp collisions at $E_{cm} = 8$ TeV with $L = 20$ fb^{-1}. See their Fig. 3 for limits.
[4] AAD 14AL search for quantum black hole formation followed by its decay to a lepton and a jet, in pp collisions at $E_{cm} = 8$ TeV with $L = 20.3$ fb^{-1}. See their Fig. 2 for limits.
[5] AAD 14C search for microscopic (semiclassical) black hole formation followed by its decay to final states with a lepton and ≥ 2 (leptons or jets), in pp collisions at $E_{cm} = 8$ TeV with $L = 20.3$ fb^{-1}. See their Figures 8–11, Tables 7, 8 for limits.
[6] AAD 13D search for quantum black hole formation followed by its decay to two jets, in pp collisions at $E_{cm} = 7$ TeV with $L = 4.8$ fb^{-1}. See their Fig. 8 and Table 3 for limits.
[7] CHATRCHYAN 13A search for quantum black hole formation followed by its decay to two jets, in pp collisions at $E_{cm} = 7$ TeV with $L = 5$ fb^{-1}. See their Figs. 5 and 6 for limits.
[8] CHATRCHYAN 13AD search for microscopic (semiclassical) black hole formation followed by its evapolation to multiparticle final states, in multijet (including γ, ℓ) events in pp collisions at $E_{cm} = 8$ TeV with $L = 12$ fb^{-1}. See their Figs. 5–7 for limits.
[9] AAD 12AK search for microscopic (semiclassical) black hole formation followed by its decay to final states with a lepton and ≥ 2 (leptons or jets), in pp collisions at $E_{cm} = 7$ TeV with $L = 1.04$ fb^{-1}. See their Fig. 4 and 5 for limits.
[10] CHATRCHYAN 12W search for microscopic (semiclassical) black hole formation followed by its evapolation to multiparticle final states, in multijet (including γ, ℓ) events in pp collisions at $E_{cm} = 7$ TeV with $L = 4.7$ fb^{-1}. See their Figs. 5–8 for limits.
[11] AAD 11AG search for quantum black hole formation followed by its decay to two jets, in pp collisions at $E_{cm} = 7$ TeV with L = 36 pb^{-1}. See their Fig. 11 and Table 4 for limits.

REFERENCES FOR Other Particle Searches

AABOUD	17B	PL B765 32	M. Aaboud *et al.* (ATLAS Collab.)
AABOUD	17D	PR D95 032001	M. Aaboud *et al.* (ATLAS Collab.)
AABOUD	17L	JHEP 1708 052	M. Aaboud *et al.* (ATLAS Collab.)
AAIJ	17BR	EPJ C77 812	R. Aaij *et al.* (LHCb Collab.)
ABLIKIM	17AA	PL B774 252	M. Ablikim *et al.* (BES III Collab.)
KHACHATRY...	17D	JHEP 1701 076	V. Khachatryan *et al.* (CMS Collab.)
KHACHATRY...	17W	PL B769 520	V. Khachatryan *et al.* (CMS Collab.)
KHACHATRY...	17Y	PL B770 257	V. Khachatryan *et al.* (CMS Collab.)
SIRUNYAN	17B	JHEP 1704 136	A.M. Sirunyan *et al.* (CMS Collab.)
SIRUNYAN	17C	JHEP 1705 029	A.M. Sirunyan *et al.* (CMS Collab.)
SIRUNYAN	17F	JHEP 1707 013	A.M. Sirunyan *et al.* (CMS Collab.)
SIRUNYAN	17J	JHEP 1708 073	A.M. Sirunyan *et al.* (CMS Collab.)
AABOUD	16	PL B759 229	M. Aaboud *et al.* (ATLAS Collab.)
AABOUD	16P	EPJ C76 541	M. Aaboud *et al.* (ATLAS Collab.)
AAD	16AI	JHEP 1603 041	G. Aad *et al.* (ATLAS Collab.)
AAD	16N	JHEP 1603 026	G. Aad *et al.* (ATLAS Collab.)
AAD	16O	PL B760 520	G. Aad *et al.* (ATLAS Collab.)
AAD	16R	PL B755 285	G. Aad *et al.* (ATLAS Collab.)
AAD	16S	PL B754 302	G. Aad *et al.* (ATLAS Collab.)
AAIJ	16AR	EPJ C76 664	R. Aaij *et al.* (LHCb Collab.)
KHACHATRY...	16BW	PR D94 112004	V. Khachatryan *et al.* (CMS Collab.)
KHACHATRY...	16K	PRL 116 071801	V. Khachatryan *et al.* (CMS Collab.)
KHACHATRY...	16L	PRL 117 031802	V. Khachatryan *et al.* (CMS Collab.)
KHACHATRY...	16M	PRL 117 051802	V. Khachatryan *et al.* (CMS Collab.)
AAD	15AN	JHEP 1507 032	G. Aad *et al.* (ATLAS Collab.)
AAD	15AT	EPJ C75 79	G. Aad *et al.* (ATLAS Collab.)
AAD	15BJ	EPJ C75 362	G. Aad *et al.* (ATLAS Collab.)
AAIJ	15BD	EPJ C75 595	R. Aaij *et al.* (LHCb Collab.)
ADRIANI	15	PRL 115 111101	O. Adriani *et al.* (PAMELA Collab.)
AGNESE	15	PRL 114 111302	R. Agnese *et al.* (CDMS Collab.)
KHACHATRY...	15F	PRL 114 101801	V. Khachatryan *et al.* (CMS Collab.)
LEES	15E	PRL 114 171801	J.P. Lees *et al.* (BABAR Collab.)
AAD	14A	PL B728 562	G. Aad *et al.* (ATLAS Collab.)
AAD	14AL	PRL 112 091804	G. Aad *et al.* (ATLAS Collab.)
AAD	14C	JHEP 1408 103	G. Aad *et al.* (ATLAS Collab.)
AALTONEN	14J	PR D89 092001	T. Aaltonen *et al.* (CDF Collab.)
AAD	13A	PL B718 860	G. Aad *et al.* (ATLAS Collab.)
AAD	13AH	PL B722 305	G. Aad *et al.* (ATLAS Collab.)
AAD	13C	PRL 110 011802	G. Aad *et al.* (ATLAS Collab.)
AAD	13D	JHEP 1301 029	G. Aad *et al.* (ATLAS Collab.)
AALTONEN	13I	PR D88 031103	T. Aaltonen *et al.* (CDF Collab.)
AALTONEN	13R	PRL 111 031802	T. Aaltonen *et al.* (CDF Collab.)
CHATRCHYAN	13	PL B718 815	S. Chatrchyan *et al.* (CMS Collab.)
CHATRCHYAN	13A	JHEP 1301 013	S. Chatrchyan *et al.* (CMS Collab.)
CHATRCHYAN	13AB	JHEP 1307 122	S. Chatrchyan *et al.* (CMS Collab.)
CHATRCHYAN	13AD	JHEP 1307 178	S. Chatrchyan *et al.* (CMS Collab.)
CHATRCHYAN	13AR	PR D87 092008	S. Chatrchyan *et al.* (CMS Collab.)
AAD	12AK	PL B716 122	G. Aad *et al.* (ATLAS Collab.)
AAD	12C	PRL 108 041805	G. Aad *et al.* (ATLAS Collab.)
AAD	12S	PL B708 37	G. Aad *et al.* (ATLAS Collab.)
AALTONEN	12M	PRL 108 211804	T. Aaltonen *et al.* (CDF Collab.)
CHATRCHYAN	12AP	JHEP 1209 094	S. Chatrchyan *et al.* (CMS Collab.)
CHATRCHYAN	12BL	JHEP 1212 015	S. Chatrchyan *et al.* (CMS Collab.)
CHATRCHYAN	12Q	PL B716 260	S. Chatrchyan *et al.* (CMS Collab.)
CHATRCHYAN	12T	PRL 108 261803	S. Chatrchyan *et al.* (CMS Collab.)
CHATRCHYAN	12W	JHEP 1204 061	S. Chatrchyan *et al.* (CMS Collab.)
AAD	11AG	NJP 13 053044	G. Aad *et al.* (ATLAS Collab.)
AAD	11I	PL B698 353	G. Aad *et al.* (ATLAS Collab.)
AAD	11S	PL B705 294	G. Aad *et al.* (ATLAS Collab.)
AALTONEN	11AF	PRL 107 181801	T. Aaltonen *et al.* (CDF Collab.)
AALTONEN	11M	PRL 106 171801	T. Aaltonen *et al.* (CDF Collab.)
ABAZOV	11I	PRL 107 011804	V.M. Abazov *et al.* (D0 Collab.)
CHATRCHYAN	11C	JHEP 1106 026	S. Chatrchyan *et al.* (CMS Collab.)
CHATRCHYAN	11U	PRL 107 201804	S. Chatrchyan *et al.* (CMS Collab.)
AAD	10	PRL 105 161801	G. Aad *et al.* (ATLAS Collab.)
AALTONEN	10AF	PR D82 052005	T. Aaltonen *et al.* (CDF Collab.)
KHACHATRY...	10	PRL 105 211801	V. Khachatryan *et al.* (CMS Collab.)
Also		PRL 106 029902	V. Khachatryan *et al.* (CMS Collab.)
AALTONEN	09AF	PR D80 011102	T. Aaltonen *et al.* (CDF Collab.)
AALTONEN	09G	PR D79 052004	T. Aaltonen *et al.* (CDF Collab.)
AALTONEN	09Z	PRL 103 021802	T. Aaltonen *et al.* (CDF Collab.)
ABAZOV	09M	PRL 102 161802	V.M. Abazov *et al.* (D0 Collab.)
AKTAS	04C	EPJ C36 413	A. Atkas *et al.* (H1 Collab.)
JAVORSEK	02	PR D65 072003	D. Javorsek II *et al.*
JAVORSEK	01	PR D64 012005	D. Javorsek II *et al.*
JAVORSEK	01B	PRL 87 231804	D. Javorsek II *et al.*
ABBIENDI	00D	EPJ C13 197	G. Abbiendi *et al.* (OPAL Collab.)
AMBROSIO	00B	EPJ C13 453	M. Ambrosio *et al.* (MACRO Collab.)
ABE	99F	PRL 82 2038	F. Abe *et al.* (CDF Collab.)
ACKERSTAFF	98P	PL B433 195	K. Ackerstaff *et al.* (OPAL Collab.)
ABE	97G	PR D55 5263	F. Abe *et al.* (CDF Collab.)
ABREU	97D	PL B396 315	P. Abreu *et al.* (DELPHI Collab.)
ACKERSTAFF	97B	PL B391 210	K. Ackerstaff *et al.* (OPAL Collab.)
ADAMS	97B	PRL 79 4083	J. Adams *et al.* (FNAL KTeV Collab.)
BARATE	97K	PL B405 379	R. Barate *et al.* (ALEPH Collab.)
AKERS	95R	ZPHY C67 203	R. Akers *et al.* (OPAL Collab.)
GALLAS	95	PR D52 6	E. Gallas *et al.* (MSU, FNAL, MIT, FLOR)
RAM	94	PR D49 3120	S. Ram *et al.* (TELA, TRIU)
ABE	93G	PR 71 2542	F. Abe *et al.* (CDF Collab.)
ASTONE	93	PR D47 4770	P. Astone *et al.* (ROMA, ROMAI, CATA, FRAS)
BUSKULIC	93C	PL B303 198	D. Buskulic *et al.* (ALEPH Collab.)
YAMAGATA	93	PR D47 1231	T. Yamagata, Y. Takamori, H. Utsunomiya (KONAN)
ABE	92J	PR D46 1889	F. Abe *et al.* (CDF Collab.)
AHLEN	92	PRL 69 1860	S.P. Ahlen *et al.* (MACRO Collab.)
VERKERK	92	PRL 68 1116	P. Verkerk *et al.* (ENSP, SACL, PAST)
AKESSON	91	ZPHY C52 219	T. Akesson *et al.* (HELIOS Collab.)
NAKAMURA	91	PL B263 529	S. Nakamura *et al.*
ORITO	91	PRL 66 1951	S. Orito *et al.* (ICEPP, WASCR, NIHO, ICRR)
ADACHI	90C	PL B244 352	I. Adachi *et al.* (TOPAZ Collab.)
ADACHI	90E	PL B249 336	I. Adachi *et al.* (TOPAZ Collab.)
AKRAWY	90O	PL B252 290	M.Z. Akrawy *et al.* (OPAL Collab.)
HEMMICK	90	PR D41 2074	T.K. Hemmick *et al.* (ROCH, MICH, OHIO+)
SAITO	90	PRL 65 2094	T. Saito *et al.* (ICRR, KOBE)
NAKAMURA	89	PR D39 1261	T.T. Nakamura *et al.* (KYOT, TMTC)
NORMAN	89	PR D39 2499	E.B. Norman *et al.* (LBL)
BERNSTEIN	88	PR D37 3103	R.M. Bernstein *et al.* (STAN, WISC)
LIU	88	PRL 61 271	G. Liu, B. Barish
BARISH	87	PR D36 2641	B.C. Barish, G. Liu, C. Lane (CIT)
NORMAN	87	PRL 58 1403	E.B. Norman, S.B. Gazes, D.A. Bennett (LBL)
BADIER	86	ZPHY C31 21	J. Badier *et al.* (NA3 Collab.)
MINCER	85	PR D32 541	A. Mincer *et al.* (UMD, GMAS, NSF)
NAKAMURA	85	PL 161B 417	K. Nakamura *et al.* (KEK, INUS)
THRON	85	PR D31 451	J.L. Thron *et al.* (YALE, FNAL, IOWA)

SAKUYAMA	83B	LNC 37 17	H. Sakuyama, N. Suzuki	(MEIS)
Also		LNC 36 389	H. Sakuyama, K. Watanabe	(MEIS)
Also		NC 78A 147	H. Sakuyama, K. Watanabe	(MEIS)
Also		NC 6C 371	H. Sakuyama, K. Watanabe	(MEIS)
BHAT	82	PR D25 2820	P.N. Bhat *et al.*	(TATA)
KINOSHITA	82	PRL 48 77	K. Kinoshita, P.B. Price, D. Fryberger	(UCB+)
MARINI	82	PR D26 1777	A. Marini *et al.*	(FRAS, LBL, NWES, STAN+)
SMITH	82B	NP B206 333	P.F. Smith *et al.*	(RAL)
KINOSHITA	81B	PR D24 1707	K. Kinoshita, P.B. Price	(UCB)
LOSECCO	81	PL 102B 209	J.M. LoSecco *et al.*	(MICH, PENN, BNL)
ULLMAN	81	PRL 47 289	J.D. Ullman	(LEHM, BNL)
YOCK	81	PR D23 1207	P.C.M. Yock	(AUCK)
BARTEL	80	ZPHY C6 295	W. Bartel *et al.*	(JADE Collab.)
BUSSIERE	80	NP B174 1	A. Bussiere *et al.*	(BGNA, SACL, LAPP)
YOCK	80	PR D22 61	P.C.M. Yock	(AUCK)
ARMITAGE	79	NP B150 87	J.C.M. Armitage *et al.*	(CERN, DARE, FOM+)
BOZZOLI	79	NP B159 363	W. Bozzoli *et al.*	(BGNA, LAPP, SACL+)
GOODMAN	79	PR D19 2572	J.A. Goodman *et al.*	(UMD)
SMITH	79	NP B149 525	P.F. Smith, J.R.J. Bennett	(RHEL)
BHAT	78	PRAM 10 115	P.N. Bhat, P.V. Ramana Murthy	(TATA)
CARROLL	78	PRL 41 777	A.S. Carroll *et al.*	(BNL, PRIN)
CUTTS	78	PRL 41 363	D. Cutts *et al.*	(BROW, FNAL, ILL, BARI+)
VIDAL	78	PL 77B 344	R.A. Vidal *et al.*	(COLU, FNAL, STON+)
ALEKSEEV	76	SJNP 22 531	G.D. Alekseev *et al.*	(JINR)
		Translated from YAF 22 1021.		
ALEKSEEV	76B	SJNP 23 633	G.D. Alekseev *et al.*	(JINR)
		Translated from YAF 23 1190.		
BALDIN	76	SJNP 22 264	B.Y. Baldin *et al.*	(JINR)
		Translated from YAF 22 512.		
BRIATORE	76	NC 31A 553	L. Briatore *et al.*	(LCGT, FRAS, FREIB)
GUSTAFSON	76	PRL 37 474	H.R. Gustafson *et al.*	(MICH)
ALBROW	75	NP B97 189	M.G. Albrow *et al.*	(CERN, DARE, FOM+)
FRANKEL	75	PR D12 2561	S. Frankel *et al.*	(PENN, FNAL)
JOVANOV...	75	PL 56B 105	J.V. Jovanovich *et al.*	(MANI, AACH, CERN+)
YOCK	75	NP B86 216	P.C.M. Yock	(AUCK, SLAC)
APPEL	74	PRL 32 428	J.A. Appel *et al.*	(COLU, FNAL)
FRANKEL	74	PR D9 1932	S. Frankel *et al.*	(PENN, FNAL)
YOCK	74	NP B76 175	P.C.M. Yock	(AUCK)
ALPER	73	PL 46B 265	B. Alper *et al.*	(CERN, LIVP, LUND, BOHR+)
LEIPUNER	73	PRL 31 1226	L.B. Leipuner *et al.*	(BNL, YALE)
DARDO	72	NC 9A 319	M. Dardo *et al.*	(TORI)
TONWAR	72	JP A5 569	S.C. Tonwar, S. Naranan, B.V. Sreekantan	(TATA)
ANTIPOV	71B	NP B31 235	Y.M. Antipov *et al.*	(SERP)
ANTIPOV	71C	PL 34B 164	Y.M. Antipov *et al.*	(SERP)
BINON	69	PL 30B 510	F.G. Binon *et al.*	(SERP)
BJORNBOE	68	NC B53 241	J. Bjornboe *et al.*	(BOHR, TATA, BERN+)
JONES	67	PR 164 1584	L.W. Jones	(MICH, WISC, LBL, UCLA, MINN+)
DORFAN	65	PRL 14 999	D.E. Dorfan *et al.*	(COLU)

INDEX

Greek letters are alphabetized by their English-language spelling. Bold page numbers signify entries in the Particle Properties Summary Tables.

Greek letters are alphabetized by their English-language spelling. Bold page numbers signify entries in the Particle Properties Summary Tables.

Greek letters are alphabetized by their English-language spelling. Bold page numbers signify entries in the Particle Properties Summary Tables.

Greek letters are alphabetized by their English-language spelling. Bold page numbers signify entries in the Particle Properties Summary Tables.

Greek letters are alphabetized by their English-language spelling. Bold page numbers signify entries in the Particle Properties Summary Tables.

Greek letters are alphabetized by their English-language spelling. Bold page numbers signify entries in the Particle Properties Summary Tables.

Greek letters are alphabetized by their English-language spelling. Bold page numbers signify entries in the Particle Properties Summary Tables.

Greek letters are alphabetized by their English-language spelling. Bold page numbers signify entries in the Particle Properties Summary Tables.

Greek letters are alphabetized by their English-language spelling. Bold page numbers signify entries in the Particle Properties Summary Tables.

Greek letters are alphabetized by their English-language spelling. Bold page numbers signify entries in the Particle Properties Summary Tables.

Greek letters are alphabetized by their English-language spelling. Bold page numbers signify entries in the Particle Properties Summary Tables.

Greek letters are alphabetized by their English-language spelling. Bold page numbers signify entries in the Particle Properties Summary Tables.

Greek letters are alphabetized by their English-language spelling. Bold page numbers signify entries in the Particle Properties Summary Tables.

Greek letters are alphabetized by their English-language spelling. Bold page numbers signify entries in the Particle Properties Summary Tables.

Greek letters are alphabetized by their English-language spelling. Bold page numbers signify entries in the Particle Properties Summary Tables.